



NIST Combinatorial Methods Center

NCMC-4: Polymer Formulations October 6-7, 2003 ♦ Bldg. 101 / Lecture Rm. A

Monday, October 6th, 2003

8:30 am Registration
Coffee & Doughnuts

8:45 am Welcome and Introductions
Eric Amis, *Polymers Division, Chief*

9:00 am Project Overview
Kate Beers, *NCMC*

9:15 am Complex Fluids from Polymer and Surfactant
Meso Phase Interactions
Robert Prud'homme, *Princeton University*

10:00 am *Coffee Break*

10:15 am A New Approach to Combinatorial Rheology
Measurements **Howard Walls**, *NCMC*

10:45 am Rapid Prototyping of Fluid Devices for
Polymer Formulations **João Cabral**, *NCMC*

11:15 am Scattering Methods Applied to High
Throughput Materials Research
Alexander Norman, *NCMC*

11:45 am *Lunch* (NIST cafeteria, Bldg. 101)

1:15 pm 3D Microscopy and Imaging as
Characterization Tools
Marcus Cicerone, *NIST Polymers*

1:40 pm Single Molecule Measurement Methods at
NIST **Angela Hight Walker**, *Optical
Technology Division, Physics Laboratory*

2:05 pm Trials and Tribulations of the Application of
HTS Methods to Evaluation of PVC
Stabilizers **Douglas Wicks**, *University of
Southern Mississippi*

2:35 pm *Coffee Break*

2:50 pm Optical Materials Library Design
Michael Doyle, *Accelrys*

3:20 pm Mapping of Generic and Application Specific
Properties of Formulations using High
Throughput Screening and Small Sample
Sensing Methods **Oleg Kolosov**, *Symyx*

4:20 pm Poster Session

6:30 pm *Dinner* (Buca di Beppo)
(122 Kentlands Blvd., Gaithersburg)

Tuesday, October 7th, 2003

8:30 am *Coffee & Doughnuts*

8:45 am Multiphase Droplet Production and
Manipulation using Microfluidics
David Weitz, *Harvard University*

9:30 am Influence of Geometrical Confinement on
Thread Breakup
Jack Douglas, *NIST Polymers*

10:00 am Measuring Dynamic Properties of Small
Scale Interfaces
Steve Hudson, *NIST Polymers*

10:30 am *Coffee Break*

10:45 am Gradient Methods for Nano-Scale Metrology
Michael Fasolka, *NCMC*

11:00 am Open Discussion: Gradient Surfaces as
Standards leader: **Kate Beers**, *NCMC*

12:00 pm *Lunch* (NIST cafeteria, Bldg. 101)

1:30 pm **NCMC lab tours, demos, etc.**

4:00 pm Meeting Over

NIST Combinatorial Methods Center

Welcome to NCMC-4: Polymer Formulations Workshop

October 6-8, 2003

National Institute of Standards and Technology
Gaithersburg, MD



NCMC Membership

20 Industrial, 1 Government and 1 Academic Partner



7 NEW Members since NCMC-3!



COMBI Group Changes

- *NEW* Group Leader: Dr. Michael J. Fasolka



Dr. Alamgir Karim
(1 year management detail)



- *NEW* Group Members:



Arnaud Chiche
(Creton, ESPCI)
Adhesion and Mechanical
Properties



Tao Wu
(Genzer, NCSU)
Polymer Formulations



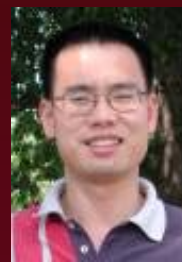
Duangrut (Mai) Julthongpiput
(Tsukruk, ISU)
SPM Model Surfaces

3 more new scientists coming in next 4 months!

NCMC Research Team



NIST Combinatorial
Methods Center



Polymer Formulations
Project



Adhesion and Mechanical
Properties Project



Division Collaborators

NCMC Focused Projects

- 2nd level of NCMC membership
- High Throughput Methods of Measuring Interfacial Tension (IFT) (S. Hudson and K. Beers)
 - Begun September 2003
 - 2 members
- High Throughput Methods of the Evaluation of Adhesion Performance (A. Forster and C. Stafford)
 - November Start (staff hire)
 - 2 members
- Integration of Modular Measurement Platform for High Throughput Analysis of Polymer Solutions and Blends (H. Walls and K. Beers)
- New Opportunities?

All research carried out in a Focused Project is non-proprietary and is intended for publication in the public domain. No proprietary information or materials will be solicited or accepted by NIST from member organizations.

Upcoming Events: COMBI Calendar

- 2003 MRS Symposium, *Combinatorial and Artificial Intelligence Methods in Materials Science II*, Dec. 1-5, 2003, Boston, MA (A. Karim, Co-organizer)
- Gordon Research Conference on Combinatorial and High Throughput Materials Science, Jan. 25-30, 2004, Santa Barbara, CA
- 2004 Adhesion Society Session, *Combinatorial Methods in Adhesion*, Feb. 15-18, 2004, Wilmington, NC (C. Stafford, Organizer)
- 2004 ACS Symposium, *Combinatorial Approaches to Materials Science*, Mar. 28-Apr. 1, 2004, Anaheim, CA (C. Davis, A. Karim, Co-organizers)
- NCMC-5: TBA, April 5 – 7, 2004, Gaithersburg, MD
- COMBI 2004, Joint NCMC-Knowledge Foundation Session on Polymer Formulations, May 3-5, 2004, DC Metro Area (M. Fasolka, Co-organizer)



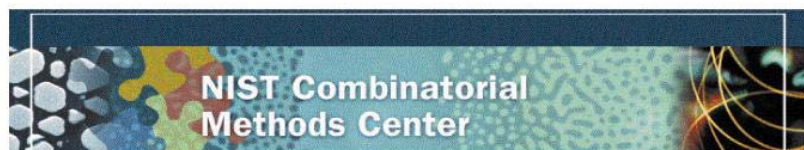
Polymer Formulations

- Complex mixtures with multiple component types
- Experience, empirical models and trial and error in the past
- Polymer mixtures and solutions, and additives play a critical role

NCMC role:

- Demonstrating simple, inexpensive, and *quantitative* high throughput and combinatorial measurements and methods
- Demonstrating innovative approaches to experimental design
- Collecting and disseminating information on combinatorial approaches and measurement methods
- Provide coordinated outreach for the NIST Labs' research activities that support this topic

NCMC-4 Agenda



NCMC-4: Polymer Formulations October 6-7, 2003 • Bldg. 101 / Lecture Rm. A

Monday, October 6th, 2003

8:30 am	Registration <i>Coffee & Doughnuts</i>	3:20 pm	Mapping of Generic and Application Specific Properties of Formulations using High Throughput Screening and Small Sample Sensing Methods Oleg Kolosov , <i>Symyx</i>
8:45 am	Welcome and Introductions Eric Amis , <i>Polymers Division, Chief</i>	4:20 pm	Poster Session
9:00 am	Project Overview Kate Beers , <i>NCMC</i>	6:30 pm	Dinner (Buca di Beppo) (122 Kentlands Blvd., Gaithersburg)
9:15 am	Complex Fluids from Polymer and Surfactant Meso Phase Interactions Robert Prud'homme , <i>Princeton University</i>	Tuesday, October 7th, 2003	
10:00 am	Coffee Break	8:30 am	Coffee & Doughnuts
10:15 am	A New Approach to Combinatorial Rheology Measurements Howard Walls , <i>NCMC</i>	8:45 am	Multiphase Droplet Production and Manipulation using Microfluidics David Weitz , <i>Harvard University</i>
10:45 am	Rapid Prototyping of Fluid Devices for Polymer Formulations João Cabral , <i>NCMC</i>	9:30 am	Influence of Geometrical Confinement on Thread Breakup Jack Douglas , <i>NIST Polymers</i>
11:15 am	Scattering Methods Applied to High Throughput Materials Research Alexander Norman , <i>NCMC</i>	10:00 am	Measuring Dynamic Properties of Small Scale Interfaces Steve Hudson , <i>NIST Polymers</i>
11:45 am	Lunch (NIST cafeteria, Bldg. 101)	10:30 am	Coffee Break
1:15 pm	3D Microscopy and Imaging as Characterization Tools Marcus Cicerone , <i>NIST Polymers</i>	10:45 am	Gradient Methods for Nano-Scale Metrology Michael Fasolka , <i>NCMC</i>
1:40 pm	Single Molecule Measurement Methods at NIST Angela Hight Walker , <i>Optical Technology Division, Physics Laboratory</i>	11:00 am	Open Discussion: Gradient Surfaces as Standards leader: Kate Beers , <i>NCMC</i>
2:05 pm	Trials and Tribulations of the Application of HTS Methods to Evaluation of PVC Stabilizers Douglas Wicks , <i>University of Southern Mississippi</i>	12:00 pm	Lunch (NIST cafeteria, Bldg. 101)
2:35 pm	Coffee Break	1:30 pm	NCMC lab tours, demos, etc.
2:50 pm	Optical Materials Library Design Michael Doyle , <i>Accelrys</i>	4:00 pm	Meeting Over

New HT&C measurement tools and strategies for characterizing complex fluids and polymer blends.

- **Plenary Lectures:**
Robert Prud'homme, Princeton University
David Weitz, Harvard University
- **NCMC Members:**
Douglas Wicks, University of Southern Mississippi
Michael Doyle, Accelrys
Oleg Kolosov, Symyx

NIST Combinatorial Methods Center

Polymer Formulations

Kate Beers, project leader

Group Members

J. T. Cabral, A. I. Norman,
H. J. Walls, T. Wu

Collaborators

S. Hudson, Processing Characterization Group
C. Stafford, NCMC



Project Development

Meeting NCMC Member Needs

- Polymer Formulations is the first project developed in direct response to discussions with members of the NCMC.

Project Objective

- To develop HT or combinatorial methods for measuring properties, such as *viscosity*, *interfacial tension*, *stability*, *compatibility and reactivity*, of polymeric mixtures involving multiple component types

Approach

- Develop *modular, rapid and small scale* fluidic reactors, mixing devices and measurement techniques
- Fabricate small scale instrumentation for testing complex fluid properties

COMBI Group Toolset

Mapping Crossed Gradients in Thin Films

Continuous Gradient Specimens



- Gradual and steady change in a property as a function of distance

NCMC Gradient Specimens

- Properties of interest to materials researchers
- Tailored gradient scope and steepness
- Reproducible fabrication

Crossed-Gradient Combinatorial Libraries

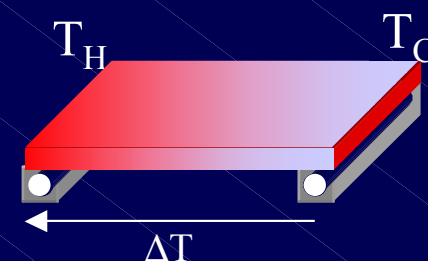
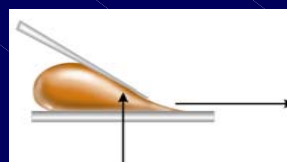
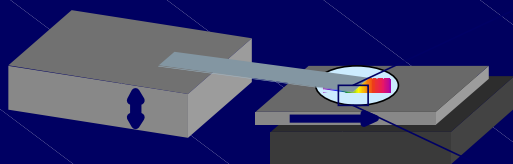
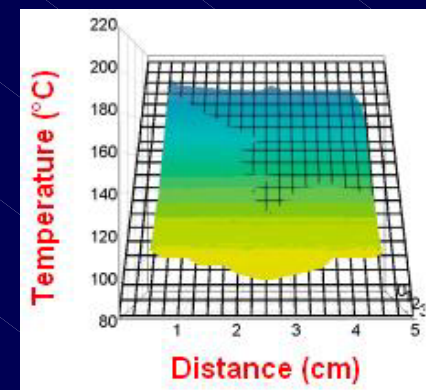
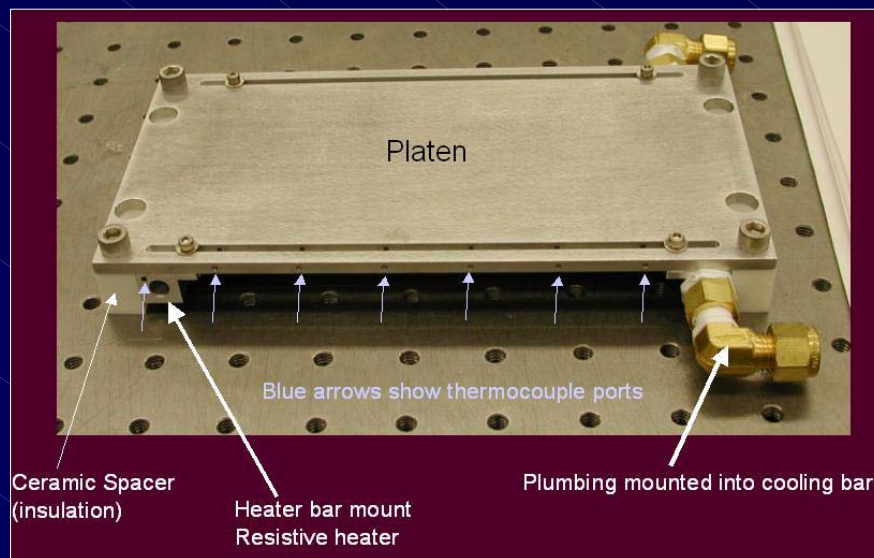


- Orthogonal arrangement of 2 gradient specimens
- Includes every combination of 2 variables within scope of gradients

COMBI Group Toolset

Variables:

- Film thickness
- Temperature
- Crosslink density
- Surface chemistry
- Crystallinity
- Composition
- Surface Patterns



ASK FOR MORE
DETAILS
DURING THE
LAB OPEN
HOUSE!

Formulations Toolset - Needs

Mixing / Processing – Fabrication

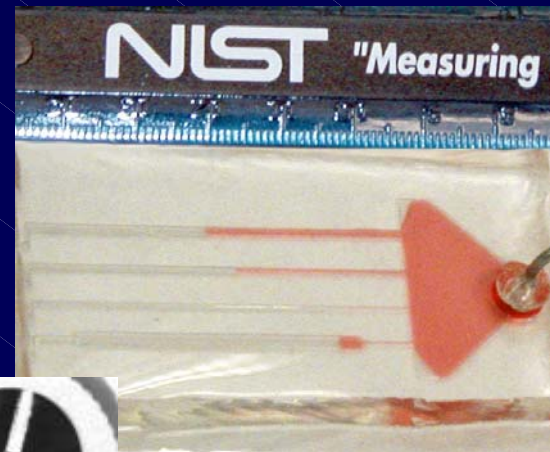
- Active vs. passive mixing, solvents, concentrations, temperature

Characterization / Properties Measurements

- Rheology
- Interfacial behavior
 - Interfacial tension measurements
- Mapping phase diagrams
 - Scattering platforms

How to build new tools?

- Length scales
- Materials
- Static vs. dynamic libraries
- Cheap, fast and flexible



H. Walls



Design Strategies

Why meso- and micro-scale fluidics?

- Increasing demand for smaller length scales ($\text{g} \rightarrow \mu\text{g}$)
- Expensive additives
- Sampling COMBI libraries

Less emphasis on library fab. until measurement tools are developed

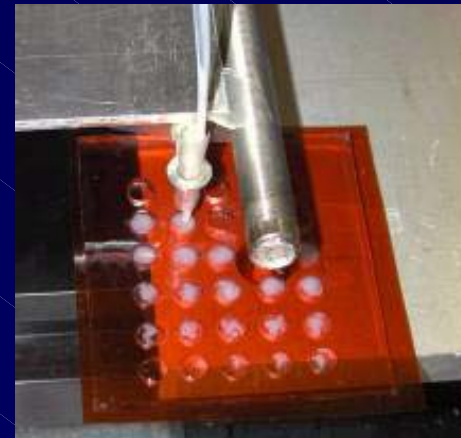
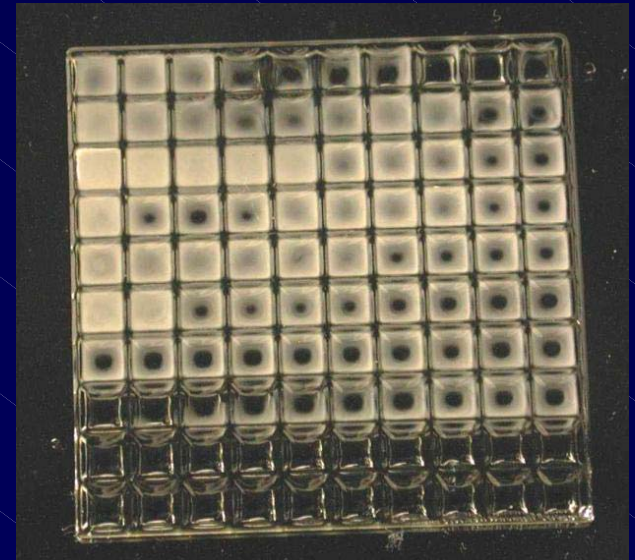
- Few examples

Connection to existing NCMC and NIST resources

- Adhesion and Mechanical Properties Project

Creativity and Innovation

- Integration



J. Cabral and
A. Norman

Measurement Method Development

Fluid – fluid interfaces

- Modeling
- 4-roll mill analog



HT Rheology

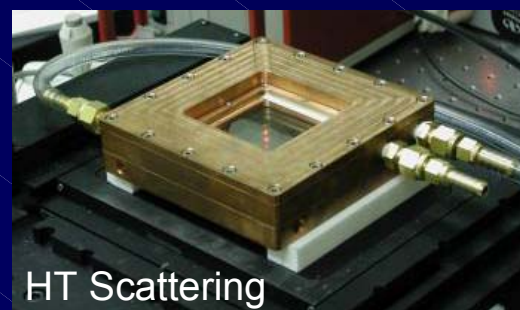
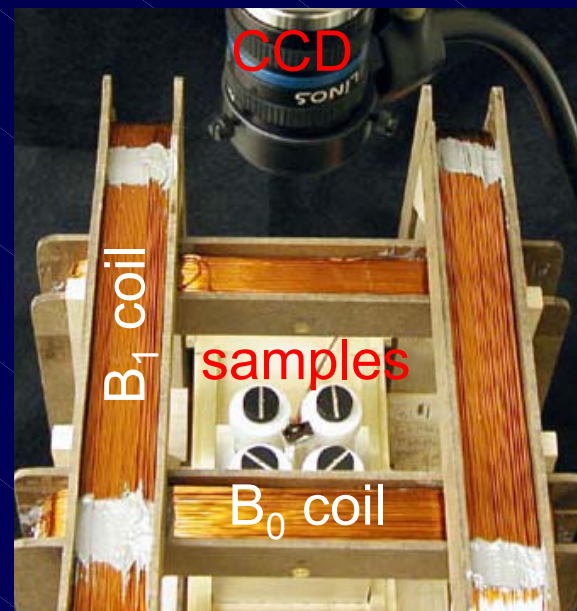
- Progressive down-scaling

Phase mapping (emulsions and blends)

- Modeling
- Scattering tools

Future Areas / Collaborations

- Solid – fluid interfaces
- Leveraging other NIST resources
 - 3-D Imaging, SM³



NCMC-4: Polymer Formulations



NIST Combinatorial Methods Center

NCMC-4: Polymer Formulations
October 6-7, 2003 • Bldg. 101 / Lecture Rm. A

Monday, October 6th, 2003

8:30 am	Registration Coffee & Doughnuts	3:20 pm	Mapping of Generic and Application Specific Properties of Formulations using High Throughput Screening and Small Sample Sensing Methods Oleg Kolosov, Symyx
8:45 am	Welcome and Introductions Eric Amis, Polymers Division, Chief	4:20 pm	Poster Session
9:00 am	Project Overview Kate Beers, NCMC	6:30 pm	Dinner (Buca di Beppo) (122 Kentlands Blvd., Gaithersburg)
9:15 am	Complex Fluids from Polymer and Surfactant Meso Phase Interactions Robert Prud'homme, Princeton University	Tuesday, October 7th, 2003	
10:00 am	Coffee Break	8:30 am	Coffee & Doughnuts
10:15 am	A New Approach to Combinatorial Rheology Measurements Howard Walls, NCMC	8:45 am	Multiphase Droplet Production and Manipulation using Microfluidics David Weitz, Harvard University
10:45 am	Rapid Prototyping of Fluid Devices for Polymer Formulations João Cabral, NCMC	9:30 am	Influence of Geometrical Confinement on Thread Breakup Jack Douglas, NIST Polymers
11:15 am	Scattering Methods Applied to High Throughput Materials Research Alexander Norman, NCMC	10:00 am	Measuring Dynamic Properties of Small Scale Interfaces Steve Hudson, NIST Polymers
11:45 am	Lunch (NIST cafeteria, Bldg. 101)	10:30 am	Coffee Break
1:15 pm	3D Microscopy and Imaging as Characterization Tools Marcus Cicerone, NIST Polymers	10:45 am	Gradient Methods for Nano-Scale Metrology Michael Fasolka, NCMC
1:40 pm	Single Molecule Measurement Methods at NIST Angela Hight Walker, Optical Technology Division, Physics Laboratory	11:00 am	Open Discussion: Gradient Surfaces as Standards leader: Kate Beers, NCMC
2:05 pm	Trials and Tribulations of the Application of HTS Methods to Evaluation of PVC Stabilizers Douglas Wicks, University of Southern Mississippi	12:00 pm	Lunch (NIST cafeteria, Bldg. 101)
2:35 pm	Coffee Break	1:30 pm	NCMC lab tours, demos, etc.
2:50 pm	Optical Materials Library Design Michael Doyle, Accelrys	4:00 pm	Meeting Over

Elucidating issues in complex fluid behavior

NCMC approaches:

- HT Rheology
- Device fabrication and design strategies
- Phase mapping (emulsions and blends)

Measurement tool inspiration at NIST

- 3-D imaging and SM³

NCMC Members

- Formulation screening

NCMC-4: Polymer Formulations

NIST Combinatorial Methods Center

NCMC-4: Polymer Formulations
October 6-7, 2003 • Bldg. 101 / Lecture Rm. A

Monday, October 6th, 2003

8:30 am	Registration <i>Coffee & Doughnuts</i>	3:20 pm	Mapping of Generic and Application Specific Properties of Formulations using High Throughput Screening and Small Sample Sensing Methods Oleg Kolosov, Symyx
8:45 am	Welcome and Introductions Eric Amis, Polymers Division, Chief	4:20 pm	Poster Session
9:00 am	Project Overview Kate Beers, NCMC	6:30 pm	Dinner (Buca di Beppo) (122 Kentlands Blvd., Gaithersburg)
9:15 am	Complex Fluids from Polymer and Surfactant Meso Phase Interactions Robert Prud'homme, Princeton University		
10:00 am	Coffee Break		
10:15 am	A New Approach to Combinatorial Rheology Measurements Howard Walls, NCMC		
10:45 am	Rapid Prototyping of Fluid Devices for Polymer Formulations João Cabral, NCMC		
11:15 am	Scattering Methods Applied to High Throughput Materials Research Alexander Norman, NCMC		
11:45 am	Lunch (NIST cafeteria, Bldg. 101)		
1:15 pm	3D Microscopy and Imaging as Characterization Tools Marcus Cicerone, NIST Polymers		
1:40 pm	Single Molecule Measurement Methods at NIST Angela Hight Walker, Optical Technology Division, Physics Laboratory		
2:05 pm	Trials and Tribulations of the Application of HTS Methods to Evaluation of PVC Stabilizers Douglas Wicks, University of Southern Mississippi		
2:35 pm	Coffee Break		
2:50 pm	Optical Materials Library Design Michael Doyle, Accelrys		

Tuesday, October 7th, 2003

8:30 am	Coffee & Doughnuts
8:45 am	Multiphase Droplet Production and Manipulation using Microfluidics David Weitz, Harvard University
9:30 am	Influence of Geometrical Confinement on Thread Breakup Jack Douglas, NIST Polymers
10:00 am	Measuring Dynamic Properties of Small Scale Interfaces Steve Hudson, NIST Polymers
10:30 am	Coffee Break
10:45 am	Gradient Methods for Nano-Scale Metrology Michael Fasolka, NCMC
11:00 am	Open Discussion: Gradient Surfaces as Standards leader: Kate Beers, NCMC
12:00 pm	Lunch (NIST cafeteria, Bldg. 101)
1:30 pm	NCMC lab tours, demos, etc.
4:00 pm	Meeting Over

Complex fluids in microfluidic channels

- Droplet formation and control
- Thread Breakup
- Experimental design and measurements

Surface gradients

- Metrology tools
- From SAMS to polymers

NCMC Laboratory Open House



Ryebuck Shearer

If I don't shear a tally before I go

My shears and stones in the river

I'll throw

And I'll never open Sawbees or take

another blow

Till I prove I'm a ryebuck shearer



Two Problems in Polymer Self-Assembly: Making Drug Nanoparticles and Making Polymer-Surfactant Mesophases

Robert K. Prud'homme
Brian Johnson, Walid Saad,
Bing-Shiou Yang, Debra Auguste
Dept. Chemical Engineering
Princeton University



Making Drug NanoParticles with Block Copolymers

Targets: Low Solubility Solutes

- ♦ Flavors
- ♦ Dyes / Pigments
- ♦ Fine Organics
- ♦ Pharmaceuticals
- ♦ Vitamins

Why Nanoparticles?

- ♦ Increased Solubilization Rate:

$$\text{Rate} \propto \sum A_i (C_{\text{sat}} - C_{\text{bulk}})$$

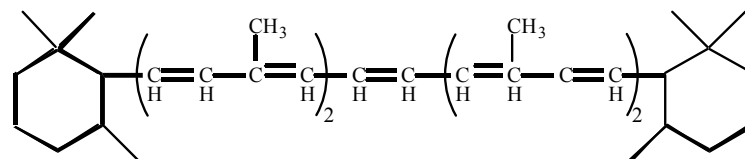
- ♦ Passive Targeting Tumors with Anti-Cancer Drugs

Model Systems:

- ♦ b-carotene

Pro vitamin A and food dye

BASF - US patent 5700471, 1997

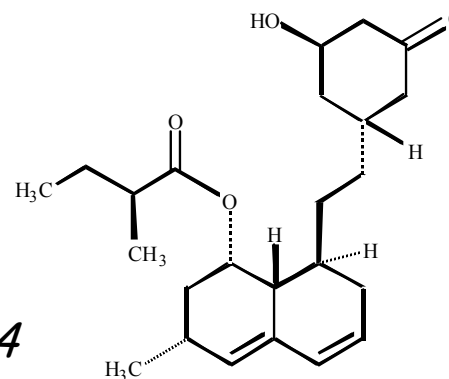


- ♦ Lovastatin

Pharmaceutical

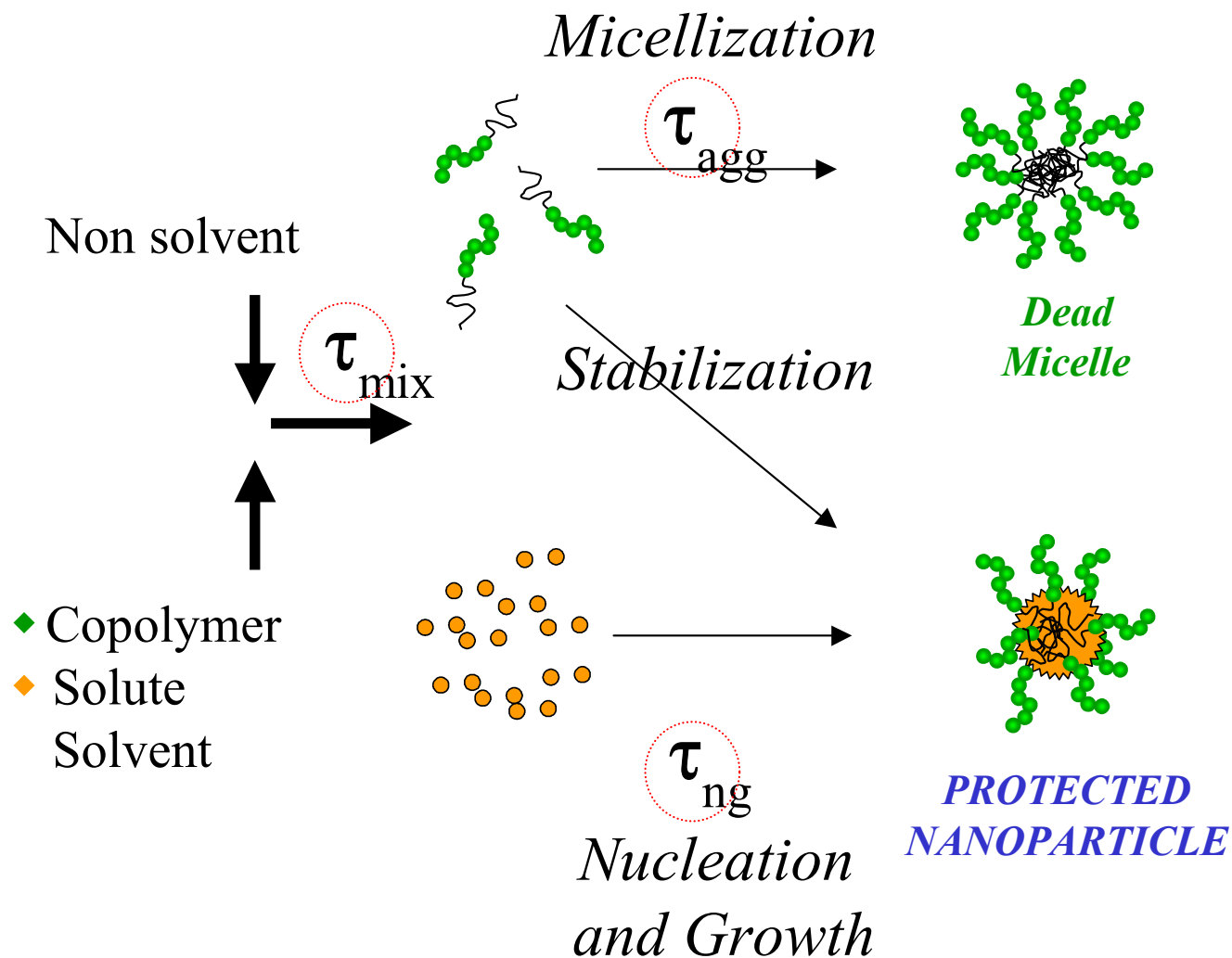
AICHE Journal Vol. 42, No. 7, 1801

Merck - US Patent 55314506, 1994





Competitive Micellization and Precipitation Kinetics



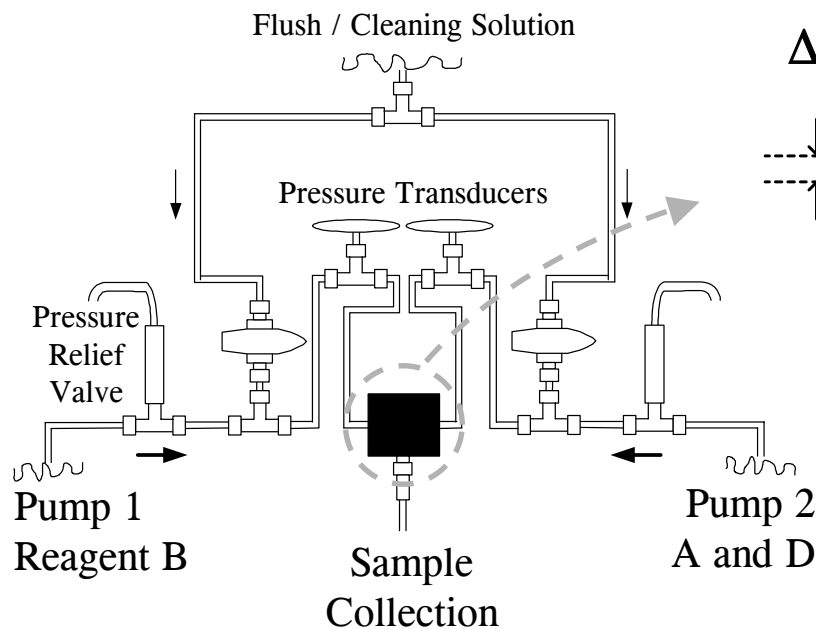


I. CONFINED IMPINGING JETS (CIJ) MIXER for PROCESS DEVELOPMENT

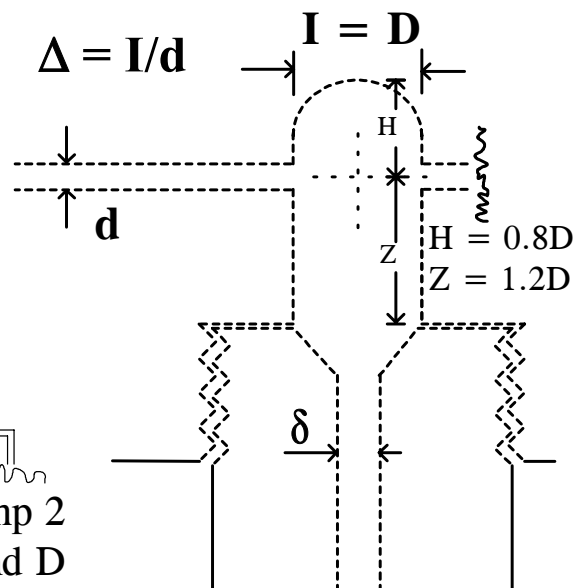
Syringe Pump



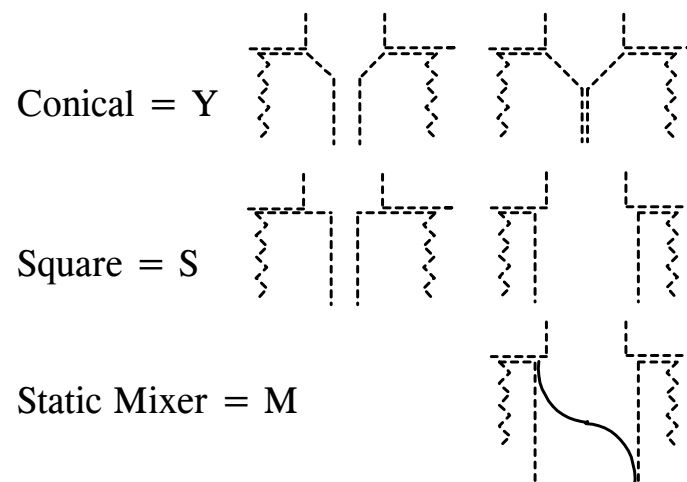
Fluid Delivery



Mixing Heads: $d = 0.25$ to 1 mm
 $\Delta = 4.8$ to 19



Outlet Configurations



Key Features

- ◆ Expect $\tau_{\text{mix}} < 10$ ms
- ◆ Small (micro) scale < 100 ml / run
- ◆ Simple & accurate operation, 0.5 ms motor

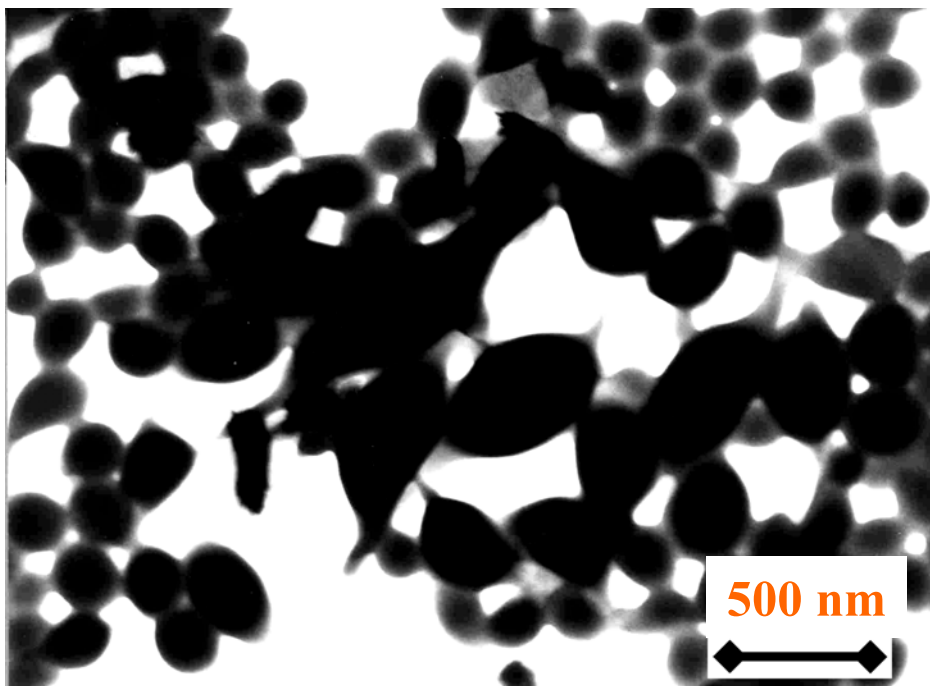
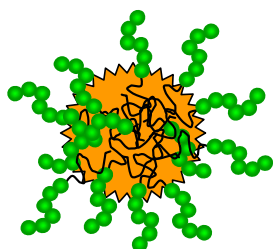


Polymer Protected vs Unprotected Particle Growth



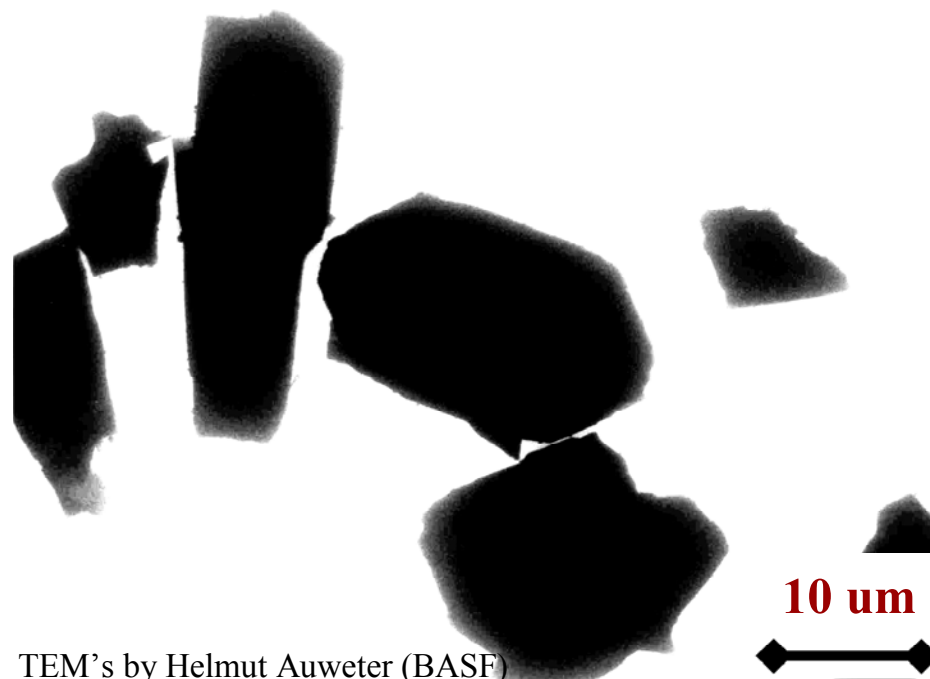
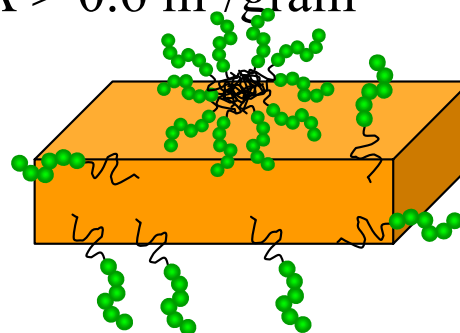
Flash Precipitation

Image analysis = 249 nm
Light diffraction = 370 nm
SSA = 22 m²/gram



“Typical” Precipitation

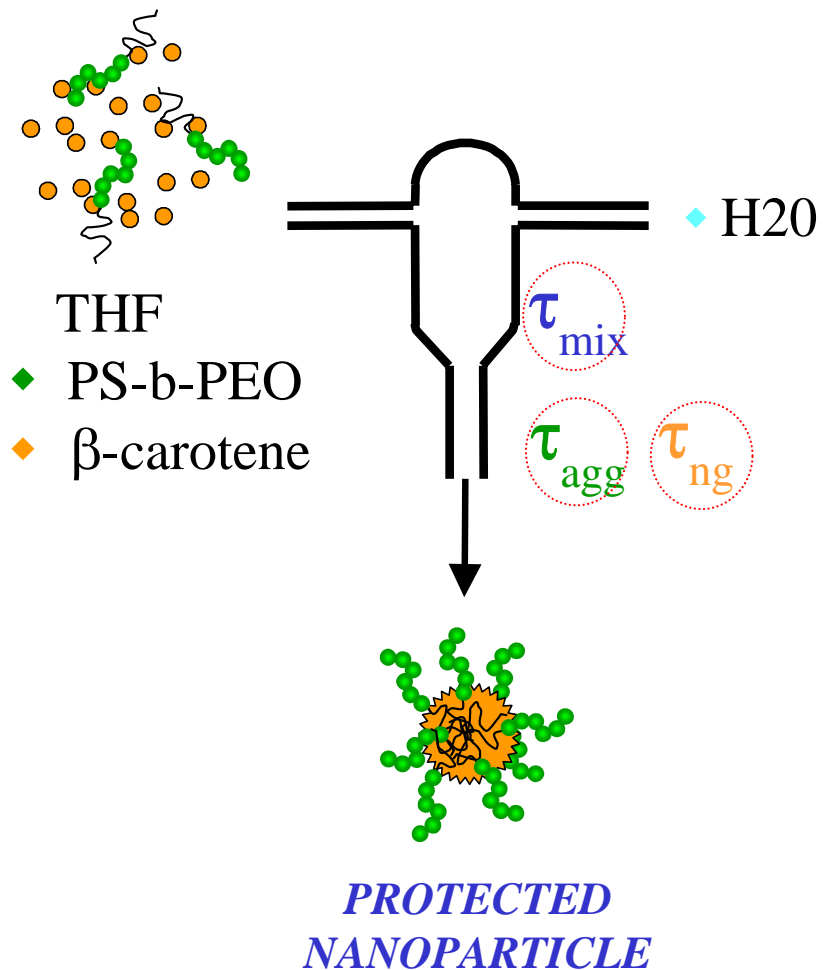
Image analysis > 10 μ m
Light diffraction > 10 μ m
SSA > 0.6 m²/gram



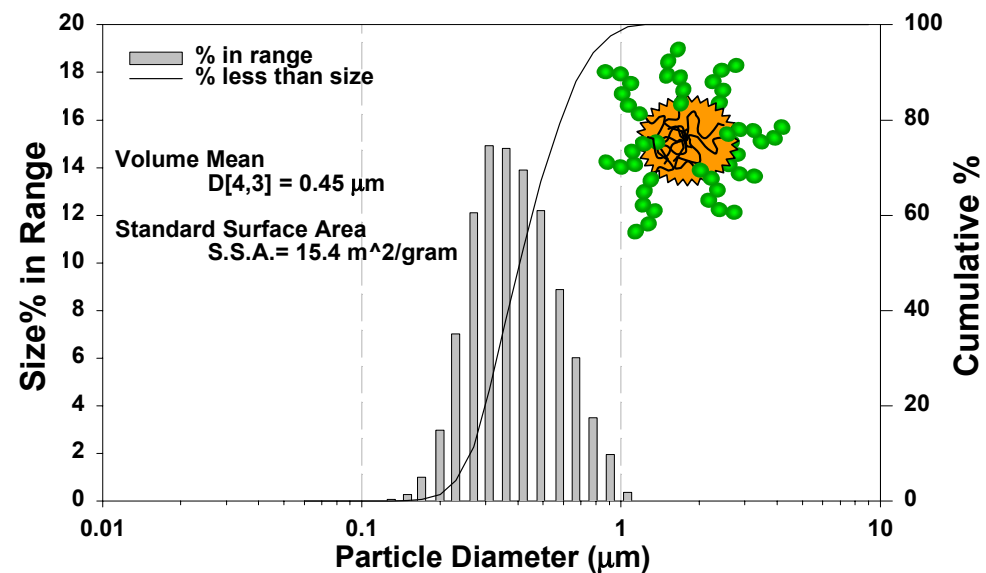
TEM's by Helmut Auweter (BASF)



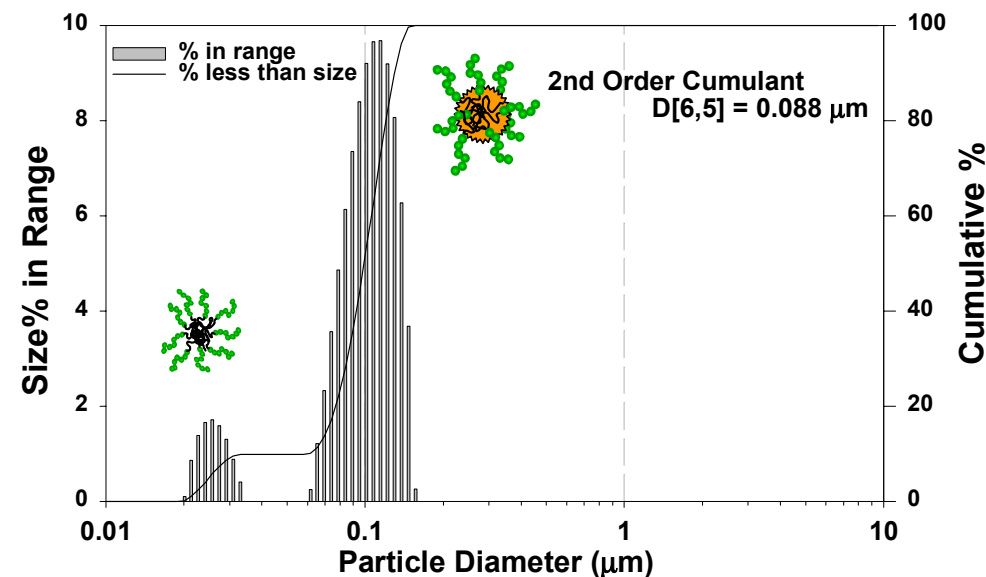
“FLASH” Precipitation of Nanoparticles - High throughput and > 2 wt% active



CIJ mixer - 2.8 m/s, (2.6 wt% drug, 0.4 wt% Copolymer)

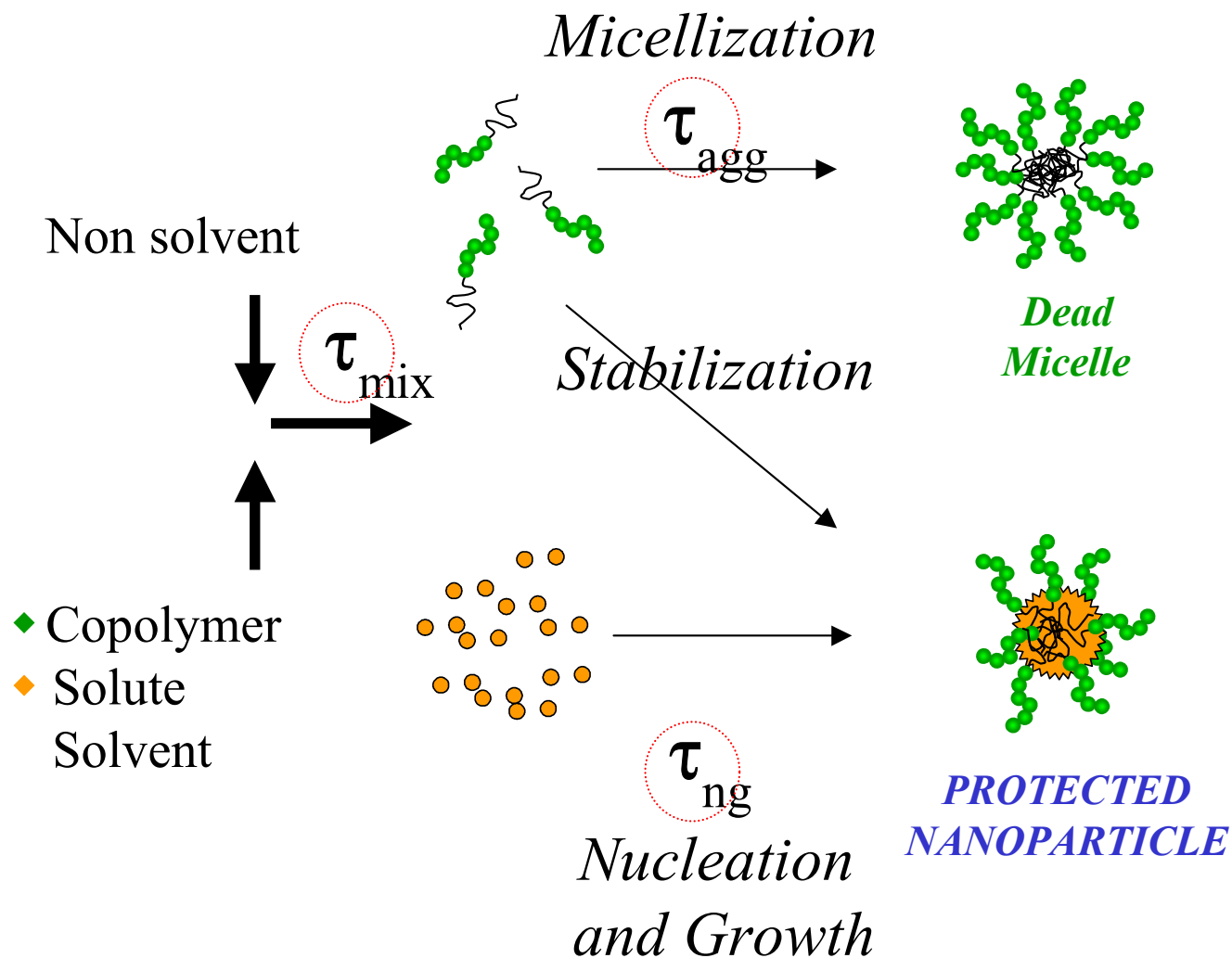


Change Inputs to Process





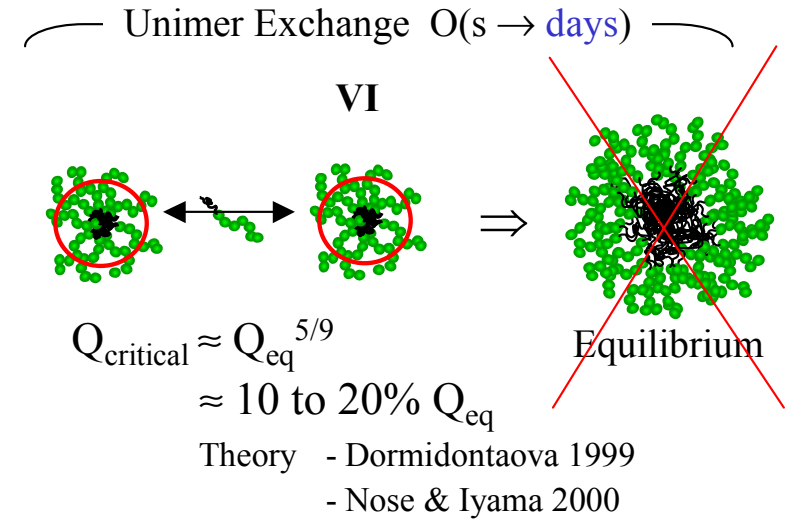
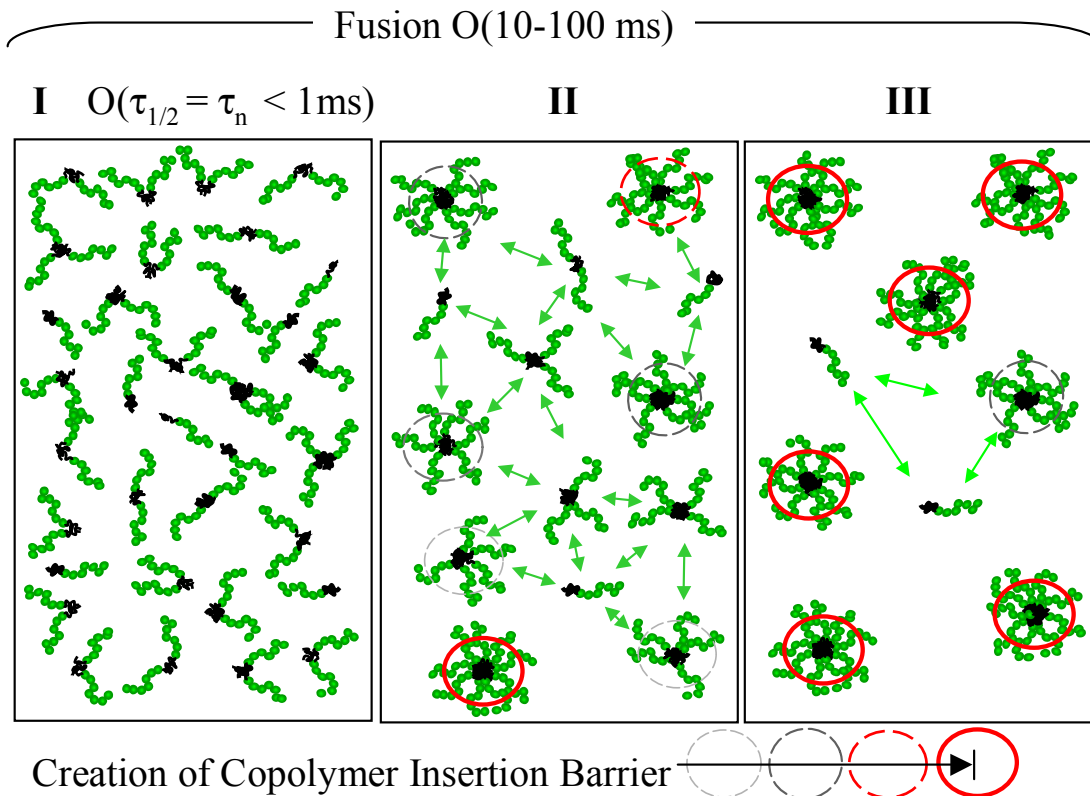
Competitive Micellization and Precipitation Kinetics





Aggregation Mechanism / Times: “homogeneous” $\tau_{mix} \ll \tau_{agg}$

Diffusion Limited Fusion to a Critical Size = Overlapping Brush

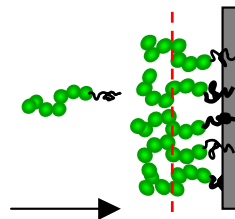


Required Observations:

1. $\tau_{agg} = O(\text{ms})$
2. Size $\neq f(\text{time})$ - *stable*
3. Size = Small $\ll 200 \text{ nm}$
4. Size = $f(\text{Insertion Barrier})$
5. Size $\neq f(C_p)$
6. $\tau_{agg} \propto \text{diffusion limited}$

III IV Overlapping Brush Penetration - $O(s)$

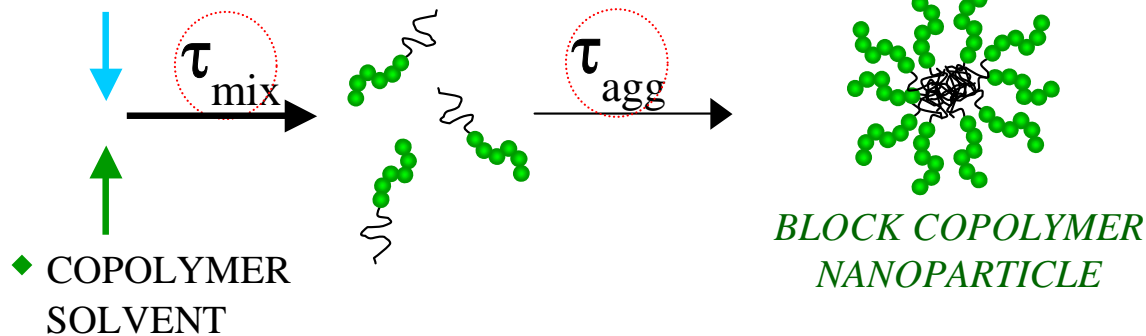
For Flat Surface
(Theory - Ligore and Libler 1990)





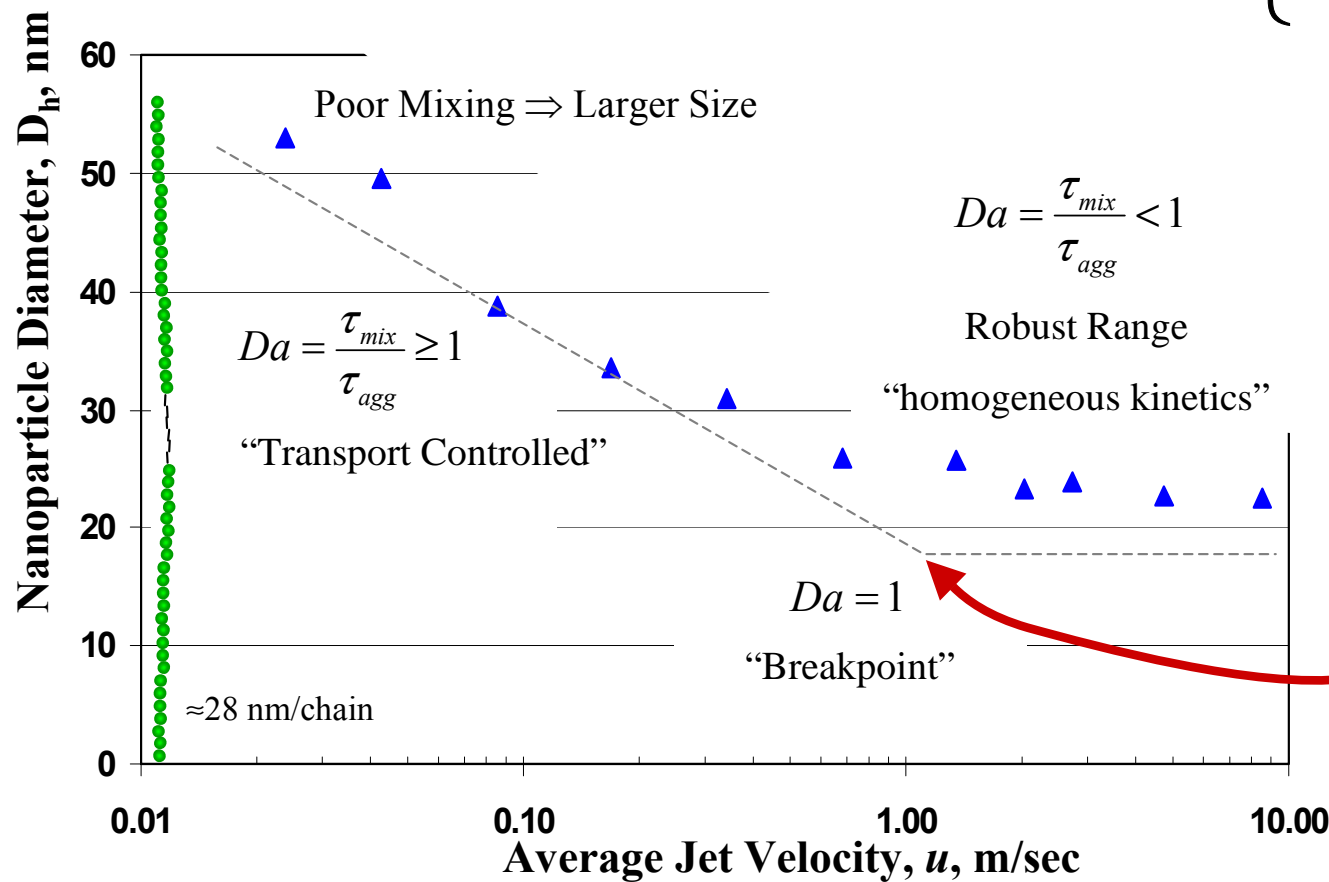
MIXING SENSITIVE PROCESS - Precipitation of Block Copolymers

◆ NON SOLVENT



Size =

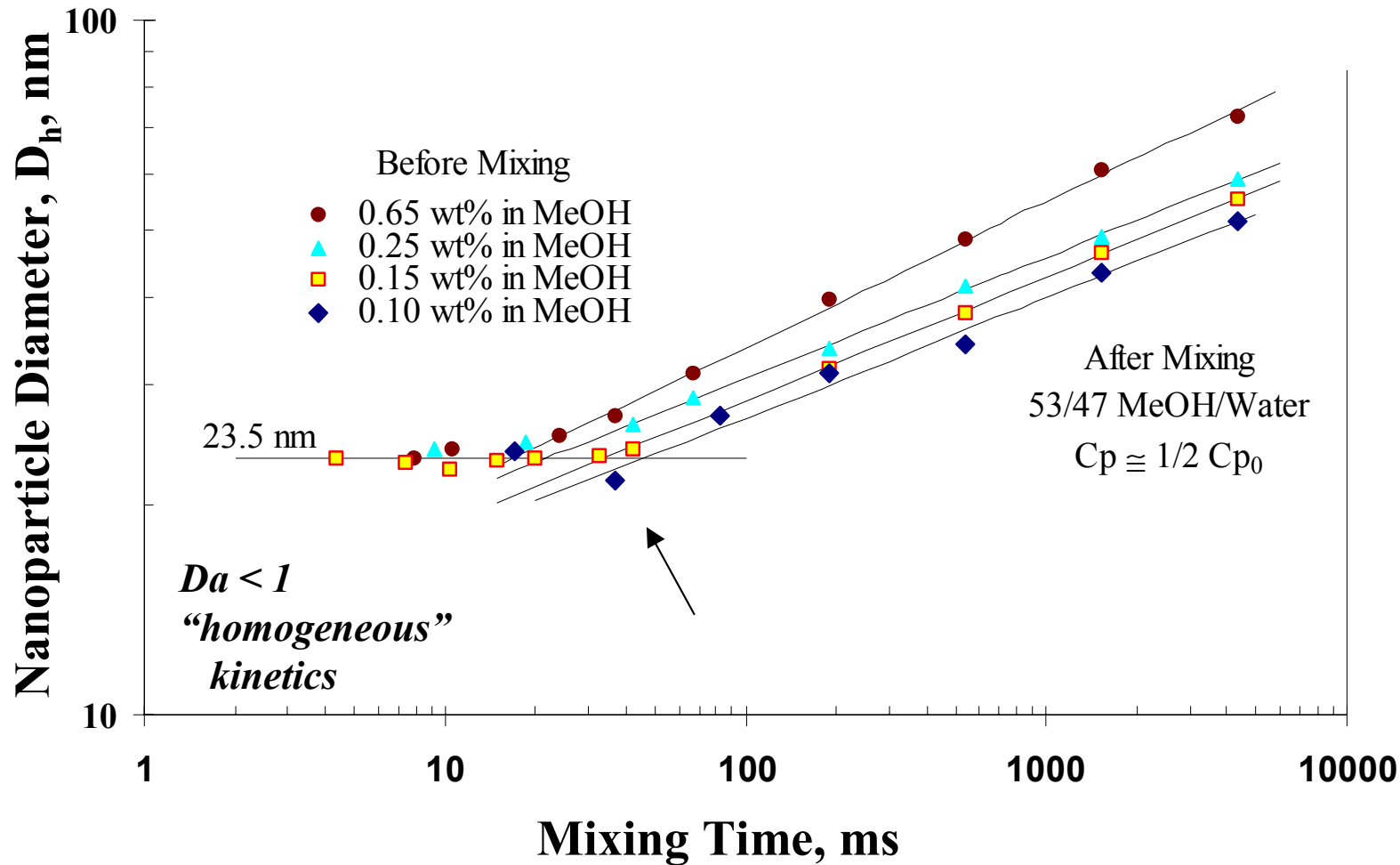
$$fn \left\{ Da = \frac{\tau_{mix}}{\tau_{agg}} \right\}$$



$\tau_{micelle} = 15$ ms



Effect of Polymer Concentration

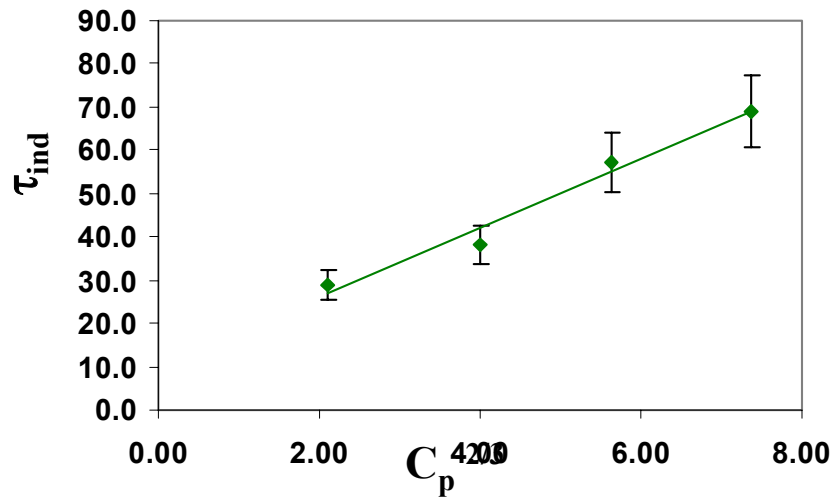


- Particle size independent of polymer concentration.
- Closed aggregation model for thermodynamics



♦ Diffusion Controlled

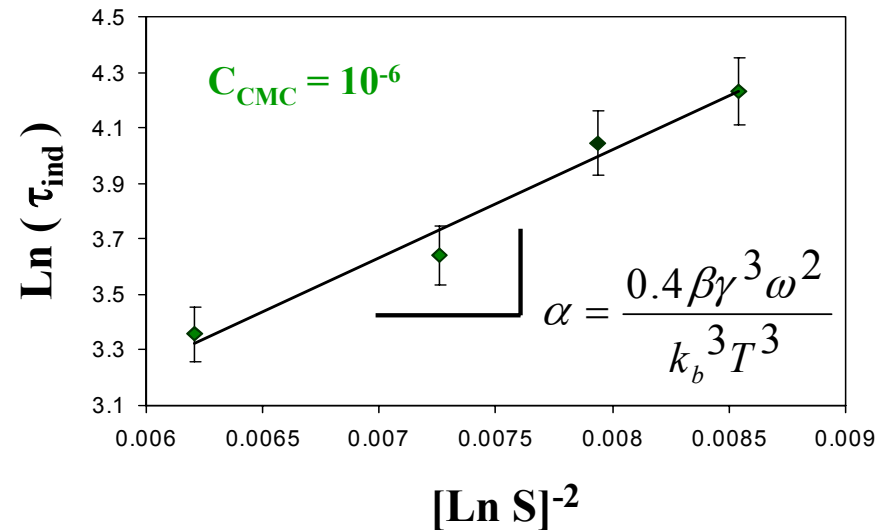
$$\tau_{ind} \propto \frac{L^2}{D_p} \propto \frac{1}{D_p C_p^{-2/3}}$$



♦ Conventional Precipitation

$$\ln(\tau_{ind}) = K_1 + \alpha \left[\ln \left(\frac{C_p}{C_{cmc}} \right) \right]^{-2}$$

(Sohnel & Mullen 1988)

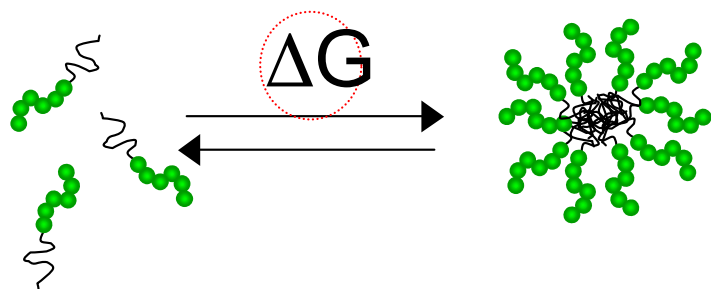


- Diffusion controlled: $C_p^{-2/3}$
- Effective particle surface energy: $\gamma_{eff} = 2.3 \text{ mJ/m}^2$

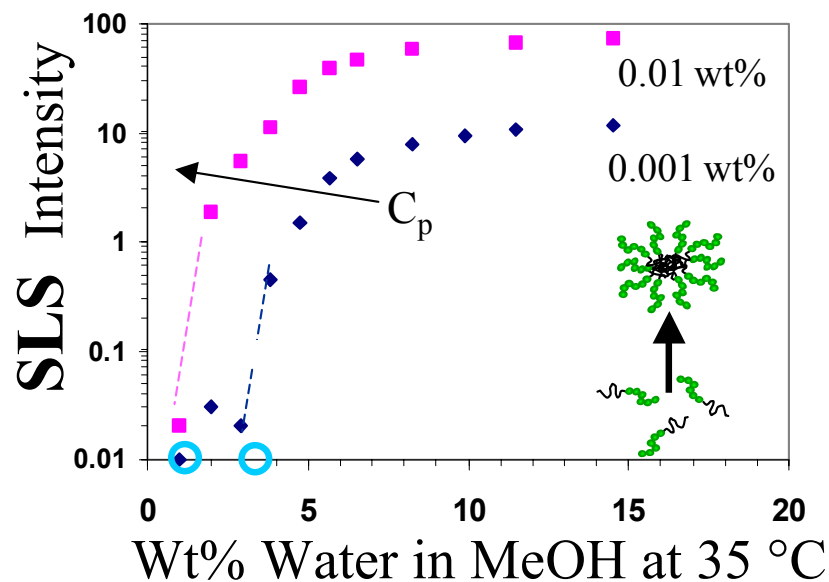


Thermodynamics of Assembly

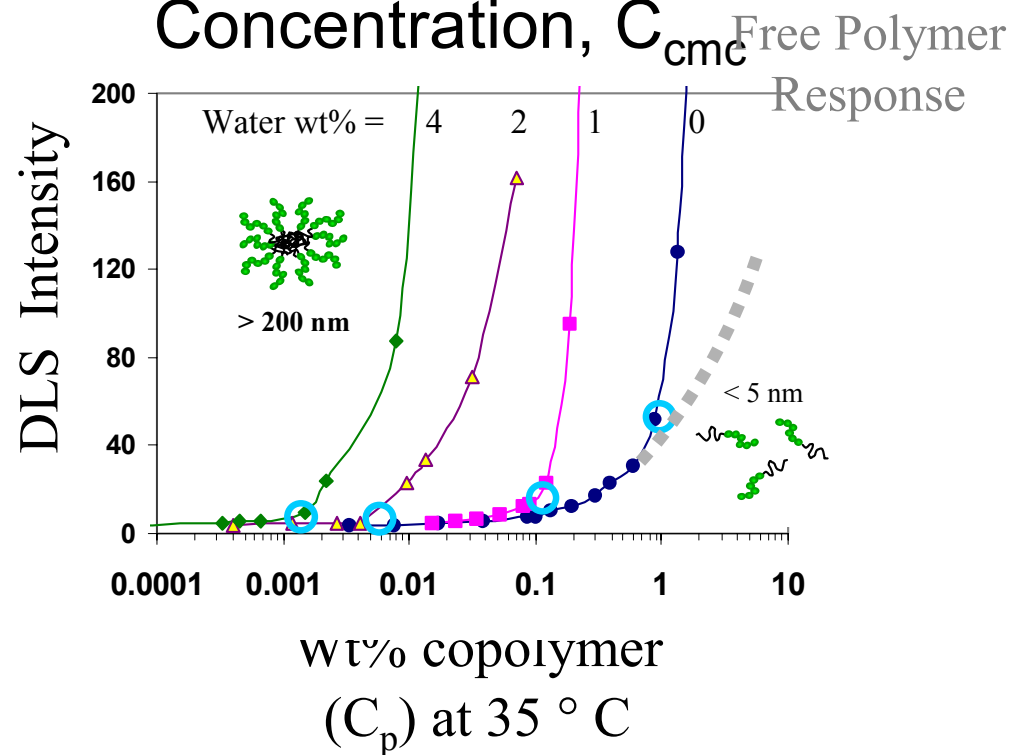
CMC of PBA(59)-b- PAA(104), 7.5k-b-7.5k via Light Scattering



♦ Critical Water Content

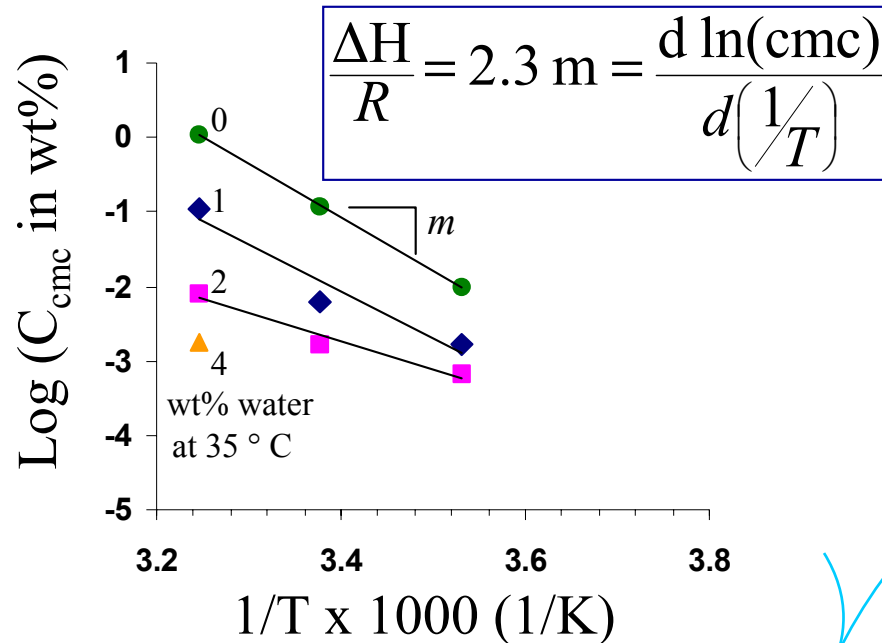


♦ Critical Micelle Concentration, C_{cmc}

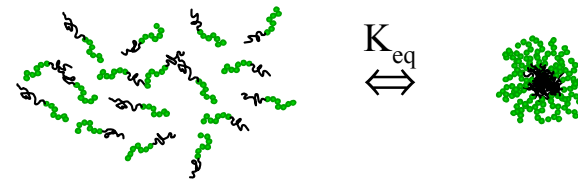




♦ CMC (35 to 10°C)



♦ Closed Association Model



$$\Delta G = RT \ln(\text{CMC})$$

Eisenburg (1997)
Tuzar (1976)

wt% ΔG° ΔH° $-T\Delta S$ ΔS°

Water kJ/mole kJ/mole kJ/mole kJ/mole K

0	-23	-136	113	-0.38
1	-29	-119	91	-0.30
2	-33	-71	38	-0.13

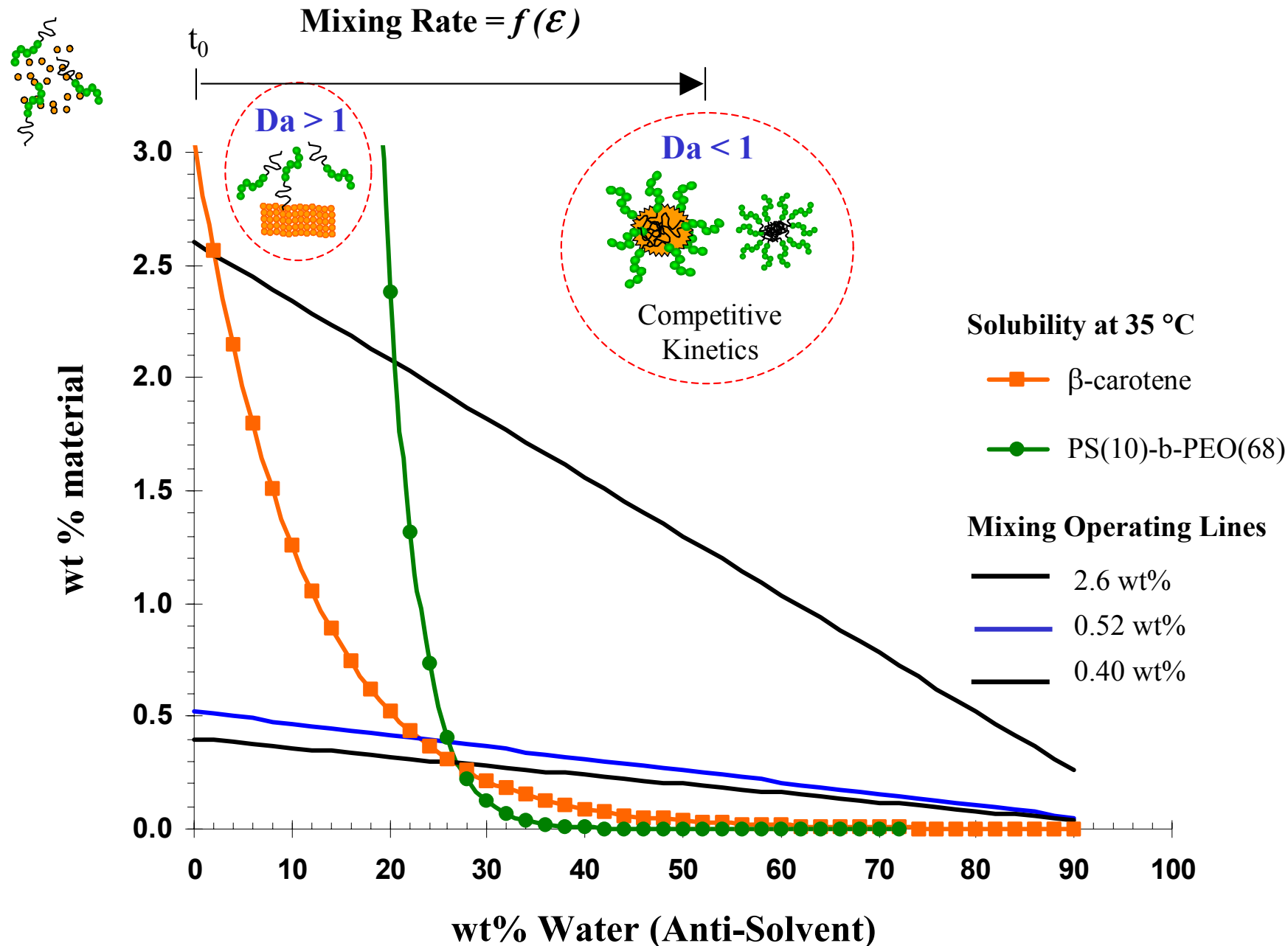
298 K

After Mixing = 53% MeOH

- ♦ Use $C_{\text{cmc}} \cong 10^{-6} \text{ wt\%}$
- ♦ $S_0 = 10^4 \text{ to } 10^5$



Flash NanoPrecipitation - Mixing Operating Lines vs. Solubility





Summary:

- 1) *Impinging jets provide scalable, high throughput, homogeneous, high supersaturation*
- 2) *Block copolymers provide controlled/arrested particle growth: narrow PSD, ~100 nm*
- 3) *Balance time scales:
 $t_{\text{mixing}} < t_{\text{nuc/growth}} \sim t_{\text{micellization}}$*

Future Objectives:

- 1) *Block copolymer property optimization?*
- 2) *Bio-compatible polymers*
- 3) *Release kinetics*
- 4) *Drying/rehydration?*
- 5) *Ostwald ripening?*



Bob, Dottie, Brad and Bobby Uluru



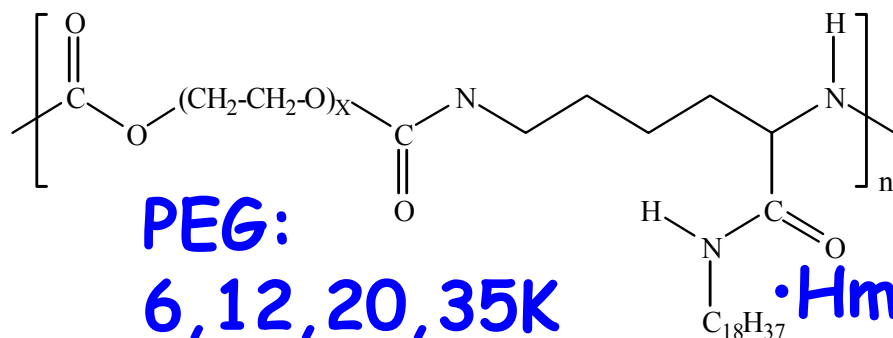


Outline

- Interactions with Lamellar Phases
 - Phase behavior
 - Shear induced onions
- Interactions with Vesicles and Liposomes
 - Protection
 - Rheology



Hydrophobically Modified Polymers



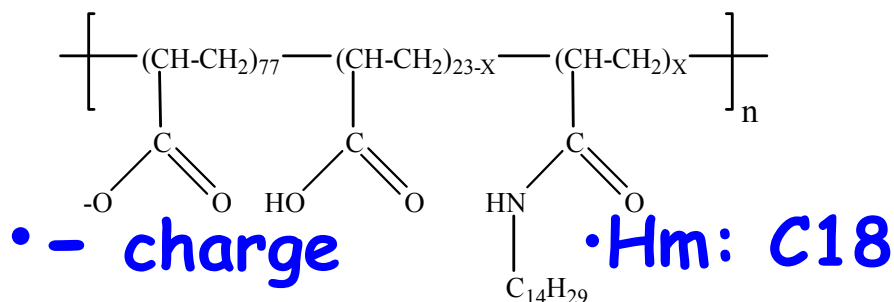
PEG:

6,12,20,35K

•Hm: C18

Hm-PEG

Poly(PEG lysine-stearylamine) (PEG-LS)



• - charge

•Hm: C18

***Hydrophobically modified
polyacrylic acid (HM-PAA)***

Hm-PAA

- Yang, Prud'homme, *Langmuir* (2001)
- Yang, ... Prud'homme *Langmuir* (2001)
- Ashbaugh, ... Prud'homme *Coll and Polym Sci* (2002)



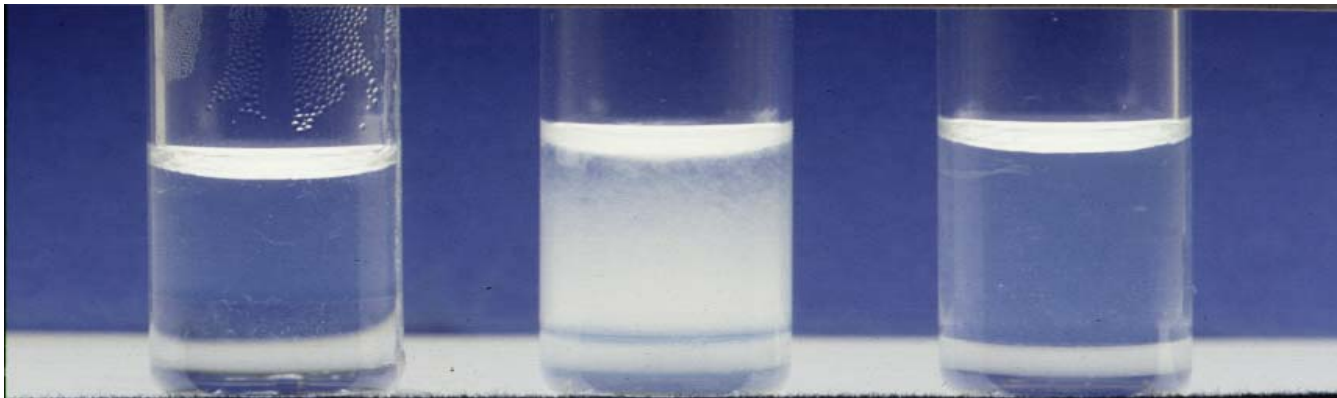
Phase Behavior

Phase identification:

L_{α} : optically anisotropic (i.e. birefringent).

L_3 : optically clear and isotropic.

$L_{\alpha 1}/L_{\alpha 2}$: visually turbid, shows one interface between two birefringent phases after centrifugation.



Surfactant
Lamellar
Solution

Surfactant
Lamellar Solution

+

PAA

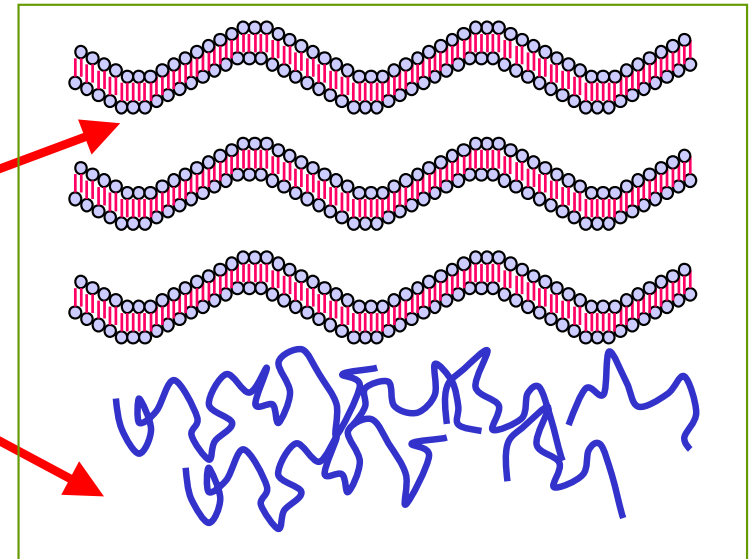
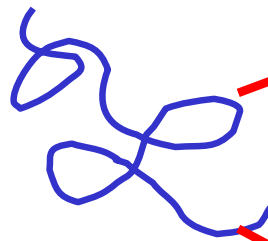
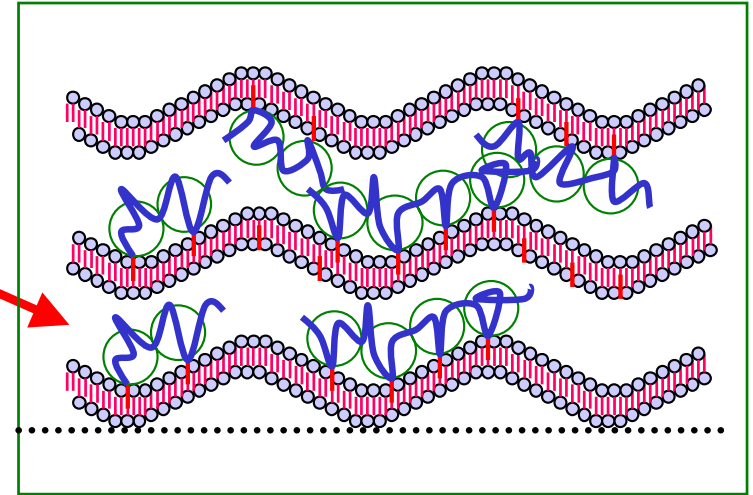
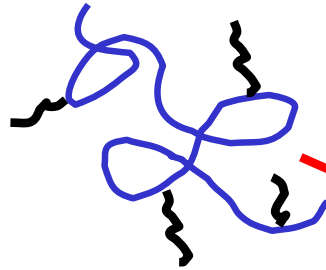
Surfactant Lamellar
Solution

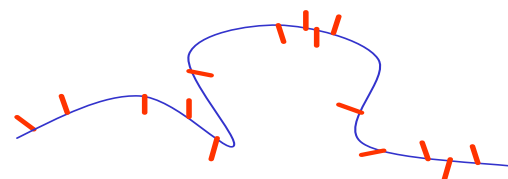
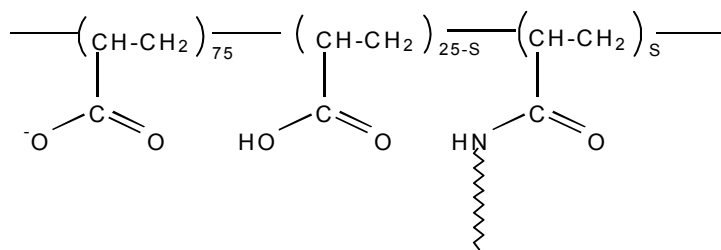
+

HMPAA—
3 mol% hydrophobe
substituted

Polymer-Lamellar Phase Separation

- Polymer does not want to lose configurational entropy (Casasa, deGennes)
- Compensate entropy loss with hydrophobic energy gain *via* association



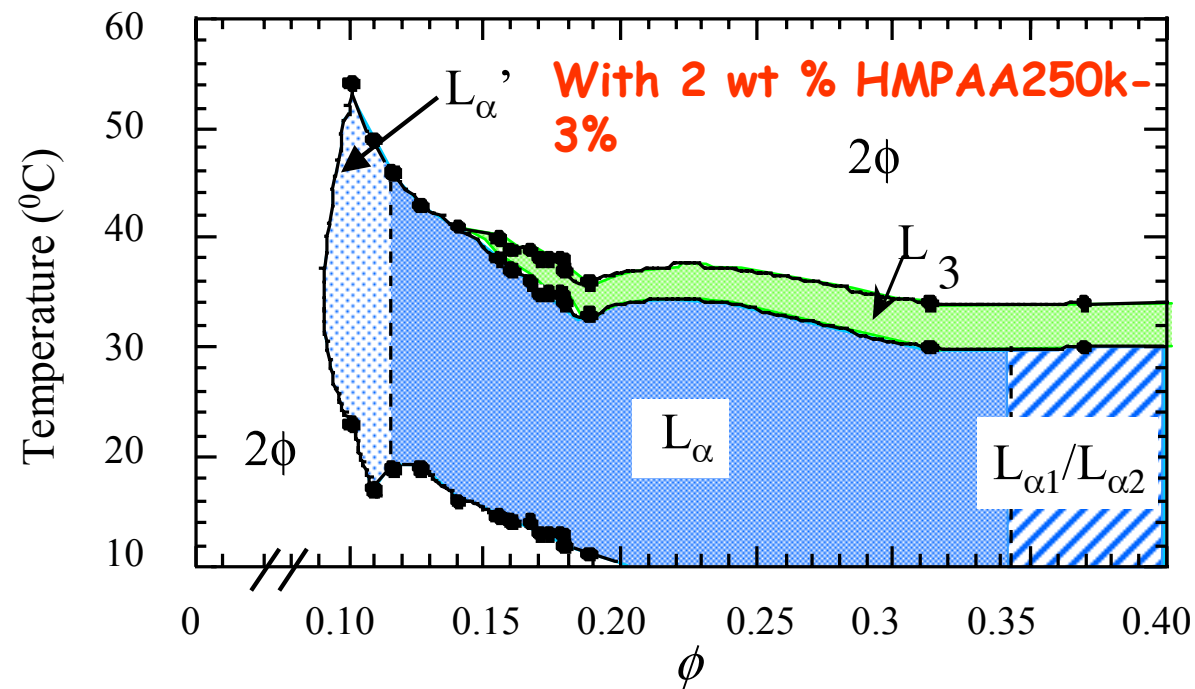


Random spacing

Name (Abbreviation)	M _w (lg/mole)	M _w /M _n	Hydrophobe Substitution level	Hydrophobe Length
HMPAA3% α 250kpoC ₁₄	250	2	3%	C ₁₄
HMPAA3% α 140kpoC ₁₄	140	2	3%	C ₁₄
HMPAA1.5% α 250kpoC ₁₄	250	2	1.5%	C ₁₄



Hm-Polymer/Surfactant Phase Diagrams

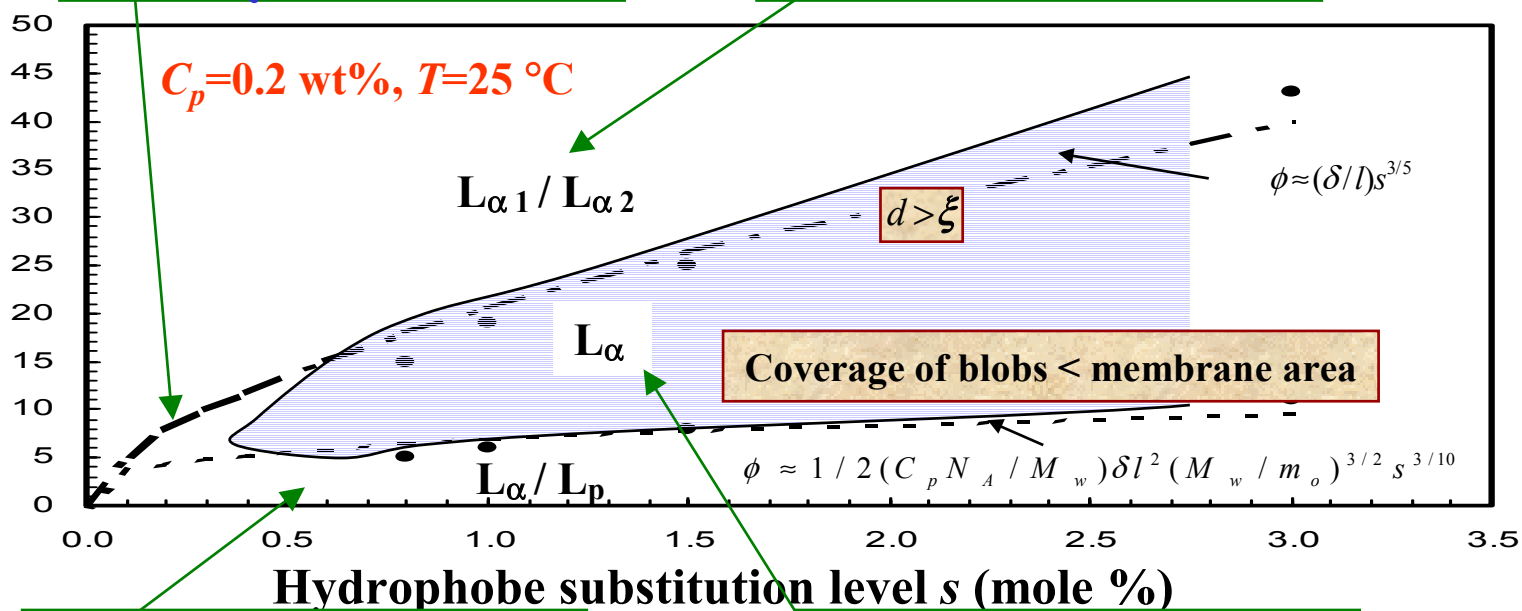


- $C_{12}E_5$: wide lamellar phase region around 60°C
- C_6OH : lamellar phase region at room temperature
- $NaCl$: screen charge-charge repulsion of the polymer

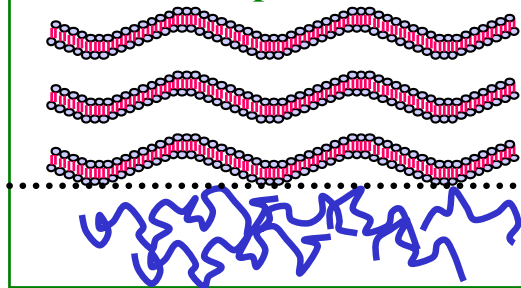


Phase Behavior

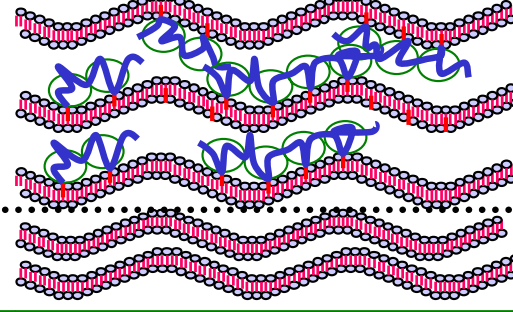
Membrane volume
fraction ϕ (%)



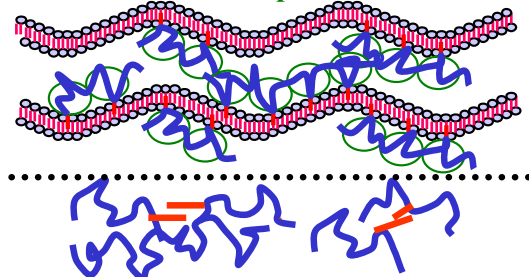
Phase Separation



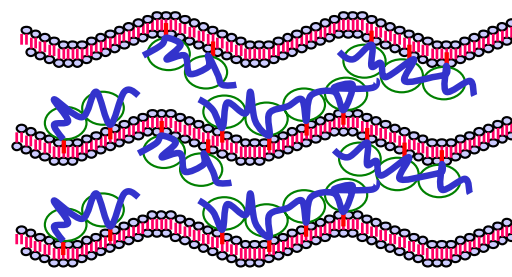
$L_{\alpha 1} / L_{\alpha 2}$



L_{α} / L_p



Polymer Doped L_{α}



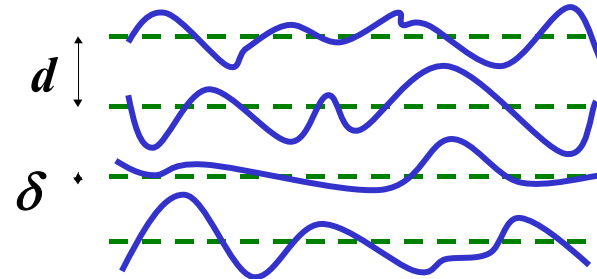


Neutron Scattering: Membrane Rigidity

$$I(q) \propto |q - q_0|^{-1+\eta}$$

$$\eta = \frac{q_0^2 k_B T}{8 \pi \sqrt{\kappa B} / d}$$

Peak divergence analysis

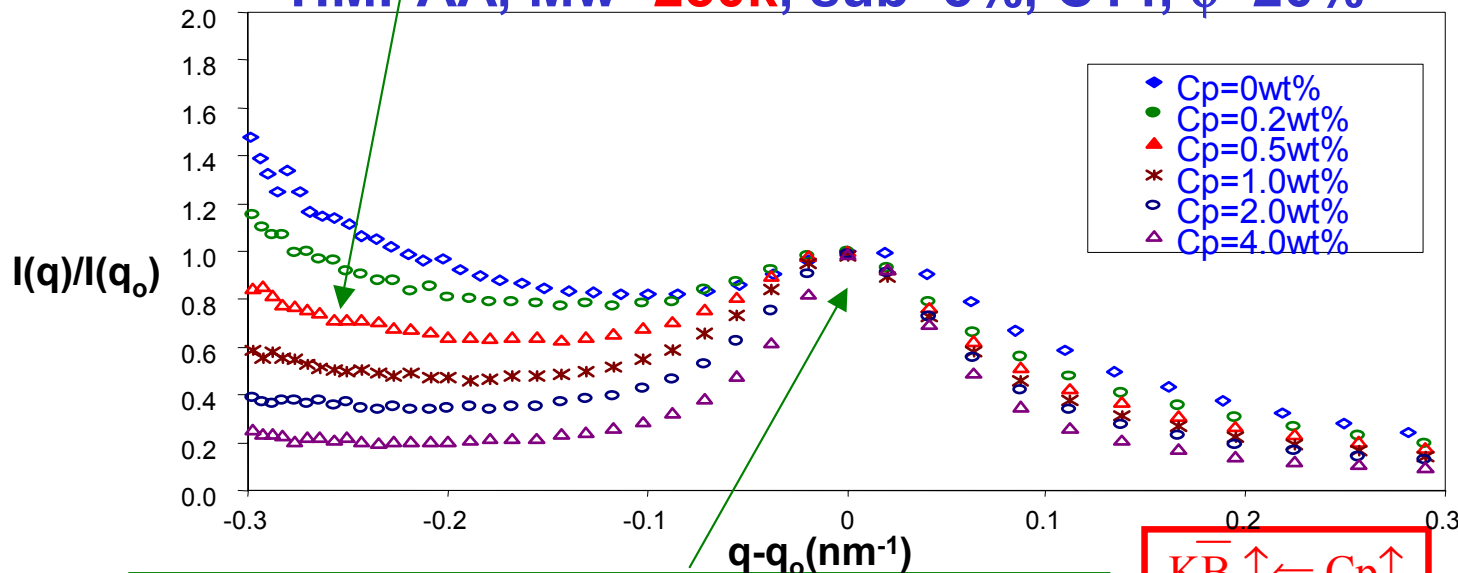


κ : bilayer mean bending modulus
 B : layer compression modulus
 κB : rigidity of the lamellar phase

Scattering intensity at small angle $I(q \rightarrow 0) \propto 1/B$

$B \uparrow \Leftarrow C_p \uparrow$

HMPAA, Mw=250k, sub=3%, C14, $\phi=20\%$



Bragg peak narrower $\Rightarrow \eta$ smaller $\Rightarrow \kappa B$ bigger

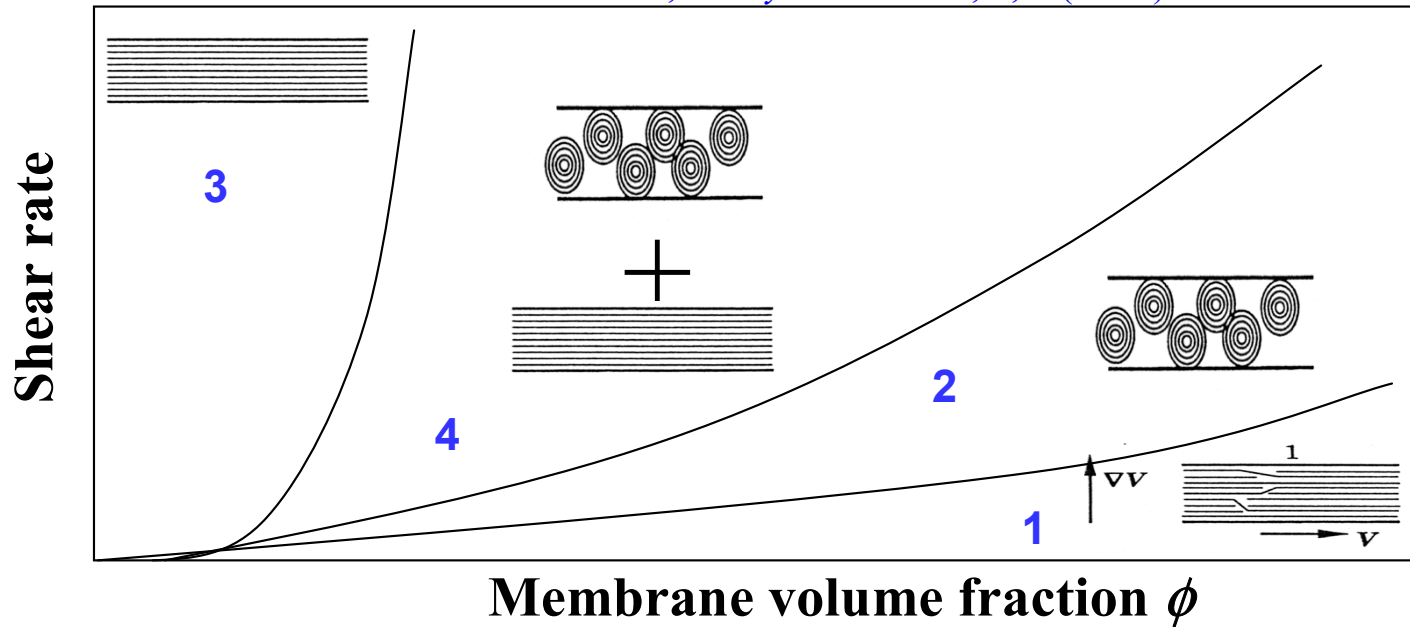
$\kappa B \uparrow \Leftarrow C_p \uparrow$



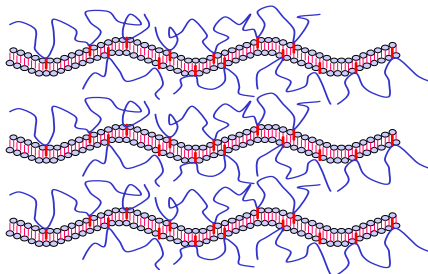
Shear-Induced Multilamellar Vesicles

Orientation Diagram

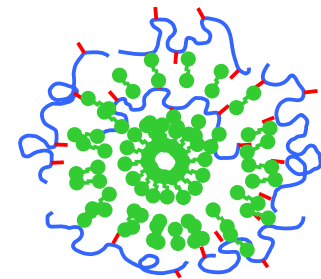
Diat and Roux, *J. Phys. II France*, 3, 9 (1993)



Lamellar Phase

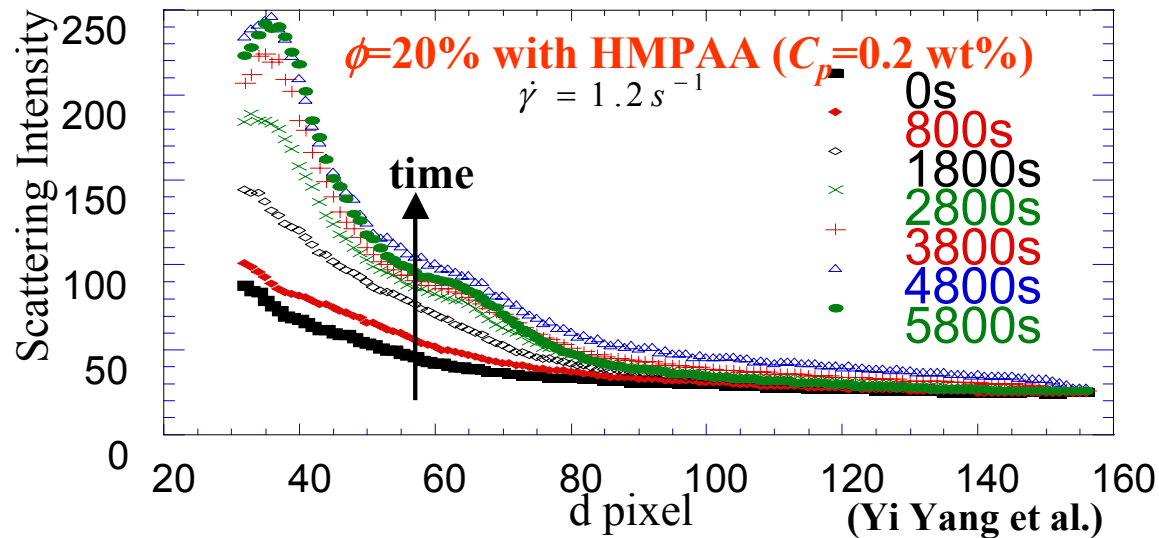
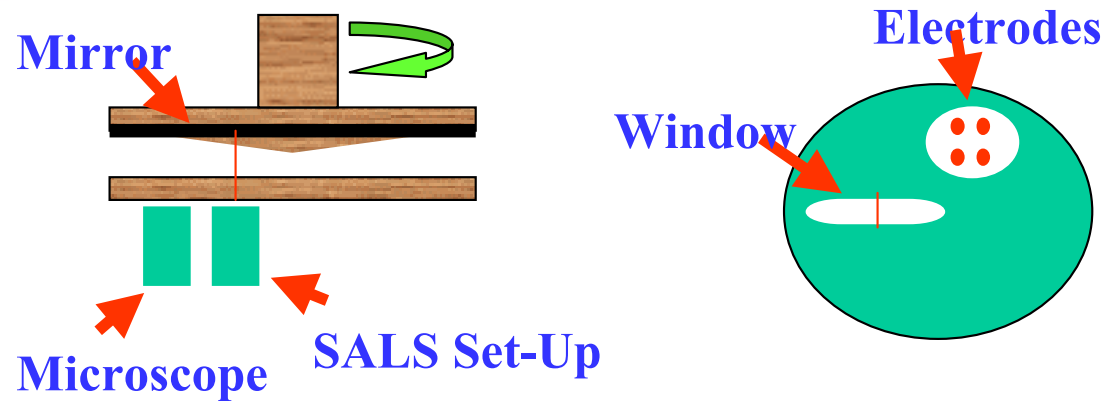


- 1. Disordered Lamellar Phase
- 2. **Onion Phase**
- 3. Oriented Lamellar Phase
- 4. Coexistence of Oriented Lamellar Phase and Onion Phase





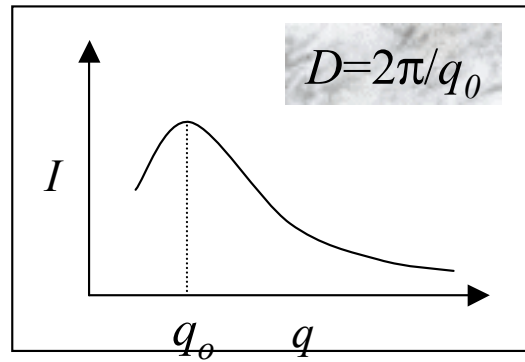
Onion formation—Rheoviscometer



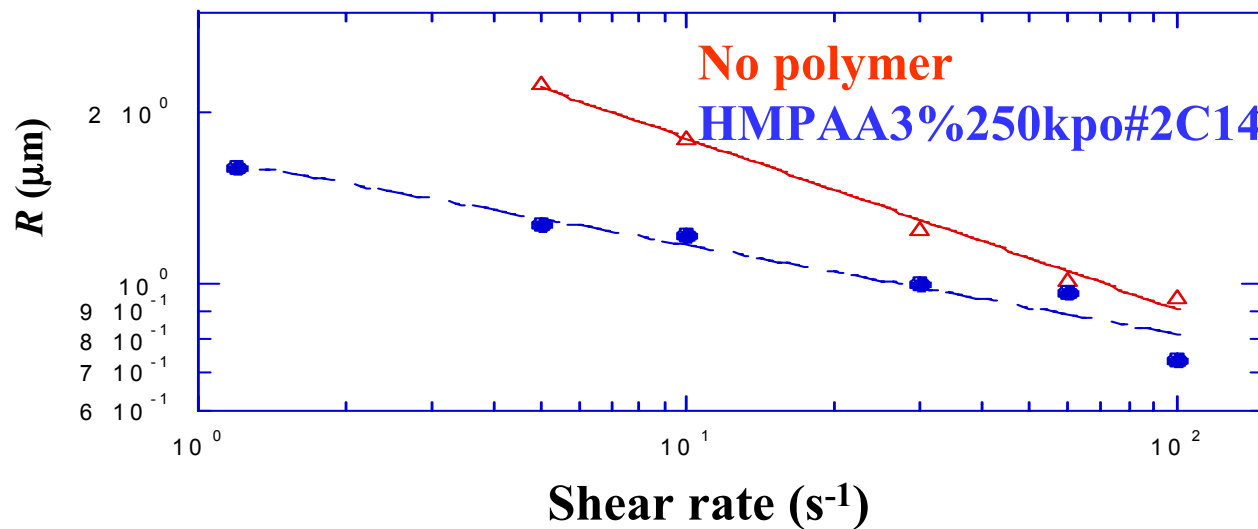
- The reference solution (without polymer) does not show a clear MLV peak under shear.
- MLV peak starts to show up after half hour under shear
- Volume fraction of onions increases with shearing time
- HMPAA doped membrane solution shows monodispersed MLV peak during shear and the structure exists several weeks



Onion size-Light scattering



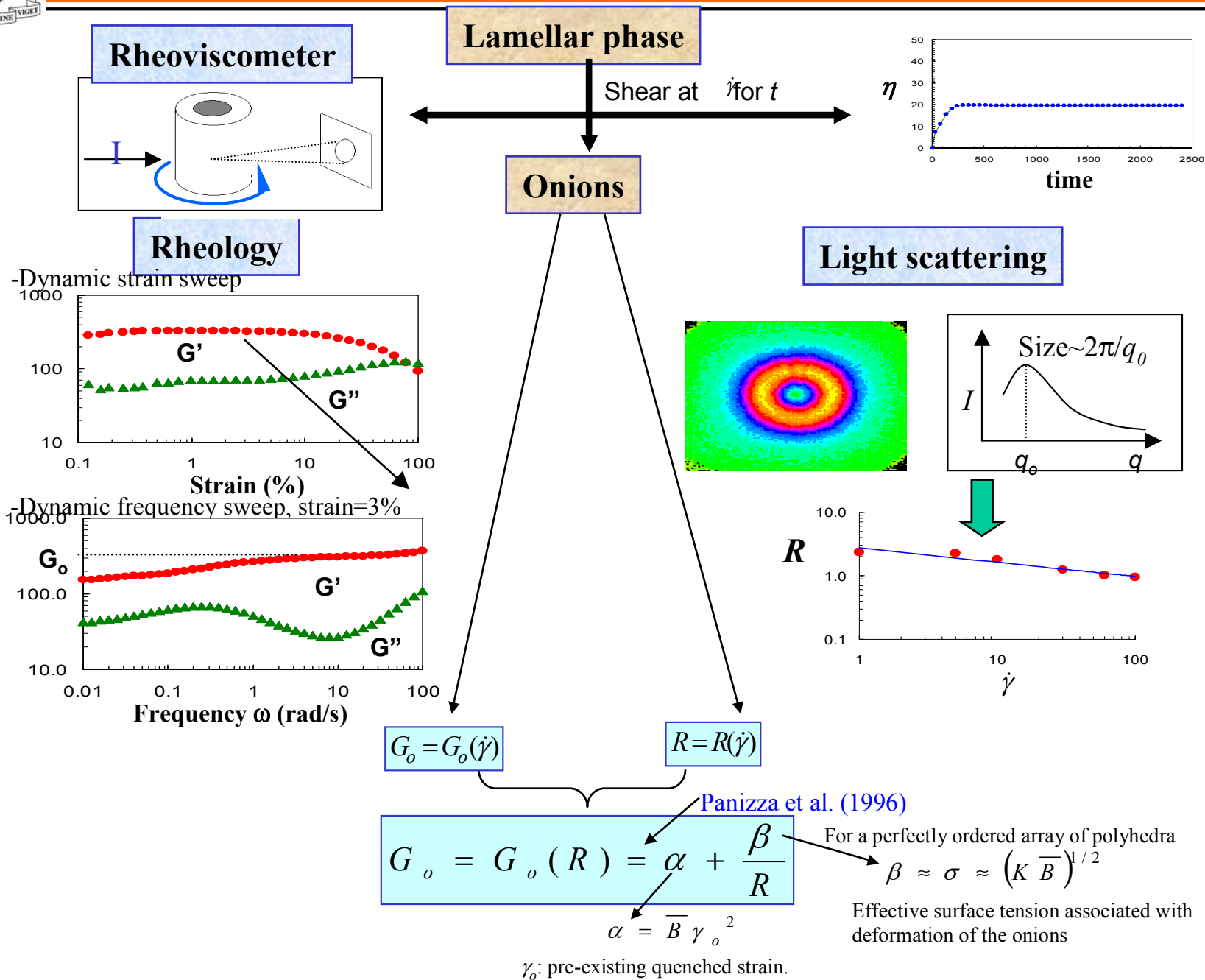
MLV size calculated by peak position



- Size of MLV decreases with shear rate
- MLVs can be controlled by shear time and shear rate



Experimental strategy





Conclusions

- *Shear induced multilamellar vesicles can completely encapsulate vesicle contents*
- *Hydrophobically modified polymers increase ease of vesicle formation*
- *Hydrophobically modified polymers increase the stability of vesicles*
- *Sizes of vesicles can be tailored by shear rate*

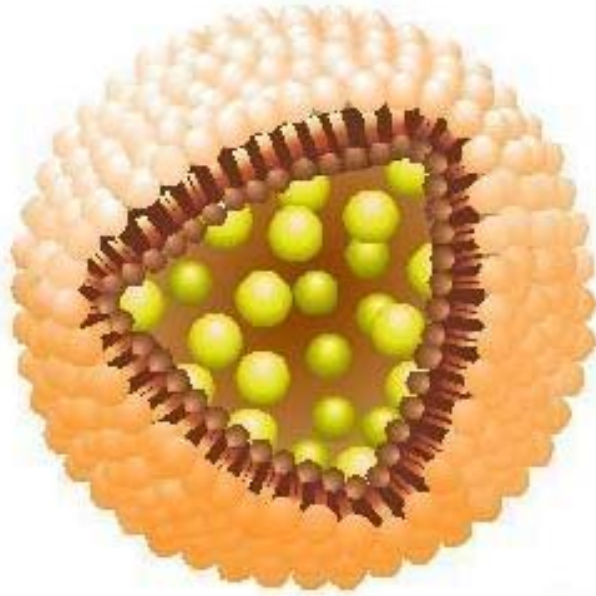


Liposomes and Vesicles with Hm-Polymers

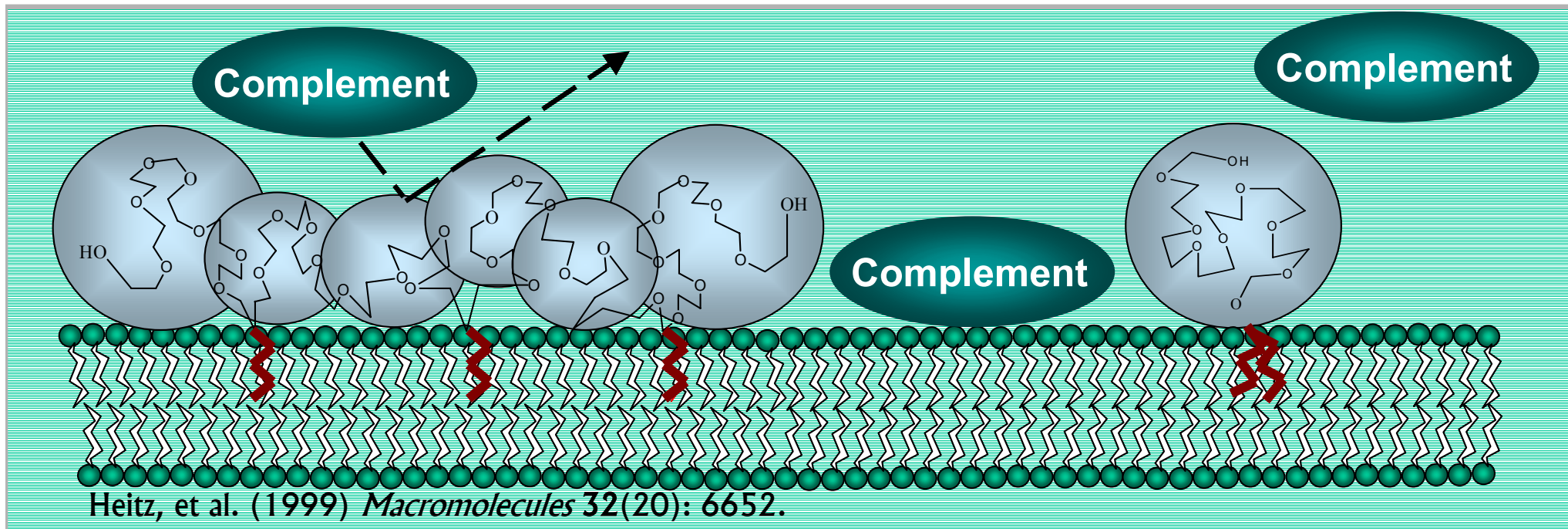
- Definitions of Liposomes and Vesicles
- Reasons for Polymer Addition
 - Rheology Control
 - Deposition and Protection
 - Triggered Release



Multiply-attached polymer protected liposomes



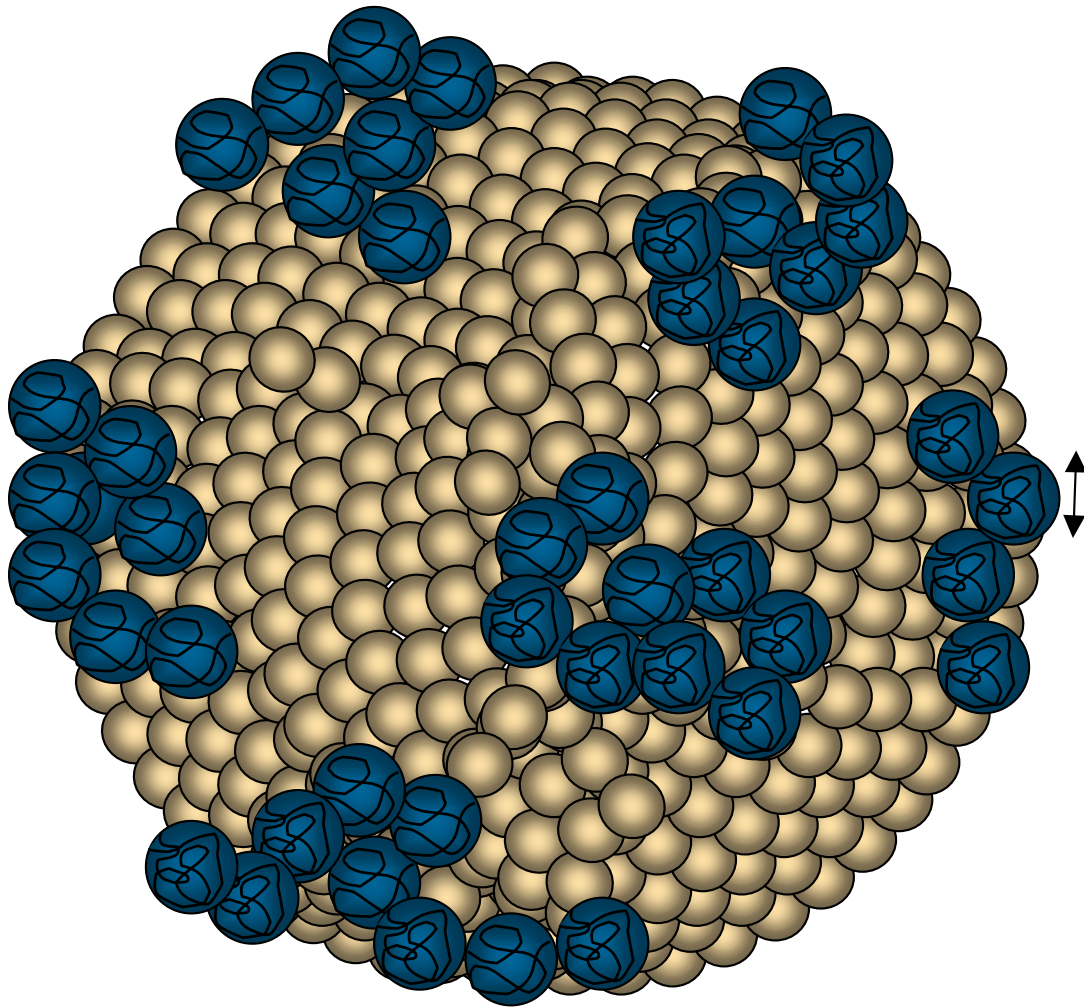
- Delivery of drugs and DNA
- Protection from immune recognition





Define surface coverage

Fractional Coverage (F_c) = $\frac{\text{area covered by polymer}}{\text{lipid area}}$



$$\Gamma^* = \frac{\text{mg polymer}}{\text{m}^2 \text{ lipid area}}$$

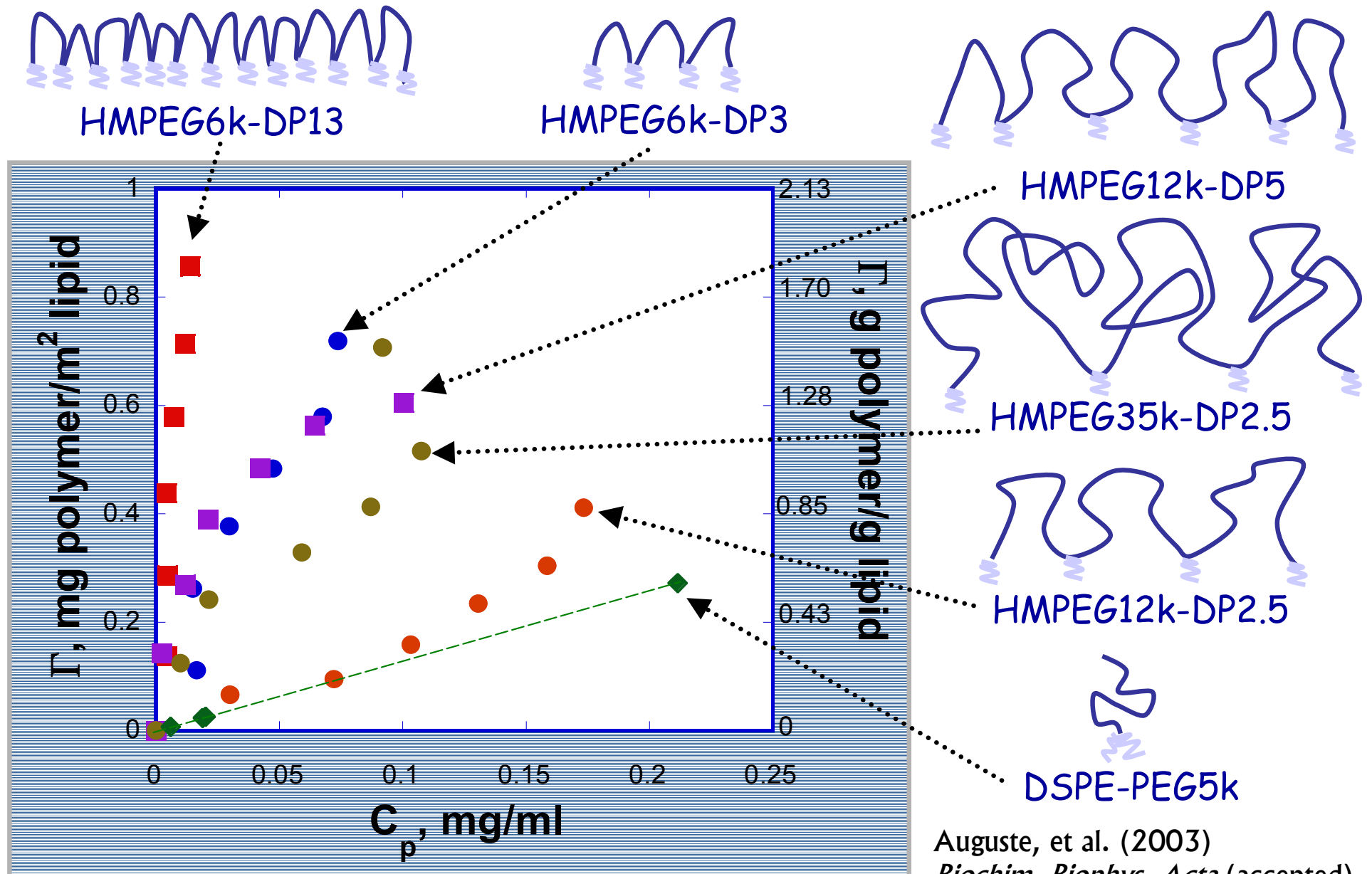
$$\xi = 0.076m^{1/2} \text{ (nm)}$$

$$\xi_{\text{PEG5k}} = 5.0\text{nm}$$

$$D_{\text{liposome}} = 100\text{nm}$$



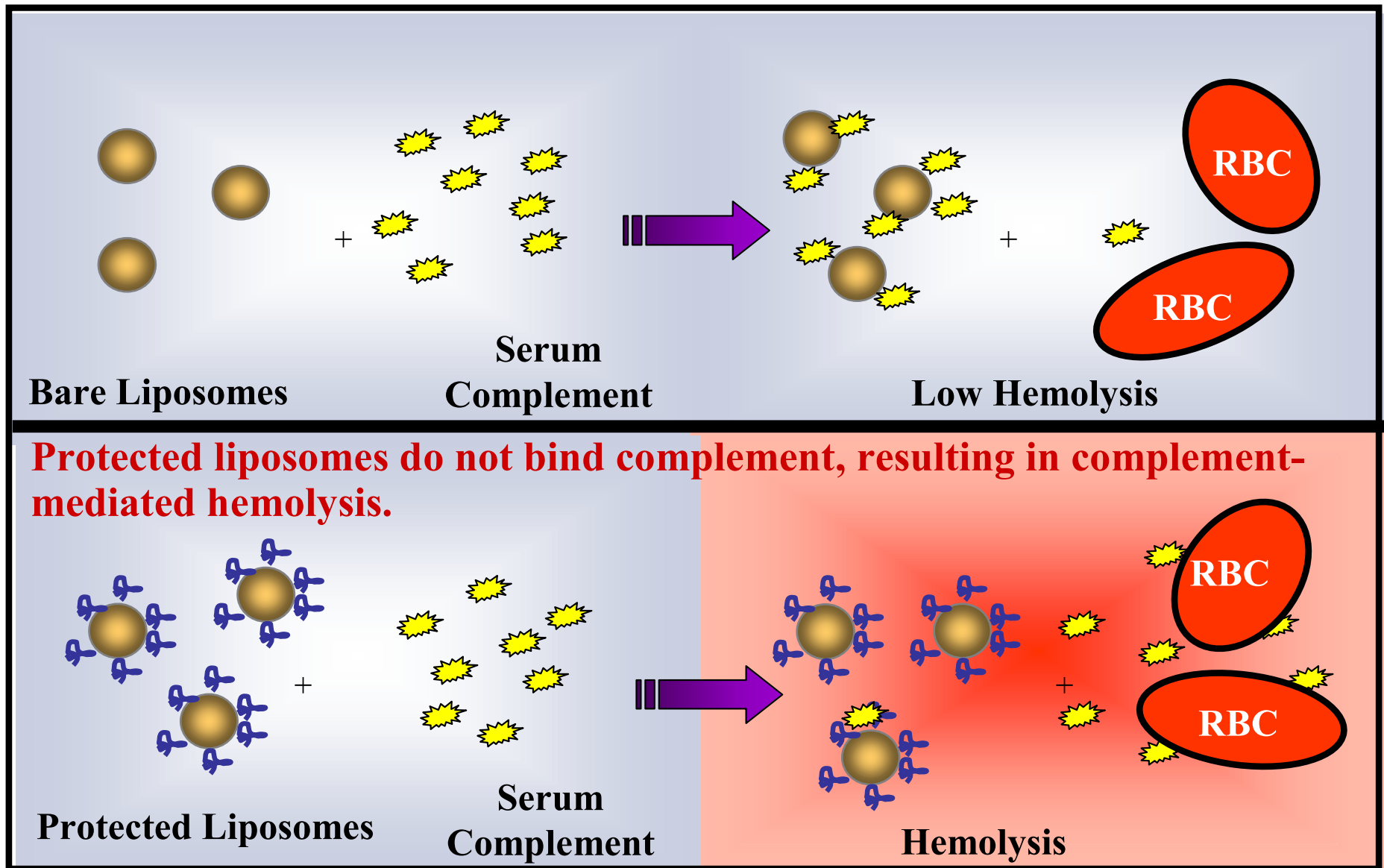
HMPEG Adsorption



Auguste, et al. (2003)
Biochim. Biophys. Acta (accepted).



Complement Assay



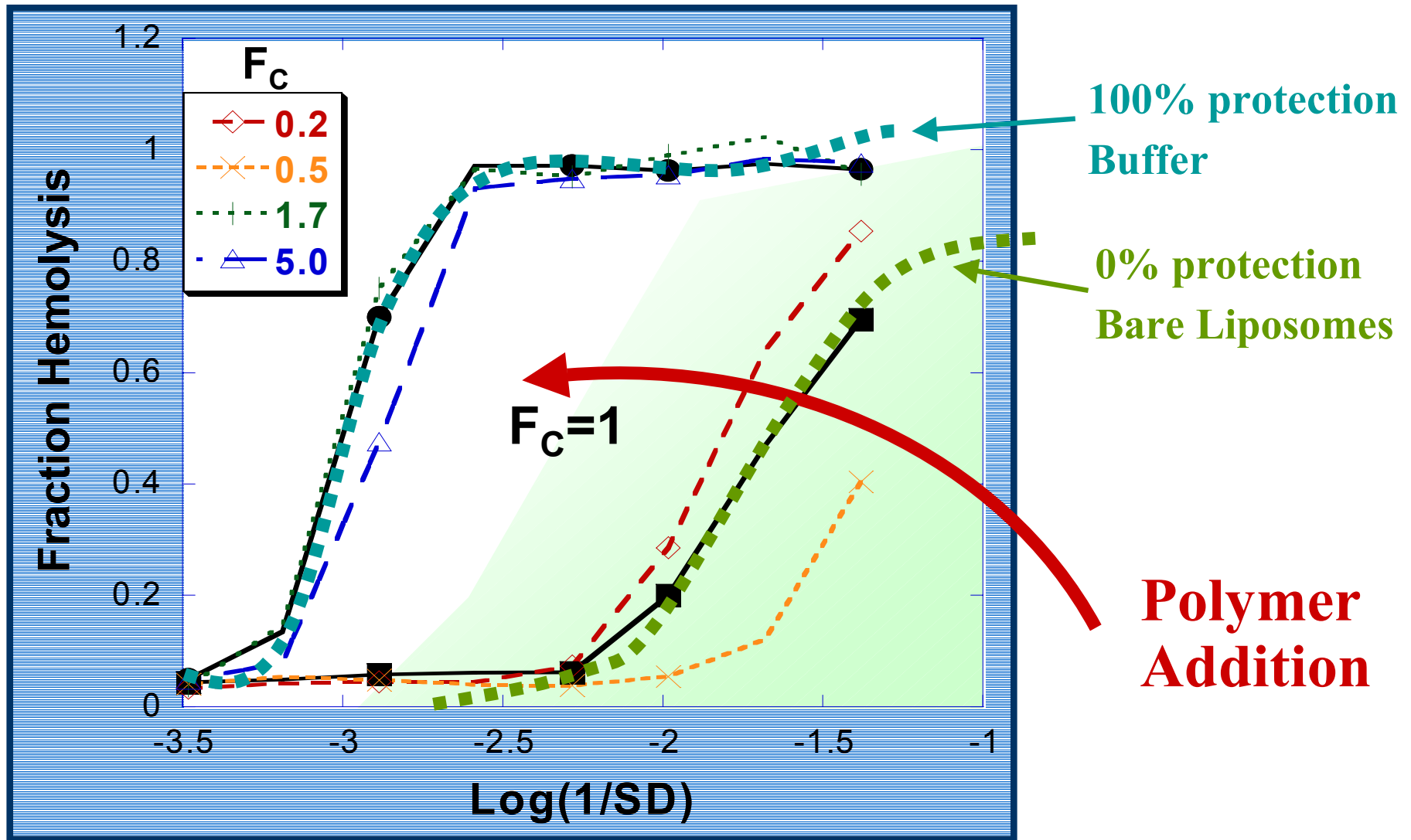
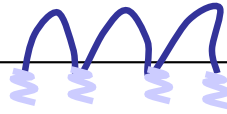
Modified from Ahl, et al. (2002). Elan Drug Delivery Poster Presentation.

Bare liposomes bind complement, which minimizes hemolysis.



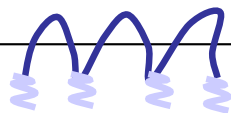
Protection from complement

HMPEG6k-DP3

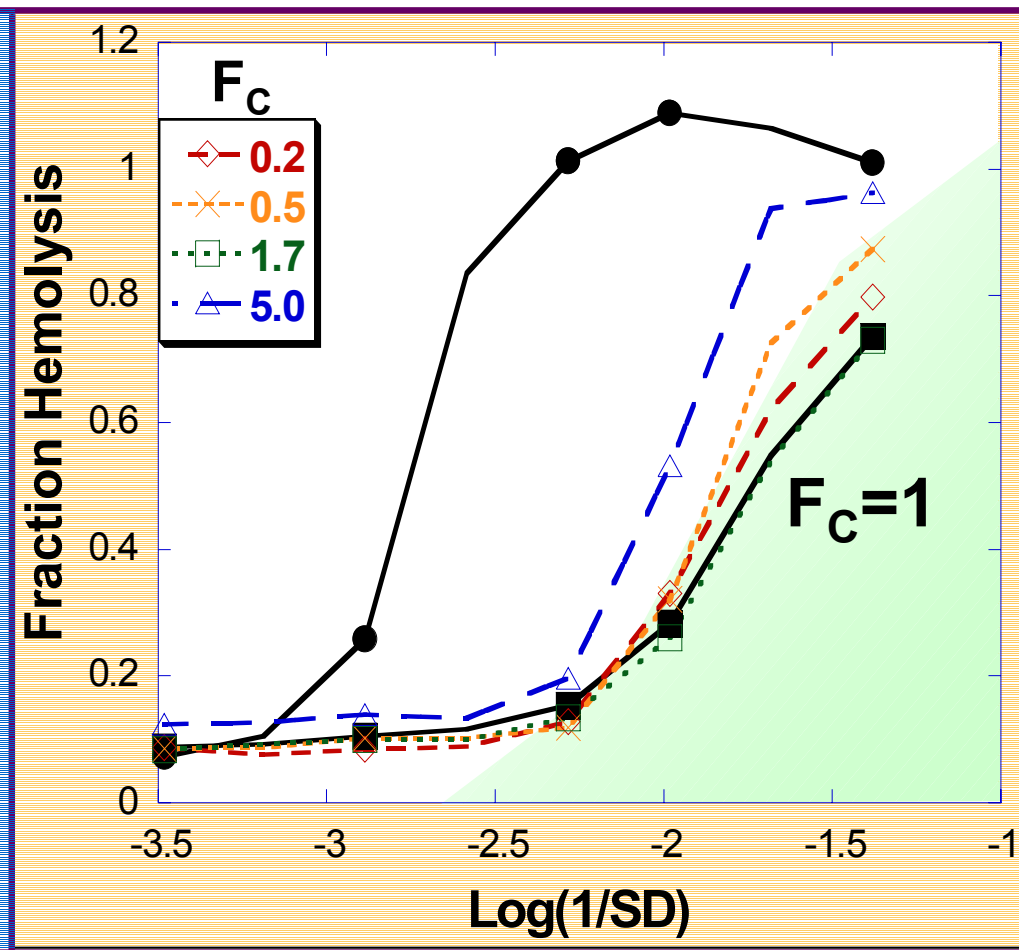
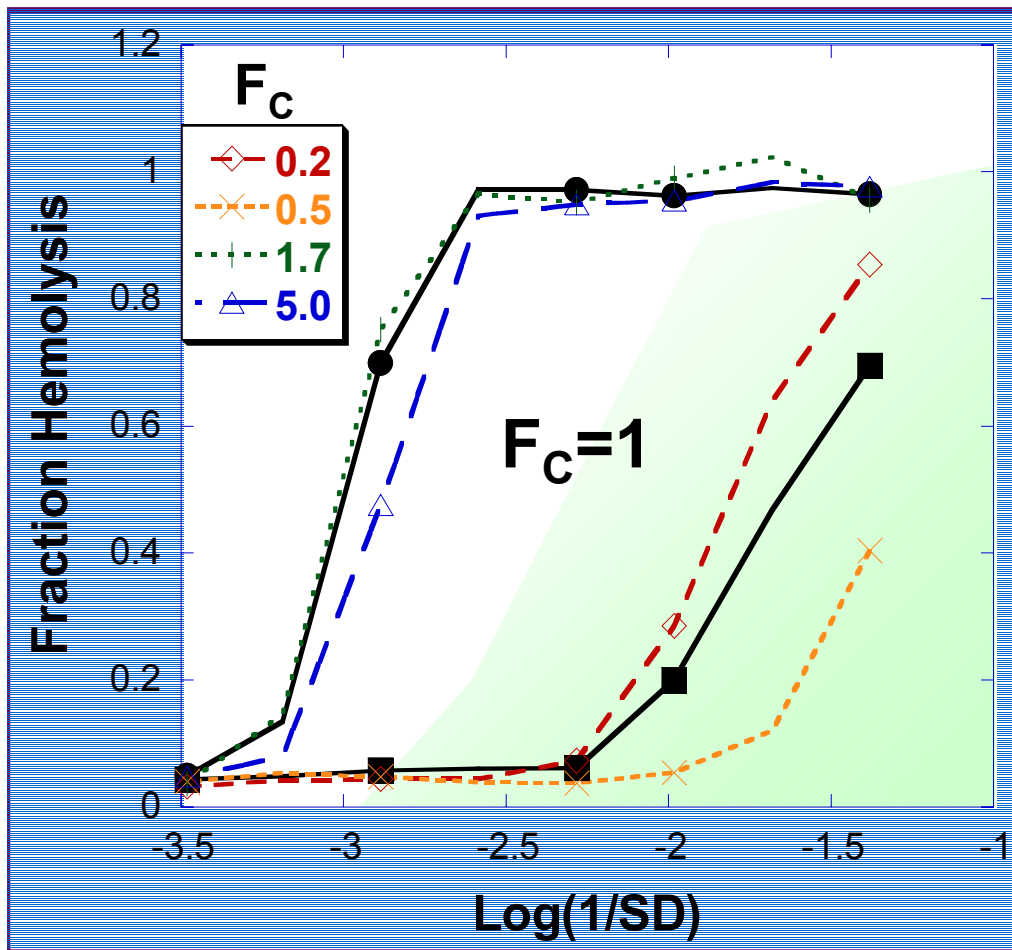
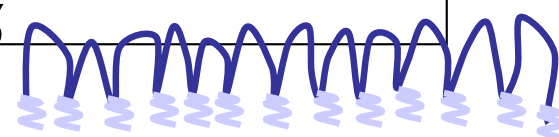


Increasing number of anchors

HMPEG6K-DP3



HMPEG6k-DP13

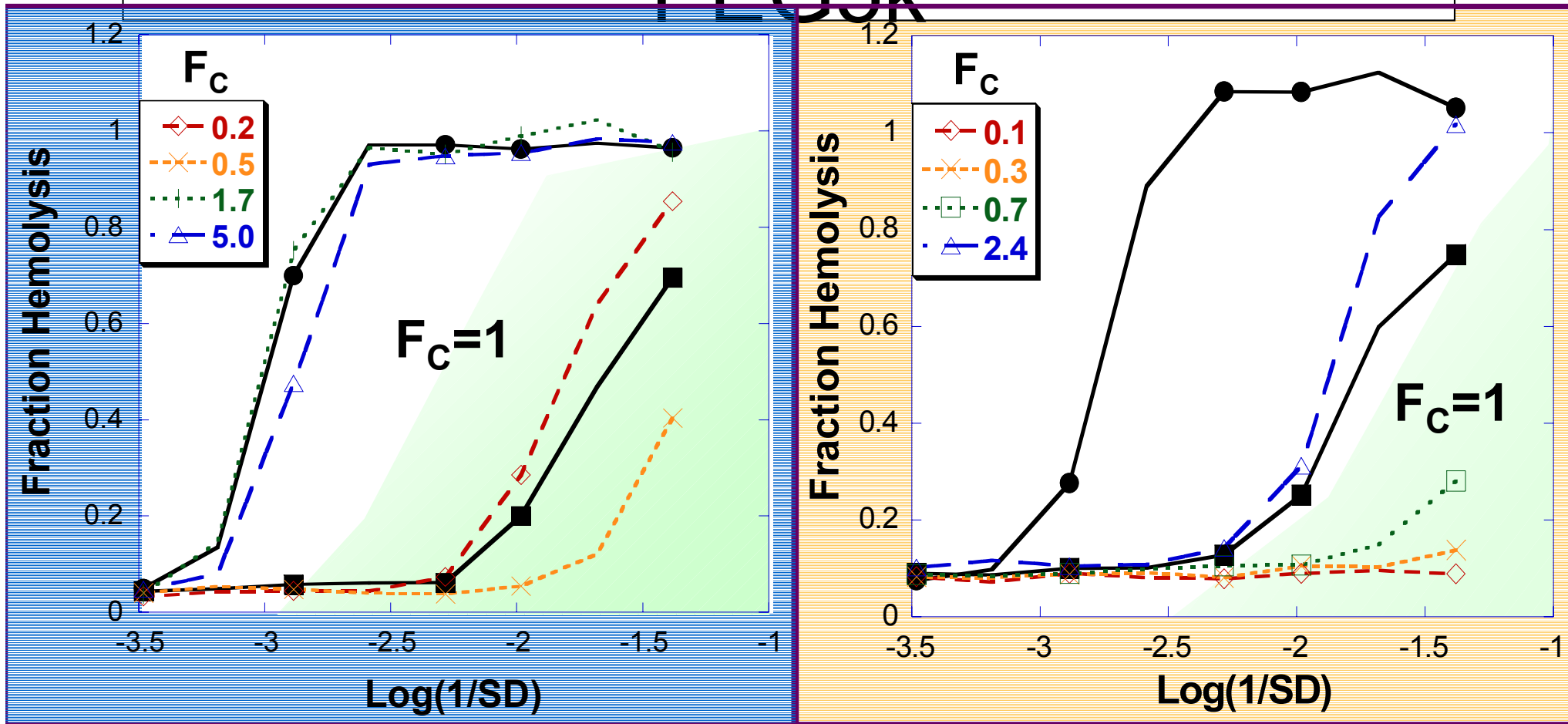


More anchors does not improve shielding from complement.



HMPEG6K-DP3

Benchmark against DSPE-PEG5k



Cooperativity increases protection relative to DSPE-PEG5k.

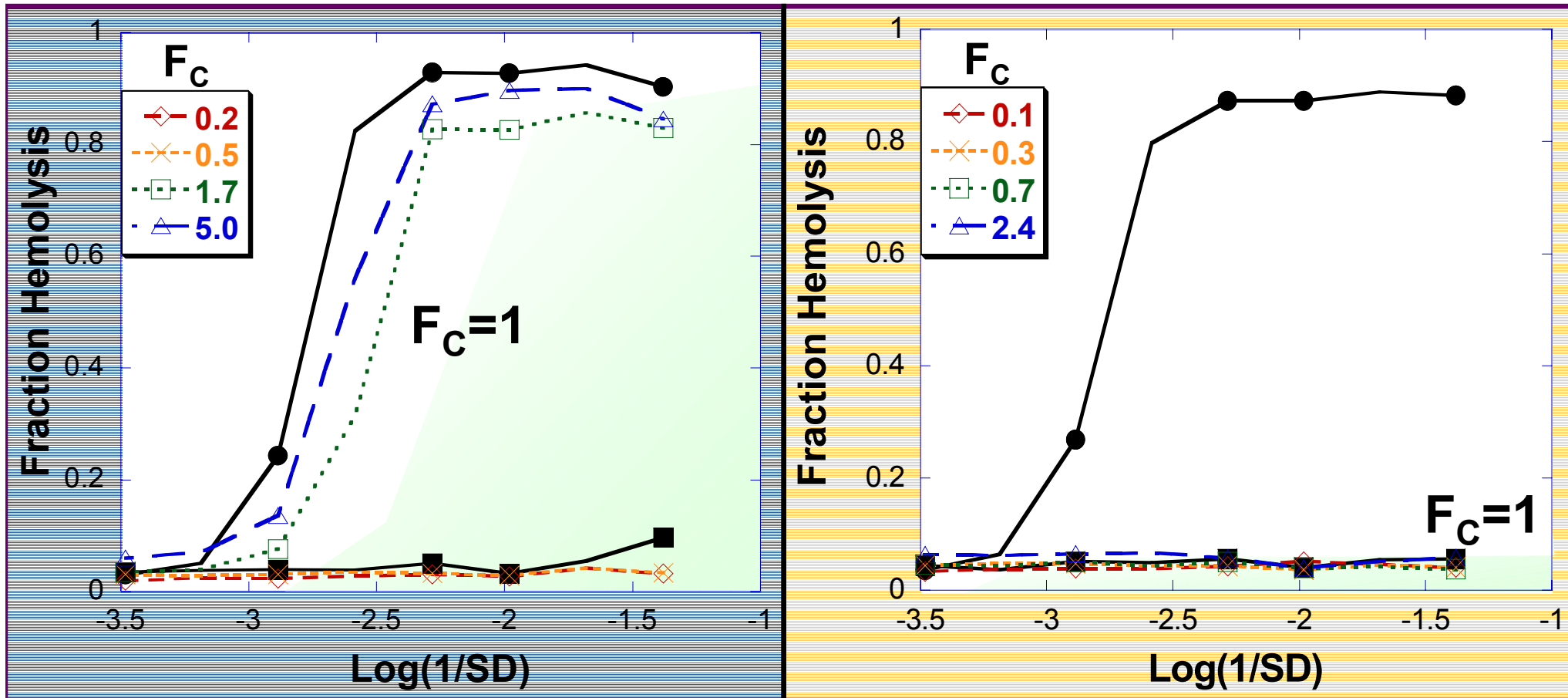
12 hr incubation tests extended

HMPEG6k-DP3



protection

DSPE-PEG5k

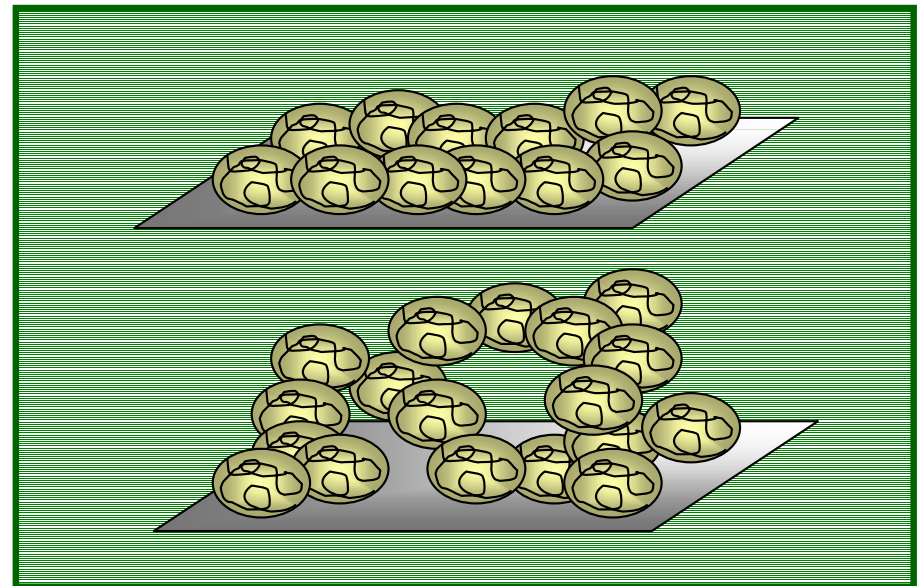
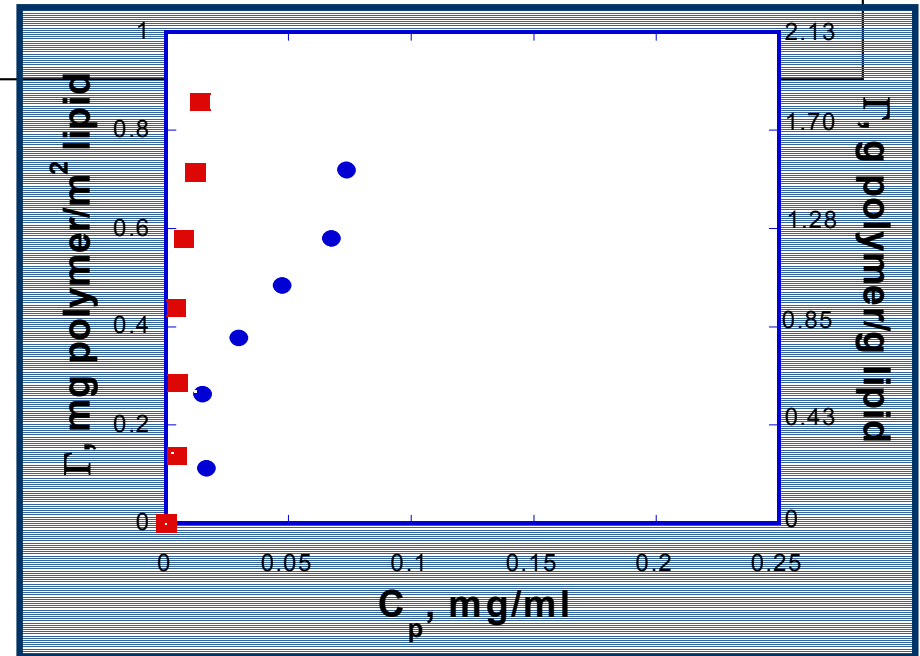


Cooperative anchoring protects over 12 hours.



Efficient packing

- **HMPEG6k-DP13** **adsorbs** strongly, $K=78.1$ (mg/m²/mg/ml)
- **HMPEG6k-DP3** adsorbs less strongly, $K=6.1$ (mg/m²/mg/ml) but **protects** from complement binding
- Inter and intra molecular associations vs. mobility on surface

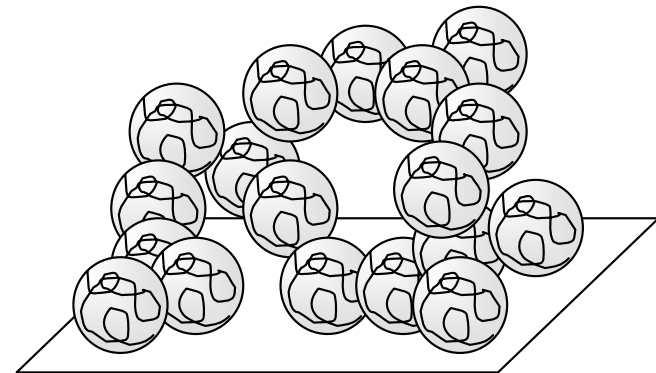
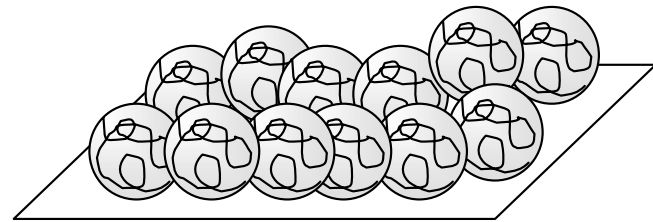




Conclusions: of HmPEG Protection

- Looked at 6K - 35K PEG
- Look at 1-13 Loops
- Higher binding alone does not guarantee protection
- PEG-lipids partition off surface
- Conformation and mobility in the adsorbed PEG layer is essential. Too high levels of cooperativity give frozen states.

Cooperative and strongly bound



Too cooperative: frozen



• Summary

- Hydrophobically modified polymers provide strong association without phase separation. Multipoint, cooperative attachment.
- Misciblize surfactant phases. Control multi-lamellar vesicle formation and stability
- Control protection of unilamellar liposomes from complement binding



Prof. Robert K. Prud'homme
Princeton University

Prof. Bill Russel,

Hank Ashbaugh: Los Alamos Labs

Bing Shiou Yang: BMS

Sonny Panmai: Merck

Debra Auguste, Kathleen Boon, Melinda Huang

Continuing Research: Electrostatically-Modified PEG

Benefits

- Triggered release of polymer from surface
- Gene delivery
- DODAP neutral above pH 7, positive below

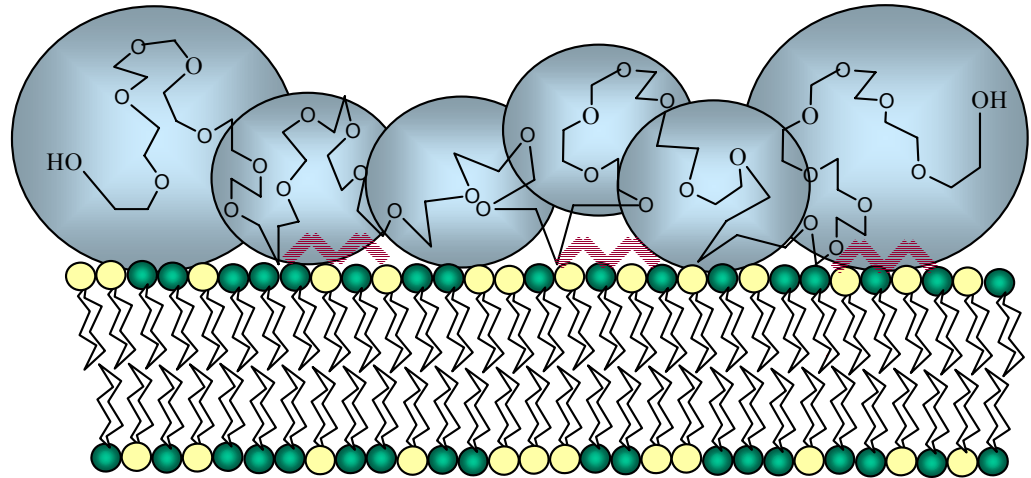
Anchors

- DMA, Polylysine, Protamine

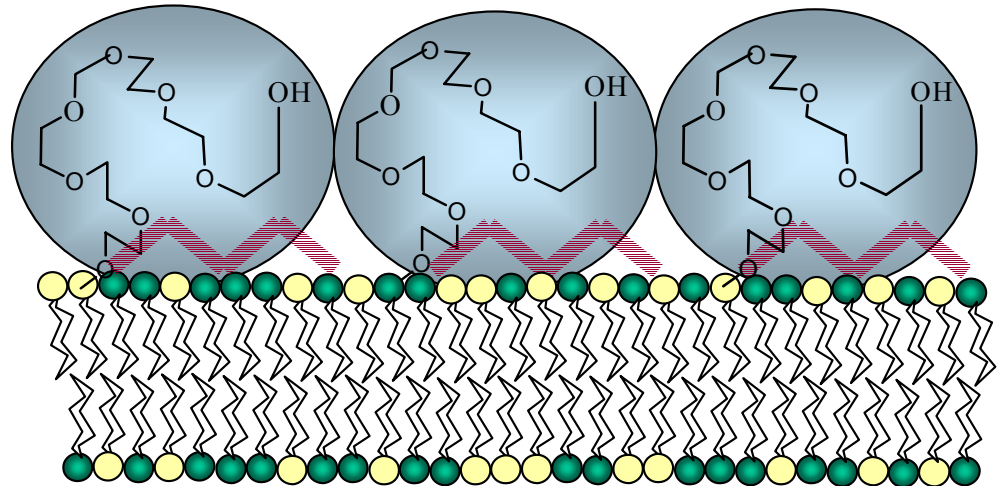
Tim Demming

Steve Armes

Multiply attached EMPEGs

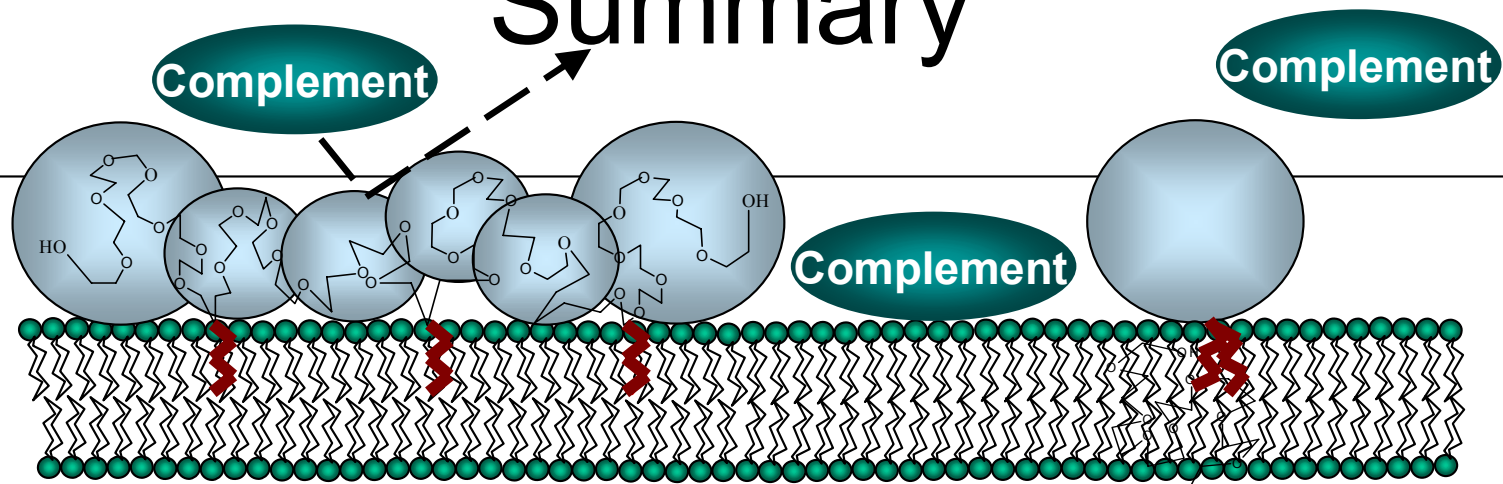


Singly attached EMPEGs





Summary



Heitz, et al. (1999) *Macromolecules* 32(20): 6652.

Cooperative binding attributes

- Binding affinity increases with number of anchors.
- HMPEGs are post-added at levels exceeding that of DSPE-PEG5k.

Complement protein binding

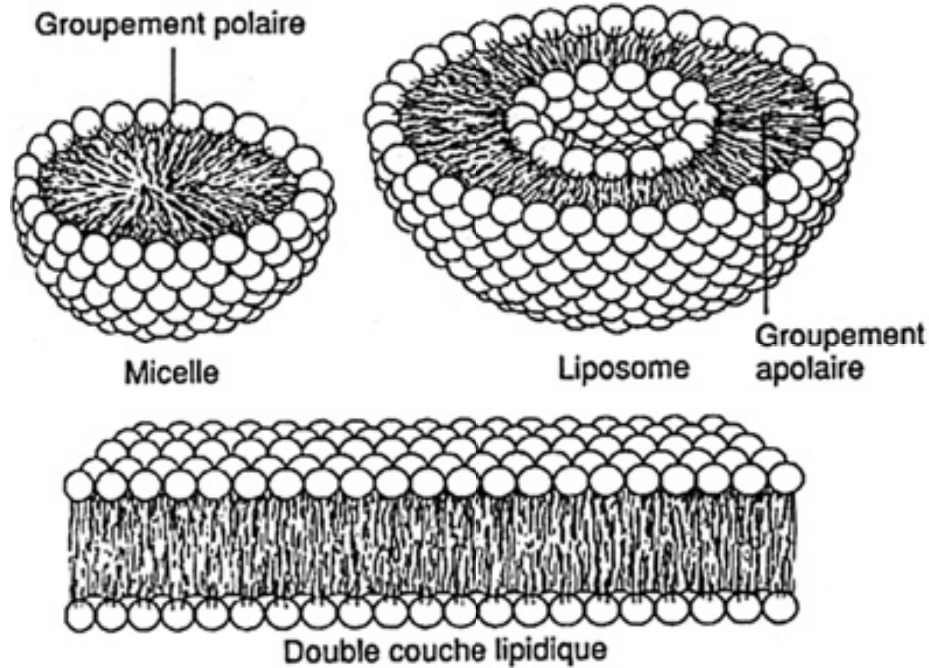
- Irreversible binding (HMPEG6k-DP3 vs. DSPE-PEG5k)
- PEG packing efficiency and mobility
- Trade-off between solubility and cooperative anchoring (HMPEG6k-DP3 & HMPEG12k-DP5)



Liposomes and Vesicles

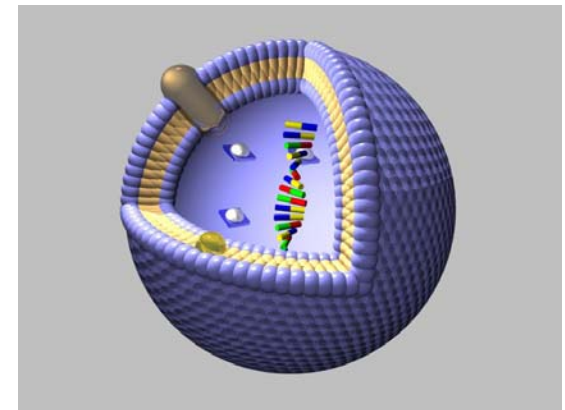
- Micelle

- Vesicle or Liposome



- Lamellar Bilayer

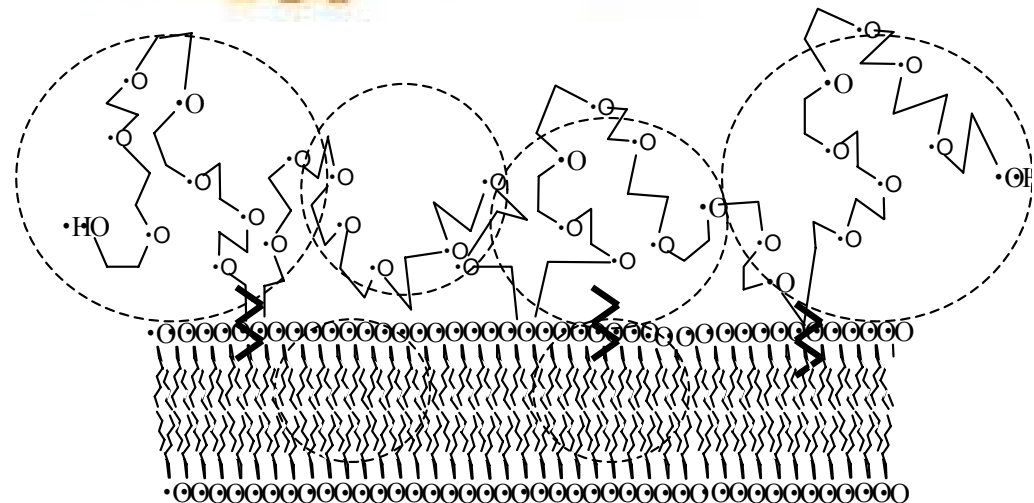
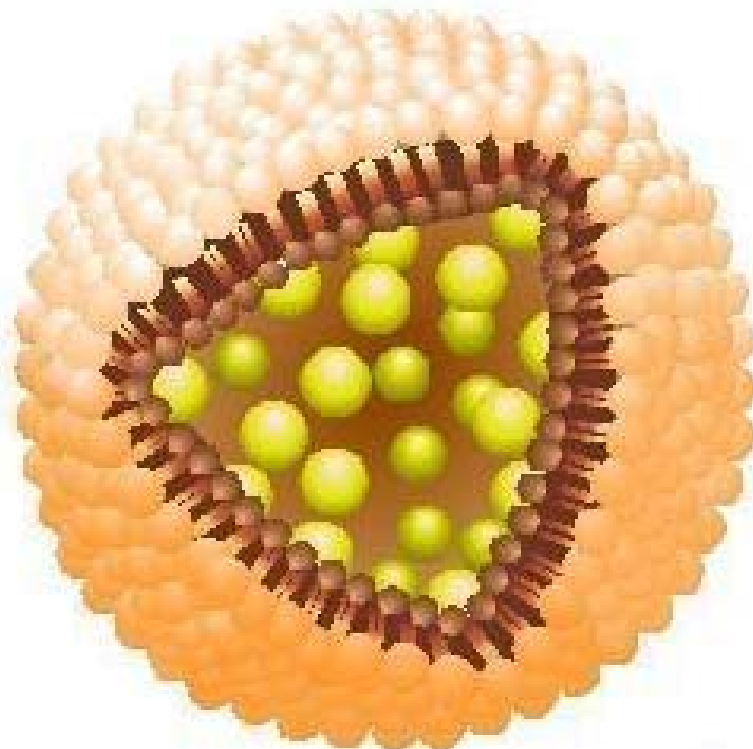
- Containers for drugs, fragrances, DNA





Liposome PEG Protection of Drug and DNA Delivery

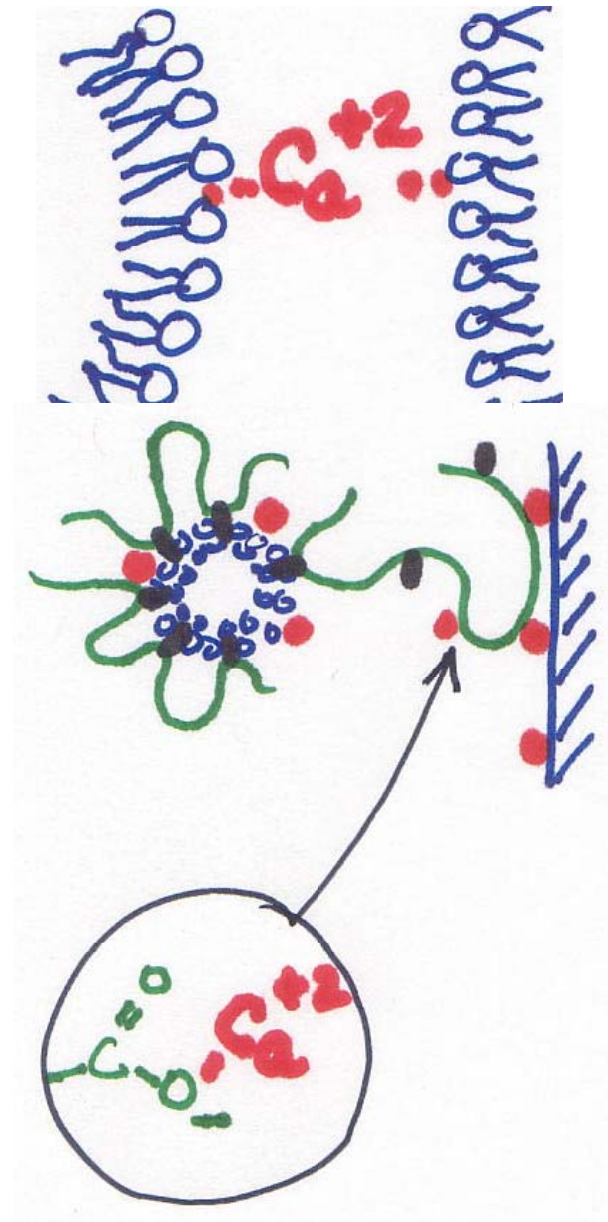
- *PEG-Lipid (Stealth Liposomes) provide longer circulation time in vivo.*
- *PEG prevents protein binding and recognition by the immune system*
- *PEG-lipids partition off surface*
- *PEG-lipids must be included in the liposome formation process*





Protection of Vesicles from Calcium-induced Rupture

- Calcium induces rupture of anionic vesicles by electrostatic fusion
- Hm Polymers can provide a steric barrier to prevent fusion: hm-PAA, and hm-PEG



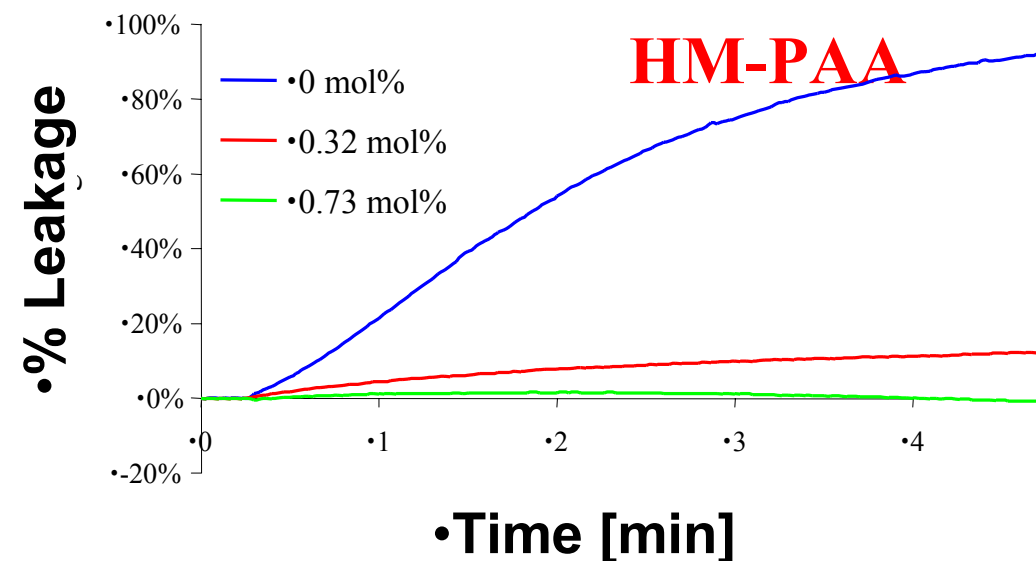
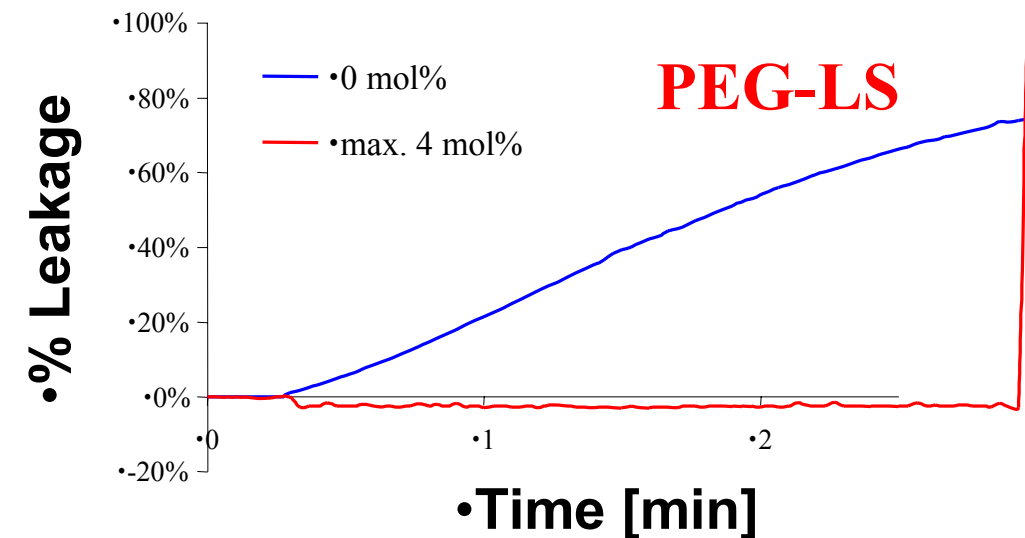


Results: Effect of Polymers on PE:PS Stability against Ca^{2+} -induced Rupture

• Percent leakage as a function of time after the addition of 7mM CaCl_2 to 34 μM PE:PS

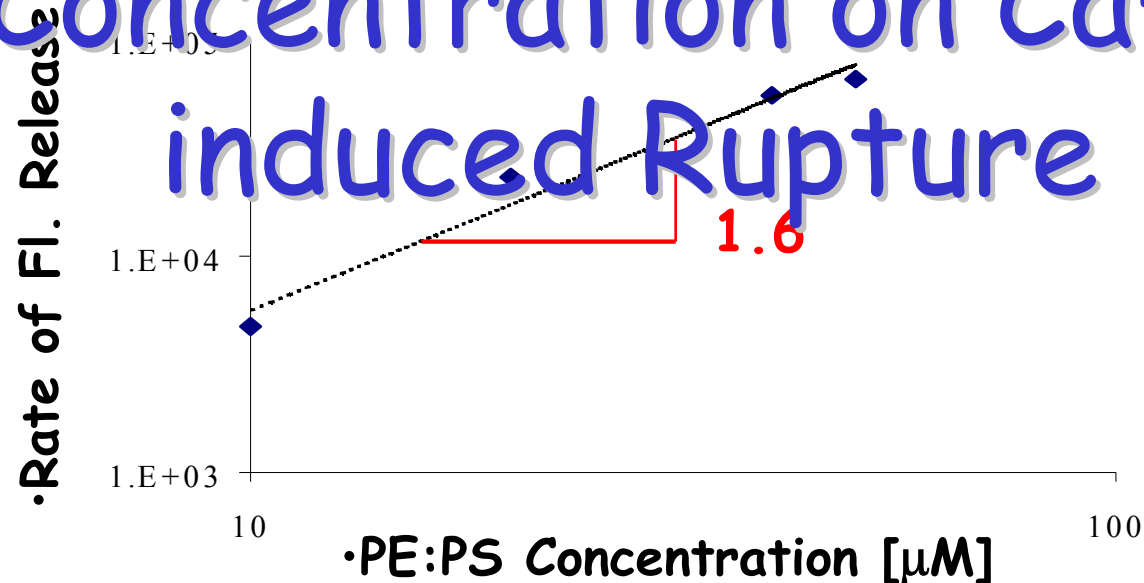
• In all cases, polymers stabilized PE:PS liposomes against Ca^{2+} -induced rupture

• Hm-PAA adsorbed on glass surfaces as stable vesicles





Results: Effect of Lipid Concentration on Ca^{2+} -induced Rupture



- Data yields : $\text{rate}_{\text{leakage}} \propto [\text{vesicle}]^{1.6}$
- Vesicle-vesicle aggregation seems to be a necessary precursor to rupture
- If vesicle-vesicle interaction is necessary for liposome rupture, then: $\text{rate}_{\text{leakage}} \propto [\text{vesicle}]^2$
- Data excludes a single vesicle mechanism



- Aqueous suspension of PE:PS (1:1) lipids (5mM) in 60mM calcein (fluorescent dye) extruded ten times through two 0.1 μ m polycarbonate filters at room temperature and 220-270psi
- unentrapped calcein removed using a desalting column
- Liposome size: diameter = 100nm
- Calcein-entrapped PE:PS liposomes diluted with



Formation of Spontaneous Unilamellar Vesicles

Mixtures of Anionic and Cationic Surfactants

7

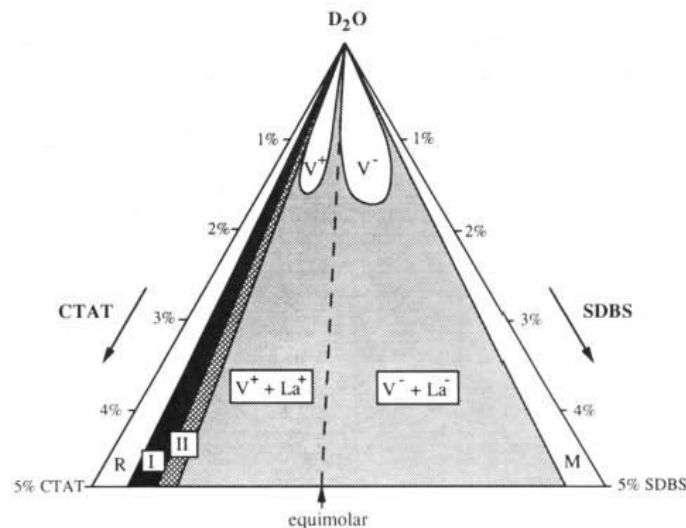


Figure 7. Ternary phase diagram of CTAT/SDBS/D₂O at 28 °C. Nomenclature used is the same as for Figure 1.

Non-stoichiometric mixtures of anionic and cation surfactant form vesicles

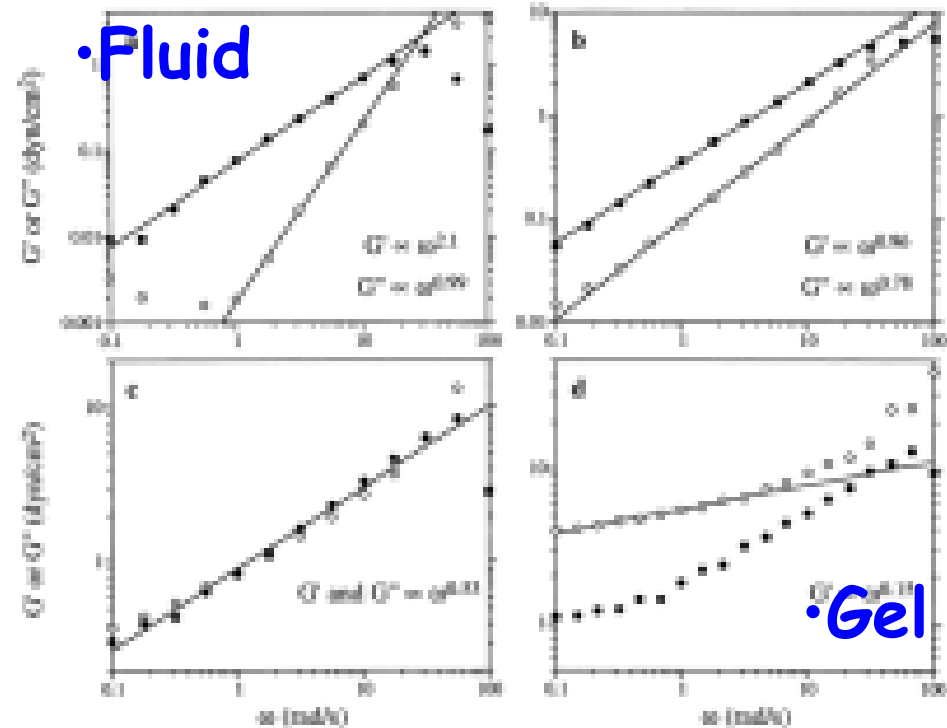
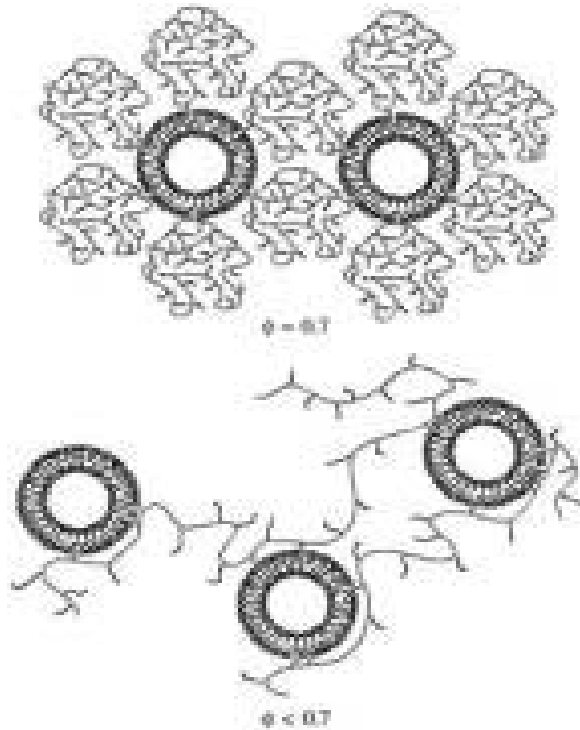
Very dilute (2%) phases.

Kaler, et al. JPC (1992)



Vesicle Gels: Hm

Vesicle systems can be bridged by hydrophobically modified polymers to create gels while still preserving the vesicle phase. (Ashbaugh, Bohn, and Prud'homme *Coll and Polym* 2002)



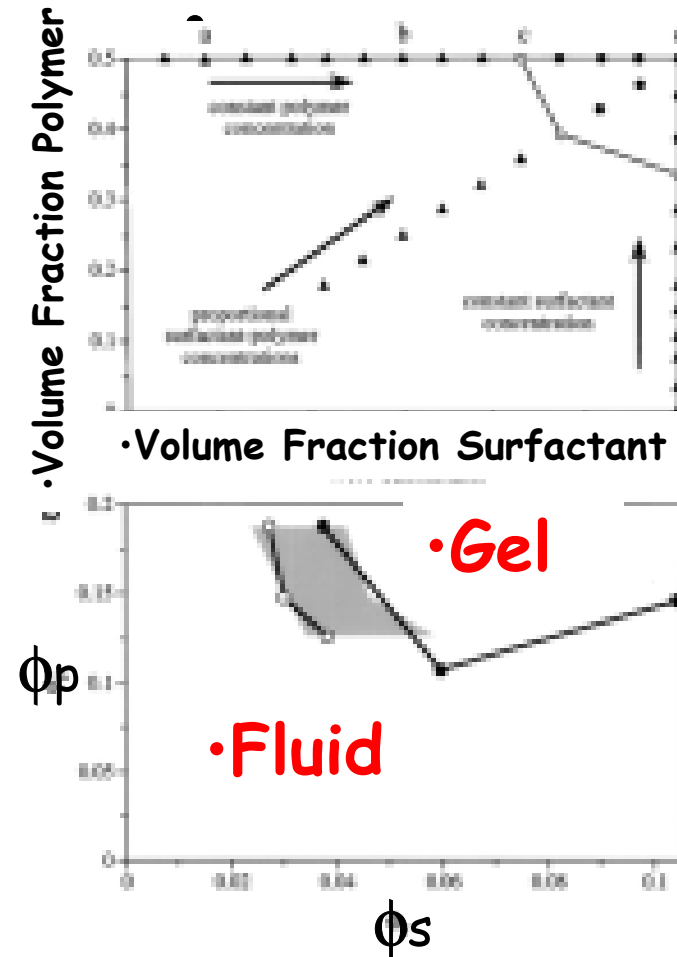


Volume Fraction at

• Gelation is by percolation

• Without Hm-Polymer- Phase Separation

• With Oppositely Charge Polymer- Phase Separation





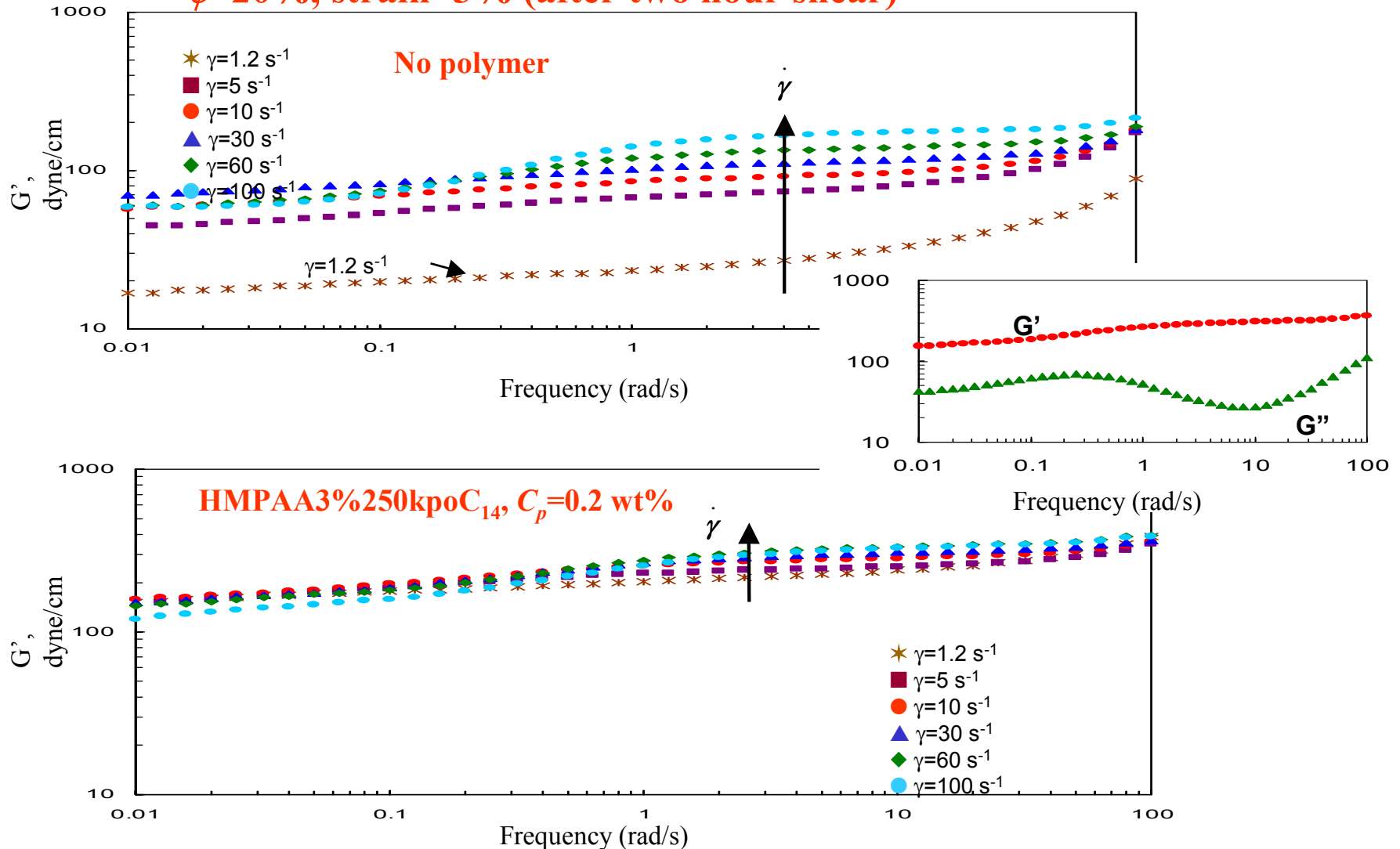
Conclusions

- Tuned Self-Assembly can be used to control inter-particle interactions
 - Nano-particles: blocked aggregation, used hydrophobic interactions
 - Wax Control: blocked aggregation, used co-crystallization



Rheological Properties of Onions

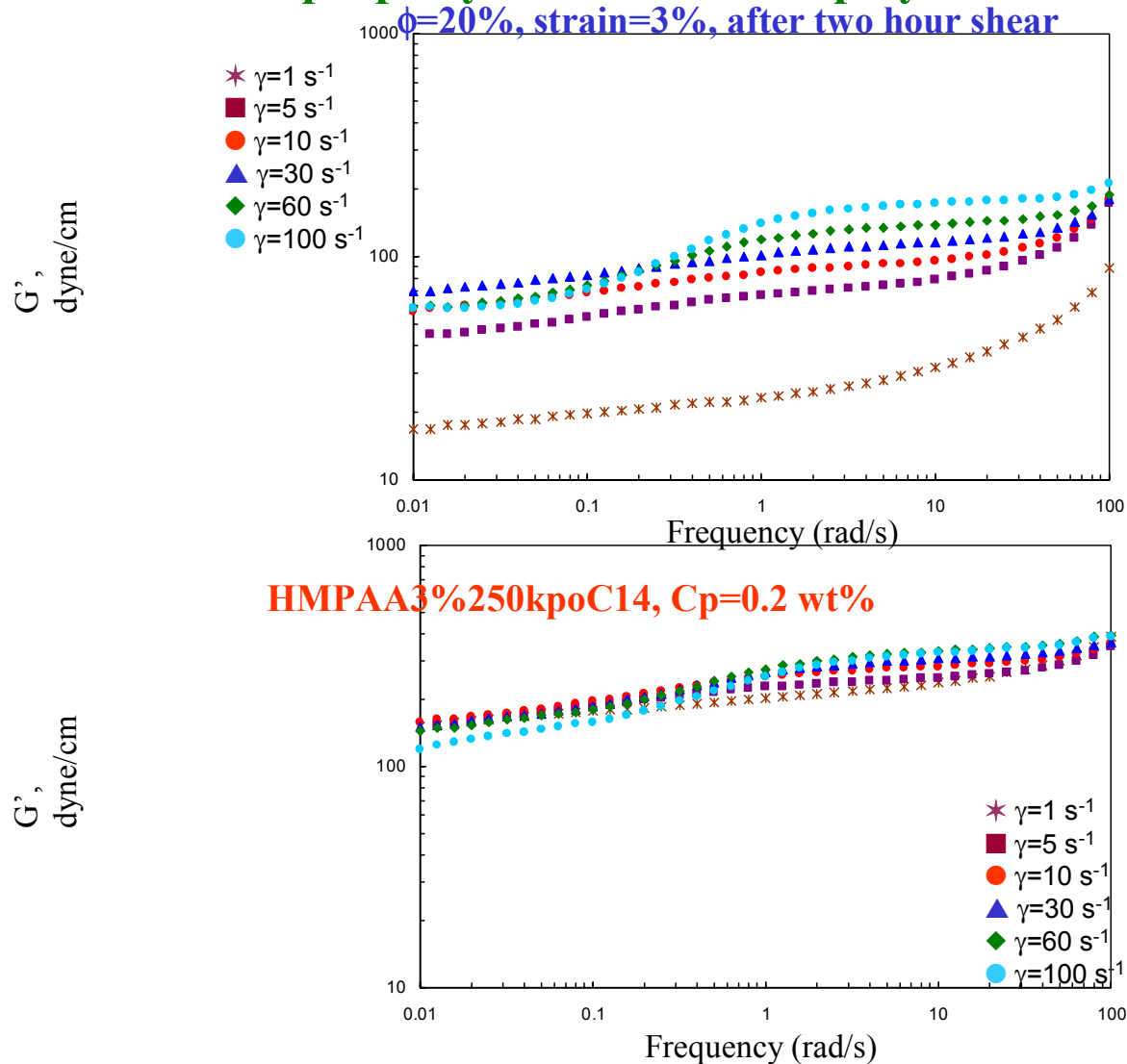
$\phi=20\%$, strain=3% (after two hour shear)



- Onions are a viscoelastic medium. $G' > G'' \rightarrow$ onions are more elastic than viscous.
- Bare membrane system doesn't form onions at $\dot{\gamma} = 1.2 \text{ s}^{-1} \leftarrow$ liquid like behavior.
- Plateau modulus G_0 is higher for polymer doped systems.
- Shear rate dependence of the G_0 of the polymer doped onions is less significant than that of onions made from bare membranes.



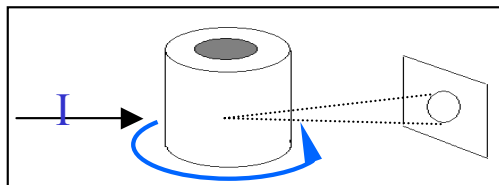
Onion property — Effect of hm-polymers



- Bare membrane system doesn't form onions at $\gamma=1 \text{ s}^{-1}$ ← liquid like behavior.
- Plateau modulus G_0 is higher for polymer doped systems.
- Shear rate dependence on the G_0 of the polymer doped onions is smaller than that of bare membrane onions.

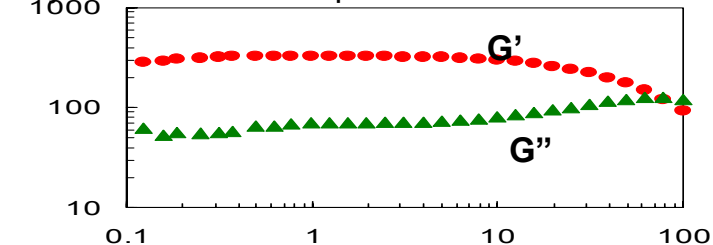


Opto-viscometer

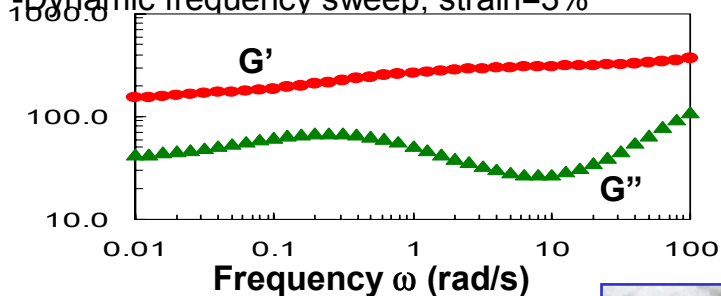


Rheology

-Dynamic strain sweep



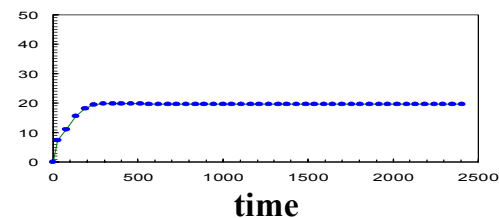
-Dynamic frequency sweep, strain=3%



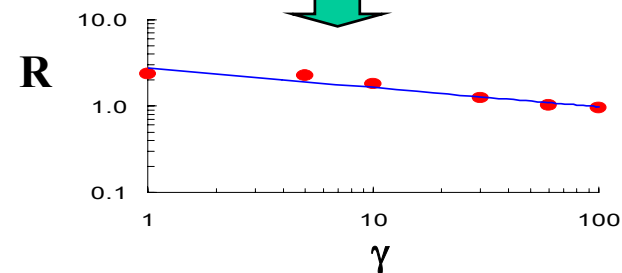
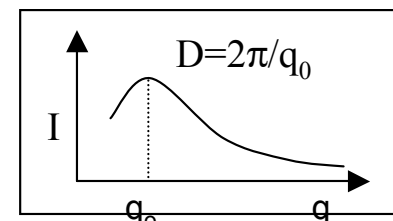
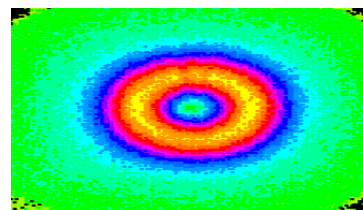
Lamellar phase

Shear for two hours at certain η
shear rate γ

Onions



Light scattering



$G_0 = G_0(\gamma)$

$R = R(\gamma)$

$G_0 = G_0(R)$

$$G_o = \alpha + \frac{\beta}{R}$$

$$\alpha = \frac{\gamma_o}{B} \gamma_o^2$$

γ_o : pre-existing quenched strain.

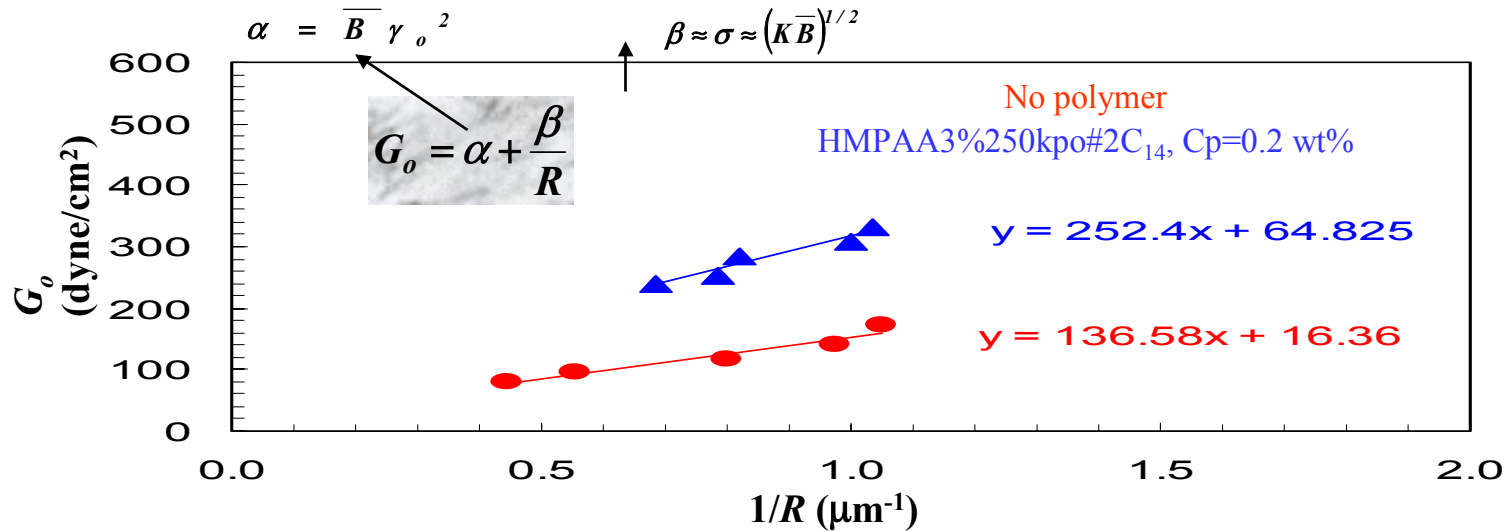
Effective surface tension associated with deformation of the onions

For a perfectly ordered array of polyhedra

$$\beta \approx \sigma \approx (KB)^{1/2}$$



Onion \leftrightarrow Lamellar Phase



Onion Phase

$$G_o = G_o(R)$$



Lamellar Phase

$$(\kappa \overline{B}, \overline{B})_{\text{Polymer doped membrane}} > (\kappa \overline{B}, \overline{B})_{\text{Bare membrane}}$$

SANS

$$\kappa \overline{B}, \overline{B} \uparrow \longleftrightarrow C_p \uparrow$$

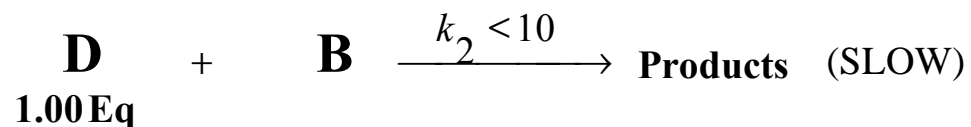
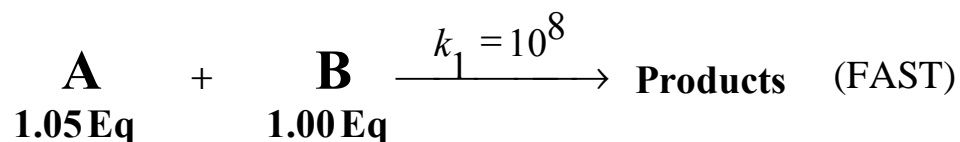
- Elastic properties of onions and corresponding lamellar phase are consistent.



III. Known $\tau_{process}$ ✓

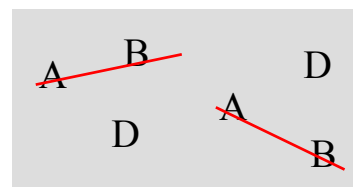
Competitive Reactions as a “Chemical Ruler”

Competitive(Parallel) Reactions



Homogeneous
kinetics

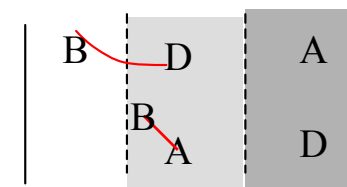
$$\tau_{mix} \ll \tau_{rxn}$$



vs.

Transport
controlled

$$\tau_{mix} \geq \tau_{rxn}$$



Characteristic Reaction Time

$$\tau_{rxn} = \frac{1}{k_2 C_{Bo}}$$

$$Da = \frac{\tau_{mix}}{\tau_{rxn}}$$

Conversion of
Slow Reaction

$$X = 1 - \frac{C_D}{C_{Do}}$$

Relative Mixing
Intensity $\frac{1}{Da} = \frac{\tau_{rxn}}{\tau_{mix}}$

$$X = f(Da)$$

0 100%
Conversion of Limiting Reagent

KEY: When τ_{mix} scaled correctly $X_{100\%} = f(Da)$ is unique

A New Approach to Combinatorial Rheology Measurements

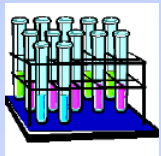
Toward quick measurements of the
complex viscosity of multiple, small
samples of polymer solutions

Howard J. Walls, Robert Berg, Kate Beers, Eric Amis, & Alamgir Karim



The Need for High Throughput Rheology

Development or tuning a polymer formulation inherently involves experimentally exploring a multi-parameter space.



composition



temperature



time

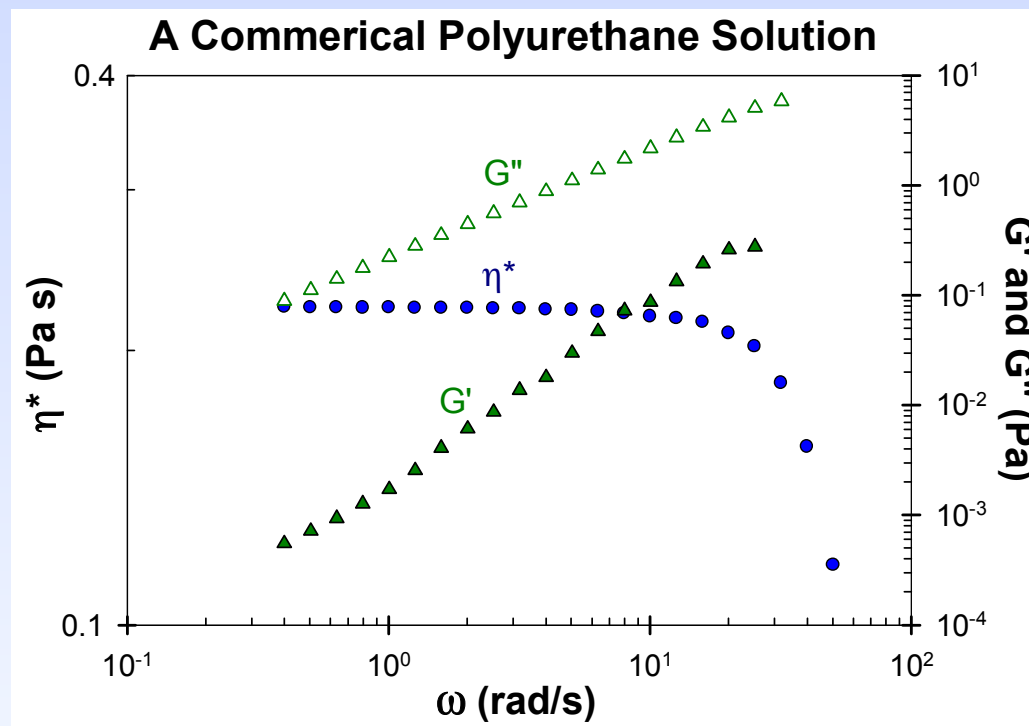
processing,
pressure,
etc.

other factors



η , G' , G''

What are the
final Properties?





Viscosity/Rheology Measurement

Considerations in selecting a measurement method:

- 1) Sample size
- 2) Total range in viscosity η
- 3) Sensitivity, precision, accuracy
- 4) Range in η measurable for single configuration of the instrument
- 5) Validity of measurement for your samples and application

Technique	Volume (mL)	η max (Pa s)	η range (decades)	Viscoelasticity
Rotational rheometer	0.4~1	Gels (100+)	4-5	Yes
Capillary viscometer	0.5~10	~10	~1	No
Falling/rolling ball viscometers	0.2~10	~10	~2	No
Quartz crystal resonators	0.2~2	~1+	2~3	Yes
Micro-rheology: DWS, particle tracking	0.01~0.3	Gels (10+)	3~4	Yes



High Throughput Rheology (HTR) Options

Possible high throughput viscosity & rheology measurements

(in literature, patented, or available for purchase)

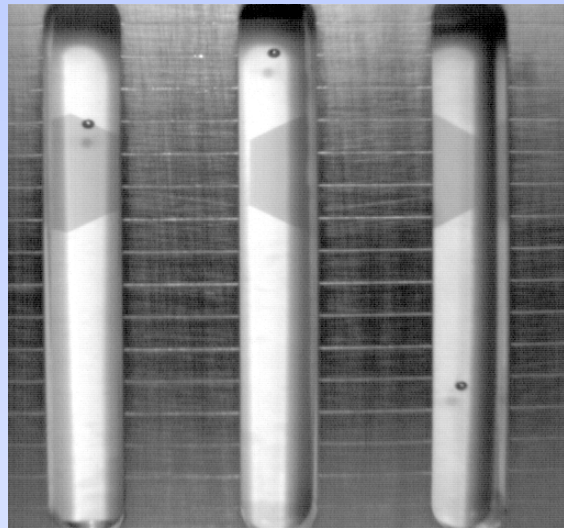
- Automated rolling ball capillary viscometer with auto sampler
 - 1 sample at a time, modest sample size, no dynamic measurements
- Rotational Rheometer with automatic sample changer
 - 1 sample at a time, several mL sample size, dynamic and broad range
- Multi capillary tube viscometer
 - Multi sample method, narrow range for single config., not dynamic
- Quartz crystal resonators
 - Single and multi sample, high frequency

Note: for rolling/falling ball, capillary, and quartz resonators ρ_f must be known, however in some cases $\eta \times \rho_f$ or $\eta \div \rho_f$ may be measured.

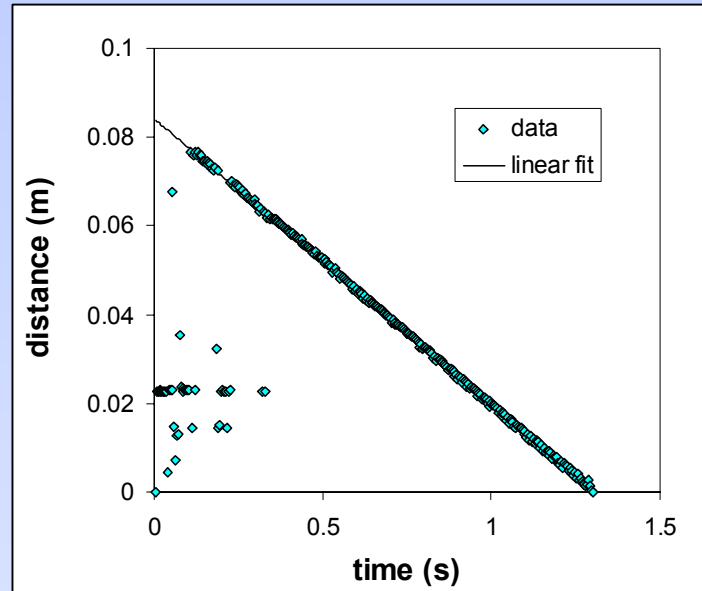


History of NCMC Efforts in HTR

- Multi-falling ball viscometer



CCD
&
IDL



$$\eta \sim \frac{2gr^2(\rho_b - \rho_f)}{9V_\infty}$$

Sample #	η (Pa s)	Re #
1	0.587	0.0324
2	1.078	0.0096
3	0.269	0.155

- Milli-fluidics device $\eta \sim \frac{\pi r^4}{8L} \frac{\Delta P}{Q}$

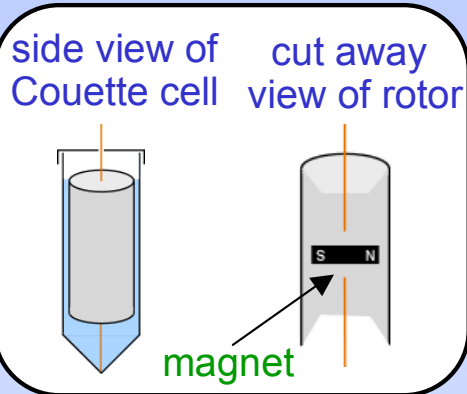


use CCD to measure fluid travel time
in channels of known dimensions

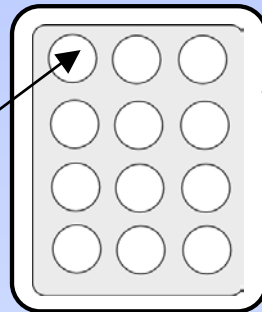


The New Idea for HTR: Combi Rheometer

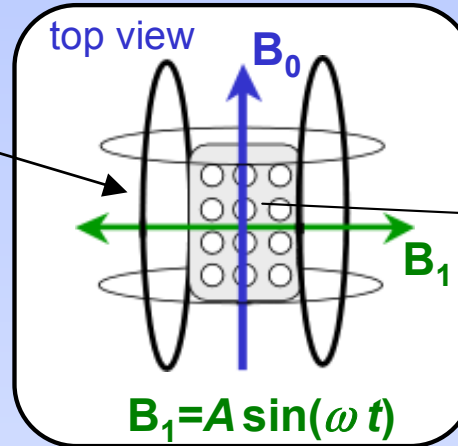
sample test cell



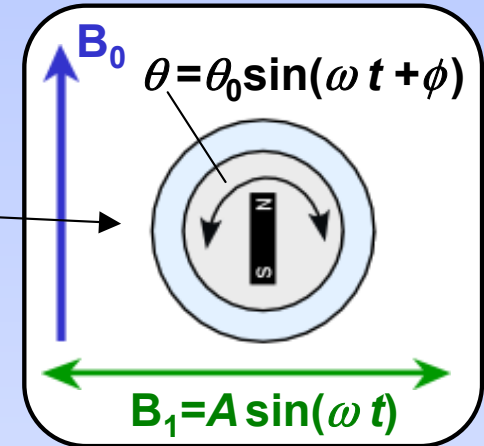
sample array



2 axis Helmholtz coil



sample response

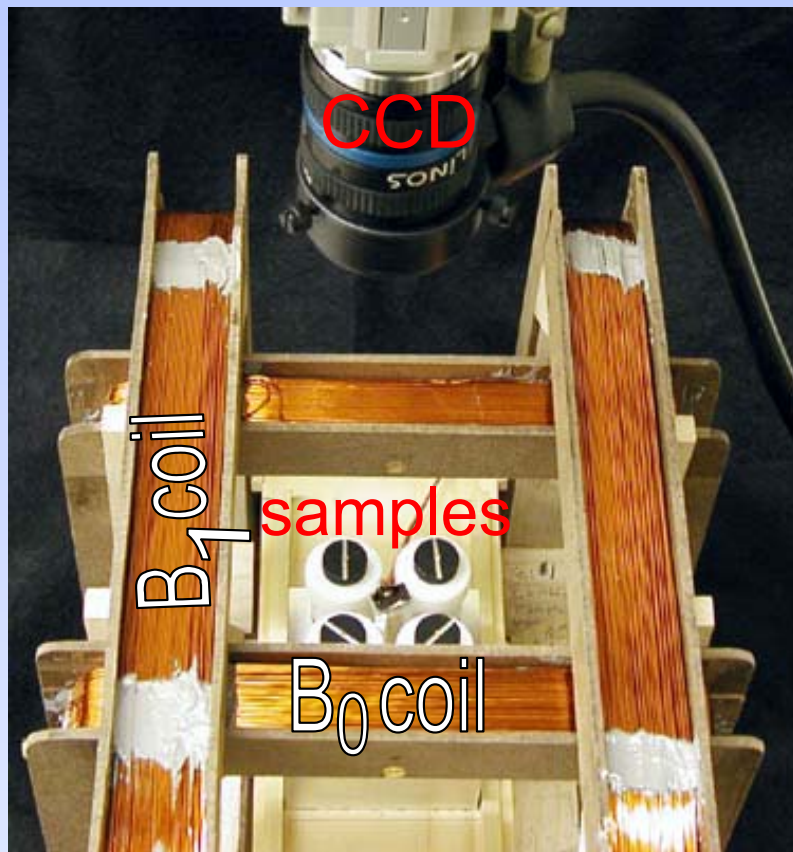


- Description

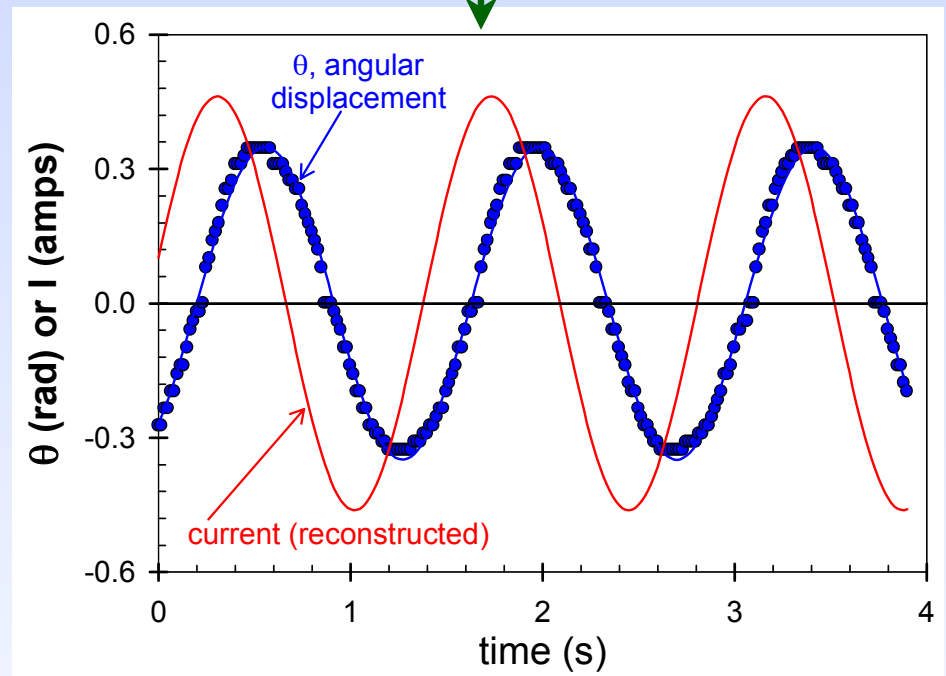
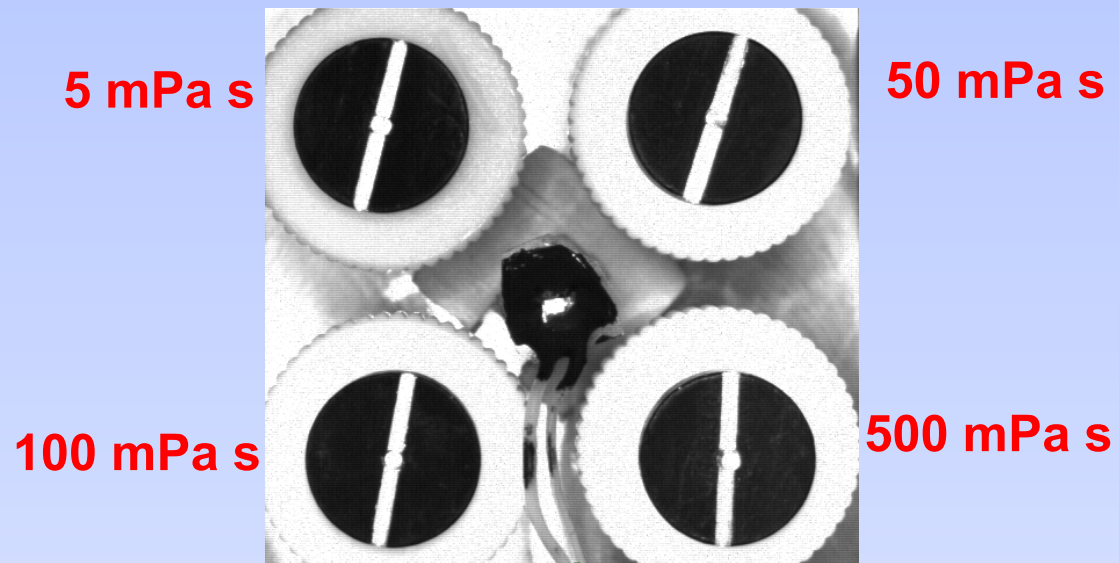
- Cylinder (a rotor) immersed in solution with rheology to be measured.
- Bar magnet embedded in rotor aligns with a static magnetic field B_0 from Helmholtz coil.
- Oscillating magnetic field B_1 applied via orthogonal Helmholtz coil.
- Viscosity (η) and viscoelasticity (η' , η'') of the fluid influences amplitude and phase response of the rotor.



The Prototype



The LED indicates the current sign and zero crossing, giving the phase lag between the current signal and rotor response.





HTR – Principle of Operation

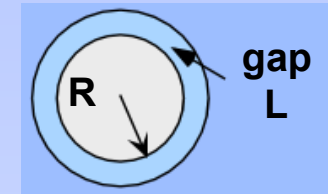
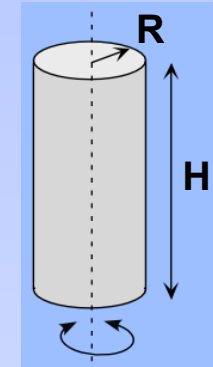
$$N(t) = K\theta + \nu\dot{\theta} + I\ddot{\theta}$$

↑
torque

↑
torsion spring constant

viscous dissipation

↑
moment of inertia



$$\theta(t) = \theta_0 e^{i\omega t}$$

$$N(t) = N_0 e^{i\omega t}$$

- K – determined by B_0 field and system parameters

- I – physical dimensions: $I \approx \frac{\pi}{2} \rho_{cylin} R^4 H$

- ν –viscosity and elasticity: $\nu \approx \frac{2\pi R^2 H \eta}{\tanh(kL)}$; $k = \frac{1+i}{\delta}$;

$$\delta = \left[\frac{2\eta}{\rho_f \omega} \right]^{1/2}$$

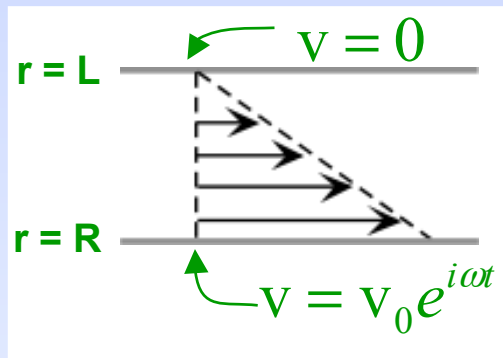
viscous
penetration length



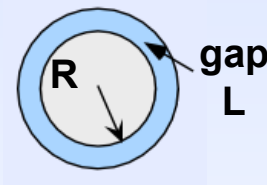
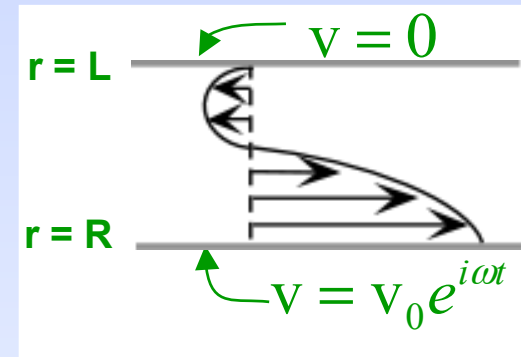
HTR – Principle of Operation

- Design considerations and knobs that can be turned
 - B_0 (static field) affects K and thus the resonance frequency.
 - B_1 (oscillating field) affects θ_0 and thus the shear rate.
 - L (gap) affects the velocity profile and thus the uniformity of the shear field.

$$\underline{L \ll \delta}$$



$$\underline{L \geq \delta}$$

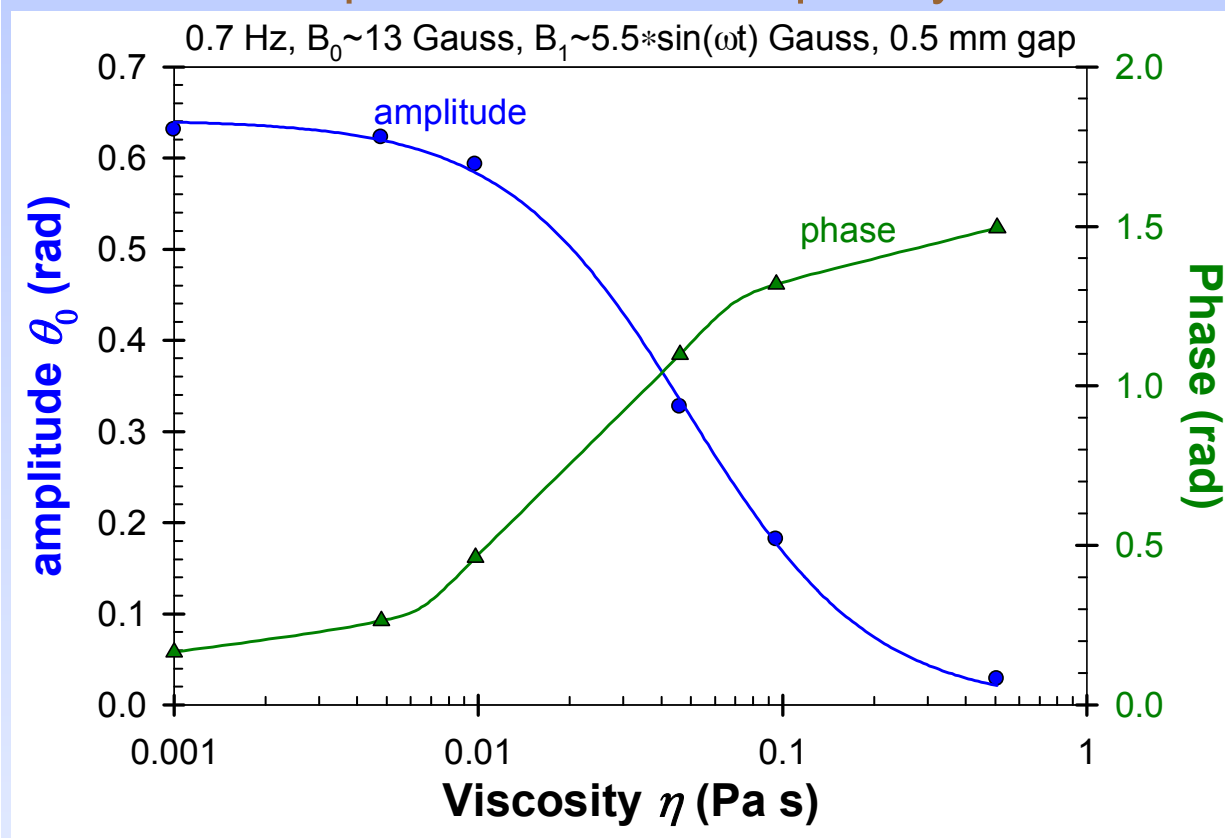


$$\delta = \left[\frac{2\eta}{\rho_f \omega} \right]^{1/2}$$



Preliminary Results: a calibration curve

Viscosity affects amplitude and phase at fixed frequency



➤ A “Combi” Viscometer

- Simultaneous measurement of 4 samples.
- Low, variable frequency.
- Zero shear viscosity (η_0) from amplitude or phase.

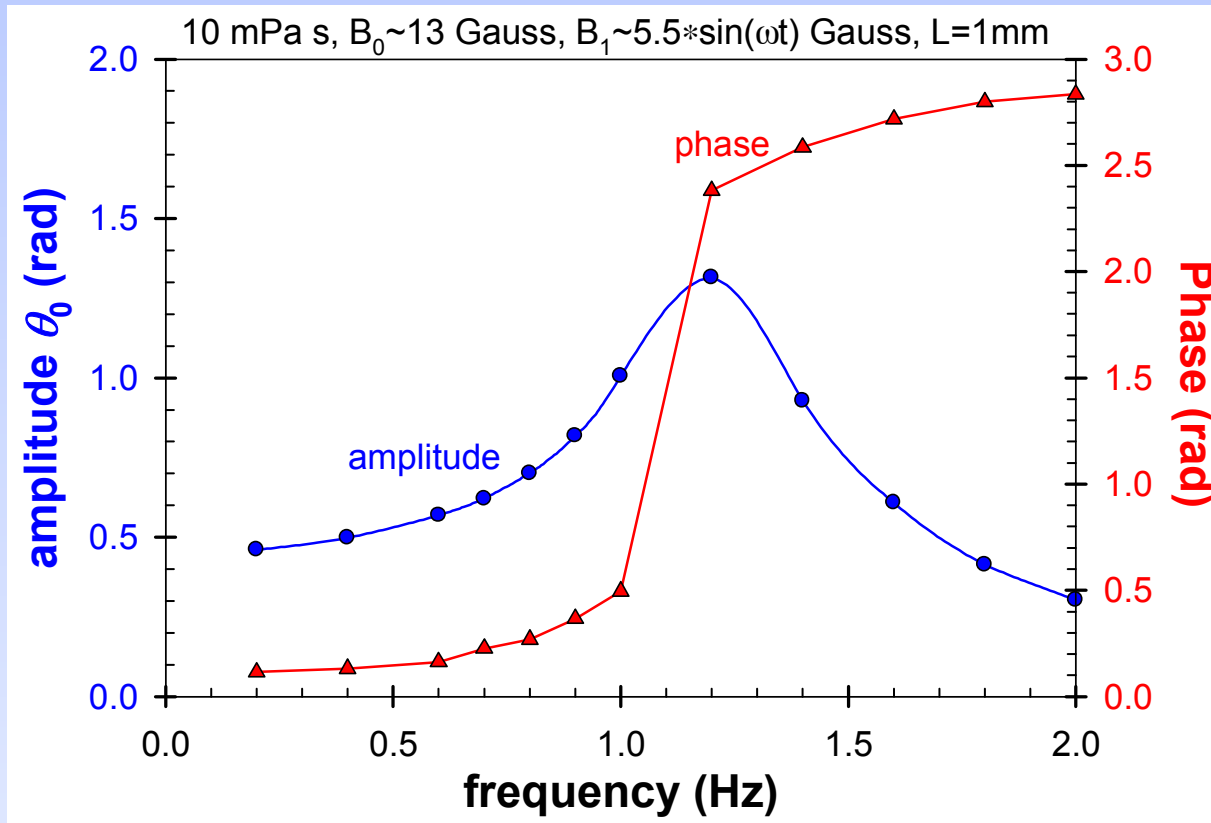
• Considerations

- **Uniformity of magnetic field:** less than 2 percent deviation in volume used.
- **Interaction:** no observable change in results if 1 to 4 cells are present.
- **Cell construction:** cells are dissimilar (cal. curve for each cell needed).



Preliminary Results: frequency sweeps

Frequency sweep for 10 mPa s

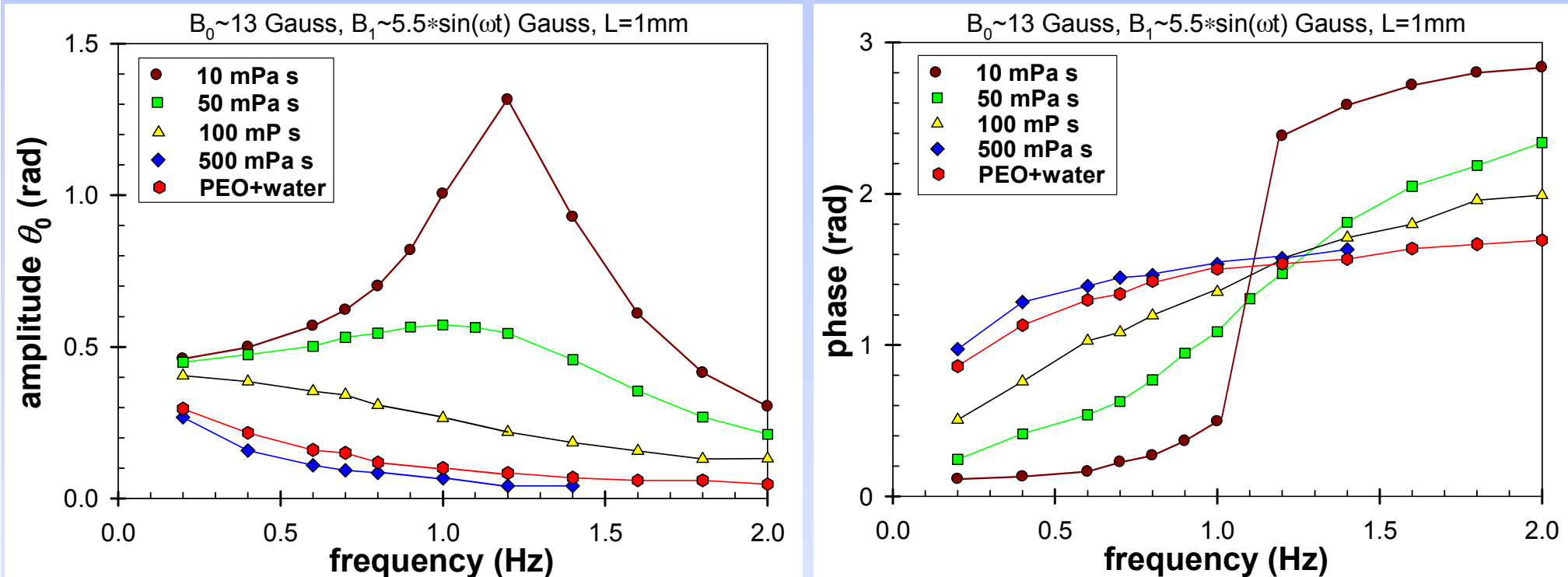


- Damped oscillator resonance
 - Low Q oscillators provide sensitivity to η over a broad frequency range.
 - Two variables allow determination of complex viscosity (η'' , η').
 - Developing an algorithm to calculate η'' , η' from the amplitude and phase response to the known applied force.



Preliminary Results: frequency sweeps

Frequency sweeps for Newtonian standards and a viscoelastic fluid

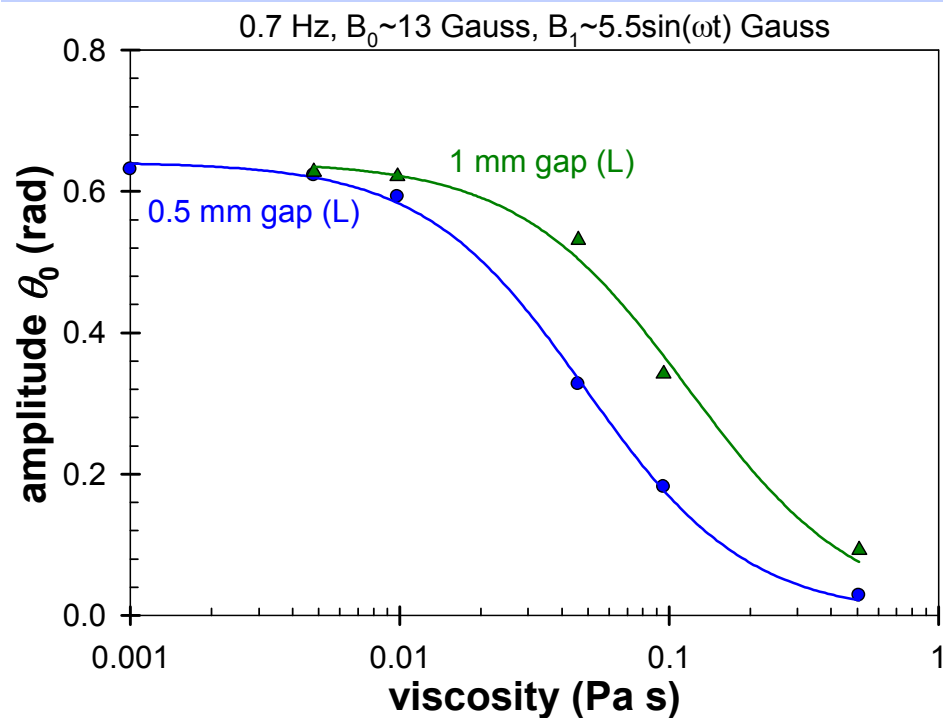


- Low freq amplitude results for PEO+water agree with results from traditional rheometer ($\eta \sim 280$ mPa s).
- Above 1.3 Hz (~ 8.2 rad/s) PEO+water phase curve suggests presence of η'' ; trad. rheometer results indicate $\eta'' \sim 0.1 \times \eta'$ at this freq.
- Working on increasing frequency range and signal to noise ratio.

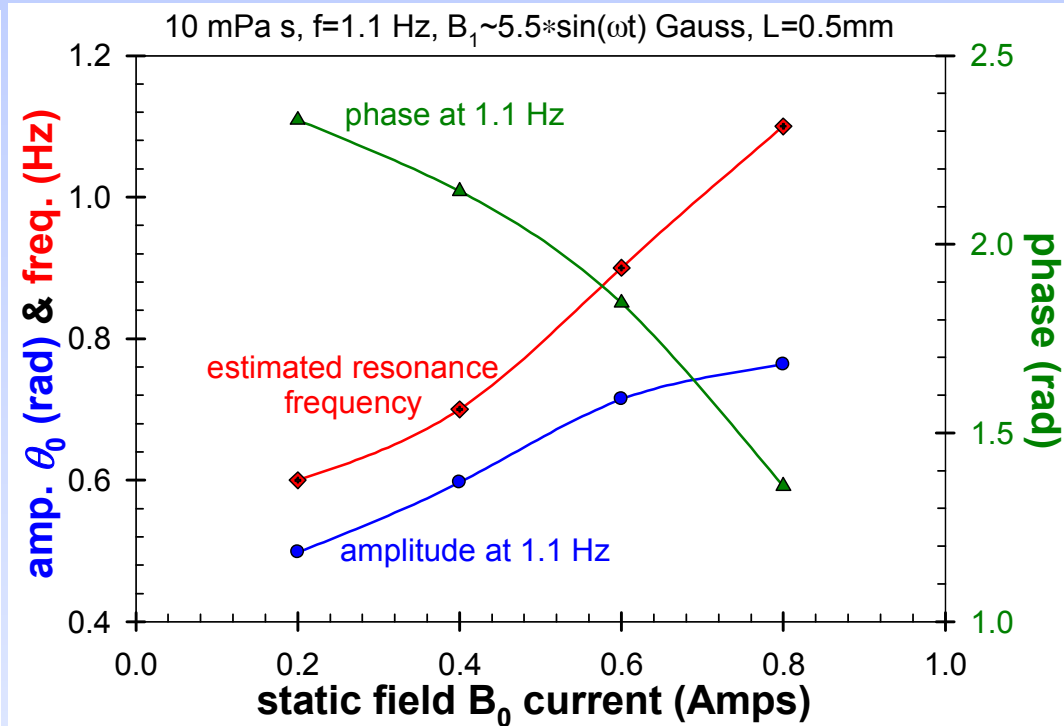


Preliminary Results: effect of L and B_0

Effect of gap L at fixed freq.



Effect of B_0 for fixed freq. and shift in resonance frequency



- Tuning the system

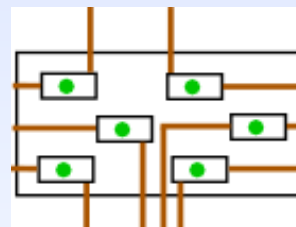
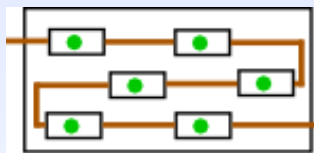
- Larger gap improves sensitivity for high viscosity samples.
- B_0 and B_1 can be adjusted to optimize the measurement.



HTR – Challenges and the Future

- Review of goals
 - Multi sample technique that is scalable.
 - Small sample size ($\sim 300 \mu\text{L}$).
 - Ability to measure η and η^* , G^* across broad range (3-4 decades).
- Short term hurdles
 - Improve amplitude and phase sensitivity with bi-colored disk and new image analysis algorithm.
 - Reduce stiction/friction with new Couette cells, improving bearing design.
 - Measure the complex viscosity of a viscoelastic standard.
- Next device, where we would like to go
 - Further idea of array of oscillators but scale down to the $\sim 300 \mu\text{L}$ goal.
 - Use milli-fluidic technology, especially our rapid templating technique.

Milli-fluidic rheometer
for gradient flows



Milli-fluidic rheometer
for discrete samples

Rapid prototyping of fluidic devices for polymer formulations

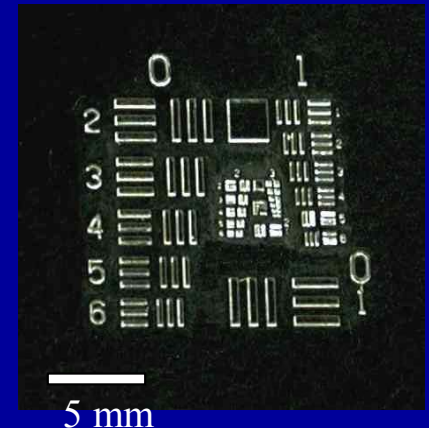
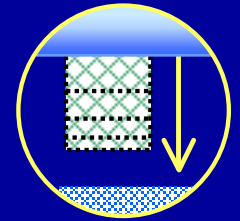


João T. Cabral, Polymers Division, NIST

Outline



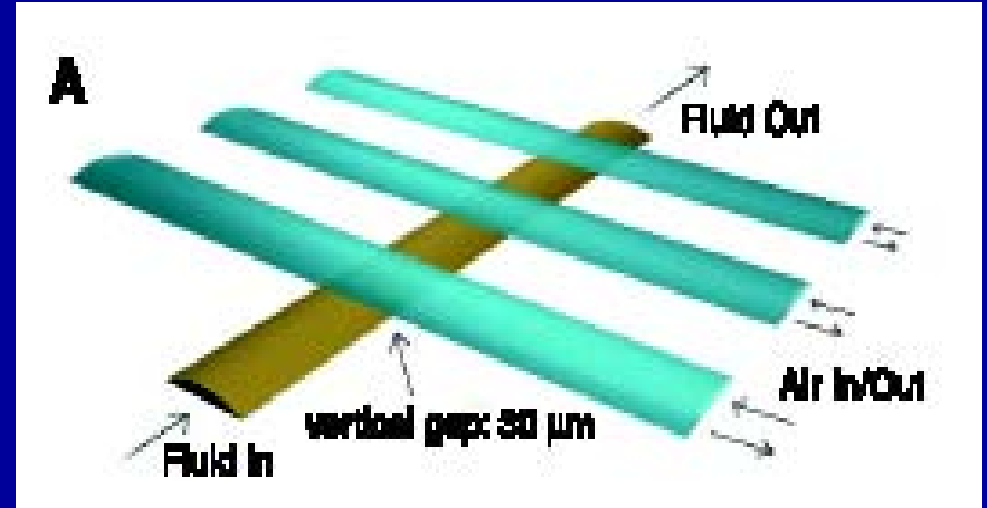
- Microfluidics & developments
- Fabrication overview
- Millifluidics and polymer formulations
- Novel rapid prototyping
 - Frontal photopolymerization
 - Open & Closed-faced configurations
 - Control of vertical and lateral dimensions
 - Devices
- Conclusions



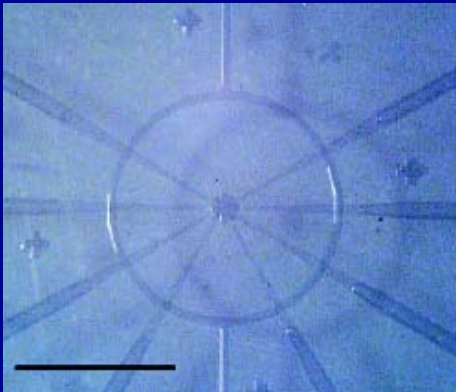
Microfluidics developments



- Valves
- Pumps
- Mixers (passive and active)
- Flow control
- Surfaces & Instabilities
- Integration



(Quake)

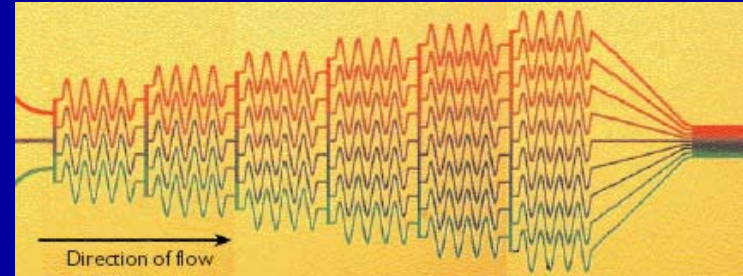


types: pneumatic, liquid, magnetic, hydrogel, optical.
elastomer: complete sealing, low actuation forces, spatial density.
pumps: peristaltic, rotary, capillary.

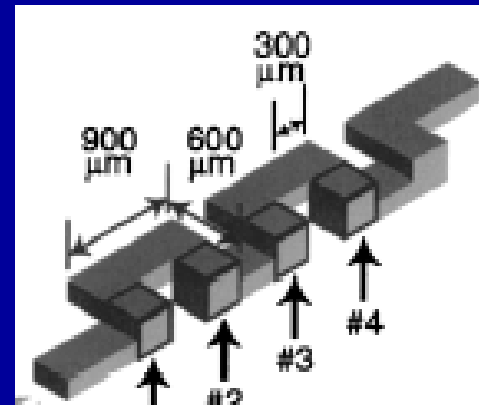
Microfluidics developments



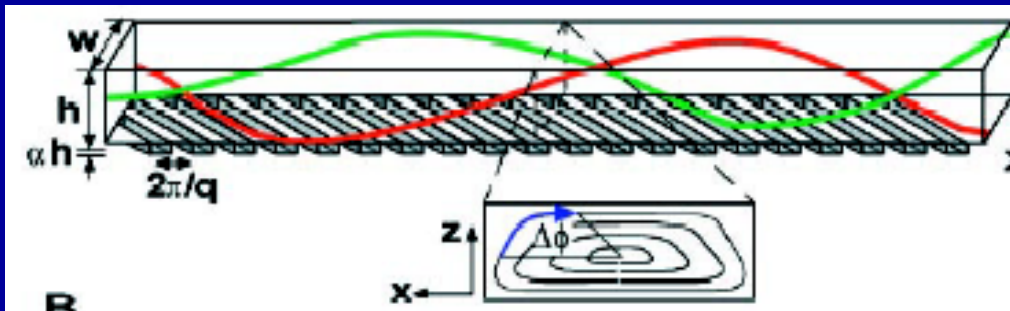
- Valves
- Pumps
- Mixers (passive and active)
- Flow control
- Surfaces & Instabilities
- Integration



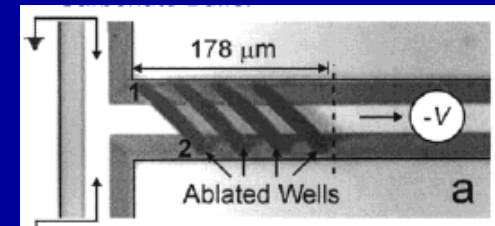
(Whitesides)



(Beebe)



(Whitesides, Adjari, Stone)

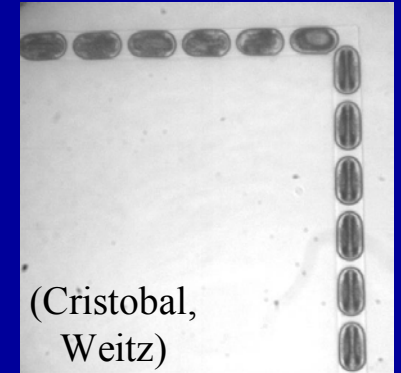
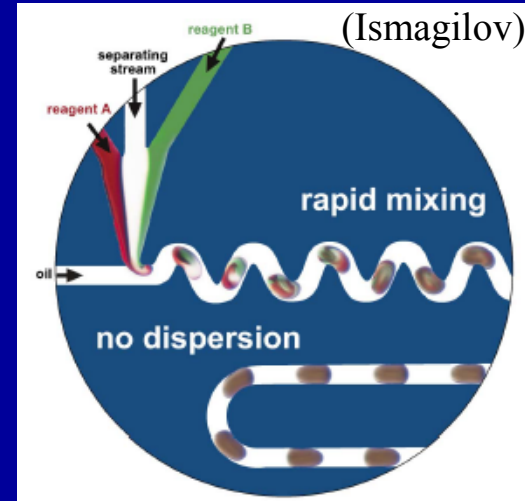


(Locascio)

Microfluidics developments

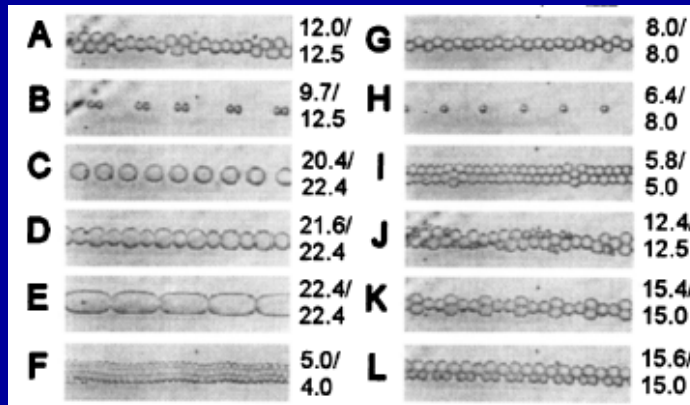


- Valves
- Pumps
- Mixers (passive and active)
- Flow control
- Surfaces & Instabilities
- Integration

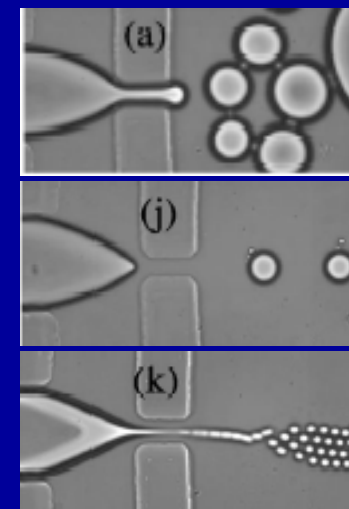


confined mixing inside moving droplets

T-channel



(Quake)



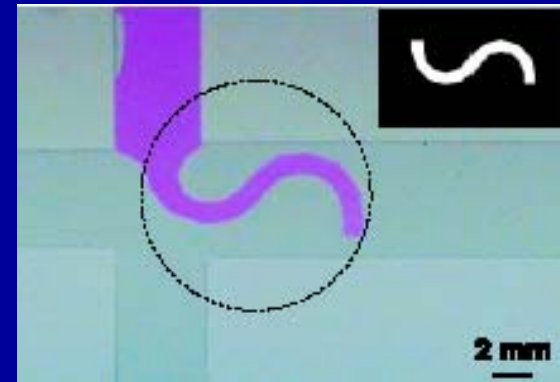
flow
focusing

(Stone)

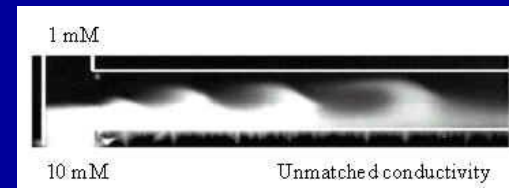
Microfluidics developments



- Valves
- Pumps
- Mixers (passive and active)
- Flow control
- Surfaces & Instabilities
- Integration



(Beebe)

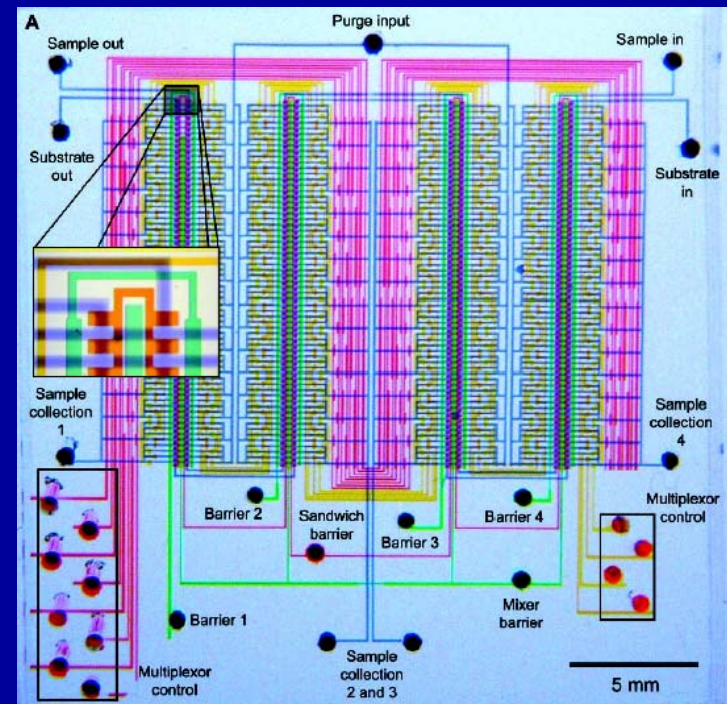


(Santiago)

Microfluidics developments



- Valves
- Pumps
- Mixers (passive and active)
- Flow control
- Surfaces & Instabilities
- Integration

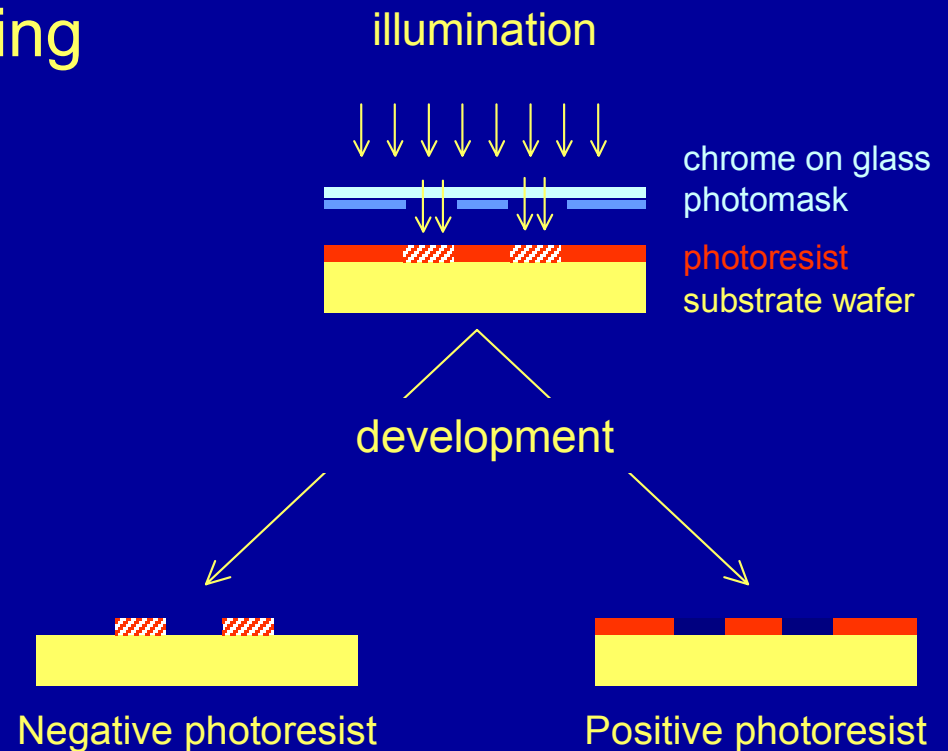


(Quake)

Device fabrication



- Photolithography (UV, X-ray, e-beam)
- Laser ablation
- Injection molding, Embossing
- Printing (solid object)
- Micromachining & MEMS
- Soft lithography



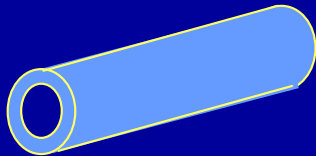
Polymer formulation devices



Fluidic devices

- reduction sample volume
- reduction time/cost
- miniaturization/portability
- pumps, valves, in & outlets, seals
- flow control
- transparency / detection

Poiseuille flow



$$Q = \frac{\pi \Delta P}{8 \eta L} R^4$$

(simple viscous flow)

Polymer-specific devices

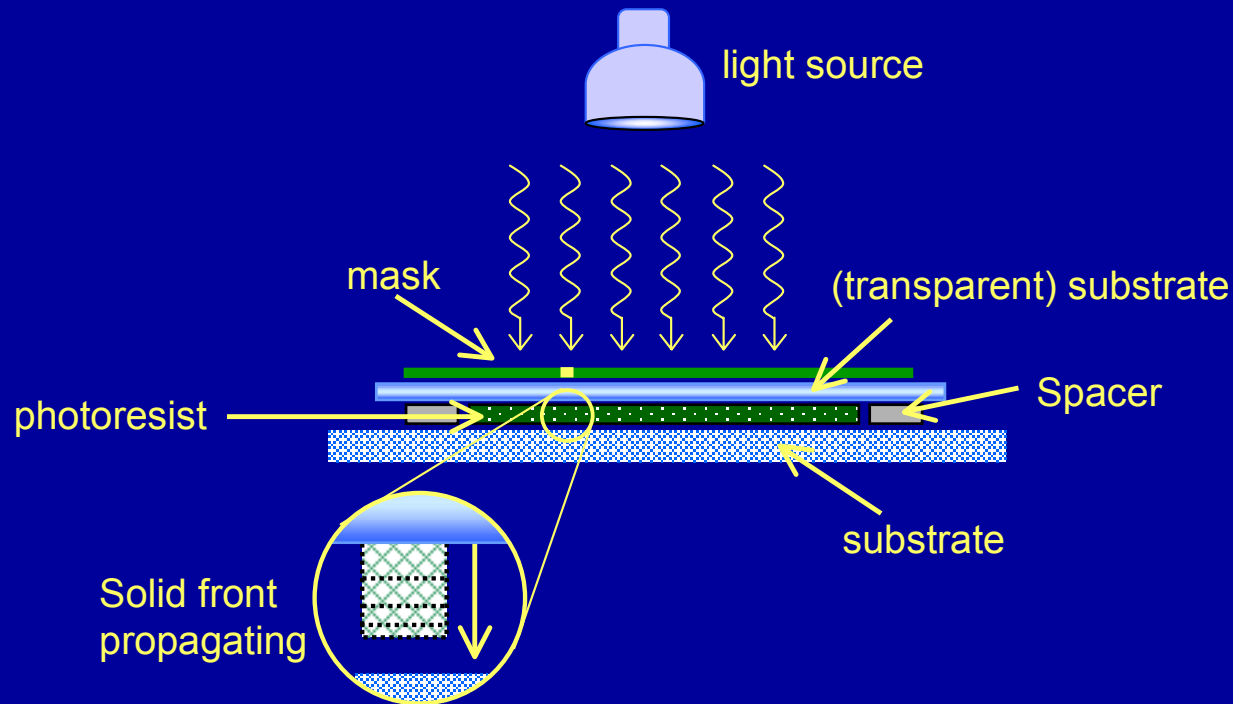
- solvent resistance
- dimensions?
- viscoelasticity?
(elastic turbulence, $Wi \sim 1/L \uparrow$)
- Finite size/ hydrodynamic effects.
- Detection / analysis: LS & OM

millifluidics

Rapid prototyping

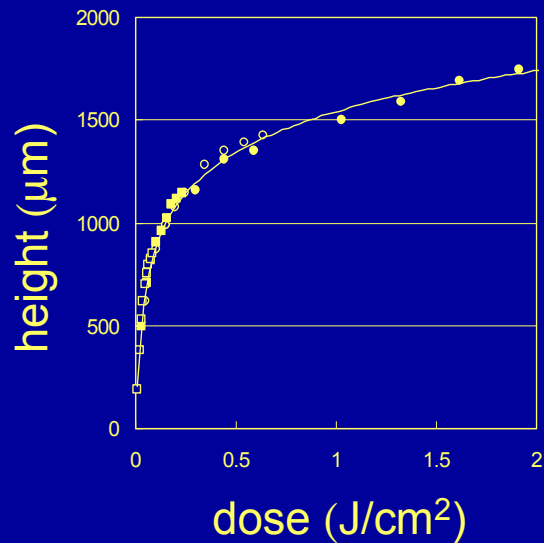
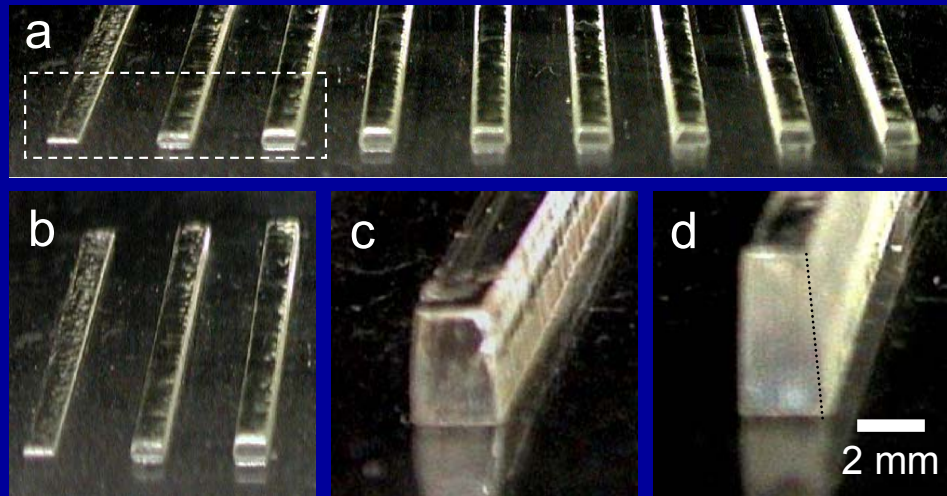
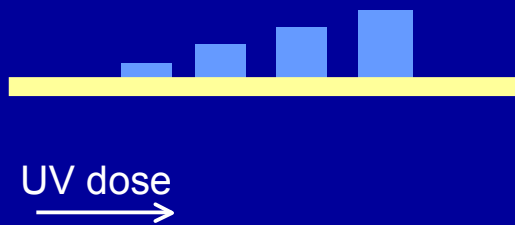


Contact photolithography



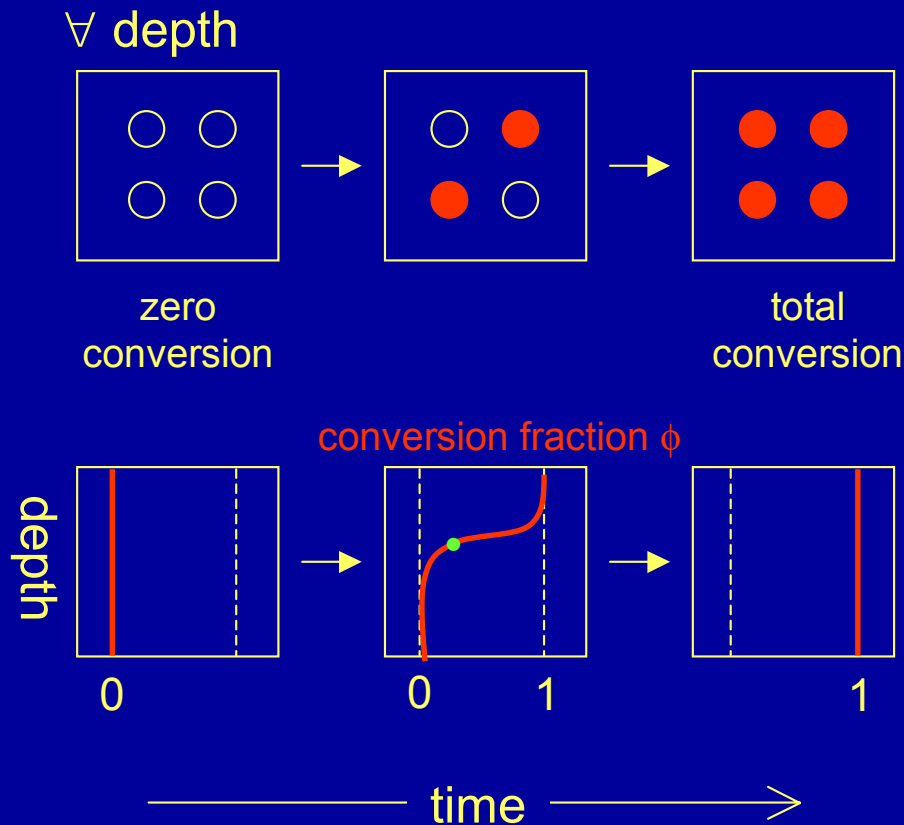
Suitable resists: *multifunctional thiolene-based optical adhesives,
UV 365nm cross-linkable*

Frontal photo-polymerization



Sharp front: accurate height control using dose (or exposure time) \neq spin coating

Model frontal photo-polymerization I



model

$$\begin{cases} \frac{\partial \phi(x,t)}{\partial t} = K[1 - \phi(x,t)]I(x,t) \\ \frac{\partial I(x,t)}{\partial x} = -[\mu_0[1 - \phi(x,t)] + \mu_\infty \phi(x,t)]I(x,t) \\ \phi(x,0) = 0, \quad I(0,t) = 1 \end{cases}$$

ϕ conversion fraction, I light intensity,
 μ_0 and μ_∞ initial and final attenuation coefficients,
 K conversion rate, ϕ_C solid threshold,
 x depth, t time.

Solid threshold $\begin{cases} \phi(x,t) > \phi_C, & \text{solid} \\ \phi(x,t) < \phi_C, & \text{liquid} \end{cases}$

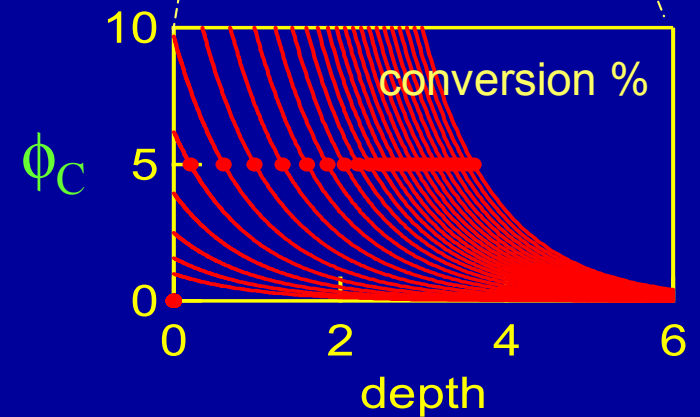
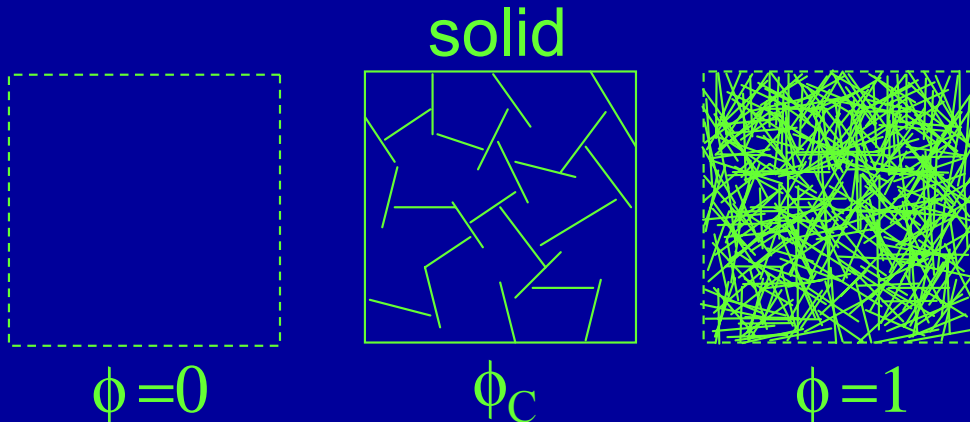
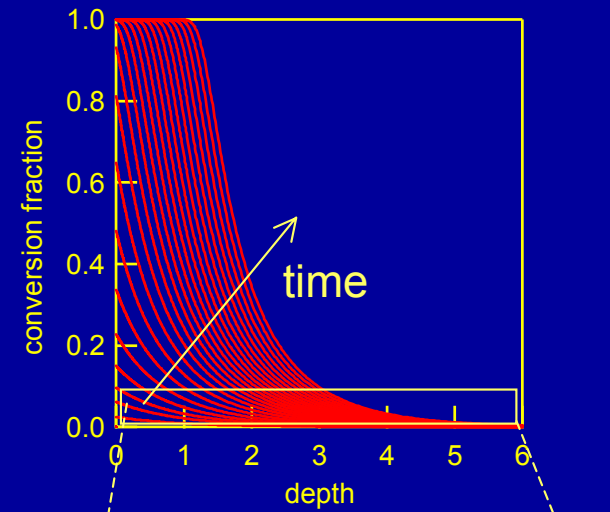
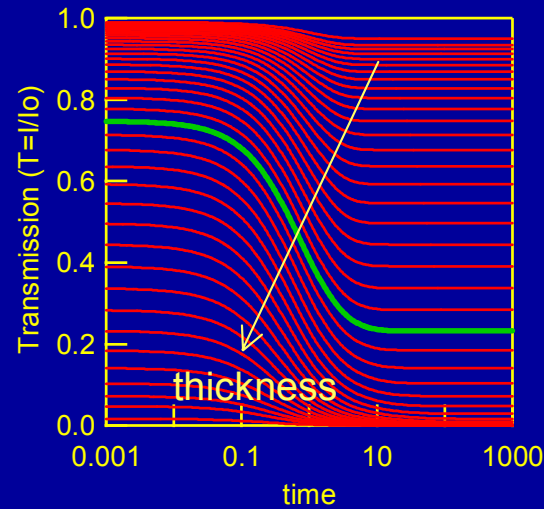
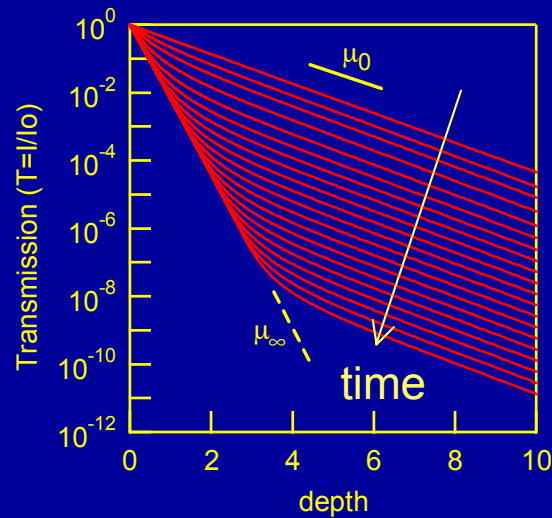
$$\left\{ \begin{array}{ll} \mu_0 > \mu_\infty (=0) & \text{log-log (linear)} \\ \mu_0 = \mu_\infty & \text{log} \\ \mu_0 < \mu_\infty & \text{log-log} \end{array} \right\} \text{fronts!}$$

Considerable attenuation, negligible mass transfer

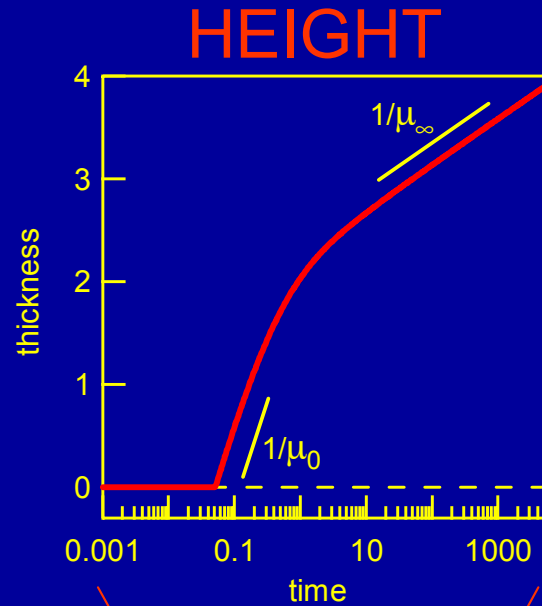
Model frontal photo-polymerization II



partial photo-“darkening” ($\mu_{\infty} > \mu_0$)

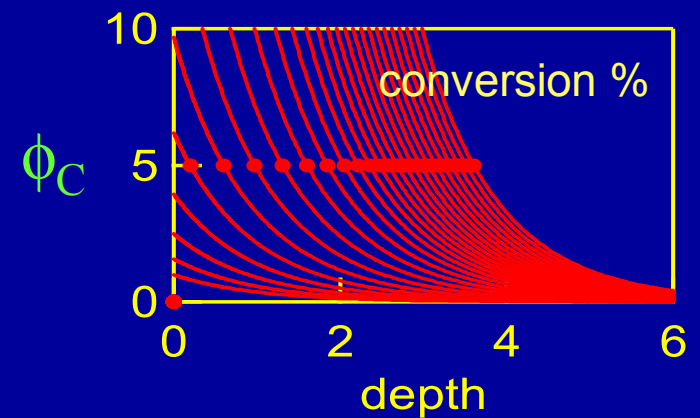
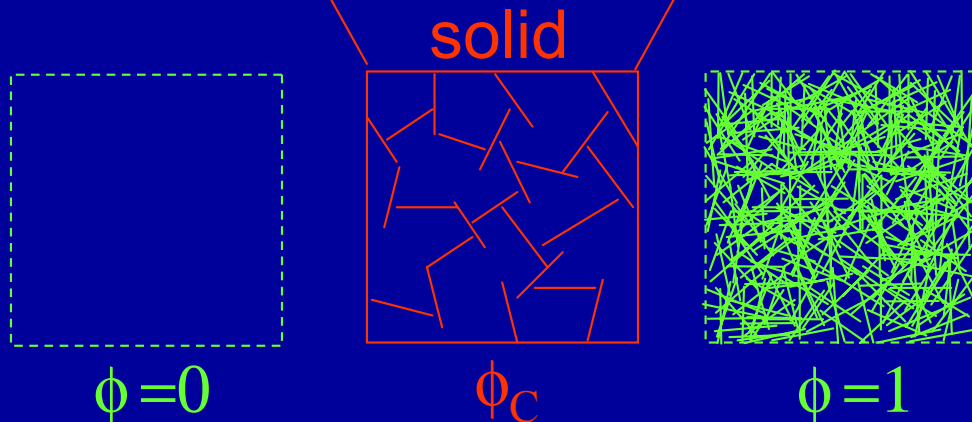


Model frontal photo-polymerization III

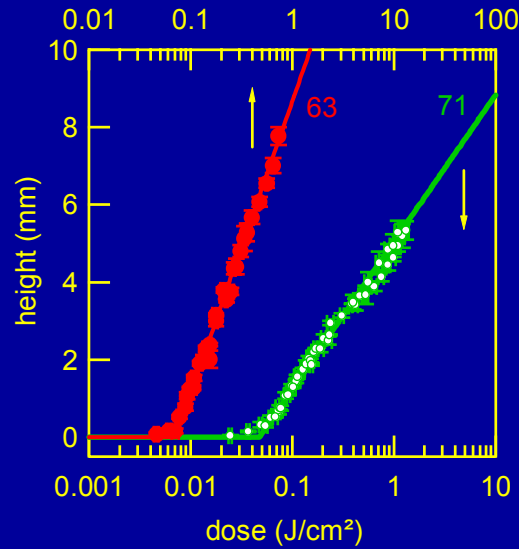


$$height = \frac{\ln(t/\tau)}{\bar{\mu}}$$

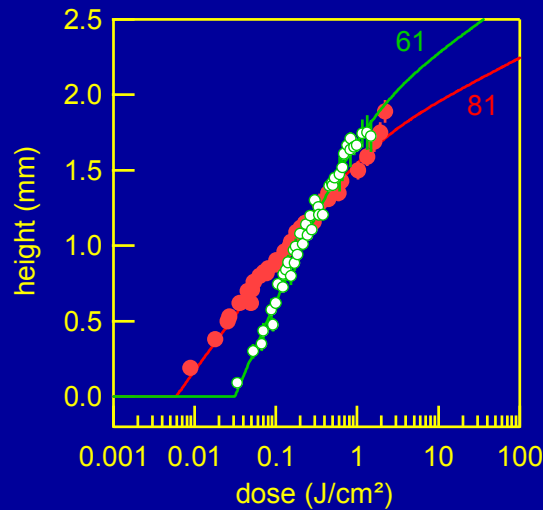
$$induction\ time \equiv \frac{\ln[1/(1-\phi_C)]}{K}$$



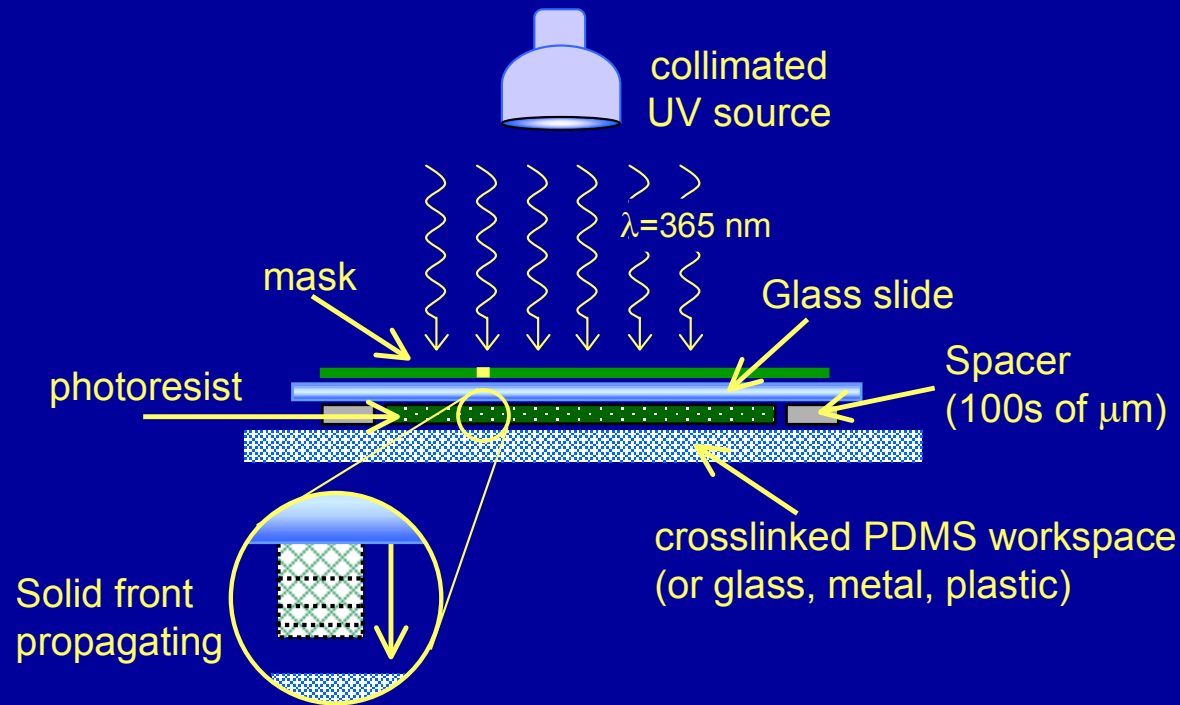
Resist choice – data



Control of vertical dimensions



Rapid prototyping



1. pre-cure

UV exposure for 10s
of seconds



2. wash

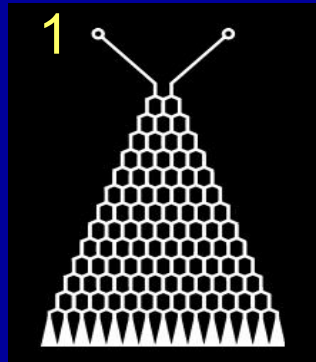
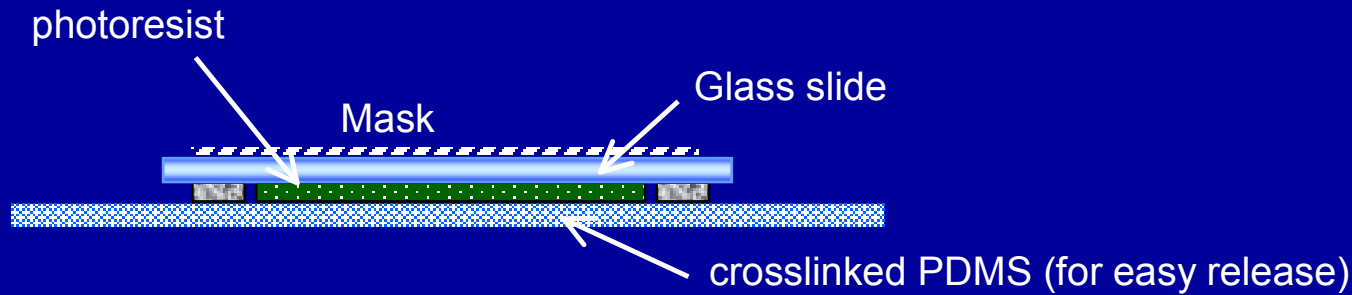
remove uncrosslinked
adhesive (ethanol/acetone)



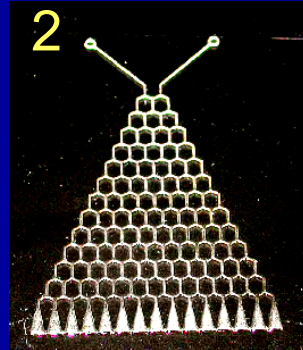
3. post-cure

UV exposure and
heat (aging) cure

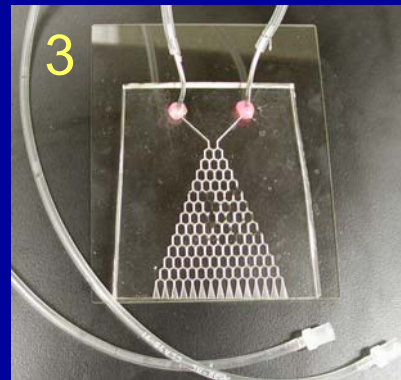
Open-face configuration



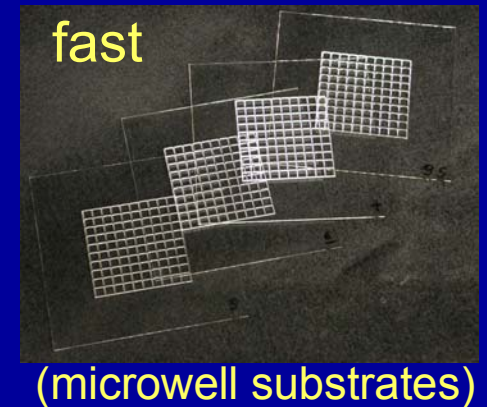
mask



master
(glass/adhesive mold)

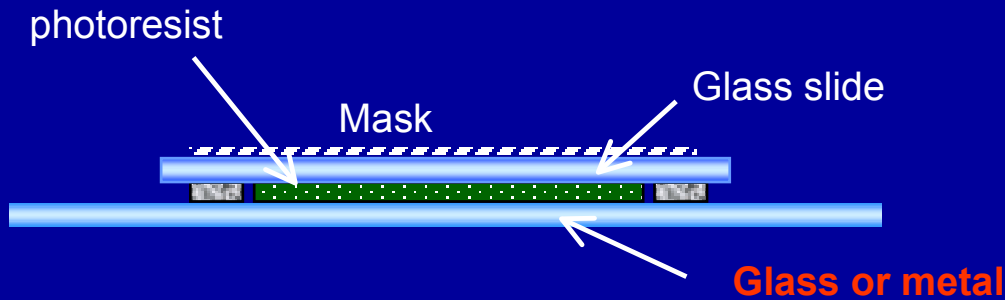


PDMS replica
(sealed against glass)

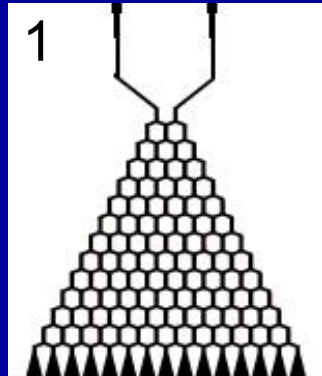


- fast replication
- convenient interfaces with tubing/pumps
- suitable for aqueous applications **BUT incompatible with most solvents.**

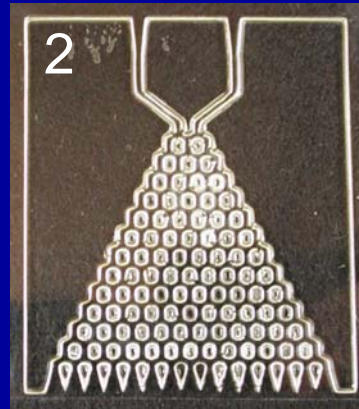
Closed-face configuration



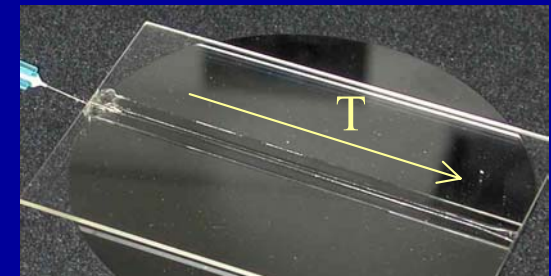
resist wash: 200-1000 cps



UV mask



Glass/adhesive/glass



Glass/adhesive/silicon

Devices entirely fabricated of crosslinked polymer matrix (sealed against glass/metal)

- optical transparency
- resistance to toluene, methanol, hexane, MEK...
- glass/metal seal

Lateral dimensions



800 μm

Channel width

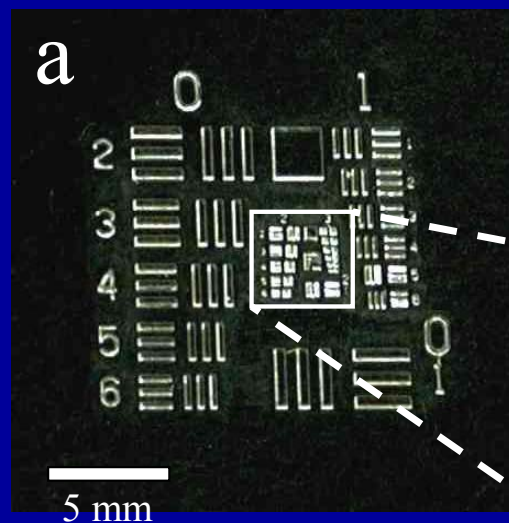
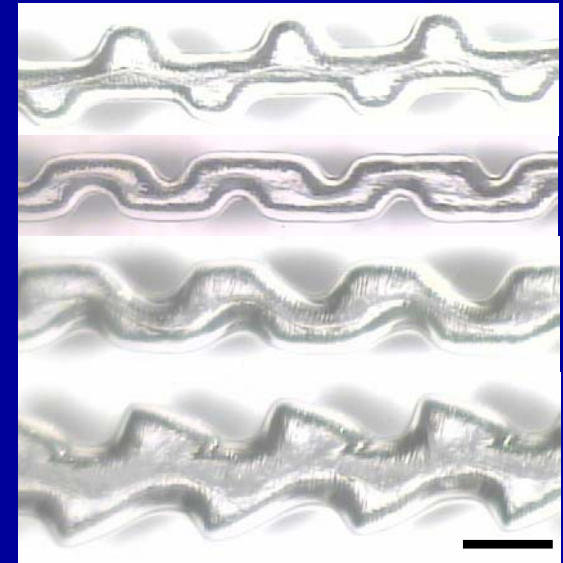


hundreds μm & above

defined by:

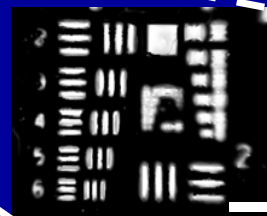
- Printing resolution on mask
- Light source collimation (illumination distance)

Topographically patterned channels



USAF 1951

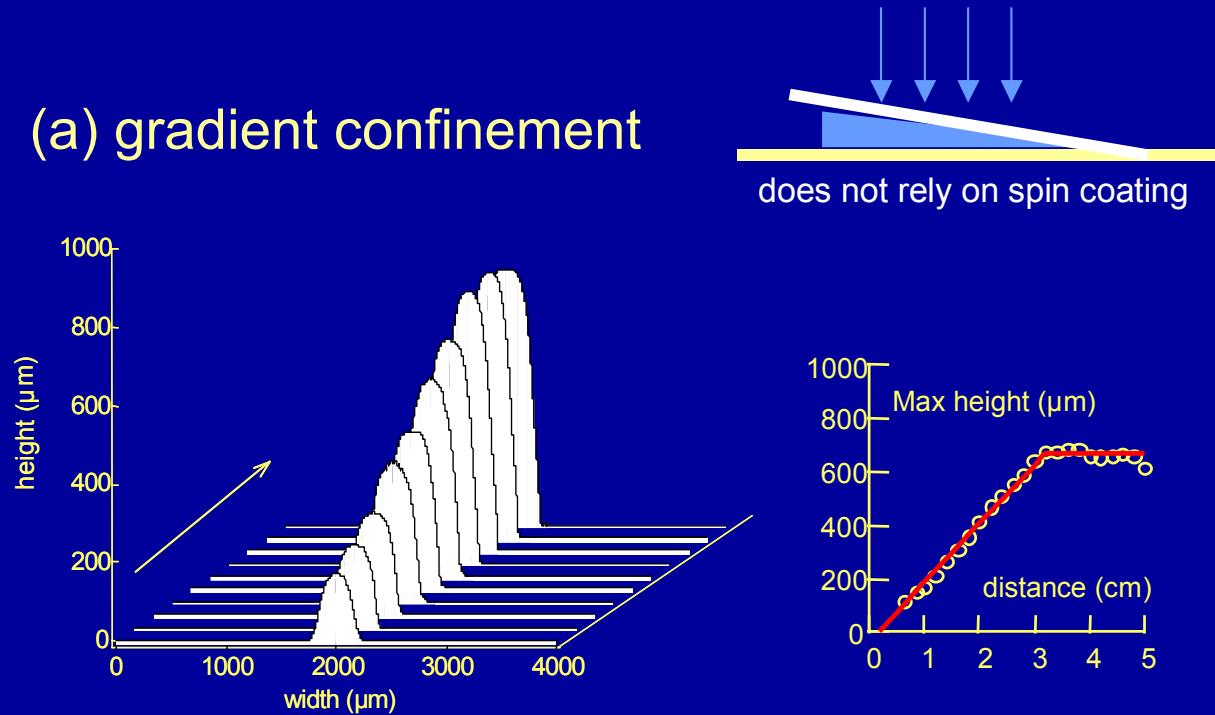
($n=17$, group +2, element 6),
70 μm wide lines



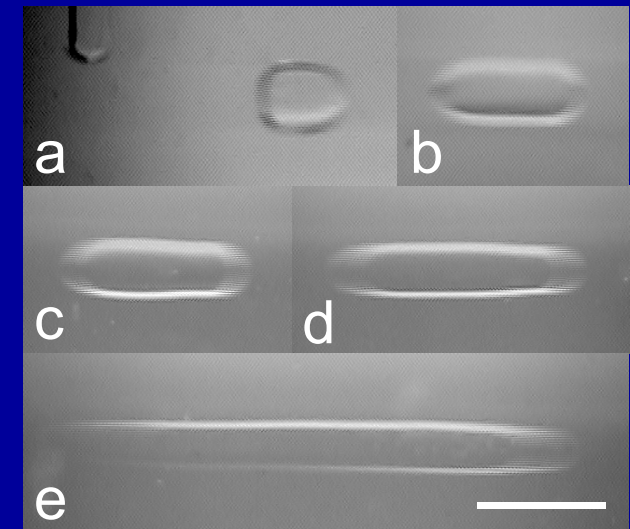
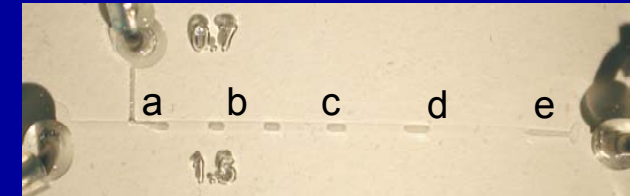
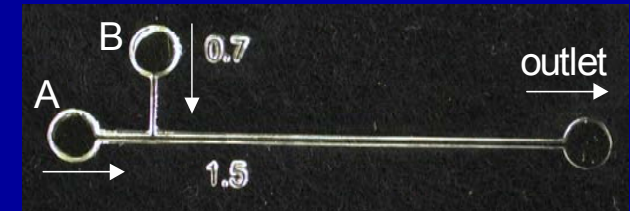
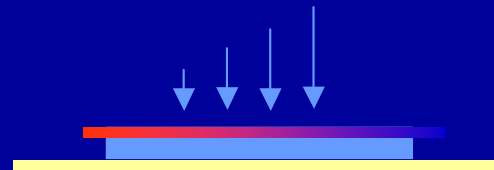
Height gradients



(a) gradient confinement

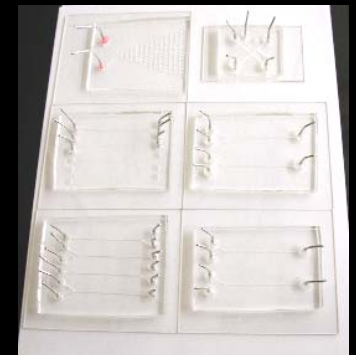
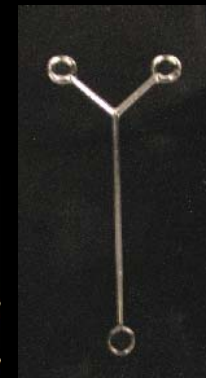
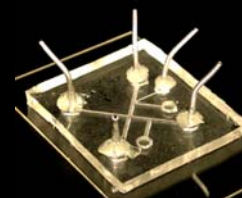
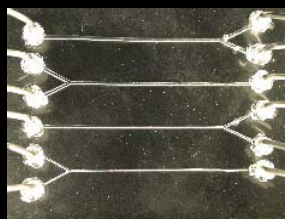
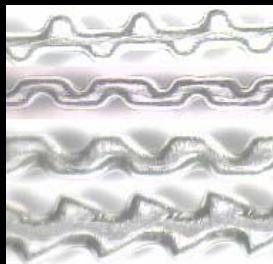
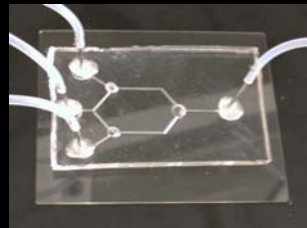
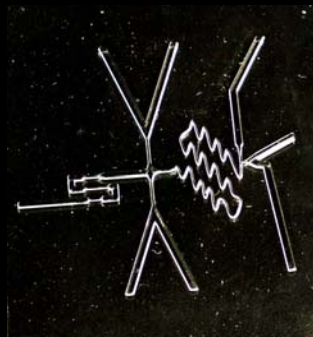
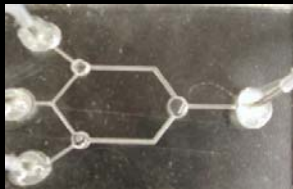
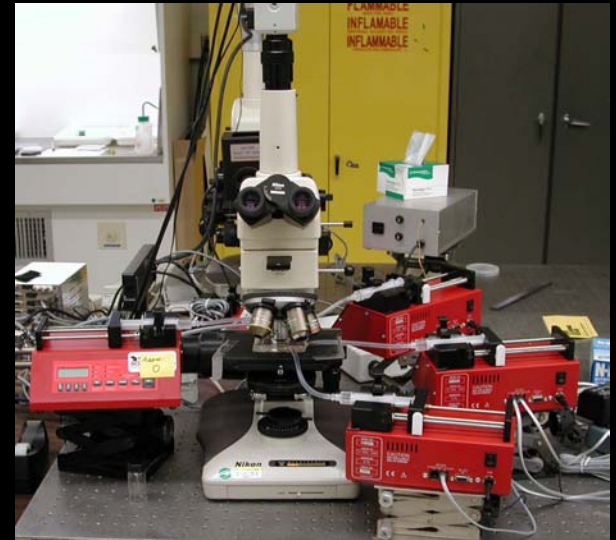
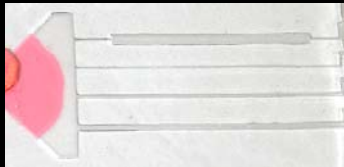
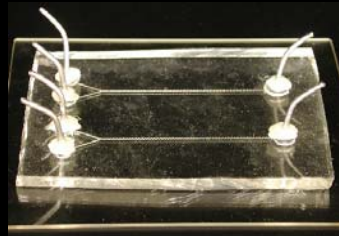
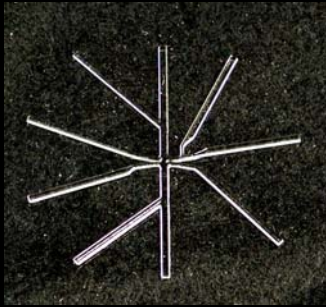
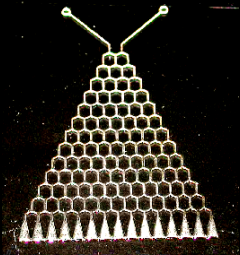


(b) gradient optical density mask



extensional flow gradient.

Devices

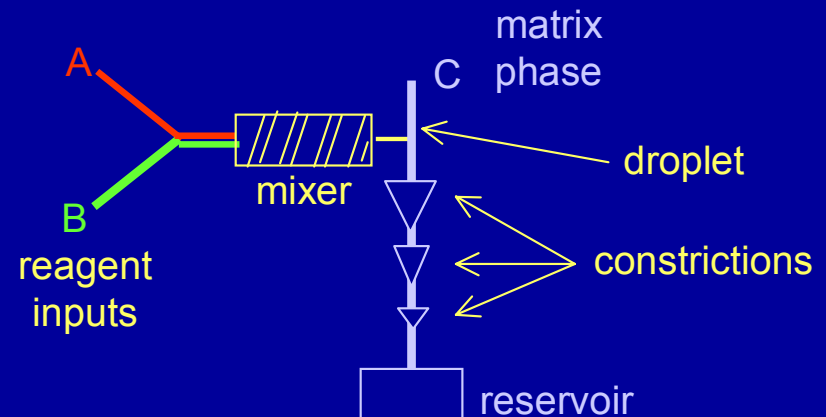
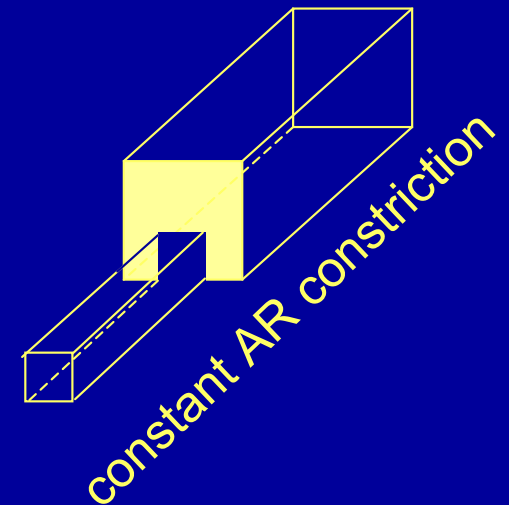
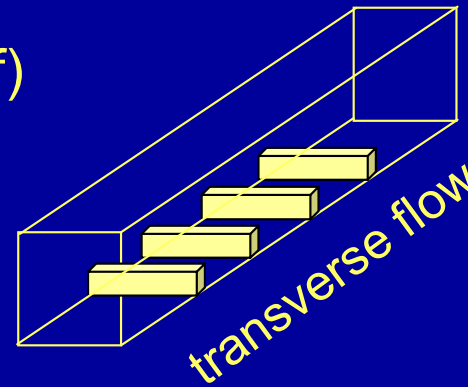


Conclusions



Novel Rapid Prototyping method

- Solvent resistant devices
- sealed (against glass, metal, itself)
- coupled (connectors, pumps)
- transparent (detection)
- high pressure
- rapid fabrication (prototype iteration)
- pseudo-3D, multilayer patterning



Acknowledgments



- Jack Douglas, Steve Hudson, Vladimir Entov (model)
- Chris Harrison and Steve Hudson (fabrication)
- Alamgir Karim and Eric Amis

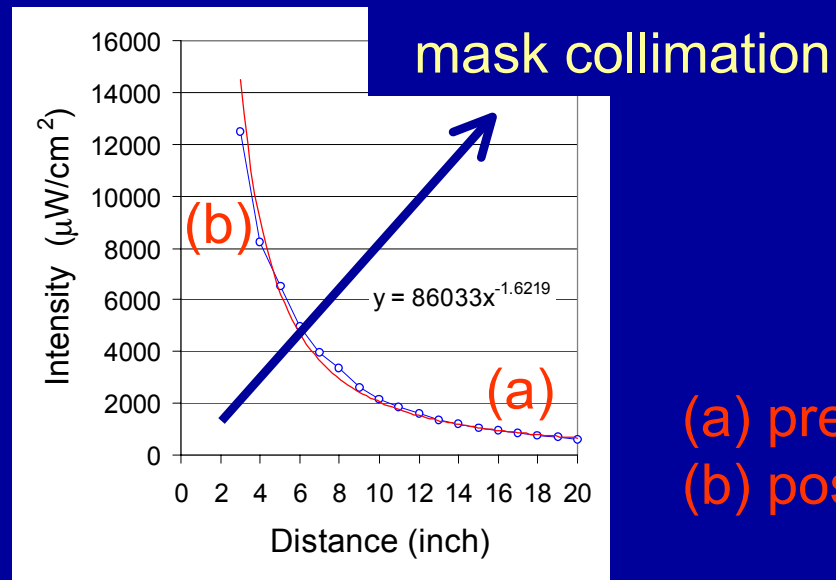
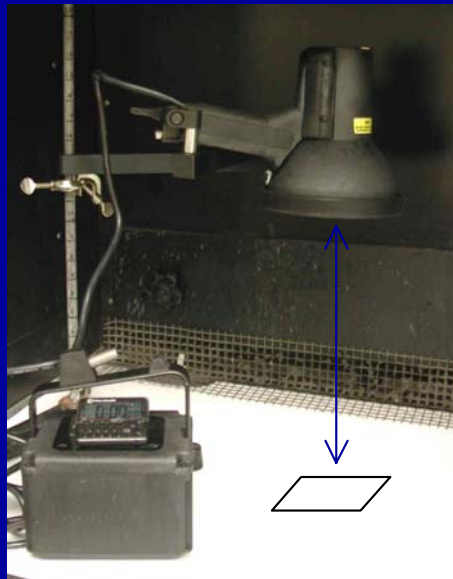
Light sources



collimated flood
illumination system

low-cost
flood lamp

100W
mercury
 $\lambda \sim 365\text{nm}$



Microfluidics developments



$Re = \rho \cdot \text{velocity} \cdot \text{length} / \text{viscosity}$.
dimensionless
number which
relates inertial
forces to viscous
forces

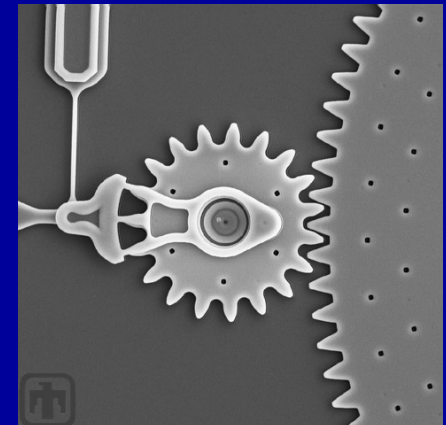
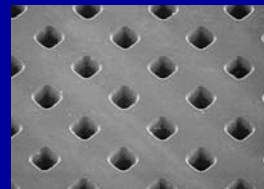
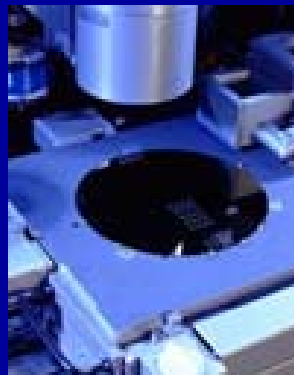
$Re = VL/\nu$, where V is velocity,
 L is characteristic size and ν is
kinematic viscosity of the
fluid.

The degree of nonlinearity in
the mechanical properties is
expressed by the Weissenberg
number, $Wi = V \lambda / L$,
which is a product of
characteristic rate of
deformation and the relaxation
time, λ .

Device fabrication



- Photolithography (UV, X-ray, e-beam)
- Laser ablation
- Injection molding, Embossing
- Printing (solid object)
- Micromachining & MEMS
- Soft lithography



Scattering Methods Applied to High Throughput Materials Research

Alexander I. Norman, João T. Cabral,
Derek L. Ho*, J. Keith Harris#,
Alamgir Karim, and Eric J. Amis



*- NIST Center for Neutron Research.

#- Dow Chemicals, Midland, MI 48674
and Chemistry Dept., Michigan State
University, East Lansing, MI 48824.

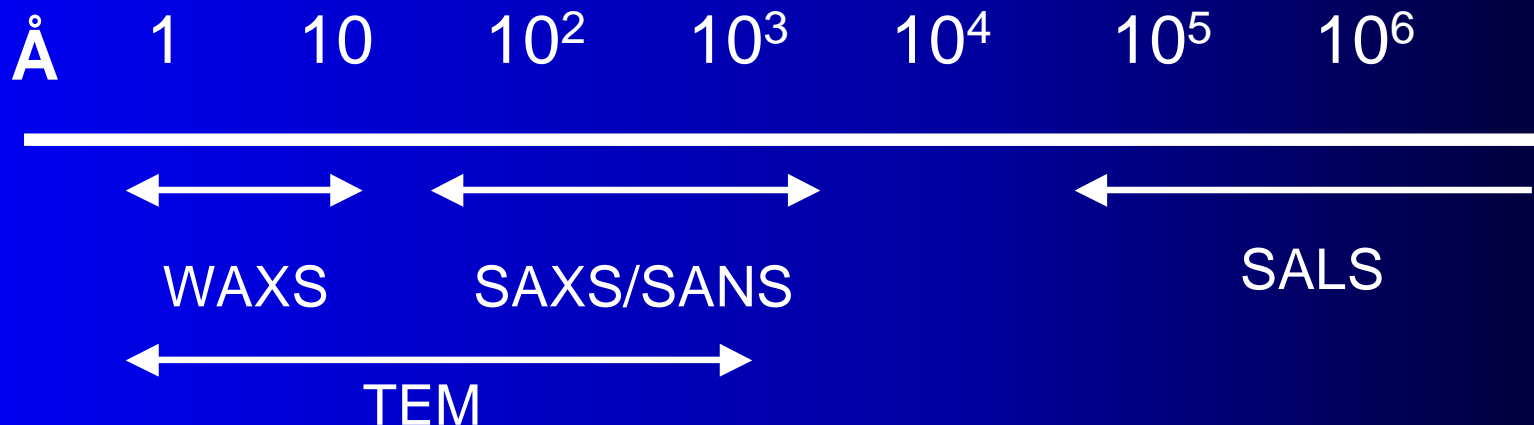
NIST Combinatorial Methods Center



Value of Scattering

- Acquisition times vary from typically a fraction of a second to 10 mins.
- Shows data in reciprocal space, thus allowing systems to be probes at a very short length scale, e.g. sub micron level to a few Å.
- TIME – High throughput techniques considerably reduce the time taken. No need for sample changing, re-alignment etc.
- Non destructive for polymers (exception – protein degradation)

$$10^6 \text{Å} = 1 \mu\text{m}$$





Combi Scattering

Library Samples

Discrete ϕ gradients

- Bulk samples
- Probe 3D structure in real space
- Liquid dispenser

Continuous ϕ gradients

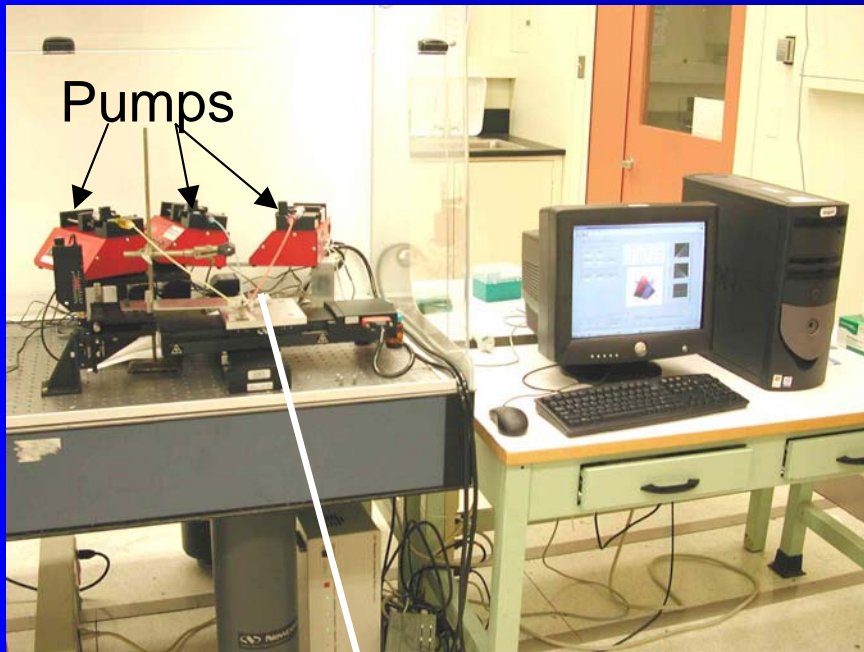
- Limited to thin films
- Probe 2D structure
- Flow coater

Time variant devices

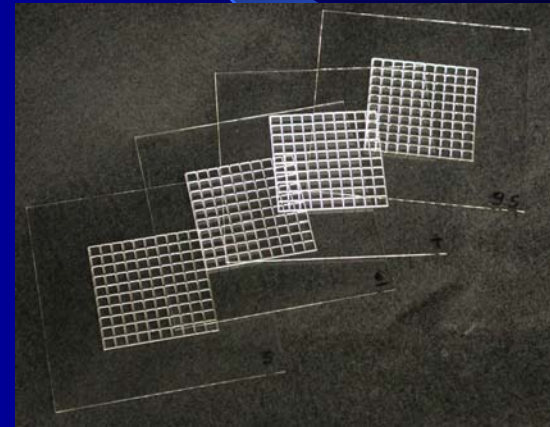
- Multi-component systems
- Monitor structure online as a function of composition
- Microfluidics



Discrete composition gradients



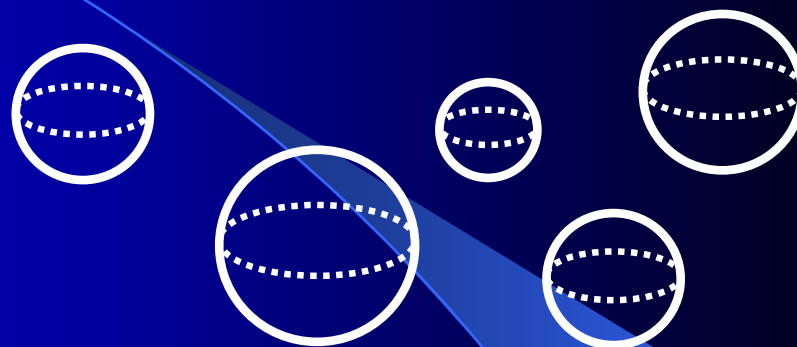
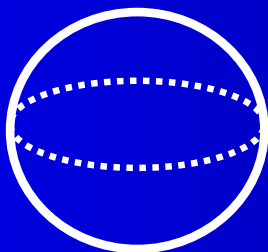
Device on motorized translation stage



Typical devices to produce a discrete composition gradient

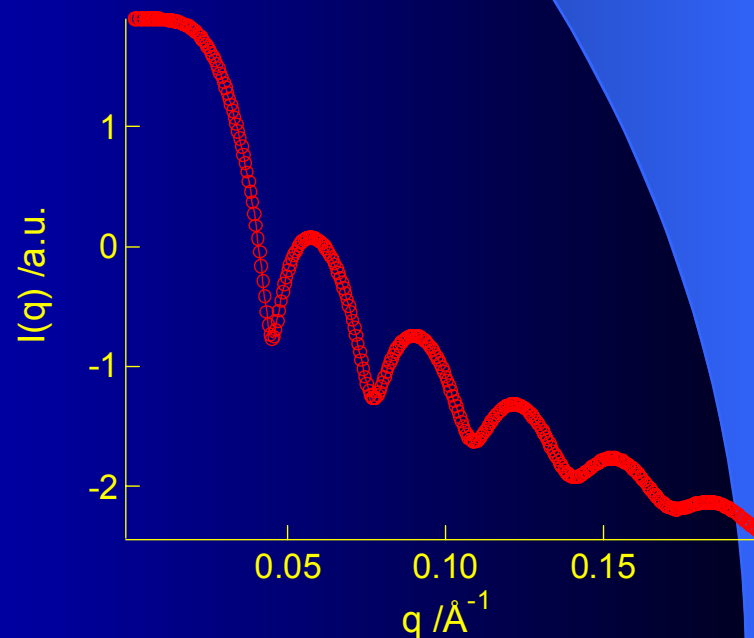
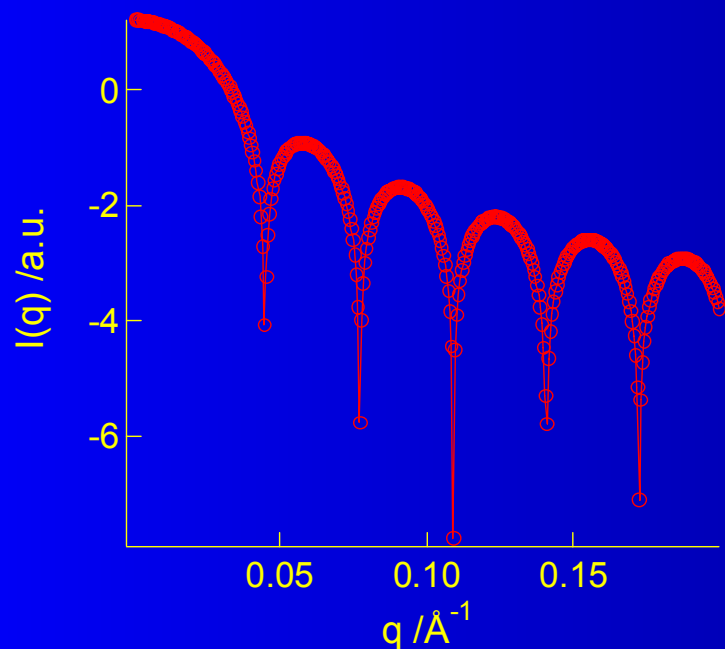


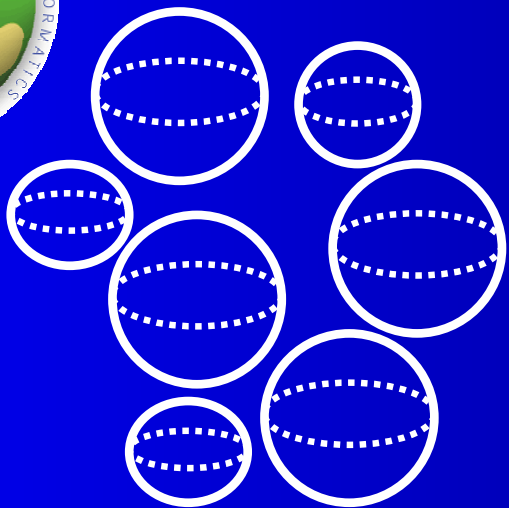
Information obtained



Monodisperse single sphere, no interaction.

Polydisperse (5%) single spheres, no interaction.

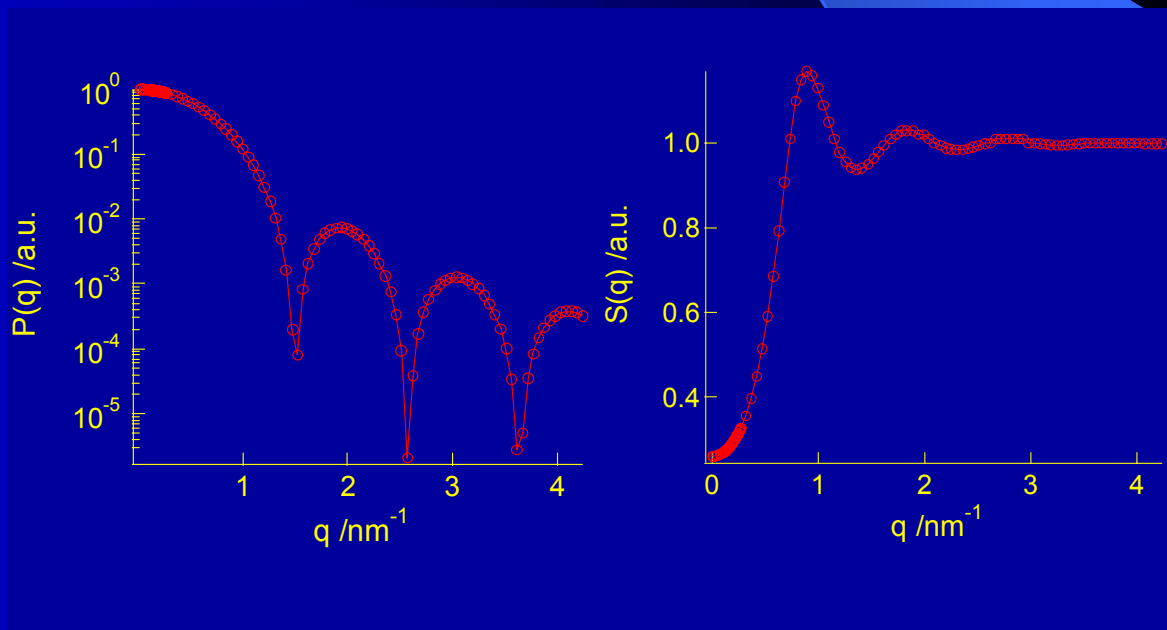
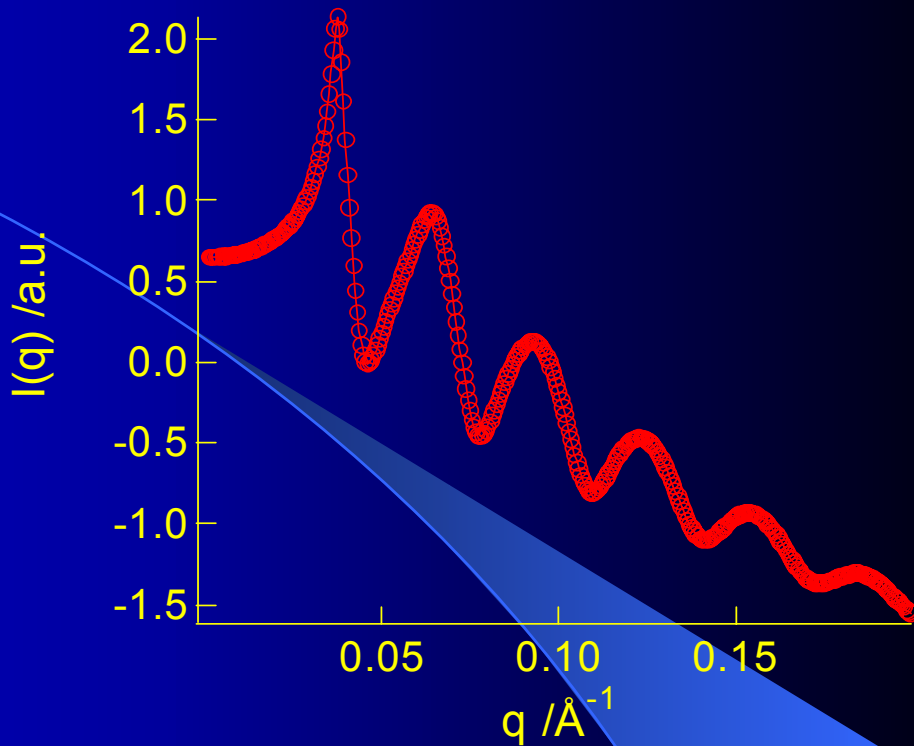




Polydisperse,
interacting spheres

$$P(q) = \left\{ \frac{3[\sin(qR) - qR \cos(qR)]}{(qR)^3} \right\}^2$$

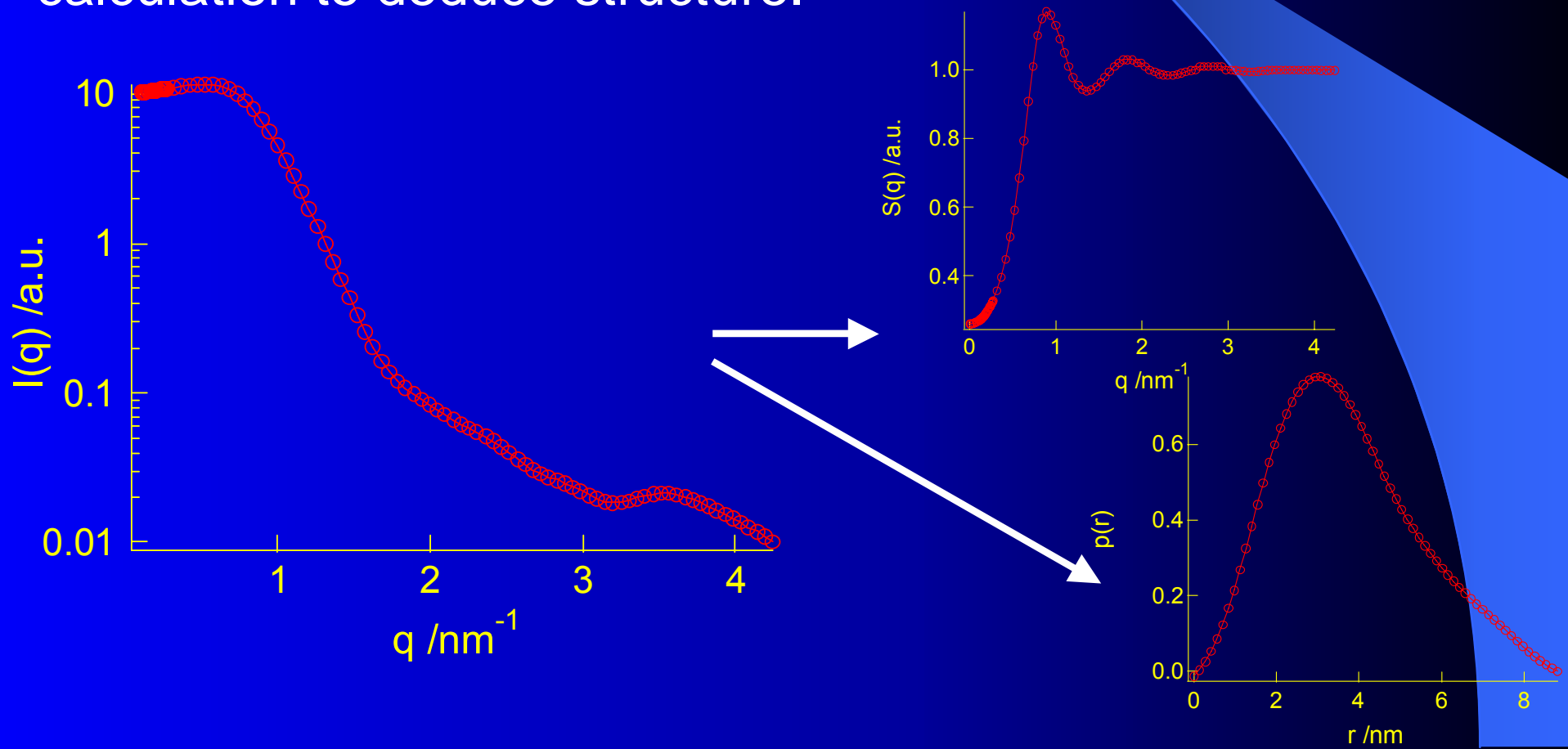
$$S(q) = 1 + 4\pi \frac{N}{V} \int_0^\infty [g(r) - 1] r^2 \frac{\sin(qr)}{qr} dr$$





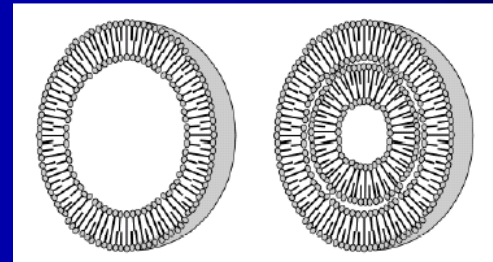
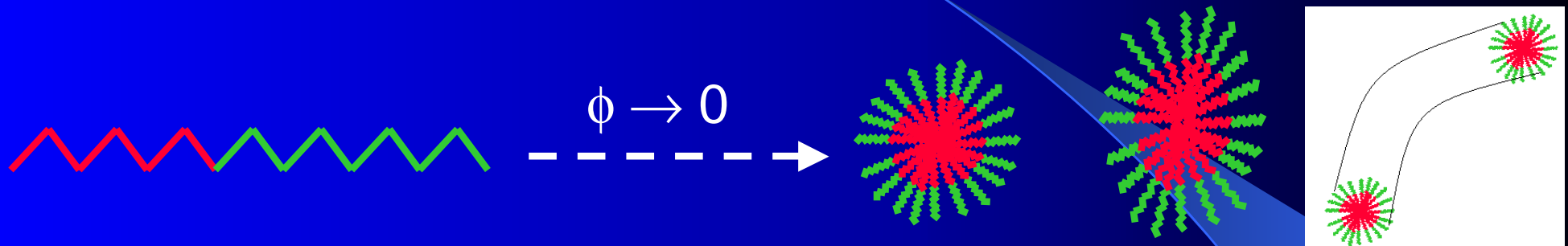
The inverse scattering problem

- Experimentally we observe $I(q)$ and perform the *inverse* calculation to deduce structure.





Model System



Vesicle formation

PBO hydrophobe

PEO head group

$$\phi = \frac{V}{l_c a_0}$$

Hydrophobe volume

CSA of head group

Hydrophobe length



Why use this system?

PEO block – $(-\text{CH}_2\text{CH}_2\text{O}-)_n$

$n = 6 \Rightarrow$ Vesicles

$n = 18 \Rightarrow$ Micelles

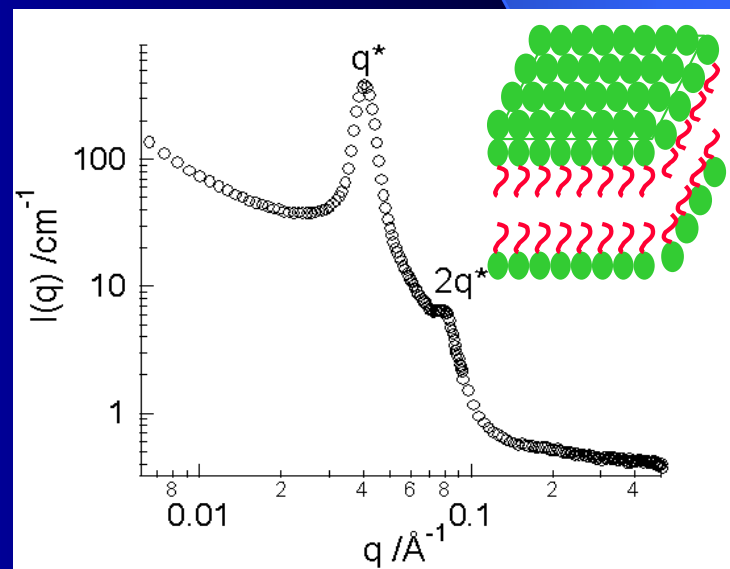
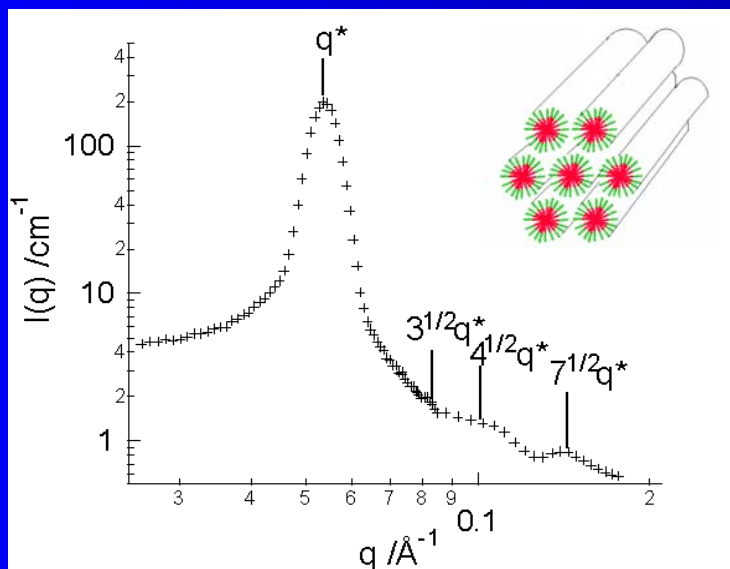
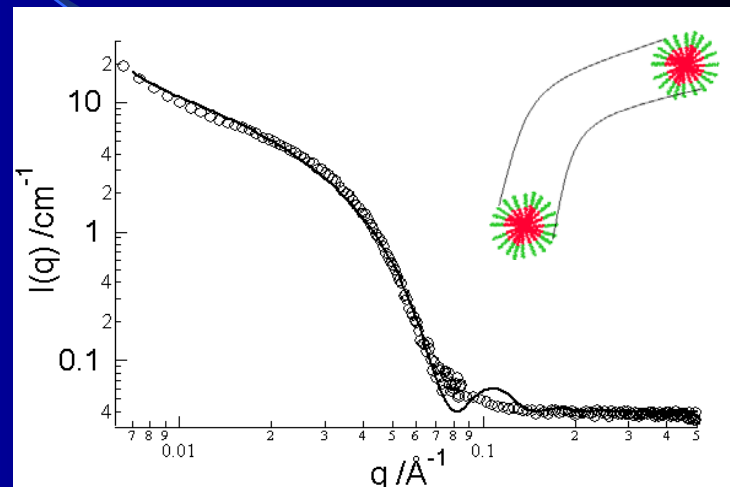
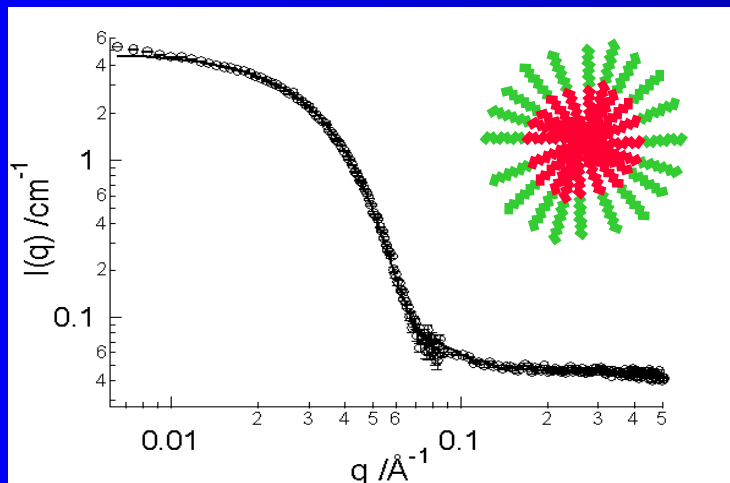
PBO block – $(-\text{CH}(\text{CH}_2\text{CH}_3)\text{CH}_2\text{O}-)_m$

$m = 9-11$

- Variety of structures formed depending on block length.
- Contrast!
- Relevance to industrial applications:
 - Personal Care Products
 - Oil Extraction
 - Drug Delivery
 - Agricultural Applications



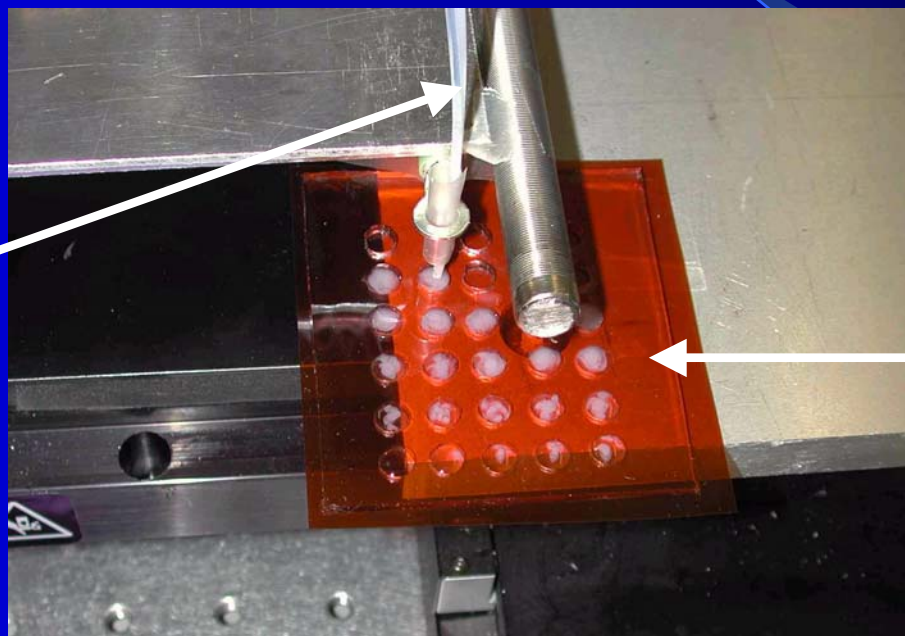
Structure determination by SAS





Combi SAXS / WAXS Study

Stock solution
of 20 wt%
EO(6) BO(11)
in H₂O and
pure H₂O.



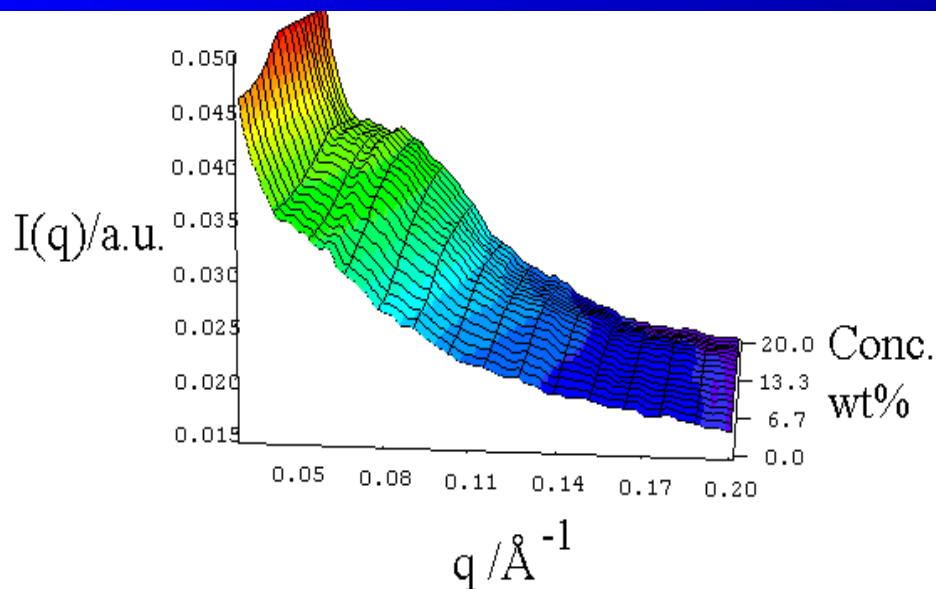
PDMS grid with
Kapton™
windows

Sample cell held vertically in front of x-ray beam and moved externally to collect 25 SAXS/WAXS data sets in less than 1hr.

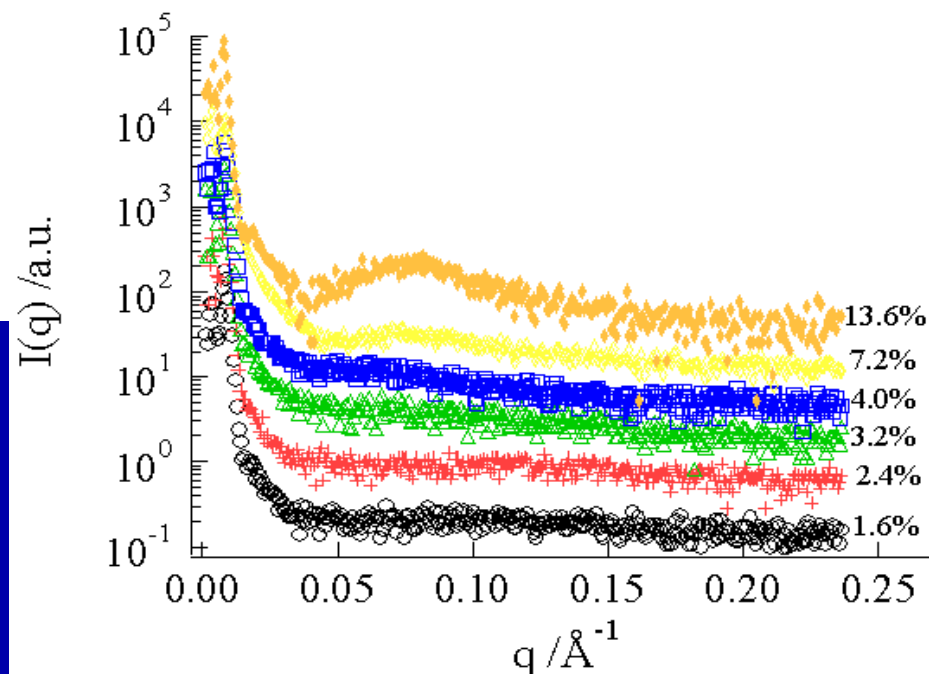
Considerable time reduction over standard methods – no need for changing samples, no re—alignment issues.



Combi library – SAXS

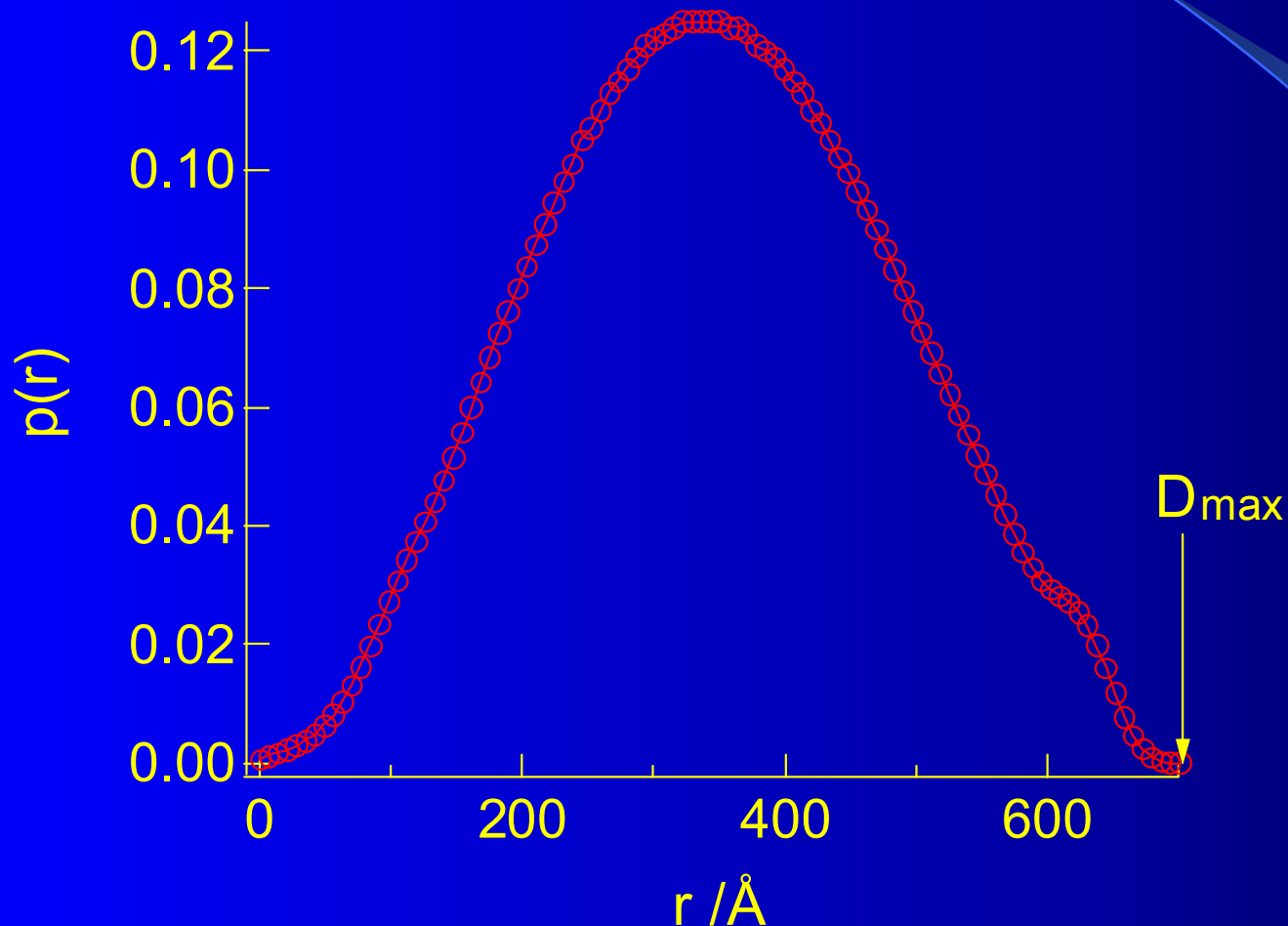


Broad SAXS peak develops (indicative of the lamellar structure within the vesicle) as the concentration increases.





Combi library – SAXS 2

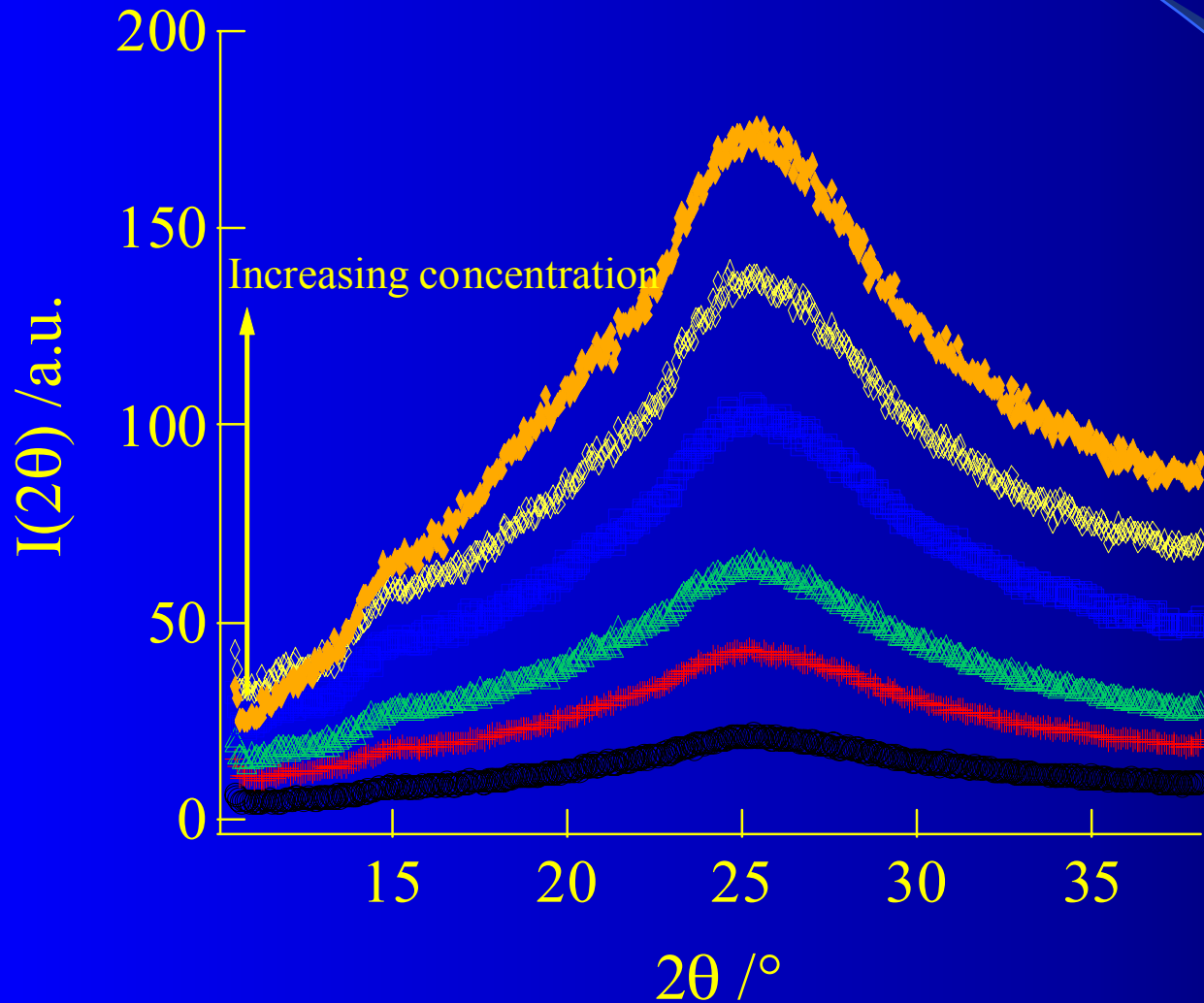


13.6 wt% EO(6)BO(11)

- Spherical $p(r)$ function.
- Larger dimensions than expected for a micelle, implying vesicle structure.
- $D_{\text{max}} = 700 \text{ \AA}$



Combi library – WAXS



No sharp Bragg reflections evident.

No change in the WAXS profile with increasing concentration.

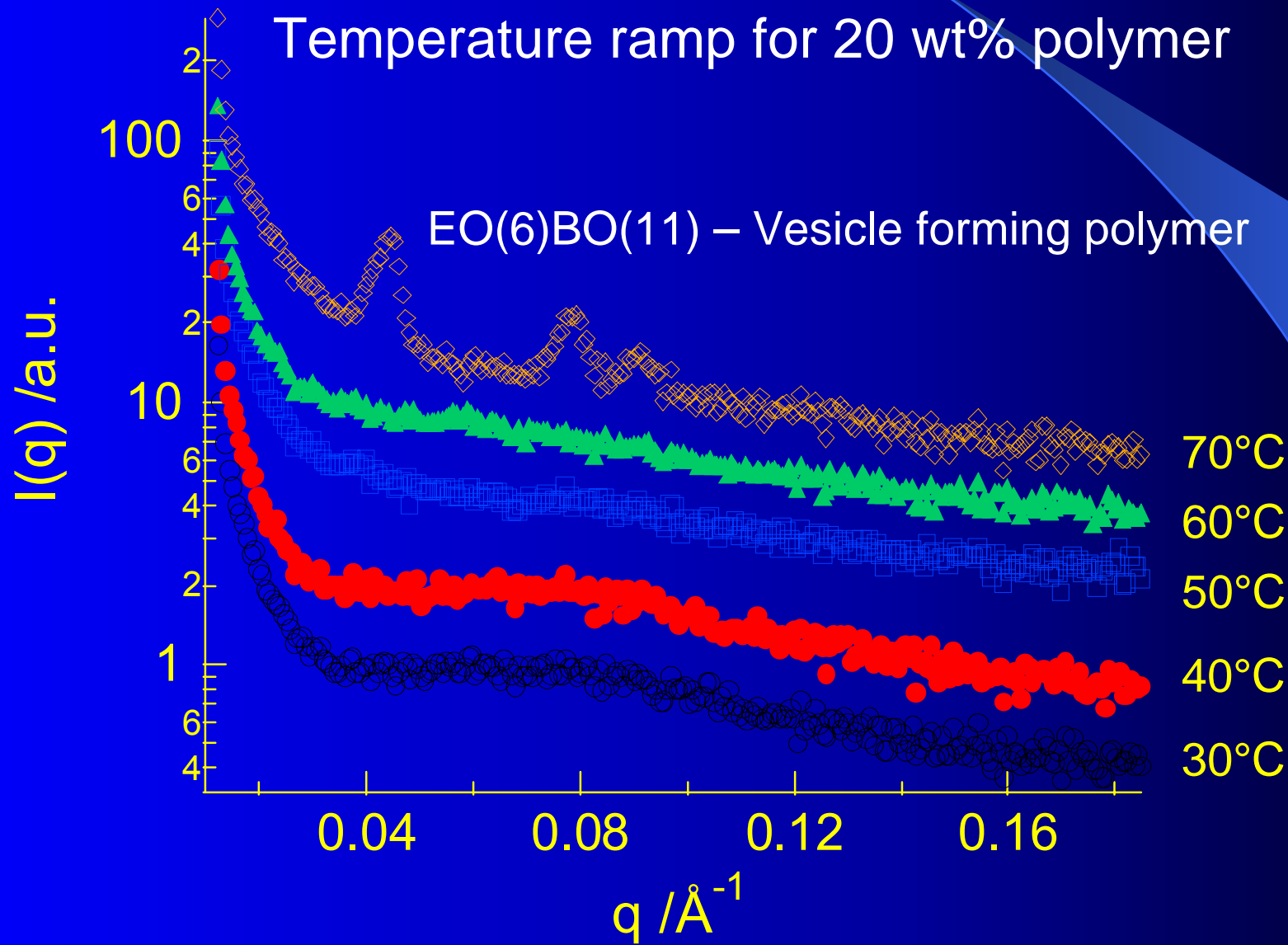
Little or 0% crystallinity in the system.



Effect of temperature

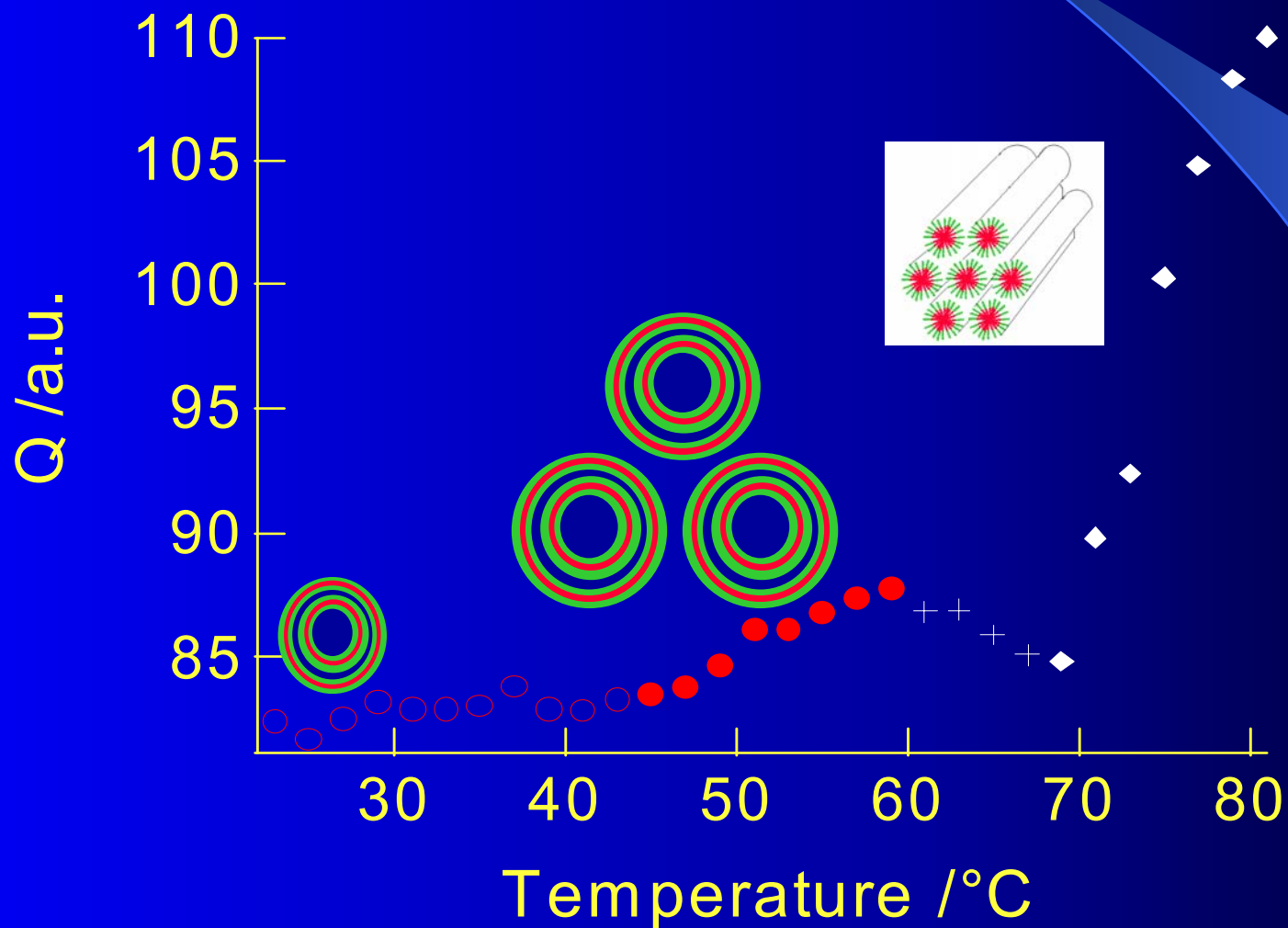
Temperature ramp for 20 wt% polymer

EO(6)BO(11) – Vesicle forming polymer



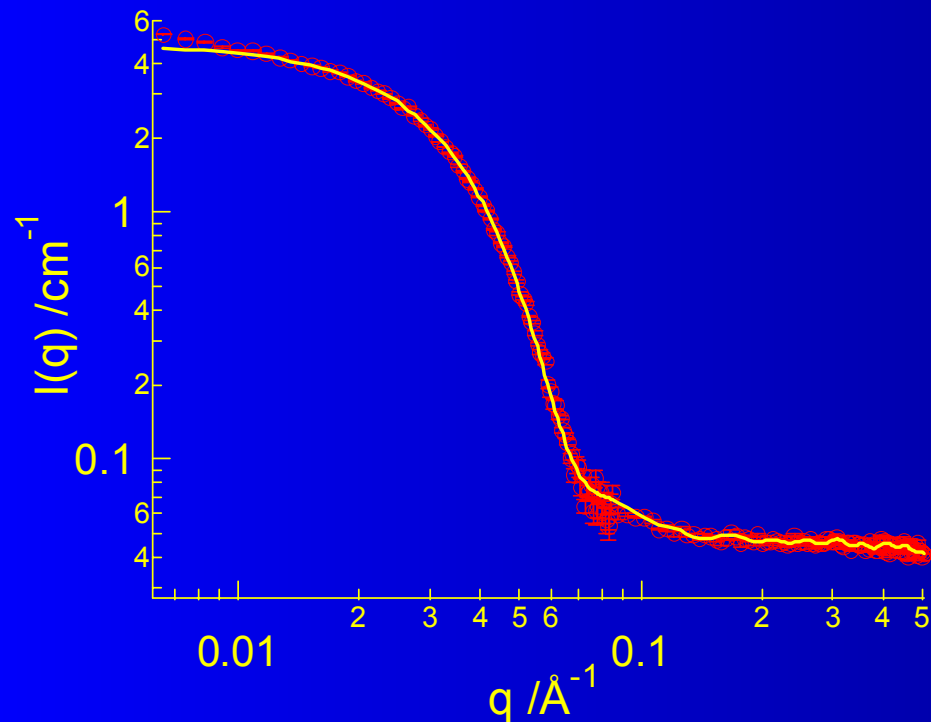


Monitoring SAXS with temperature

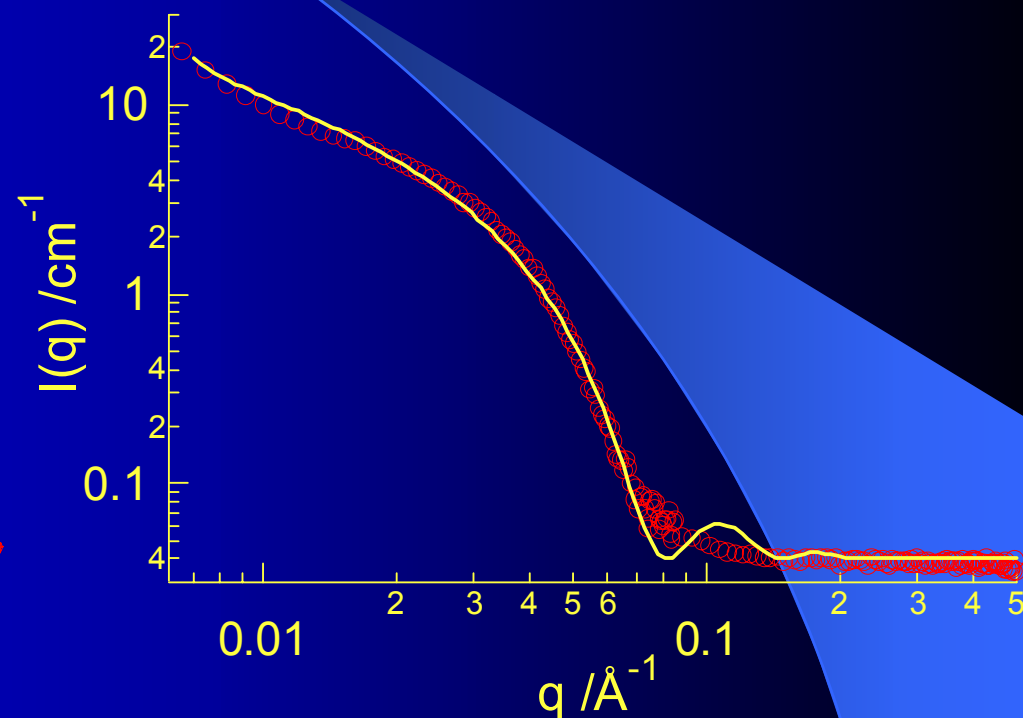
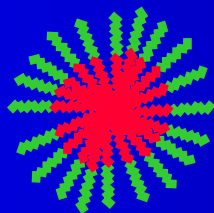




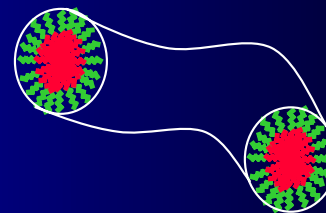
SANS study on micelles



0.2 wt% @ 10°C

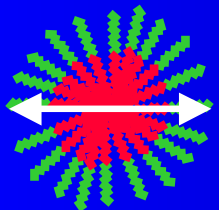
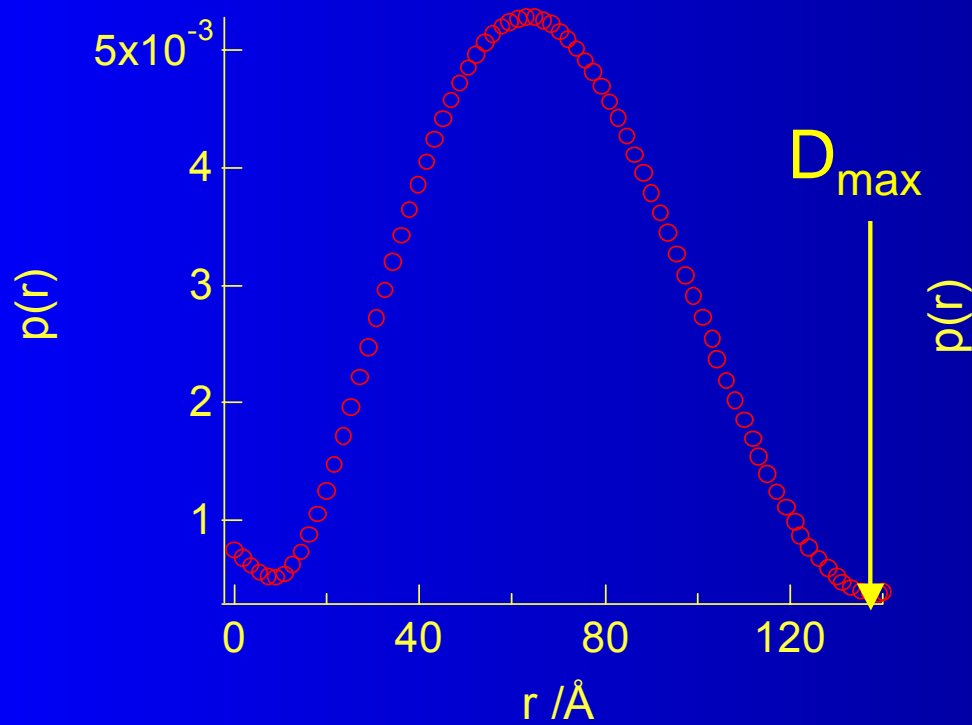


0.2 wt% @ 40°C

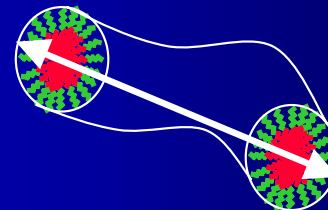
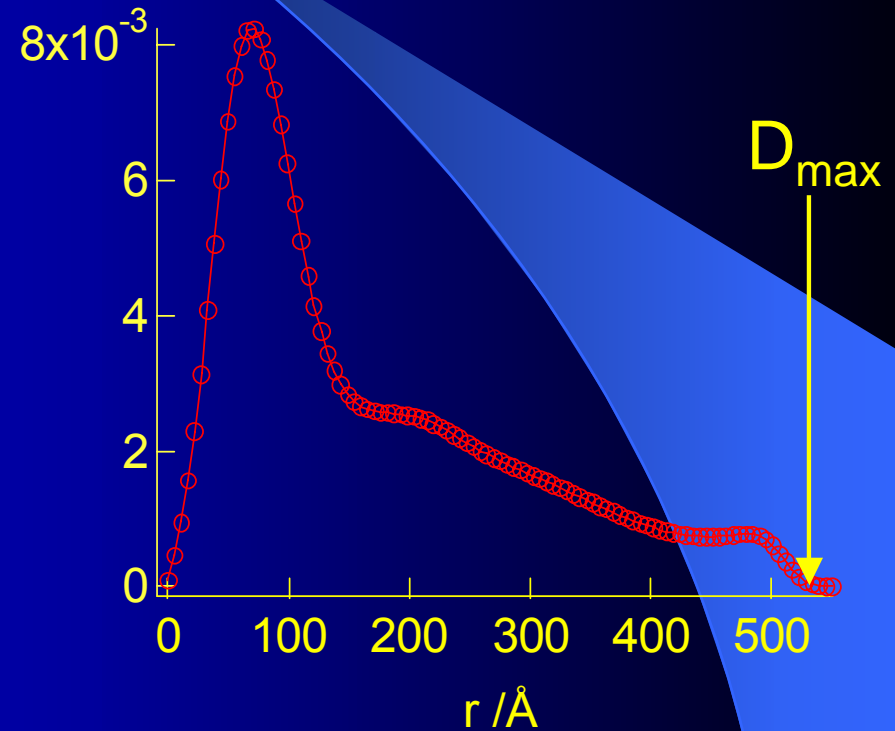




In real space



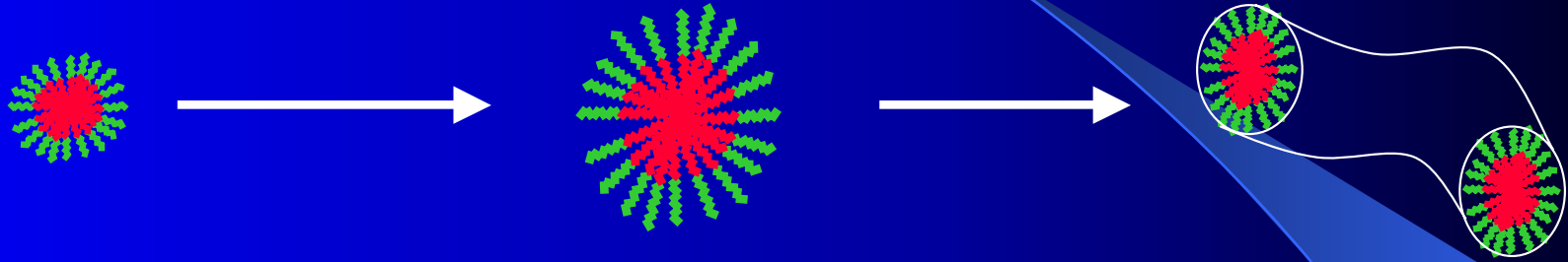
Maximum particle
dimension = 130\AA



Maximum particle
dimension = 525\AA

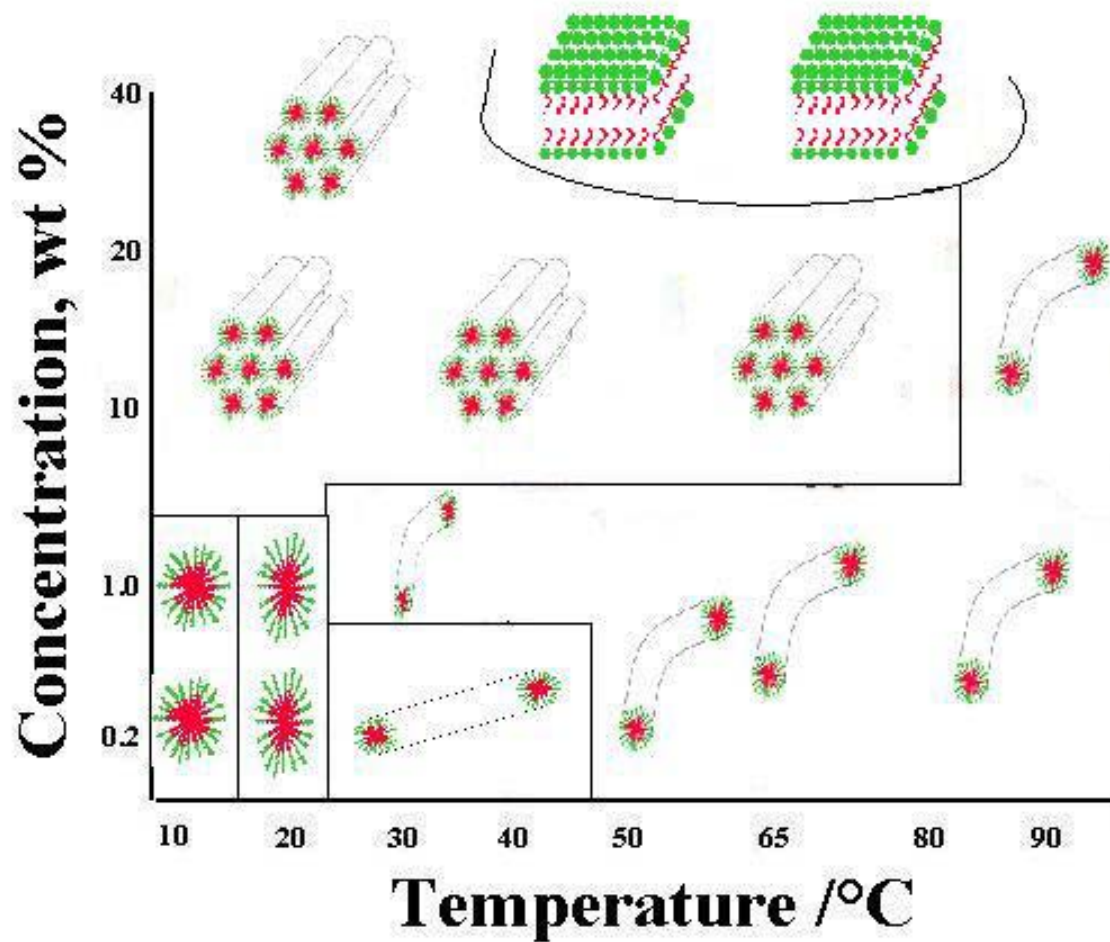


Sphere – Worm transition



Increasing temperature →

- Increasing temperature reduces the solvent quality for **PEO**.
- PEO becomes less solvated and to account for this the micelle swells.
- Eventually, this swelling will lead to an over—stretching of **PBO** in the core.
- Hence to increase in volume the micelle elongates into worm—like structures.
- Worm—like structures recognizable by birefringence.

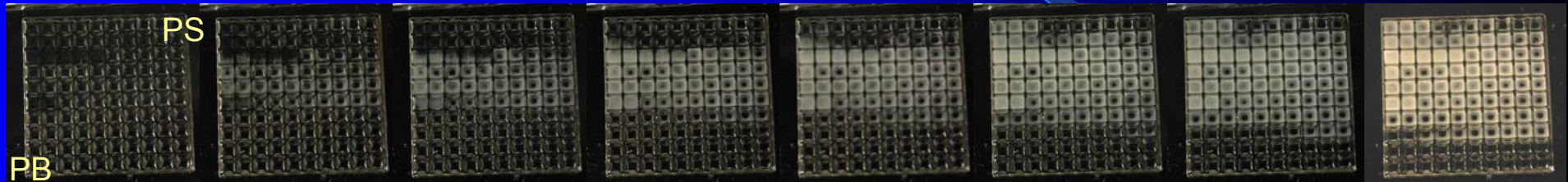




Light Scattering

145°C

→ 50°C

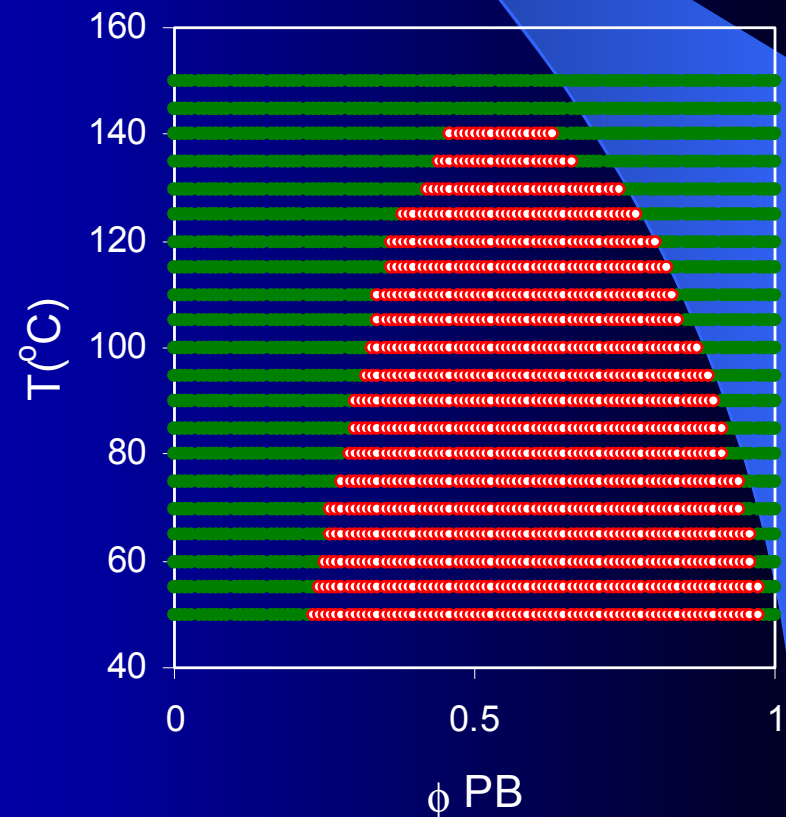


Optical turbidity study carried out on a discrete concentration gradient of a binary PS/PB blend (5K).

Phase diagram estimated.

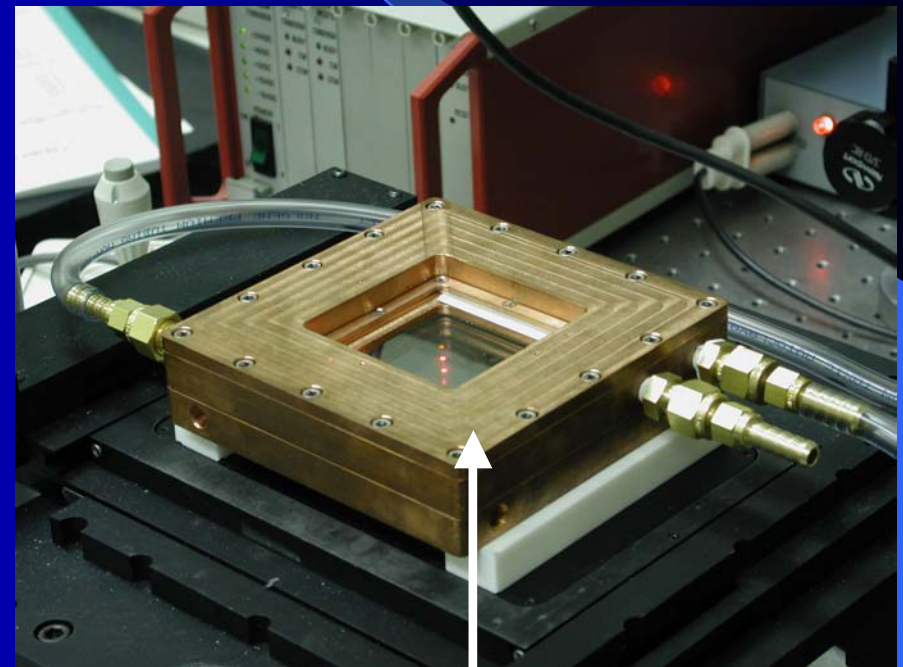
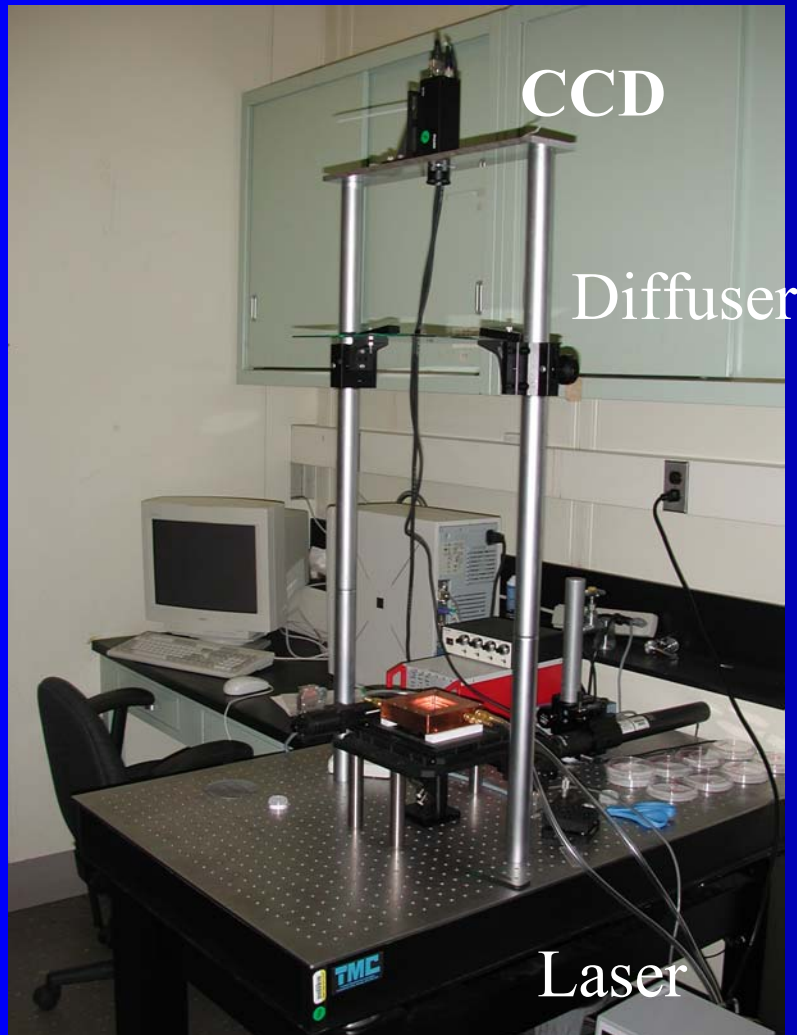
Can be carried out by SALS techniques to yield more structural information, e.g. size.

Cahn—Hilliard analysis to confirm SD mechanism.





SALS – Instrumentation



Heating stage containing
10 x 10 sample array



Future Direction

- Time variant devices to follow SALS, SAXS, SANS as the composition of components changes.
- Birefringence measurements using the established HT techniques – either by polarized light microscopy, or depolarized SALS measurements (H_v/V_v).
- Variation of ionic strength to be investigated on discrete library samples.
- Rapid phase mapping of binary and ternary polymer blends using discrete libraries.



Acknowledgements

Development of high throughput techniques – João Cabral.

X—ray scattering measurements – Sheng Lin-Gibson, Igors Sics.

SANS measurements – Derek Ho and Sheng Lin-Gibson.

Polymer samples – Keith Harris @ Dow Chemicals.

Multi-Modal Imaging

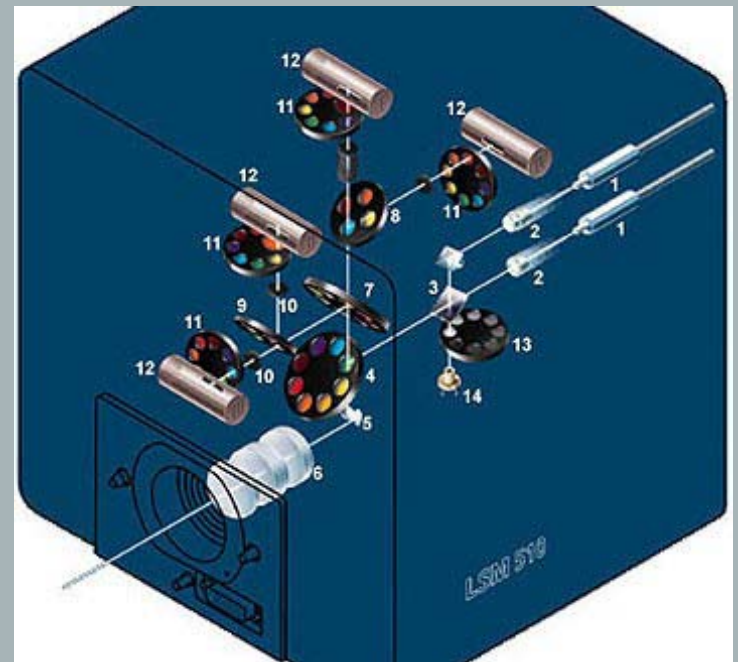
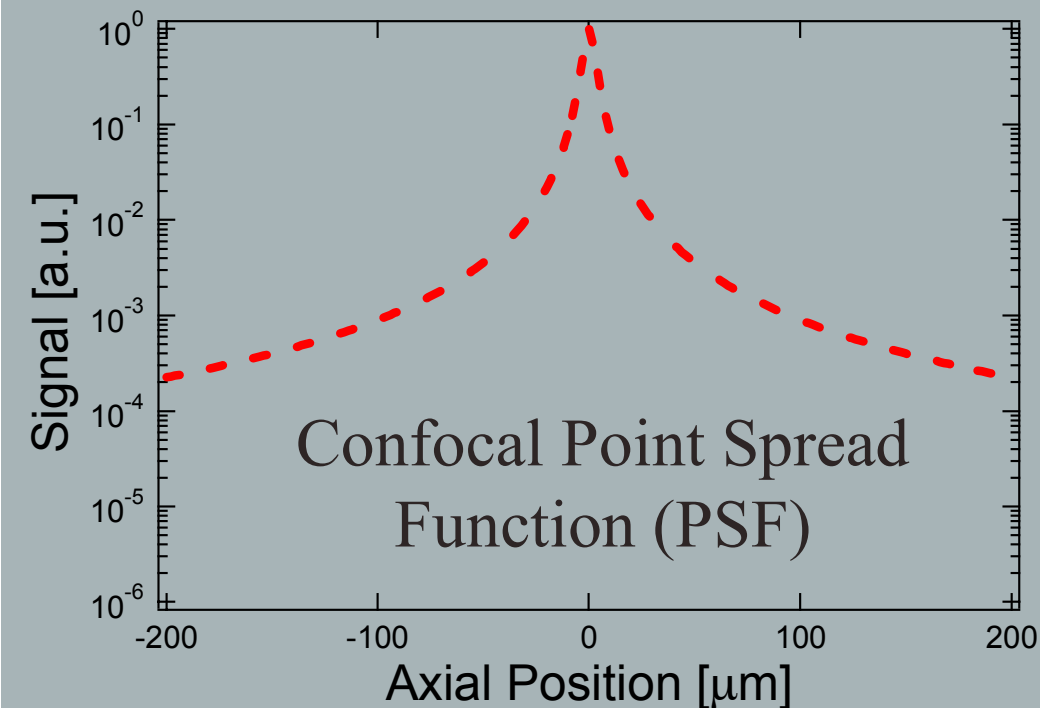
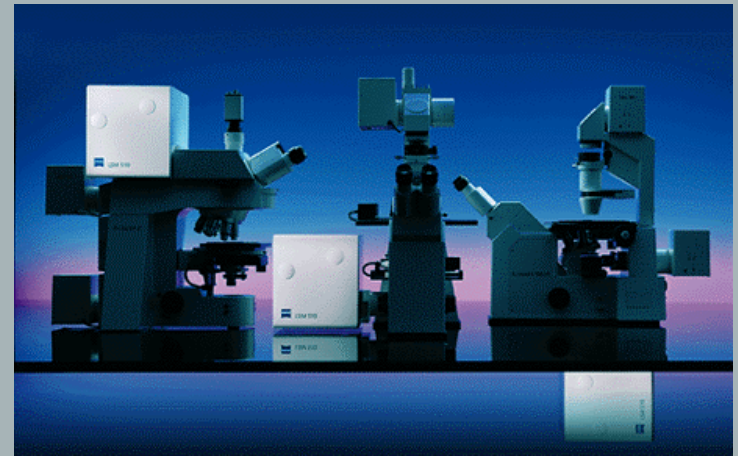
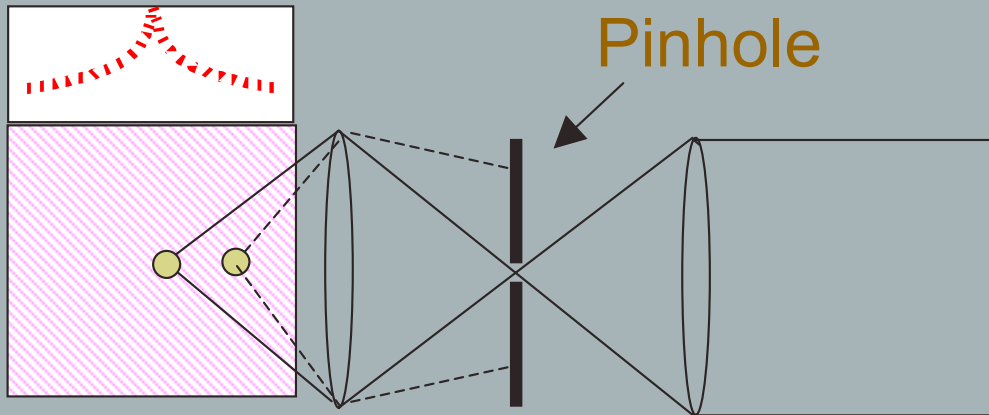
Marcus T. Cicerone

Polymers Division, NIST

Multi-Modal Imaging

- ▶ *Confocal Microscopy*
- ▶ *Infrared Microscopy*
- ▶ *Optical Coherence Microscopy*
- ▶ *Coherent Anti-Stokes Raman (CARS) Microscopy*

Confocal Microscopy



Confocal Microscopy

Data Analysis: Quantifying Deviation from Mixing

Zigzag micro-channel: 85 μm wide,
60 μm deep and 4.5 cm long.

$$D_i = \sqrt{\frac{1}{N} \sum_{i=1}^N (I_i - I_{\max})^2}^*$$

N = Number of pixels

D_i = Deviation from mixing

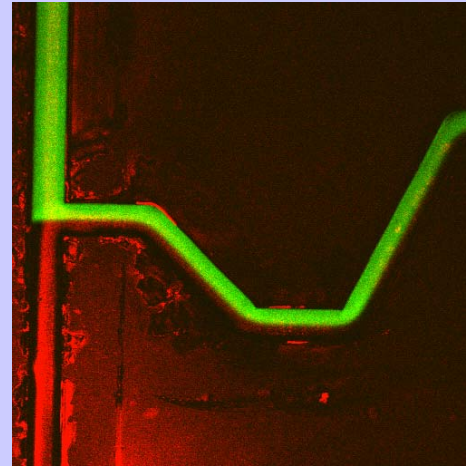
I_i = Intensity at pixel i

I_{\max} = Maximum intensity observed at
any pixel in a fully mixed system

* Liu *et al.*, J. MEMS, 2000

Deviation from mixing at points along the channel
is normalized to the corresponding value at the
channel junction

Incoming analyte stream with fluorescent
probe



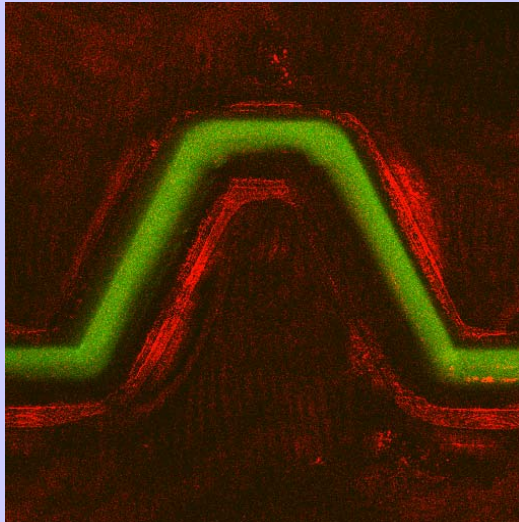
Incoming analyte stream

Flow

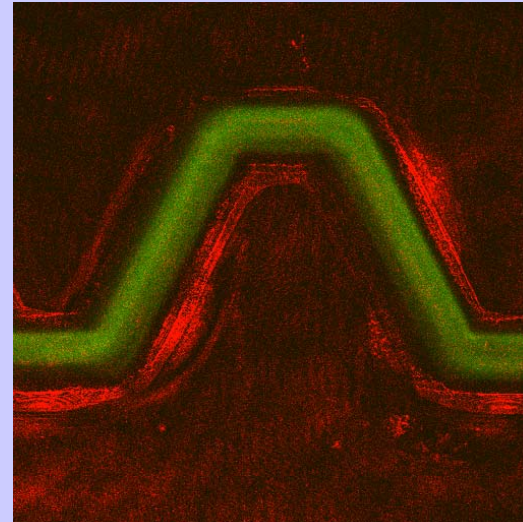
Jai A. Pathak, David J. Ross and Kalman B. Migler
NIST

Confocal Microscopy

Visual Comparison of Degree of Mixing



Sugar/Salt Solution with Rhodamine B

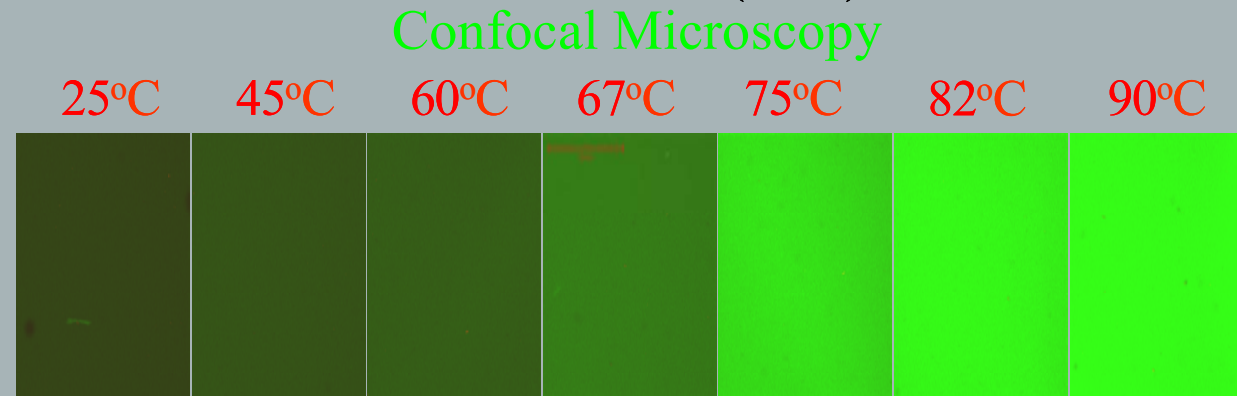
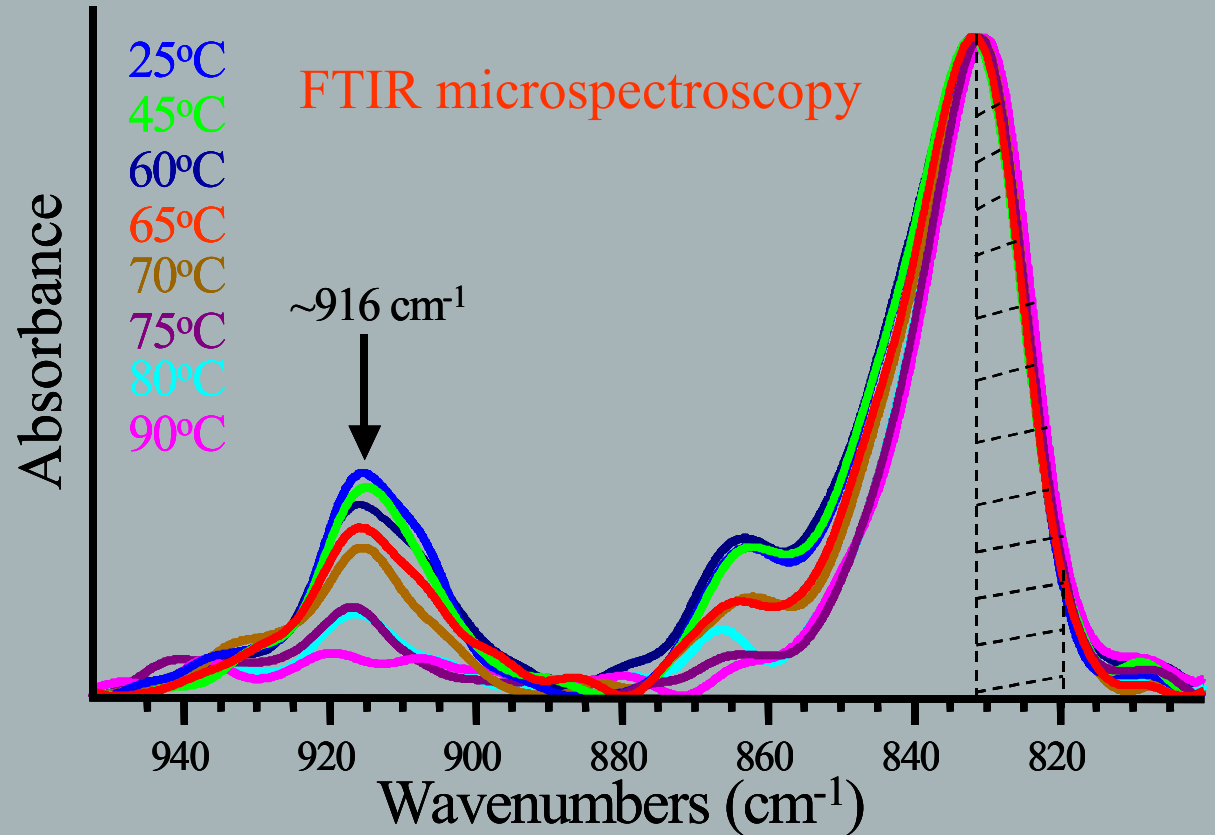
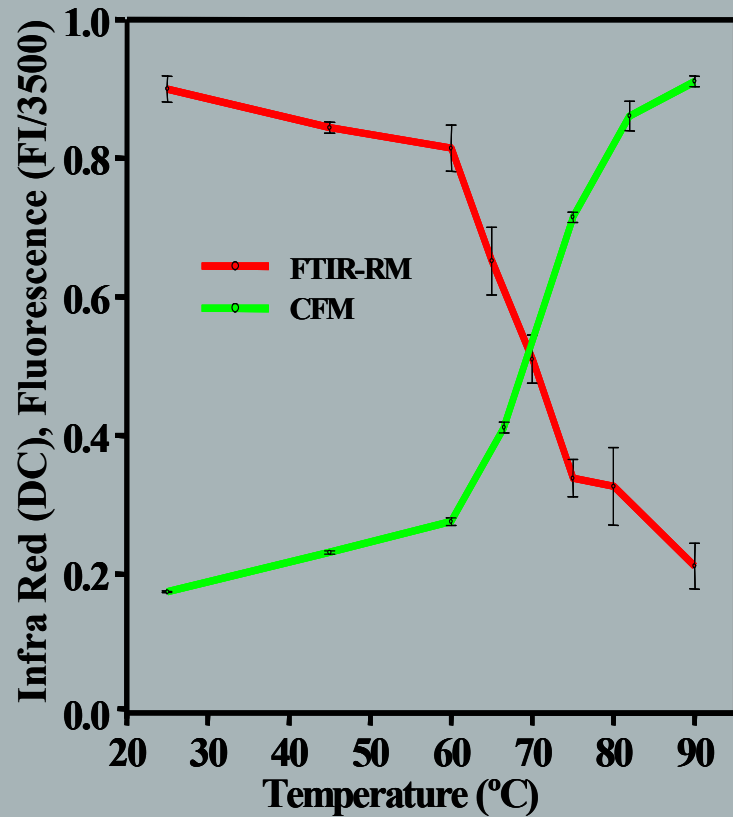


Sugar/Salt/Polyacrylamide Solution with Rhodamine B

Comparison made at $Q = 100 \mu\text{l/hr}$ and at same point on channel (3 mm from channel junction); Dashed lines are drawn to demarcate the edges of the channel

Jai A. Pathak, David J. Ross and Kalman B. Migler
NIST

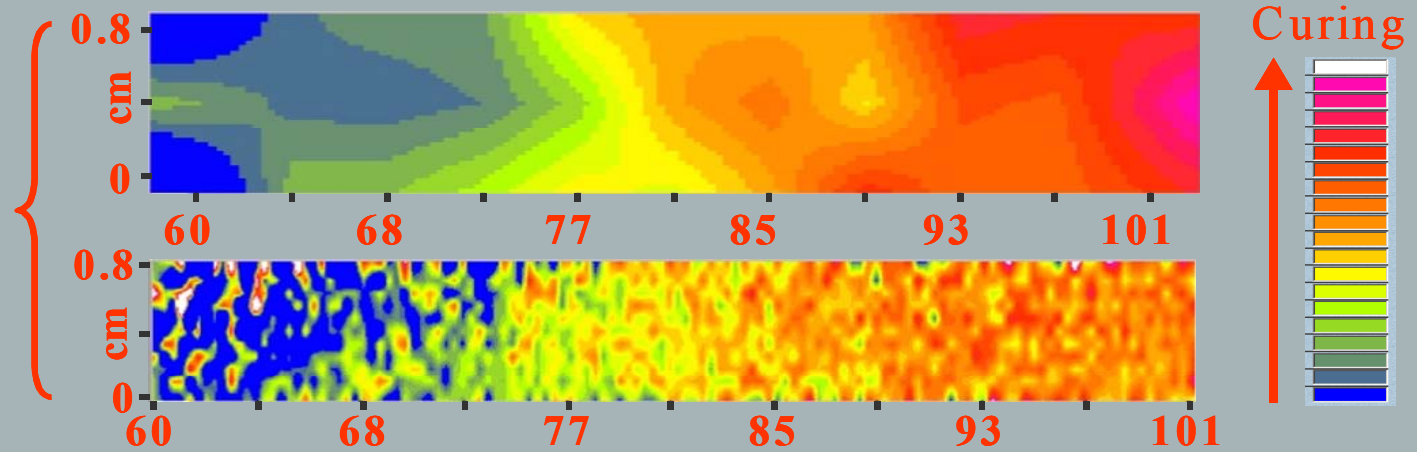
Epoxy films cured at various temperatures



Naomi Eidelman (ADAF, NIST), Aaron M. Forster (NIST)
and Dharmara Raghavan (Howard University)

Epoxy film cured for 15 minutes on a temperature gradient stage

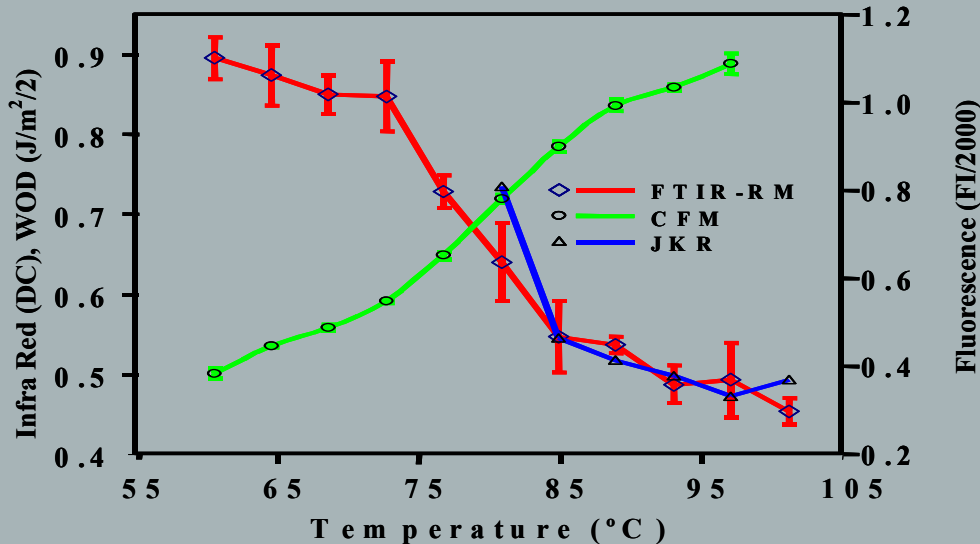
FTIR
microspectroscopy
maps



Confocal Microscopy



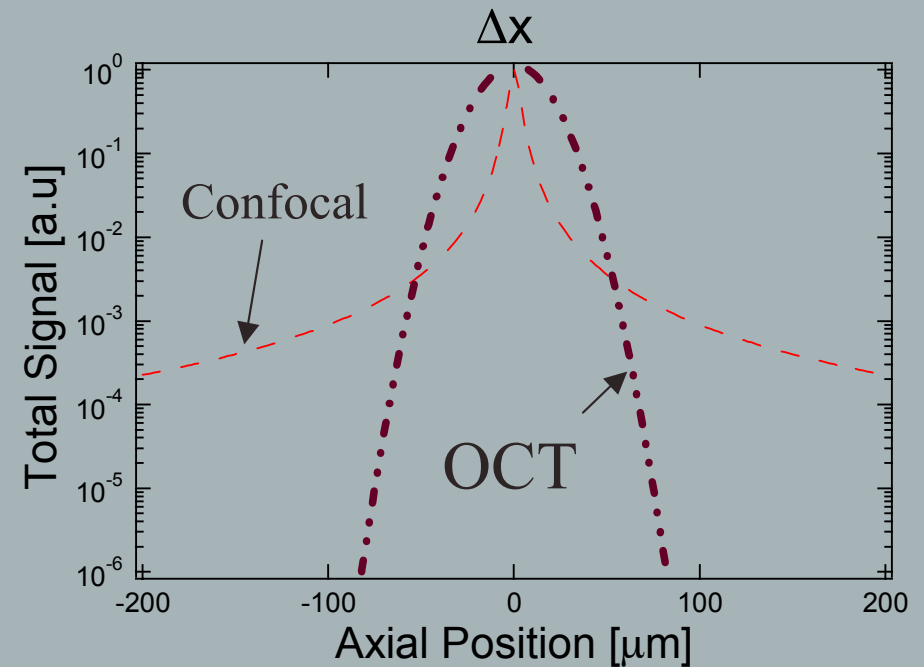
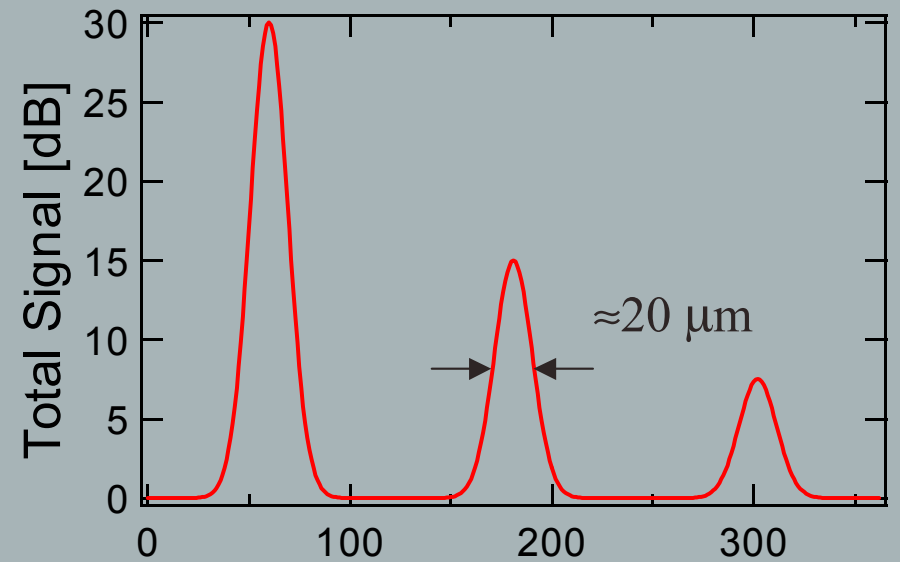
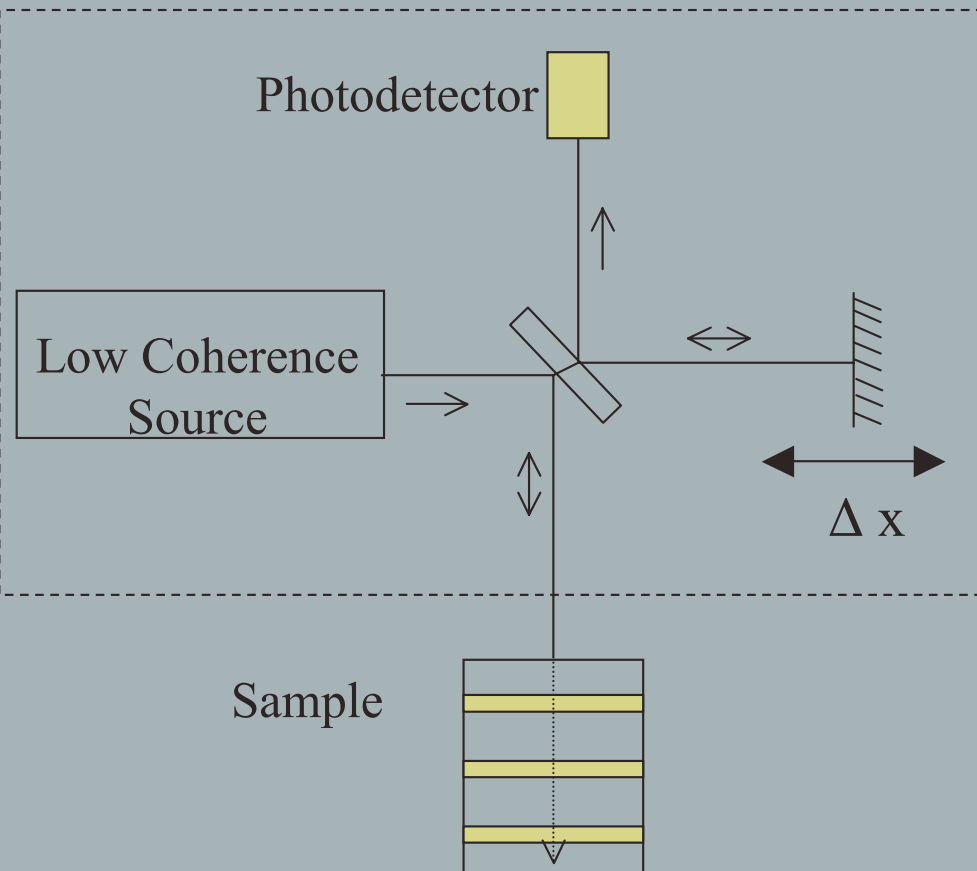
Temperature, °C



FTIR-RM, fluorescence
intensity and work of
debonding across the 15
minutes temperature gradient
cured epoxy film

Naomi Eidelman (ADAF, NIST), Aaron M. Forster (NIST)
and Dharmara Raghavan (Howard University)

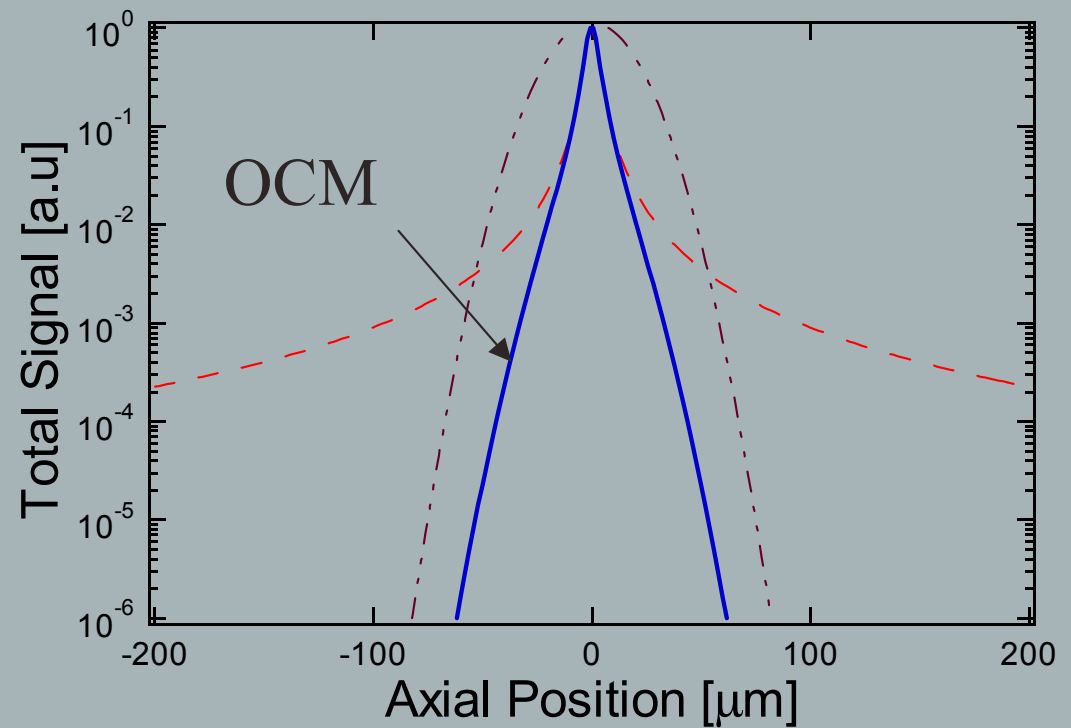
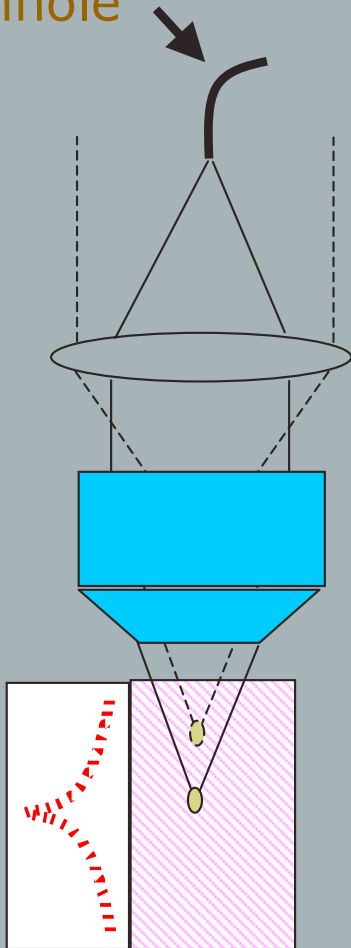
Optical Coherence Tomography



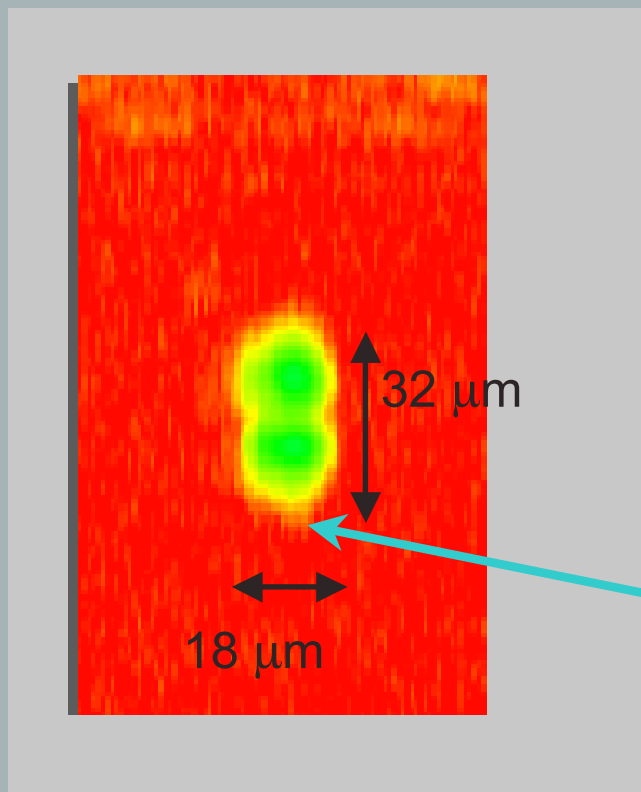
Optical Coherence Microscopy (OCM)

Single Mode Fiber
acts as pinhole

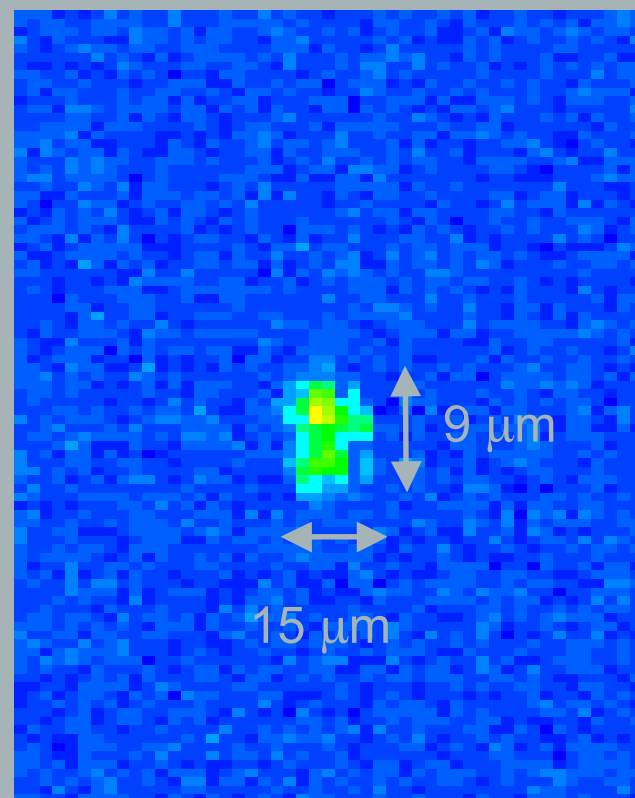
Objective



OCM



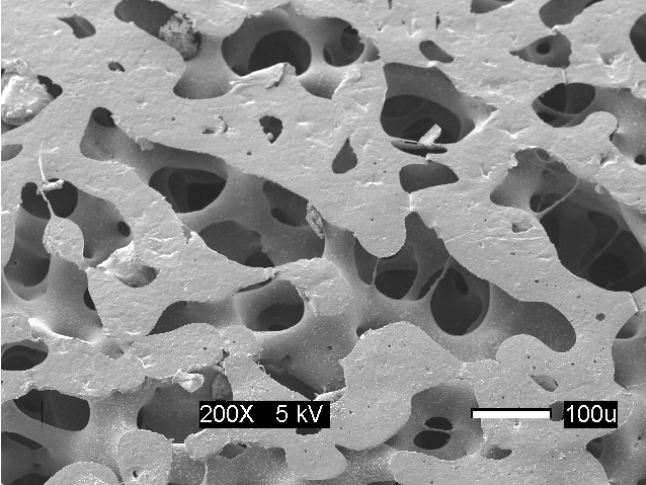
Optical Coherence
Tomography



Confocal Coherence
Microscopy

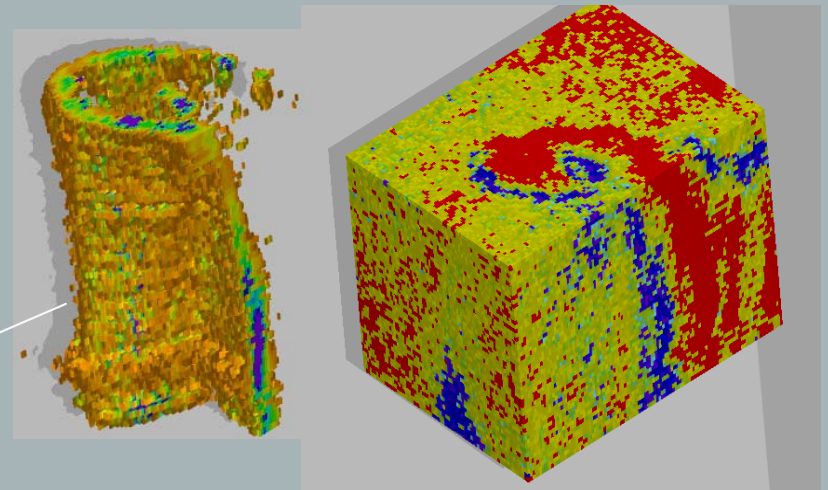
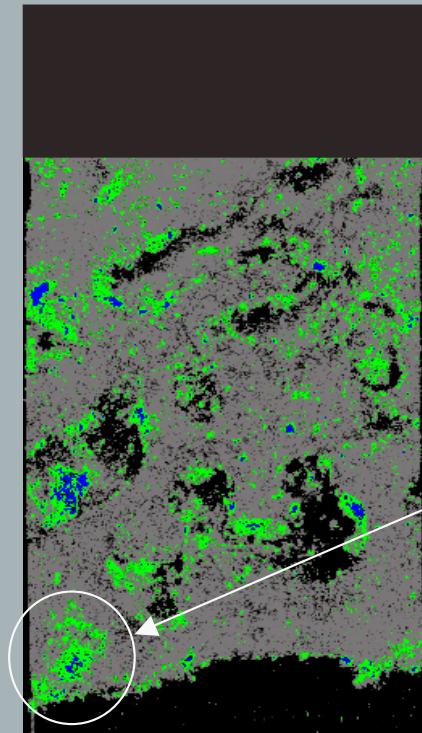
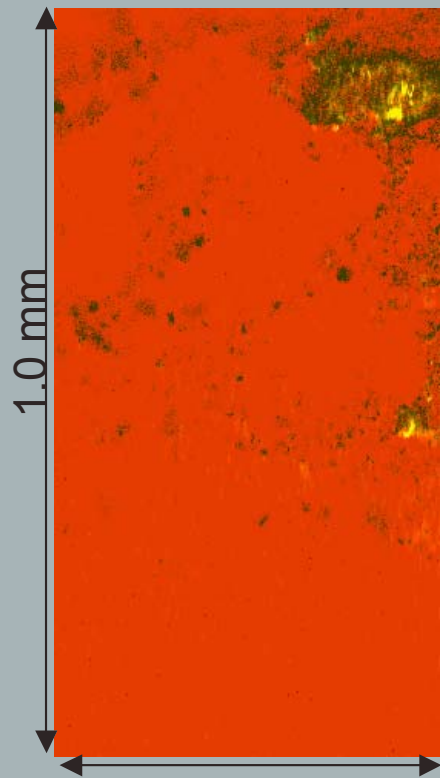
Marcus T. Cicerone, Joy P. Dunkers, and Forrest A. Landis

NIST Polymers



OCM / CFM

Poly(ϵ -caprolactone) scaffold cultured with fetal chick osteoblasts. Stained with nuclear fast red. Total depth: 330 μm .



500 μm

Marcus T. Cicerone, Joy P. Dunkers, and Forrest A. Landis

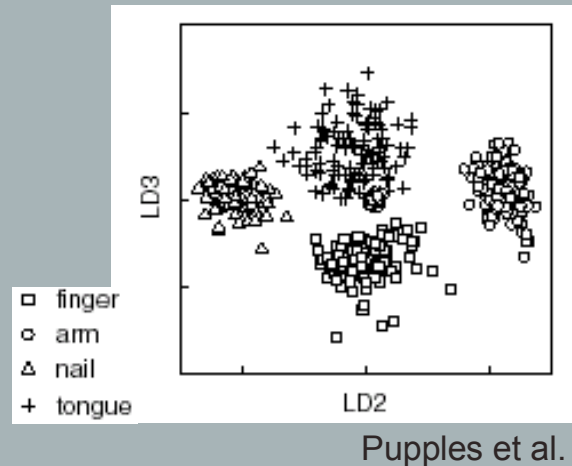
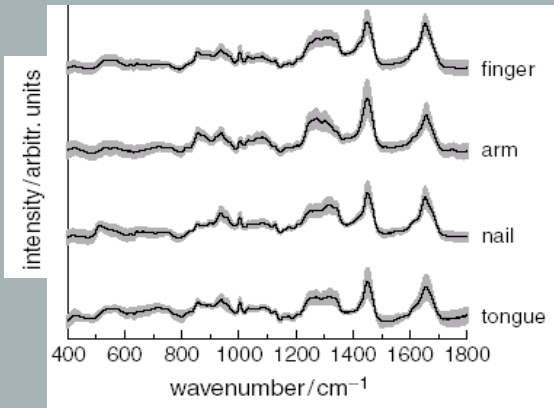
NIST Polymers



Coherent anti-Stokes Raman μ -Spectroscopy (μ CARS)

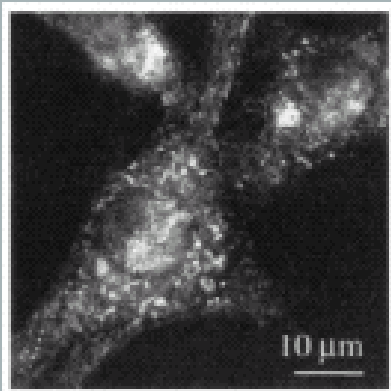
- ▶ *Rapid, high efficiency acquisition of vibrational spectra*
- ▶ *High spatial resolution: $\approx 0.2\mu\text{m}$ lateral, and $\approx 0.5\mu\text{m}$ axial*
- ▶ *Nearly non-invasive (gentle enough for rapidly dividing cells)*

μ CARS



Multivariate Analysis (MVA) allows automated discrimination between similar cell types based on full Raman spectra. Raman spectra acquisition require $\approx 5\text{s}$. This is much too slow for volumetric imaging.

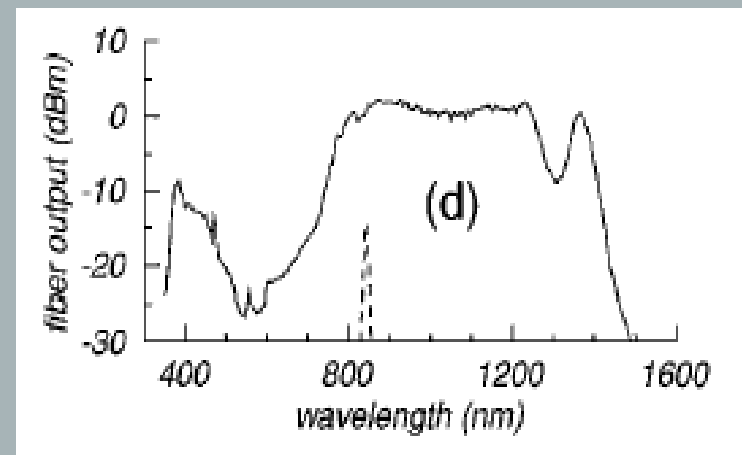
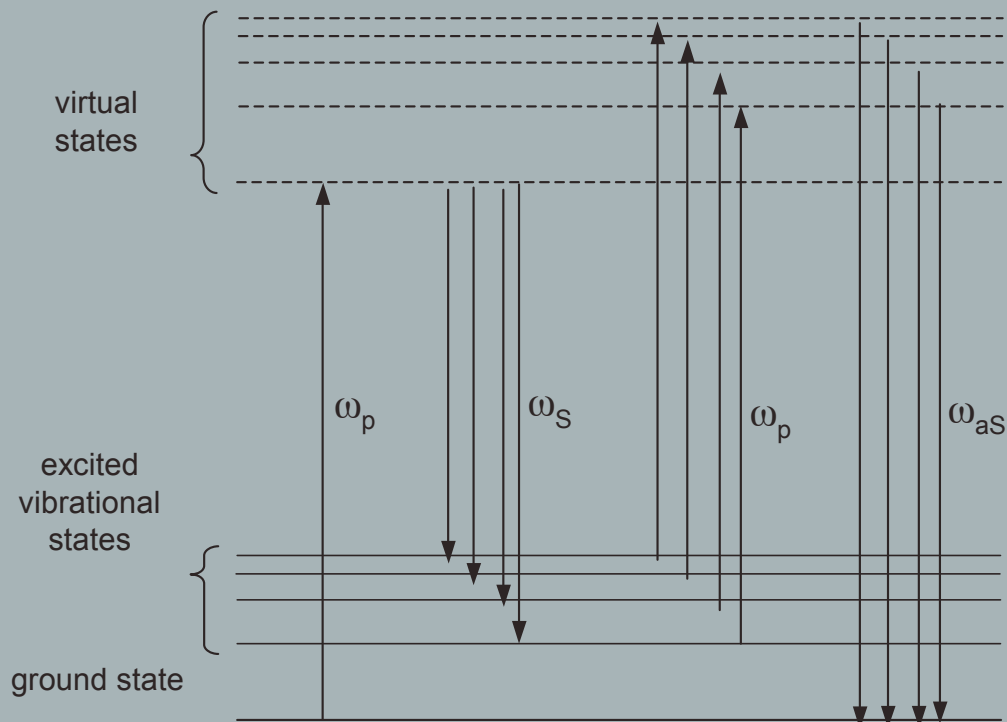
Narrowband μ CARS



Narrowband CARS can yield images at 50 μs pixelation rates, with but only a single Raman band

Xie et al.

μ CARS



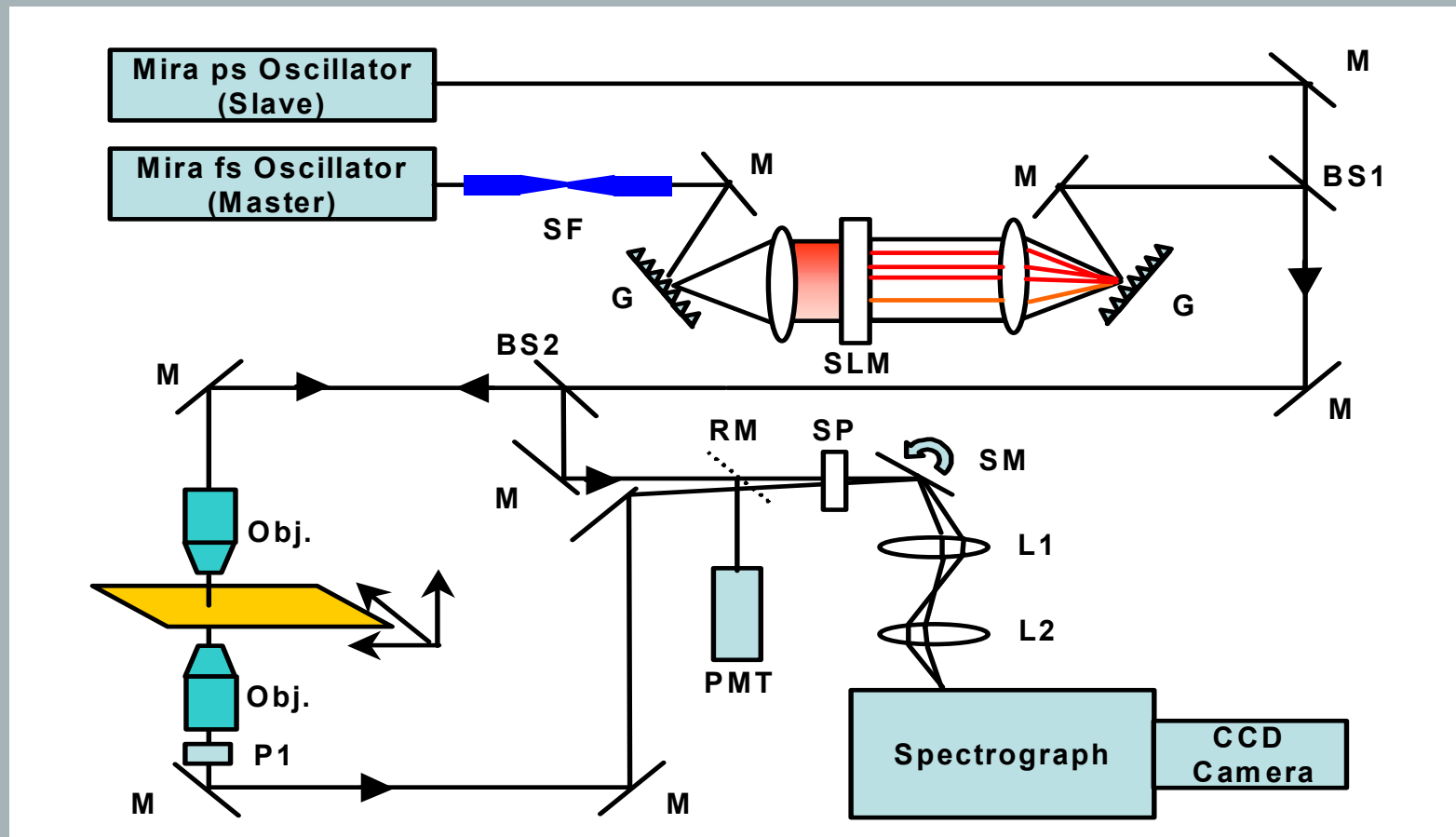
Birks et al. *Optics Letters* 2000; **25**:1415-1417

A broadband Stokes beam (ω_S) is necessary in order to produce broadband CARS spectra. This can be provided by stretched fiber continuum generation.

Marcus T. Cicerone and Tak W. Kee

NIST Polymers

μ CARS



Marcus T. Cicerone and Tak W. Kee

NIST Polymers

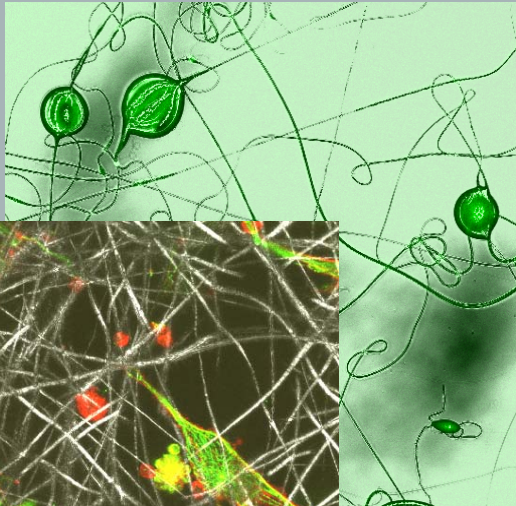
μCARS / Training

Cell Type	Stress / Signal	Ultimate Response
Mesenchymal stem cell (MCS)	FGF-2	Proliferation
MCS	TGF-β	Chondrogenic differentiation
MCS	β-glycerophosphate	Osteogenic differentiation
MCS	Indo-methacin Insulin 3-isobutyl-1-methyl-xanthine	Adipogenic differentiation
Chondrocytes	Change cell shape by culturing in electrospun nanofibrous scaffold	Redifferentiate (transform from fibroblast-like cells to chondrocytes)
MSC and Chondrocytes	Modify glucose availability	Change metabolic state
MSC and Chondrocytes	Plating onto surfaces coated with specific extracellular matrix components (e.g. fibronectin, collagen)	Interaction between extracellular matrix and membrane integrin receptors
Osteoblasts	TGF-b1	Intracellular Ca ²⁺ flux
Fibroblasts	Cytochalasin	Reorganization of cytoskeleton

Marcus T. Cicerone and Tak W. Kee, NIST Polymers

Rocky Tuan, Wan-Ju Li, NIH / NIAMS

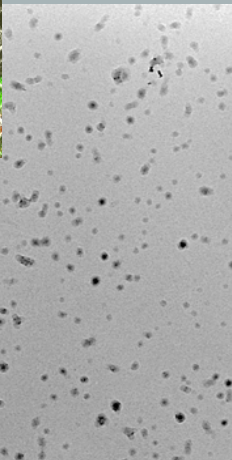
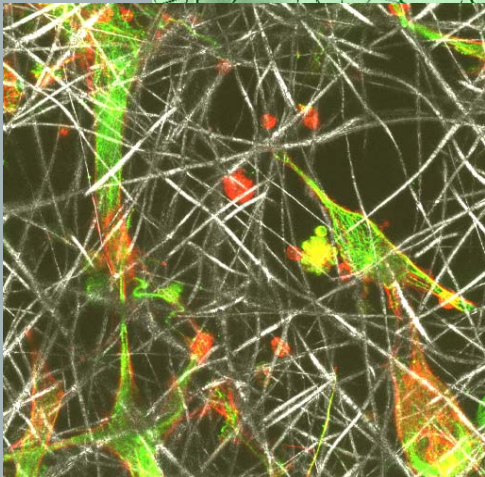
Stochastic “COMBI” For Tissue Engineering



- ▶ *We can encourage cell proliferation and differentiation by delivery of growth factors from tissue scaffolds.*

- ▶ *Cell response depends on additional factors such as availability of nutrients, local physical and chemical environment. (Geometry of scaffold, proximity to other cells, etc.)*

- ▶ *Correlate cell behavior with local environmental conditions and exposure to growth factors.*



500 nm

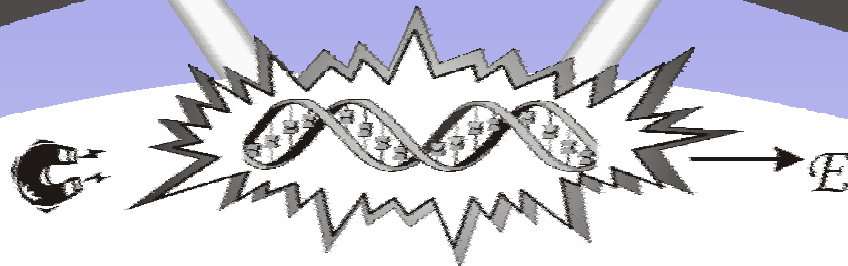
Marcus T. Cicerone and Tak W. Kee, NIST Polymers

Rocky Tuan, Wan-Ju Li, NIH / NIAMS

Bio-NEMS

SM³

Single Molecule
BioMetrology



Single Molecule Manipulation
and Measurement

SM³

SINGLE MOLECULE MANIPULATION AND MEASUREMENT

EEL



CARB



Physics Laboratory



Information Technology
Laboratory

Gaithersburg



Boulder



CARB



JILA



SM³ ...an interdisciplinary team with a common goal...



John Kasianowicz, Biophysicist
Protein Nanopores



Laurie Locascio, Biomedical Engineer
Microfluidic Systems



Lori Goldner, Physicist
Nano-Optics



Michael Gaitan, Electrical Engineer
MEMS and Nanofabrication



Angela Hight Walker, Chemical Physicist
Molecular Spectroscopy



John Marino, Biochemist
NMR Proteins



David Nesbitt, Chemical Physicist
Single Biomolecule Fluorescence



John Moreland, Physicist
Nano-Magnetics and MEMS



Vince Stanford, Mathematician
Signal Analysis

NIST Role

Measurements and Standards

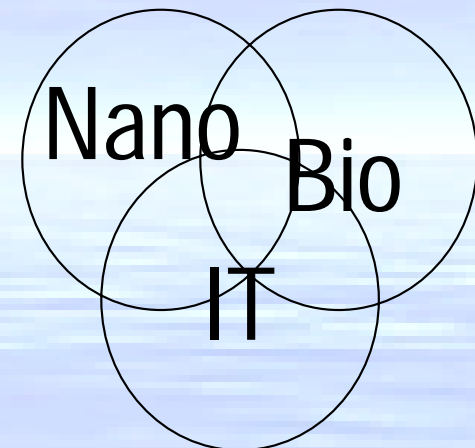
Industry trend is smaller sample size

- genomics
- proteomics
- microfluidic systems
- lab-on-a-chip
- chem/bio sensors



Converging Technologies

- Nanotechnology
- Biotechnology
- Information Technology



Why Single Molecule Measurements?

- Ensemble averaging provides incomplete information
- Many biological processes are done one molecule at a time
- Statistical distributions
- Kinetics and dynamics
- Subtle structural differences have big consequences
- High throughput



SM³ Program Objective

*To develop and integrate new measurement methods to transport and probe structure, function, and dynamics of **single biomolecules***

DNA, RNA, and Proteins

Technical Approach

NanoBioTechnology Platform

Platform based on
Nanofabrication
Molecular Assembly

Manipulation (Transport):
Fluidic Restrictions,
Beads



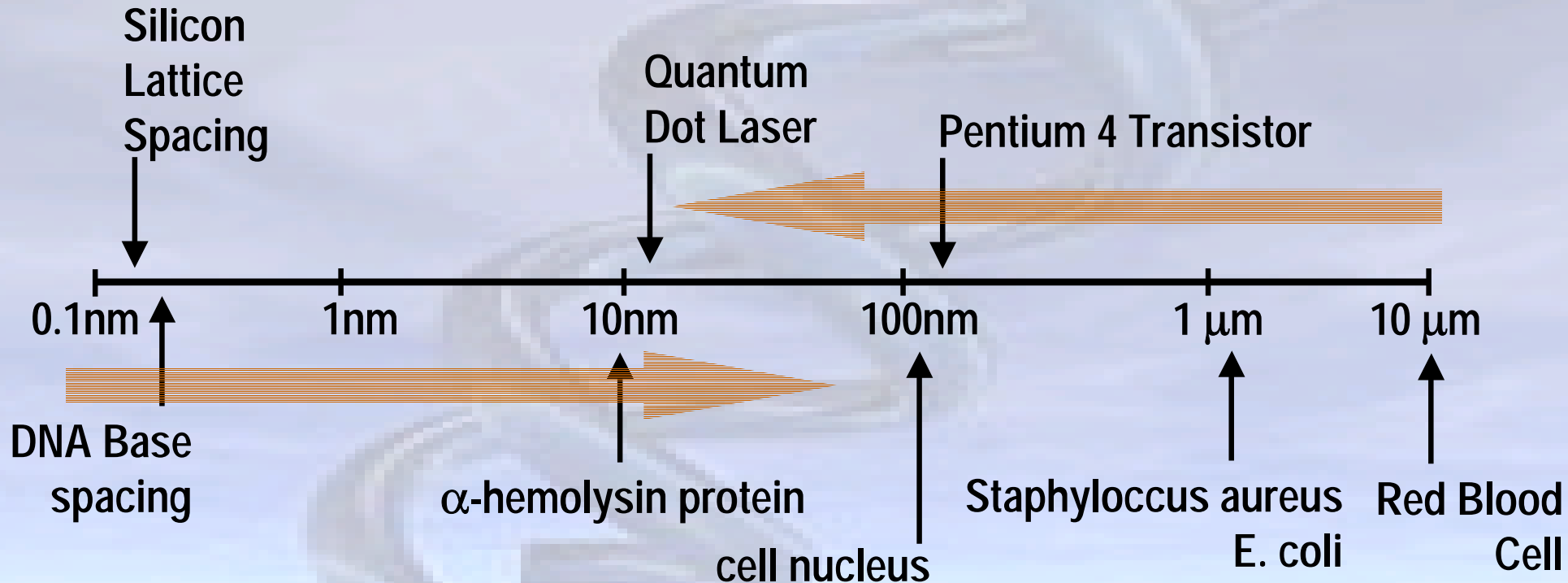
Electronics meets Biology

Measurements:
Electronic, Optical, Force

Manipulation (Capture):
Vials, Beads, Arrays

Scales

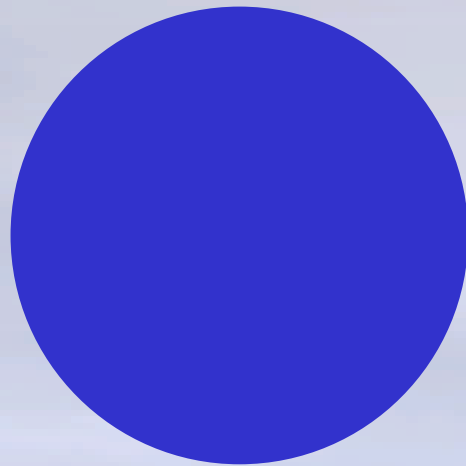
Electronics: Top-Down



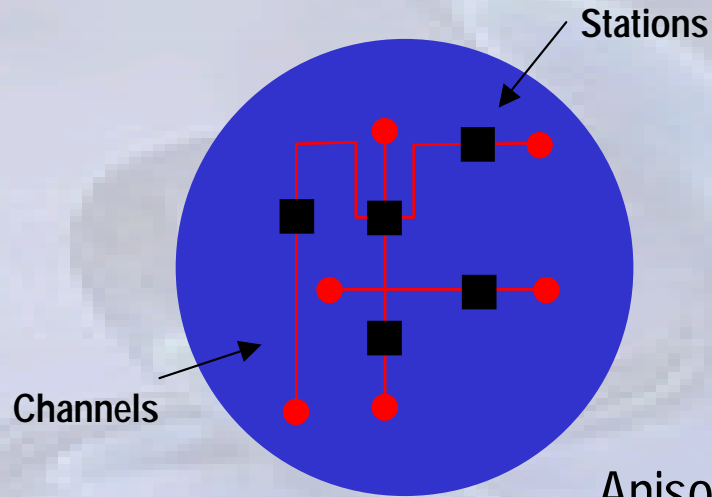
Biology: Bottom-Up

Human DNA
3 billion base pairs
1 meter total length

The Platform

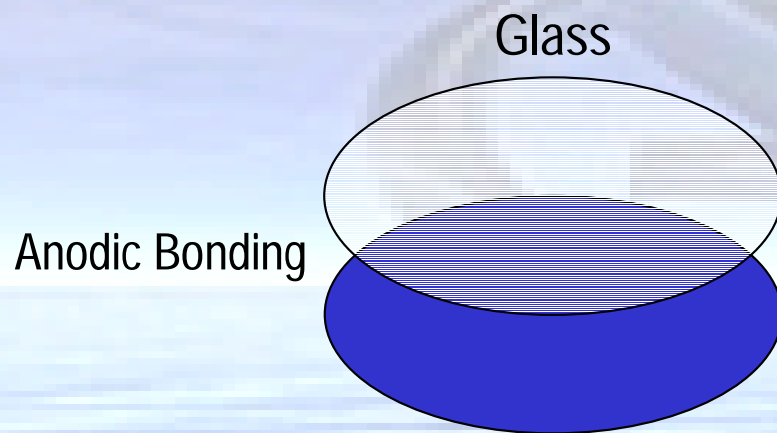


Silicon Wafer

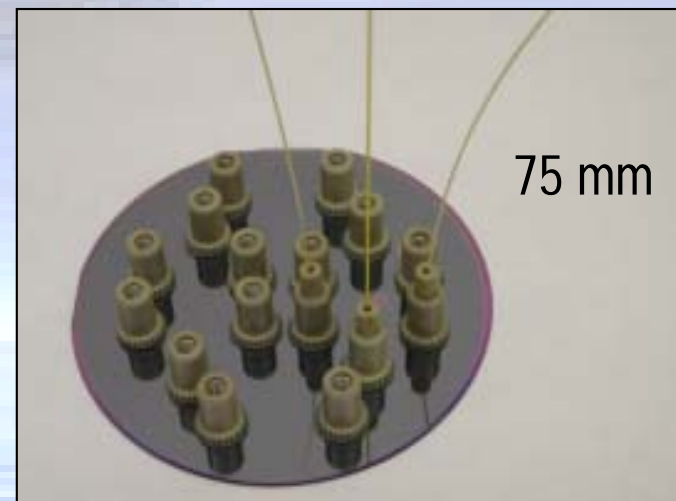


Through holes

Anisotropic Etching (Wet, DRIE)

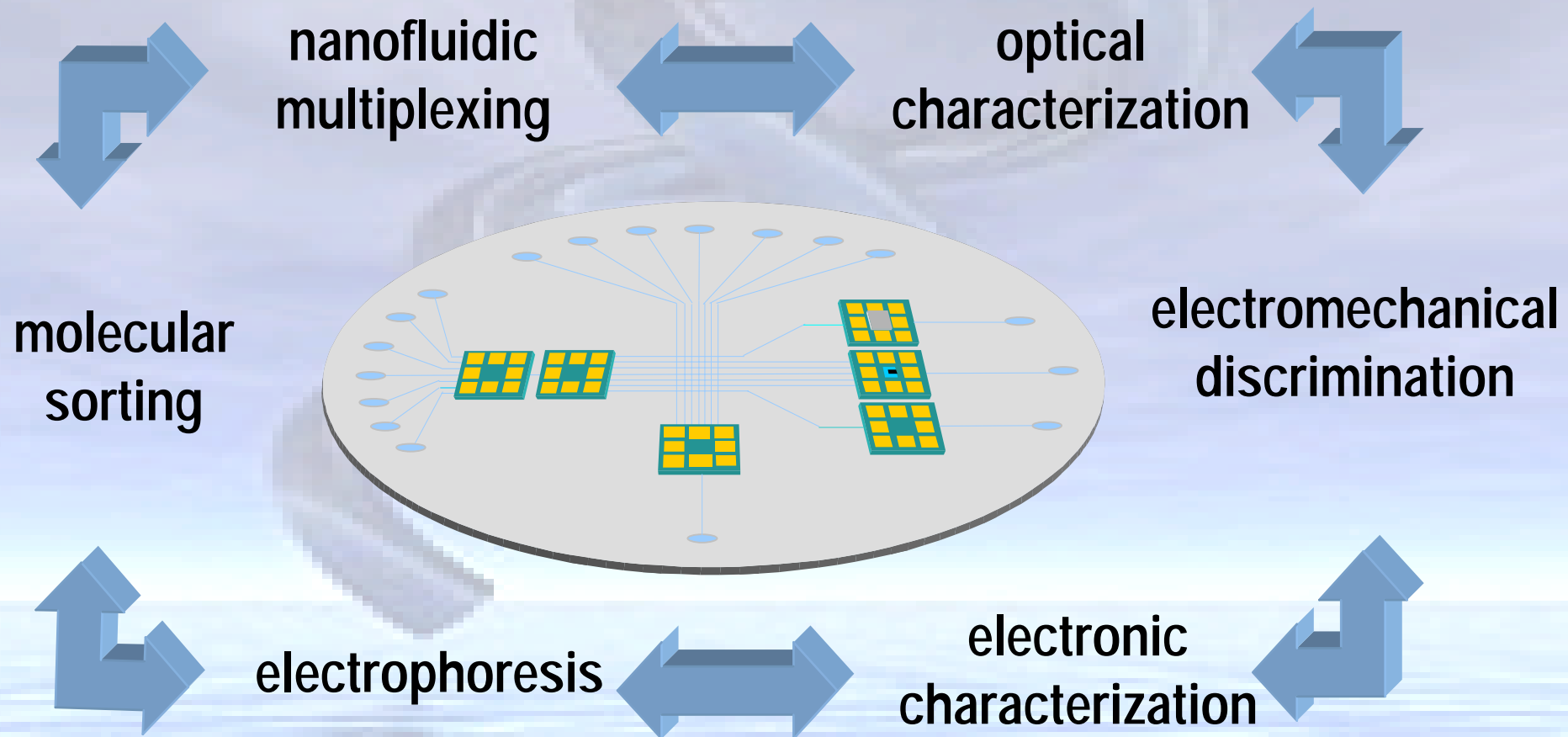


Silicon Wafer

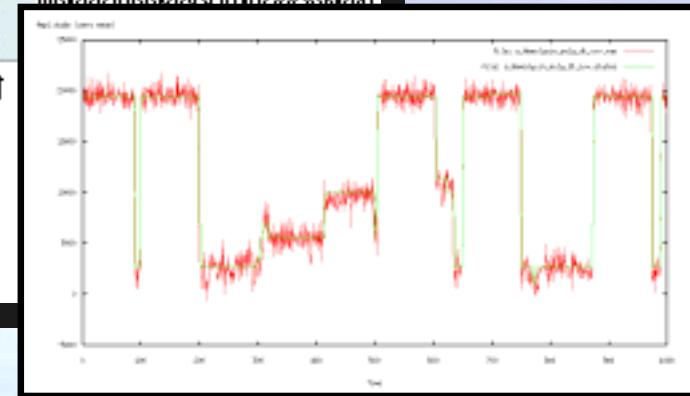
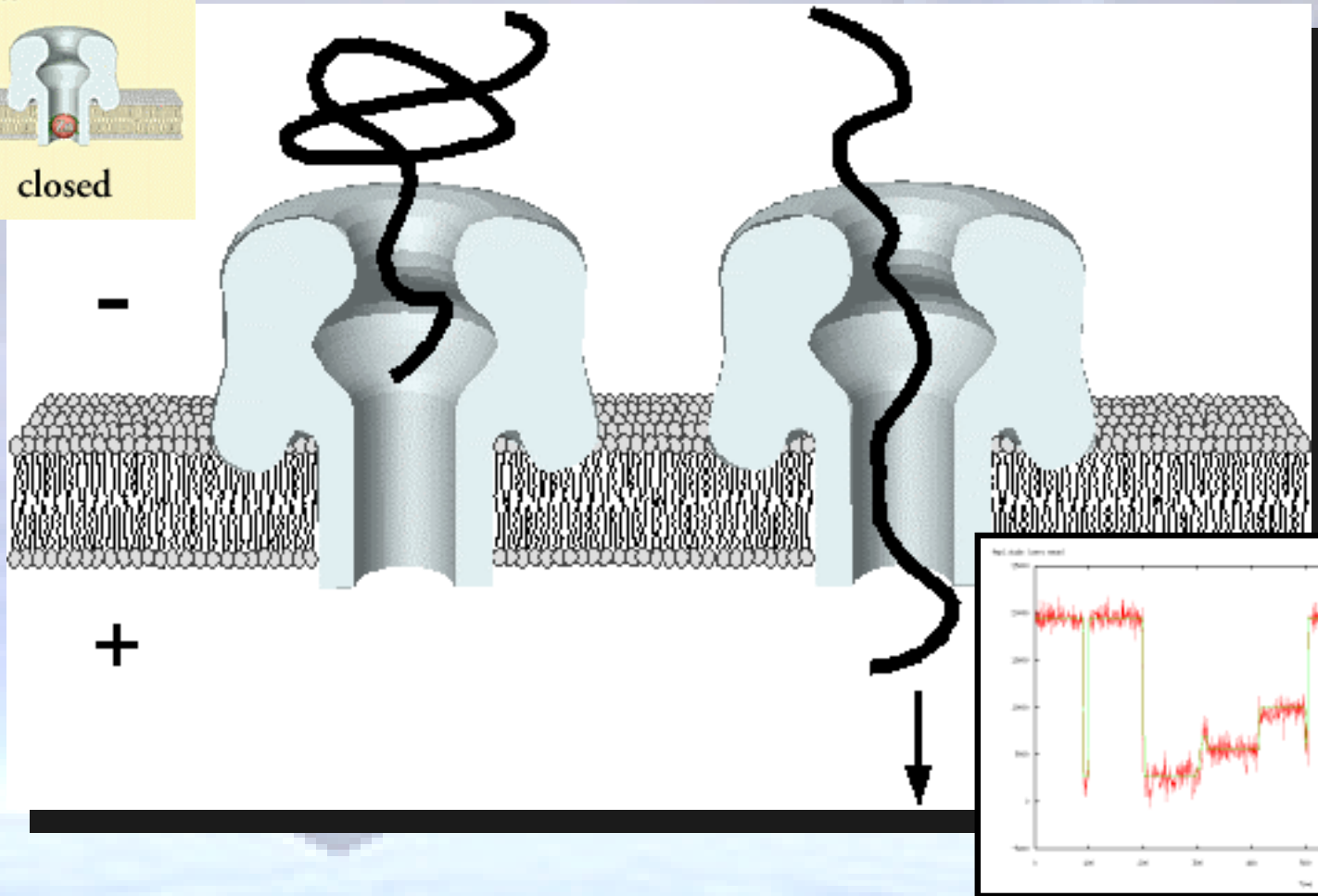
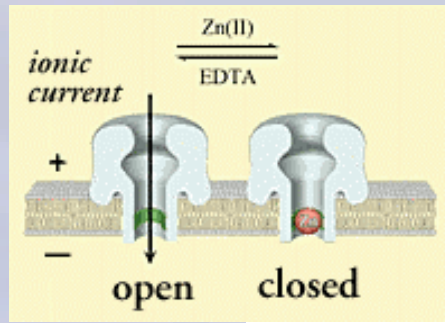


Measurements Integrated into the Platform

Single Molecule Electronic, Optical, and Force Measurements on a MEMs Platform



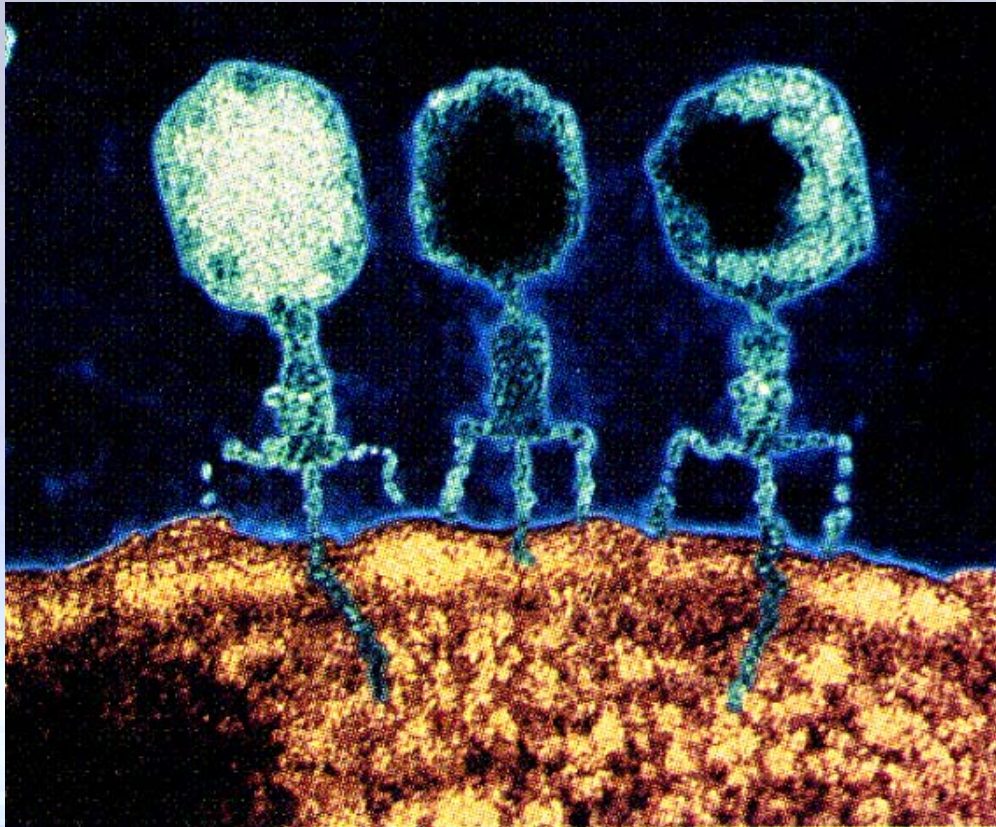
Electronic: DNA Transport Through the α HL Channel



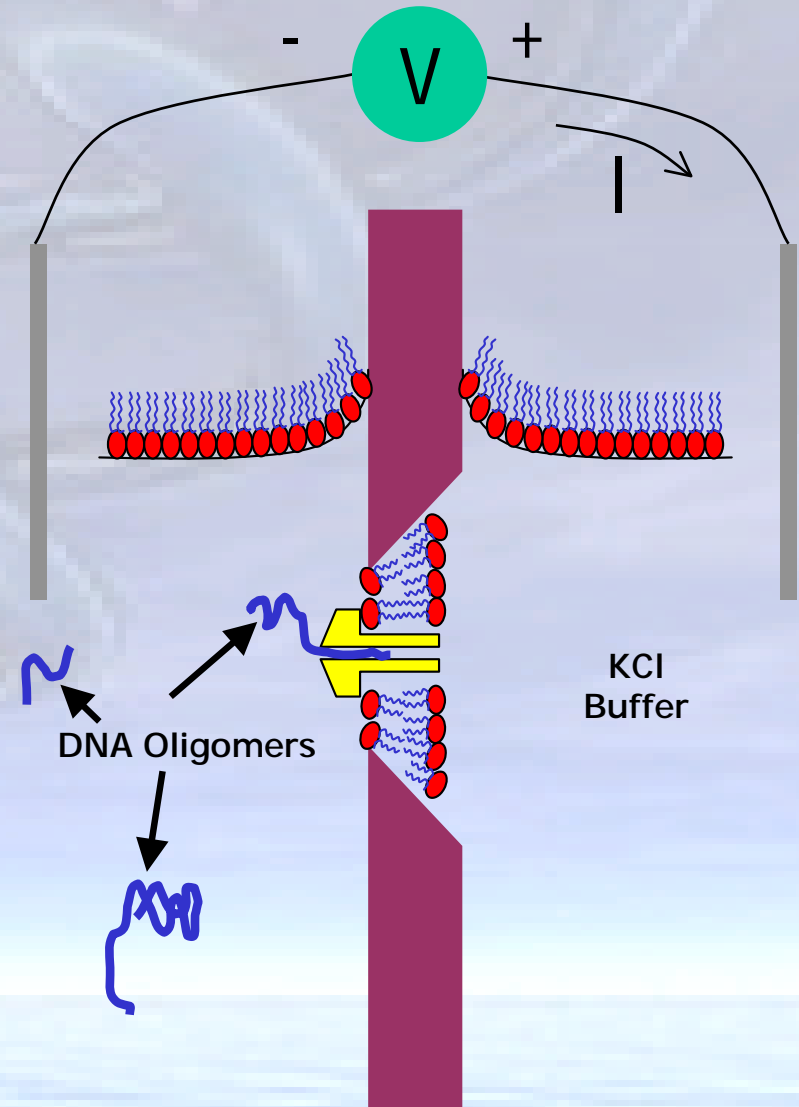
Electric field drives *individual* DNA molecules through single α HL channel

(Kasianowicz, et al. 1996. *Proc. Nat'l. Acad. Sci.* **93**, 13770)

DNA Entry Into Single Nanopores

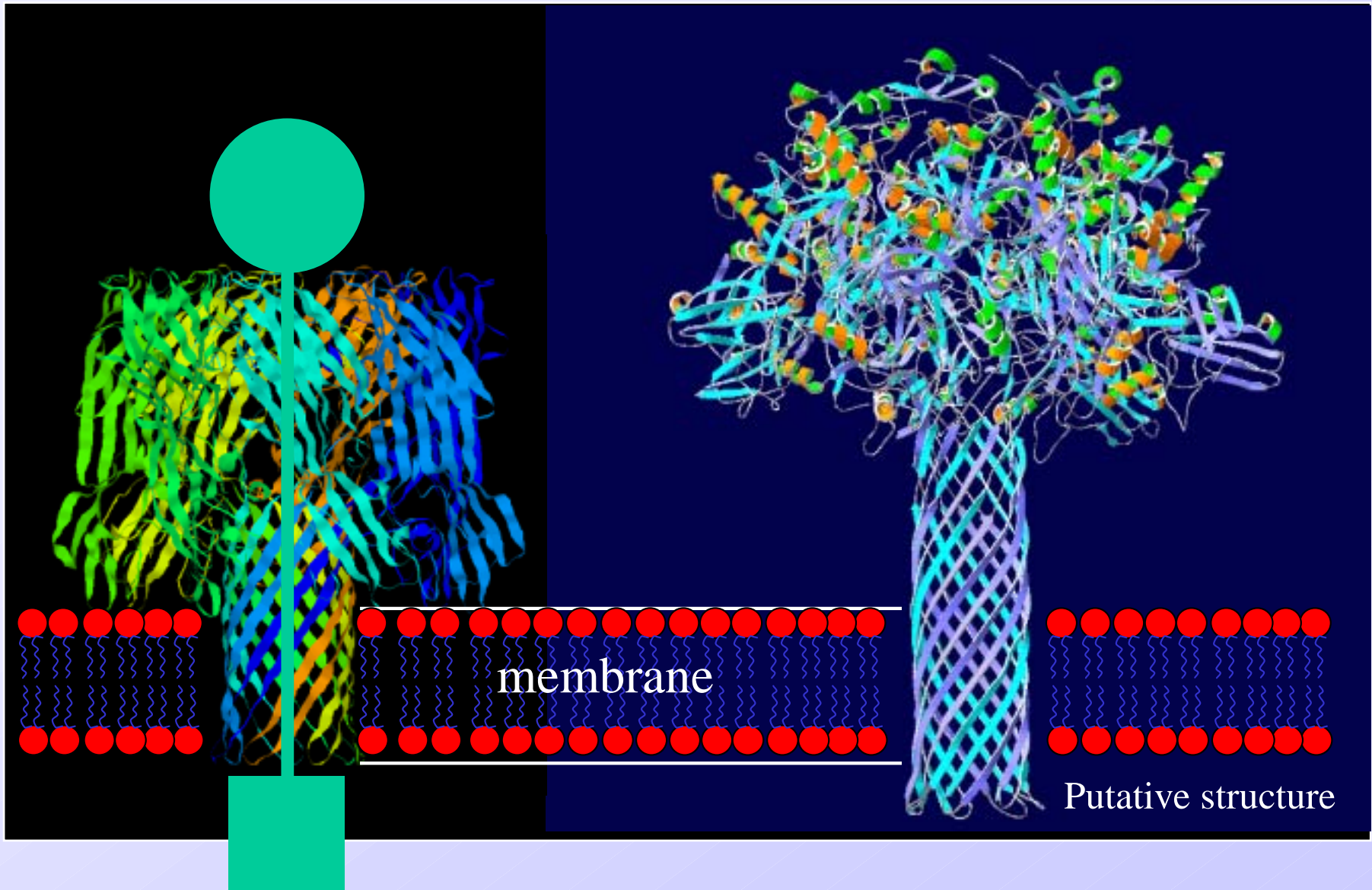


Nature



Experiment

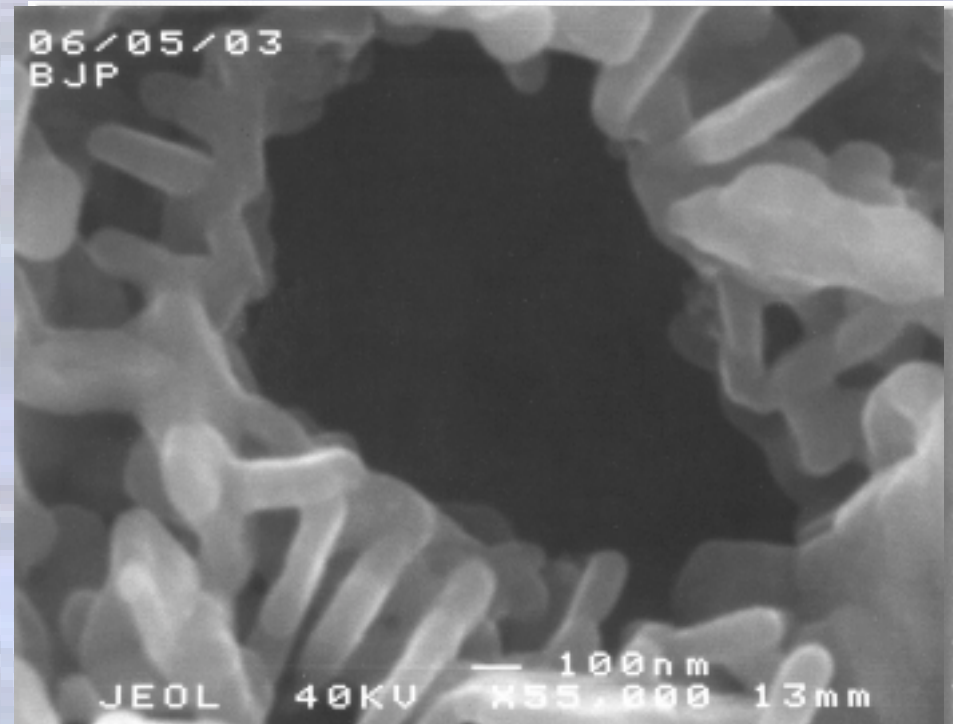
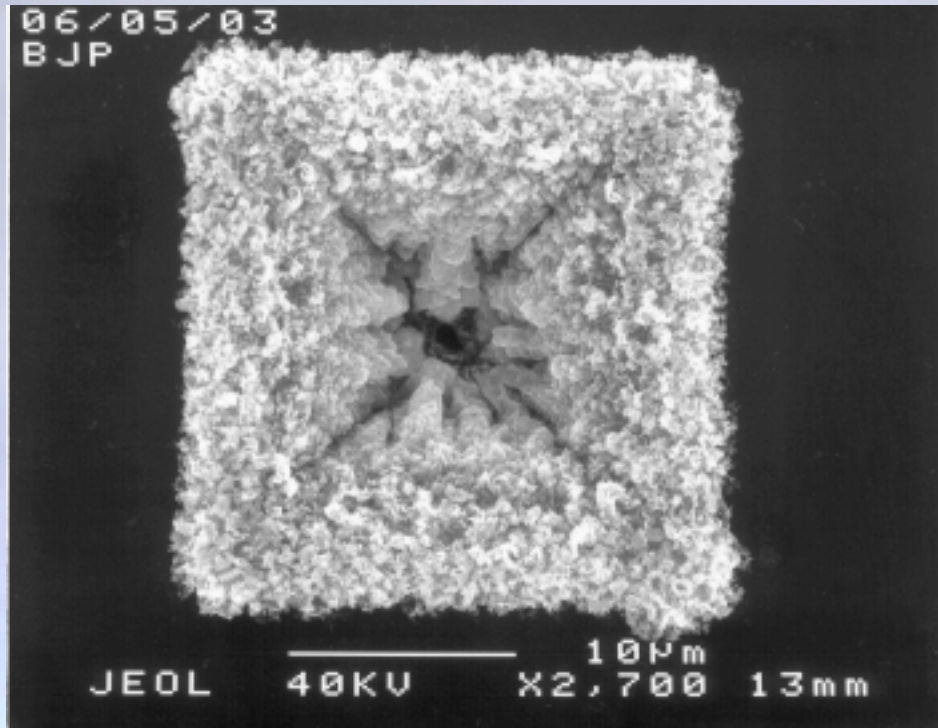
Protein Nanopores



S. aureus αHL

B. anthracis PA₆₃

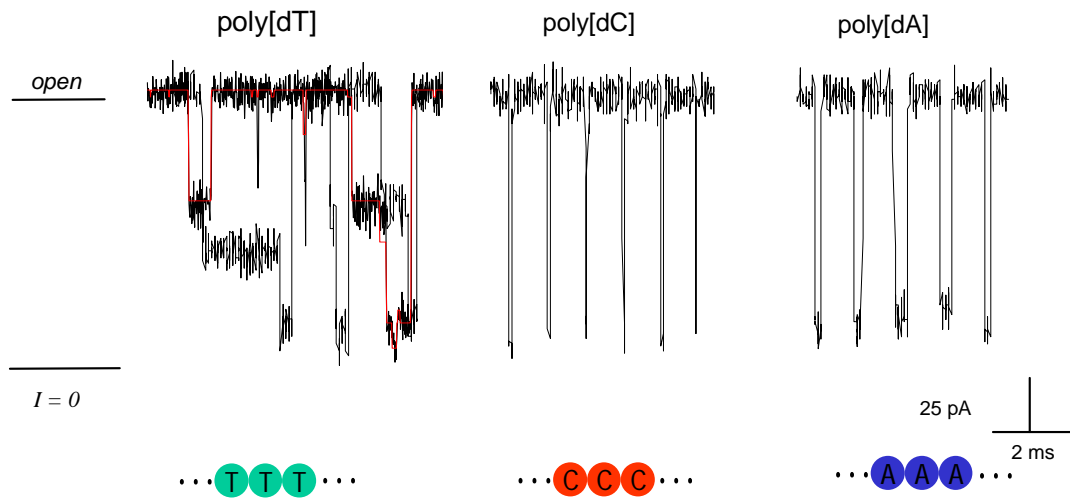
Solid State Nanopores



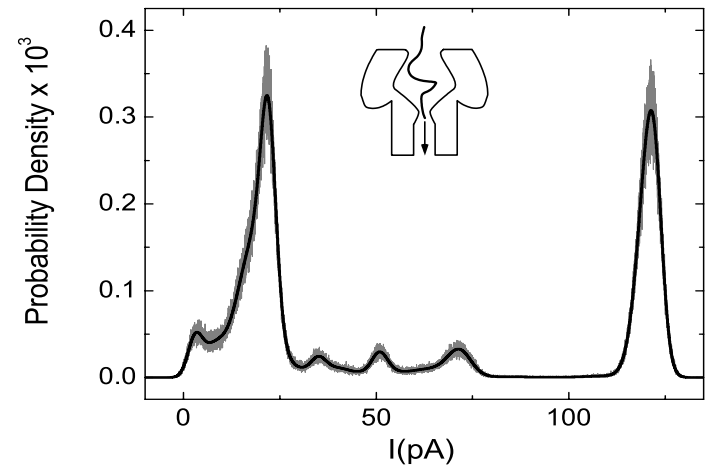
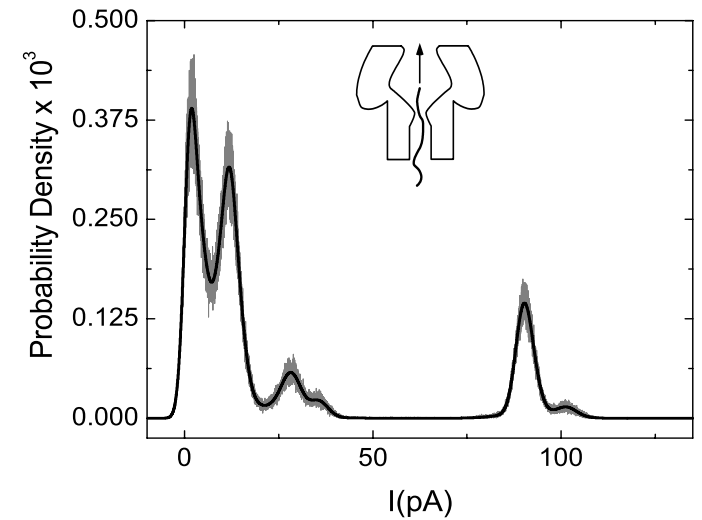
Silver Electroplated

Data Analysis

Decoding Algorithms

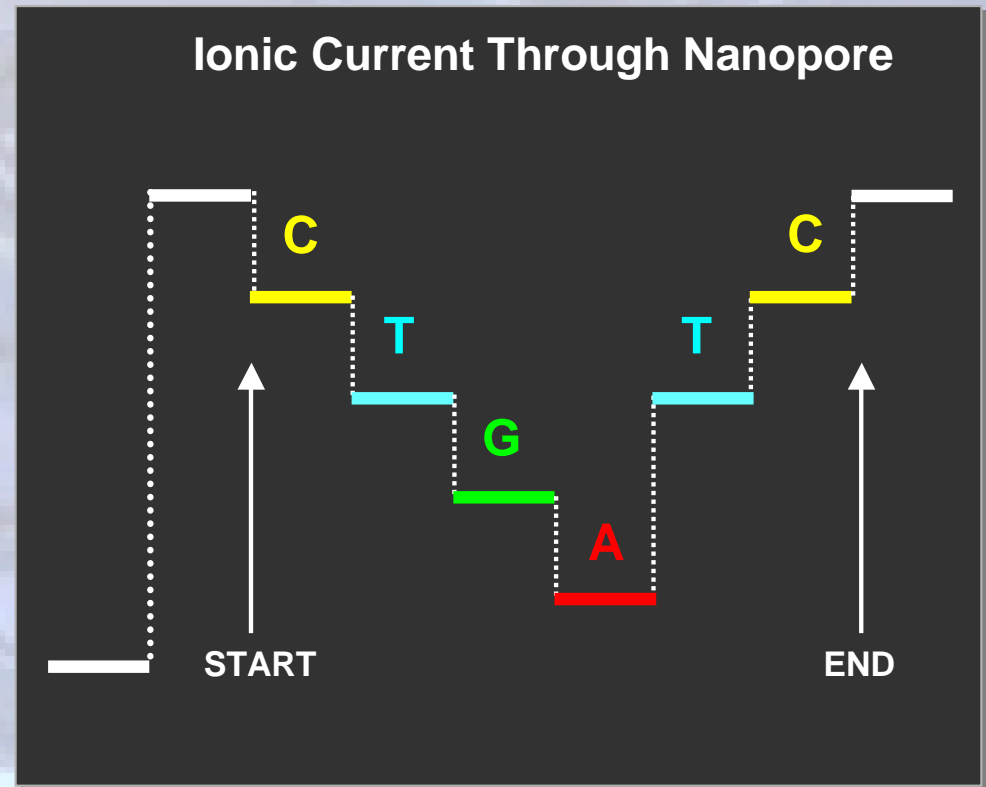
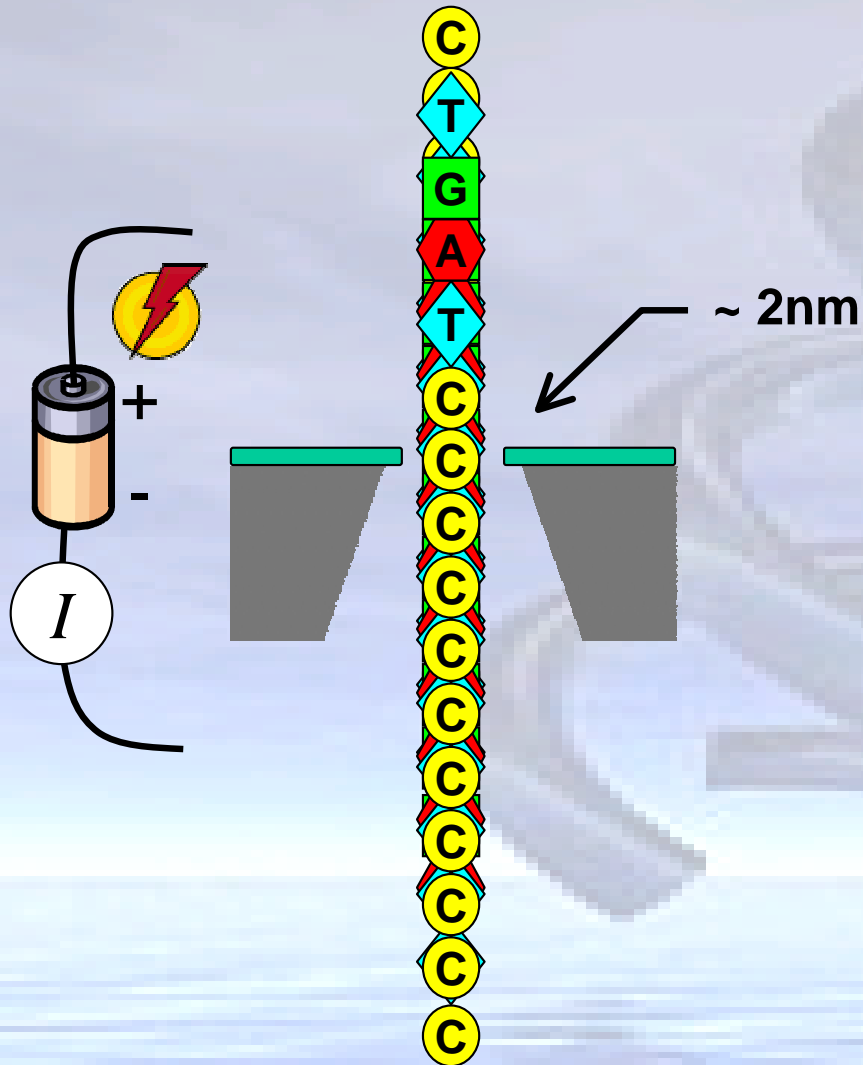


- Identical length DNA molecules cause different signals
- Signal content depends on the transport direction
- Building computer systems & software to decode information in molecules



Future Electronic Measurements

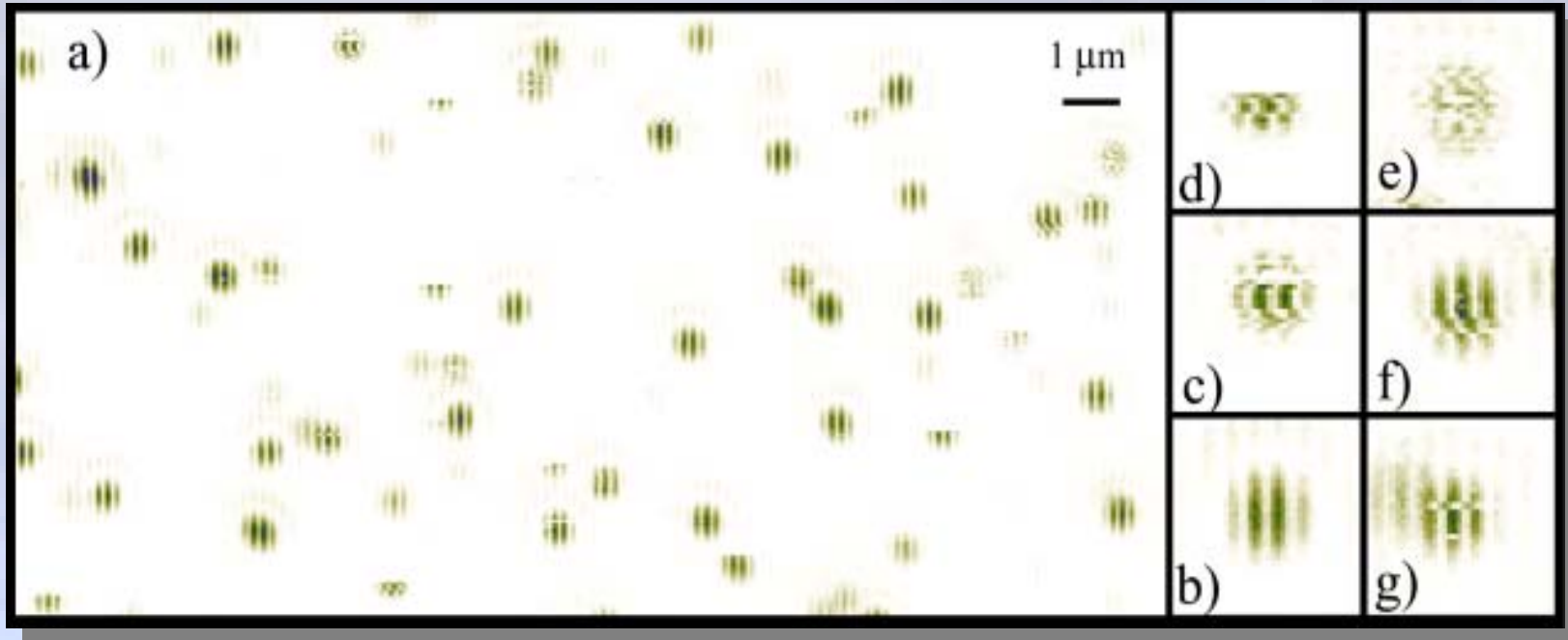
Solid-State Nanopores with base-pair resolution



Potential for Ultra-Rapid
DNA Sequencing Applications

Optical Measurements

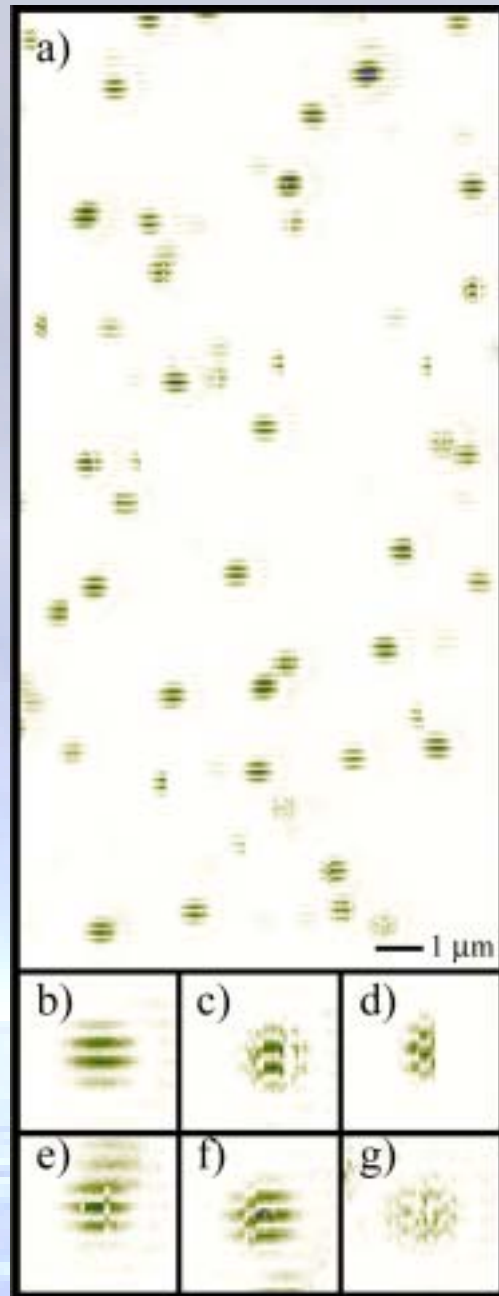
Single Molecule Fluorescence



Rotational Dynamics of Single Dye Molecules in Polymer Films

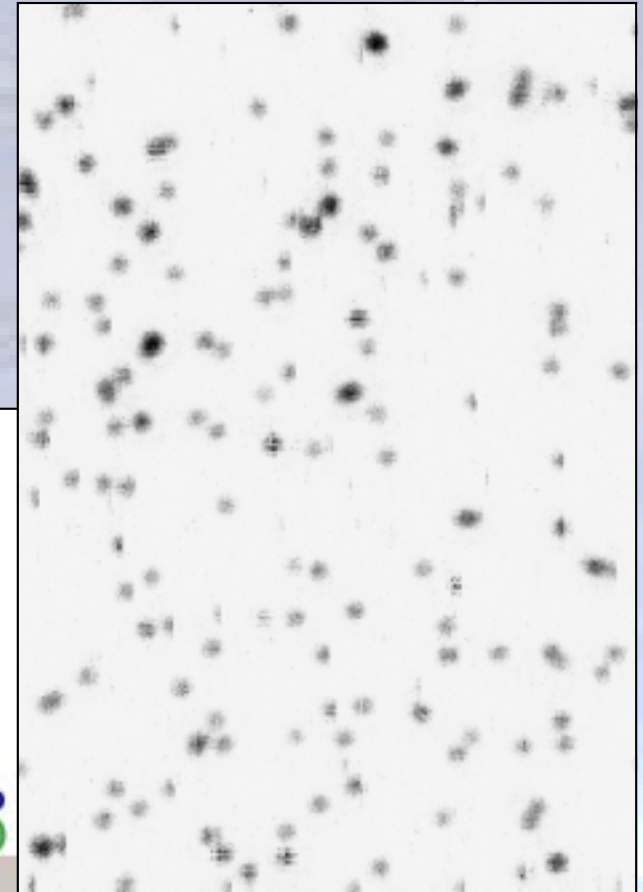
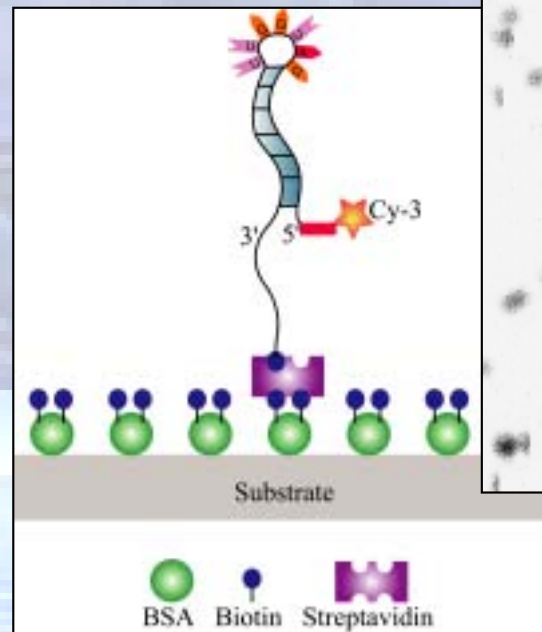
Weston KD, Goldner LS. "Orientation imaging and reorientation dynamics of single dye molecules," J PHYS CHEM B 105: (17) 3453-3462 MAY 3 2001

Activity of Surface Attached Biomolecules

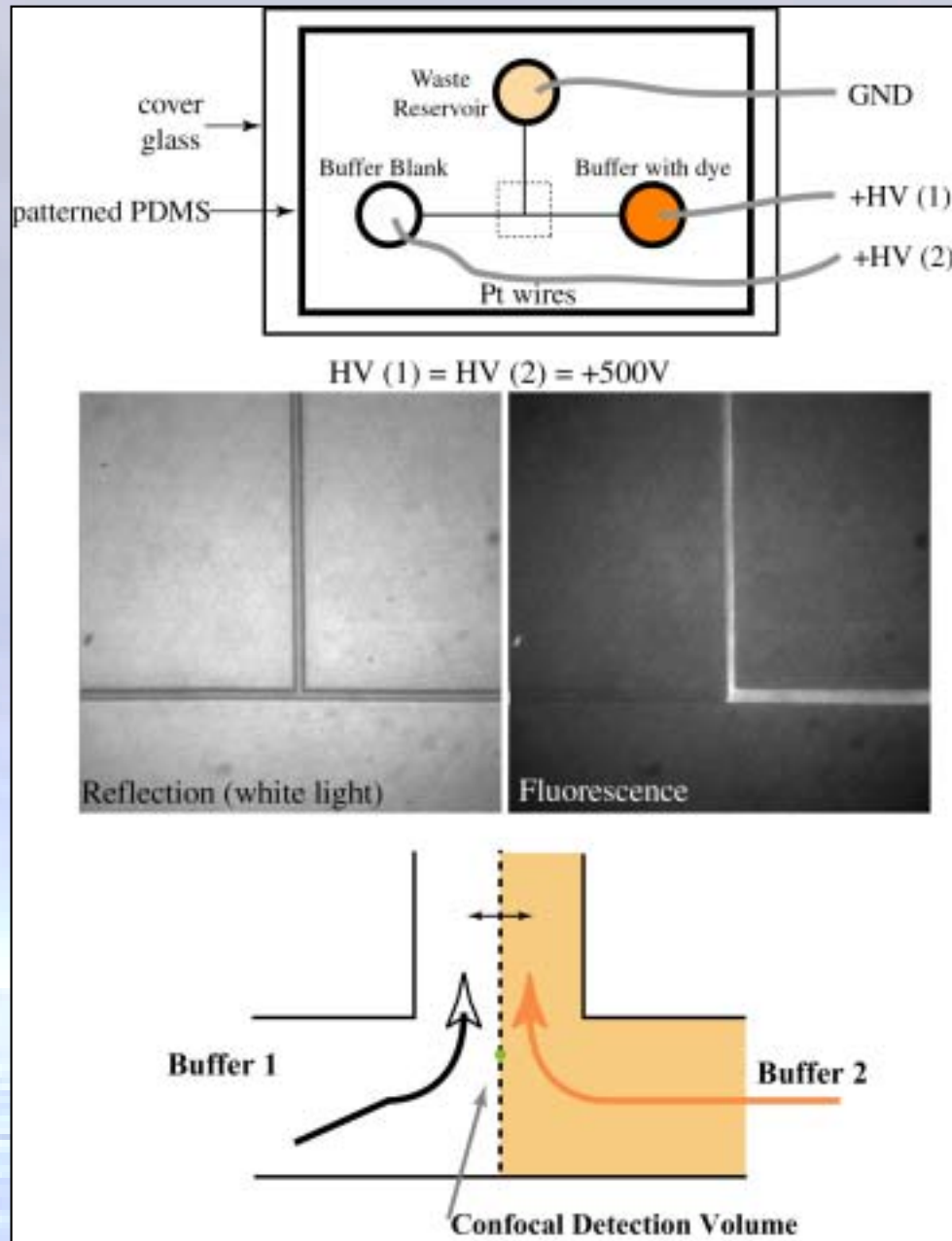


Dye
molecules in
polystyrene

RNA on
biotinylated
glass

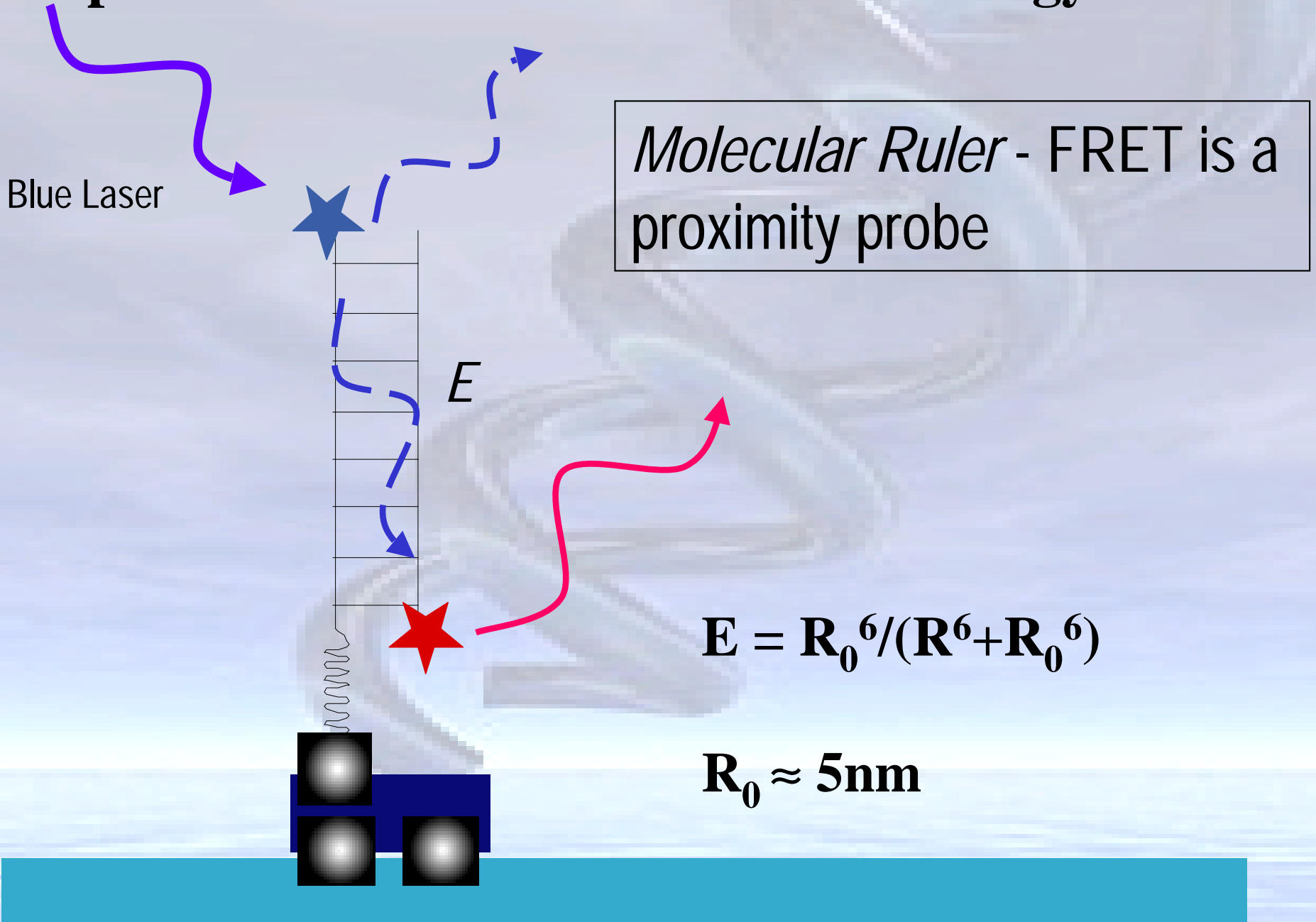


Fluorescence Integrated with Fluidics



- To demonstrate solution modulation in a microchannel device, one arm of a T device was filled with buffer and dye and the other arm was filled with blank buffer.
- Solutions from both flow toward the base of the T (waste) below.
- Electroosmotic force is used to drive the flow. Here the applied voltages HV(1) and HV(2) are held at 500 V and to drive flow.

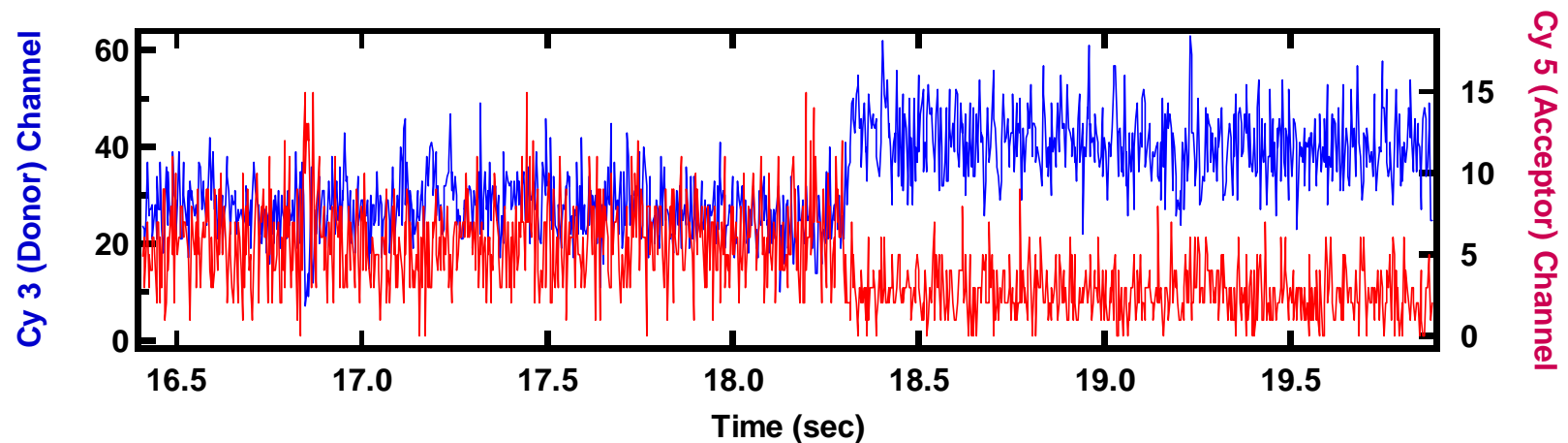
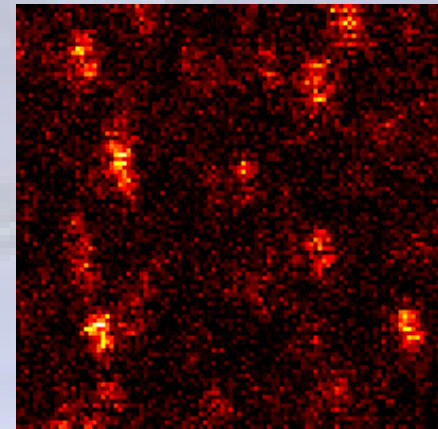
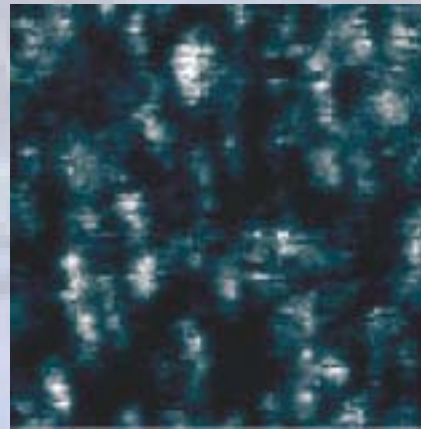
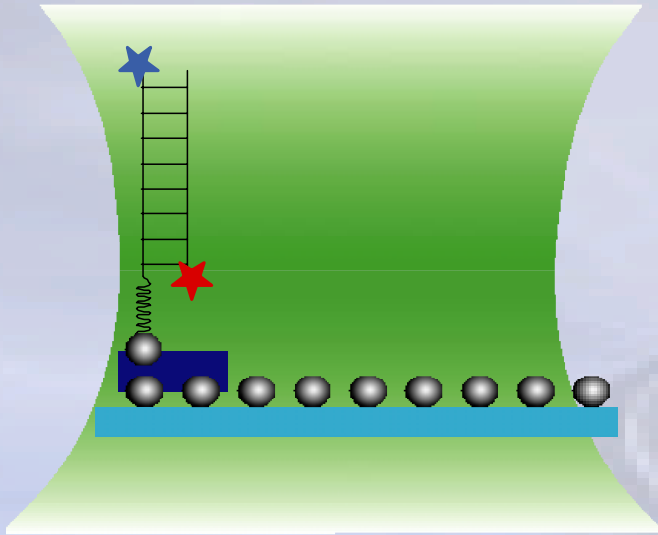
Optical: Fluorescence Resonance Energy Transfer



RNA Structural Analysis

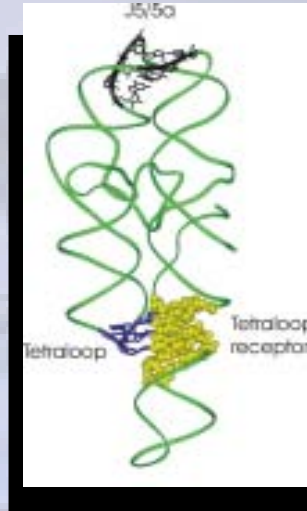
FRET on Surfaces

Simultaneous imaging of fluorescence via direct excitation of Cy3(left) and Cy5 FRET(right).

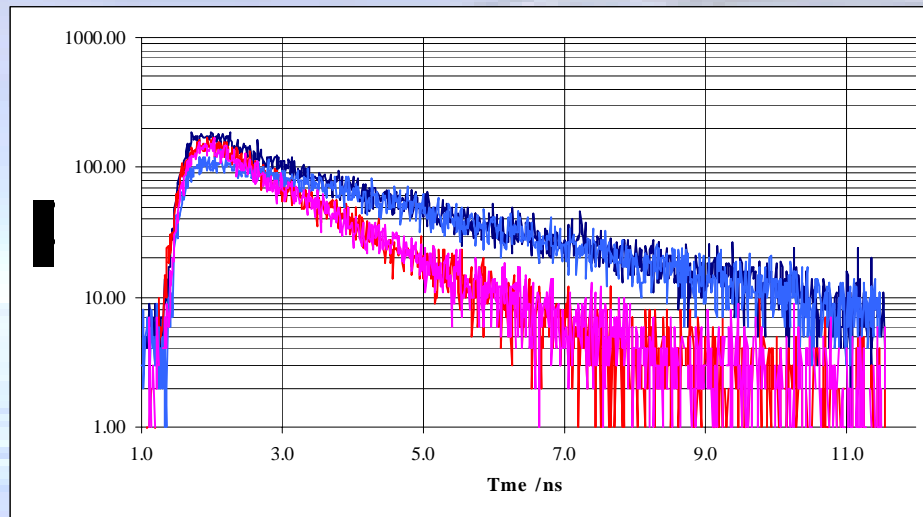


RNA Structural Analysis

FRET in Solution

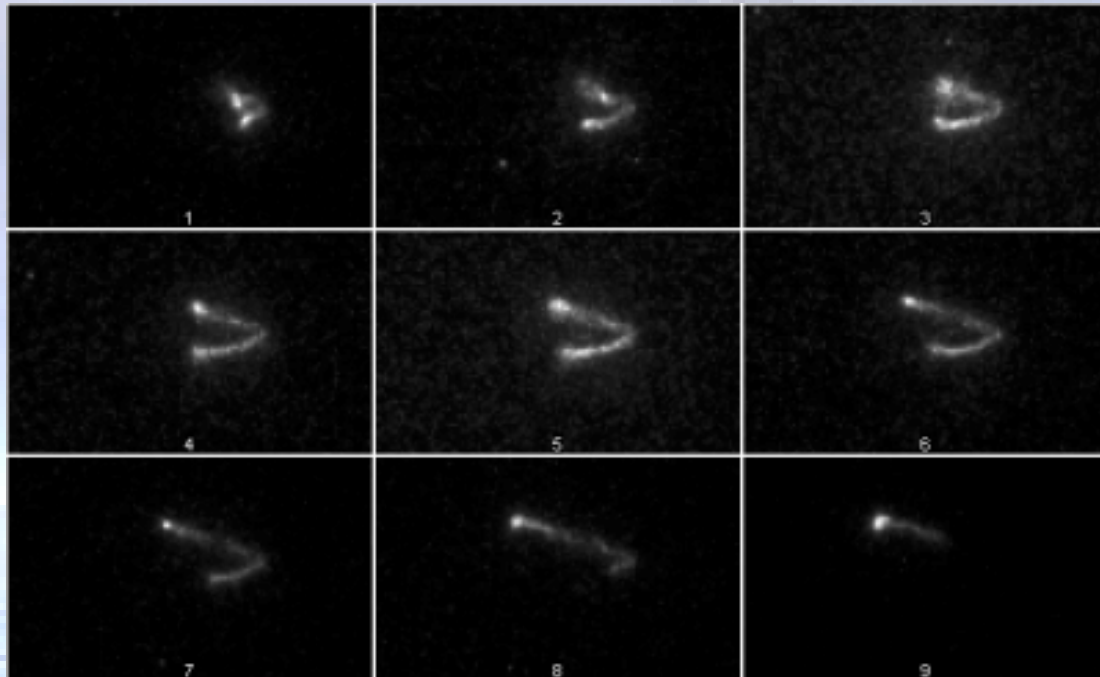


- *Burst Integrated Fluorescence (BIFL)* apparatus designed, constructed and fully operational
- *Time/color/polarization* correlated single photon fluorescence counting at *single* molecule sensitivities
- FRET studies initiated of conformational dynamics crucial to “ribozymal” function



DNA Structure and Dynamics

Single Molecule Electrophoresis

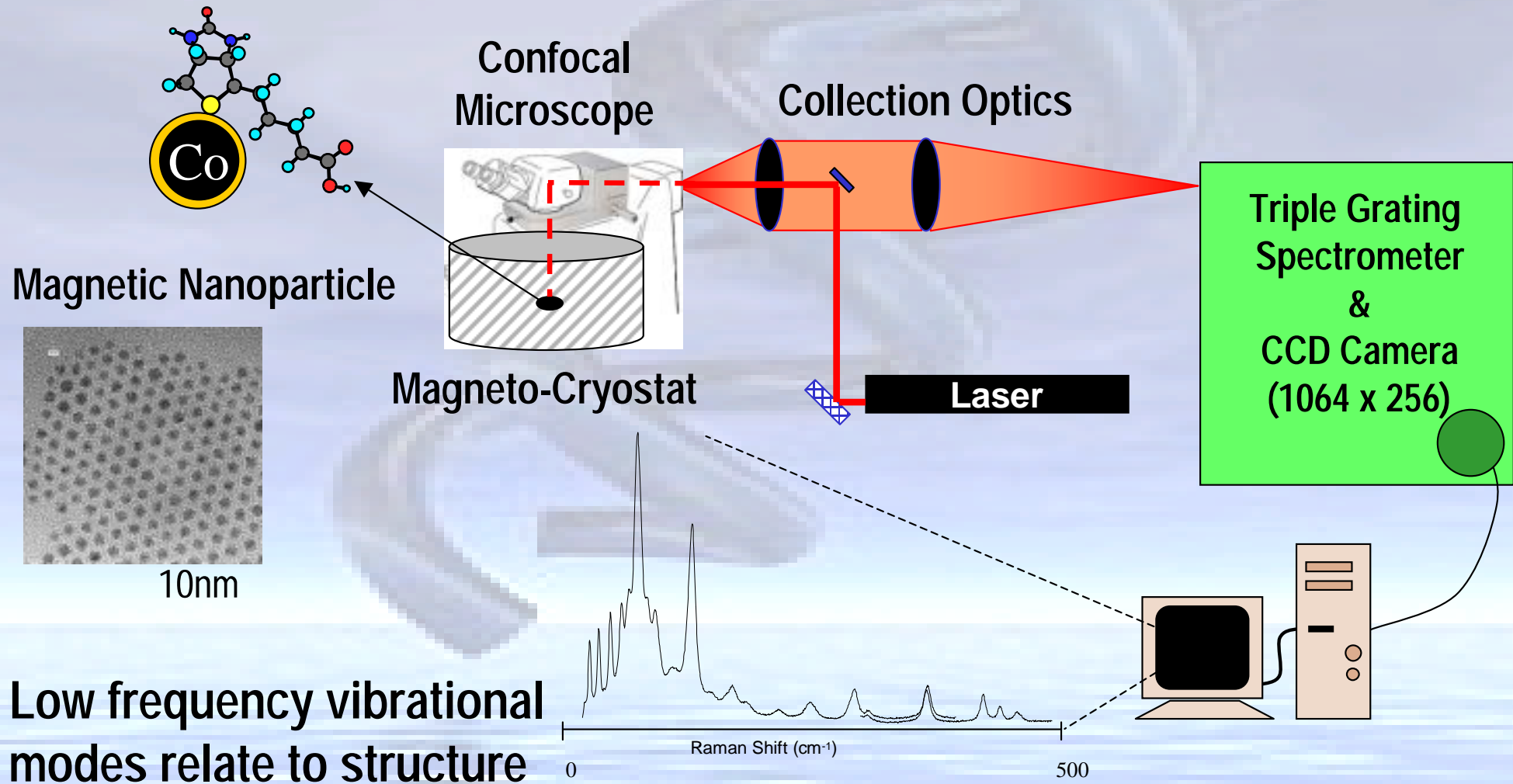


Agarose Gel

- Imaging single molecule DNA transport in fluidic restrictions.
- Transport is linked to structure.

Optical: Vibrational Spectroscopy

Surface Enhanced Raman Spectroscopy

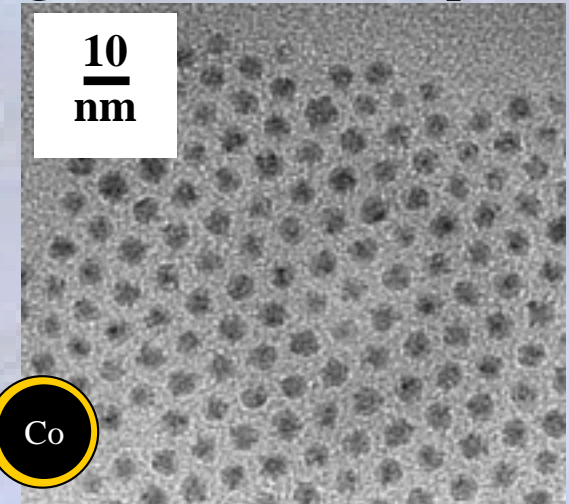


Single Molecule Vibrational Spectroscopy Surface Enhanced Raman Scattering (SERS)

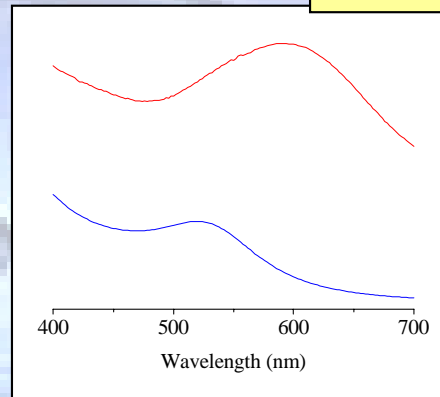
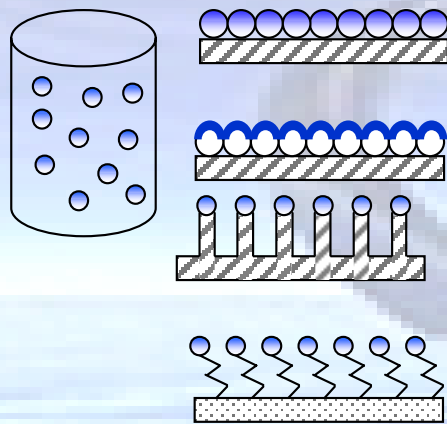
SERS is a spectroscopic technique resulting in strongly increased Raman signals from molecules which have been attached to nanometer sized metallic structures. The enhancement mechanisms, while not fully understood, are generally divided into **electromagnetic** and **chemical** effects. The dominate electromagnetic effect is directly dependent upon the optical properties of the nanostructured surface.

Goal: Quantitative SERS

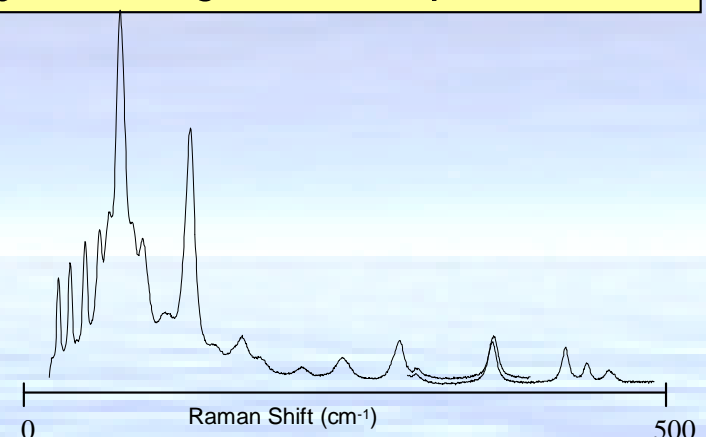
Magnetic Cobalt Nanoparticles



Need gold-coated Co nanoparticles for SM sensitivity **and** magnetic manipulation



UV-VIS of 5 nm Au nanoparticles

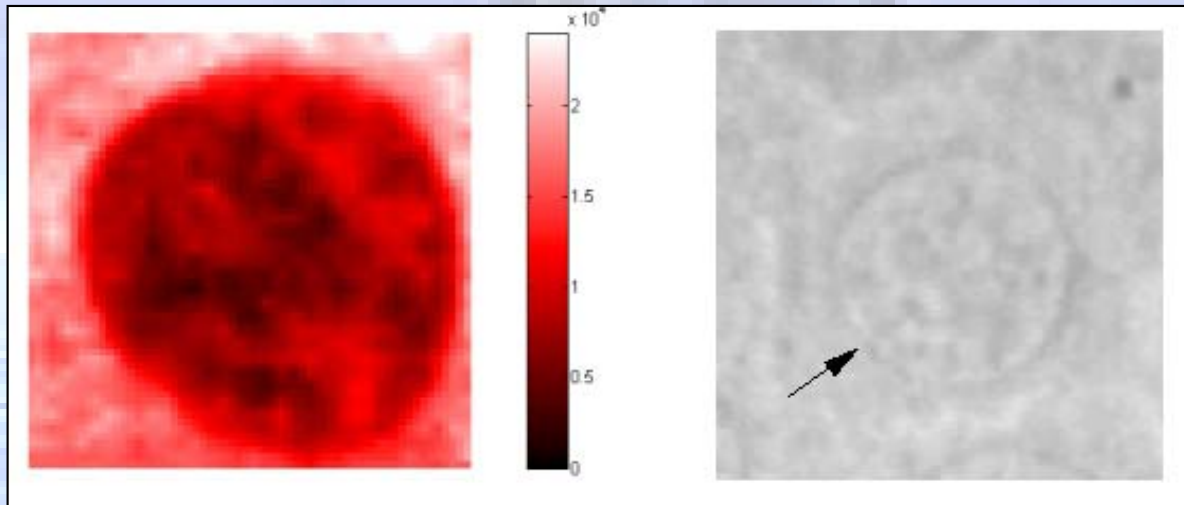
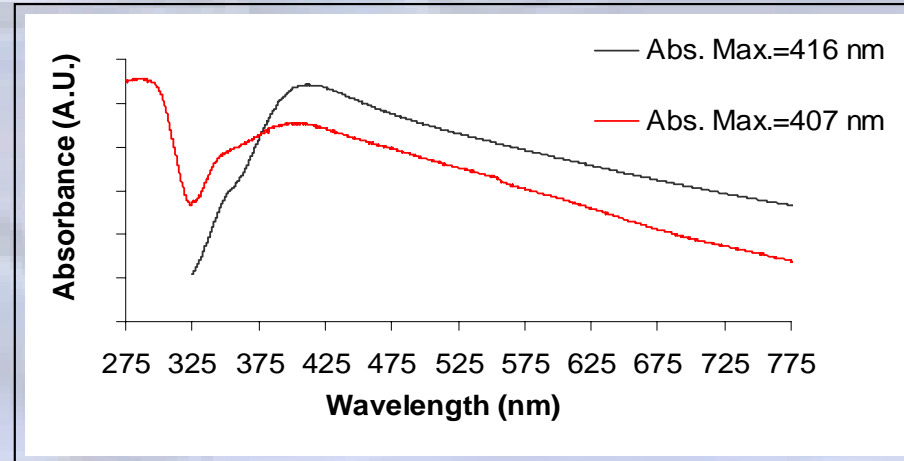
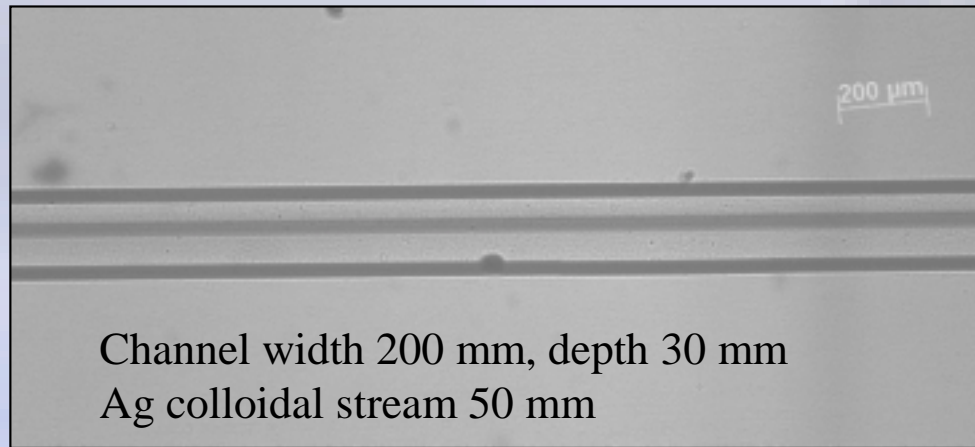


Analyzed vibrational spectra lead to **STRUCTURE!**

Concentrate on low frequency vibrational modes--**detailed structural info!!**

SM SERS: Imaging and Fluidics

Single molecule imaging in micro or nanofluidic devices with nanoparticles made "on the fly"

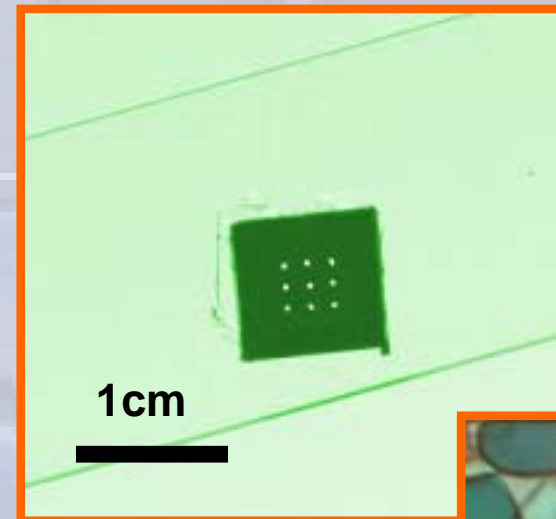
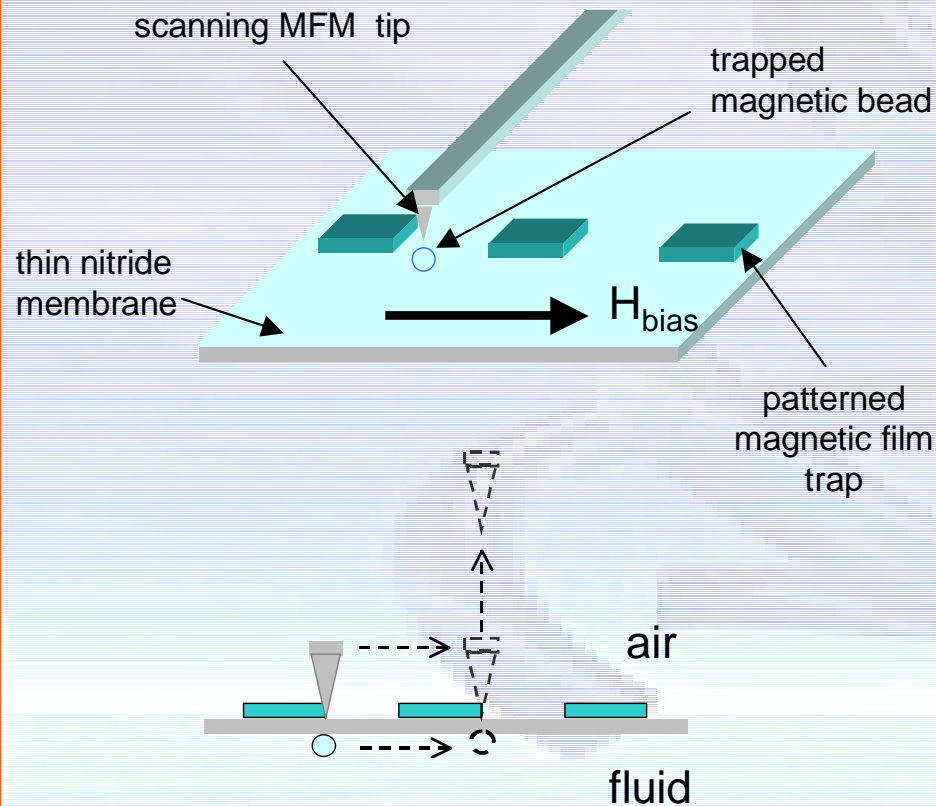


Single molecule
vibrational imaging of
biological samples on
nano structured surfaces

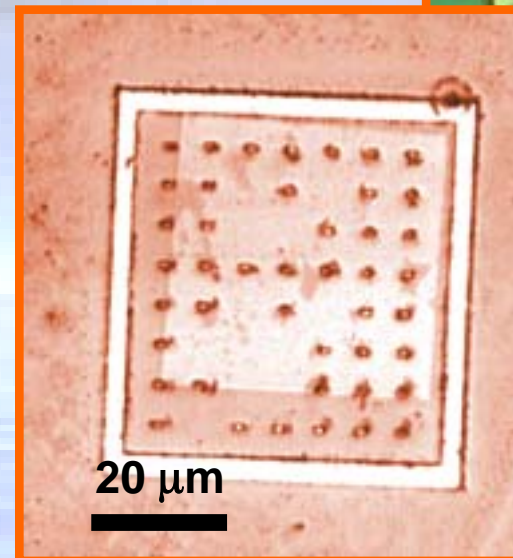
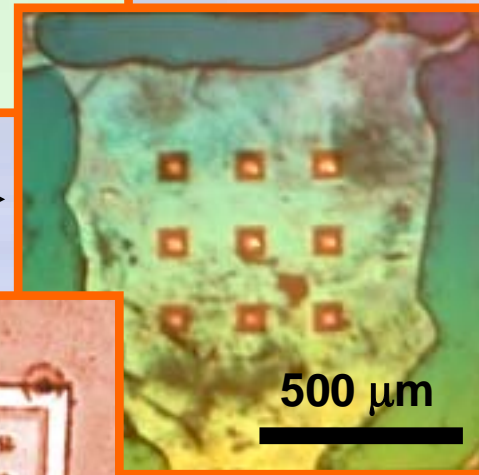
Manipulation

Micromachined magnetic trap fluid cell

Basic concept for single magnetic bead manipulation

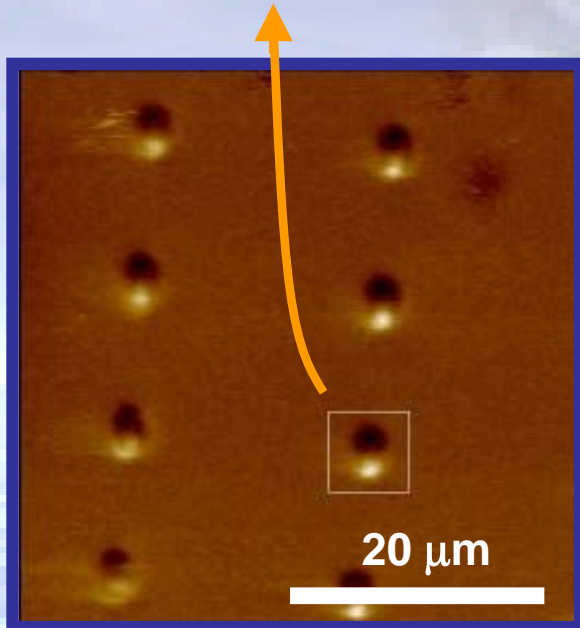
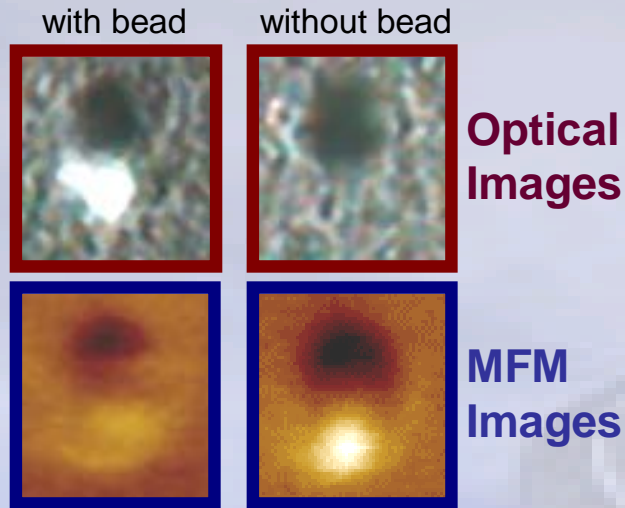


Micromachined wells in Si chip.

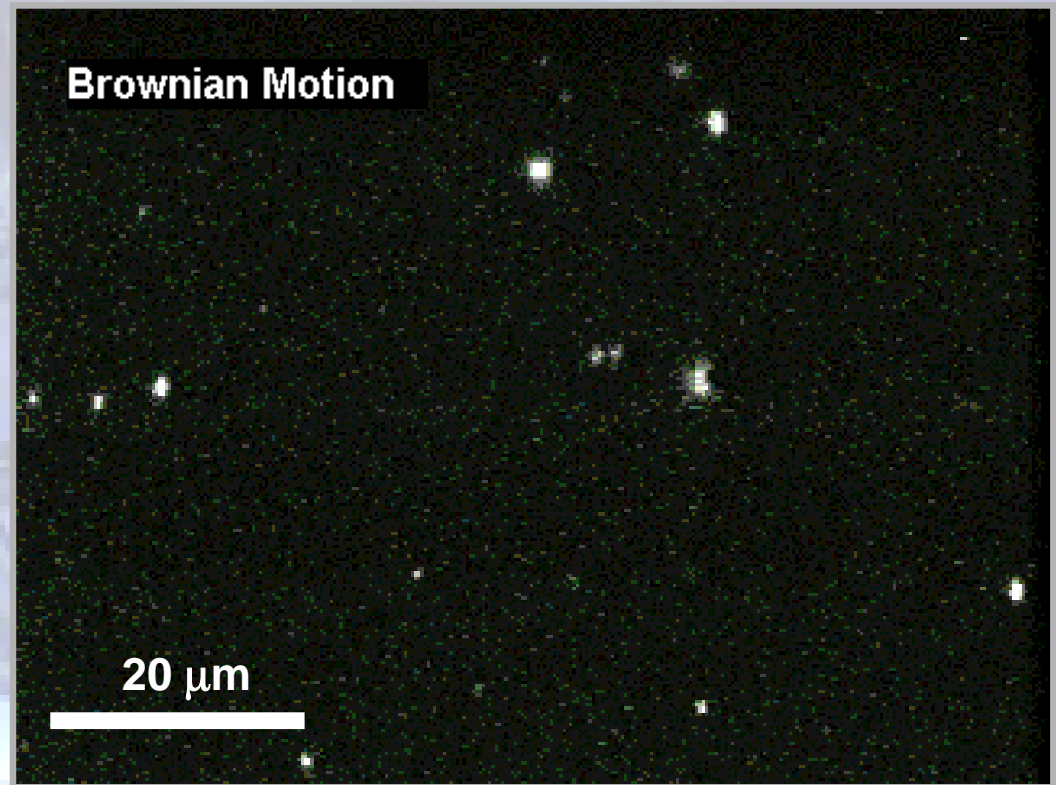


NiFe thin film traps on nitride membrane

Magnetic Bead Trapping and Position Control



Trapping magnetic beads



Fluorescence microscopy video of magnetic beads coated with FITC dye near NiFe magnetic traps with and without applied field ($H_{\text{bias}} = 1 \text{ kOe}$).

Optical/Force Measurements

Simultaneous optical & physical probes

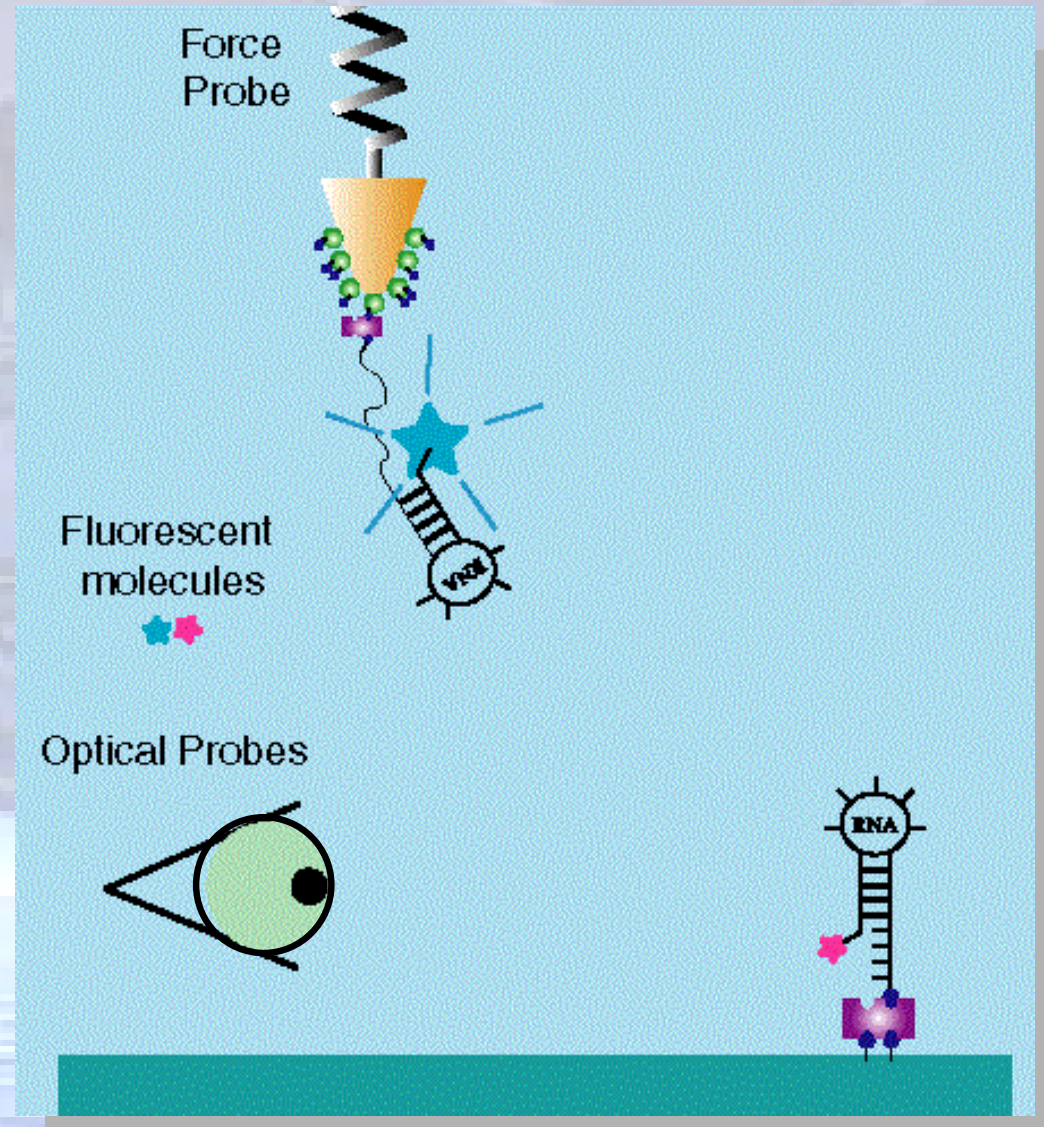
Structure & dynamics of single molecules

Optical Probes

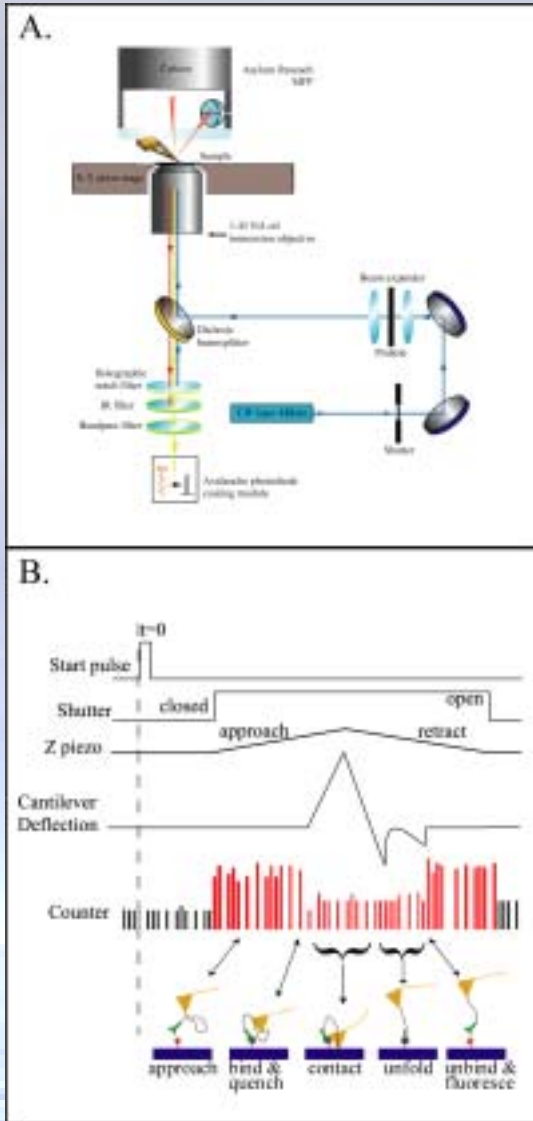
Fluorescence Resonance Energy Transfer (FRET)

Force Probes

Magnetic probes, AFM, Laser tweezers



Simultaneous force and optical measurements of single binding events

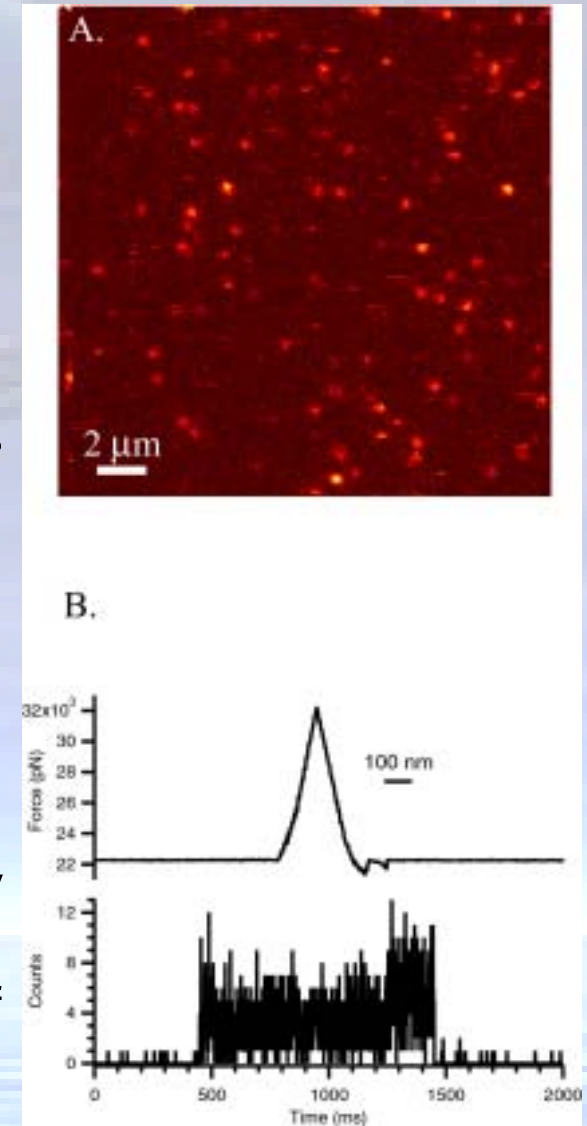


Apparatus for simultaneous force and optical measurements on single molecules

Single fluorescent antigen molecules

Illustration of data sequence

Typical simultaneously acquired force and optical data showing increase of fluorescence upon unbinding

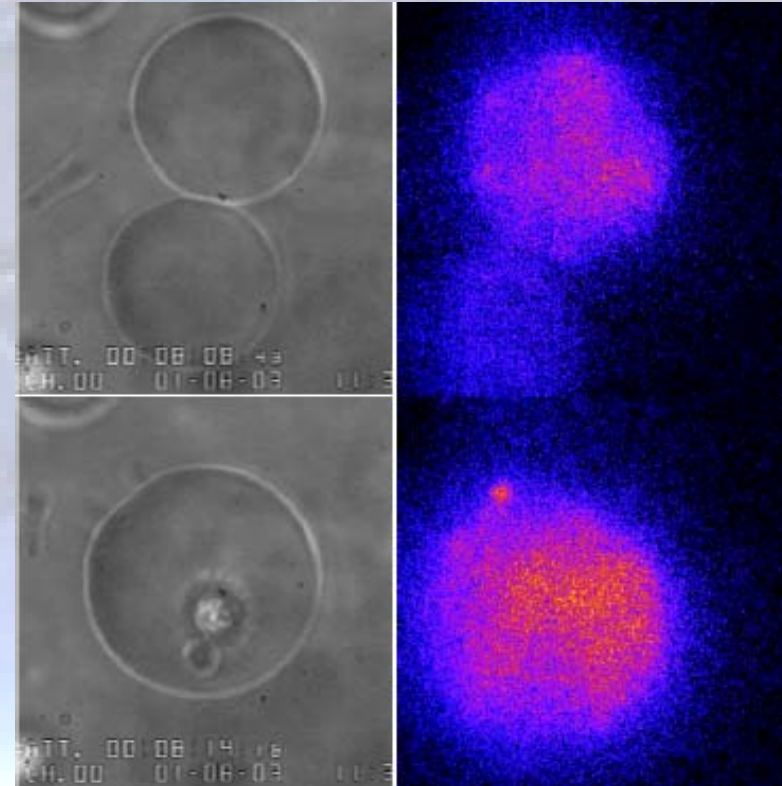


Liposomes

Nanochannels and Nanoreaction Vials



Reactants encapsulated in single liposome or in 2 separate liposomes and fused



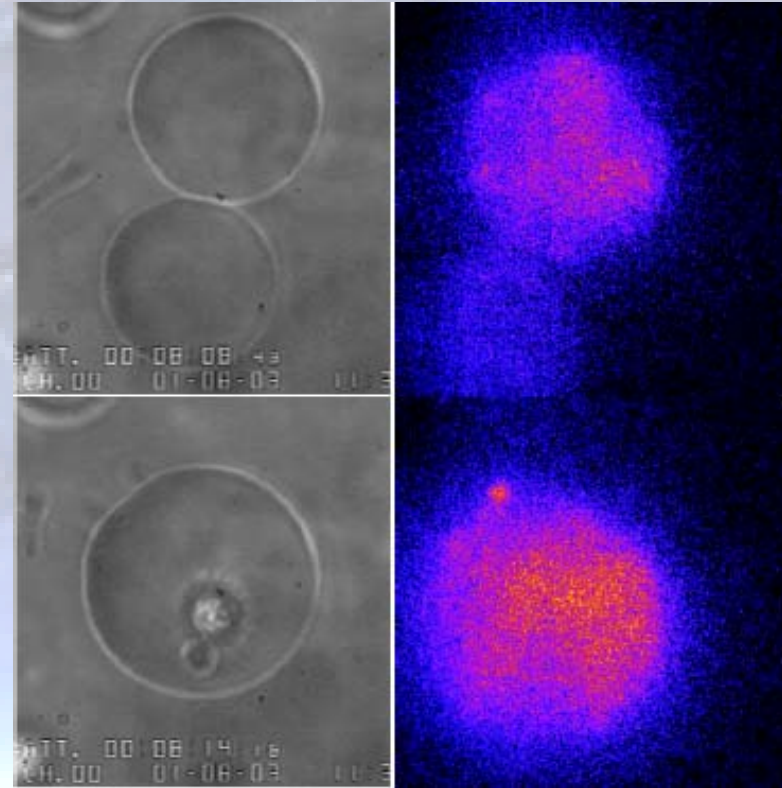
Independently controllable environment, study reaction kinetics, single molecule events

Liposomes

Nanochannels and Nanoreaction Vials

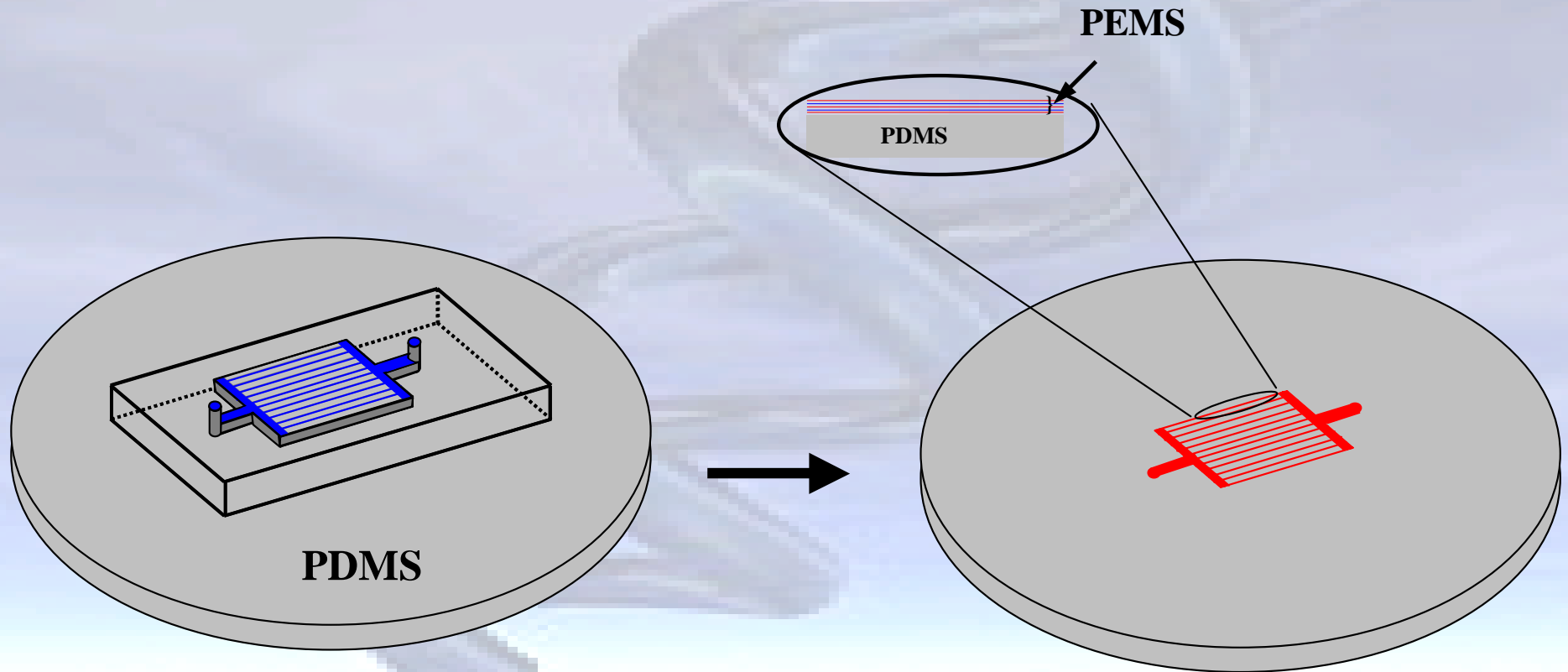


Pull a nanochannel from a liposome



Independently controllable
environment, study reaction
kinetics, single molecule events

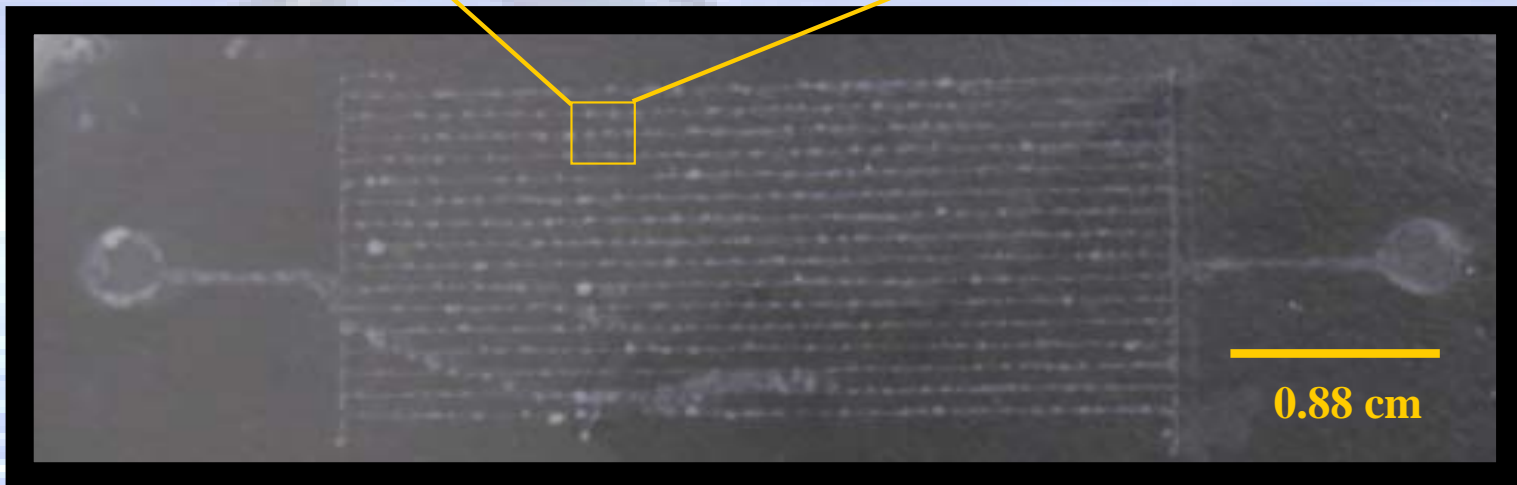
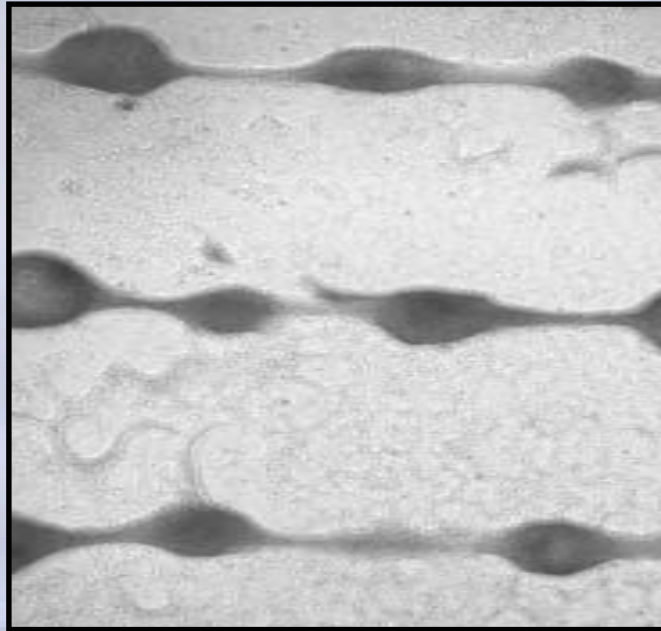
Patterning PDMS with PEMS



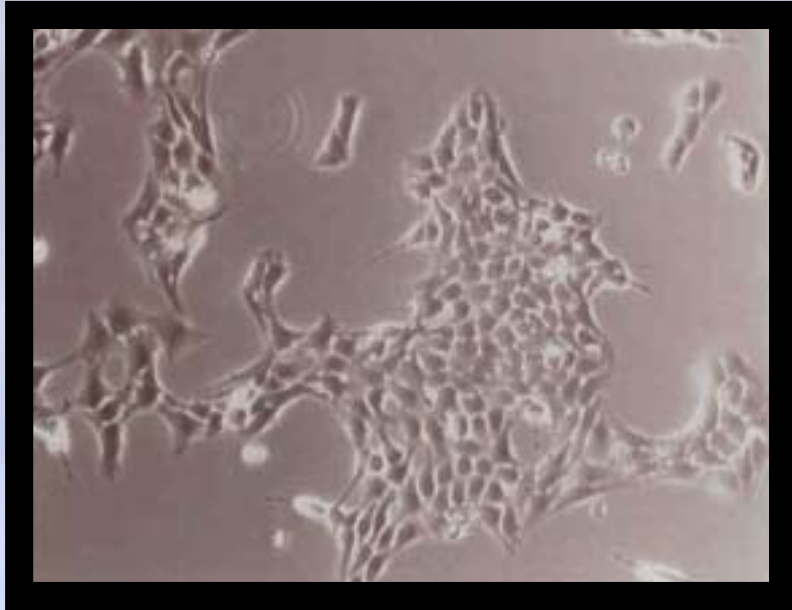
Polyelectrolyte Multilayers (PEMS)

Polydimethylsiloxane (PDMS)

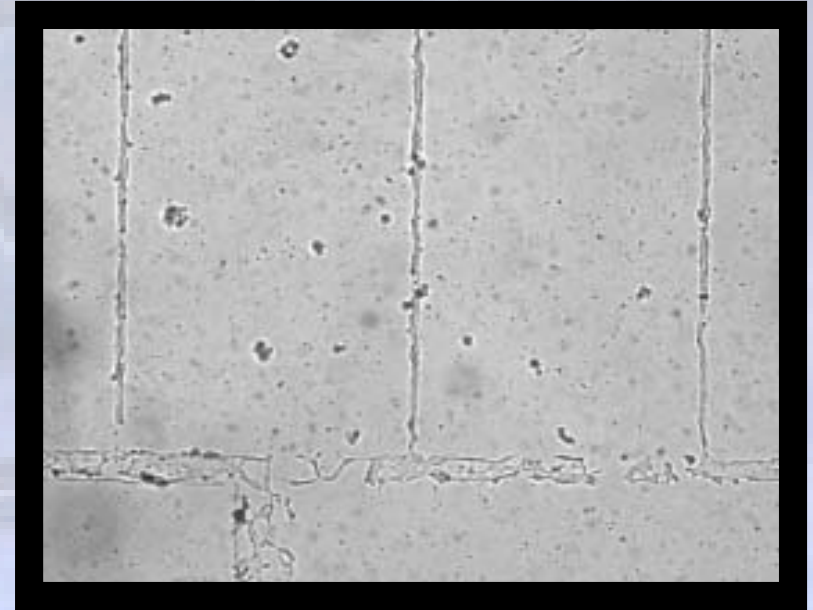
**Two weeks growth of retinal cells on poly(ethyleneimine).
Cells are covering all the polycation area.**



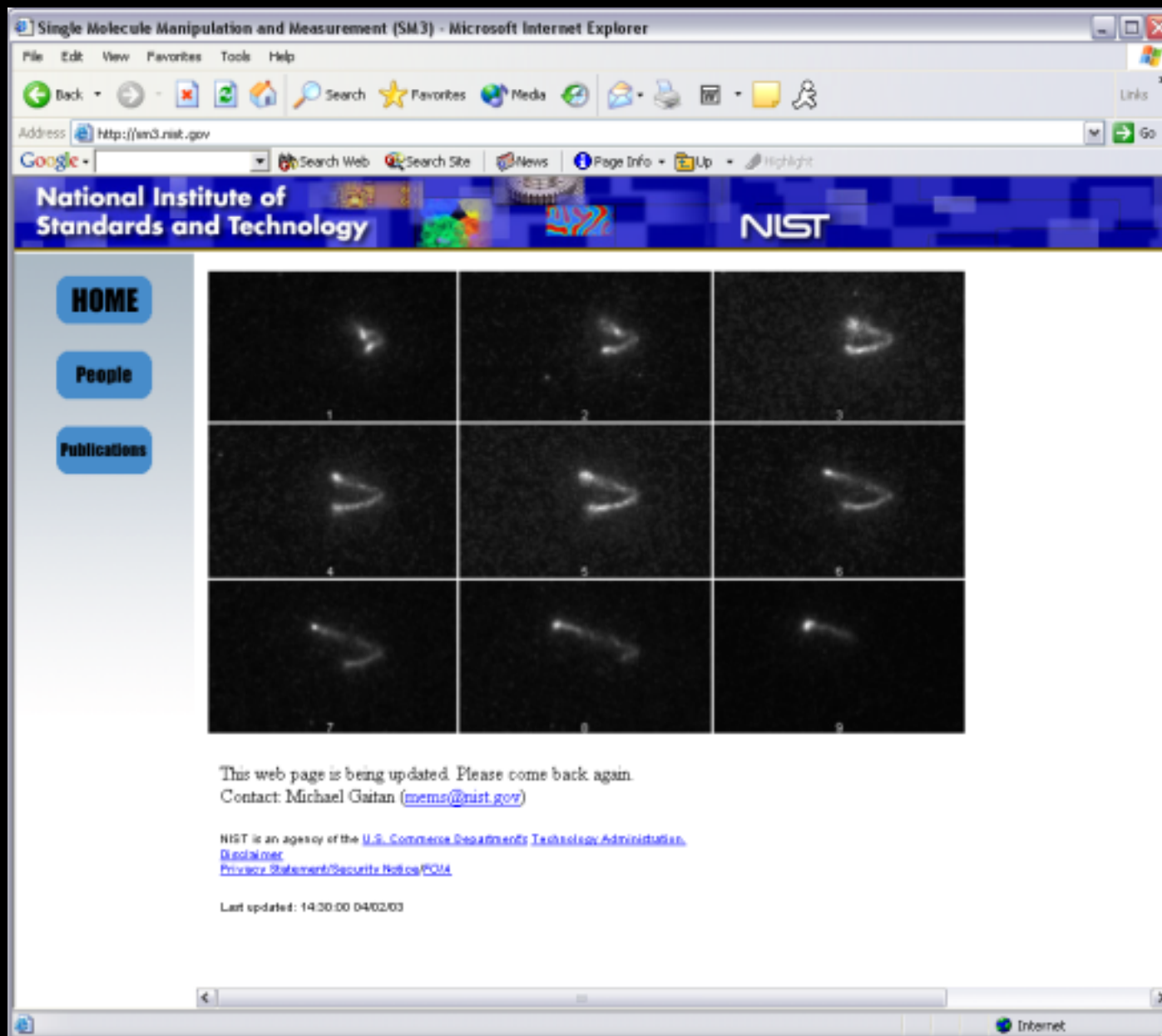
Non-Patterned Cell Growth vs. Patterned Cell Growth



Retinal cells cultured in polystyrene culture flasks.



Overnight growth of retinal cells on poly(allylamine hydrochloride) patterned lines.



<http://sm3.nist.gov>

A Successful SM³ Program Will -

Enhance US competitiveness

Europe and Japan are ahead

Build confidence in bioinformatics

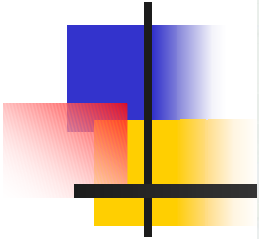
Validation tools for industry

Enable rapid commercialization

Faster, more accurate measurements

Benefit many industries

Healthcare, Nanotech, and IT



Trials and Tribulations of the Application of HTS Methods to Evaluation of PVC Stabilizers

Douglas Wicks and Chunyong Wu
University of Southern Mississippi
October 6, 2003

douglas.wicks@usm.edu



Goals

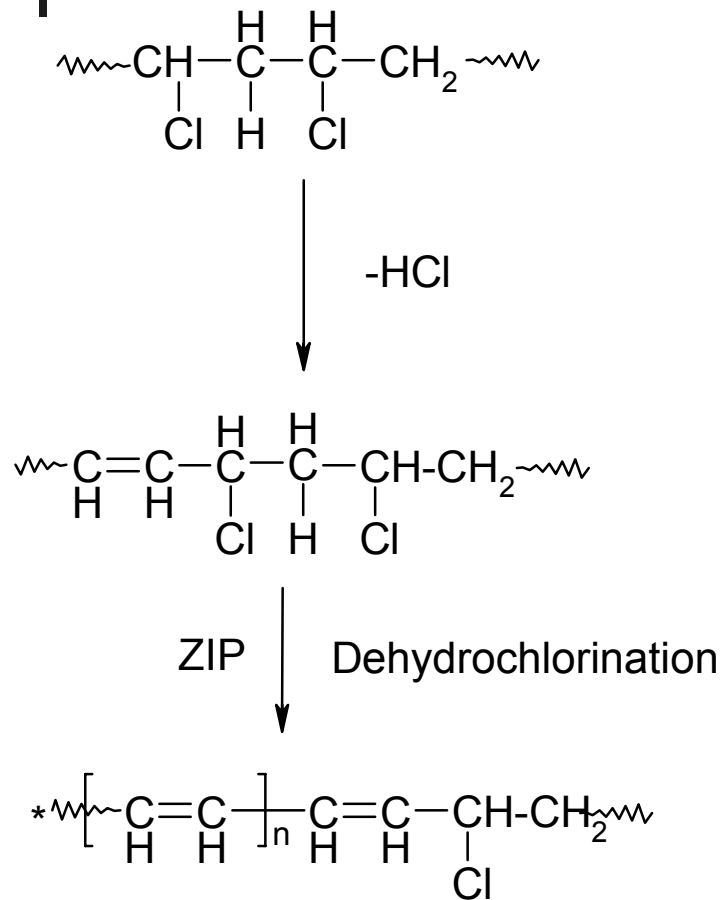
- Create protocols to select PVC stabilizers through HTS
 - Investigate fluorescence emission of PVC during thermal heating
 - Setup methods of sampling and testing
 - Investigate the impact of stabilizers on PVC degradation in terms of PVC type, stabilizer type and ratio, and heating
 - Find lead compositions based on the fluorescence emission of PVC samples



Content

- Fluorescence emission vs. PVC degradation
- Experimental
- Benchmarking of PVC stabilizers
- Sample Preparation
- Impact of stabilizers on PVC stability
 - Fluorescence Emission of PVC Resin
 - Fluorescence Emission of Flexible PVC
- Summary

PVC Degradation at High Temperatures



- Active sites for degradation:
 - Allylic chlorine: propagates dehydrochlorination zip
 - Evolution of HCl: catalyzes degradation
 - Oxygen: accelerates dehydrochlorination through formation of peroxy radicals
- Changes of PVC:
 - Formation of conjugated polyenes sequence of 5 to 30 double bonds
 - Reactive conjugated polyenes crosslink or cleave the polymer chain
 - Color changes parallel the amount of degradation running from yellow to brown to black



Heat Stabilizer for PVC

- Stabilizer groups by functionalities
 - Primary stabilizers react with allylic chlorine and methylene hydrogen
 - Secondary stabilizers scavenges hydrogen chloride
- Classes of stabilizers
 - Alkyltin: mono and dimethyl-, butyl-, and octyltin alkyl thioglycolates, mercaptopropionate and alkyl maleates
 - Mixed metal carboxylates
 - Alkyl phosphite
 - Beta-diketones
 - Epoxidized Fatty Acid Esters
 - Hydroxycarbonates of Mg and Al
- Commercial stabilizers contain combinations

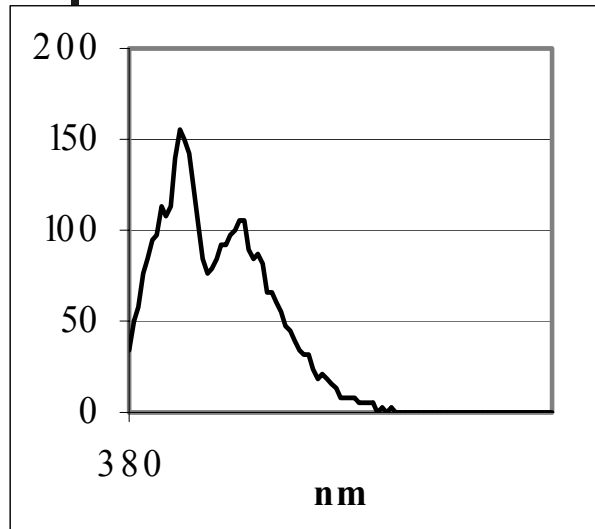


Fluorescence vs. PVC Degradation

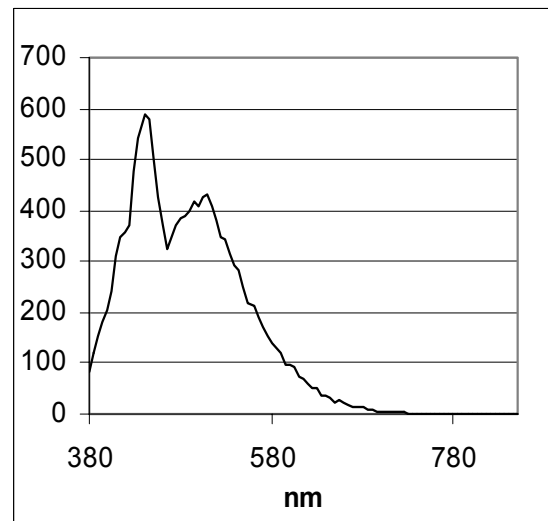
- Fluorescence emission of conjugated triene or tetraene in degraded PVC
 - Emission at 410nm under 325nm excitation
 - Norman S. Allen, John Wooler, Polym. Degrad. & Stabil, (13), 1985
 - Emission at 500nm and 720nm under 360nm excitation
 - C.E.James and R.C. Poller, Eur. Polym.J. (22),1980
- Longer polyenes in deeply degraded PVC have little fluorescence emission
- PVC without stabilizer has weaker fluorescence emission compared with PVC containing stabilizers

Fluorescence Emission of PVC Resin with 360nm excitation

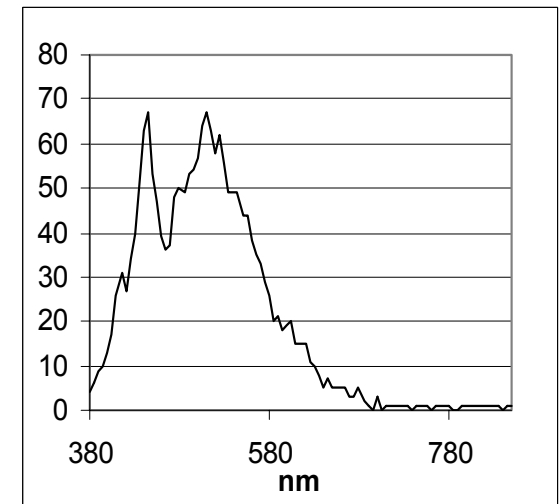
Resin: 99.5% suspension PVC Sample from Georgia Gulf



Resin without heating



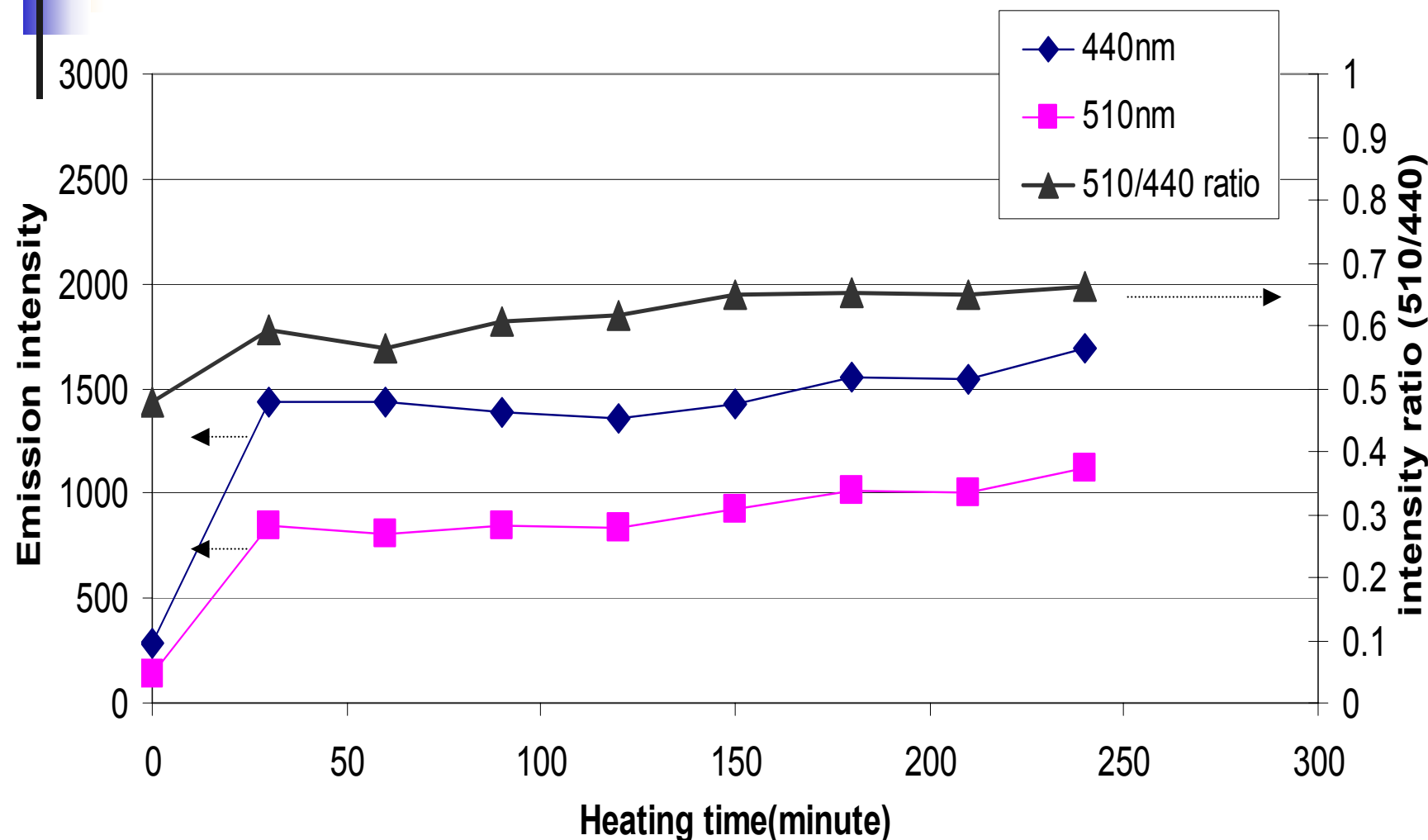
*Resin heated at 180°C
for 12 hours*



*Resin heating at 200°C
for 12 hours*

- Fluorescence Emission Peak at 440nm and 510nm
- Increased intensity with moderate degradation at 180°C
- Reduced intensity after deep degradation at 200°C
- Increased ratio between 510nm emission and 440nm emission

Fluorescence Emission of PVC Powder during Degradation at 200°C





HTS Experimental

■ Materials

- PVC resin, flexible PVC and stabilizer are provided by Georgia Gulf
- 5% or 10 % PVC was dissolved in THF
- 0.5% stabilizers was dissolved in THF

■ Microplates

- 96-well Aluminum multi-tier plates was made by USM Mechanic Shop
- 0.5ml glass flat-bottom inserts were purchased from Biotech Solutions, Inc.

■ Sampling and testing

- PVC and stabilizer mixtures were prepared by Biomek FX liquid handler from Beckman Coulter
- Solvent was evaporated by heating below 100°C with air ventilation
- PVC degradation was conducted with different intervals at 180°C and 200°C (drying ice was used to quickly cool the plates)
- Fluorescence emission at 440nm and 510nm under 360nm excitation were measured by Safire Microplate Reader from Tecan
- Data were analyzed by using Spotfire DecisionSite as query tools

PVC Materials from Georgia Gulf

PVC sample	Formulation	Function	Chemical Name	Loading(wt %)
PVC Neat Resin		Polymer	PVC	99.5~99.9
Flexible PVC	PVC resin	Polymer	PVC	69.27
	J251	Plasticizer 50/50	Di-isoheptaalkyl phthalate	28.45
			Di-isononylalkyl phthalate	
	ESO	Co-stabilier/plasticizer	Epoxidized soybean oil	2.51
	Mineral oil			0.17

PVC Stabilizers Provided by Georgia Gulf

Tradename	Usage	Vendor	Comp
Thermchek 152	Flex PVC	Ferro	Ba/Zn
BC4746S	Flex PVC	AKCROS	Ba/Cd
Mark T-201	Rigid PVC	Witco	Tin Thiols
Mark 1900	Rigid PVC	Witco	Tin Thiols
TM-404	Rigid PVC	Rohm & Haas	Tin Mercaptide
TM-2080	Rigid PVC	Rohm & Haas	Tin Thiols and Esters

Biomek FX



Safire Microplate Reader

Microsoft Excel - Book1

File Edit View Insert Format Tools Data Window XFluor4 Help


A27 =

	A	B	C	D	E	F	G	H	I	J	K	L	M	N	O	F
1	SAFIRE;	Serial number: 12901300185;	Firmware: V 2.10 04/02	SAfire;												
2	Date:					17/1/03										
3	Time:					21:22										
4																
5	Measurement mode:					Fluorescence Top										
6	Excitation wavelength:					485 nm										
7	Emission wavelength:					520 nm										
8	Excitation bandwidth:					12 nm										
9	Emission bandwidth:					12 nm										
10	Gain (Manual):					100										
11	Number of flashes:					10										
12	Lag time:					0 µs										
13	Integration time:					40 µs										
14	Plate definition file:					NUN96ft.pdf										
15	Z-Position (Manual):					4016 µm										
16																
17	Rawdata					Temperature: 26.2 °C										
18	<>	1	2	3	4	5	6									
19	A	137	149	154	147	154	255									
20	B	144	164	158	168	146	146									
21	C	151	145	144	148	145	146									
22	D	153	150	158	137	157	150									
23	E	148	140	144	148	127	136									
24	F	139	142	139	144	165	161									
25	G	145	147	146	143	150	157									
26	H	154	143	144	140	149	133									
27																
28																
29																
30																
31																
32																
33																
34																
35																

Sheet1

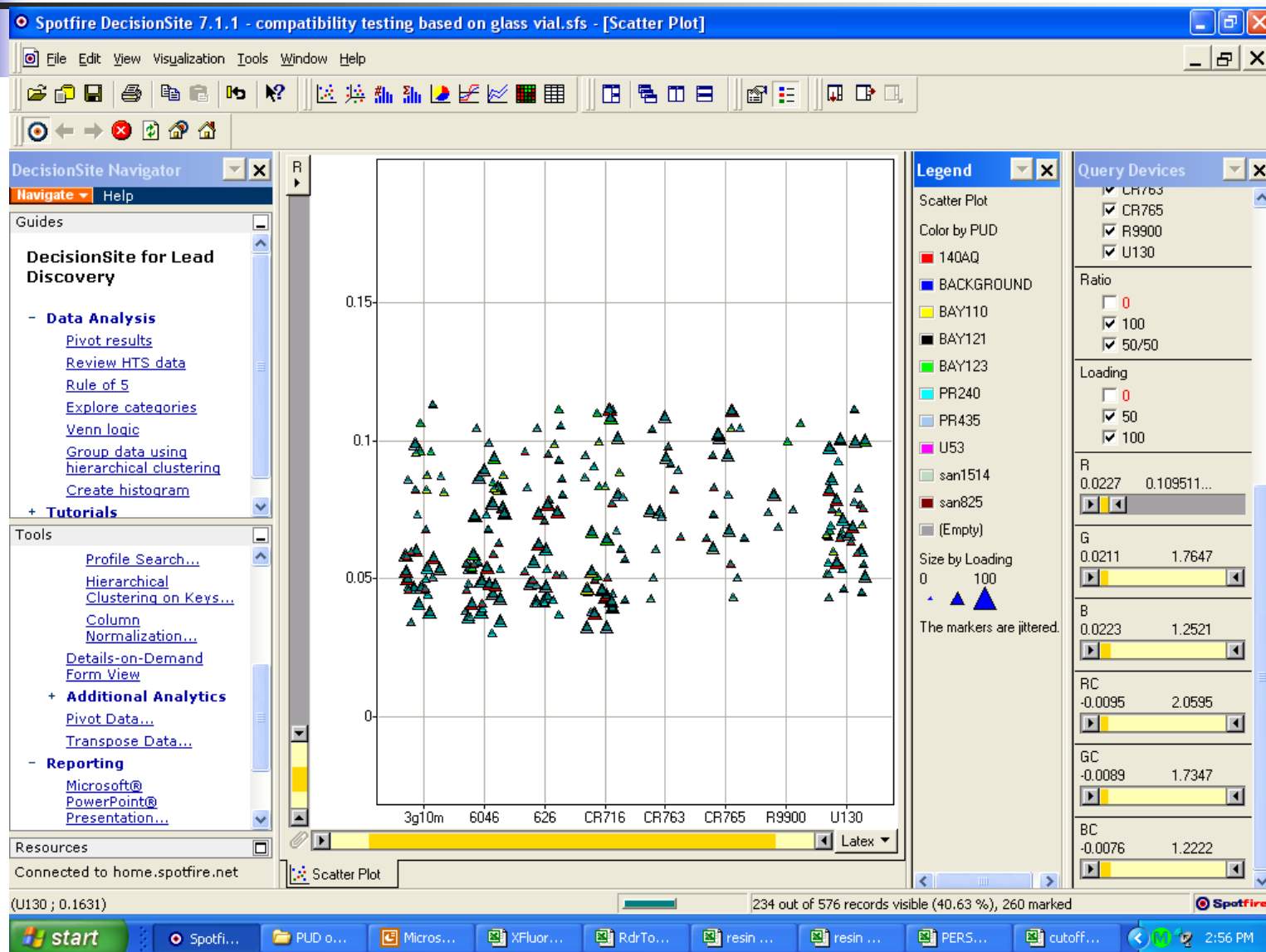
Ready NUM

start XFluor4.xls RdrTool4.xls Doc1.doc - Microsoft ... Book1 9:23 PM



SpotFire DecisionSite

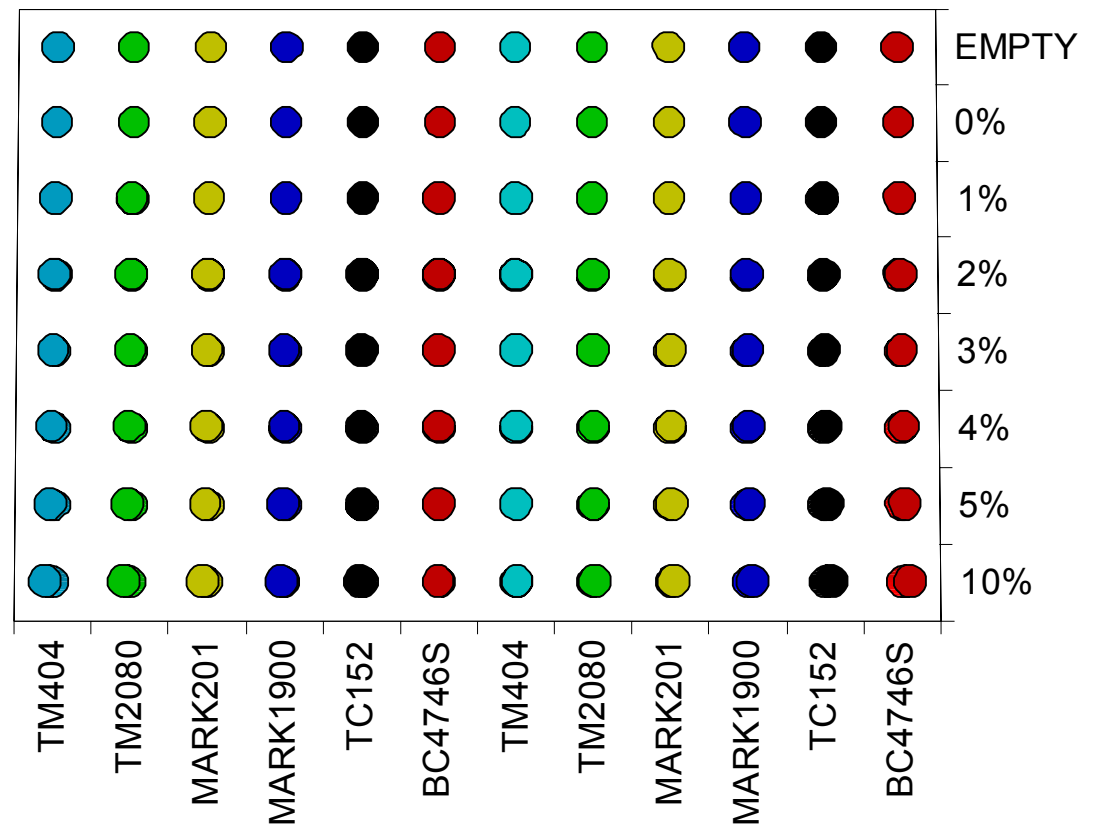
HTS@USM



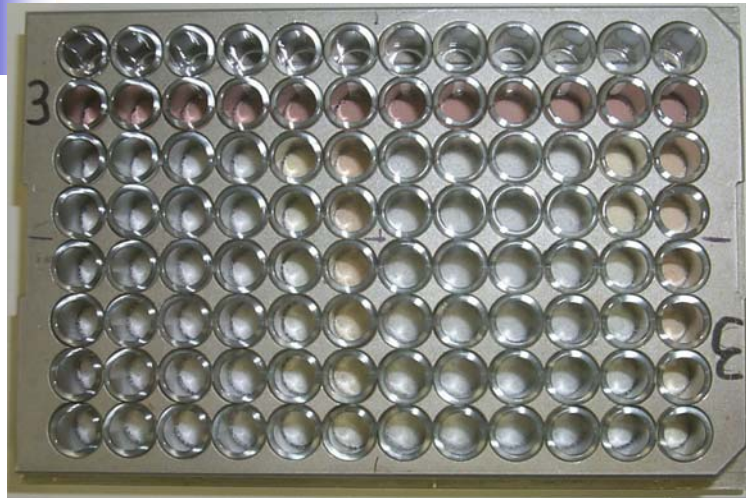
Benchmarking of PVC Stabilizers

Sample Layout on plate

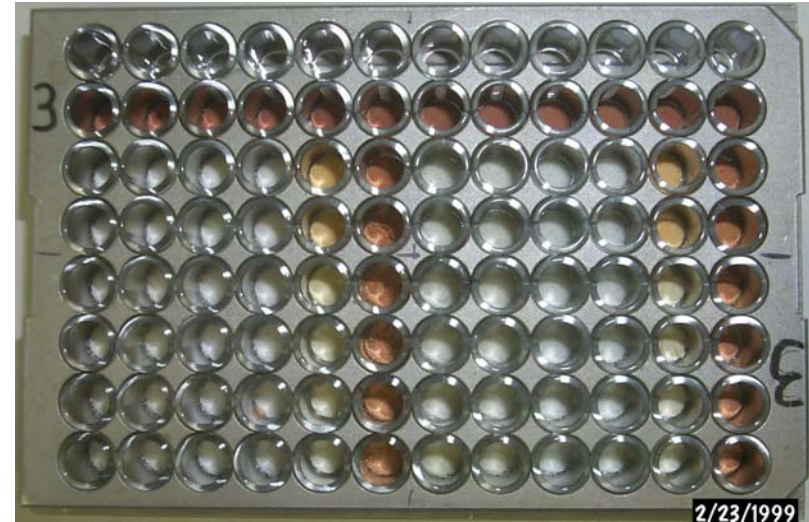
- Purpose:
 - Check qualitative impact of stabilizers on PVC degradation
- Testing Procedures
 - Mix PVC resin powder and stabilizers
 - Record fluorescence at 440nm and 510nm after heating
 - Compare Fluorescence and color change in terms of stabilizers



Coloring of Benchmarking Samples



30minutes at 200°C



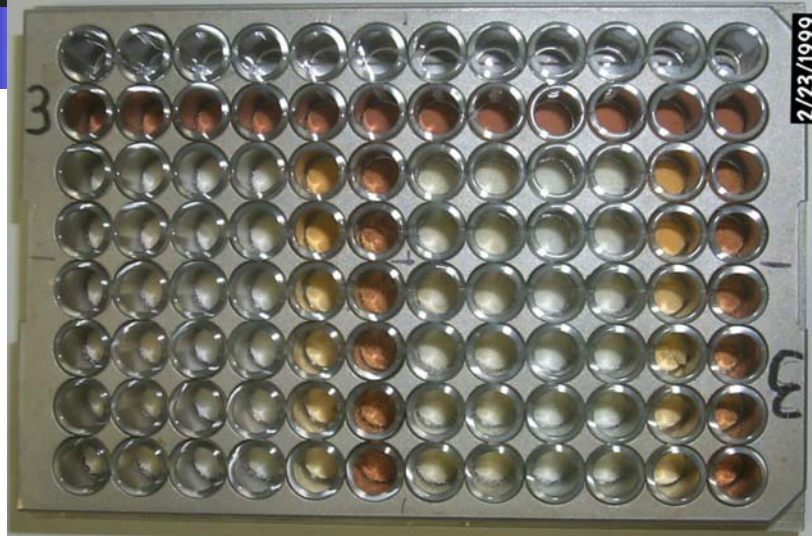
120minutes at 200°C



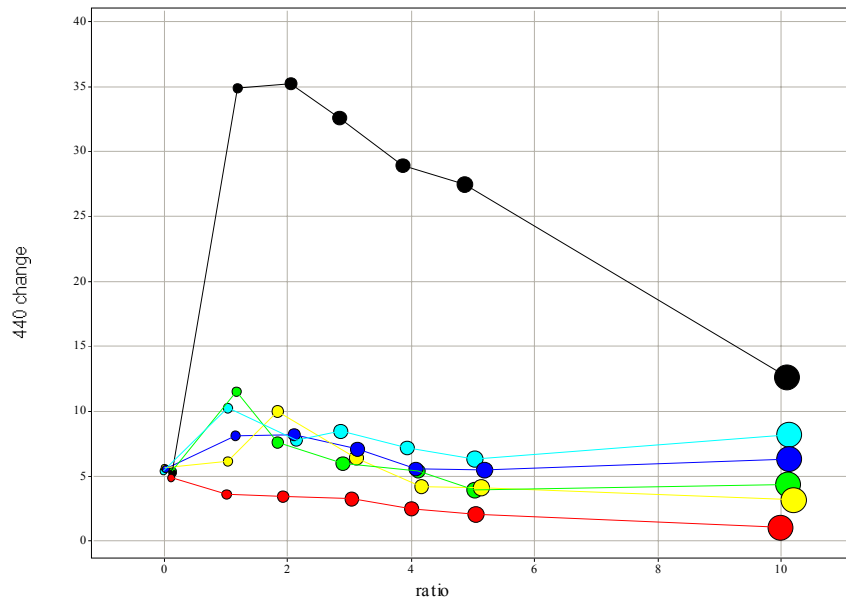
240minutes at 200°C

- Color change orders
 - BC4746S>TC152>Mark201,Mark1900>TM404,TM2080
- Less color associated with higher stabilizer ratio, as shown in samples containing TC152

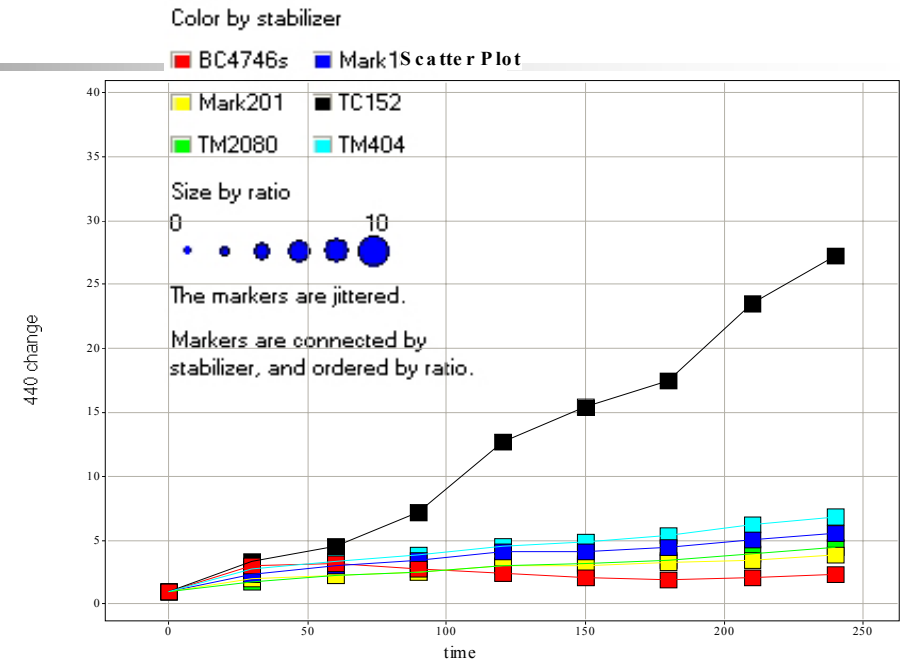
Fluorescence Emission of Benchmarking Samples



Scatter Plot



Heated at 200°C for 240minutes

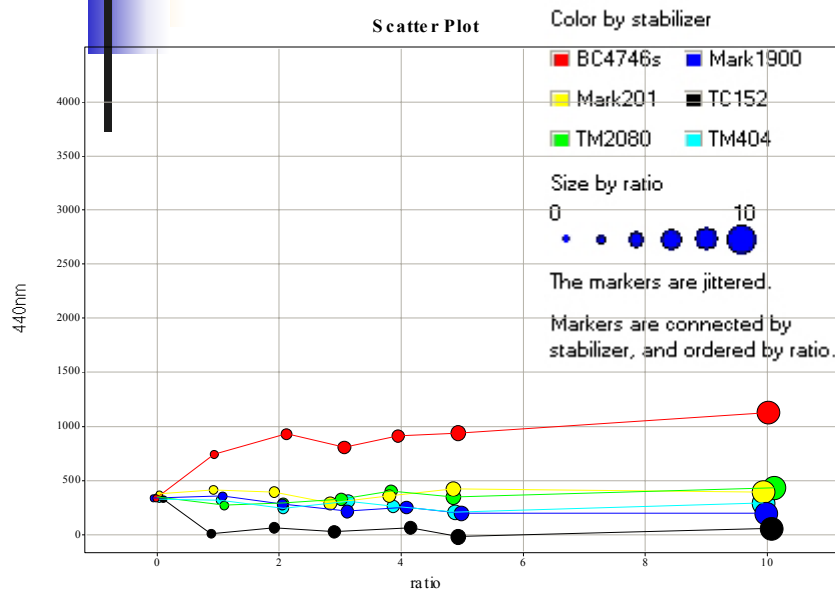


Intensity Change containing 5% stabilizers

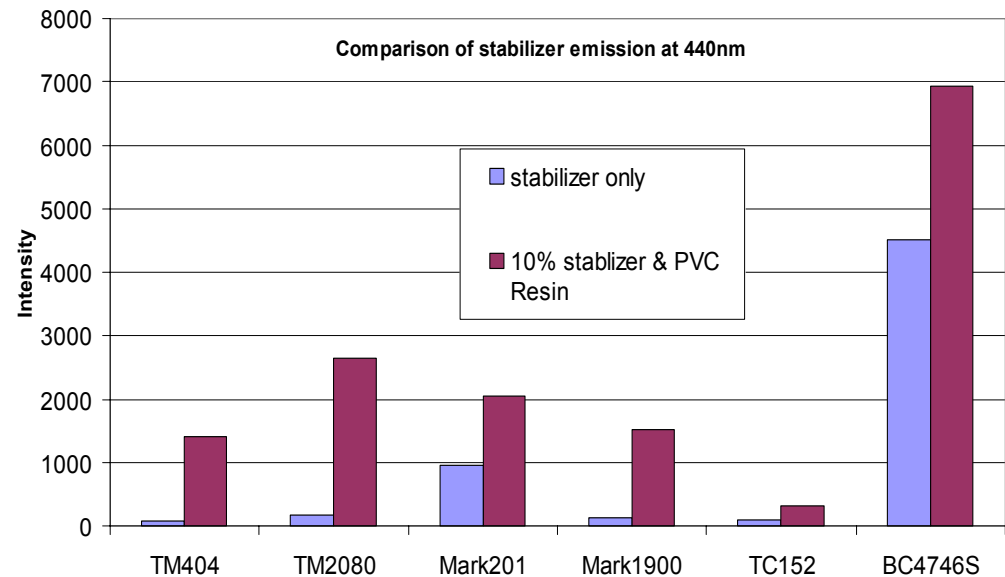
Issues:

- BC4746S: less fluorescence change but deeper color change
- TC152 shows more change by heating

Initial Fluorescence of Benchmarking Samples



Initial fluorescence emission after mixing

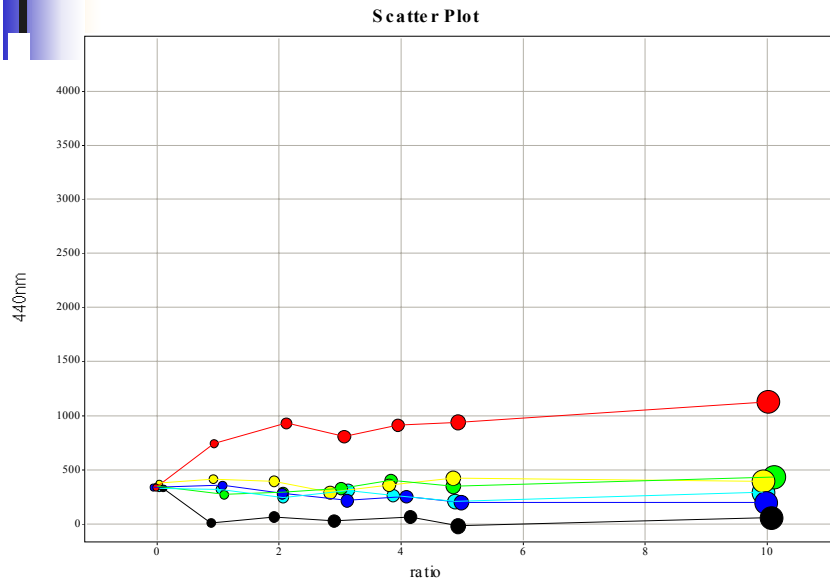


Fluorescence emission of stabilizer and samples containing 10% stabilizer

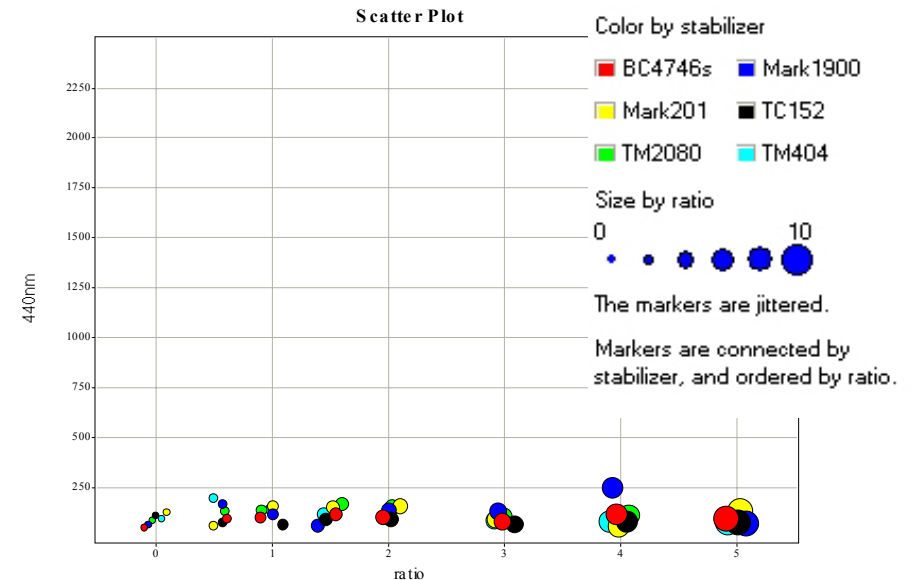
■ Fluorescence from stabilizers

- Stronger initial fluorescence emission from BC4746S
- Weaker initial fluorescence emission from TC152
- Functional compounds in stabilizers do not give off fluorescence
- Fluorescence compounds in stabilizers
 - Distillates light naphthenic in BC4746S
 - Unknown compounds as trade secrets

Comparison of Sample Preparation



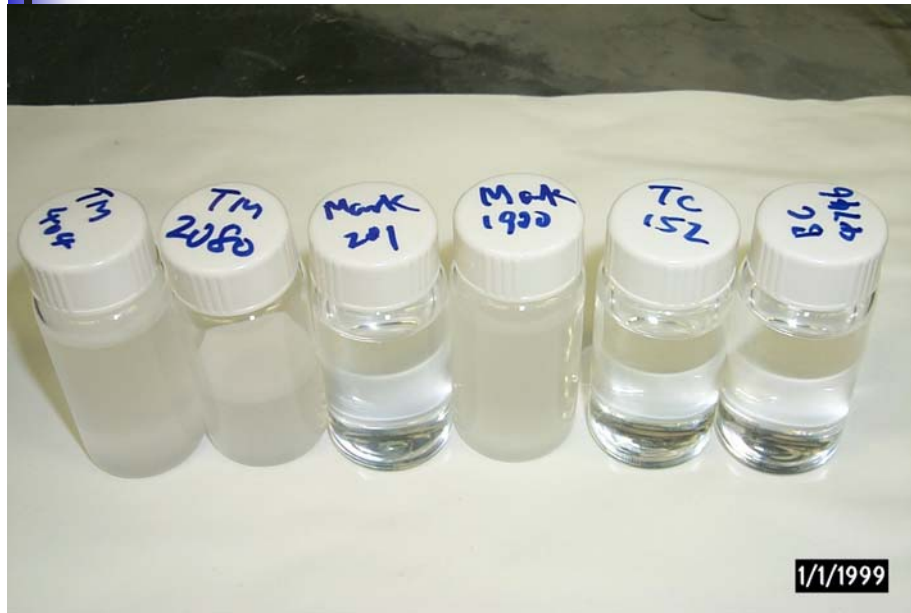
**Initial fluorescence emission
of benchmarking samples**



**Initial fluorescence emission
of samples prepared from PVC and
stabilizer solution in HTS test**

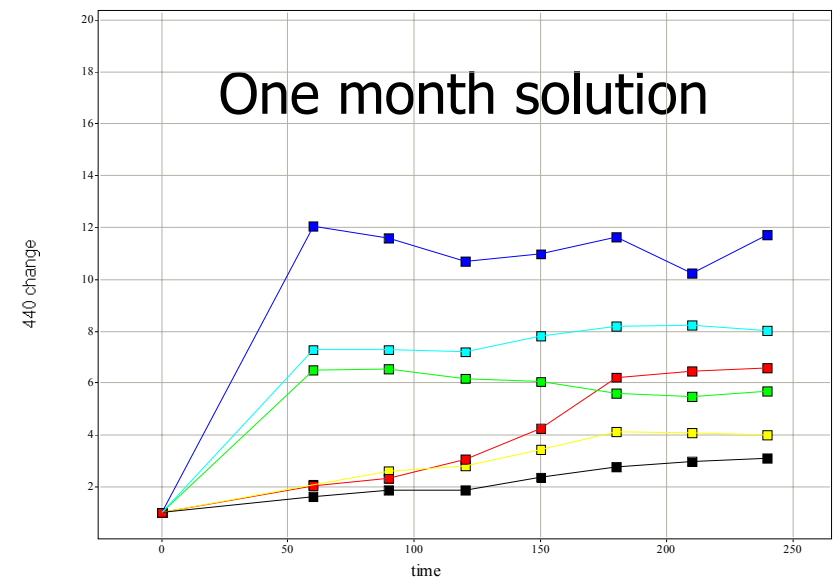
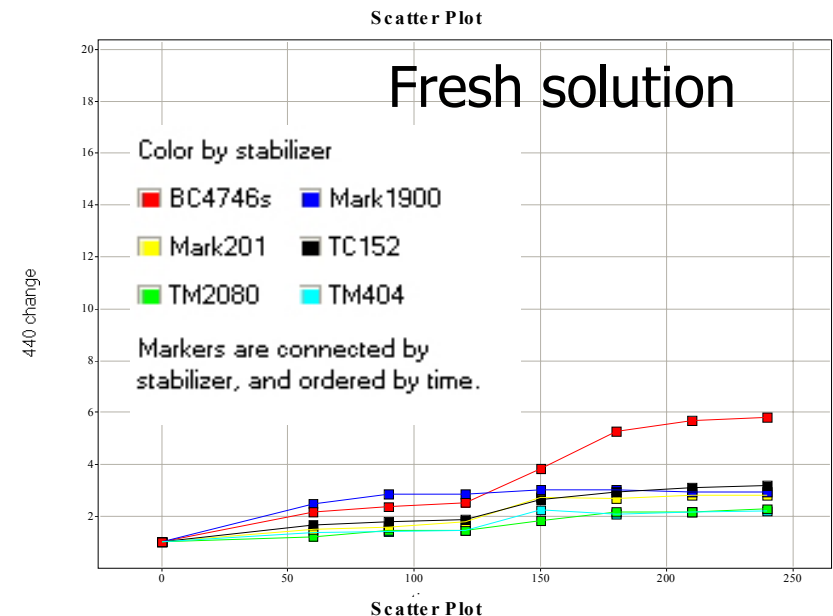
- Samples prepared from PVC solution showed similar level of initial fluorescence emission intensity for all stabilizers

Aging of Stabilizer Solutions due to Auto Oxidation

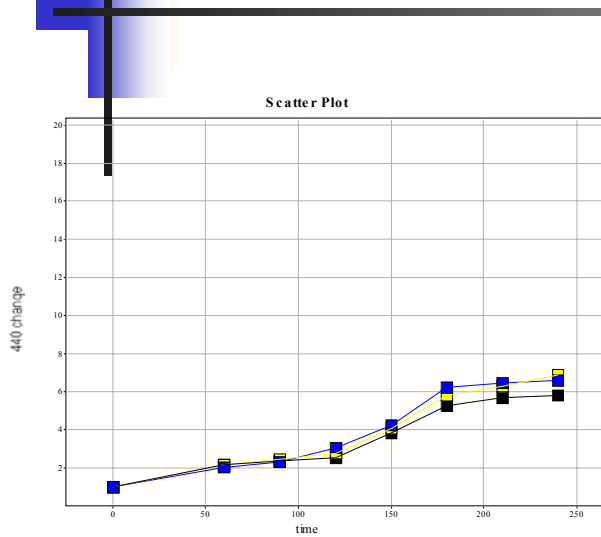


■ Issues

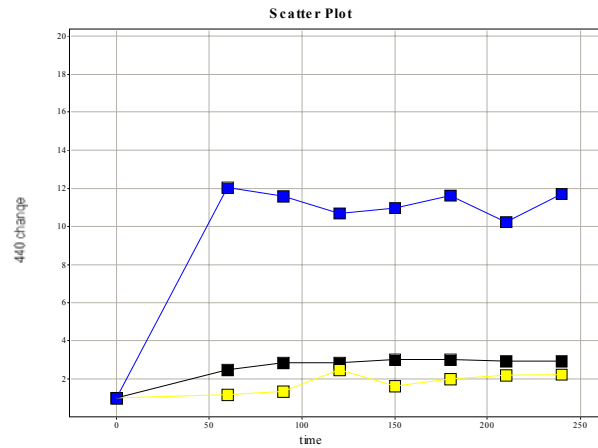
- TM404, TM2080 and Mark1900 solutions change from clear to opaque during storage
- TM404, TM2080 and Mark1900 are thioglycolates, which oxidize in air at R.T.
- Deteriorated performance for changed stabilizer solutions



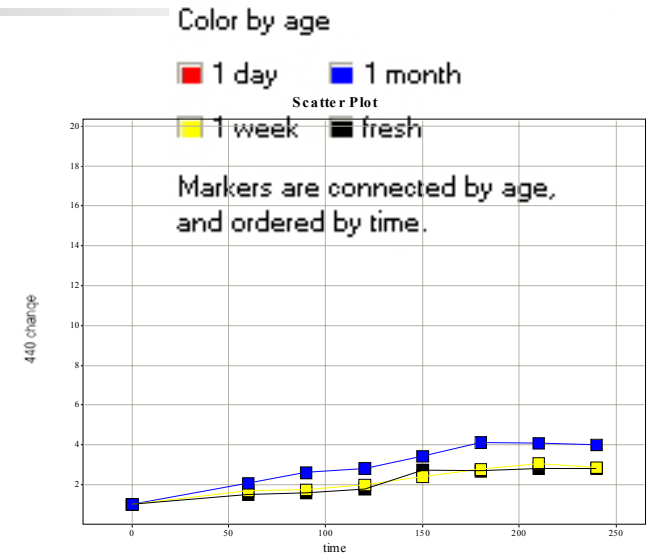
Deterioration of Stabilizer Solutions (5%)



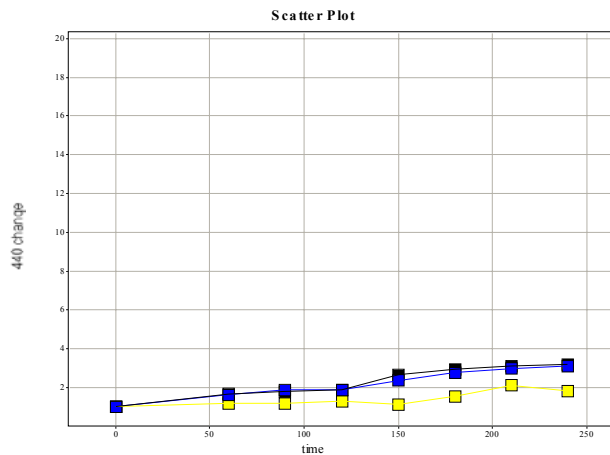
BC4746S



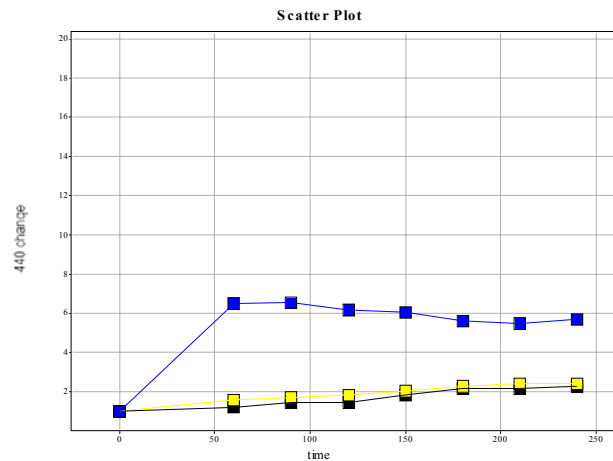
Mark1900



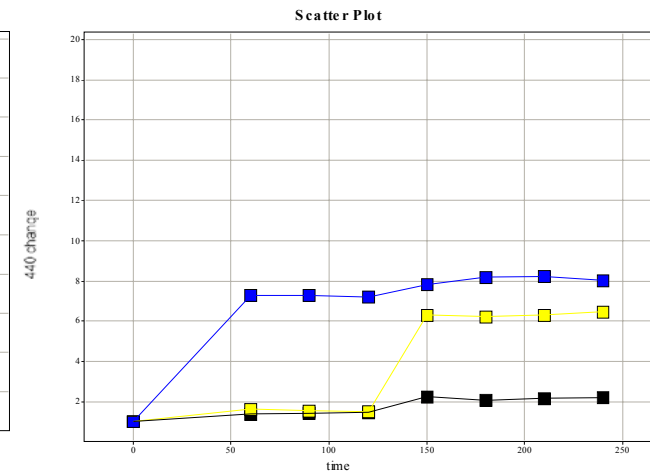
Mark201



TC152



TM2080



TM404



Impact of Stabilizers on PVC Degradation

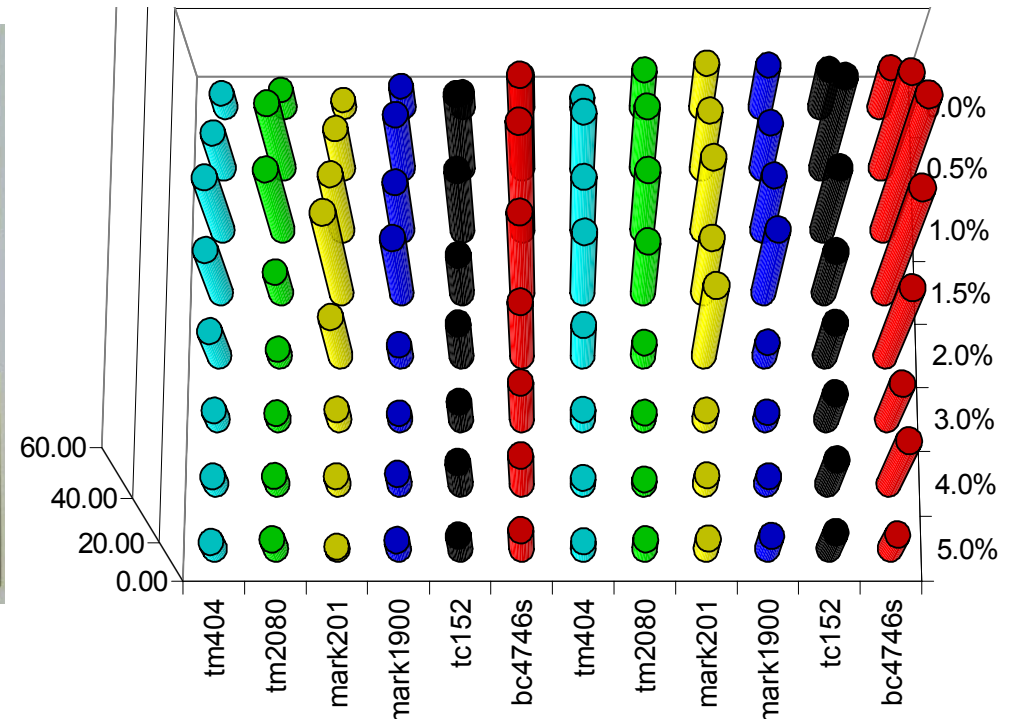
- Sample pool
 - PVC resin and flexible PVC
 - Six stabilizers
 - 8 different ratios between PVC and stabilizers
 - Duplicated sample
 - 2 heating temperatures and 10 intervals
- Data analysis based on stabilizers, ratios, and heating time
 - PVC resin heated at 180°C and 200°C
 - Flexible PVC heated at 180°C and 200°C

Color Change and Fluorescence Emission of PVC Resin after heated at 200°C for 240 minutes



tm404
tm2080
mark201
mark1900
tc152
bc4746s
tm404
tm2080
mark201
mark1900
tc152
bc4746s

Replicates



Replicates

- Color change matches the extent of fluorescence intensity change

Color by stabilizer

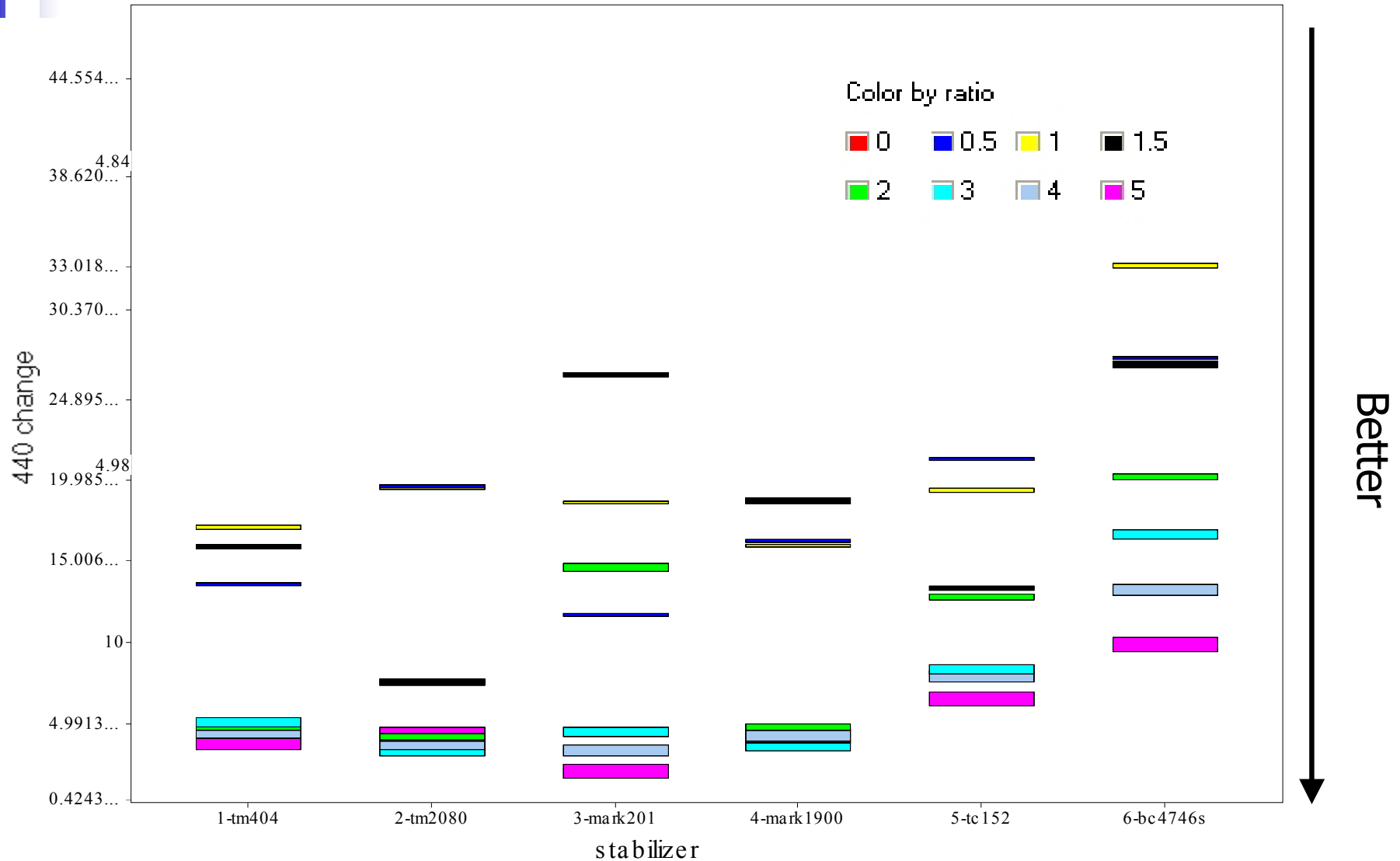
BC4746s Mark1900
Mark201 TC152
TM2080 TM404

Comparison of stabilizers in PVC Resin

after 240minute at 200°C

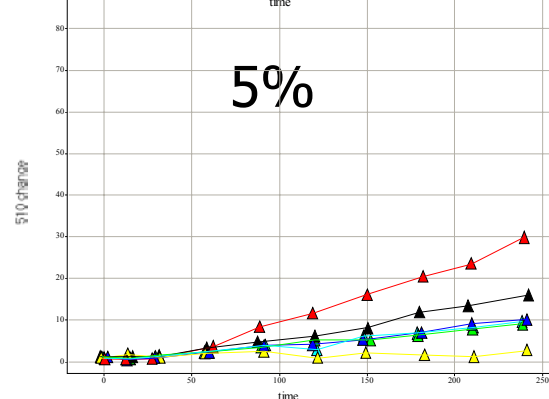
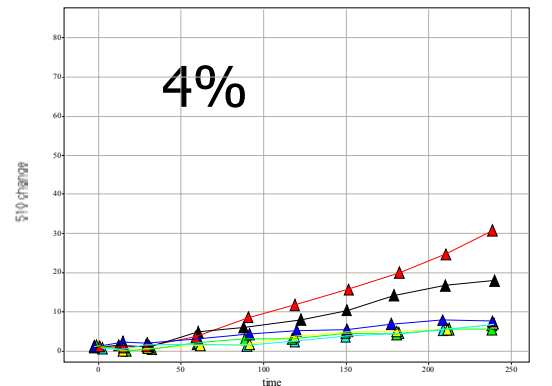
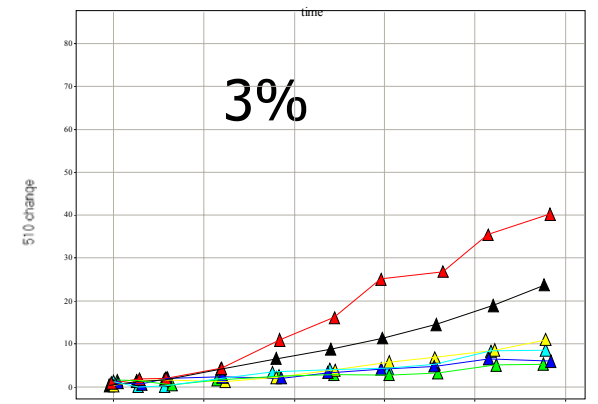
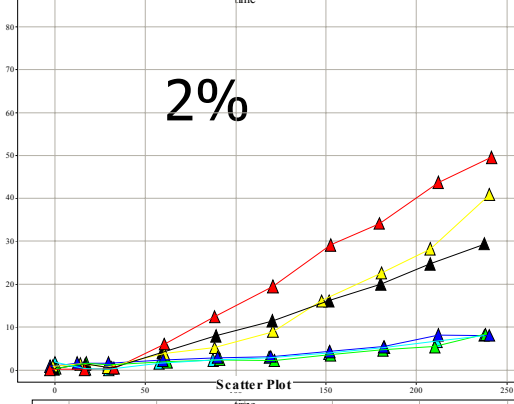
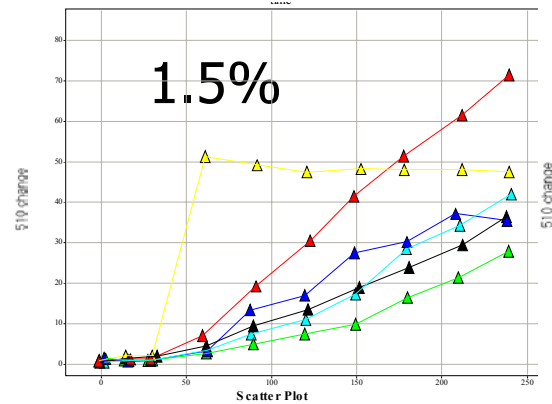
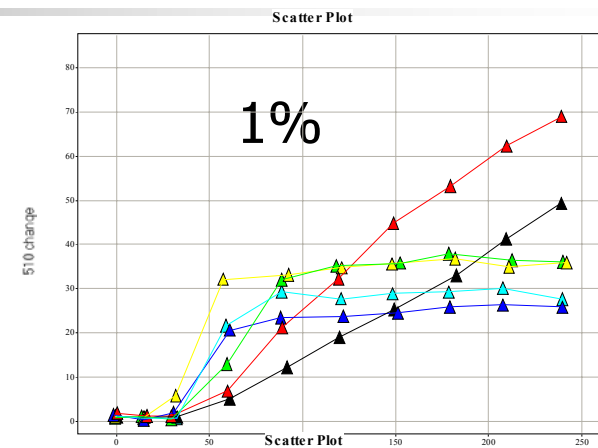
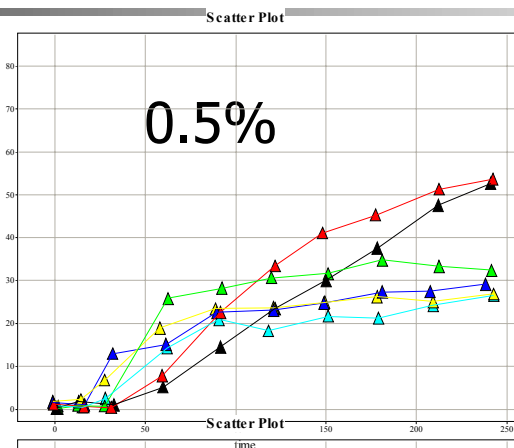
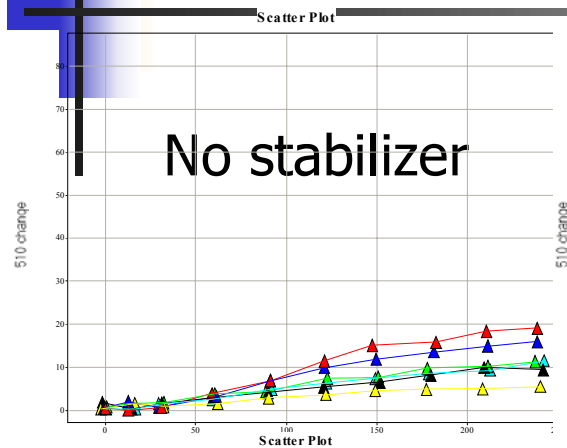
HTS@USM

Bar Chart



Fluorescence vs. Stabilizers

in Resin Heated at 200°C



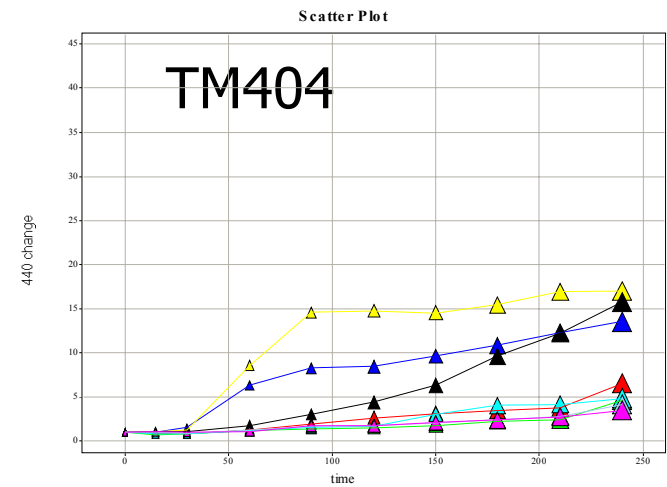
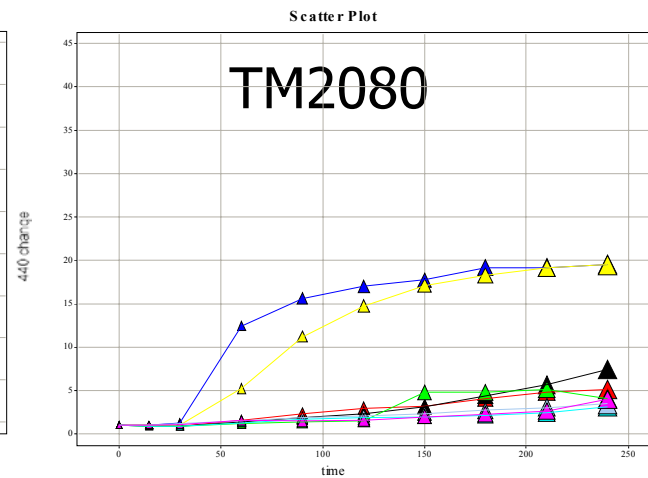
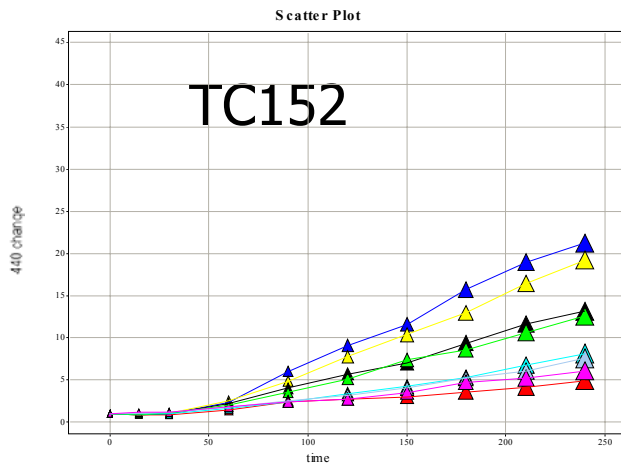
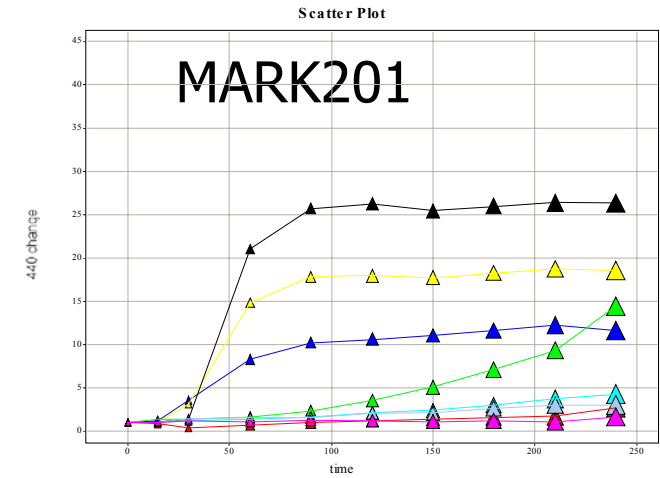
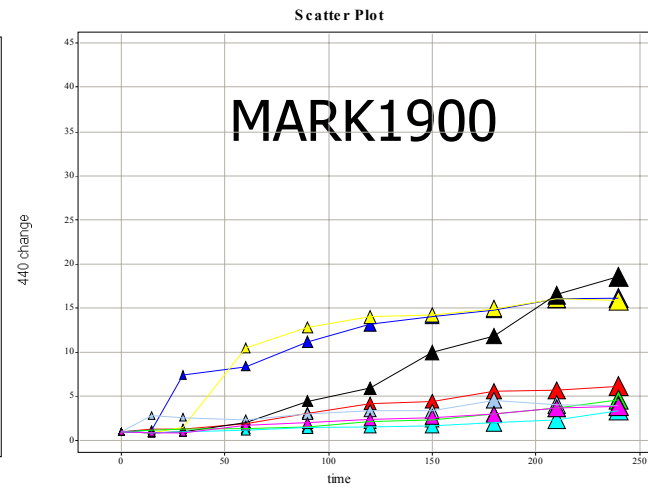
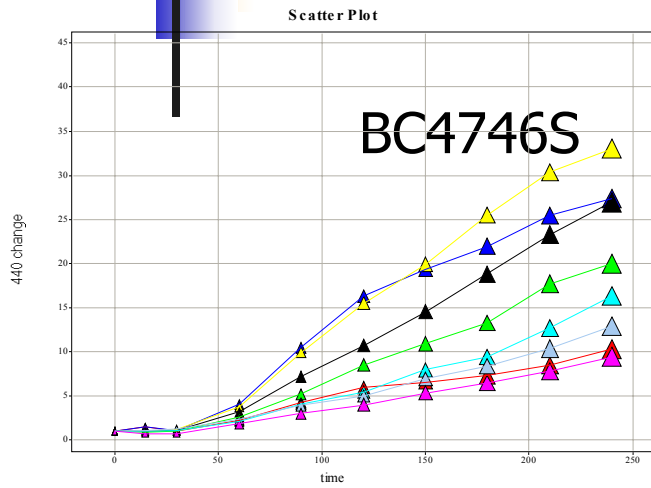
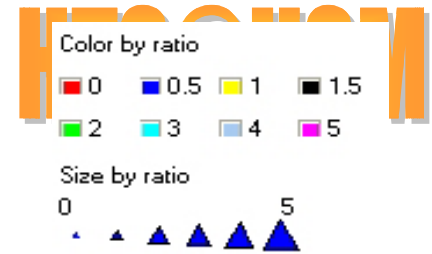
Color by stabilizer

BC4746s Mark1900
Mark201 TC152
TM2080 TM404

The markers are jittered.

Markers are connected by stabilizer, and ordered by time.

Fluorescence vs. Heating Time in Resin Heated at 200°C



Fluorescence vs. Stabilizer Ratio in Resin Heated at 200°C

Color by time

0	15	30
60	90	120
150	180	210
240		

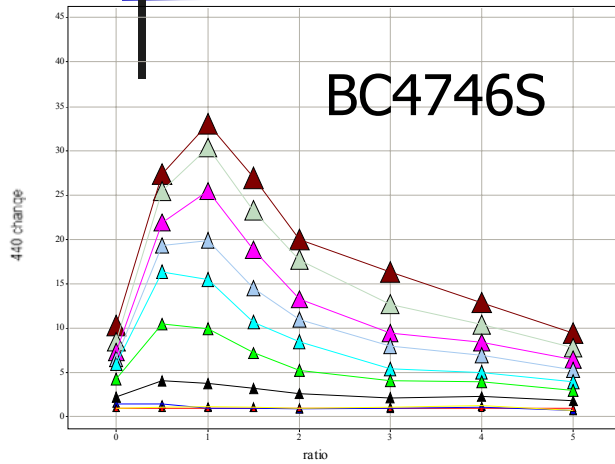
Size by time

0 240

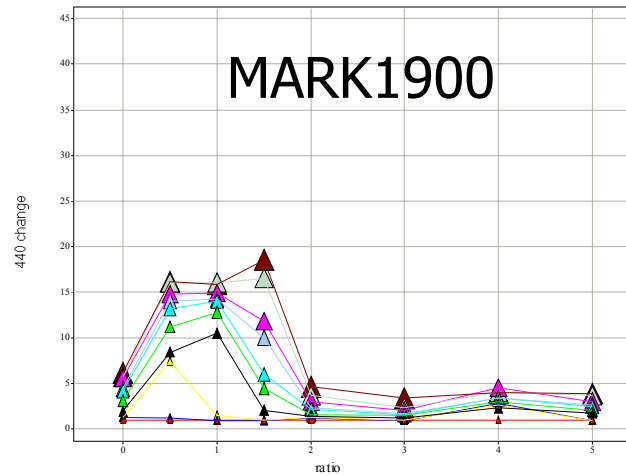
Markers are connected by time,
and Scatter Plots by ratio.



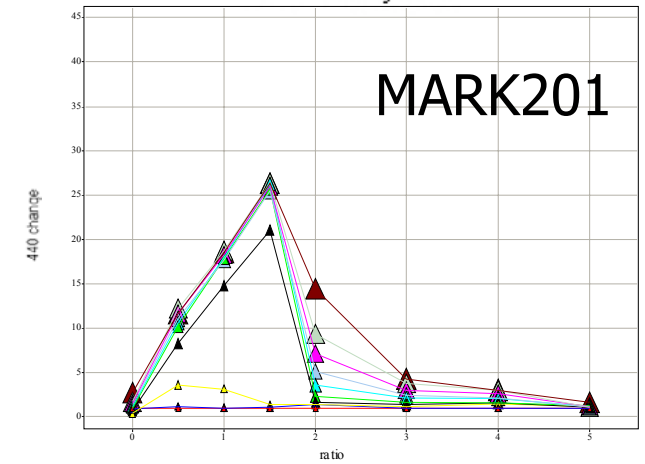
Scatter Plot



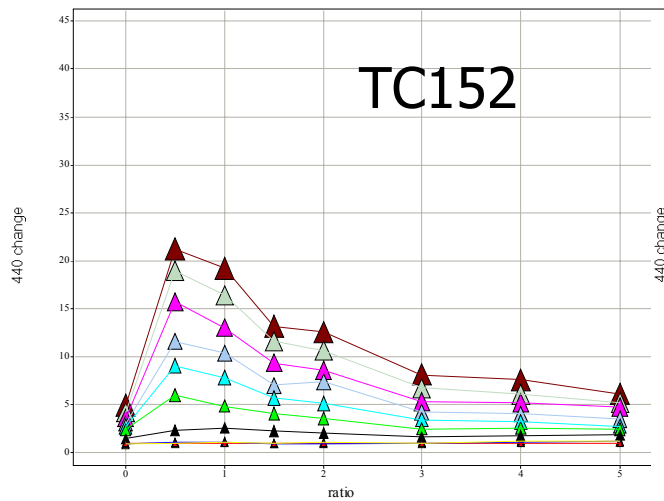
Scatter Plot



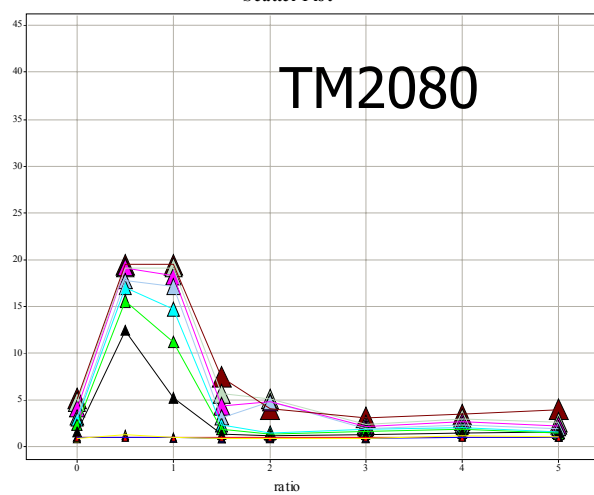
Scatter Plot



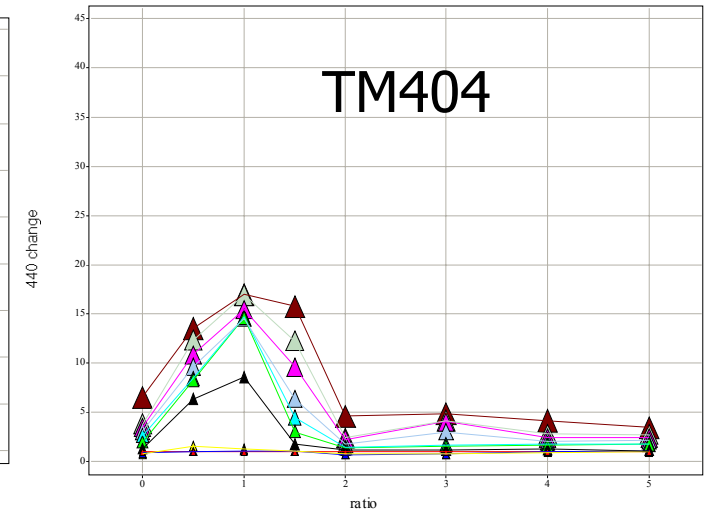
Scatter Plot



Scatter Plot



Scatter Plot

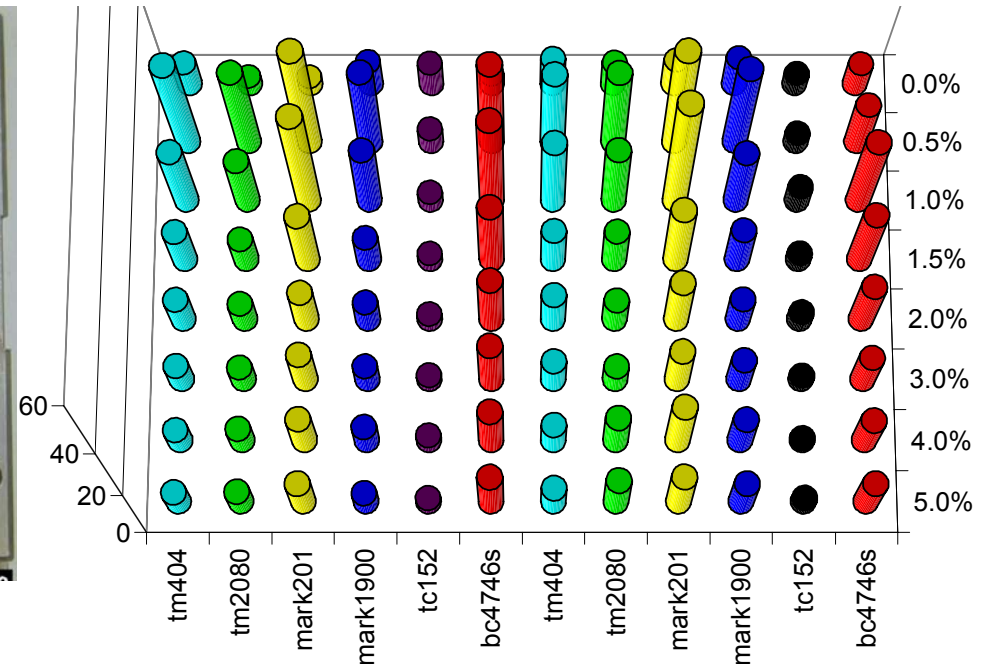


Color Change and Fluorescence Emission of Flexible PVC after heated at 200°C for 240 minutes



tm404
tm2080
mark201
mark1900
tc152
bc4746s
tm404
tm2080
mark201
mark1900
tc152
bc4746s

Replicates



Replicates

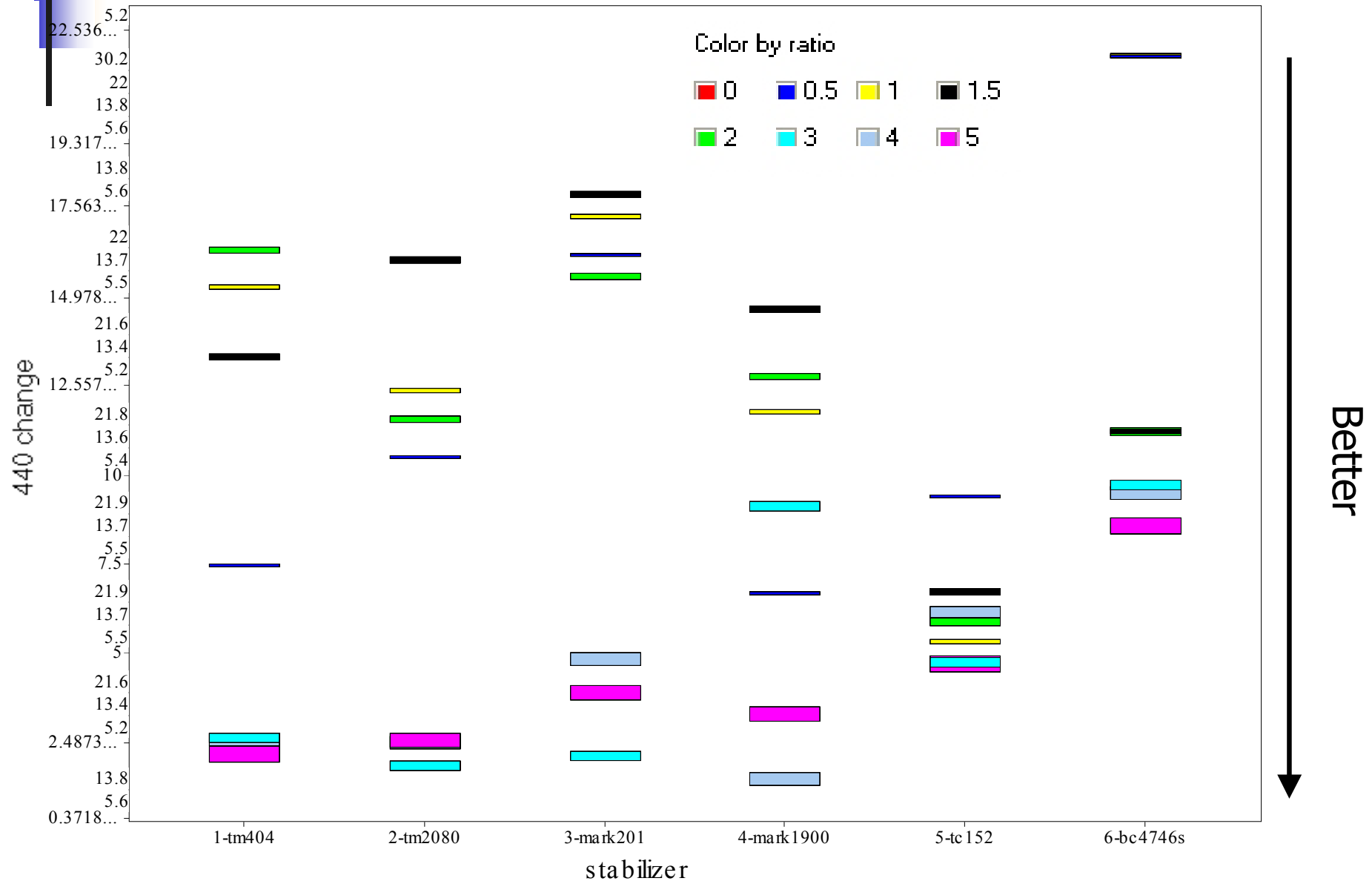
Color by stabilizer

- BC4746s
- Mark201
- TM2080
- Mark1900
- TC152
- TM404

Comparison of stabilizers in Flexible PVC after 240minute at 200°C

HTS@USM

Bar Chart



Fluorescence vs. Stabilizers

in Flexible PVC Heated at 200°C

No stabilizer

0.5%

1%

1.5%

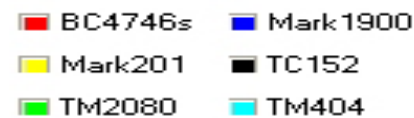
2%

3%

4%

5%

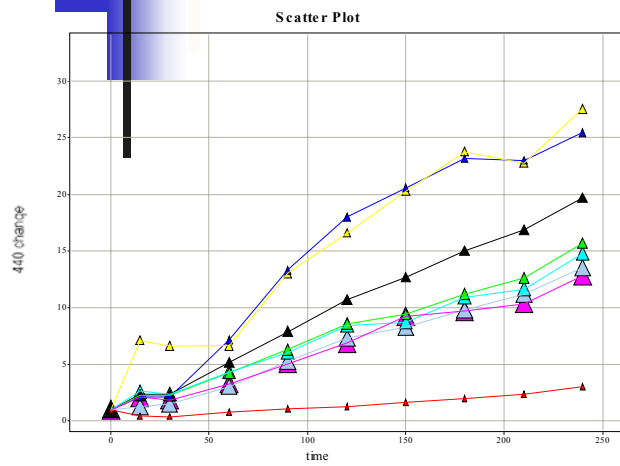
Color by stabilizer



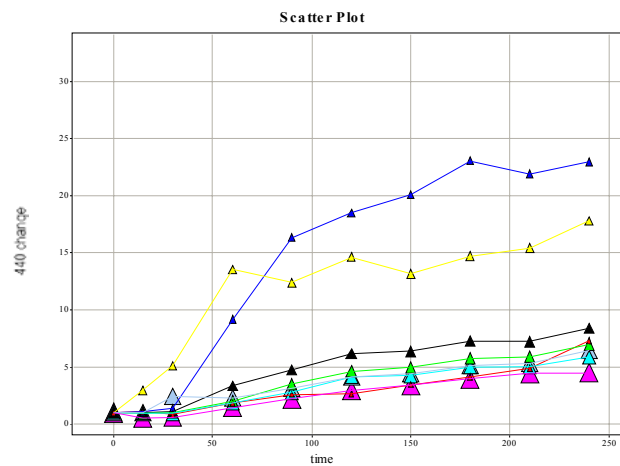
The markers are jittered.

Markers are connected by stabilizer, and ordered by time.

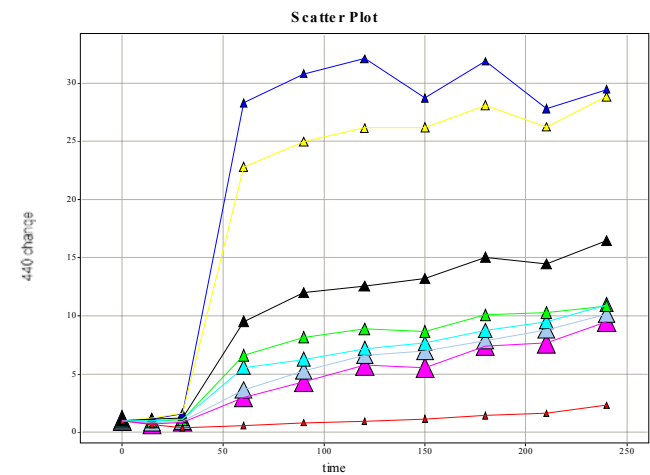
Fluorescence vs. Heating Time in Flexible PVC Heated at 200°C



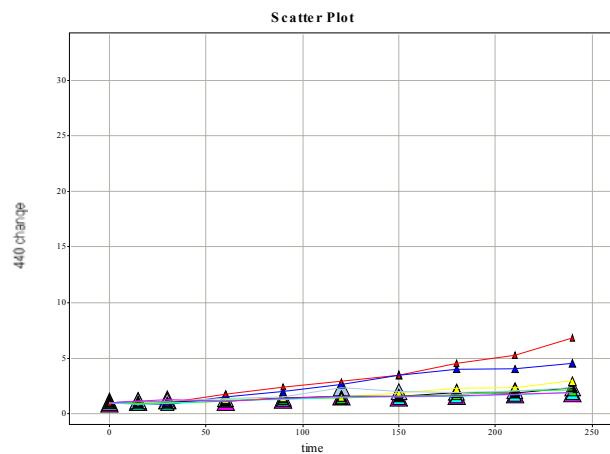
BC4746S



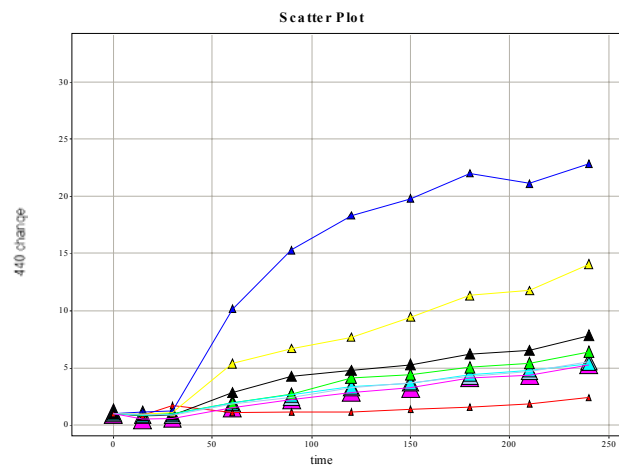
MARK1900



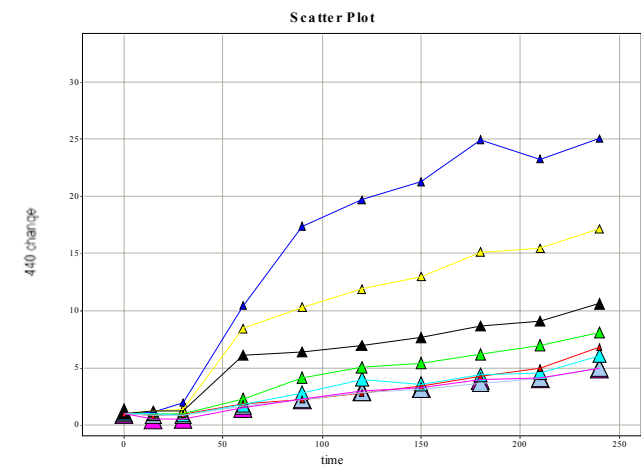
MARK201



TC152



TM2080

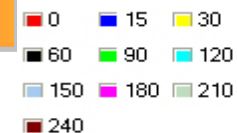


TM404

Fluorescence vs. Stabilizer Ratio in Flexible PVC Heated at 200°C



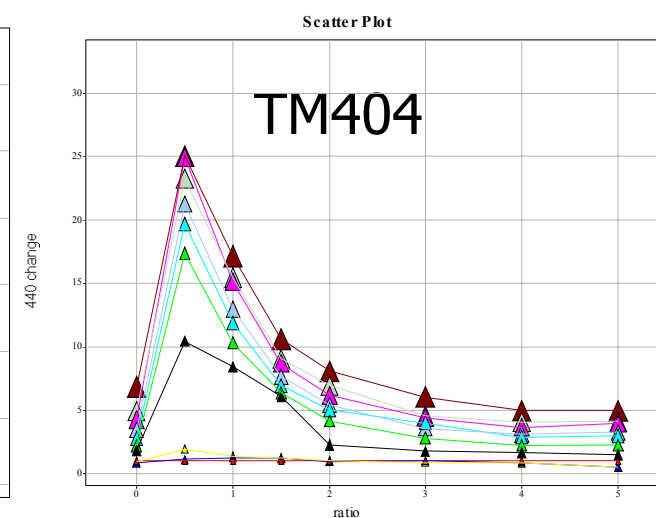
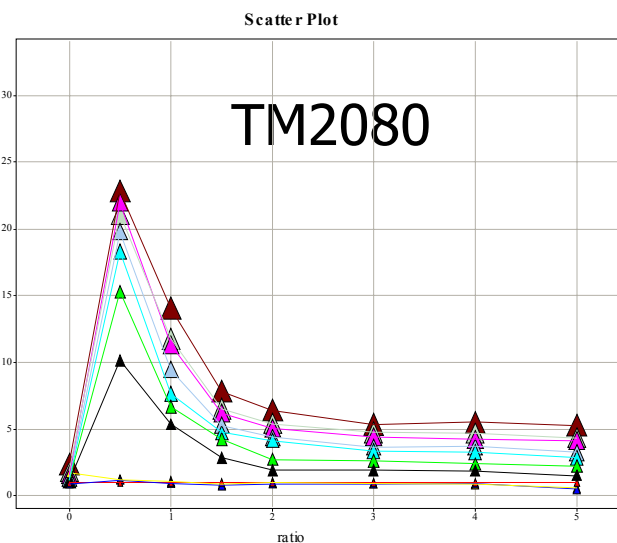
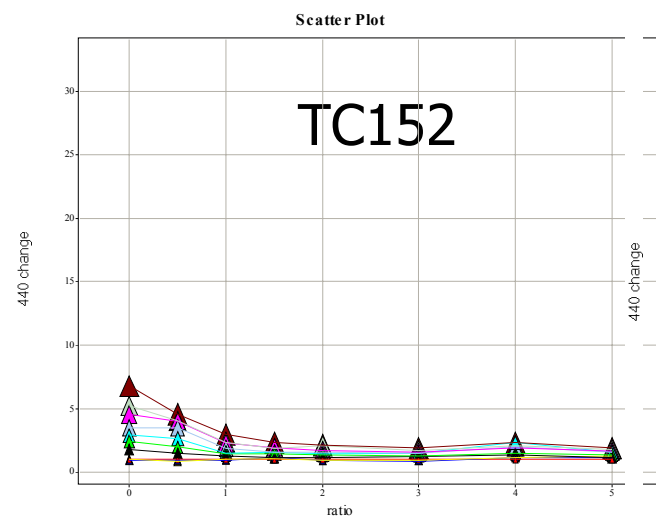
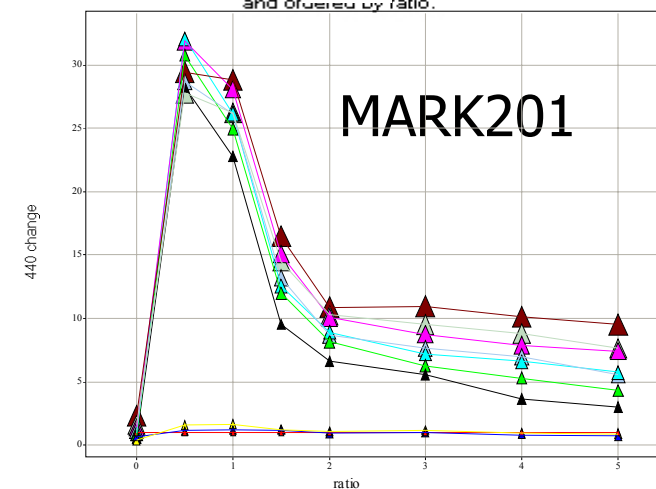
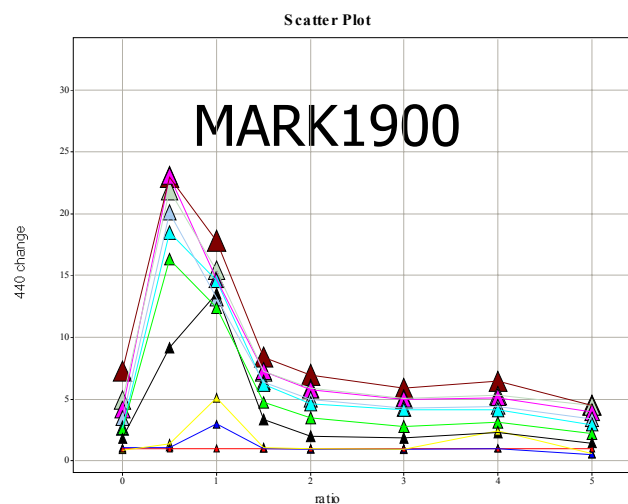
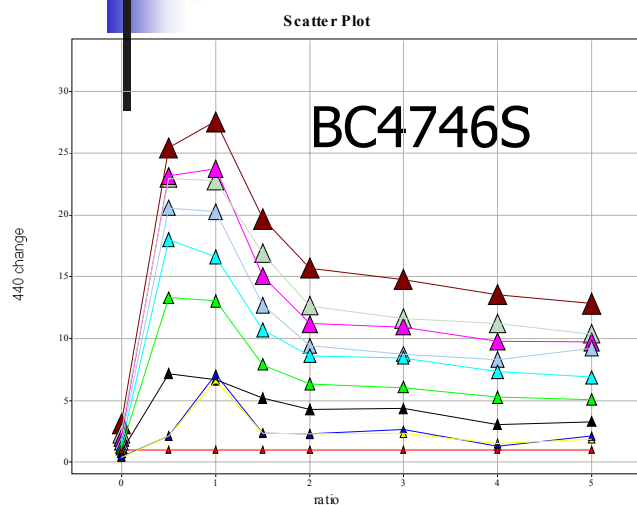
Color by time



Size by time



Markers are connected by time,
and ordered by ratio.



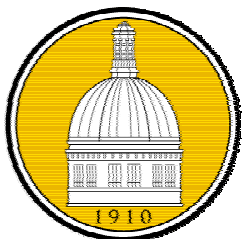


Summary

- PVC degradation can be characterized by fluorescence emission at 440nm and 510nm
- Impact of stabilizers on PVC degradation was successfully measured by the change of fluorescence emission at 440nm and 510nm
- For PVC resin, thiol functional stabilizers show better performance
 - Less than 2% stabilizers shows poor protection
 - 4% or more thiol stabilizers make efficient protection
 - 3% MARK1900 shows some difference at 180°C and 200°C
- For flexible PVC, only TC152 shows efficient protection at both 180°C and 200°C with a broad range of stabilizer ratio

Acknowledgements

- The research is funded by NSF Award 0227827
- Robert M. Hearin Support Foundation
- Henry Harris and Rogerio S. Rocchetto from Georgia Gulf Chemical





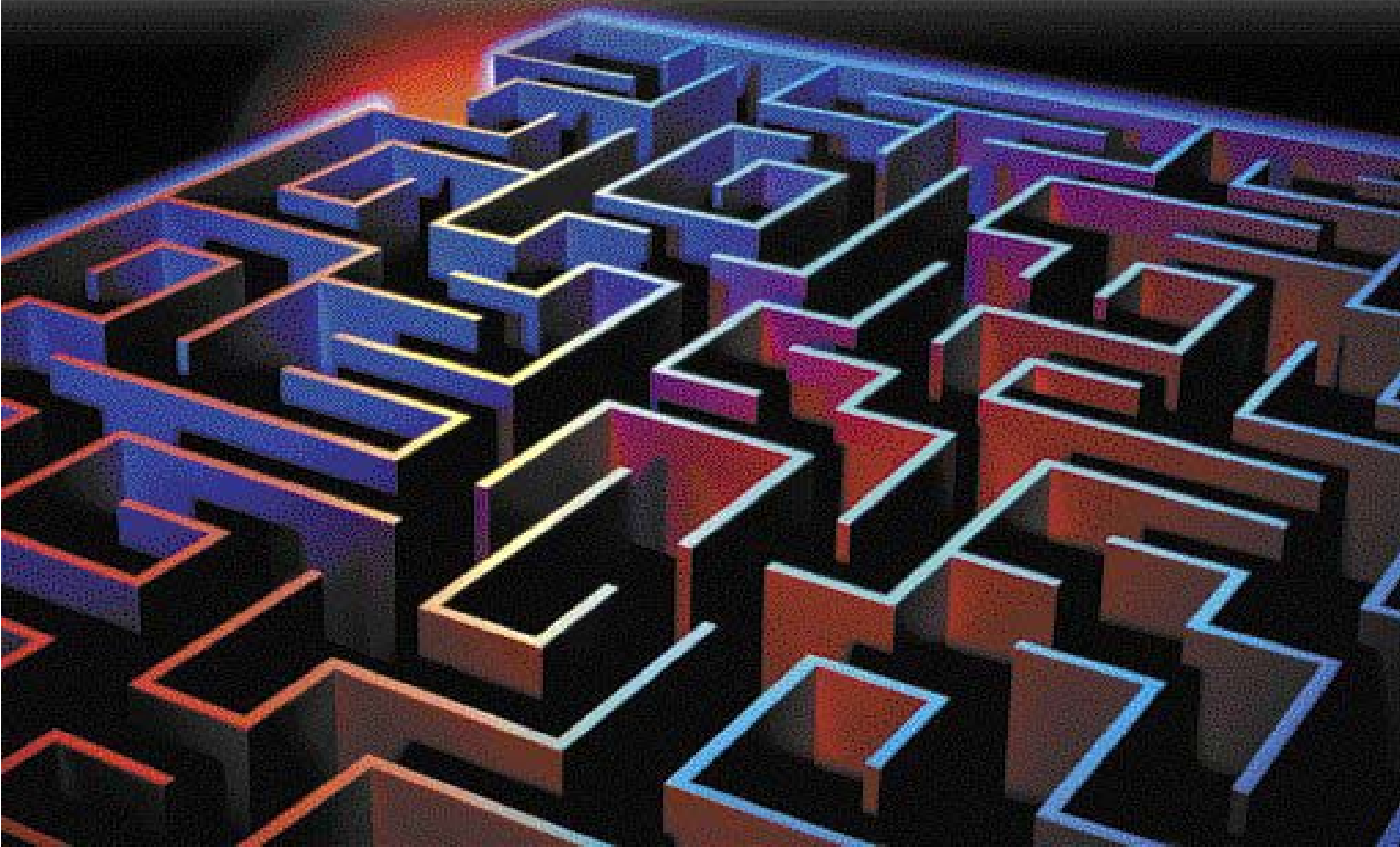
Materials Library Design

What Experiment to do next ?

“Solving the robot blues”

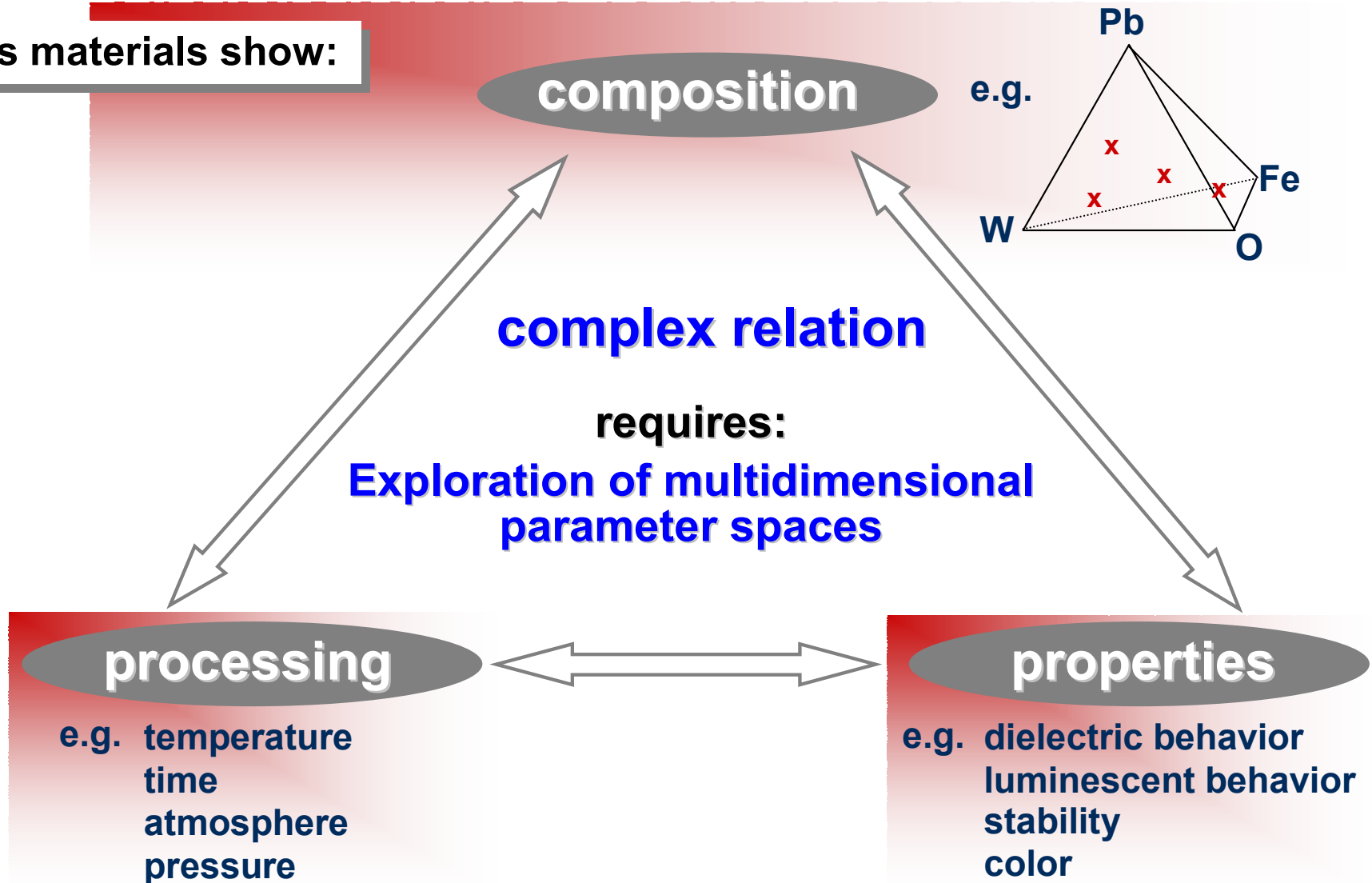
How Do I Find My Way Through?

(From Where I Am to My Goal -- Given the Range of Choices)



Combinatorial Materials Development

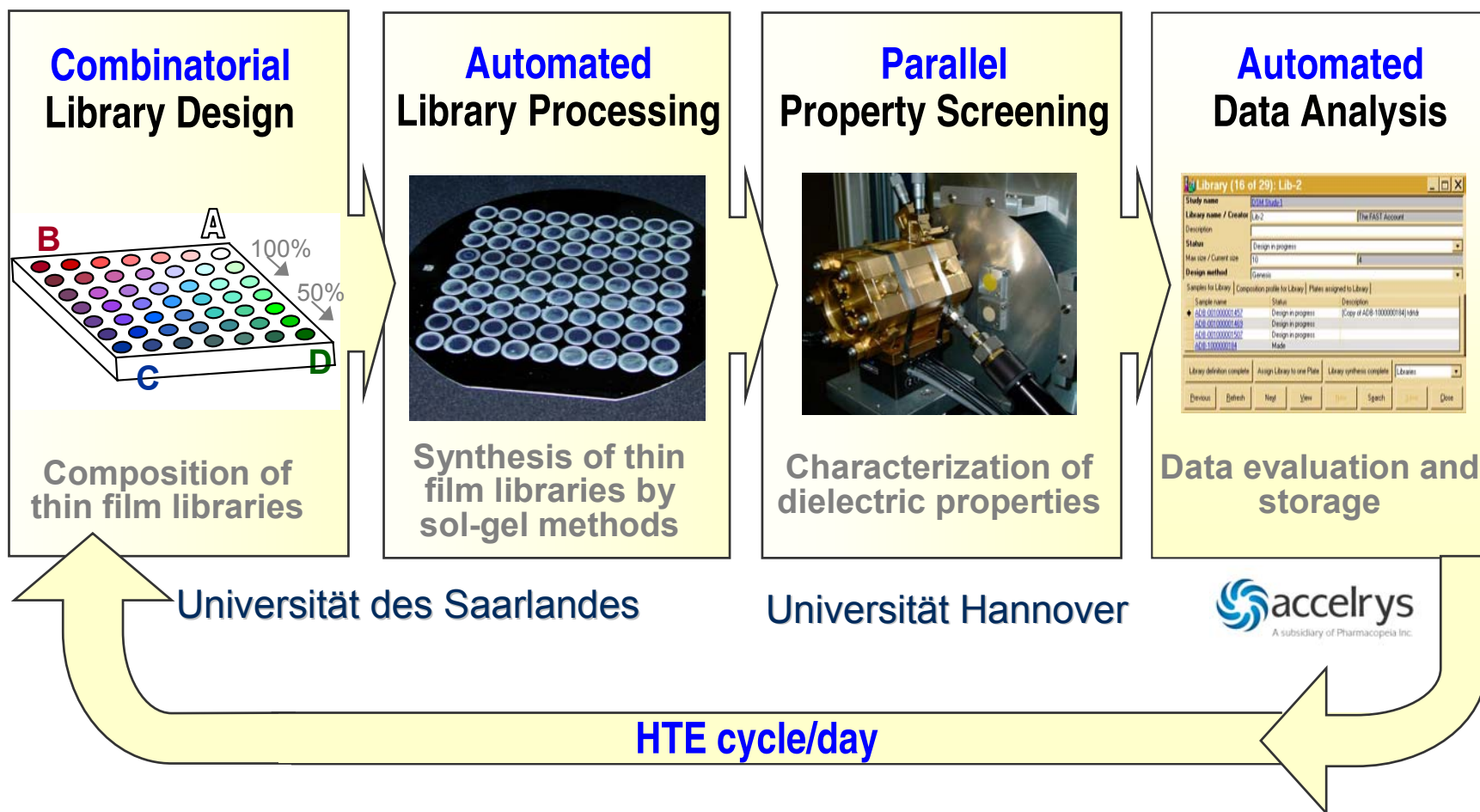
Today's materials show:



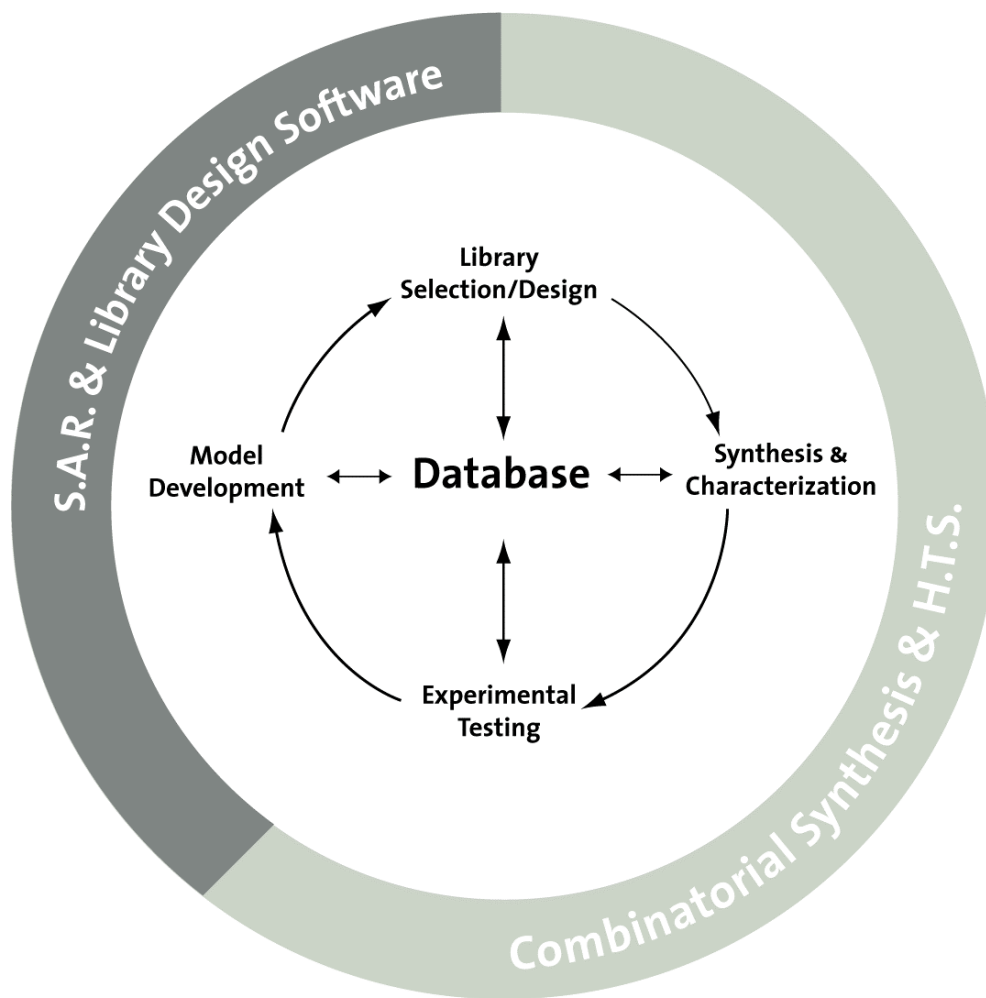
Combinatorial Methods for Microwave Dielectrics

New MW dielectrics needed for:

passive integration & miniaturization (Amplifiers, Antennas, Resonators)



The Conventional Process

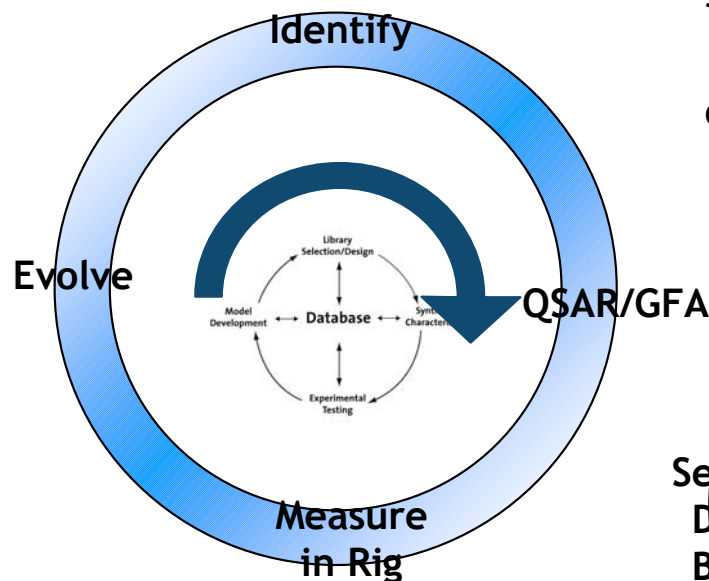
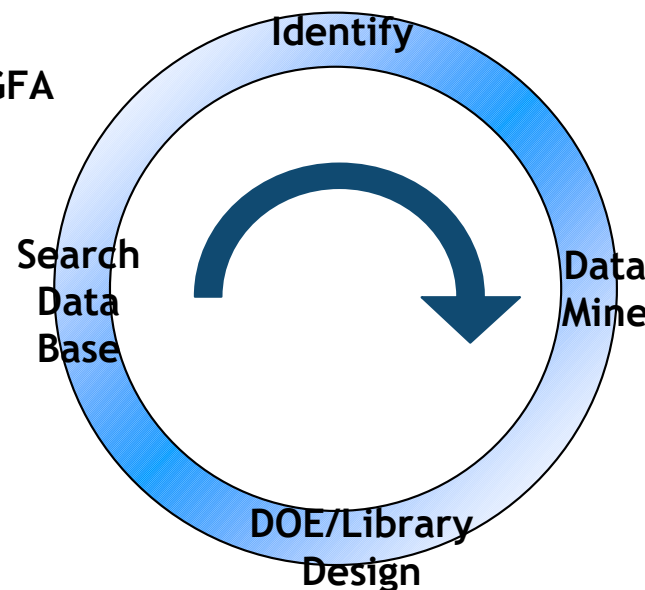


The Interlocking Domains of Combinatorial Design

Purely Data Driven

DOE and Optimization for combinatorial library design.

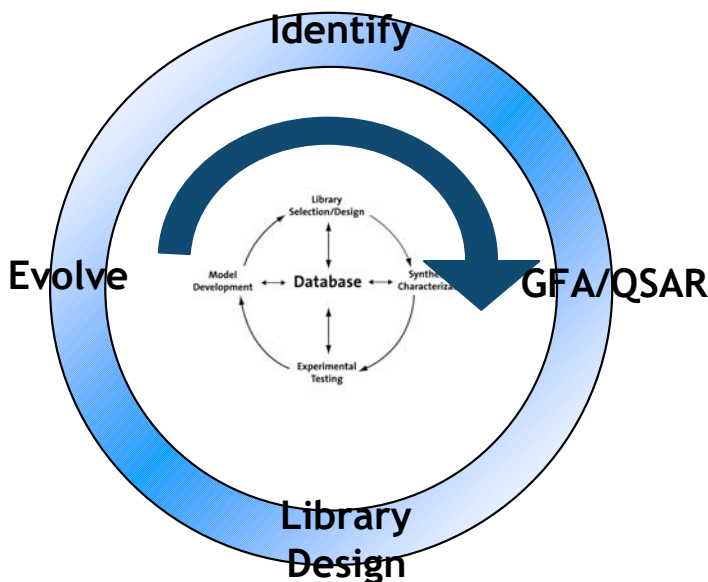
- Set up DOE
- Identify points in Data Store similar
- Use these to build model and optimize against historical data



Partially Theoretical

Optimization and combinatorial library design.

- Uses GA on experimental data from rigs to identify promising next generation



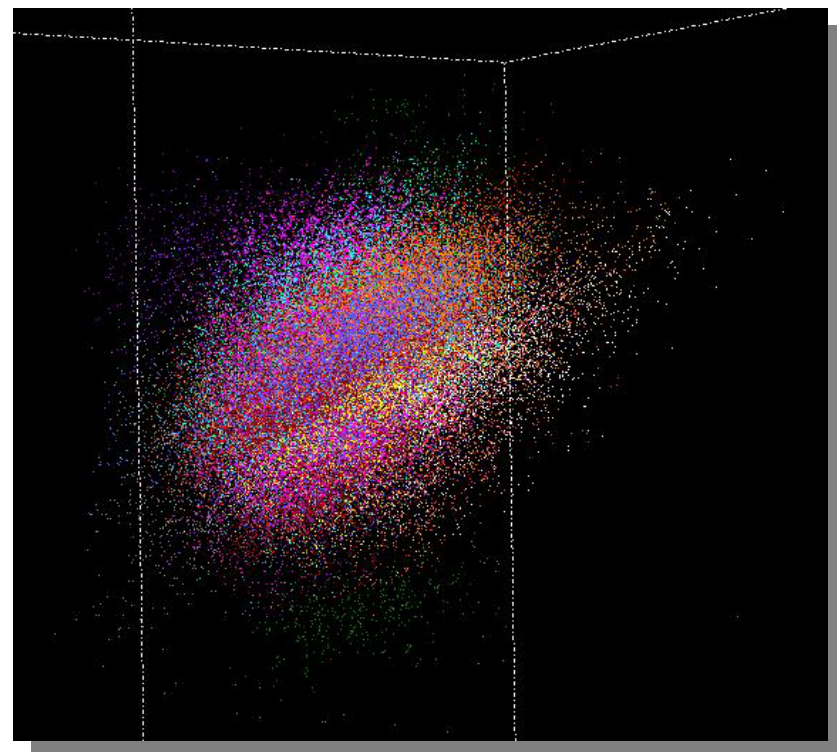
Purely Theoretical

Optimization and combinatorial library design.

- Design Property structure mapping
- The run selection to optimum using GA to drive composition to target values

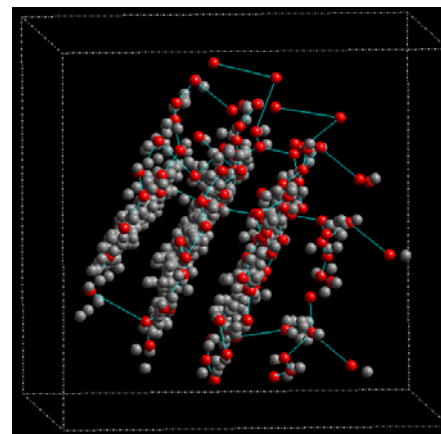
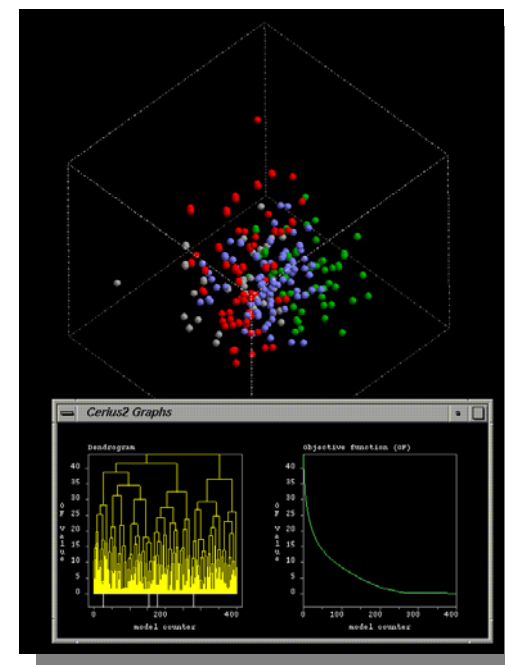
Combinatorial Library Design

- Library Specification
 - Molecular: Product or Reaction-based
 - Polymers, Heterogeneous catalysts ?
- Library Design
 - Diversity and similarity metrics
 - Similarity Selection
 - Array and mixture design
- Library Comparison
- Library Focussing
 - Active site model (atomic or abstracted)
 - QSAR Model, PCA-55 descriptors (1.6-1.8 million compounds)



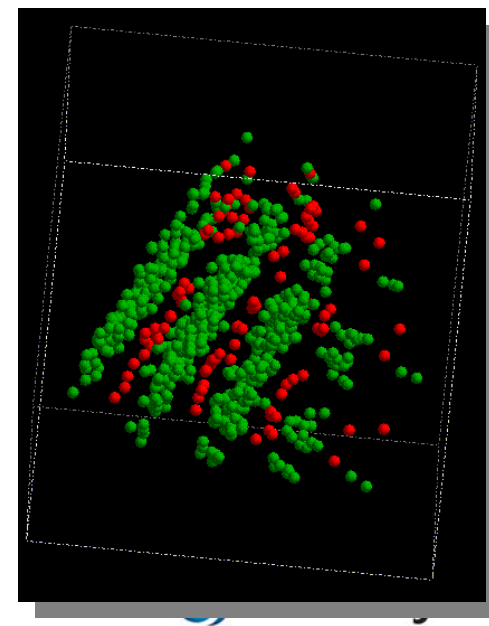
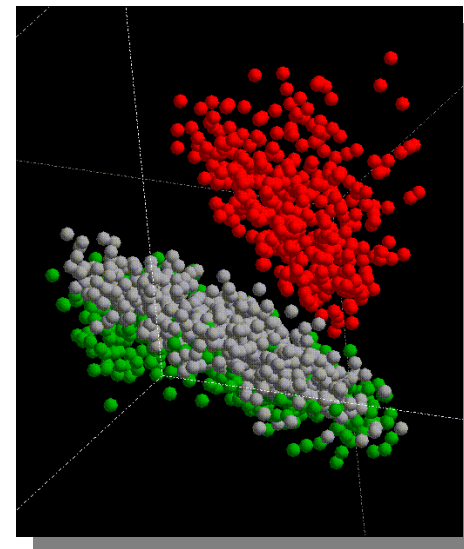
Diversity and Similarity Analysis

- Select diverse, representative and similar subsets
 - Clustering, distance-based and cell-based selections
 - Select method according to speed and accuracy
 - Validated literature methods and novel metrics
 - Include the combinatorial constraint
 - mixtures
 - arrays
 - plate selection
 - Handle million(s) of compounds

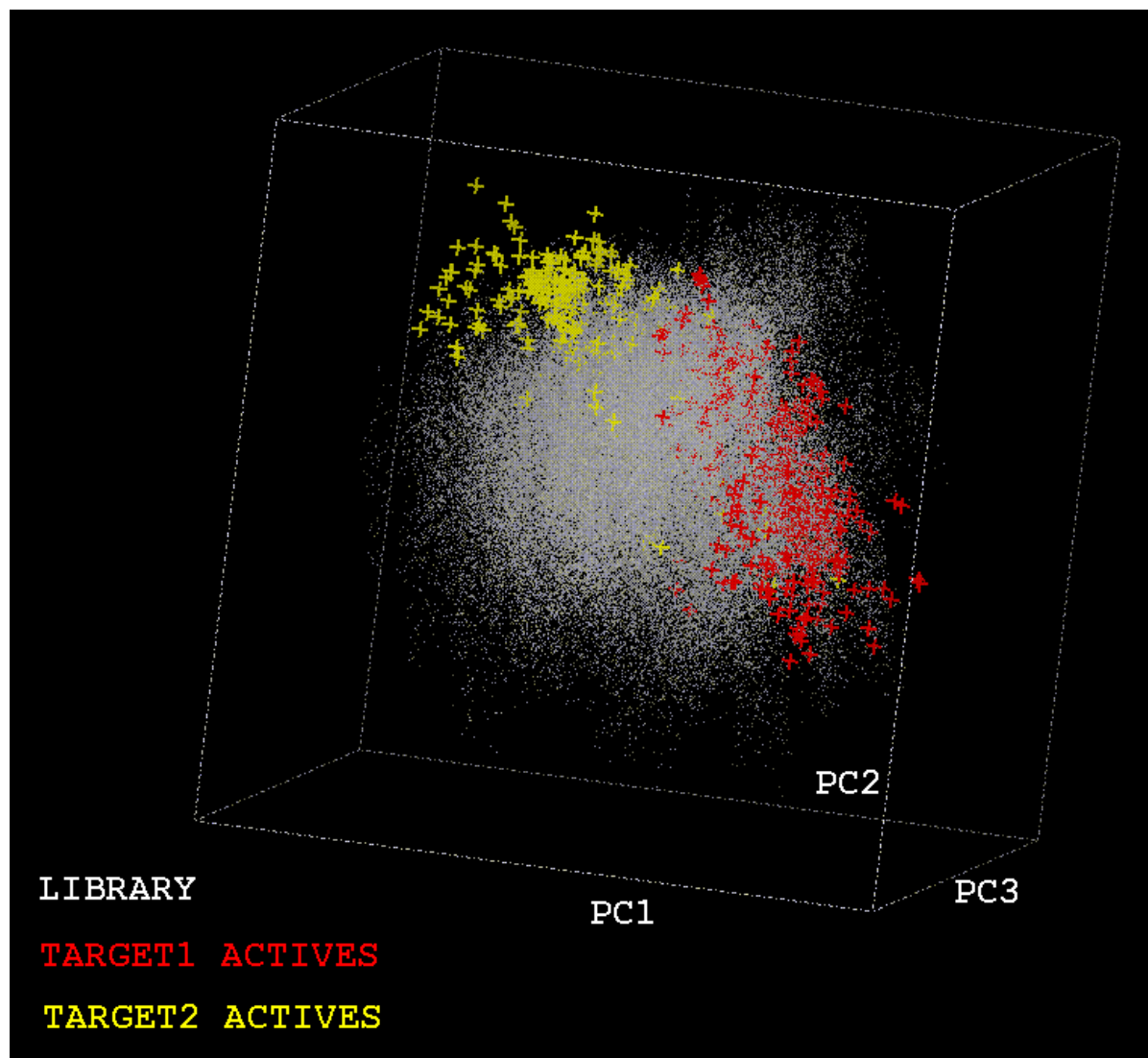


Diversity and Similarity Selection

- Compare libraries, select subsets with reference to existing sets.
 - Visualize multiple libraries in property space; compare libraries with distance histograms
 - Reference space (e.g. CAP)
 - Common space of multiple libraries
 - Select a subset from a library that is diverse in itself **and** different from anything in a second library
 - Identify holes in a library; identify compounds to fill those holes from a second library
 - File-based system for large libraries
 - 3D Chemical space



Molecular Investigation Library (140,000)



Designing Diverse and Focused Combinatorial Libraries of Synthetic Polymers

Charles H. Reynolds*

Rohm and Haas Company, 727 Norristown Road, Spring House, Pennsylvania 19477-0904

Received February 12, 1999

Molecular topology and genetic algorithm optimized quantitative structure–property relationships (QSPR) have been used to design diverse and focused libraries of synthetic biodegradable polymers. A diverse subset (17 polymers) of a 112-member virtual polymer library was selected based on the molecular topology of the repeat unit using a stochastic diversity method (SimSearch-SCA). These 17 polymers were shown to be highly representative of the two-dimensional property space for the full library where the properties of interest are glass transition temperature (T_g) and hydrophobicity as measured by the air–water contact angle (CA). The 17 polymers in the diverse library were used to derive QSPR equations for T_g and CA by using a genetic algorithm to select molecular topology descriptors for linear regression. High quality models were derived for both T_g and CA. These QSPR models were tested by comparing the computed and experimental T_g and CA values for the 95 polymers that were *not* included in the training set. Representative models give r^2 values of 0.89 and 0.92 for T_g and CA, respectively. The QSPR models were further tested by using them to build focused libraries with specific values of T_g and CA. The focused libraries were very successful in identifying polymers that fall within specified ranges of T_g and CA. This work illustrates that the same concepts of molecular similarity and diversity that have been exploited so effectively in the pursuit of small biologically active molecules can also be employed in the design of synthetic polymers, particularly in the context of parallel synthesis.

Library Focusing

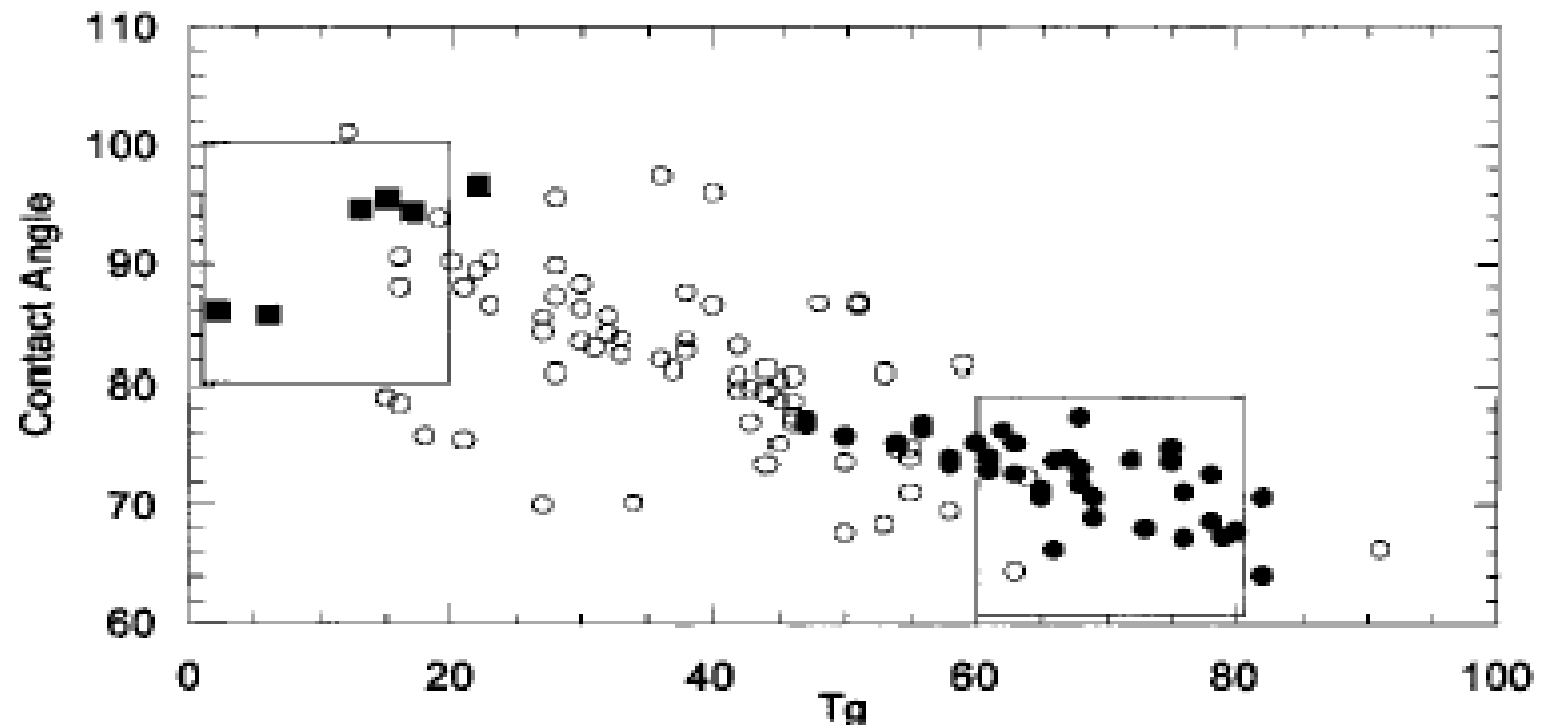


Figure 10. Map of T_g and CA property space. Two focused libraries are shown. The filled squares (**Focus1**) are a library focused on T_g between 0 and 20 °C and CA between 80 and 100° (low T_g —high CA). The filled circles (**Focus2**) are a library focused on T_g between 60 and 80 °C and CA between 60 and 80° (high T_g —low CA).

The Results

- Another way to measure the success of this focused library is to compute the number of “hits” identified for a given number of polymers synthesized and tested.
- For the low Tg-high CA focused library, [25 “hit”](#) polymers (17 in the screening library + 8 in the focused library) nets five “hits”.
- By comparison, random testing of 25 polymers from the full library of 112 possible polymers would only be expected to net [2 “hits”](#) based on the incidence of polymers in the full library that satisfy both the Tg and CA restraints.

Optimal Binary Alloys

- Johannesson, G.H. et. al., “Combined Electronic Structure and Evolutionary Search Approach to Materials Design,” Physical Review Letters 88, 255506(5) (2002)
 - Material type are four-component alloys of 32 transition, noble and simple metals in fcc- and bcc-based structures,
 - Primary Descriptor (and fitness function) was the Heat of Formation as calculated by DFT (LMTO and KKR)
 - Evolutionary algorithm encoded alloys directly:

Pt	Ru	Pd	Al
Al	Al	Zn	Zr
Hf	Hf	Ir	Ir

...

Population of 20

Optimal Binary Alloys

- Results depended on “models” used
 - With simplest fitness function,
 - All the most stable alloys preferred bcc to fcc,
 - Typically involve an equal number of early and late transition metals.
 - These are known to be not very ductile materials.
 - Impose the additional model that alloy must be more stable in fcc than in bcc in order to be “fit”
 - Noble metals (e.G. Pd and pt) become important,
 - The stable alloys are thus very expensive
 - Impose a primitive cost model, by excluding Ag, au, pd, pt, Ir
 - Stable alloys now dominated by transition metal silicides
 - Excluded Si
 - Known superalloys then appear on the list

Optimal Isomerization Catalysts

- “Development of a low temperature light paraffin isomerization catalysts with improved resistance to water and sulphur by combinatorial methods,”
Applied Catalysis A, General, 239, (2003) 35-42.
 - By means of combinatorial techniques (high-throughput catalyst preparation and testing systems, and a genetic algorithm (GA)), a search of new more tioresistant catalysts for low temperature isomerization of light paraffins has been conducted.
 - After three evolving cycles catalysts have been found that not only are active and selective but also are more resistant to deactivation by water and sulphur than the corresponding conventional ones.
 - The results have been reproduced in a pilot plant and the stability is shown.



The System Studied

- Metal oxide supports three different supports were chosen,
 - γ -Al₂O₃; ZrO₂; TiO₂.
- Acidity enhancers these components are known to generate acidity when interacting with the support.
 - The selected ones were SO₄²⁻, BO₃³⁻, PO₄³⁻ and WO_x.
 - Each catalyst consisted of only one enhancer and its percentage over the support is ranging from 0.5 to 6 wt.% for sulphur, boron and phosphorus and 0.5 to 36% for tungsten.

Five different enhancer contents were chosen.

- Promoters the promoters are introduced with different purposes
 - (a) to increase isomerization activity and selectivity,
 - (b) to decrease coke formation
 - (c) specially to improve catalyst resistance against water and sulphur poisoning.
- The preferred promoting elements are Pt, Ce, Pd, Nb, Sn, Ni and Mn.
 - The content of each metal over the support is ranging from 0.5 to 6 wt.% for all metals and in this range we have chosen five different levels.

Four acid enhancers were used to generate acidity over the supports. These acid promoters were:

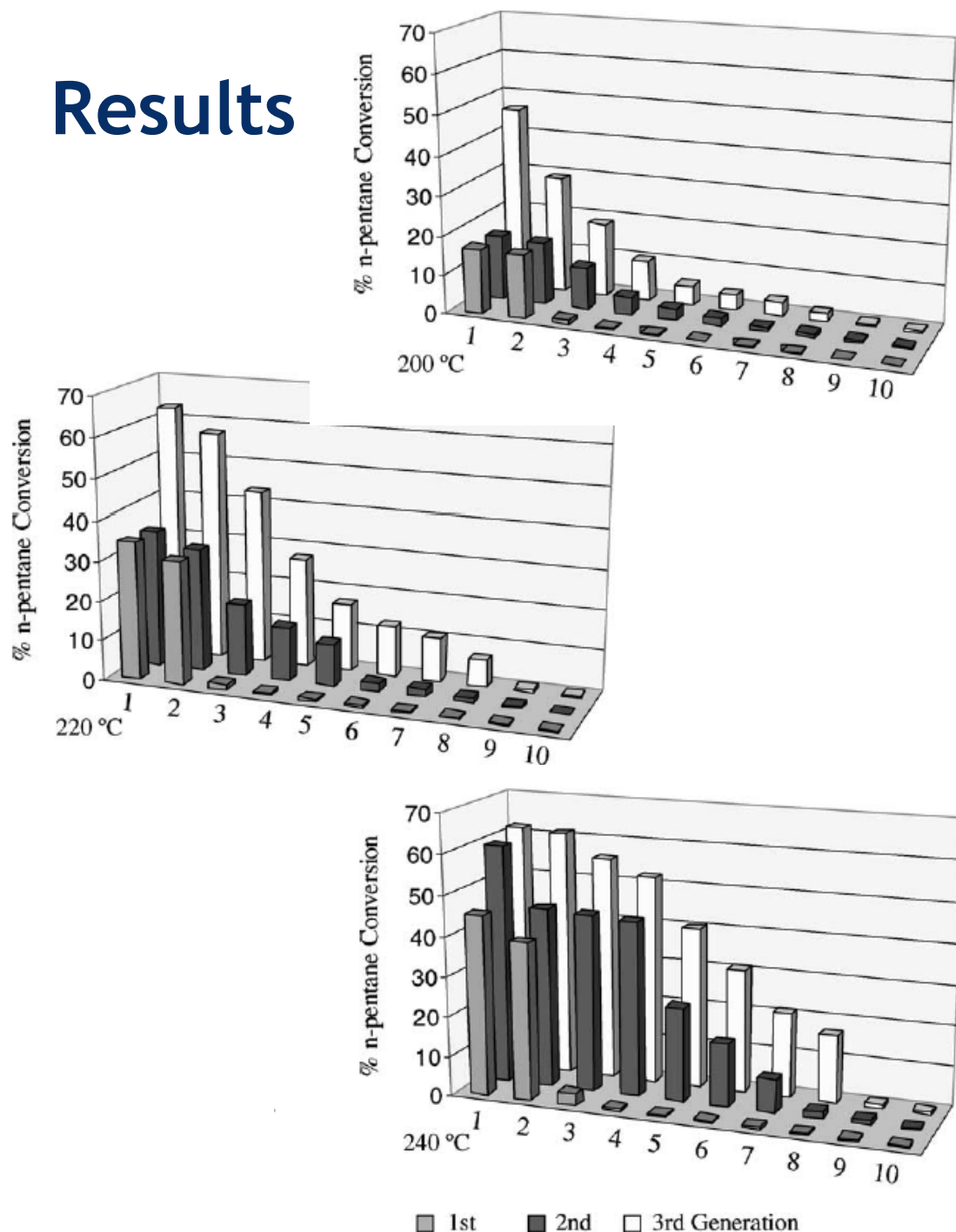
- (NH₄)₂SO₄ as a source of sulphate groups.
- H₃BO₄ as a source of borate groups.
- H₃PO₄ as a source of phosphate groups.
- (NH₄)₆H₂W₁₂O₄₀·nH₂O as a source of tungstenate groups.

2.2.3. Metallic promoter precursors

Five promoters were used:

- Ni(NO₃)₂·6H₂O as a source of Ni.
- MnCl₄·4H₂O as a source of Mn.
- SnCl₄·5H₂O as a source of Sn.
- Ce(NO₃)₃·6H₂O as a source of Ce.
- PdCl₂ as a source of Pd.
- C₁₀H₅O₂₀Nb·H₂C₂O₄ as a source of Nb.
- H₂PtCl₆ as a source of Pt.

Results



	Support	Acidity enhancer (wt.%)	Promotor (wt.%)	Promotor (wt.%)		
First generation						
1	ZrO ₂	S	1.75	Ce	0.97	Pt 0.51
2	ZrO ₂	S	2.18	Pd	1.00	Pt 0.46
3	TiO ₂	W	17.38	Mn	0.87	Pt 0.48
4	ZrO ₂	W	5.58	Ni	0.55	Pt 0.51
5	Al ₂ O ₃	W	45.57	Nb	4.60	Pt 0.52
6	Al ₂ O ₃	W	11.27	Sn	5.52	Pt 0.47
7	ZrO ₂	B	0.54	Ni	1.06	Pt 0.50
8	ZrO ₂	P	4.34	Mn	3.90	Pt 0.48
9	TiO ₂	B	0.55	Mn	0.97	Pt 0.55
10	Al ₂ O ₃	W	11.32	Ni	1.09	Pt 0.51
Second generation						
1	ZrO ₂	S	2.22	Pd	0.49	Pt 0.47
2	ZrO ₂	S	1.76	Ce	0.97	Pt 0.51
3	ZrO ₂	S	2.57	Nb	4.05	Pt 0.47
4	ZrO ₂	S	2.05	Mn	1.74	Pt 0.48
5	ZrO ₂	B	2.33	Mn	1.86	Pt 0.51
6	Al ₂ O ₃	P	1.42	Mn	7.87	Pt 0.52
7	TiO ₂	P	3.72	Ce	0.94	Pt 0.49
8	TiO ₂	S	2.55	Ni	2.05	Pt 0.49
9	TiO ₂	S	1.98	Ce	0.86	Pt 0.51
10	Al ₂ O ₃	W	39.18	Ce	0.68	Pt 0.49
Third generation						
1	ZrO ₂	S	2.21	Nb	0.48	Pt 0.56
2	ZrO ₂	S	2.15	Ce	1.18	Pt 0.48
3	ZrO ₂	S	0.59	Pd	0.52	Pt 0.56
4	ZrO ₂	S	1.81	Nb	5.11	Pt 0.42
5	ZrO ₂	S	2.44	Nb	3.96	Pt 0.52
6	ZrO ₂	S	2.63	Ce	1.10	Pt 0.47
7	ZrO ₂	S	2.55	Nb	0.88	Pt 0.48
8	ZrO ₂	S	2.09	Mn	1.13	Pt 0.48
9	ZrO ₂	P	3.32	Nb	1.01	Pt 0.44
10	TiO ₂	S	2.62	Ce	0.52	Pt 0.48

What is QSAR?

- Quantitative structure-activity relationships
- Addresses two questions:
 - What features of a molecule affect its activity?
 - What can be modified to enhance properties?
- Quantitative in that a mathematical model is used to account for the observed activity.

Birth of QSAR

⇒ 1893

“Plus ils sont solubles, moins ils sont toxiques”

Charles Richet

⇒ 1964

“Fragment and additive group contribution theory”

Hansch and Fujita

Quantitative Structure-Activity Relationship (QSAR)

Conditions: Y observations (Dependent variable)
X parameters (Independent variable)

Objective: Correlate Y with X1, X2 ...

Challenge: Variance is spread over X parameters
Find the QSAR signal...

... in a huge field of variance!

“Variations in X1, X2 ... that are correlated with changes in materials activity... and make sense!”

Concerns

Quality of Y:

“Strength of a QSAR model depends on the quality of the dependent variable”

Choice of X:

“Improper choice of independent variables often results in a poor QSAR model”

Overfitting:

“With enough parameters, you can correlate anything with anything!”

- Ideal ratio is 1 independent variable to 5 molecules

Descriptors

Descriptor Families

Topological

Fragments

Receptor surface

Structural

Information-content

Spatial

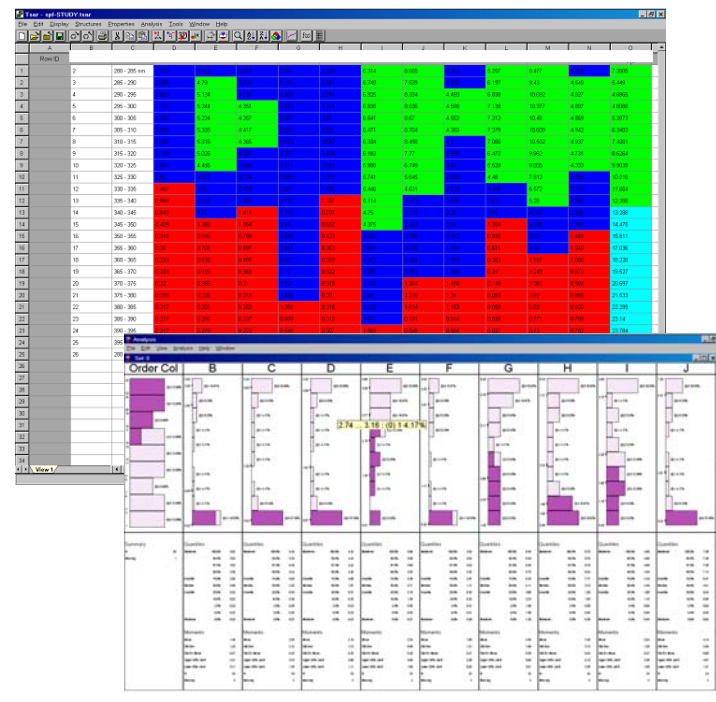
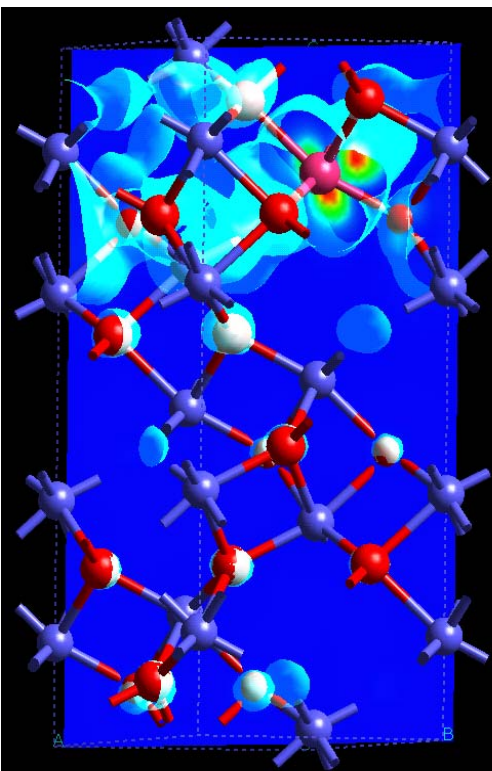
Electronic

Thermodynamic

Conformational

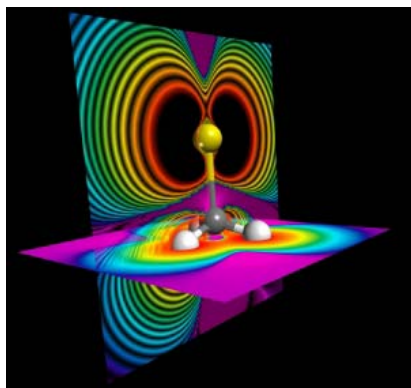
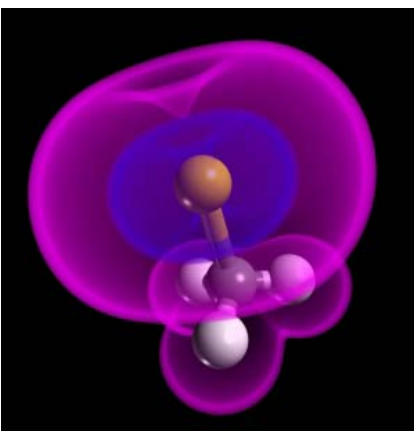
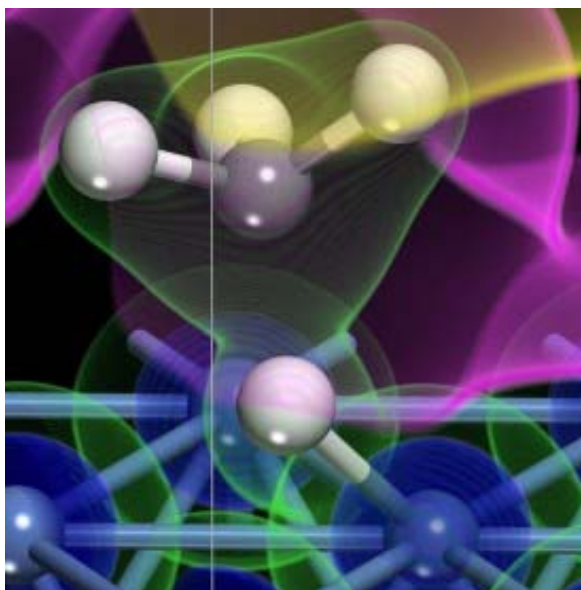
Quantum mechanical

Descriptors - calculable molecular attributes that govern particular macroscopic properties



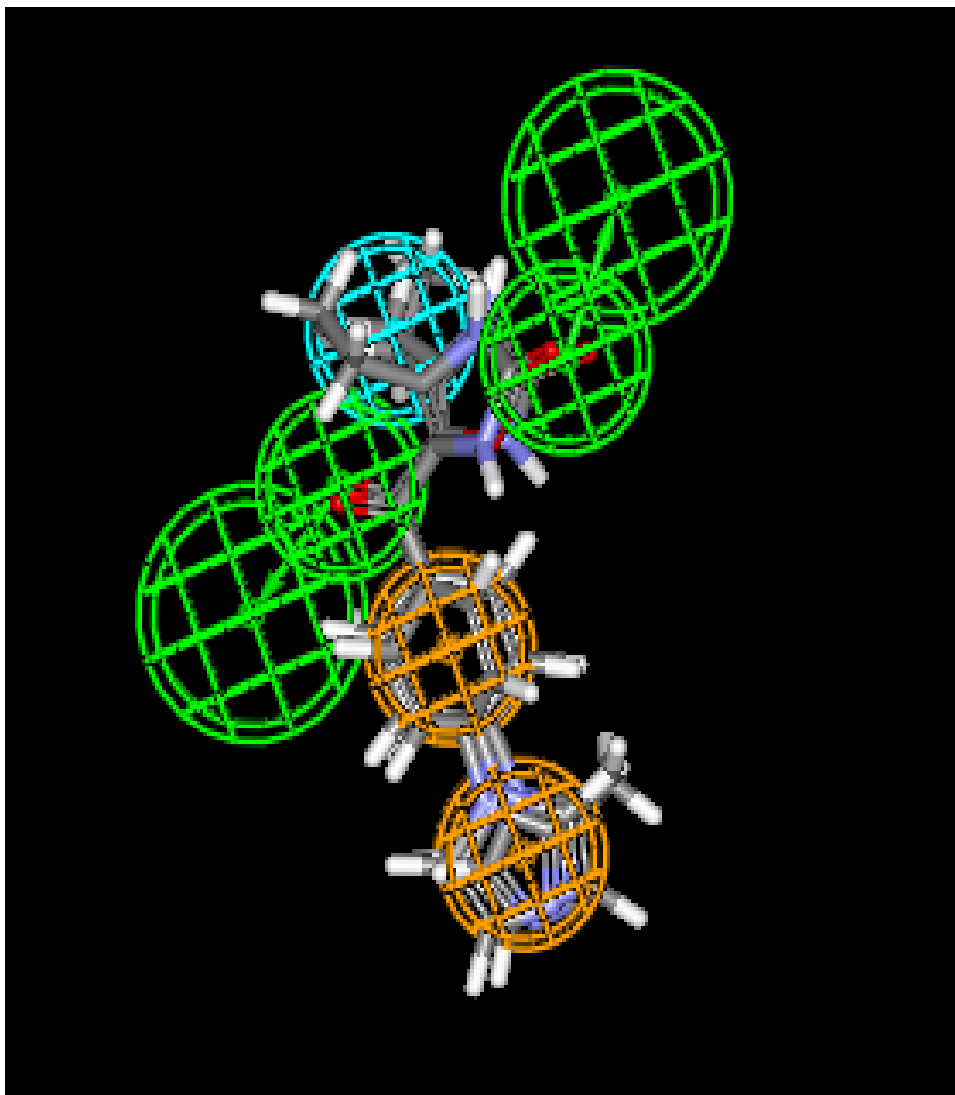
Computation Solution

QM/Catalysis Modeling



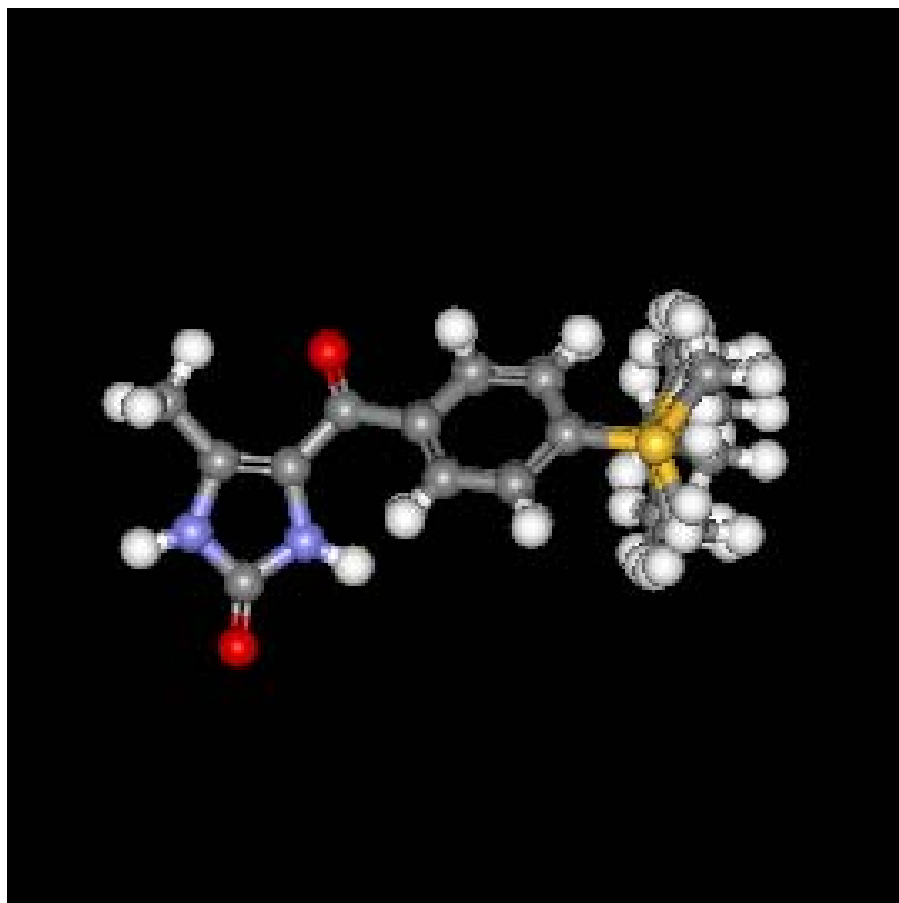
- Tools for modeling homogeneous and heterogeneous systems
 - Surface builder, organometallic sketching using fragment browser
- DMol³ for modeling gas phase, 3D periodic systems and reactions at surfaces
 - Calculate energy, geometry optimization, transition state search and optimization
 - Properties including orbitals, electrostatics, Fukui functions
- CASTEP for modeling 3D periodic systems
 - Calculate energy, geometry optimization, dynamics
 - Properties including density of states, band structure, optical properties
- VAMP semi-empirical code
 - for molecular organic and inorganic systems

Feature Based Descriptors



- Analysis of the spatial distribution of similarly charged groups and also similar chemical groups can lead to an understanding of the complex processes and chemistry in materials systems.

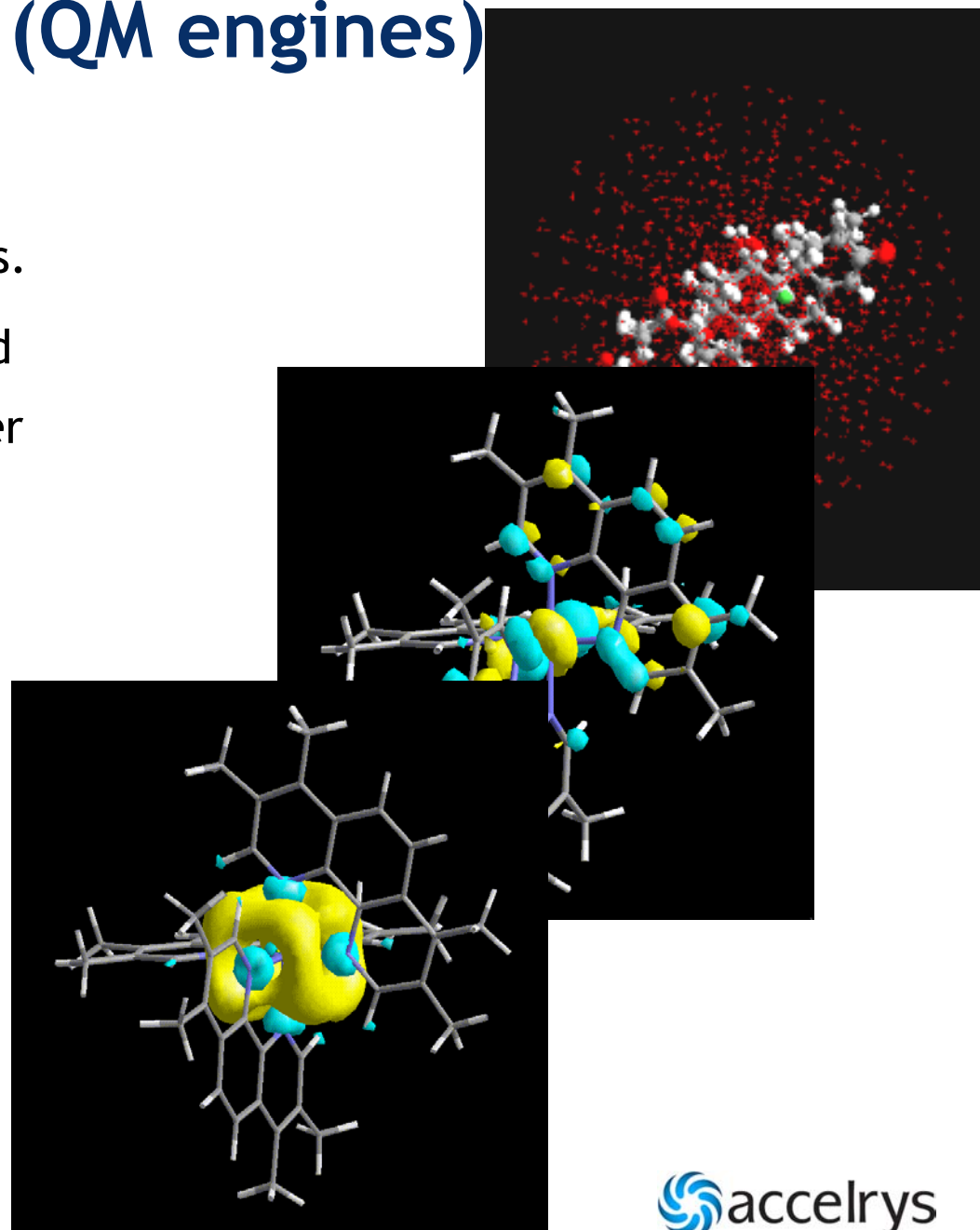
Conformation Based Descriptors



- Conformational distributions, characteristics of distribution (FWHM) moments of distributions, characteristic frequencies of distributions and ranges of properties are all important descriptors for materials modeling.

Electronic Descriptors (QM engines)

- HOMO, LUMO, other eigen values.
- Polarizability, Fukui Softness and Hardness, electron affinity, super delocalisability.
- Point charges, electron density, polarizability, multi pole-moments.
- MFA field interactions (probes, sorbants).



Analysis general: Materials Properties from Calculations - I

Structural properties

- Geometries of molecules
- Crystal structures (packing)
- Density
- Defect structures
- Crystal morphology
- Surface structures
- Interface structures

Mechanical Properties

- Compressibility
- Elastic moduli
- Thermal expansion coefficients
- Vibrational properties
- Hardness

Thermodynamic Properties

- ΔU , ΔH , ΔS , ΔG , C_p , C_v
- Binding energies
- Surface and interface energies - adhesion
- Pressure induced phase transitions
- Temperature induced phase transitions
- Phase diagrams

Transport properties

- Electrical conductivity
- Thermal conductivity
- Viscosity
- Diffusion constants
- Permeability

Chemical and other properties

- Chemical reaction rates
- Reactivity with surfaces
- UV stability

Analysis general: Materials Properties from Calculations - II

Electrical, optical, and magnetic properties

- Electron density distribution - electrical moments
- Polarizabilities, hyperpolarizabilities
- Ionization energies and electron affinities
- Electrostatic potential, work function
- Energy band structure - metal, semiconductor, insulator, superconductor
- Band gaps, band offsets at hetero-junctions
- Optical spectra
- Spin density distribution, magnetic moments, crystalline magnetic anisotropy
- Magneto-optical properties (Kerr rotation)
- NMR chemical shifts
- Dielectric response
- Luminescence
- Fluorescence

Chemical and other properties

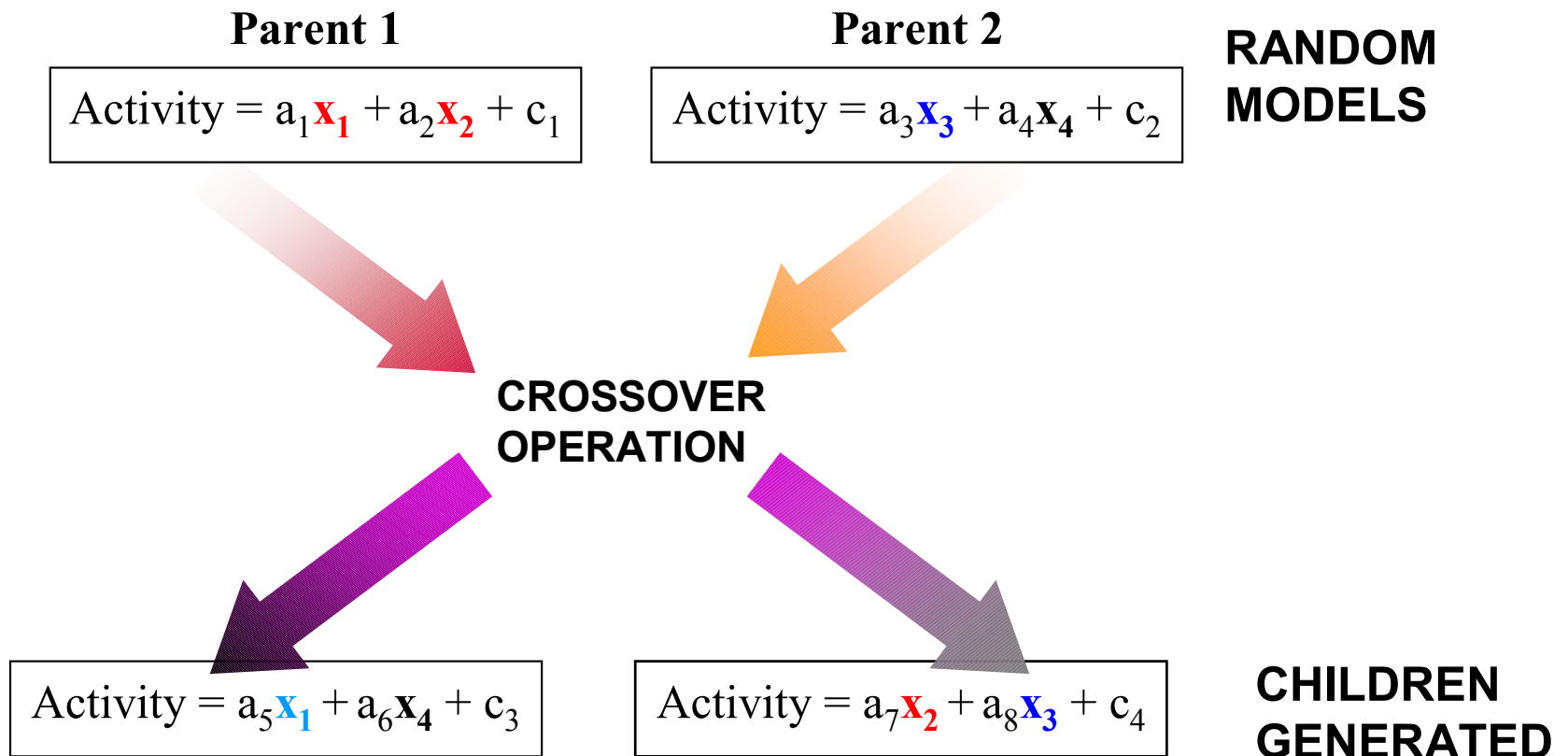
- Chemical reaction rates (catalytic properties, corrosion, electro-chemistry)
- Reactivity with surfaces
- UV stability

Genetic Algorithm

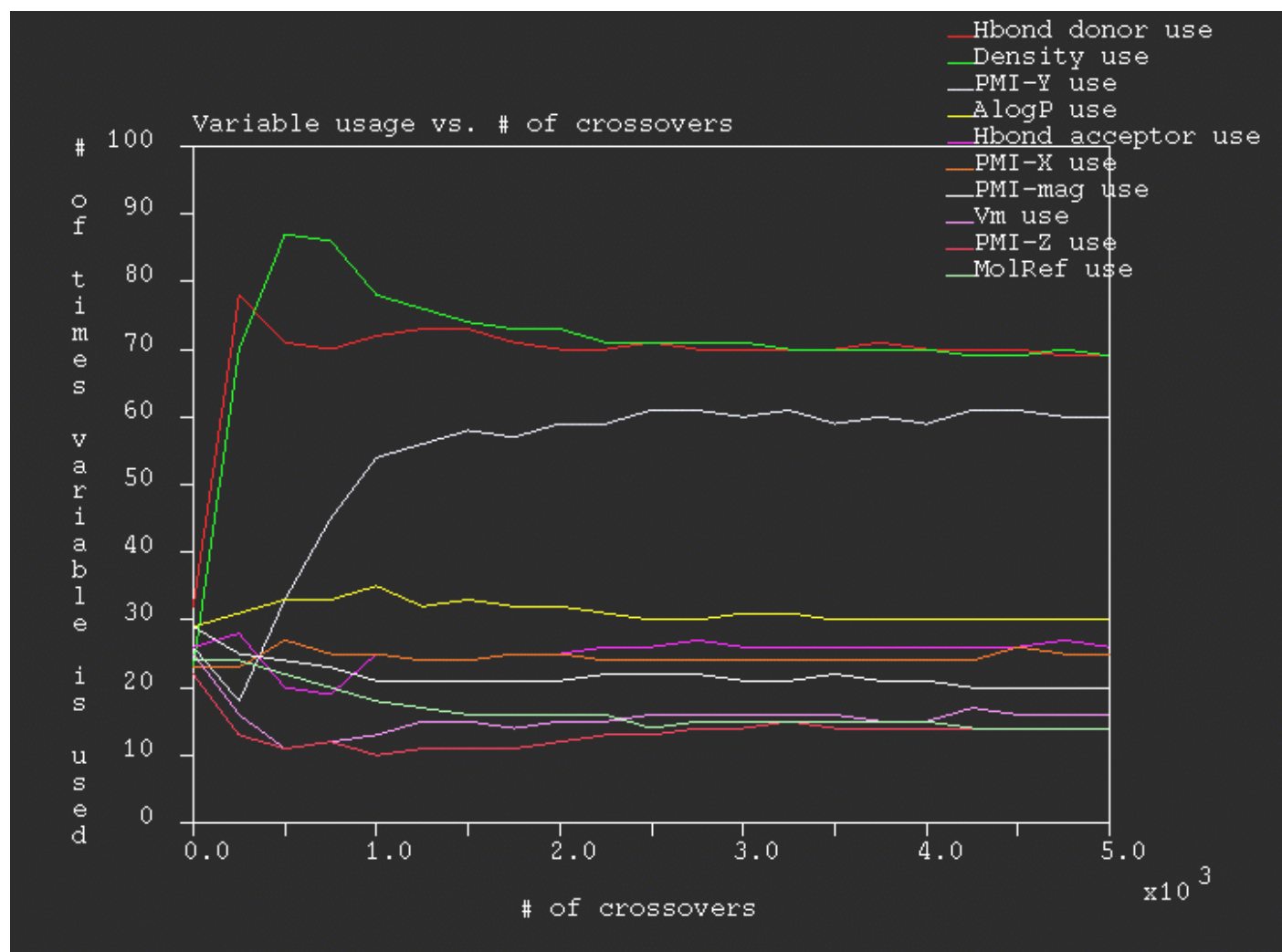
- *“Computer Simulation of Darwin's Theory”*
- Advantages
- Evolutionary algorithm (better models)
- Multiple models
- Prevents overfitting (LOF measure)
- Linear and higher order polynomial models
- Automatic outlier removal (spline)
- Monitor descriptor usage by crossover plot



Genetic Algorithm Flow Chart



GA Variable Usage



Good Principles for Setting up GA

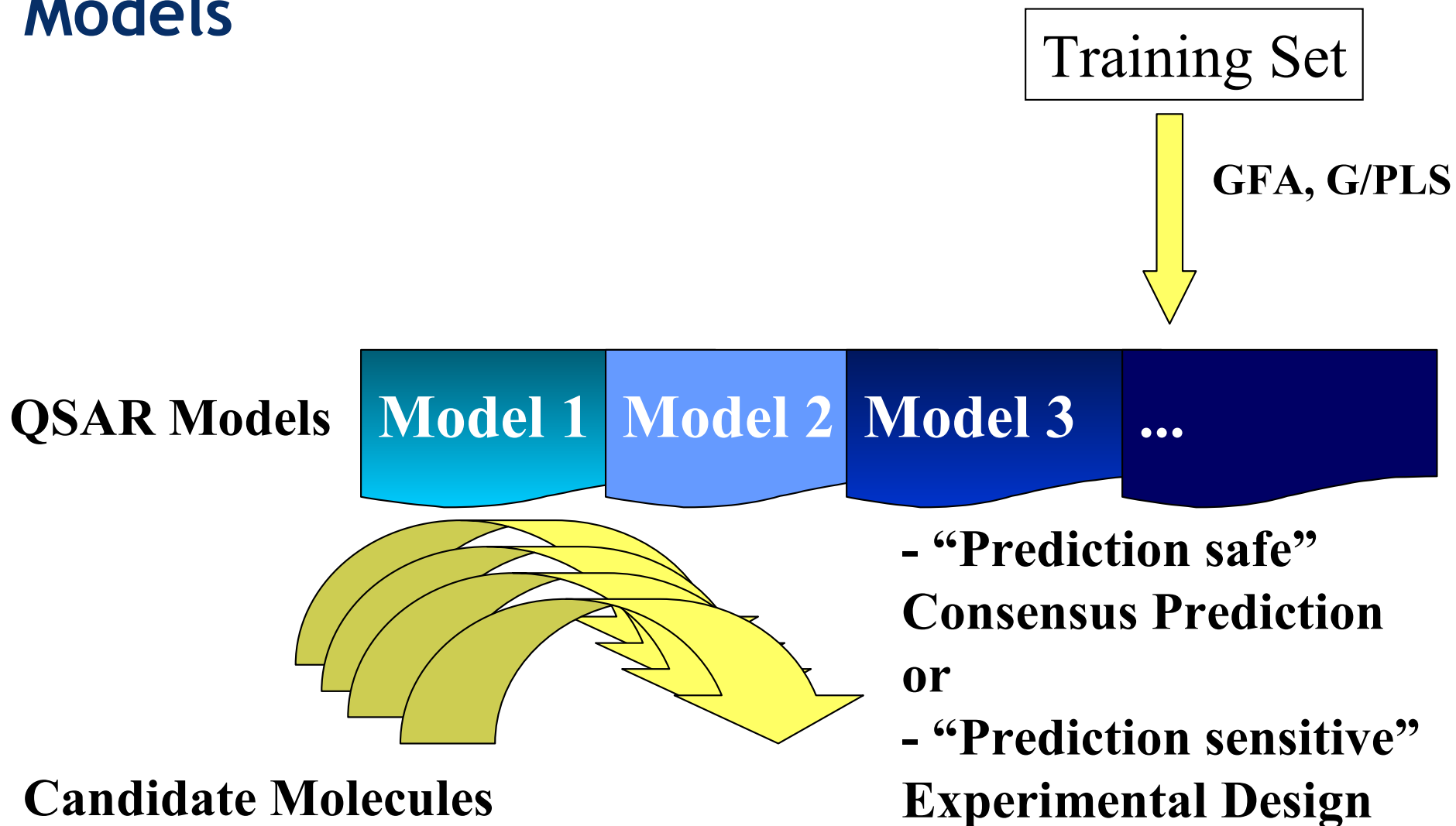
Equations:

1. Each descriptor involved in 1-5 equations
2. Start with simple terms (linear)

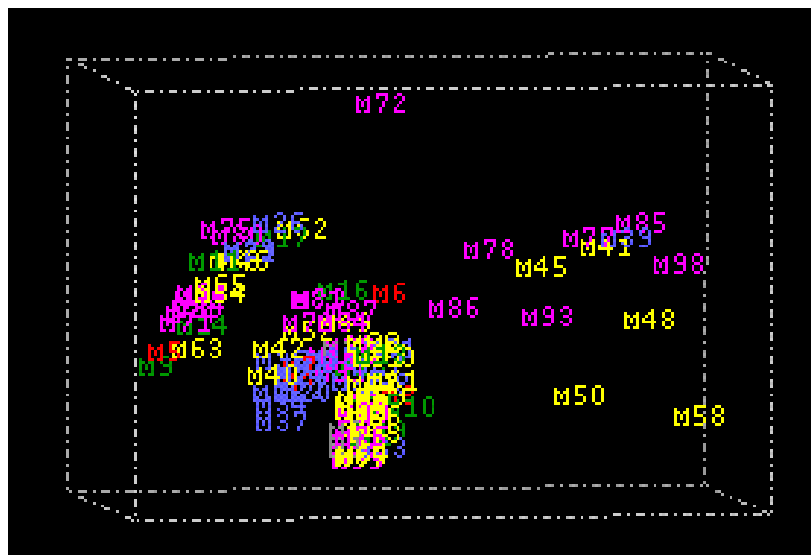
Evolution:

1. Use 10-50 times more iterations than equations
2. Check variable usage for convergence
3. Adjusting the smoothing factor

The Real Power of GFAs: Multiple QSAR Models

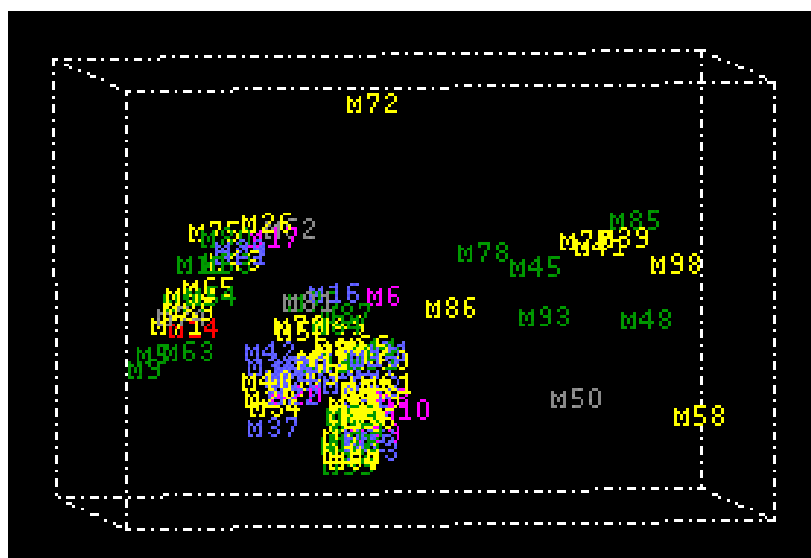


Graphical Analysis of Models



a

Models can be colored by LOF(a) or Adj. R^2 (b)

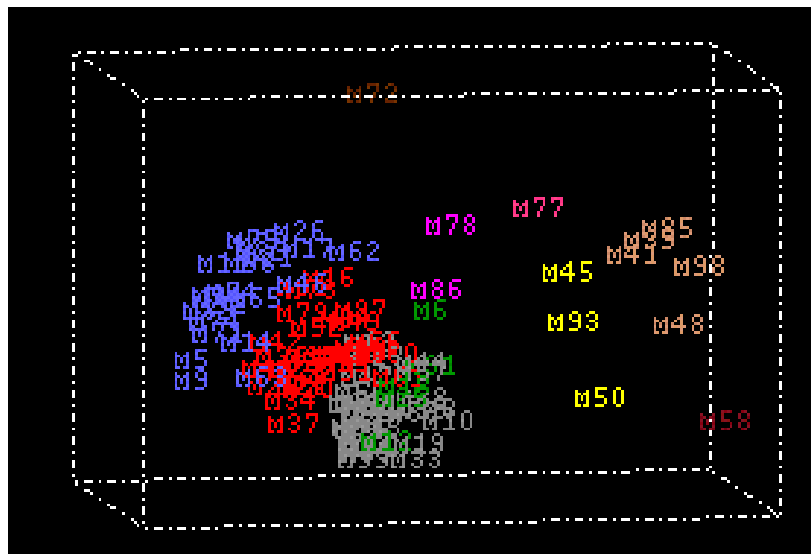


b

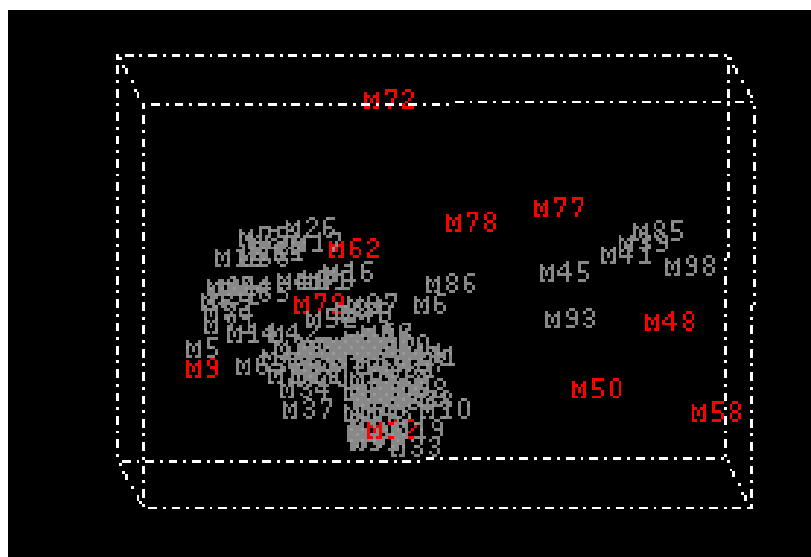
Other possible coloring schemes:

- F-test values
- Nvars
- R
- LSE

Clustering/Selection of Models

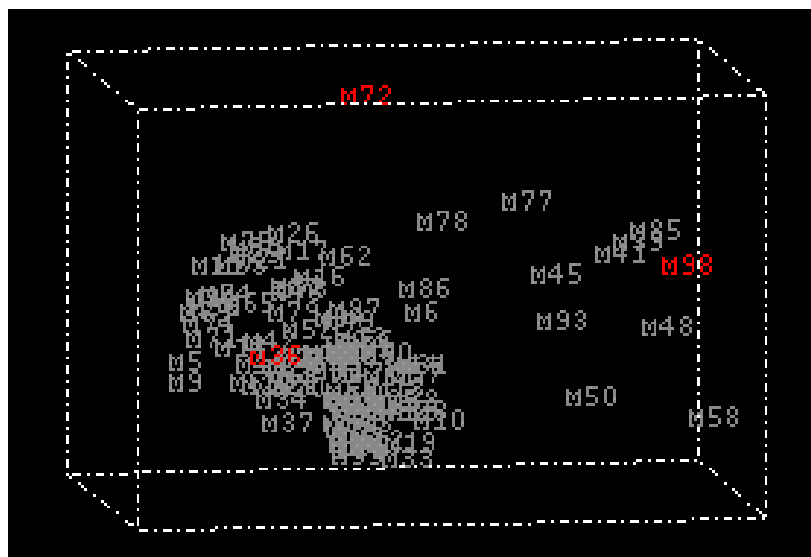


Clustering of models

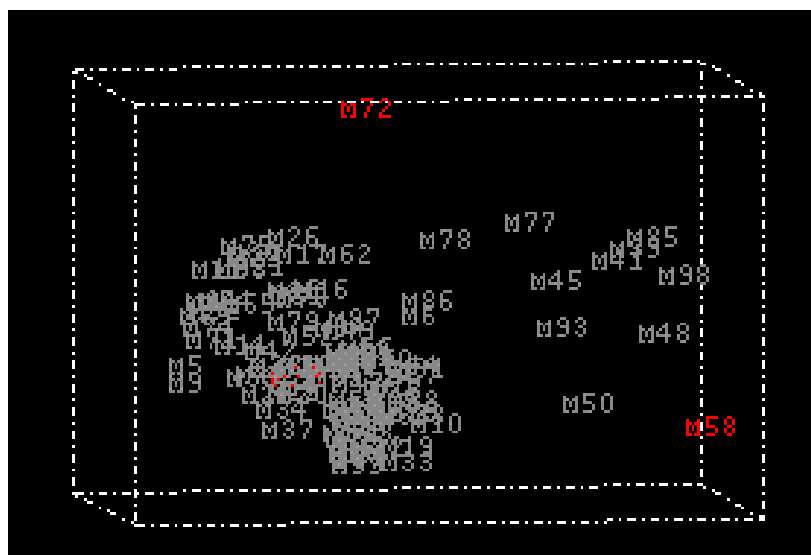


**Selection of 10
diverse models**

Representation of Basis Models



**Initial Selection:
M36, M98, M72**

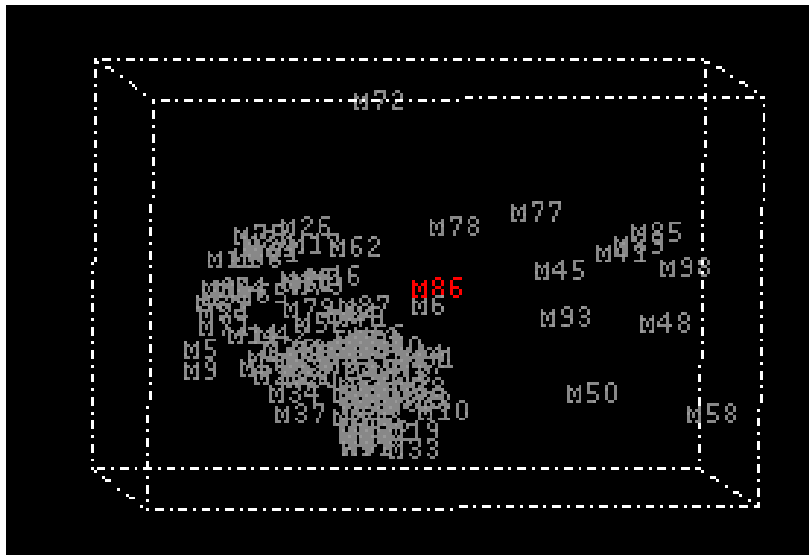


**Alternate Selection:
M23, M58, M72**

Identification of Consensus Model

Objective:

- Select a “central” model with minimal contradictions vs other possible models



Consensus Model:
M86

Use in Experimental Design

Objective:

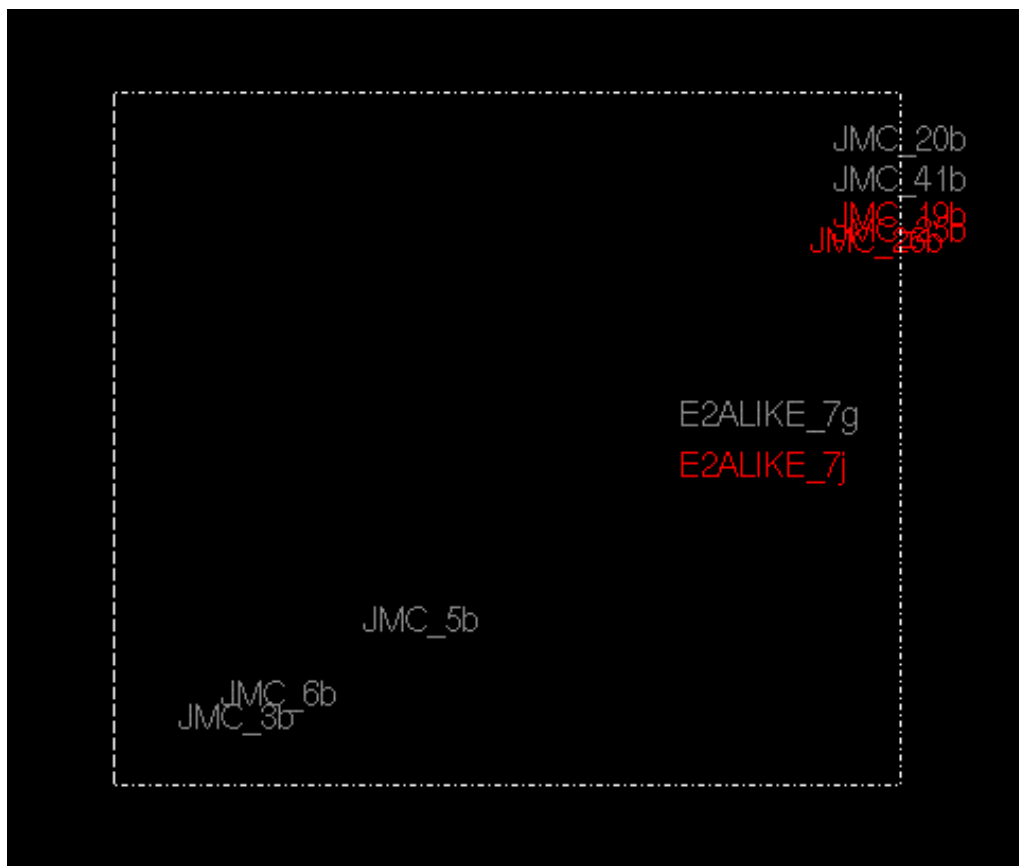
- Identify orthogonal models (basis models) corresponding to radically different prediction schemes
- Identify compounds which are “prediction safe”:
Predicted active by selected models

or

- Identify compounds which are “prediction sensitive”:
Predicted differently across selected models

Experimental Design

Compare predictions from models 15 and 35



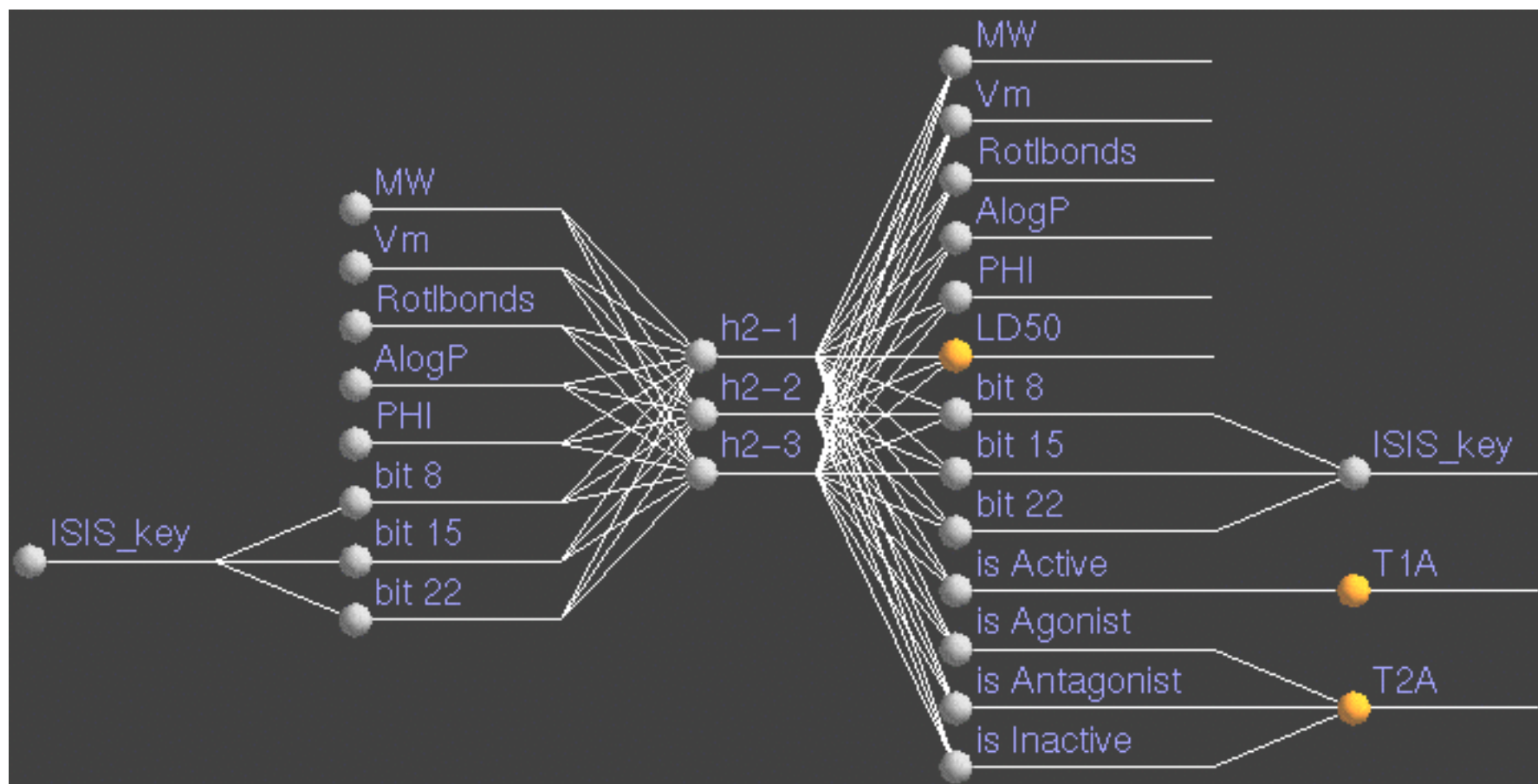
Diagonal:
Predicted same

Off Diagonal
Predicted different

Other 'new' techniques

- Neural networks (McCulloch and Pitts, 1943)
- Rule induction (Quinlan, 1986)
- Expert systems (molecular mechanics, *etc.*)
- New statistical methods (continuum regression)
- Hybrid systems

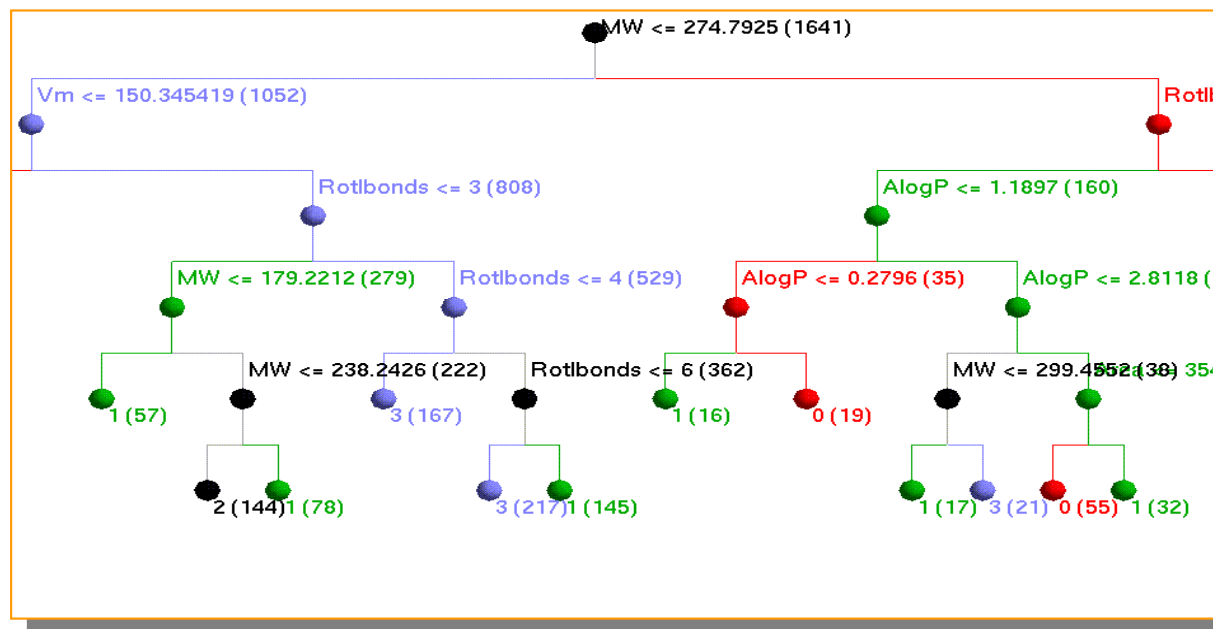
Backpropagation Network Review



- Layers of nodes, connections between layers
- Pre/post-processing of fingerprints/categoricals
- $L \rightarrow R$: prediction, $R \rightarrow L$: training/weight update

VHTS: Recursive Partitioning

- SAR and Activity Prediction from HTS data - recursive partitioning
 - Categorical dependant (screening) data
 - Categorical (e.g. fingerprint) or continuous independent data
 - Decision tree to best isolate members of each class
 - Weighting by classes
 - Various splitting rules: impurity, two-ing, greedy split



Thin Layer Polymer Systems

Collaborators:

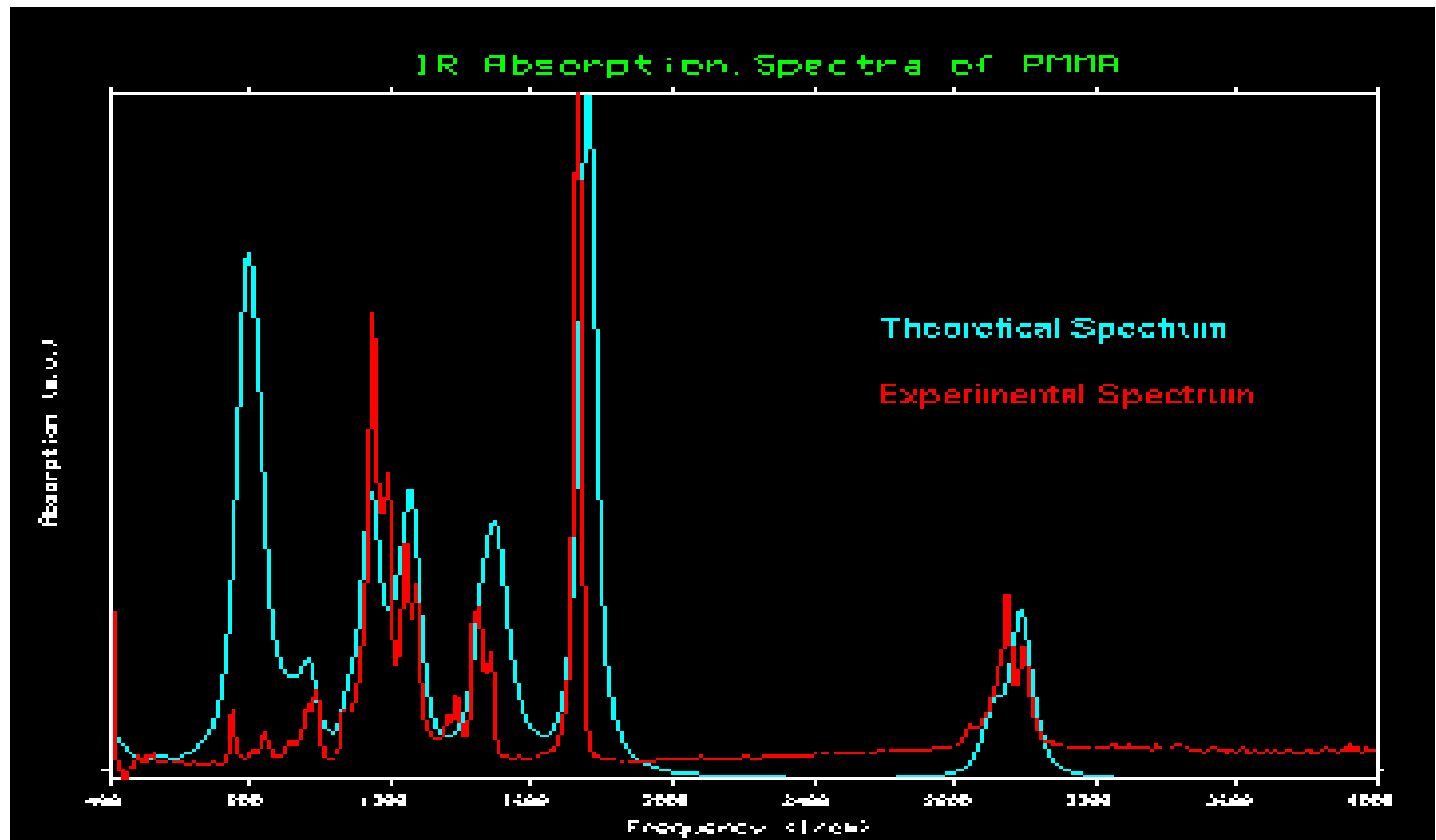
CEA – *Armand Soldera*

Accelrys – *Peter Gravil*

Optical Coatings

- Researchers at CEA/Le Ripault, France, needed a tool which could predict the transmission, adsorption and reflection of a given film in advance of manufacturing the material
- Using Accelrys' software they were able to design a library polymers with specific optical properties in the UV, Visible and IR spectral range. They also validated their focusing algorithms which were based on quantum chemistry tools
 - A Soldera, J.P. Dognon, "Infrared Absorption Spectras of Polymers from Classical Molecular Simulation², submitted to "12th European Symposium on Polymer Spectroscopy", Lyon, France.

Optical Coatings



Carbon nanotubes in Flat-Panel Displays – *effect of adsorbates*

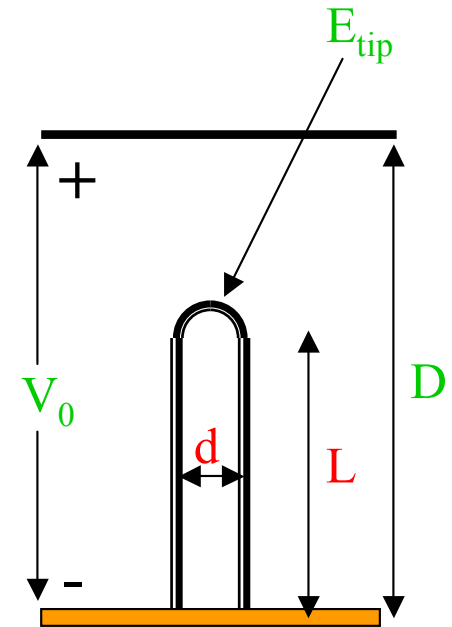
Collaborators:

Motorola -- *Paul Von Allmen*

Accelrys -- *J. Andzelm, N. Tanpipat*

Nanotubes as field-emission devices

- High length-to-width ratio makes metallic nanotubes behave like antennas
 - Aspect ratio can be as high as 10^5
 - Very high fields can occur at tube tip
 - Electron emission can occur at fields as low as 0.3 eV/\AA
- Aligned nanotubes can be used as Flat-Panel displays
 - Researchers have invented advanced fabrication methods for patterning aligned nanotube films on glass or silicon substrates

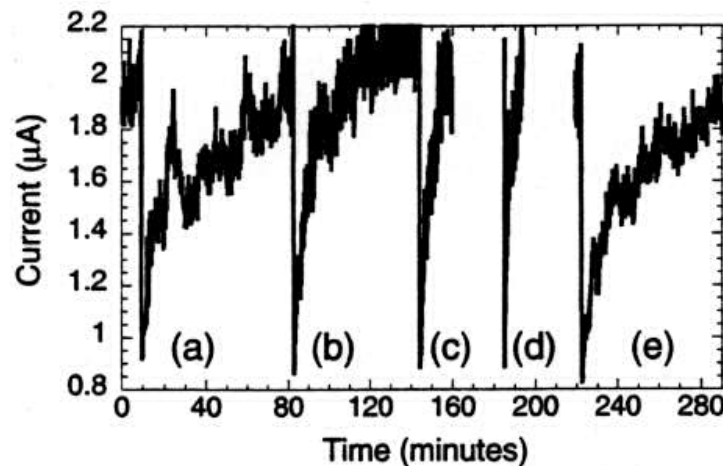


$$E_0 = V_0/D$$

$$E_{\text{tip}} \sim E_0(L/d)$$

There's a need to lower operating voltage!!!

Adsorbate effects on field emission

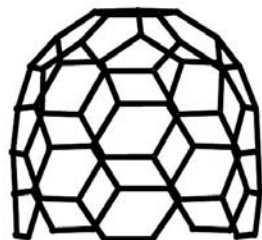


Dean et al., *J. Vac. Sci. Technol. B* 17, 1959 (1999).

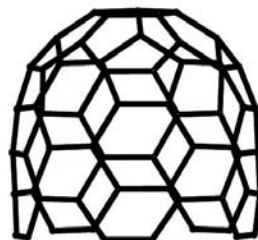
FIG. 4. The effect of water partial pressure on the recovery time of field emission current after heating the emitter to 900 K. (a) 5×10^{-9} Torr H_2O , (b) 5×10^{-8} Torr H_2O , (c) 4×10^{-7} Torr H_2O , (d) 5×10^{-6} Torr H_2O , and (e) 2×10^{-9} Torr H_2O after 3 h of pumping after measurement of (d).

- Water molecules present at the nanotube tip significantly enhance field-emission current
- Higher water concentration has stronger effect
- The water molecules are stable up to $T \sim 900$ K
- Non-polar molecules like H_2 does not have appreciable effect

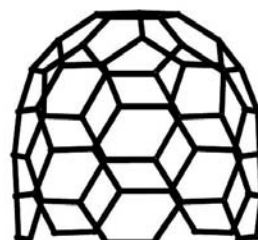
Modeling of adsorbates on nanotube tip



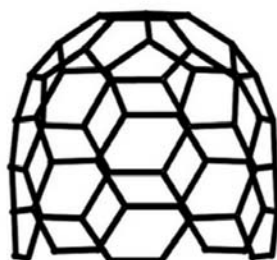
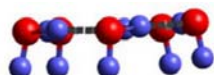
H₂ flat



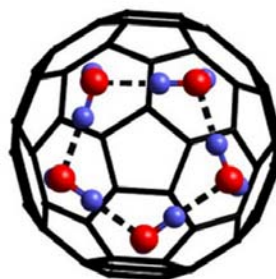
H₂ upright



Water down



*5 Water adsorbates
(side view)*



*5 Water adsorbates
(top view)*

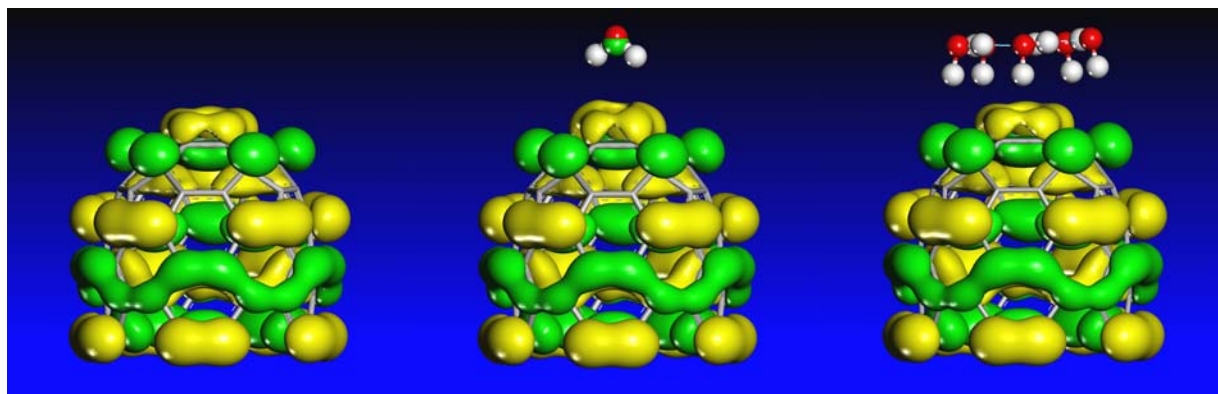
- (5, 5) Armchair tube
- 3-layer stem capped by a C₆₀-half
- Dangling bonds at stem-end were not H-saturated
- C-atoms at open end fixed
- Concentrated E-field at tip represented by a uniform field of $E_{FE} \sim 1 \text{ eV/\AA}$.
- Accelrys' DFT code DMol³

www.accelrys.com/mstudio/dmol3.html

How does adsorbed water effect field emission?

<i>System</i> (at $E = 1 \text{ eV/\AA}$)	<i>Ionization Potential</i> (eV)	<i>Position of HOMO</i> (eV)
<i>Free Nanotube</i>	6.4	- 5.1
<i>1 Water on Nanotube</i>	6.3	- 5.0
<i>5 Water on Nanotube</i>	5.8	- 4.5

- HOMO remains confined to nanotube \Rightarrow emission occurs from nanotube
- Shape of HOMO not affected significantly by adsorbates
- However:
 - HOMO becomes more unstable in presence of water
 - Instability increases with # adsorbed water
 - Instability correlates perfectly with a decrease in Ionization Potential



HOMO of isolated nanotube, nanotube + 1 water; nanotube + 5 water

Ionization Potential vs. adsorbate dipole moment

<i>Adsorbate</i>	<i>Dipole Moment (Debye)</i>	<i>Ionization Potential (eV)</i>
H ₂	0.0	6.40
HCl	1.0	6.36
H ₂ O	2.0	6.30
HCN	3.0	6.20
LiH	5.9	6.12

SnO₂ nanoribbons as chemical sensors

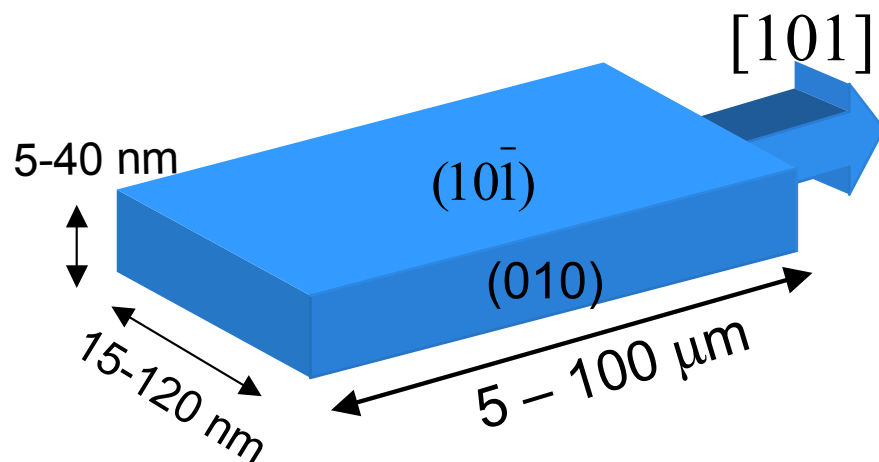
Collaborators:

Brookhaven -- *J. Rodriguez*

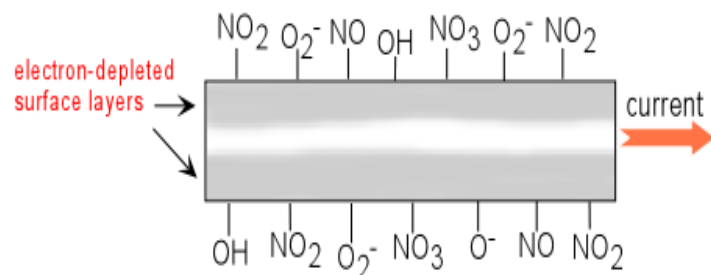
UC, Berkeley -- *M. Law, J. McKinney, P. Yang*

Accelrys -- *P. Kung*

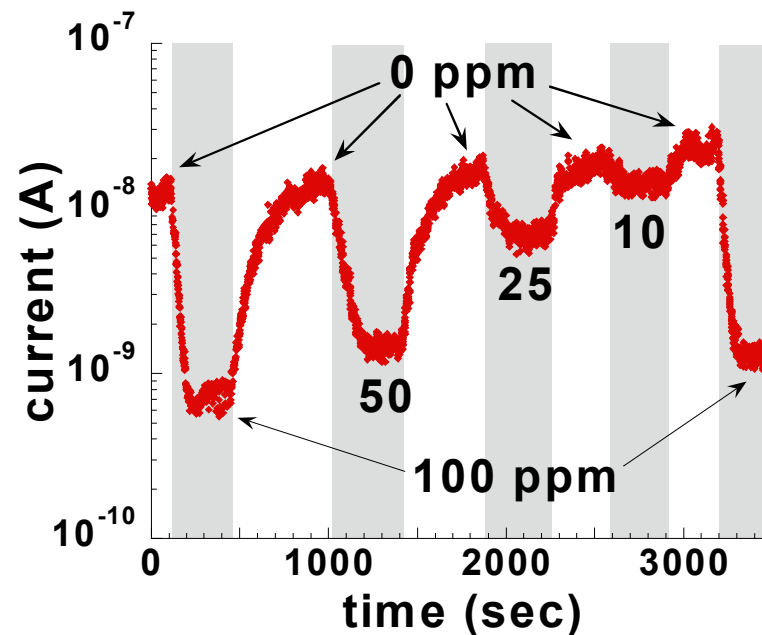
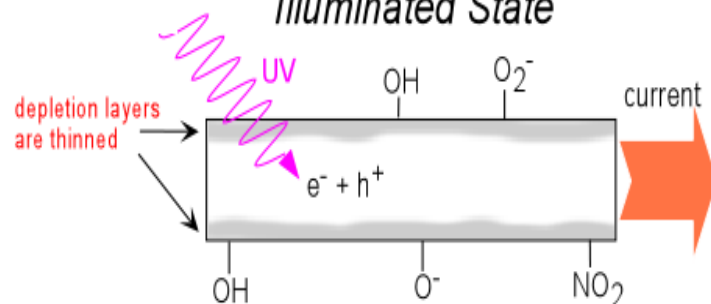
SnO₂ Nanoribbons as Gas Sensor



Dark State



Illuminated State



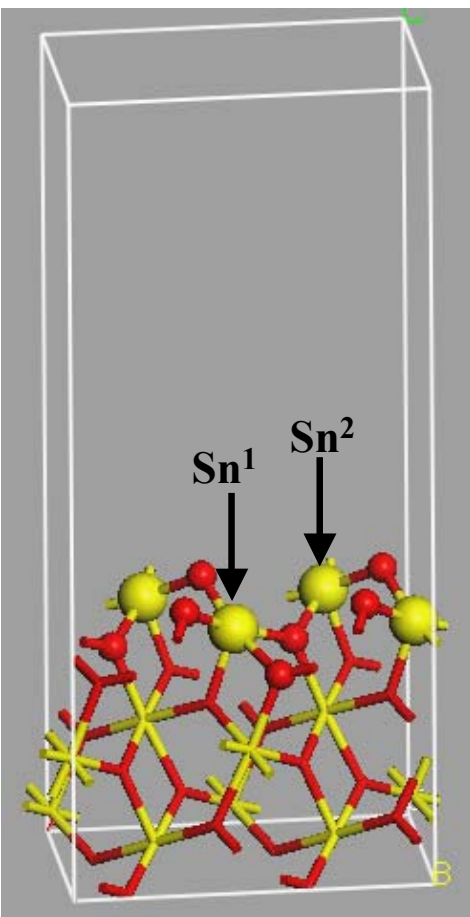
NO₂ adsorption lowers conductance

- Surface & bulk O-vacancies lead to *n*-type doping of the nanoribbon
- Chemisorption of NO₂ withdraws electrons from nanoribbon & lowers conductivity

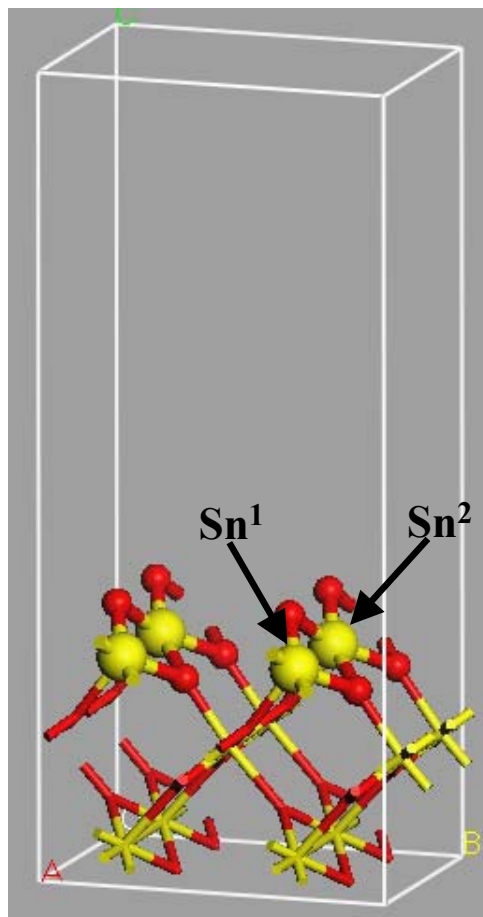
Re-usability

- Photodesorption by UV makes NO₂ adsorption reversible & restores conductivity

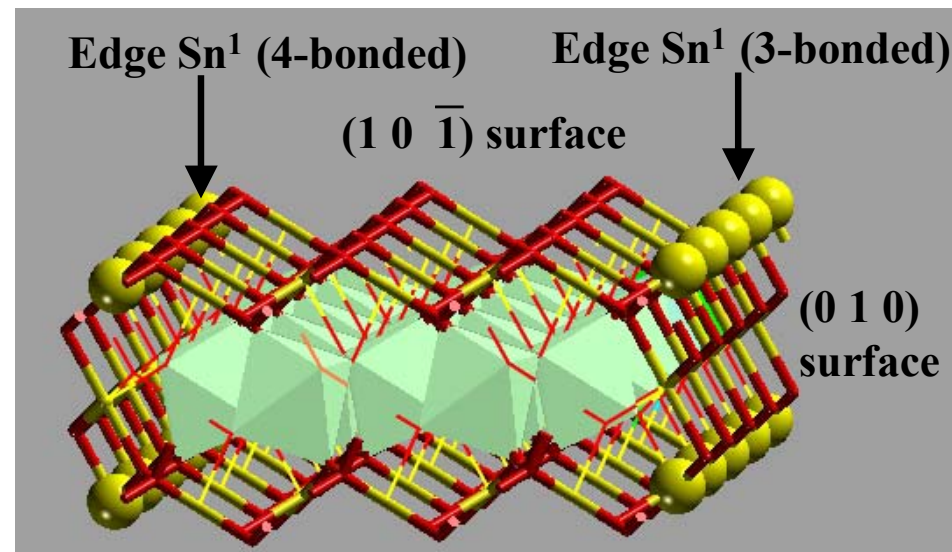
Modeling the Nanoribbon



(1 0 $\bar{1}$) surface



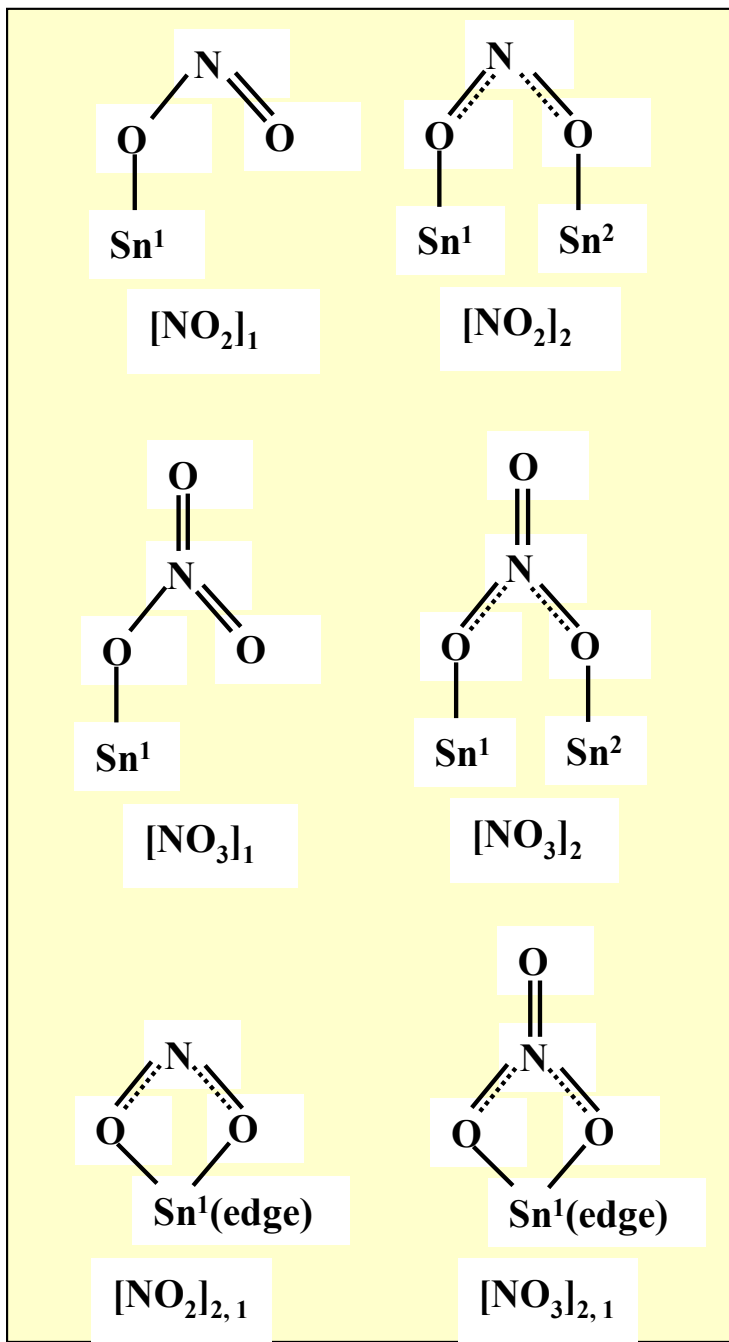
(0 1 0) surface



Nanoribbon edges

- Three separate models for (10 -1), (010), and nanoribbon edge
 - Surfaces terminated by *5fold*-coordinated Sn linked by *2fold*-coordinated bridging O
 - Edges terminated by *3fold* or *4fold*-coordinated Sn-atoms
- Adsorbate structures, binding energies, charge transfer computed by DMol³
 - Adsorbates: NO₂, O₂, CO

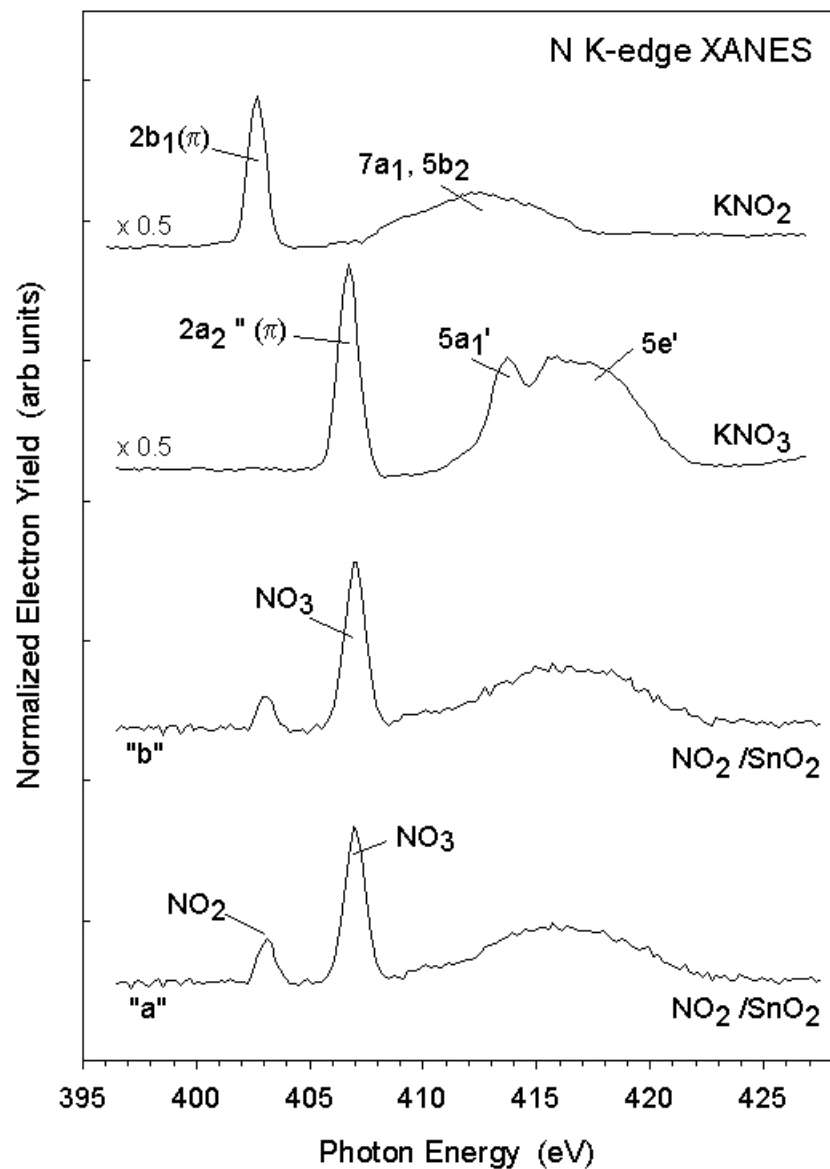
Binding at defect-free surface



Surface	Adatom structure	Binding Energy ^{a)} (kcal/mol)	Net charge Transfer (el)
(1 0 $\bar{1}$)	[O ₂]	1.4	0.00
	[CO] ₂ , Sn, O	12.9	+0.10
	[NO ₂] ₁	11.2	-0.17
	[NO ₂] ₂	13.8	-0.17
	[NO ₂] ₂ , Sn, O	2.8	+0.05
	[NO ₃] ₁	14.3	-0.30
	[NO ₃] ₂	25.5	-0.41

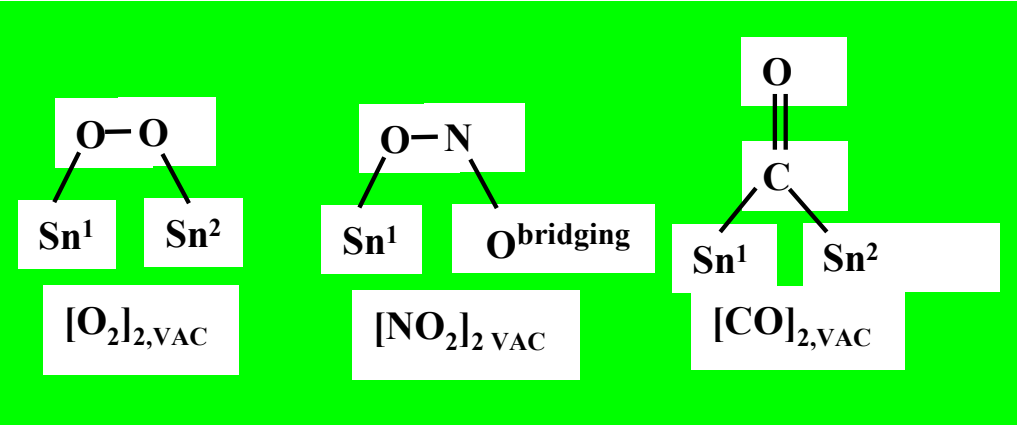
- O₂ has no effect on *defect-free* surface
- CO increases conductance
- 2-bonded NO₂ is slightly more stable than 1-bonded NO₂
 - NO₂ can freely walk along Sn-rows
- NO₂ + NO₂ → NO₃ + NO
 - 2-bonded NO₃ is strongly bound & immobile
 - NO is weakly bound

Confirmation of surface NO_3^{**}



****Performed at the *National Synchrotron Light Source @ Brookhaven National Lab***

Effect of surface O-vacancies

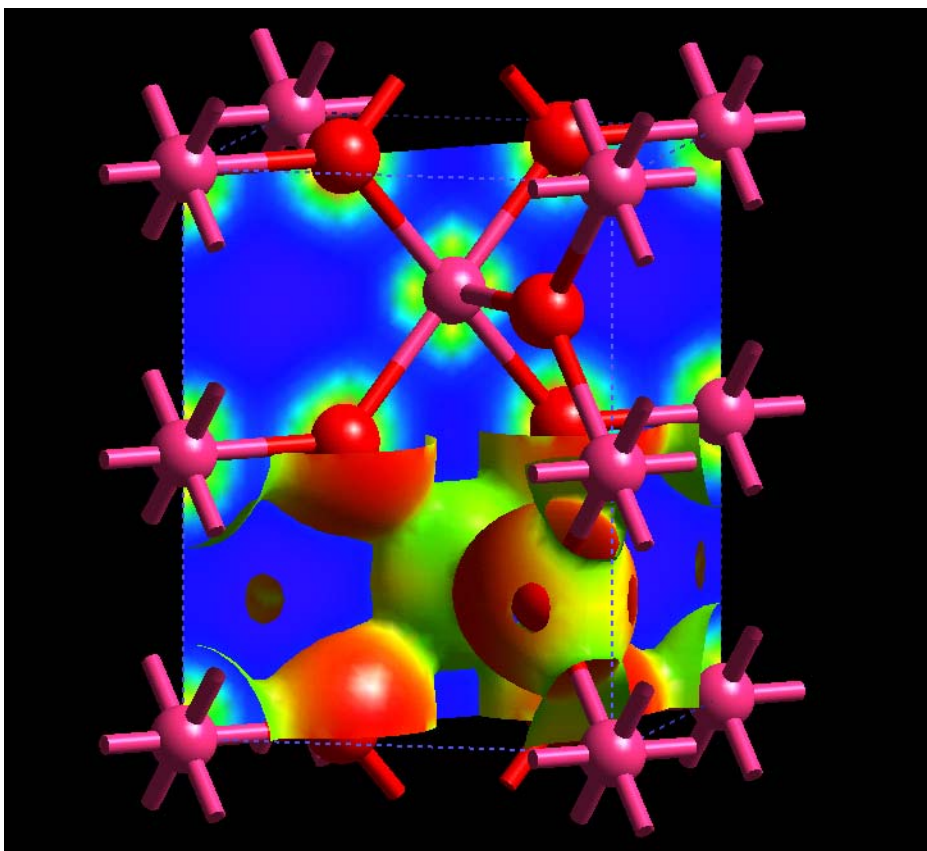


<i>Adatom structure</i>	<i>Binding Energy (kcal/mol)</i>	<i>Net charge Transfer (el)</i>
[O ₂] _{2, vac}	38.5	-0.88
[NO ₂] _{2, vac}	41.4	-0.51
[CO] _{2, vac}	6.1	-0.10

Summary:

- All adsorbate structures involves one or more bonds to surface Sn-atoms. Binding increases in the following sequence:
 - (010) < (10-1) < 3-fold-edge < 4-fold-edge
- O₂ adsorption leads to a significant drop in conductance only if surface O-vacancies are present
 - adsorbs as a peroxide bridge at a vacancy site
 - weak physisorption on a defect-free surface
- CO has higher binding to defect-free surface
 - should lead to an increase in conductance
- Adsorbed NO₂ should be mobile on the flat surfaces, until converged to NO₃ by a second NO₂
 - NO₂ + NO₂ → NO₃ + NO
 - NO has weak binding (< 2 kcal/mol) and should desorb easily
 - Surface NO₃ confirmed by XANES spectroscopy

β -MnO₂ Pyrolusite



$P4_2/mnm$ space group

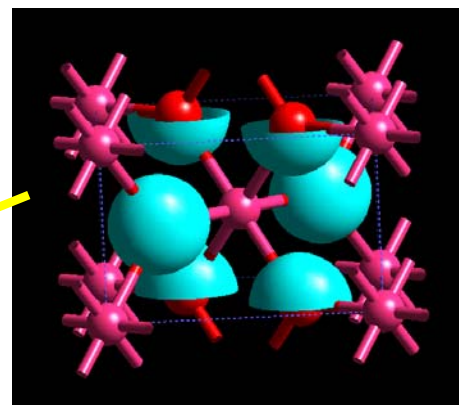
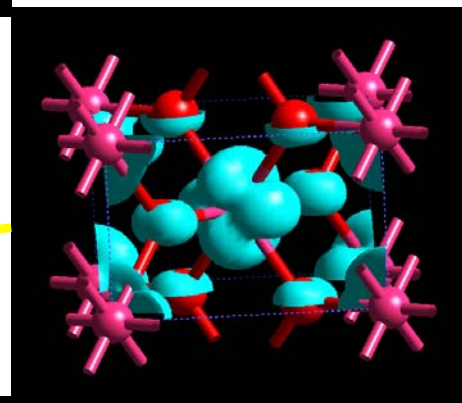
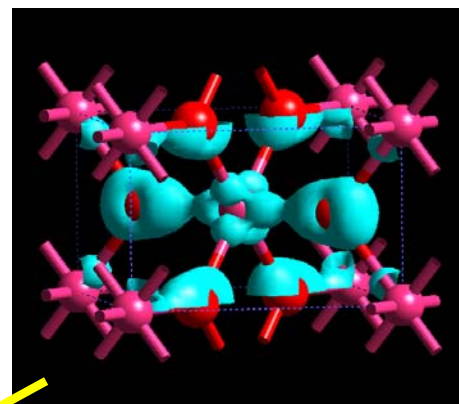
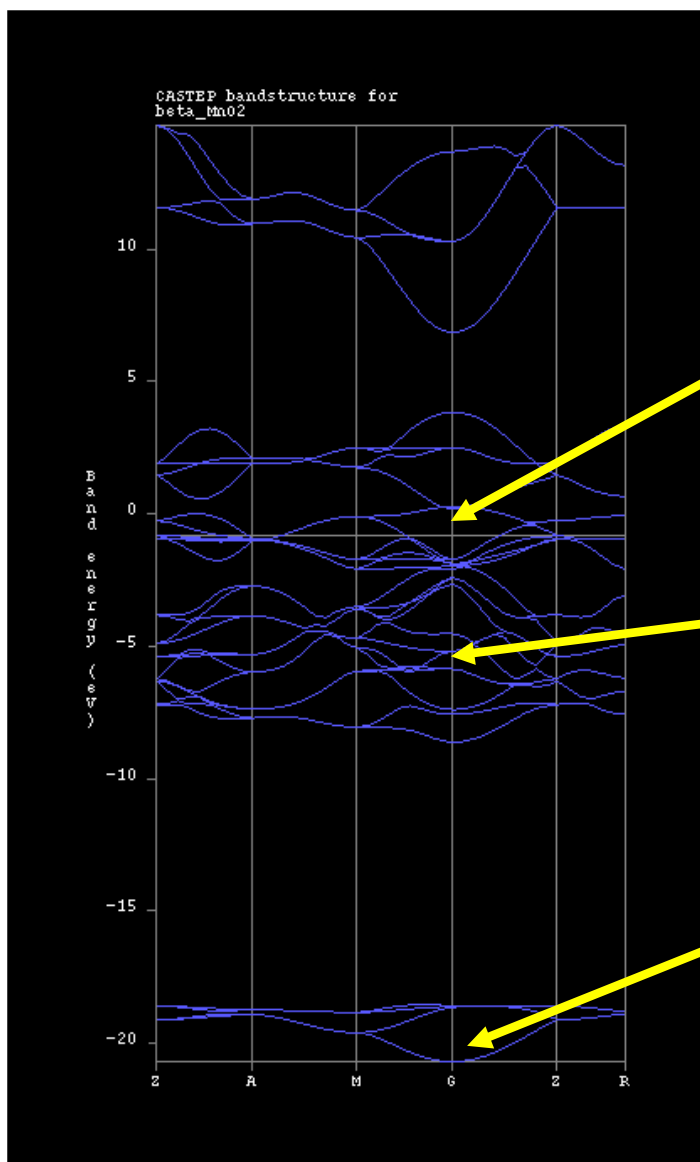
2 MnO₂ units/cell

[1x1] tunnel structure

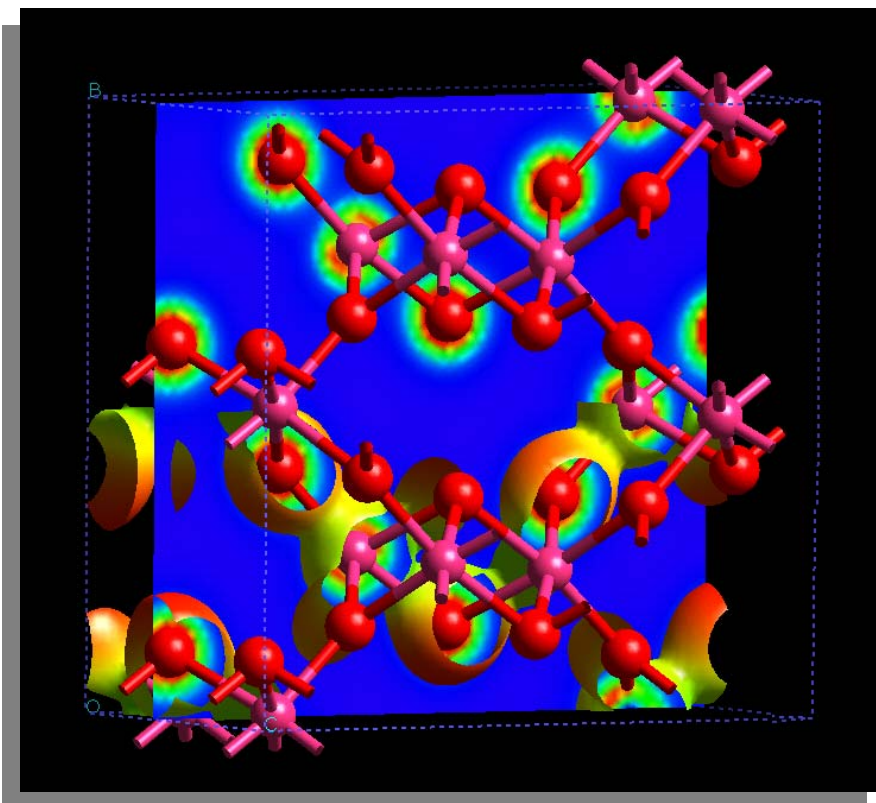
Corner and edge sharing
(MnO₆) octahedra

	<i>Experiment</i>	<i>Theory</i>	<i>Error</i>
<i>a</i>	4.3983	4.483	1.9%
<i>c</i>	2.8730	2.806	-2.3%
<i>u</i>	0.3052	0.297	-2.6%

β -MnO₂ Electronic Structure



MnO₂ Ramsdellite



Pbnm space group

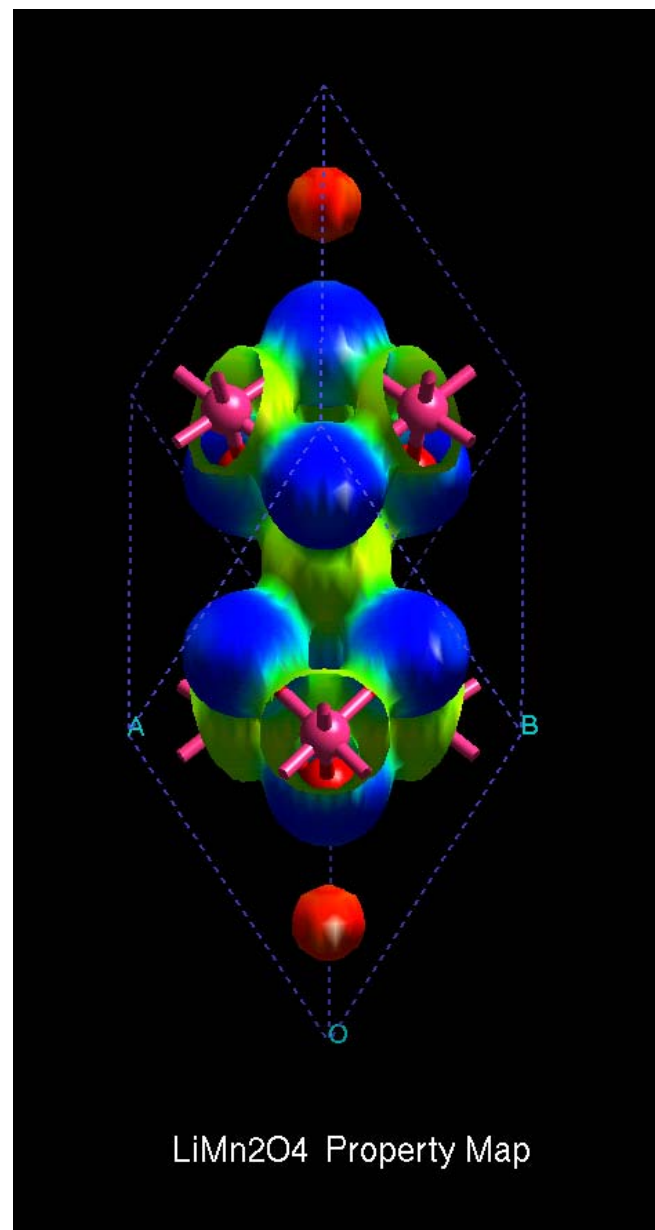
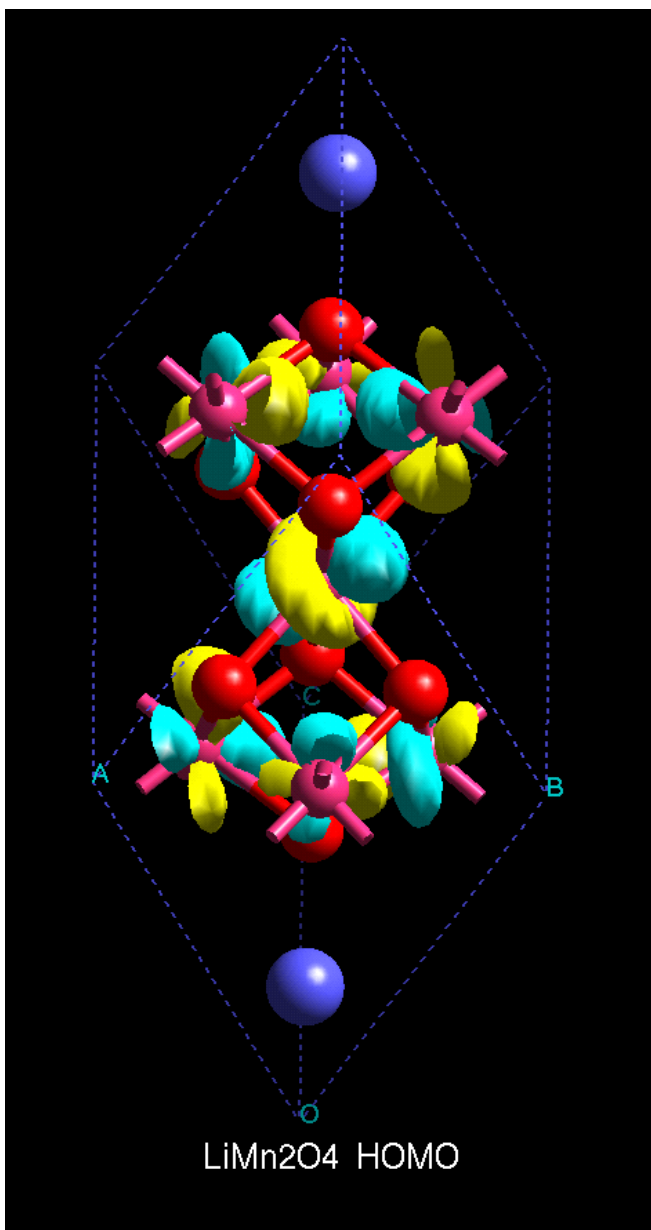
4 MnO₂ units/cell

[2x1] tunnel structure

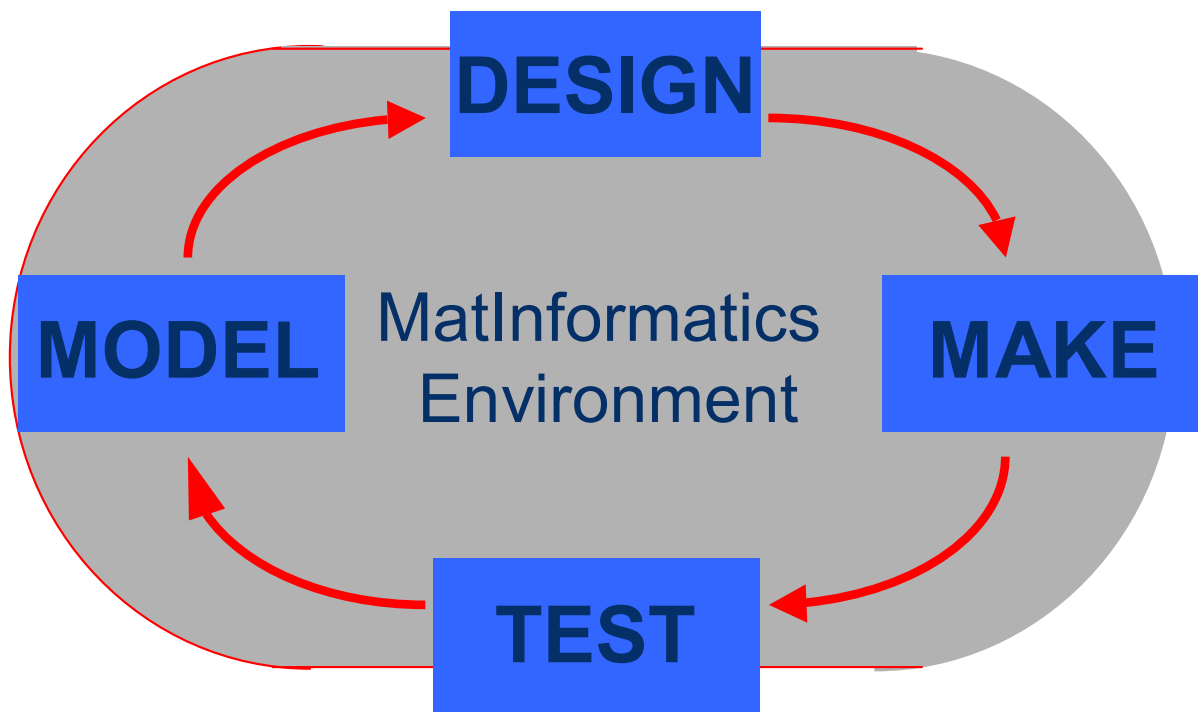
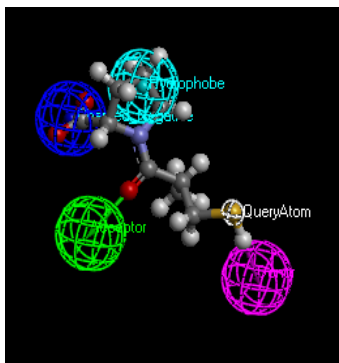
**Corner and edge sharing
(MnO₆) octahedra**

	<i>Experiment</i>	<i>Theory</i>	<i>Error</i>
<i>a</i>	9.270	9.422	1.6%
<i>b</i>	4.533	4.622	2.0%
<i>c</i>	2.866	2.787	-2.7%

Electronic properties of LiMn_2O_4

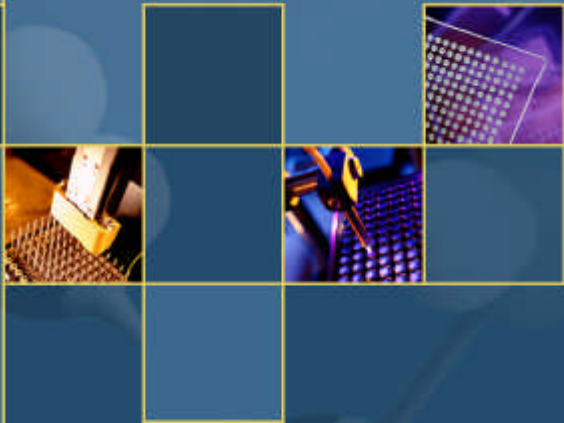


The Final Word.....



“Knowledge is of no value unless you record
what you’ve learnt”

N. Machiavelli



Properties screening of materials and formulations using HTS methods and sensors

Oleg Kolosov, Miroslav Petro, and Leonid
Matsiev.

NIST, October 2003

Symyx Technologies, Inc.



Outline

High throughput combinatorial toolkit at Symyx (polymers and inorganic materials)

- Generic discovery workflows
- Software integration

High Throughput Measurements

- High Throughput Screens - bridging the gap (Synthesis - Formulation – Processing - Sample preparation)
- Material Properties Sensors

Example of the discovery workflow for polymer materials

Conclusions



Outline

High throughput combinatorial toolkit at Symyx (polymers and inorganic materials)

- Generic discovery workflows
- Software integration

High Throughput Measurements

- High Throughput Screens - bridging the gap (Synthesis - Formulation – Processing - Sample preparation)
- Material Properties Sensors

Example of the discovery workflow for polymer materials

Conclusions



Combinatorial methodology

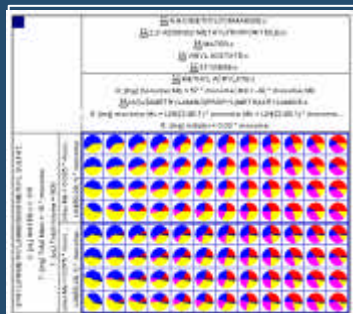
In general, combinatorial approach brings certain benefits of

- speed, resulting in de-bottlenecking the whole idea-to-product process and leading to earlier opportunities for material development
- chance to compare like with like experiments within the same library, thus revealing qualitative trends much easier,
- significant reduction of the cost per experiment via effectively populated combinatorial space,
- lower amount of material per experiment needed in miniaturized instrumentations,
- improved breadth of intellectual property protection



Polymer Synthetic workflow

Design arrays of over
3000 polymers



Symyx software (Library
Studio™, Impressionist™)
for designing libraries and
controlling automation

Synthesize and disperse in
polar media



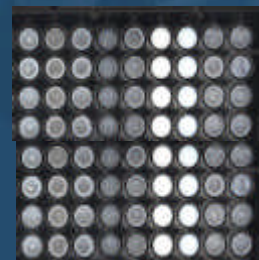
Typical synthesis scale: 96
different 100 mg samples
made at controlled
temperature, pressure

Measure M_w , M_w/M_n



Symyx RapidX GPC™

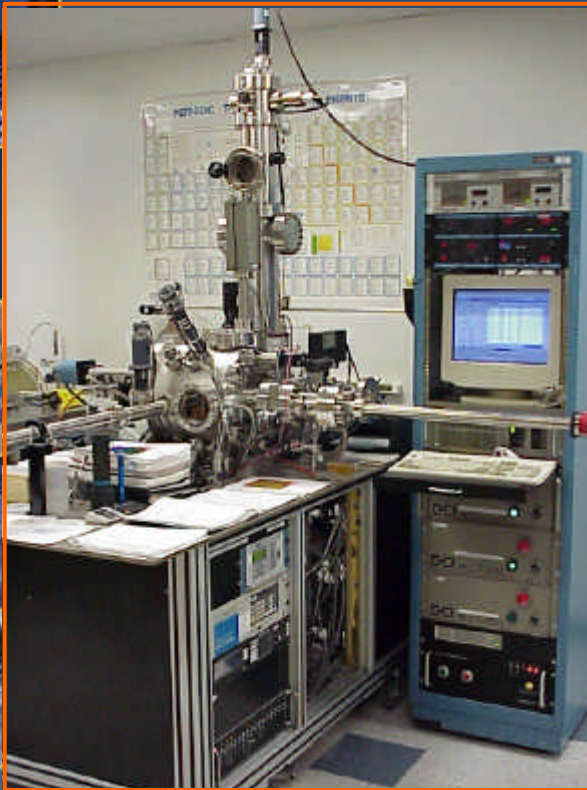
Check solubility



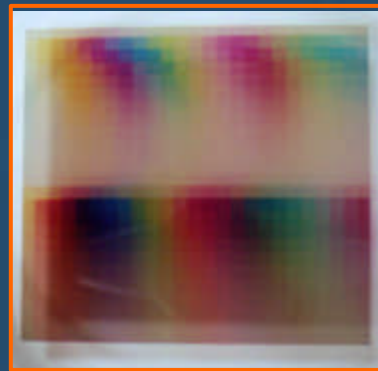
Automated
turbidity



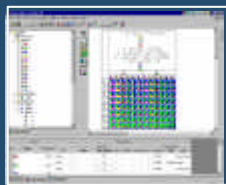
Combinatorial Sputter Deposition



Magnetron RF/DC sputtering
Automated target exchange
Up to 40 starting materials
Dynamic shutter system
Full system automation
Seamless database interface



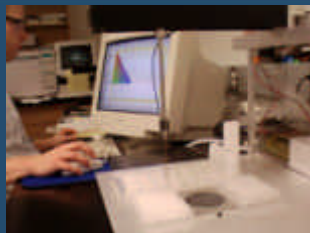
Exploration by the Combinatorial Solution Synthesis Approach



Library Design



Starting precursors / solutions



Microtiter plate

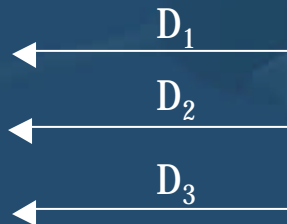
Characterization and high throughput screening



X-ray Diffraction



Library of ceramic materials on 3 inch silicon wafer

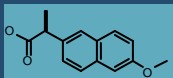


Treated substrates (silicon, quartz....), 121 - 144 regions

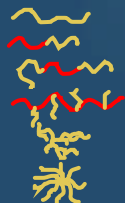
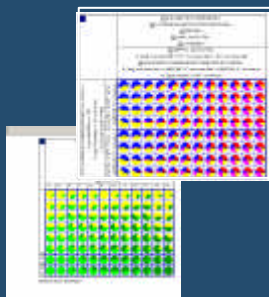


Dispersion Formulations Workflow

Active Compound



Design and Synthesize
Arrays of Dispersants



Disperse Materials
in Parallel



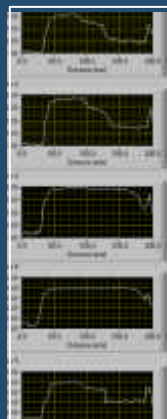
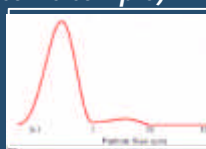
Ultrasonic Homogenizer

Solubility (turbidity)



Orbital Shaker

Characterize Arrays of Materials in
Parallel (Particle Size, Stability, and
Solubility, etc. *using same sample*)

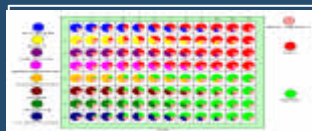


Hits and
Leads

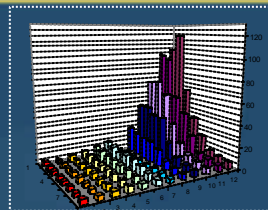


Solubility Workflow

**LIBRARY
DESIGN**



**DATA
ANALYSIS**



DISPENSE SUBSTRATE

96 Samples/Run



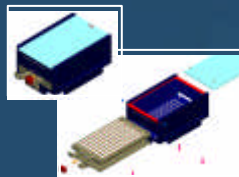
48,000-60,000 Experiments/Year



QUANTIFY



DISPENSE SOLVENTS



EQUILIBRATE/SEPARATE



Outline

High throughput combinatorial toolkit at Symyx (polymers and inorganic materials)

- Generic discovery workflows
- Software integration

High Throughput Measurements

- High Throughput Screens - bridging the gap (Synthesis - Formulation – Processing - Sample preparation)
- Material Properties Sensors

Example of the discovery workflow for polymer materials

Conclusions



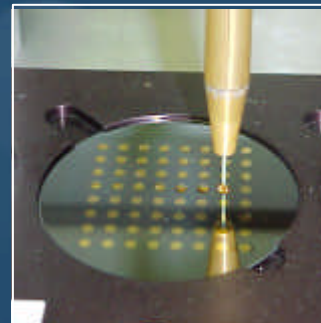
Polymer Properties Measurement



Rapida GPC®



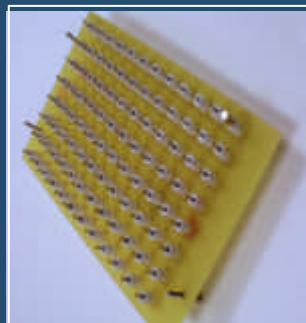
SAMMS™ Thermal Analysis



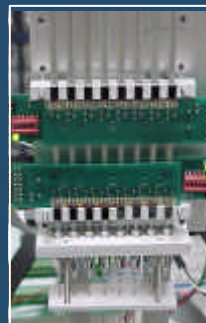
Rapida FT-IR™



Parallel DMTA™



Parallel Viscometer™



Parallel Viscometer™

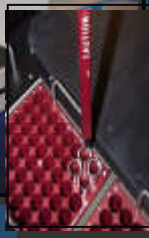


Rapida DLS™



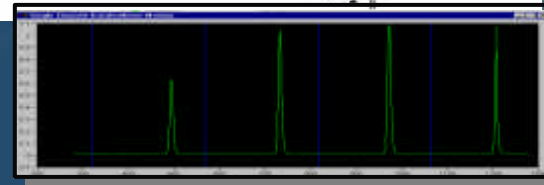
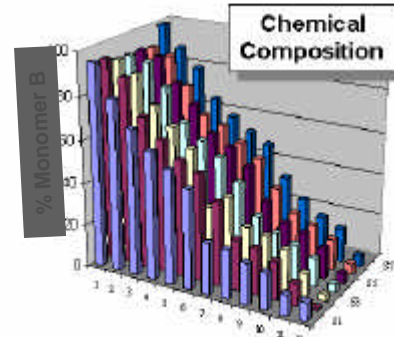
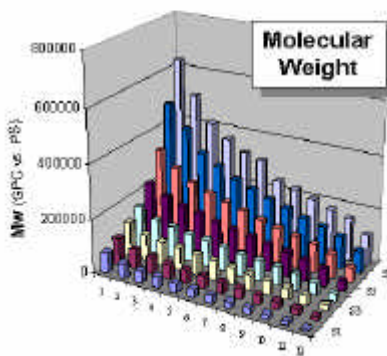
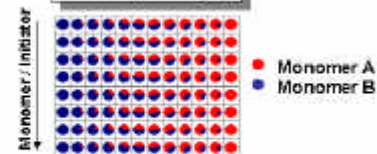
Molecular Weight and Composition screen

Symyx Rapid[®]GPC™



- Diverse library of random copolymers
- Molecular weight by Rapid[®]GPC™
- Chemical composition by Rapid[®]HPLC™

Library Design

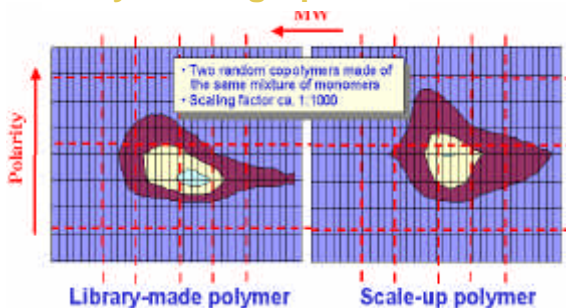


- Molecular weight distribution, Chemical composition distribution, Conversion, Yield, Purity, Other properties (eg optical)



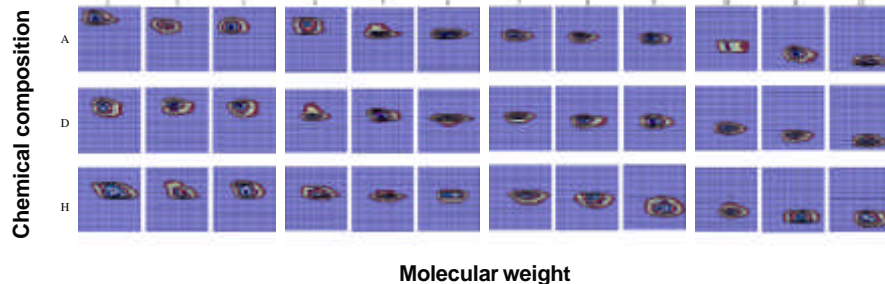
From Symyx' Polymer to Scale-Up and Production Optimization

Polymer fingerprints



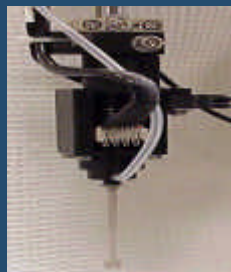
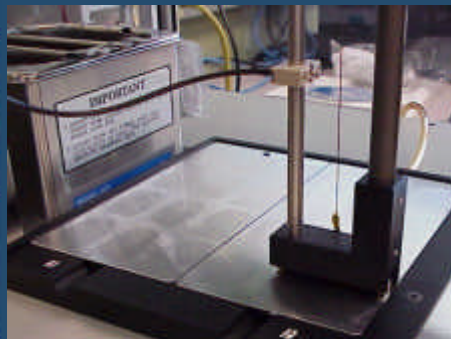
- Symyx' proprietary polymer fingerprinting technology allows rapid optimization of the polymer scale-up process and minimize a risk of the polymer property drift

Rapid optimization of the scale-up process conditions

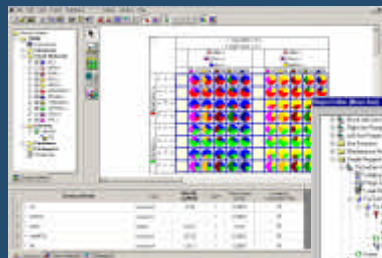


Polymer Coating formulation - sample preparation - measurements

Coating Deposition & Analysis



Design Tool — Library Studio®



Impressionist™ Procedure for execution



Polymerization



Formulation , Viscosity Index and Surface Energy

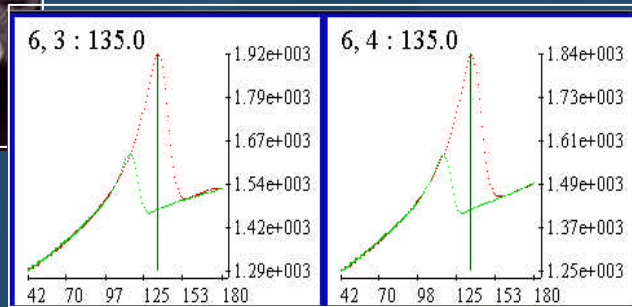
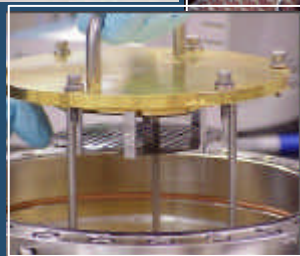
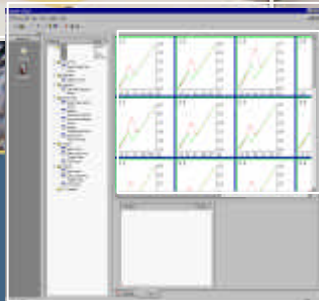
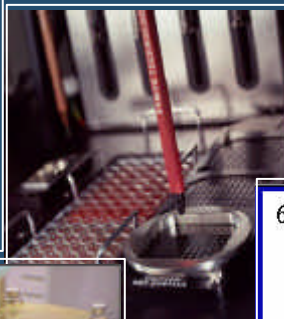


SAMMS™ - Sensor Array Modular Measurement System

Rapid calorimetric determination of polymer glass transition temperatures and melting points.

Sample mass » 1-10 mg. » 15 to 120 seconds per sample.

- 15-60 seconds per sample
 - Comparable to 90 minute DSC for T_m, T_g
- 128 samples in 30-120 minutes
 - 384 samples per day
 - 96,000 experiments annually



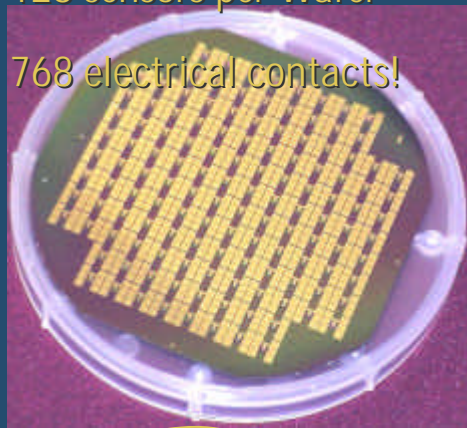
SAMMS – Test Head and Individual Sensor

Wafer temperature control

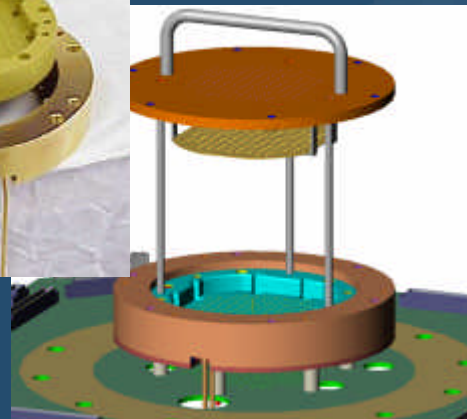
Thermal isolation for PCB

128 sensors per Wafer

768 electrical contacts!

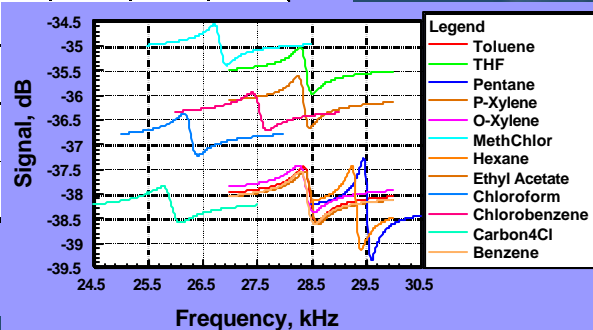
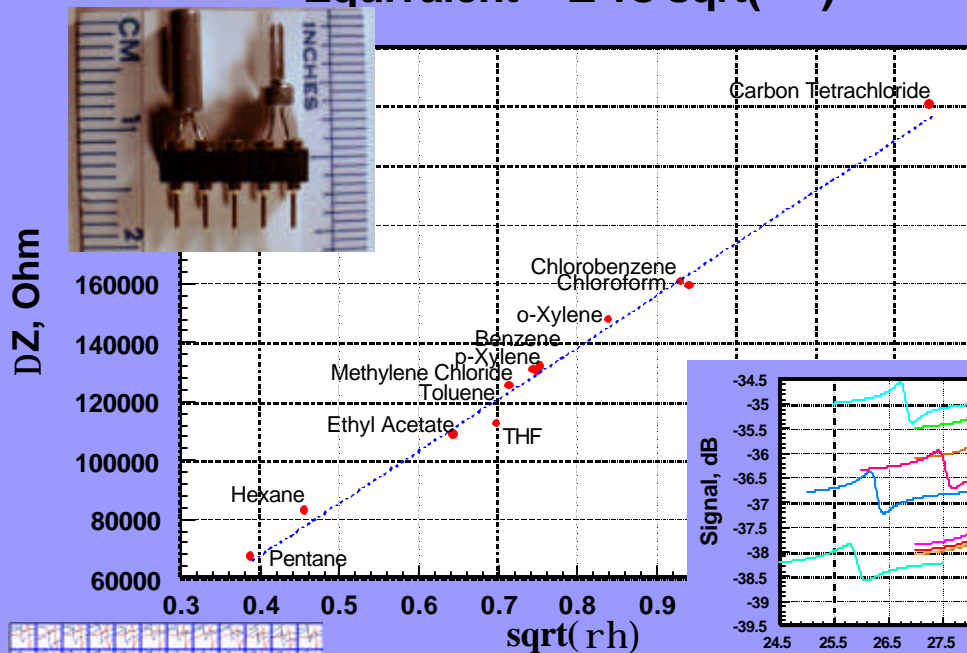


Sample mass $\ll 1$ mg
Film thickness $\sim 1\text{-}10$ μm



Viscosity and Density Sensors

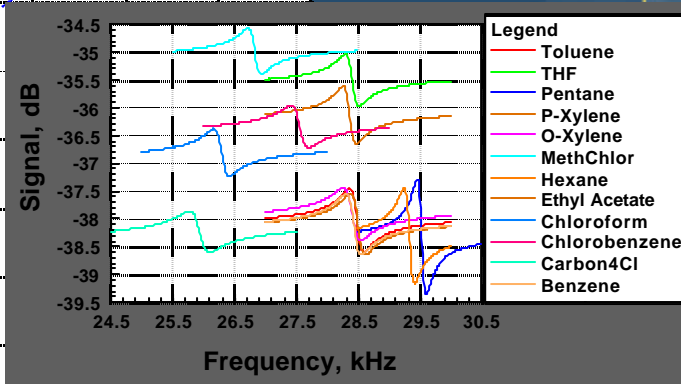
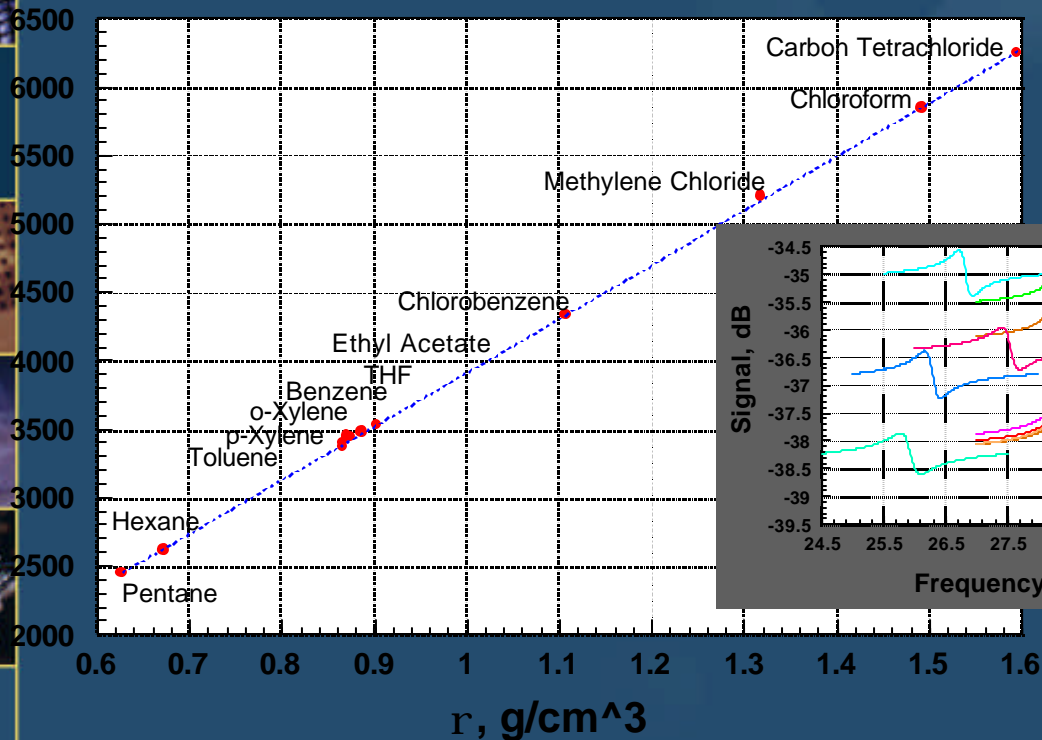
Equivalent DZ vs sqrt(rh)



TF Sensor Response to Liquid Density

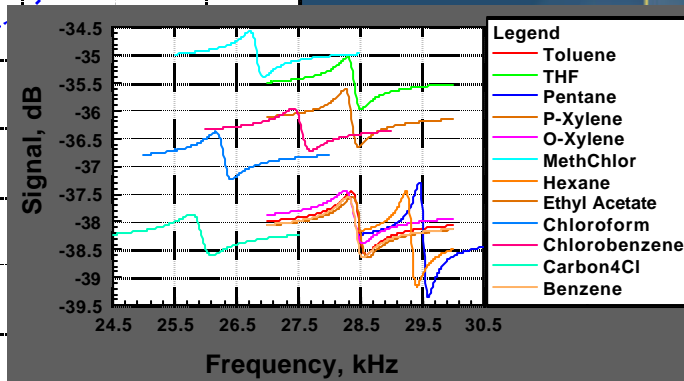
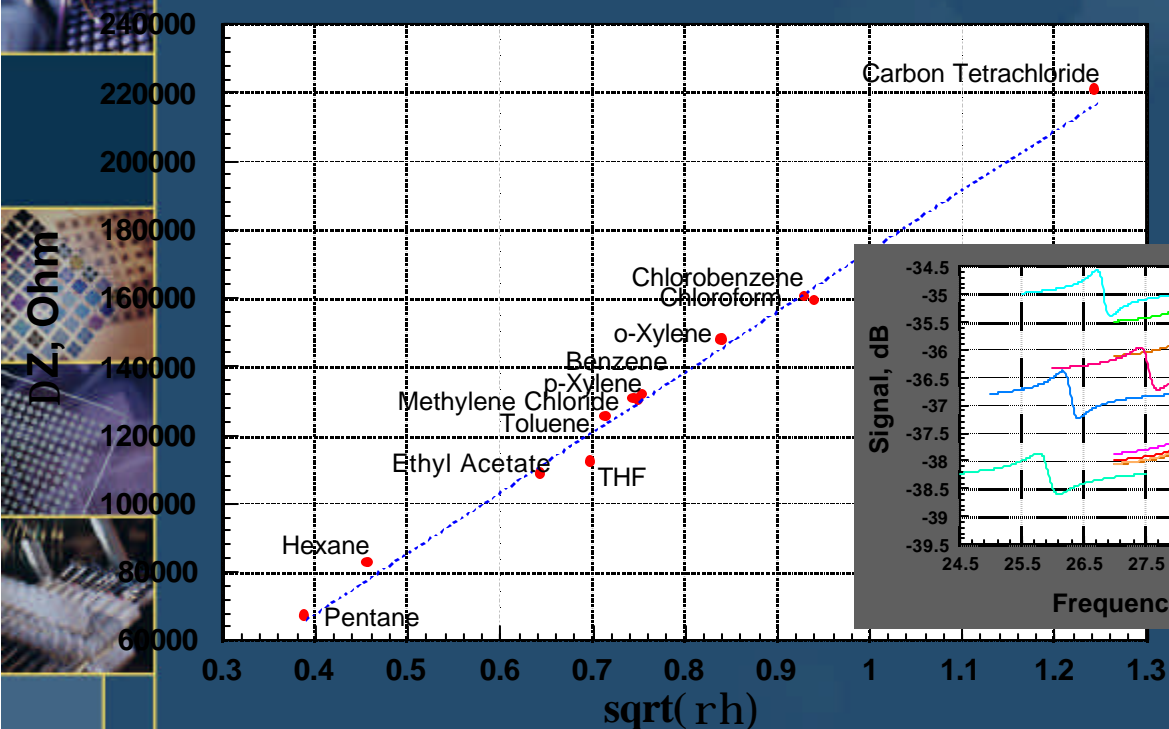
Equivalent DL vs Specific Weight

DL, H

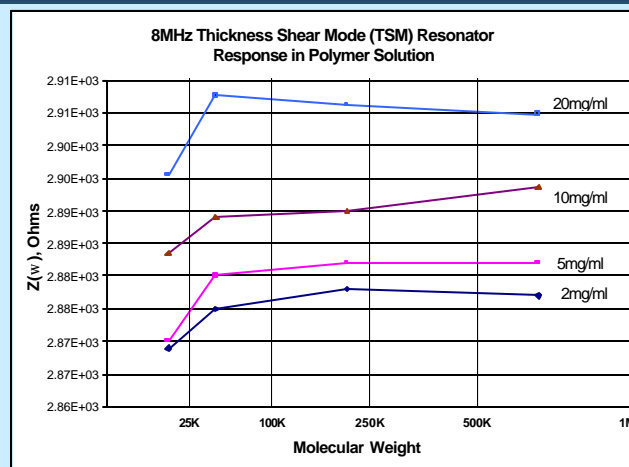
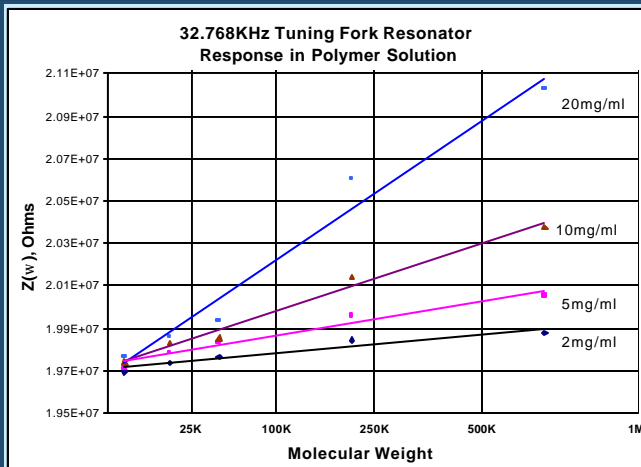


TF Sensor Response to Liquid Viscosity

Equivalent DZ vs sqrt(rh)



Sensitivity to Molecular Weight



© Symyx Technologies, Inc. 2000-2003. Proprietary Information. All rights reserved.

Tuning Fork Resonator

Highly sensitive to both polymer concentration and molecular weight

TSM Resonator

Limited sensitivity to polymer concentration and virtually insensitive to molecular weight



TF Sensor Response in Gases

In Air at ambient conditions: $c \sim 330\text{m/s}$, $\rho \sim 1.3 \text{ kg/m}^3$, $\eta \sim 1.708\text{E-}3 \text{ mP*s}$

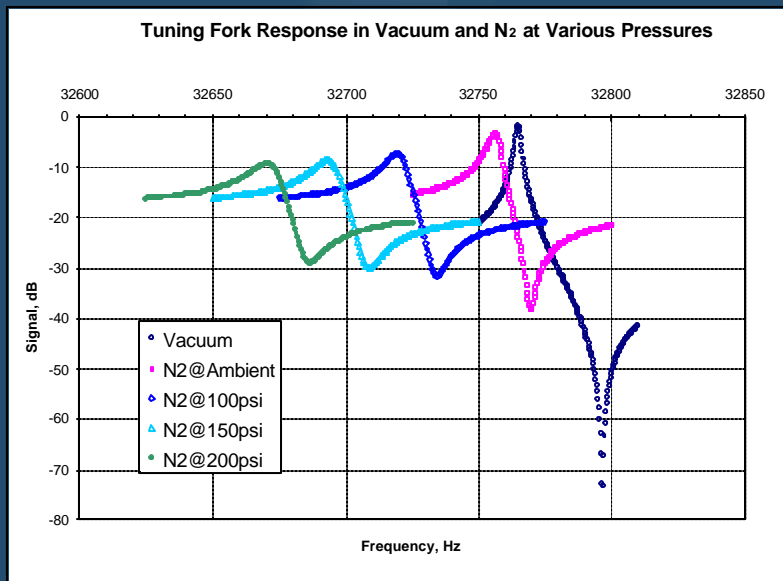
	Size l	$f_{\text{res.}}$	l	$a^{\text{res}}(1V_{\text{RMS}})$	d	$Re \sim$	
Tuning Fork		$\sim 2\text{mm}$	32KHz	10mm	$\sim 30\text{nm}$	11.4 mm	0.9

Gas	Viscosity, cPs (0 C, 101 kPa)
-----	----------------------------------

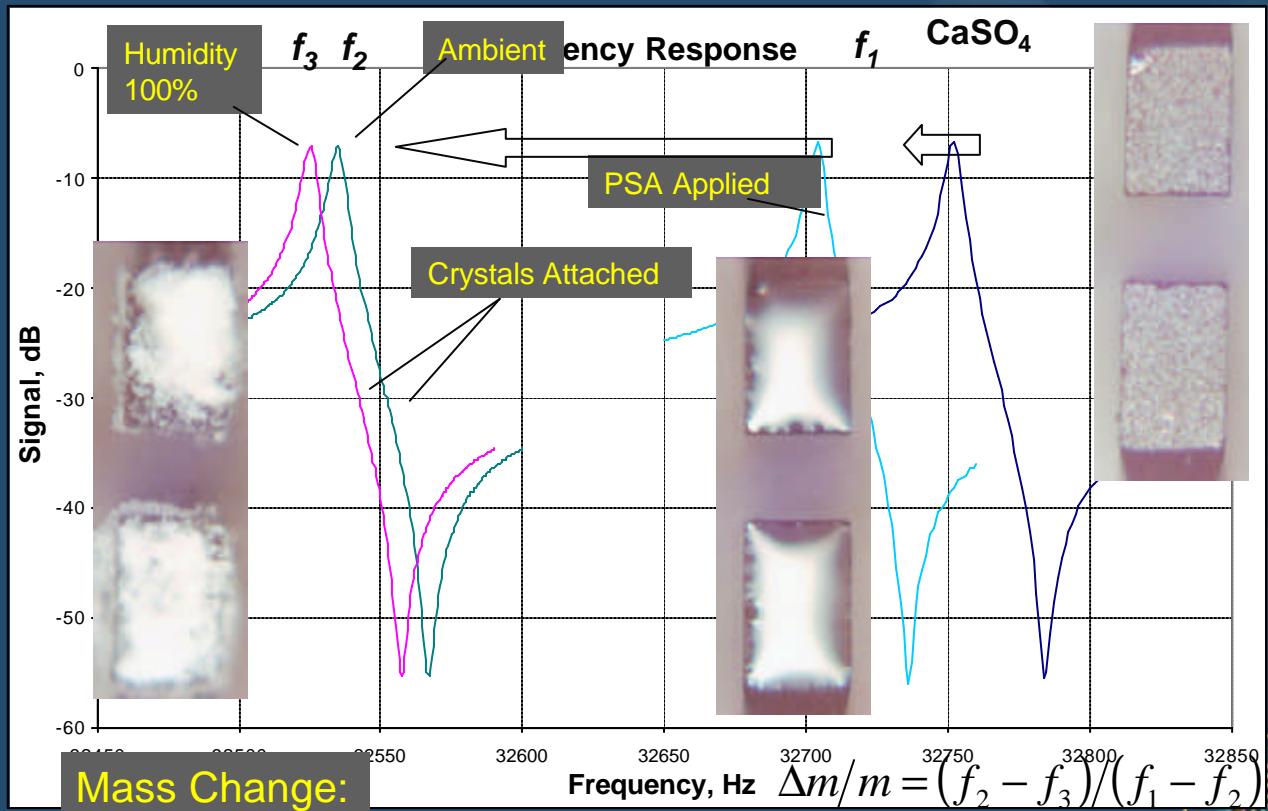
Air	1.708E-03
Carbon dioxide	1.390E-03
Helium	1.860E-03
Hydrogen	8.345E-04
Methane	1.026E-03
Nitrogen	1.660E-03
Oxygen	1.919E-03

$$r = \frac{1}{m} \frac{P}{RT}$$

$$h = \frac{1}{3\sqrt{2}s} \sqrt{\frac{8mkT}{p}}, s = pd^2$$



TF as a Nanobalance



Outline

High throughput combinatorial toolkit at Symyx (polymers and inorganic materials)

- Generic discovery workflows
- Software integration

High Throughput Measurements

- High Throughput Screens - bridging the gap (Synthesis - Formulation – Processing - Sample preparation)
- Material Properties Sensors

Example of the discovery workflow for polymer materials

Conclusions



The discovery workflow

The Goal and the Challenge

The ultimate goal was

- to create a new polymer platform for bioactive containing formulations with enhanced and prolonged delivery of active material to the human tissue.

The challenge was

- a great complexity of mutual interactions among various components of a multicomponent system, usual in such applications





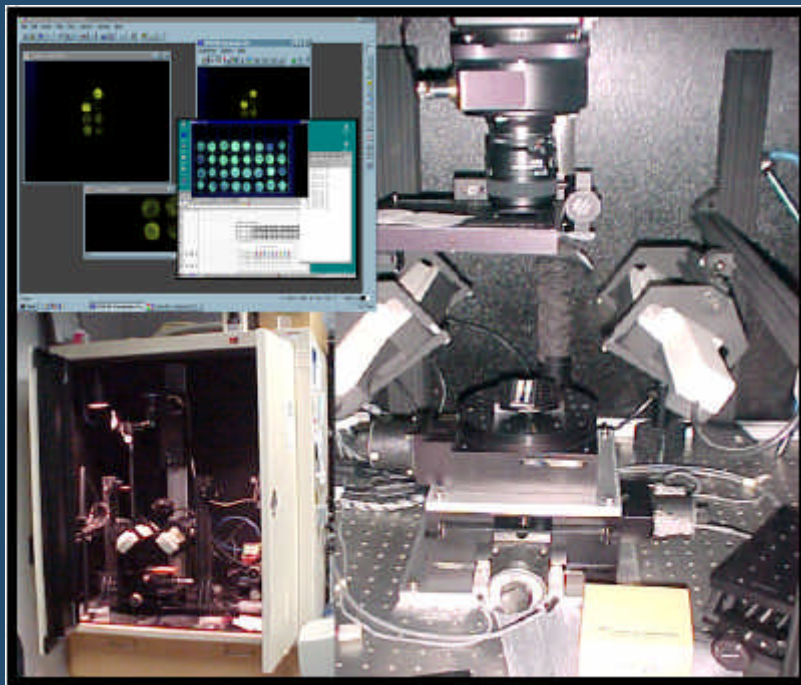
Symyx Proprietary

Instrumental setup used for monitoring bioactive retention



Instrumental setup used for monitoring bioactive retention and release on/from real living tissue. A section of the living tissue is provided in individual vial (left image) assembled in indexed position libraries (right image).

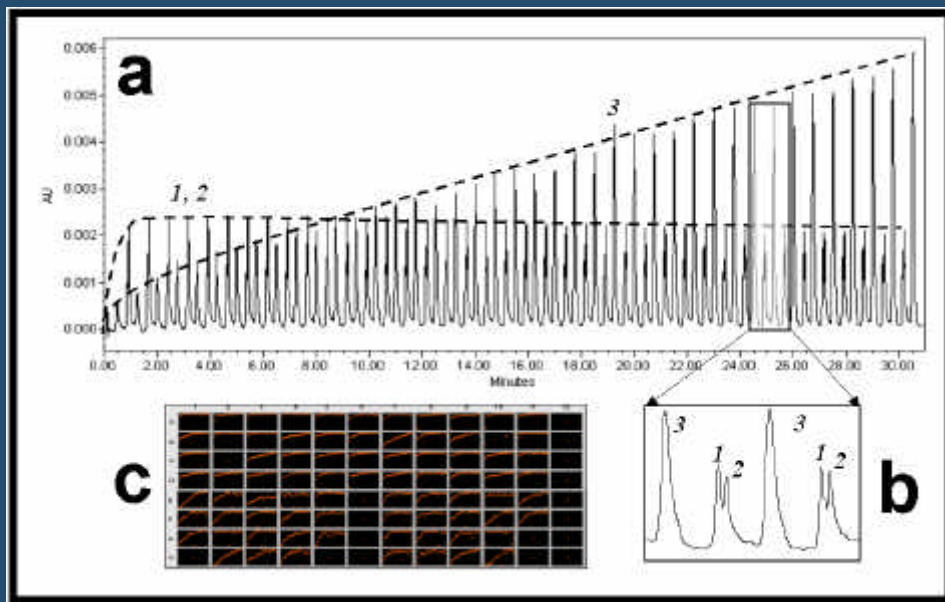
Optical Screening Station



Symyx hardware and software used for fluorescence imaging of tissue mimics. In the left upper corner are examples of the libraries for testing polymer affinity to the substrates in the data processing software.



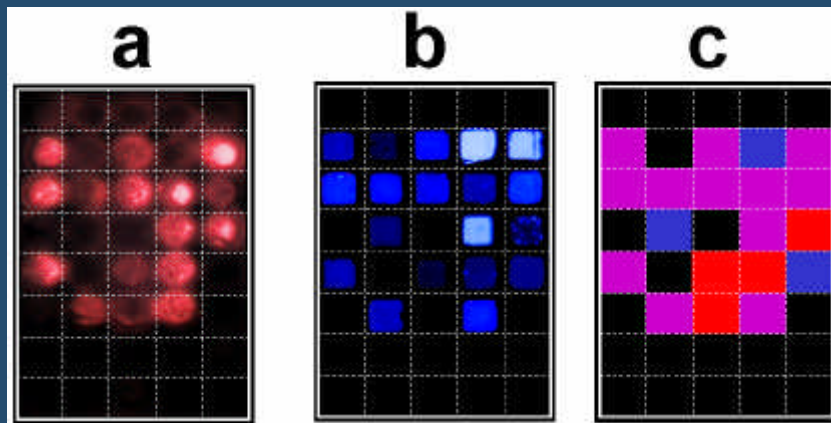
Symyx System for Bioactive Retention and Release



Example of data output obtained by Symyx system for bioactive retention and release. Raw chromatograms (a), zoom showing the separation of individual components (b) and collection of reduced data for diversity of formulations (c). The individual peaks in the chromatogram correspond to small molecules (1,2) and polymer (3).



Hit selection using screening data on polymer substantivity to substrates

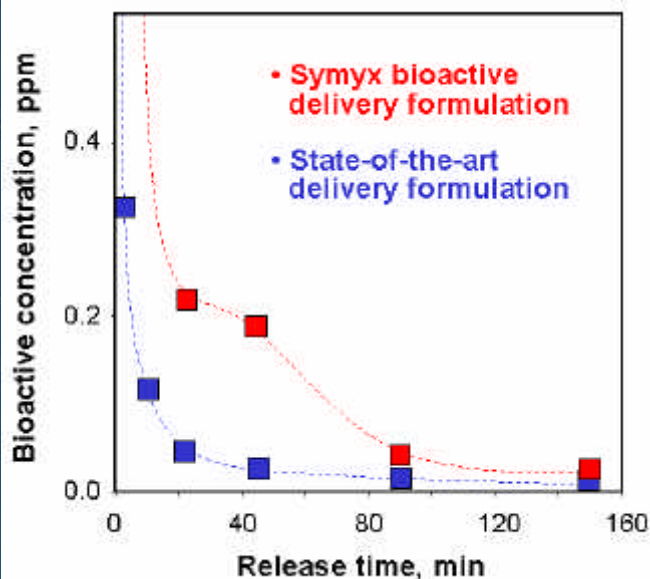


Representing the tissue-1 as object of preferred delivery (a) and the competitive tissue-2 (b).

Resulting hit map (c) shows distribution of polymers into the four different categories – the polymers selectively substantive to a first tissue type (red), selectively substantive to a second tissue type (blue), substantive to both tissue types (purple) and those of no substantivity (black). The brightness of the spots corresponds to a quantity of the polymer retained. Colors in the images represent the type of tissue used and do not possess any other information value.



Release profiles for the bioactive



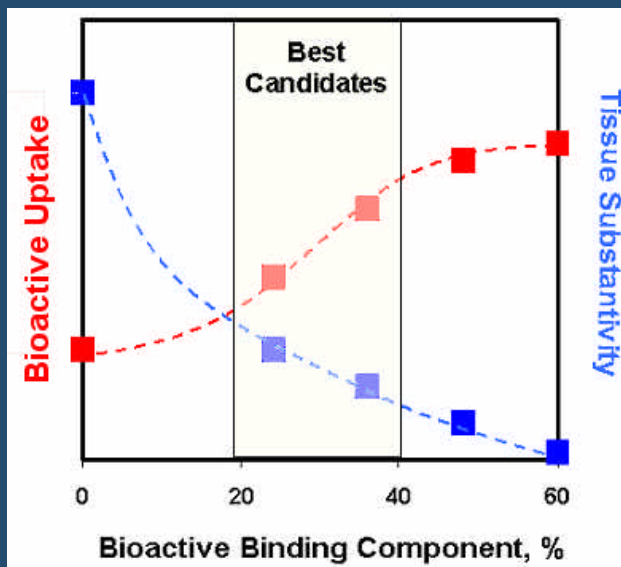
Release profiles for the bioactive delivered from

- the state-of-the-art formulation (in blue)
- versus the analogous formulation containing the best performing polymer candidate as identified in this study (in red).

The same amount of the bioactive delivered in both cases. Bioactive extraction performed under the open dynamic conditions with multiple replacements of biological fluid over the biological tissue.



Optimization of Formulation

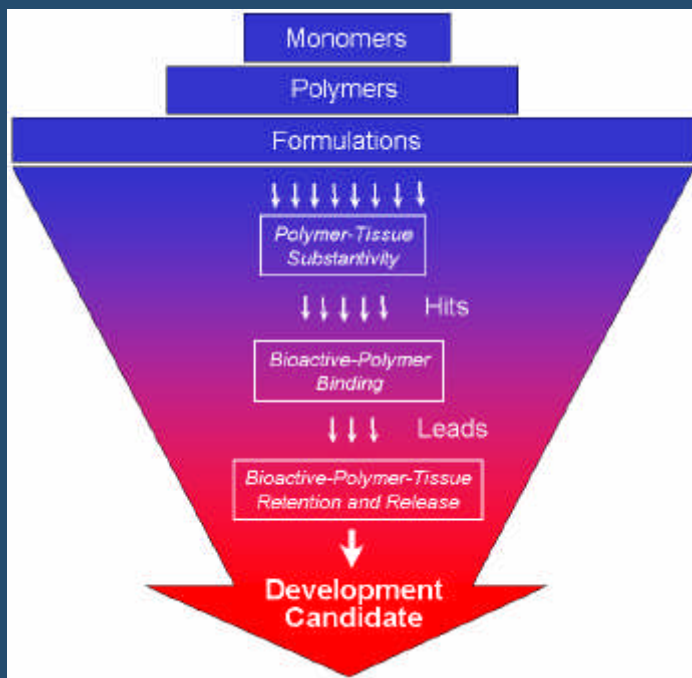


Comparison of bioactive uptake (red) and tissue substantivity (blue) as a function of the content of bioactive binding component in the polymer.

- The highlighted region (yellow) represents the best compromise between the uptake and substantivity.



Polymer Discovery Workflow



Overall scheme of the discovery workflow targeting the bioactive delivery agents.



Acknowledgement

All Symyx employees

Especially to

MingJun Liu, Han-Ting Chang, Dominique Charmot
(synthesis and formulations),

Son Hoai Nguyen, Sigrid Kuebler, Mary Beth Kossuth, Tom
McWaid, Eric Carlson, Earl Danielson (polymers HT screening)

James Bennett (material properties sensors), Marty Devenney,
and Henry Weinberg.



Production and Manipulation of Complex Fluid Structures with Microfluidics

Dave Weitz Harvard

Darren Link, Andy Utada, Zhengdong Cheng,

Galder Cristobal, Erwan Grasland-Mongrain

Howard Stone, Michael Brenner, Shelly Anna

Whitesides group

- Microfluidics for production of monodisperse emulsions
- Control of droplet size distribution
 - Passive Breakup of drops
- Electric Fields
 - Electro-flow-focusing
 - Droplet manipulation
- Multiple emulsions with microfluidic control

Structured Fluids

- Most products are structured fluids
 - Emulsions, Colloids, Polymers, Surfactants
 - Mixtures of all of these
- How to control structure, function?
- Key is mixing, structuring
- Precise control of minute quantities of fluids
 - Encapsulate in single drop; control at drop level
- Use microfluidic techniques
 - Control fluids, mixing; control quantities
 - Control structure

The microfluidic advantage

Rapid prototyping

Direct visualization

Low Reynolds number:

$$\frac{\text{inertial stress}}{\text{viscous stress}} = \frac{\rho U^2}{\eta U / d} = \frac{\rho U d}{\eta}$$

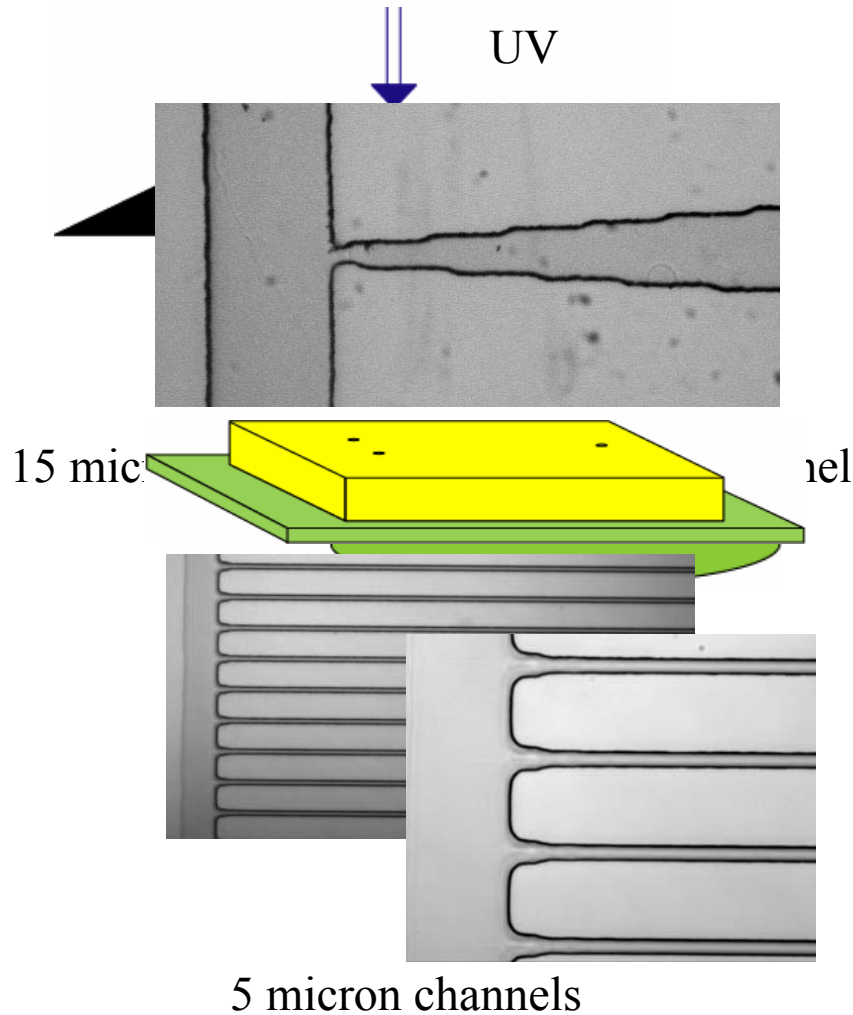
neglect momentum

Laminar flow

Microfluidics with Soft-Lithography

- Pioneered by George Whitesides
- Fabricated into silicone – PDMS
- Mold pattern
- Very high turn-around
 - Ideal for prototyping
- PDMS is oil wet, not water wet
 - Limitations for mixed solvent

Soft Lithography



Clean silicon wafer

Spin coat photoresist

Align mask

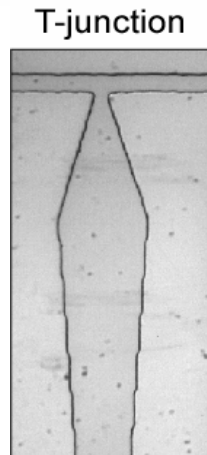
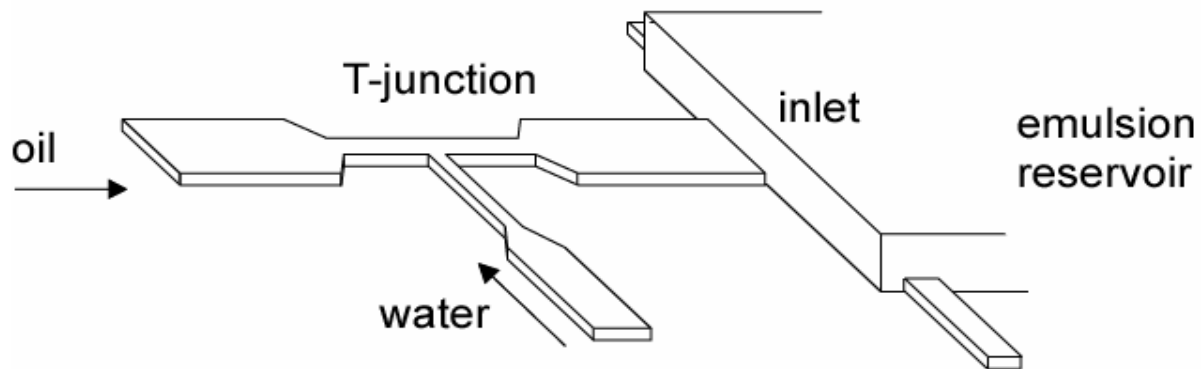
UV exposure

Develop

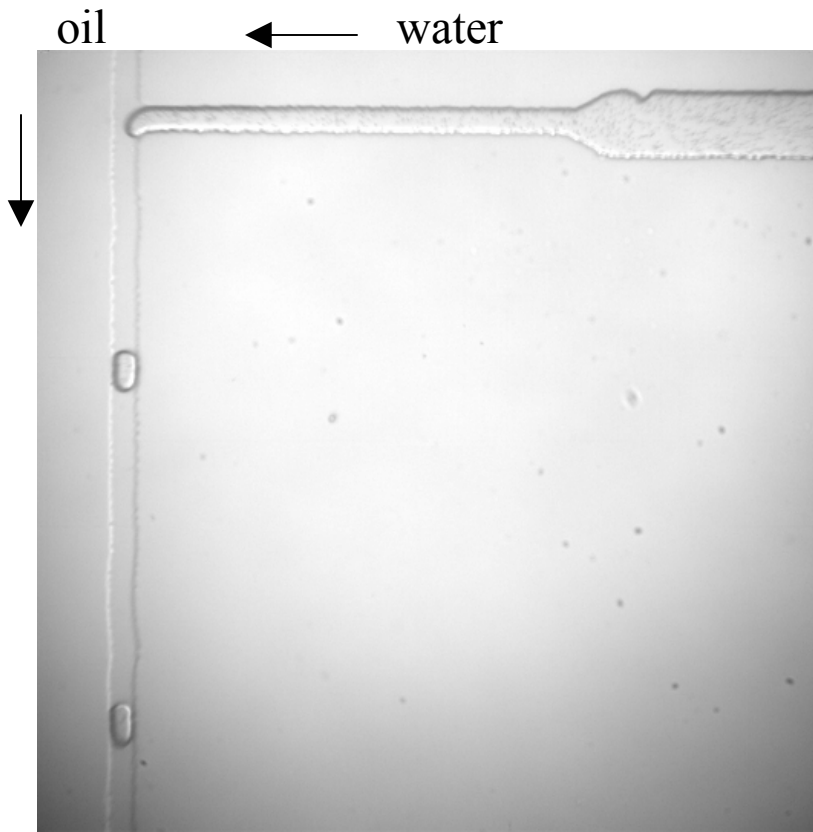
Relief mold rubber

Seal on glass

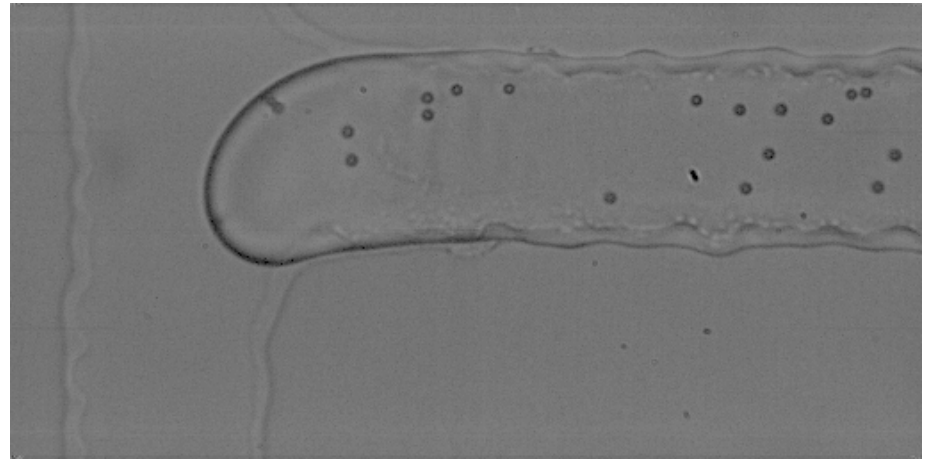
Microfluidic emulsions



Dynamics of break off



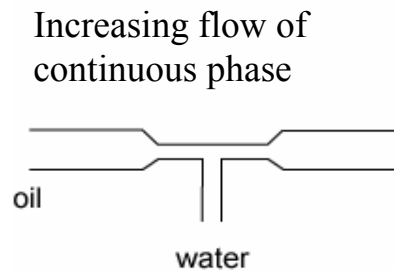
30 micron channels



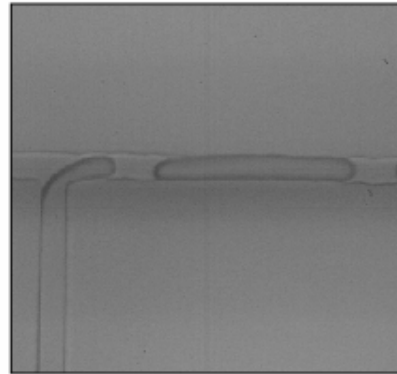
capture: 7100 fps
playback: 20 fps

3000 drops/second
1L in 40 days

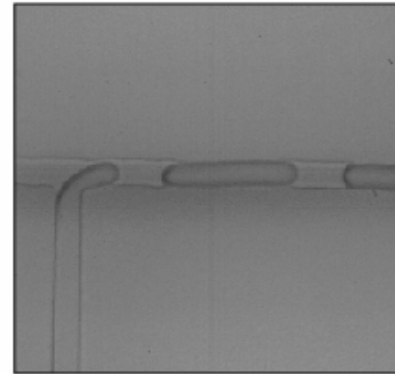
Drop break off



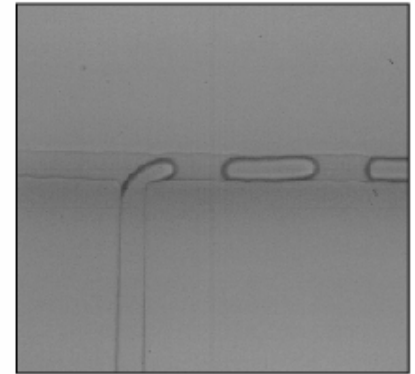
25 $\mu\text{l/hr}$
60 $\mu\text{l/hr}$



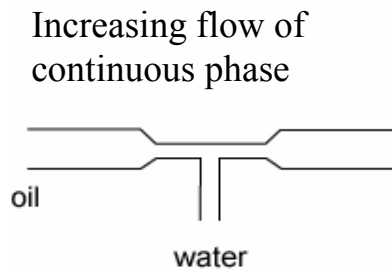
50 $\mu\text{l/hr}$
60 $\mu\text{l/hr}$



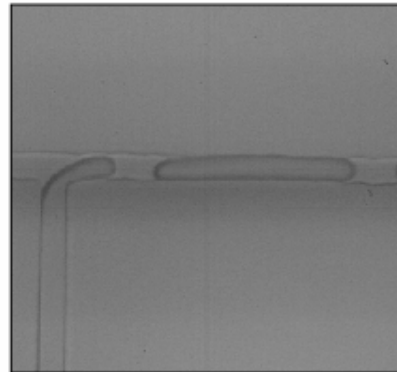
63 $\mu\text{l/hr}$
60 $\mu\text{l/hr}$



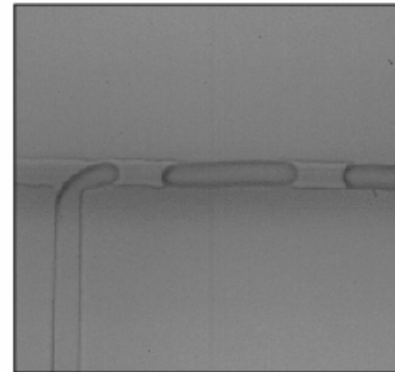
Drop break off



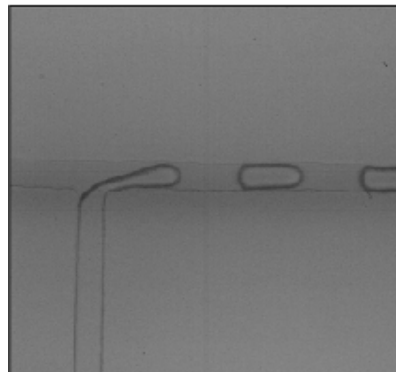
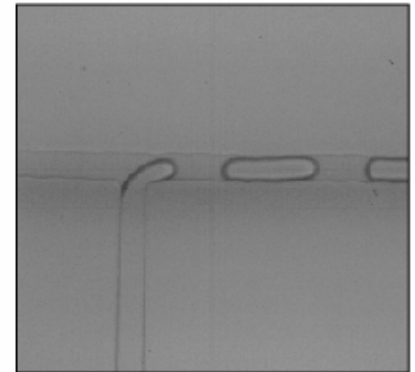
25 μ l/hr
60 μ l/hr



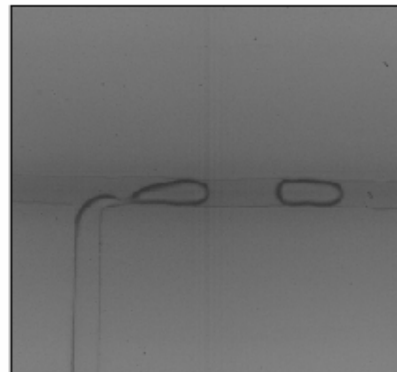
50 μ l/hr
60 μ l/hr



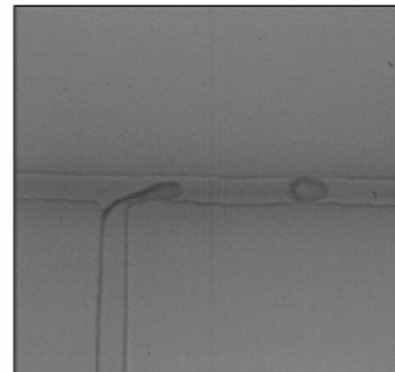
63 μ l/hr
60 μ l/hr



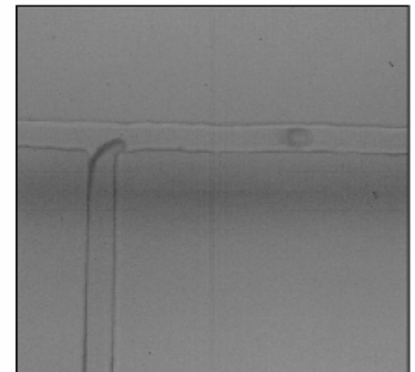
125 μ l/hr
60 μ l/hr



250 μ l/hr
60 μ l/hr



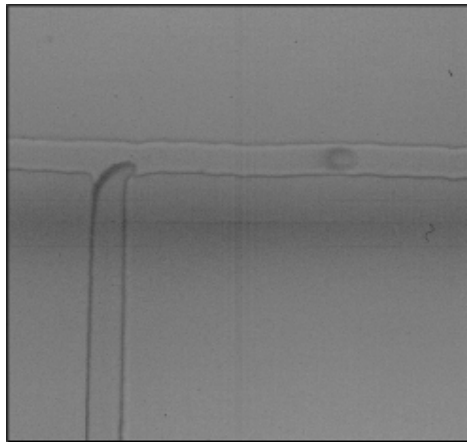
500 μ l/hr
60 μ l/hr



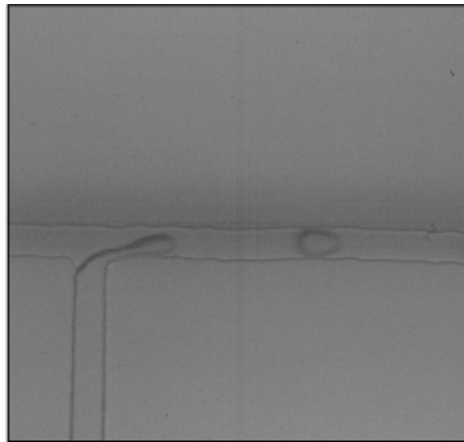
750 μ l/hr
60 μ l/hr

Control Size by Relative Flow

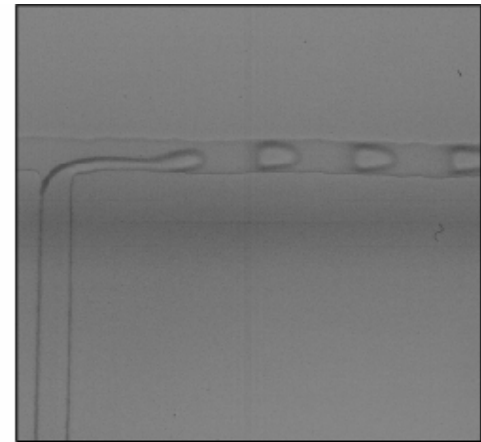
Increasing flow of
dispersed phase



750 μ l/hr
60 μ l/hr



750 μ l/hr
120 μ l/hr

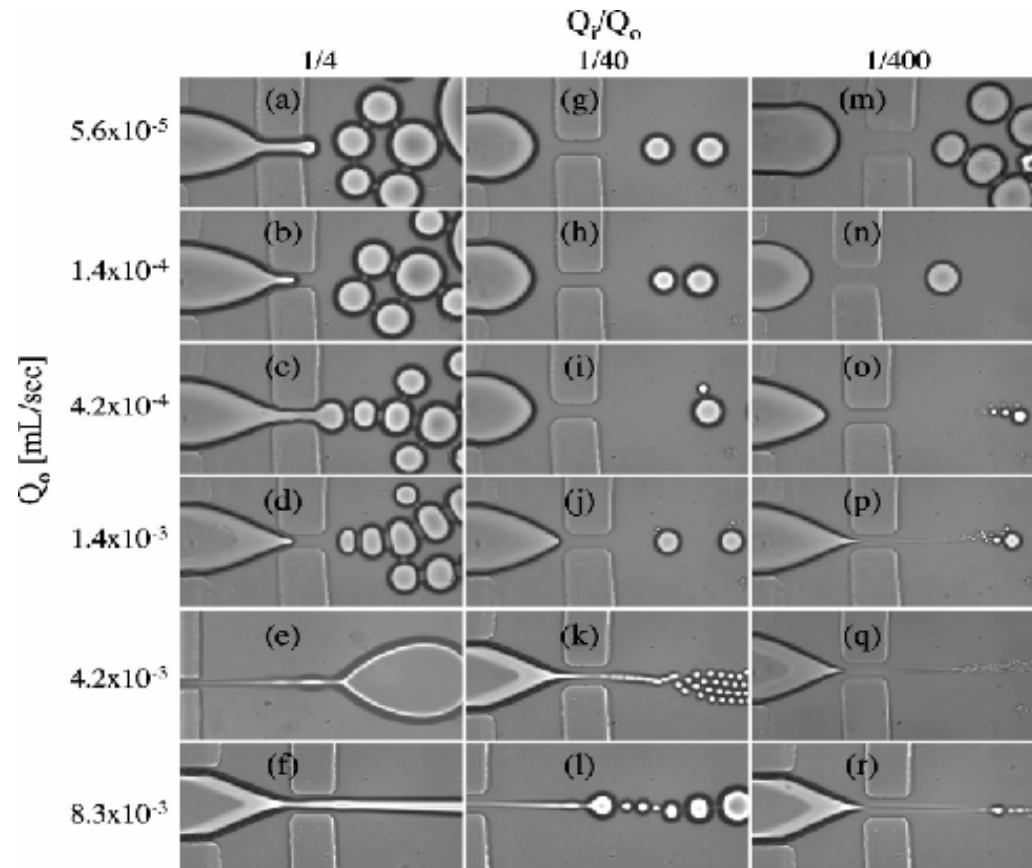
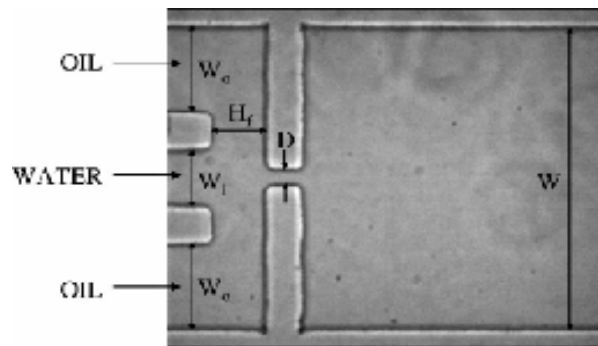


750 μ l/hr
300 μ l/hr

Formation of dispersions using “flow focusing” in microchannels

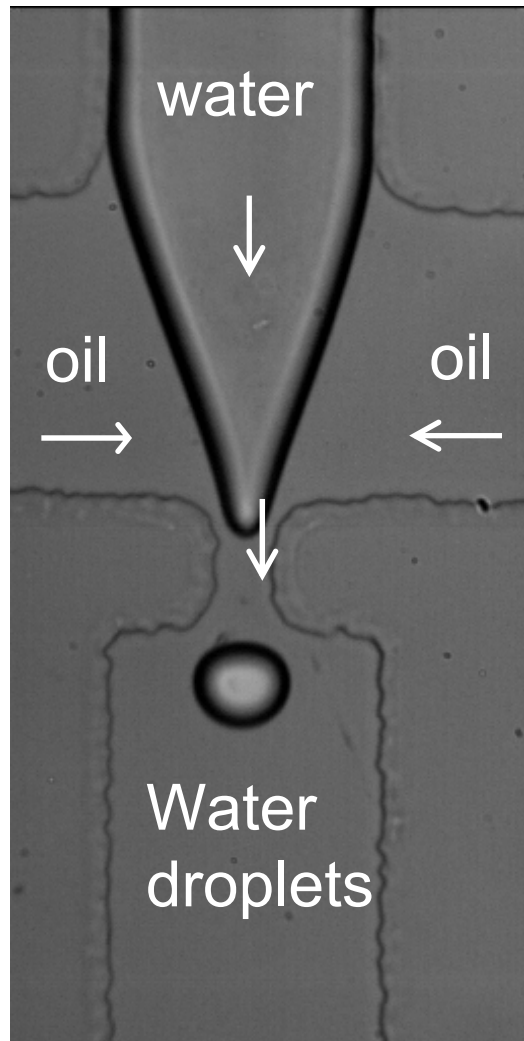
Shelley L. Anna, Nathalie Bontoux, and Howard A. Stone

Appl. Phys. Lett. 82, 364 (2003).



Flow Focusing with Microfluidics

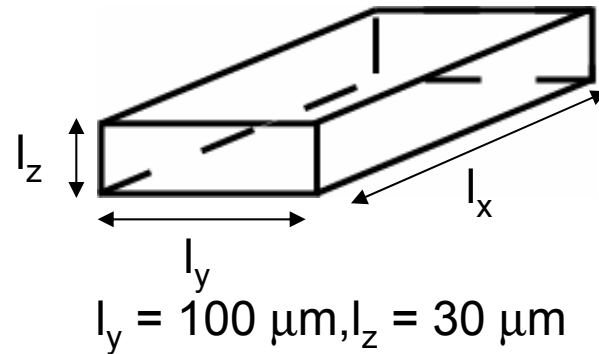
Flow-focusing



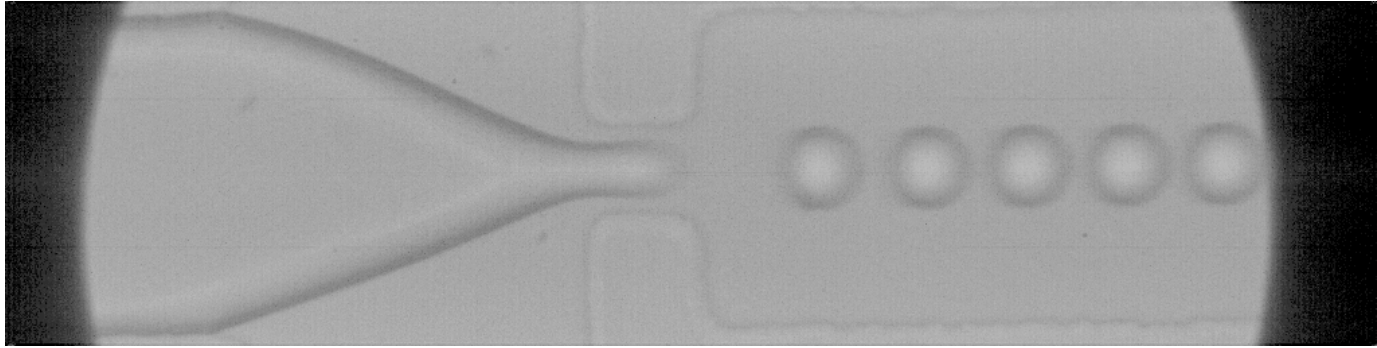
Why droplets?

- meter and transport of fluids
- reaction chambers
- templates to design materials

Rectangular Channels

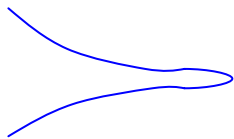


Droplet Formation by Flow Focusing

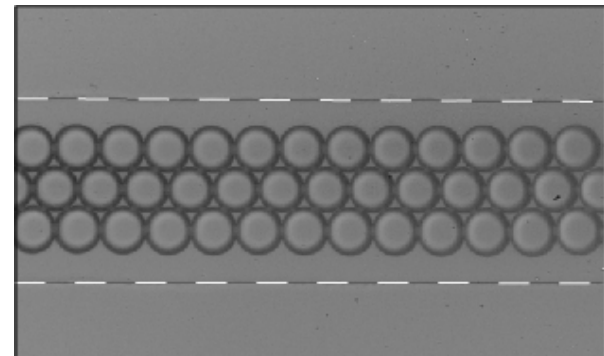


Water flow rate: $265 \mu\text{l/hr}$ ($\sim 2.5\text{cm/s}$)

10,000 drops/s

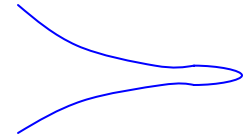
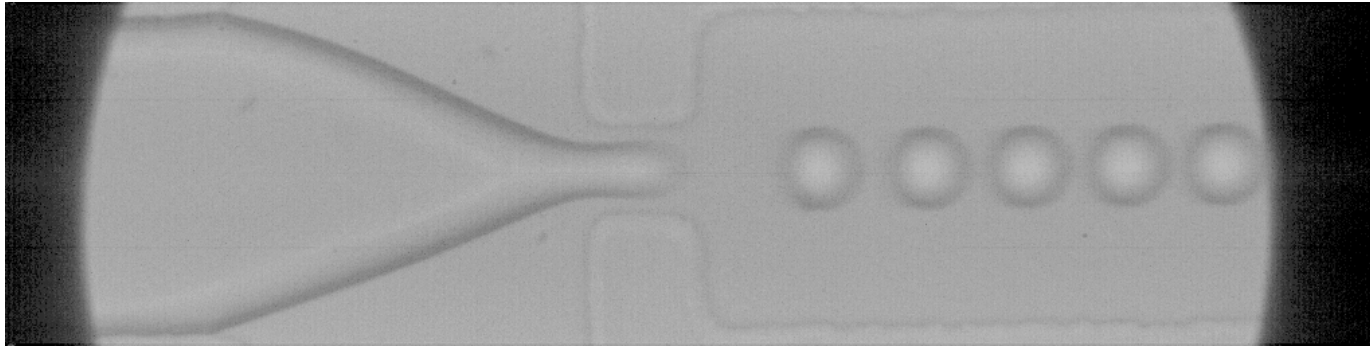


Tip stays at a single position



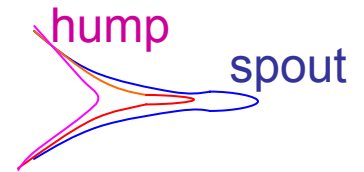
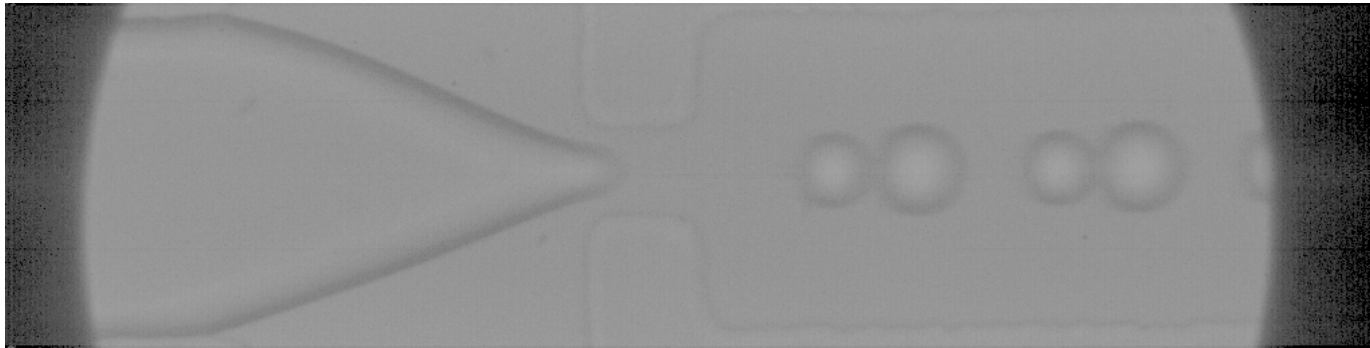
Very monodisperse droplets

Hump-spout transition

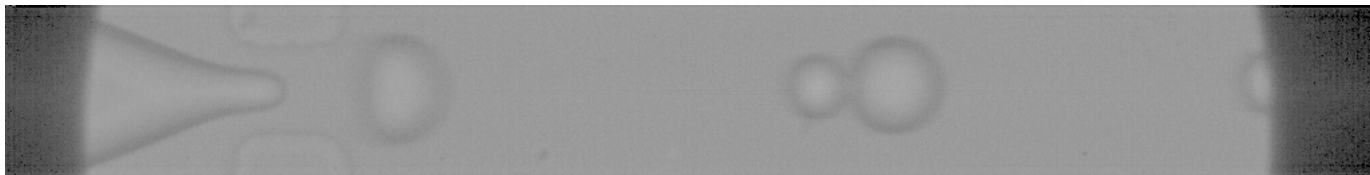


Tip stays at a single position

Water flow rate: 265 $\mu\text{l/hr}$ ($\sim 2.5\text{cm/s}$)

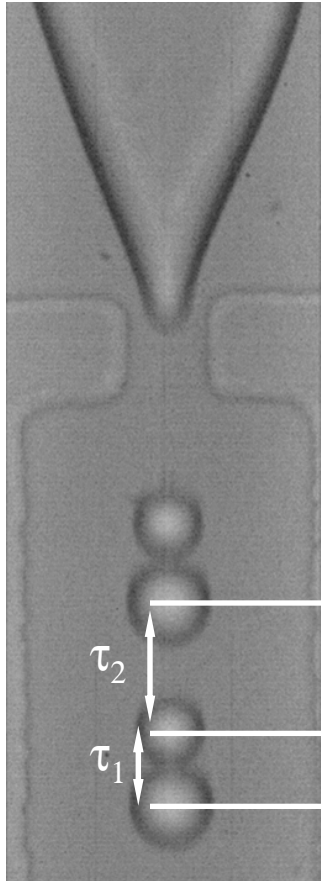


Tip moves

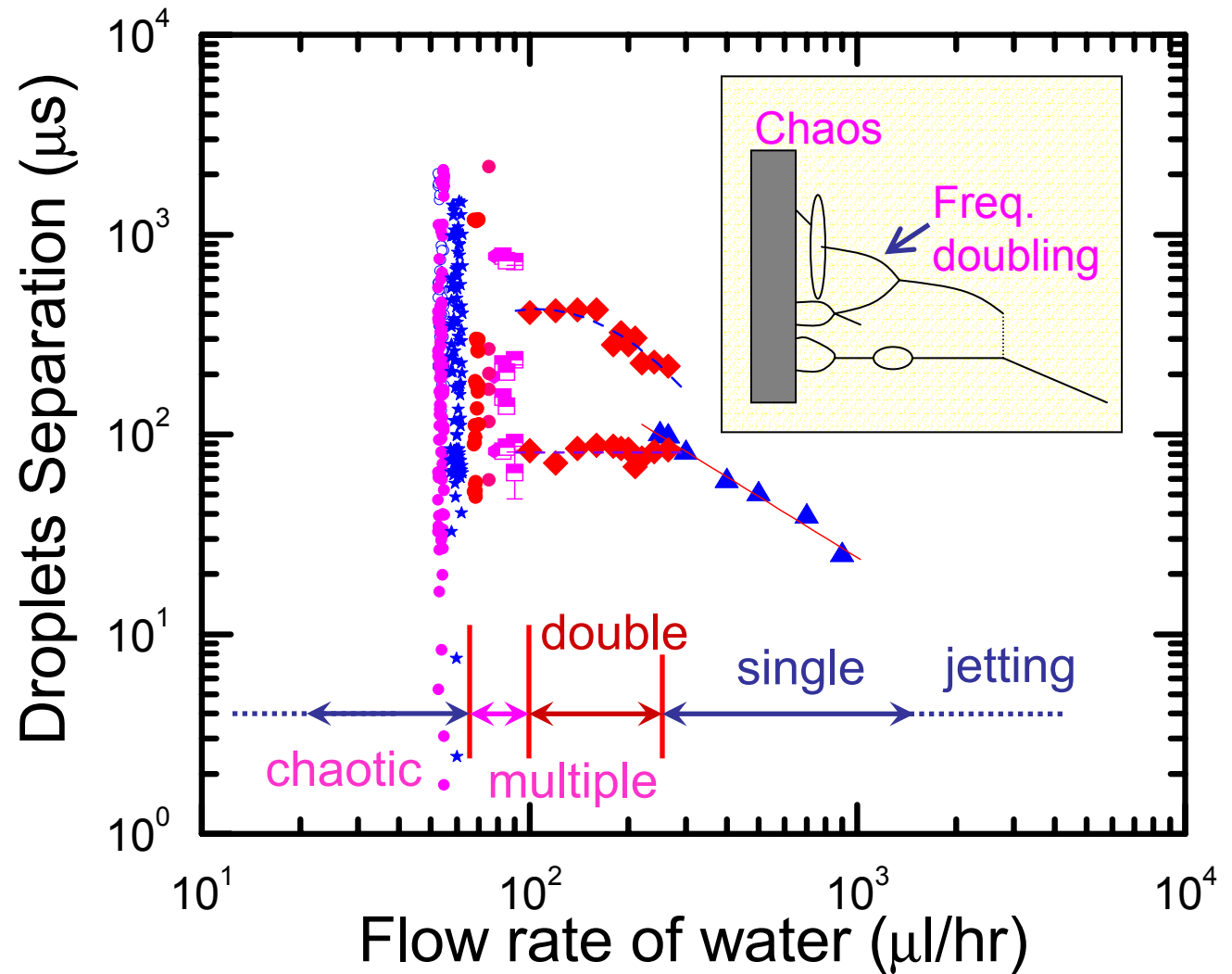


Water flow rate: 110 $\mu\text{l/hr}$ ($\sim 1\text{cm/s}$)

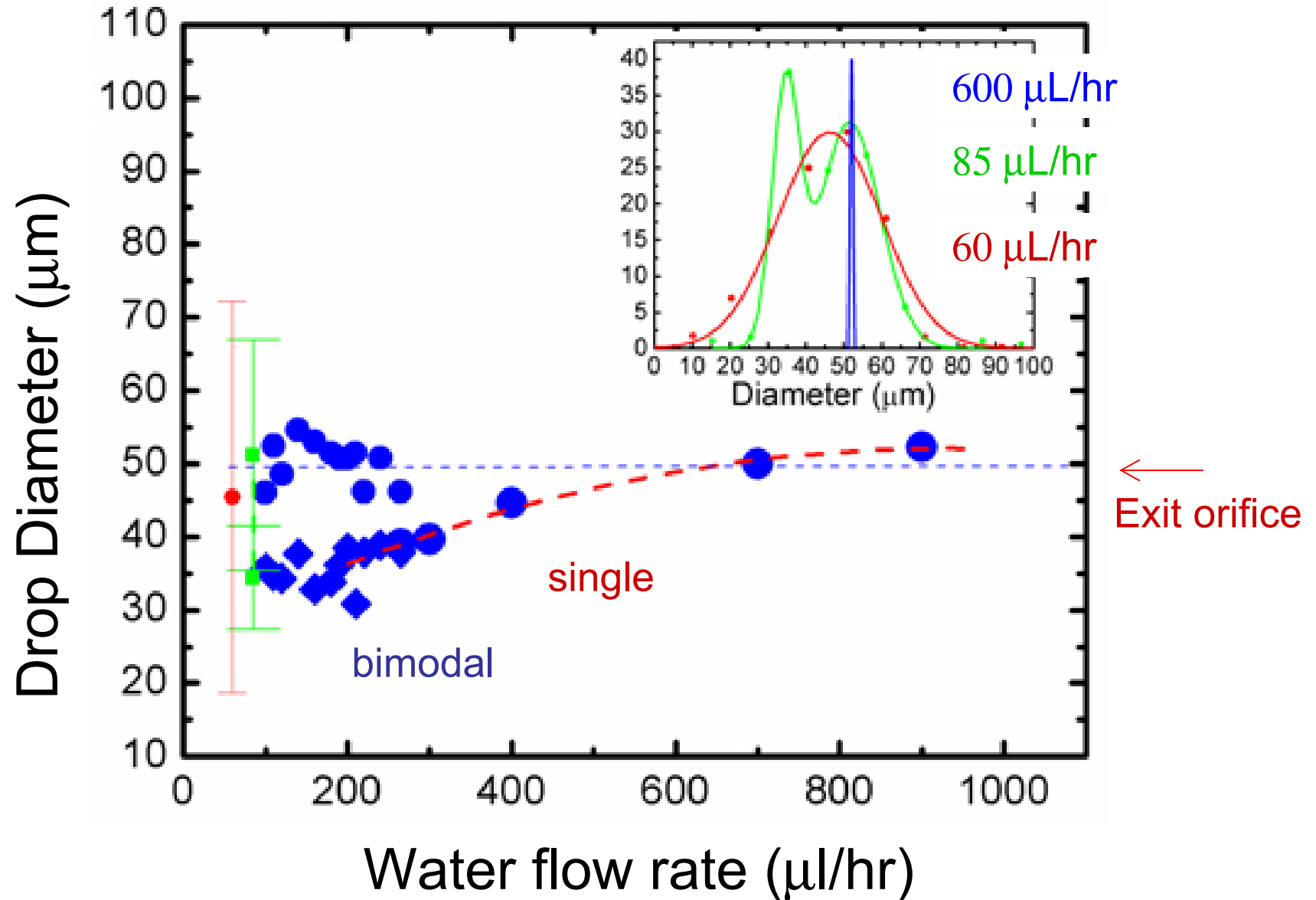
Dynamics bifurcation of droplets production



oil: 1000 $\mu\text{l/hr}$
 $\sim 9\text{cm/s}$

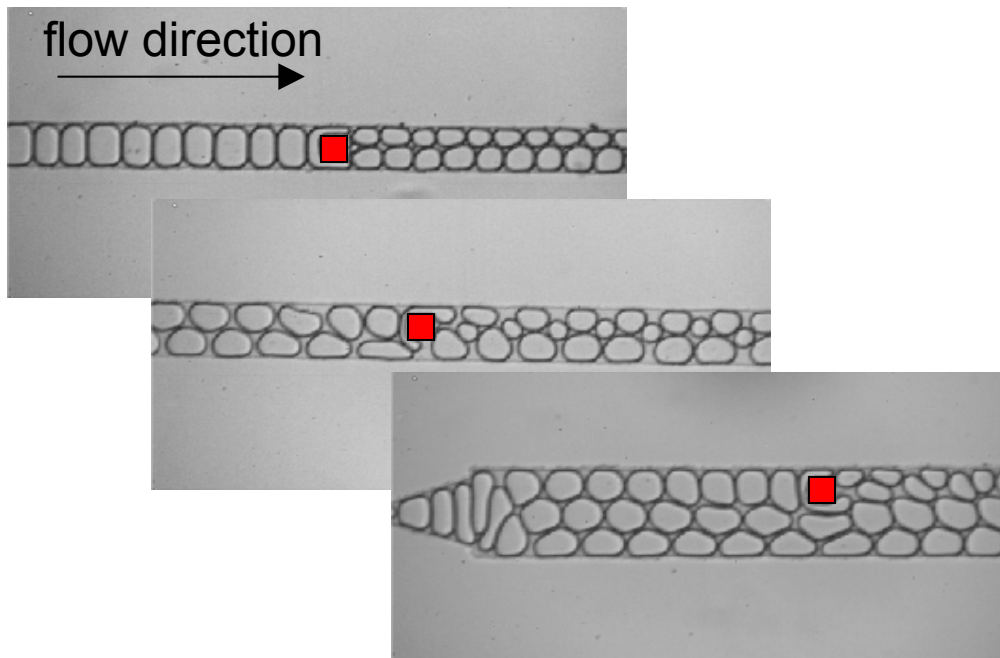
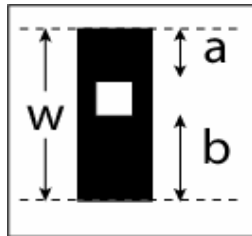


Size of water droplets by flow focusing

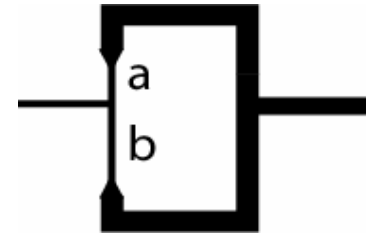


Manipulating the size distribution: fission

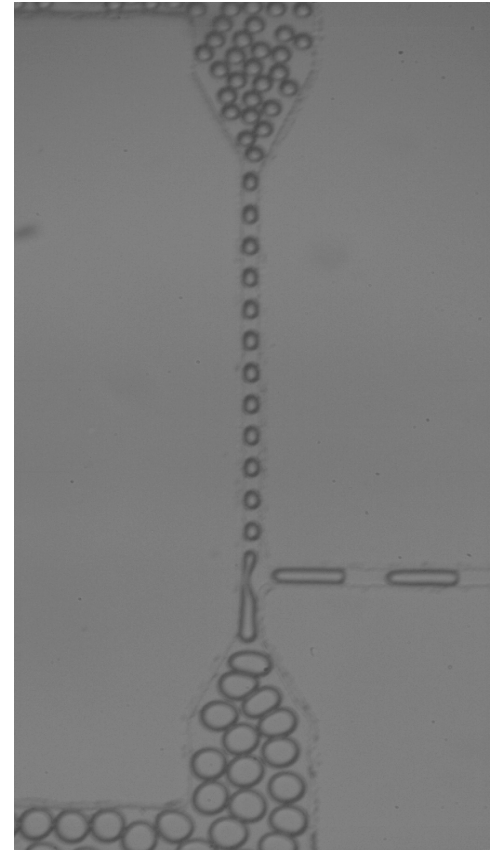
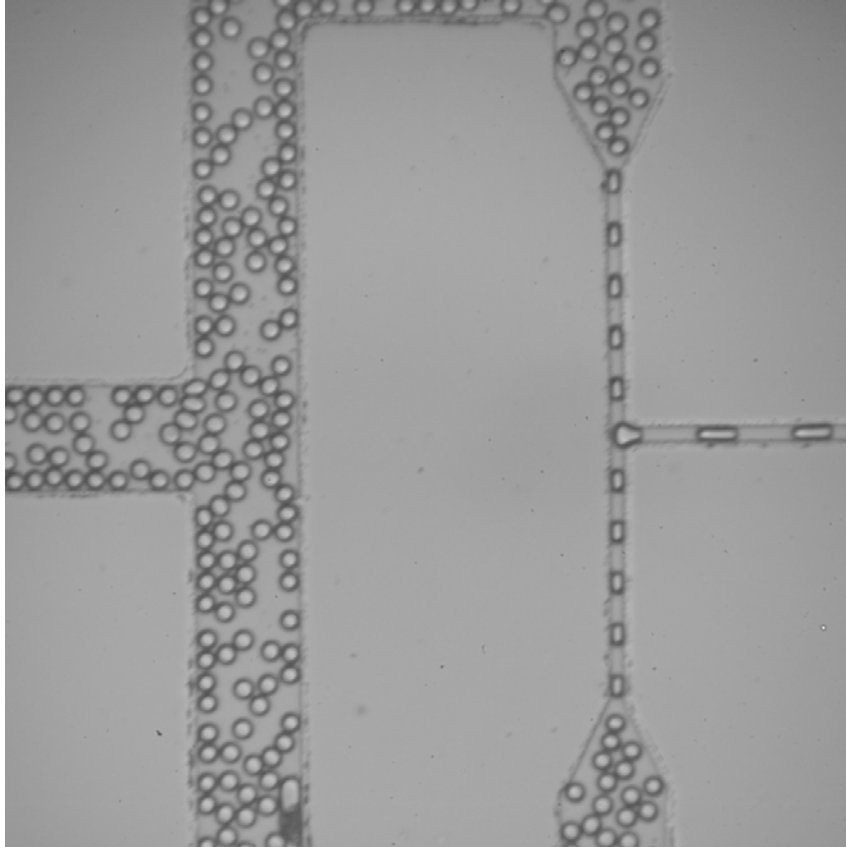
Obstruction mediated breakup



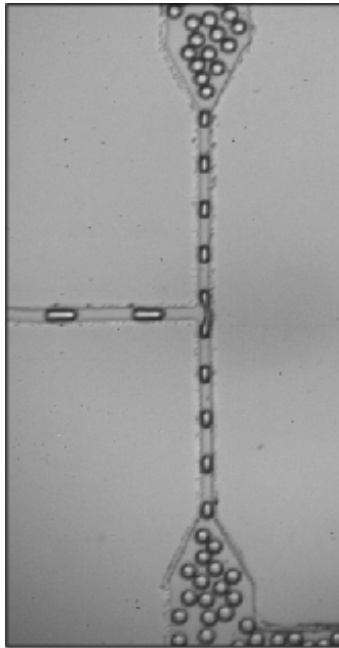
Extensional flow breakup



Symmetric and asymmetric extensional flows

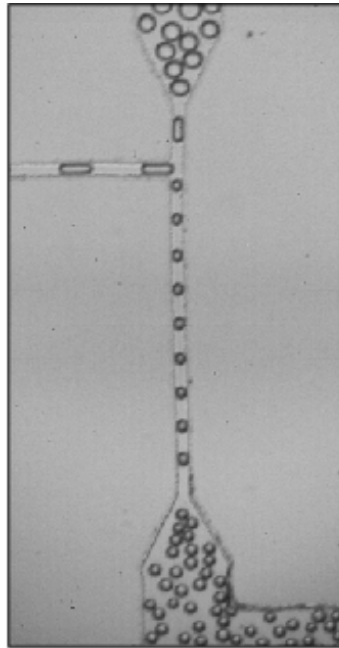


Passive break-up



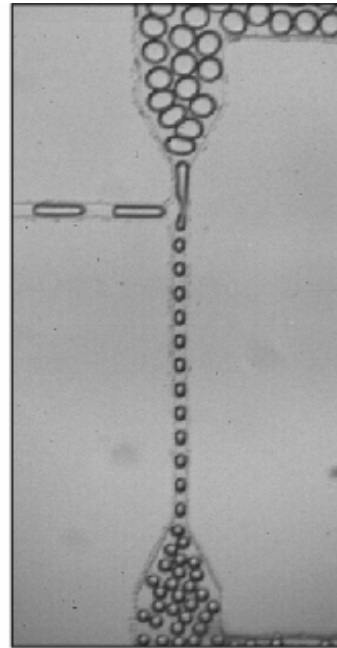
500-500 T

1:1



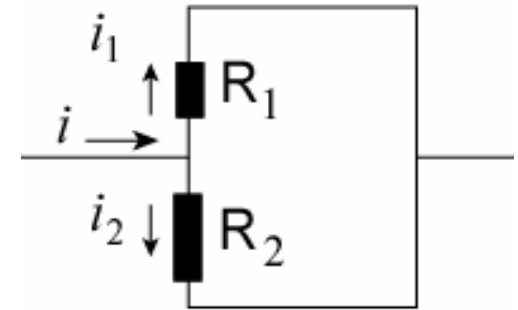
160-540 T

2:3



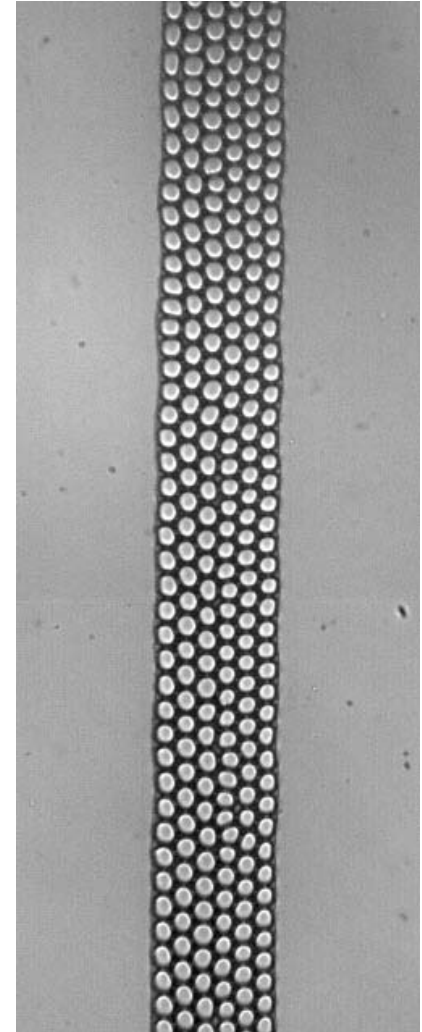
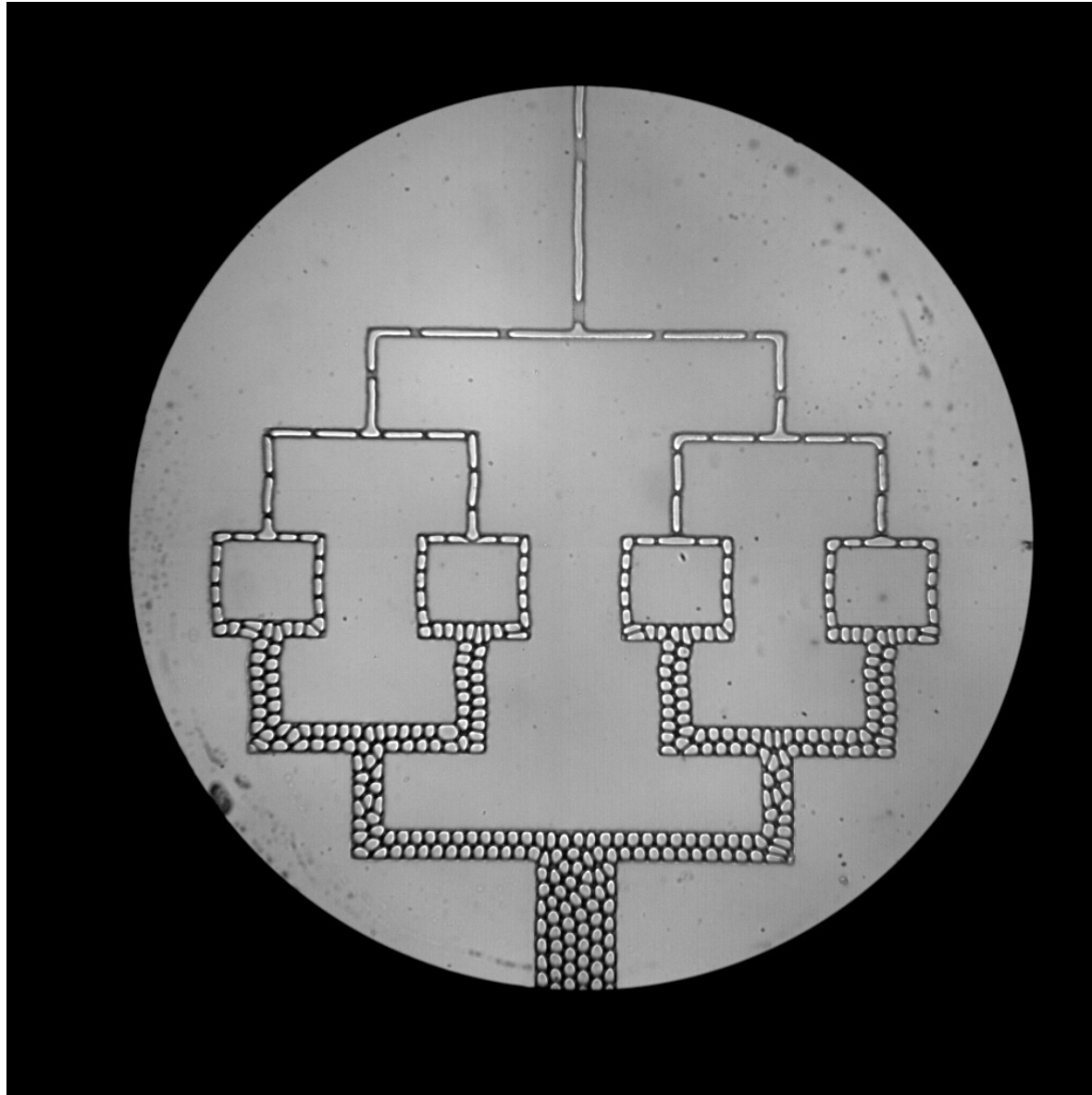
100-800 T

1:2

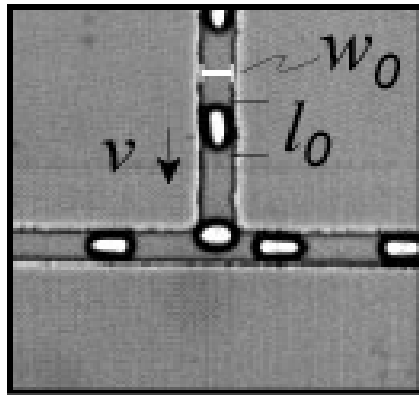


pressure – voltage
flow rate – current
flow resistance – resistance

High Volume Fraction Monodisperse Emulsions



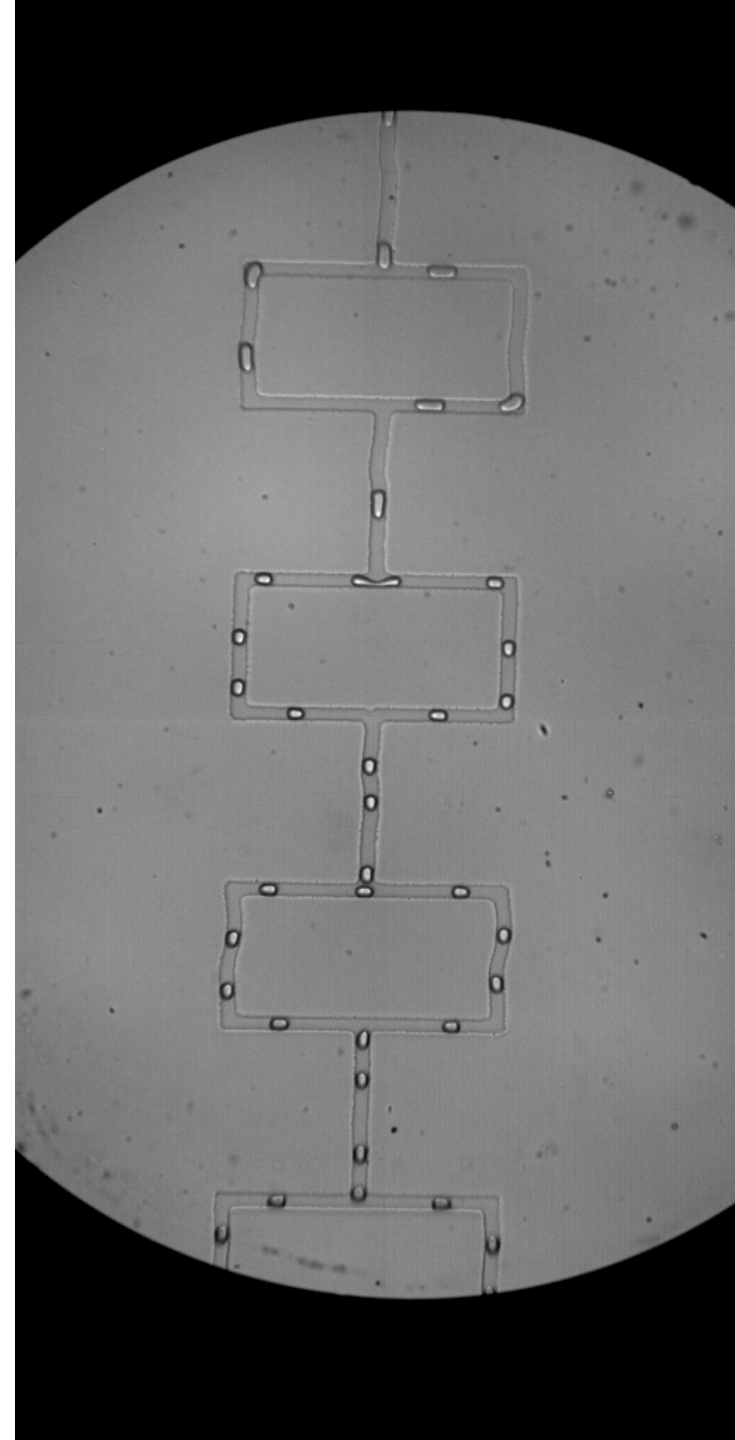
Critical flow for breaking drops



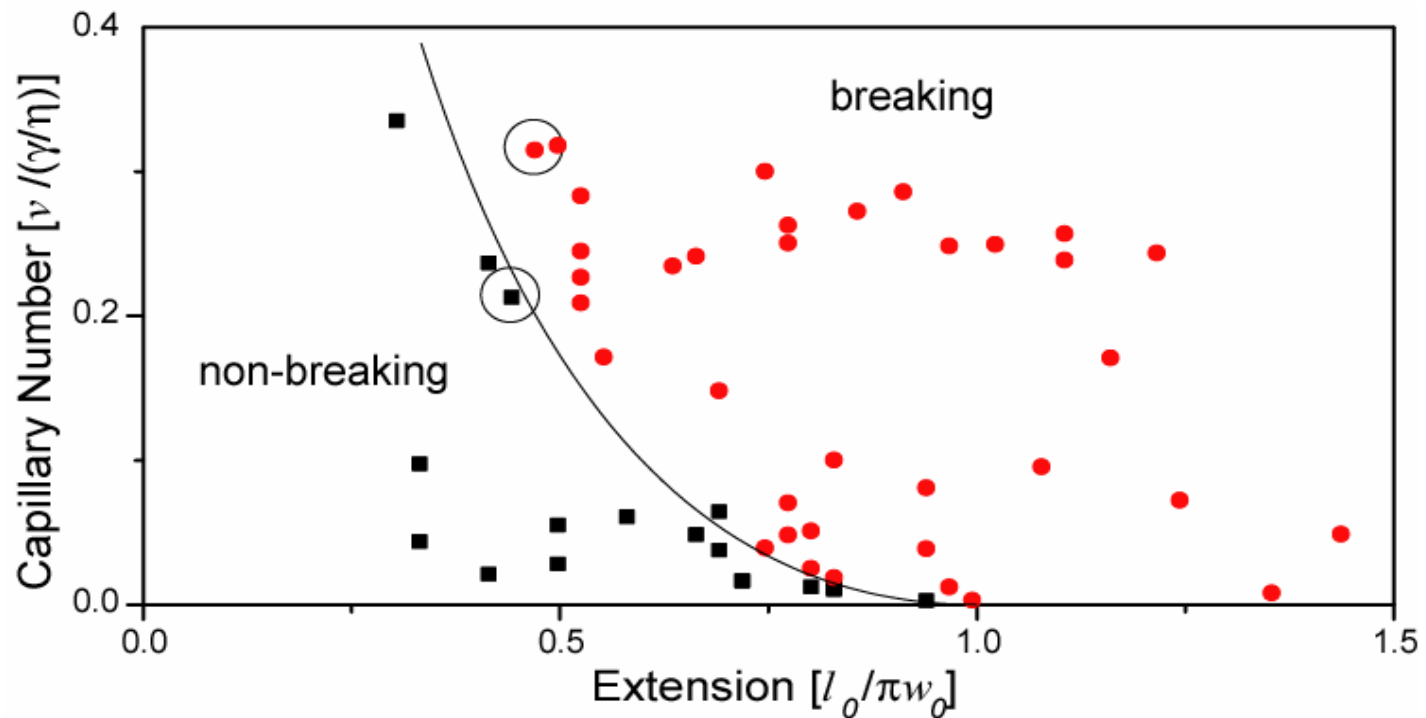
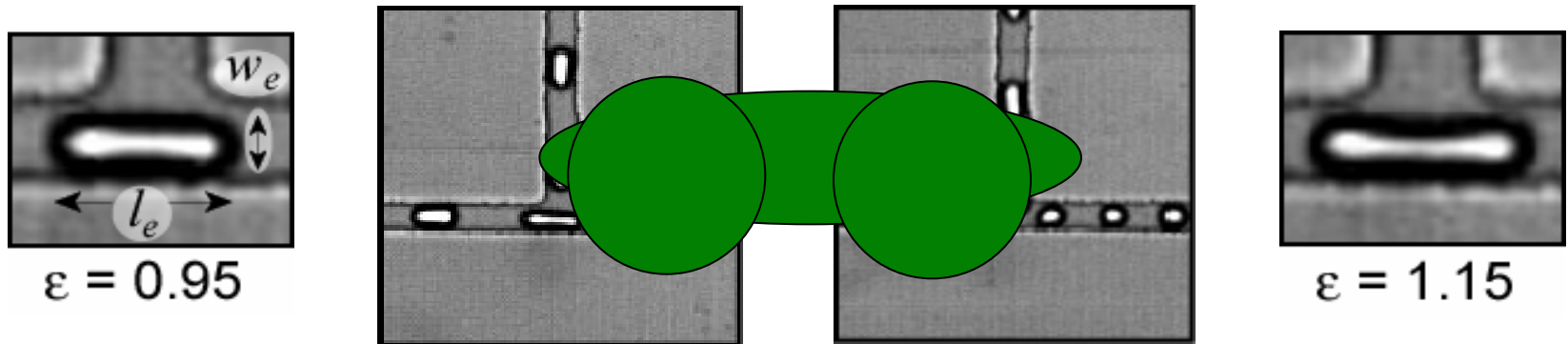
capillary number = $\frac{\text{viscous force}}{\text{surface tension}}$

$$C_G = \frac{\eta G a}{\gamma} = \frac{\eta v}{\gamma}$$

$$\text{extension} = \frac{\text{length}}{\text{circumference}} = \frac{l_0}{\pi w_0}$$



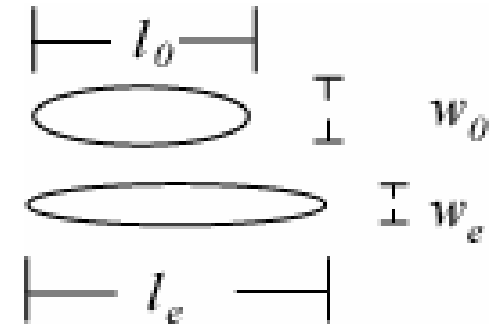
Rayleigh-Plateau instability



The forces of passive breakup

Viscous force stretching the drops

$$C_G \propto \left(\frac{l_e}{a} - \frac{l_0}{a} \right)^2$$



Conservation
of volume

$$l_0 w_0^2 \approx l_e w_e^2$$

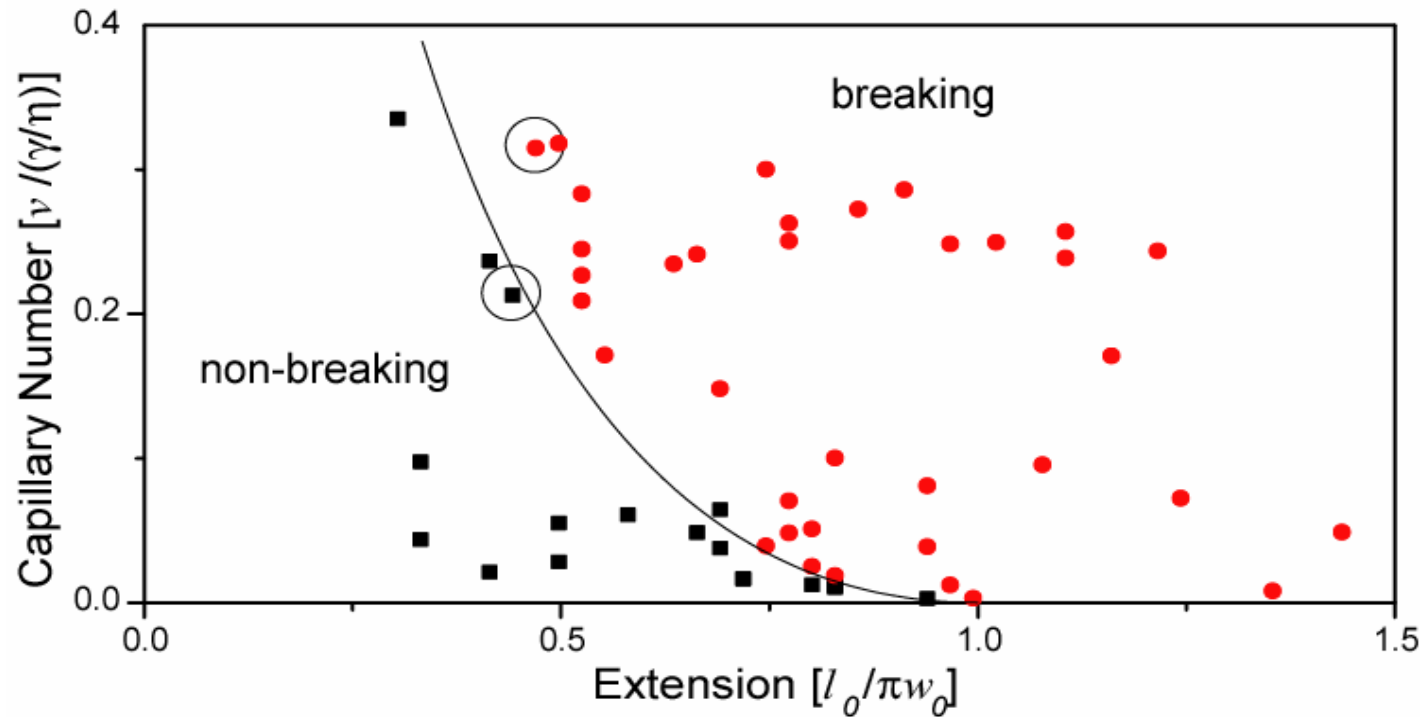
$$l_e = \pi w_e$$

$$\mathcal{E}_0 = \frac{l_0}{\pi w_0}$$

critical capillary number

$$C_{cr} \propto \mathcal{E}_0 (\mathcal{E}_0^{-2/3} - 1)^2$$

Critical capillary number

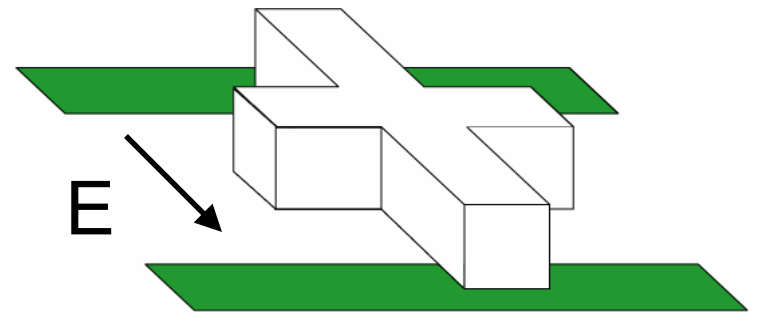
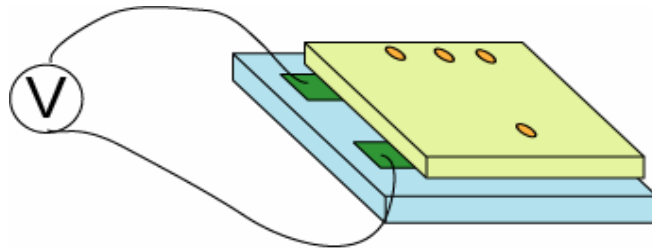
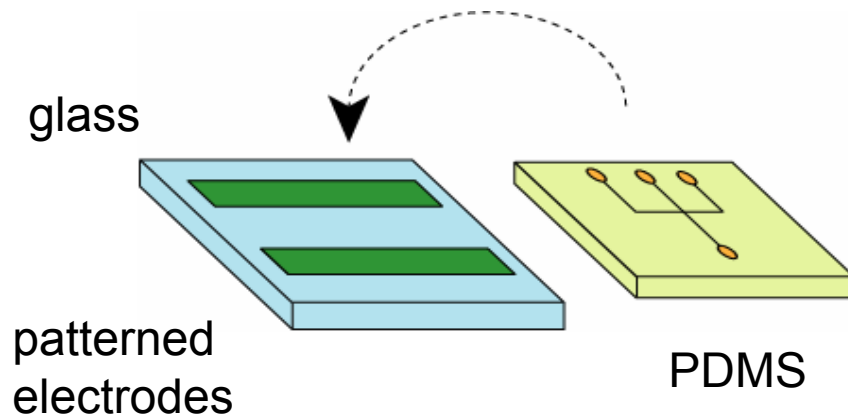


$$C_{cr} \propto \mathcal{E}_0 (\mathcal{E}_0^{-2/3} - 1)^2$$

Never get much smaller than the channel diameter

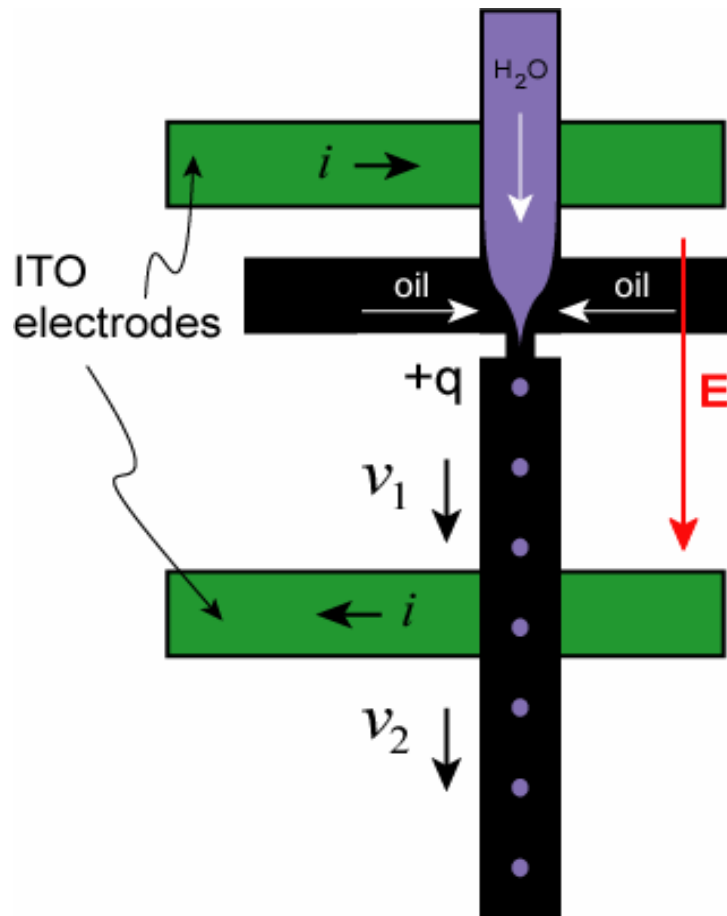
Need larger forces!

Making small drops: Electric fields



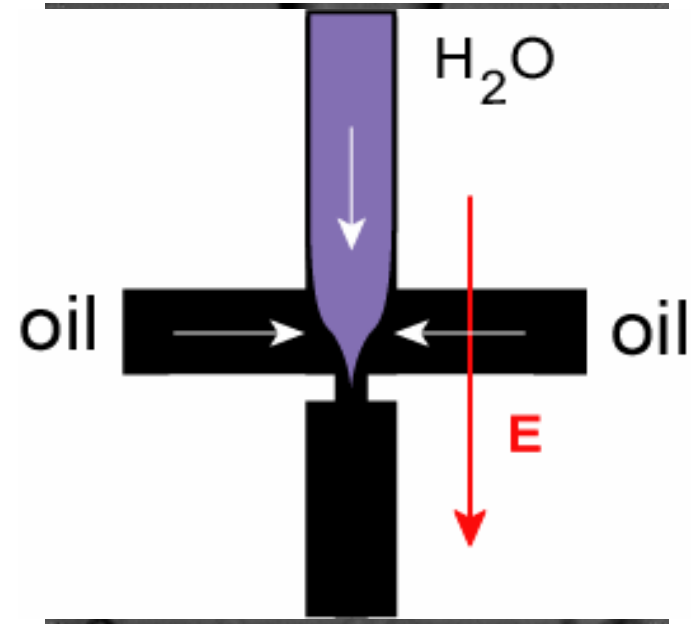
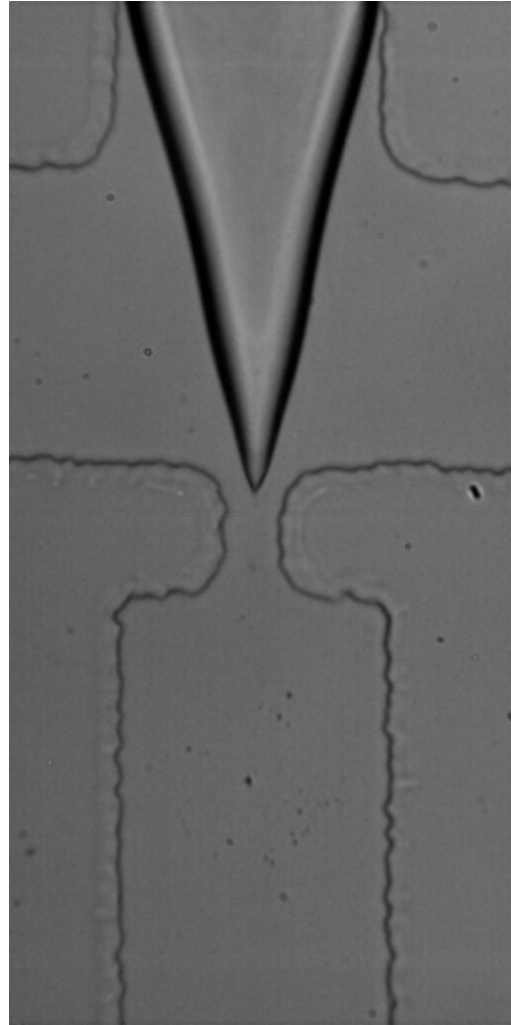
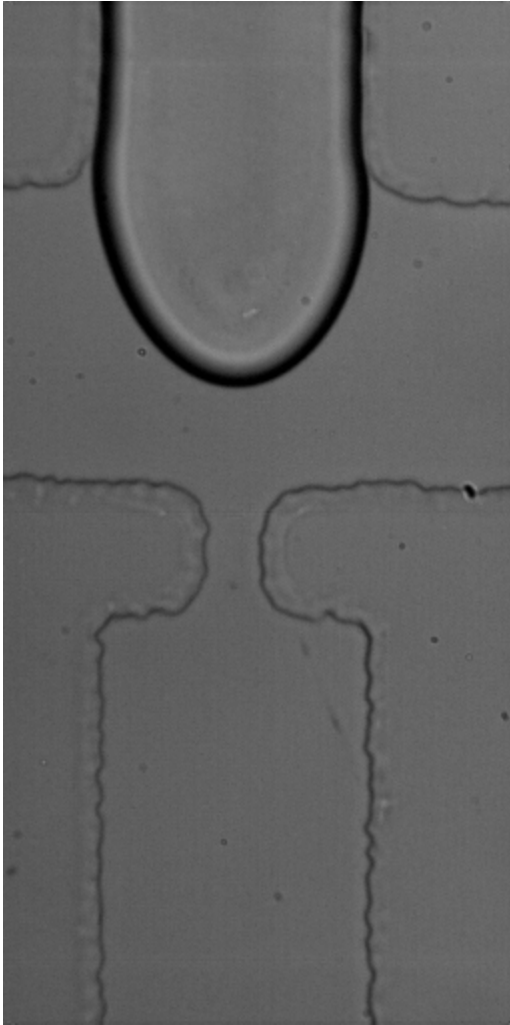
0.5 mm and 1 mm gaps
0 – 2500 V

Electro flow-focusing devices



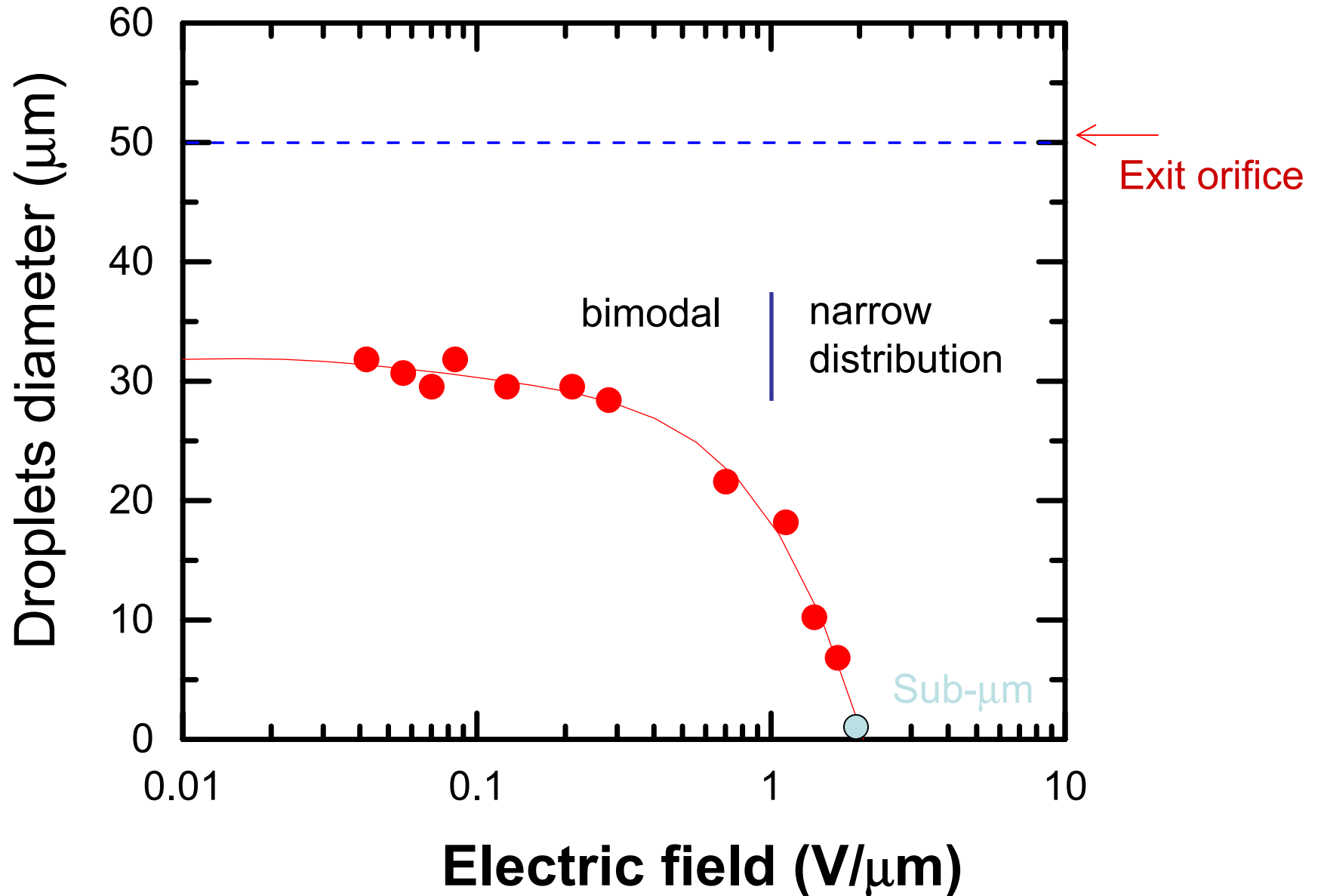
Pulling drops off
with an electric field

Electro flow-focusing

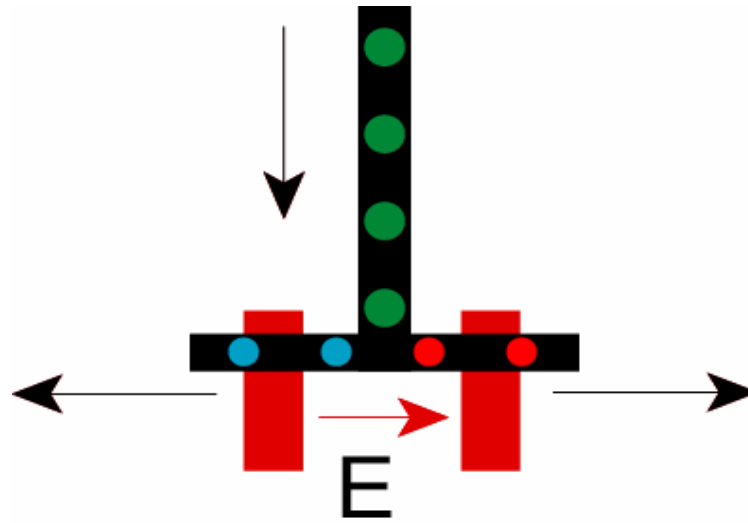


$$E = 2V/\mu m$$

Size of water droplets by electro flow focusing



Neutral drops in a field

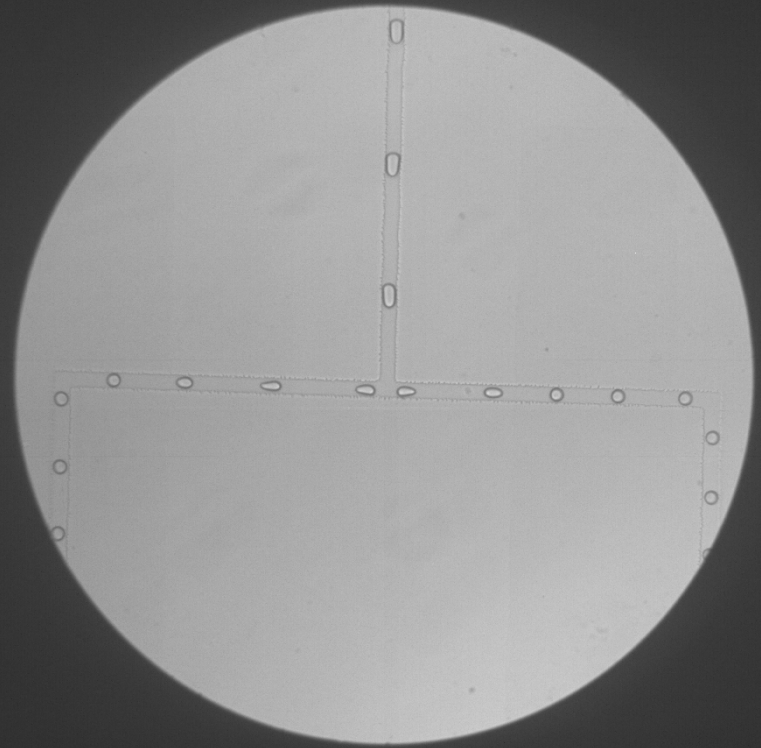


Uncharged droplets

$E=0$

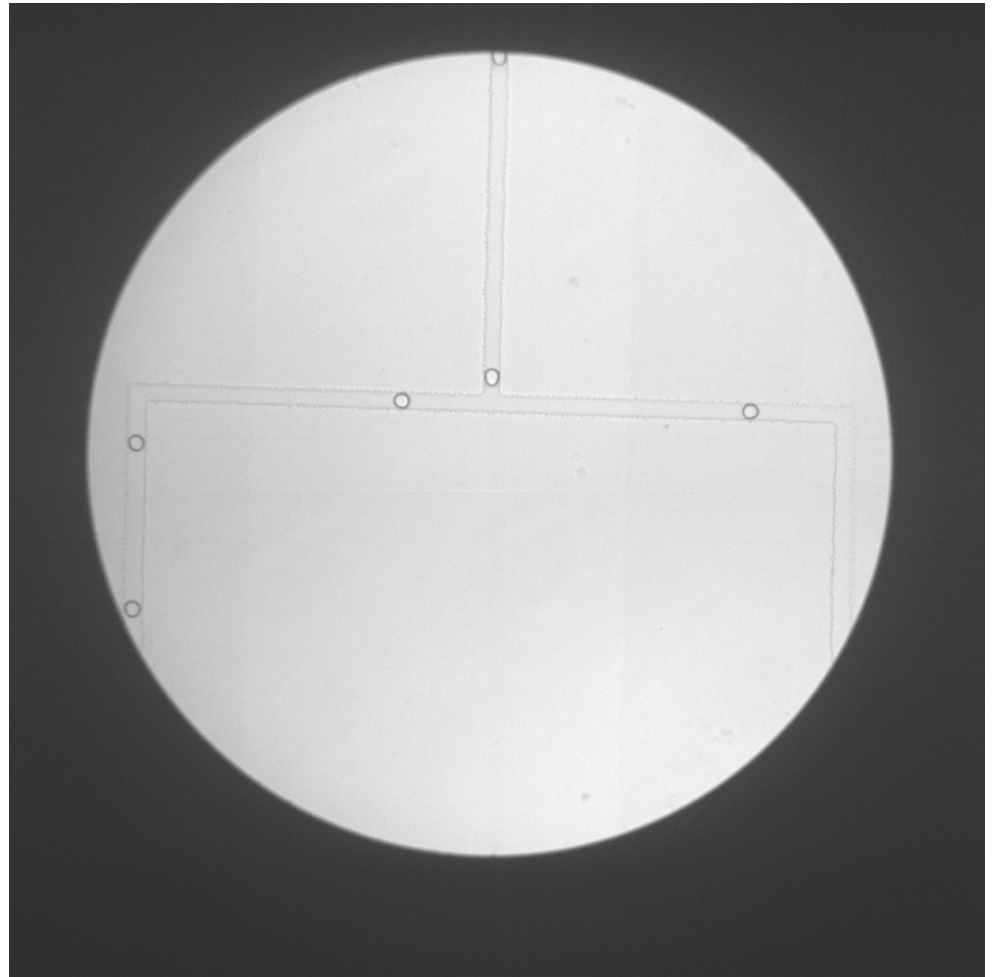
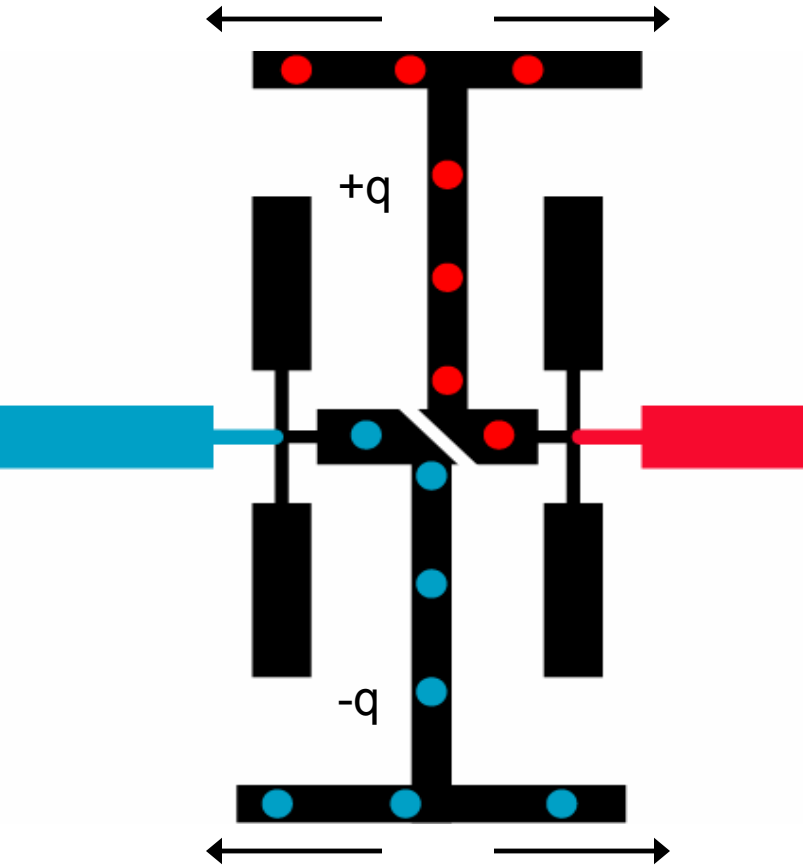


$E=1.4 \text{ V}/\mu\text{m}$

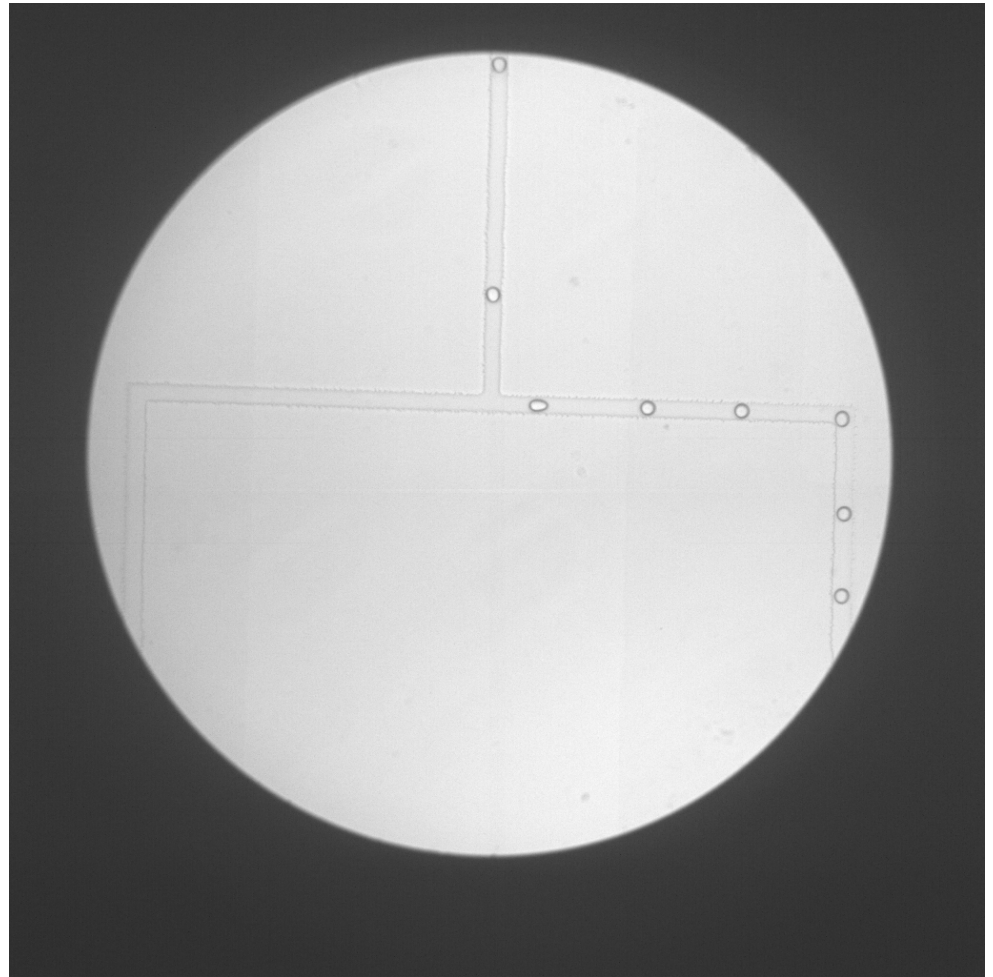
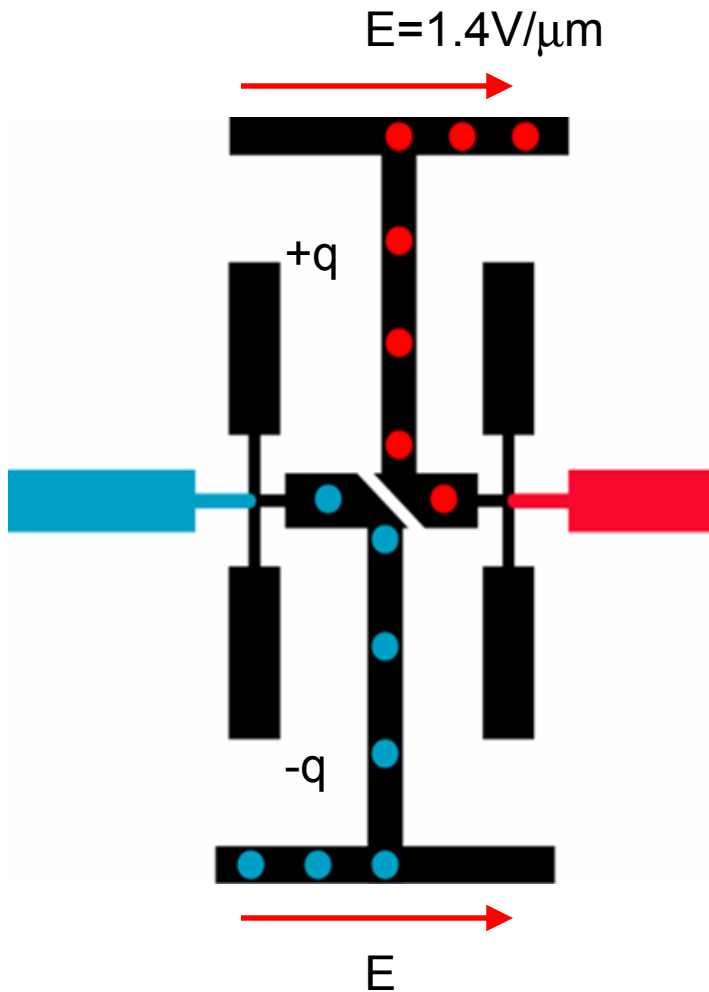


Droplet steering

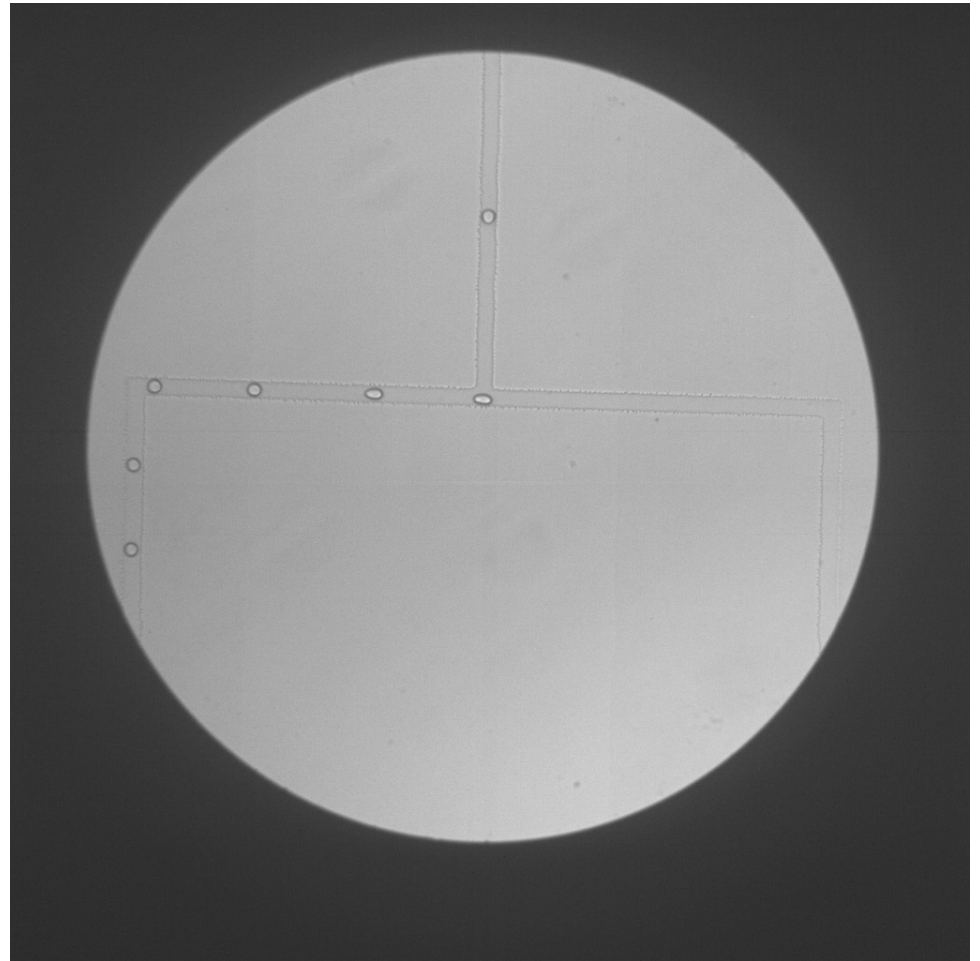
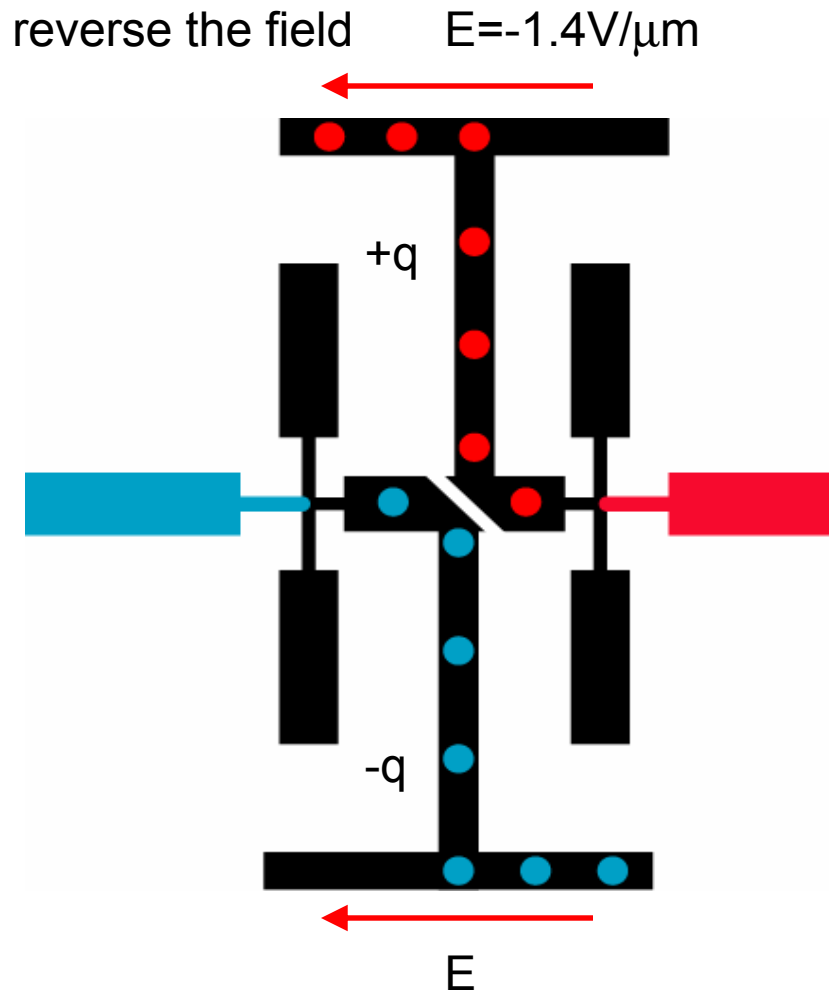
no electric field at bifurcation



Droplet steering



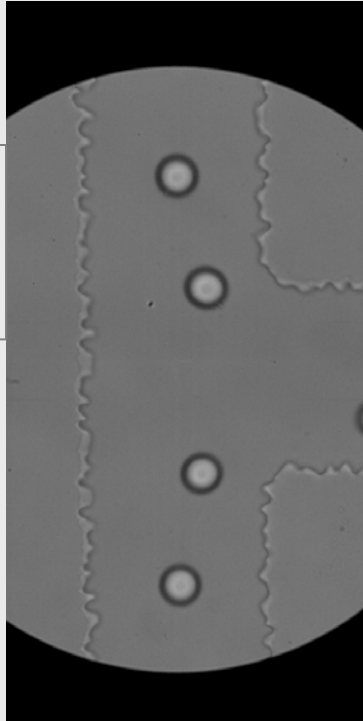
Droplet steering



Recombination: Can we put drops back together again?

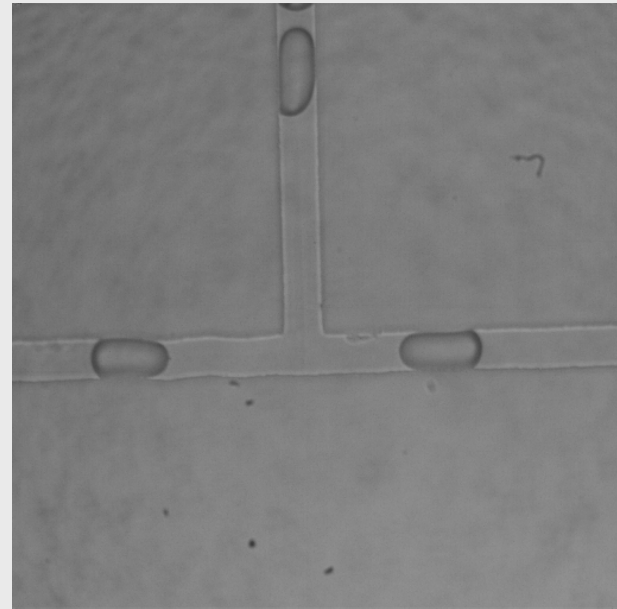
Small drops

Oil: 100 $\mu\text{L}/\text{h}$
Water: 10 $\mu\text{L}/\text{h}$



Big drops

Oil: 100 $\mu\text{L}/\text{h}$ Water: 50 $\mu\text{L}/\text{h}$



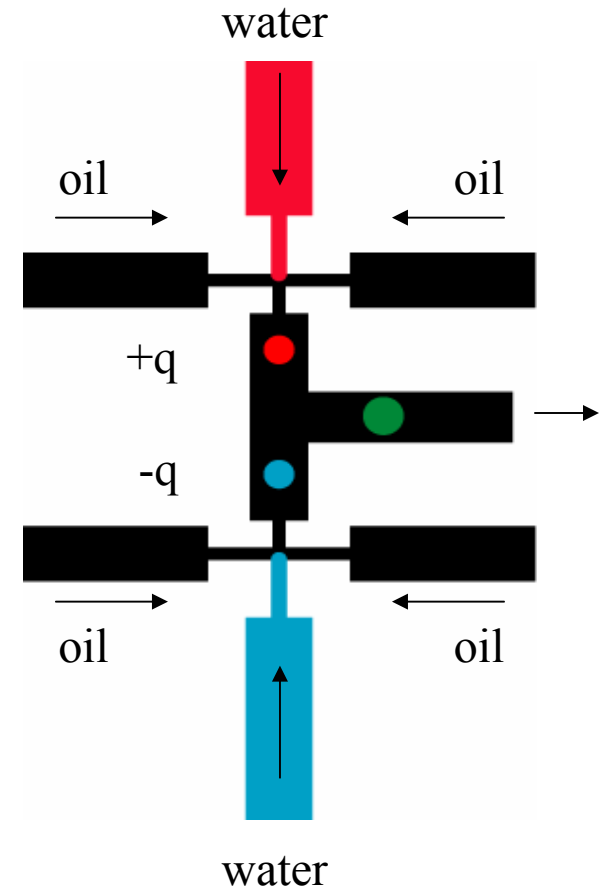
Close-up

Oil: 60 $\mu\text{L}/\text{h}$
Water: 20 $\mu\text{L}/\text{h}$

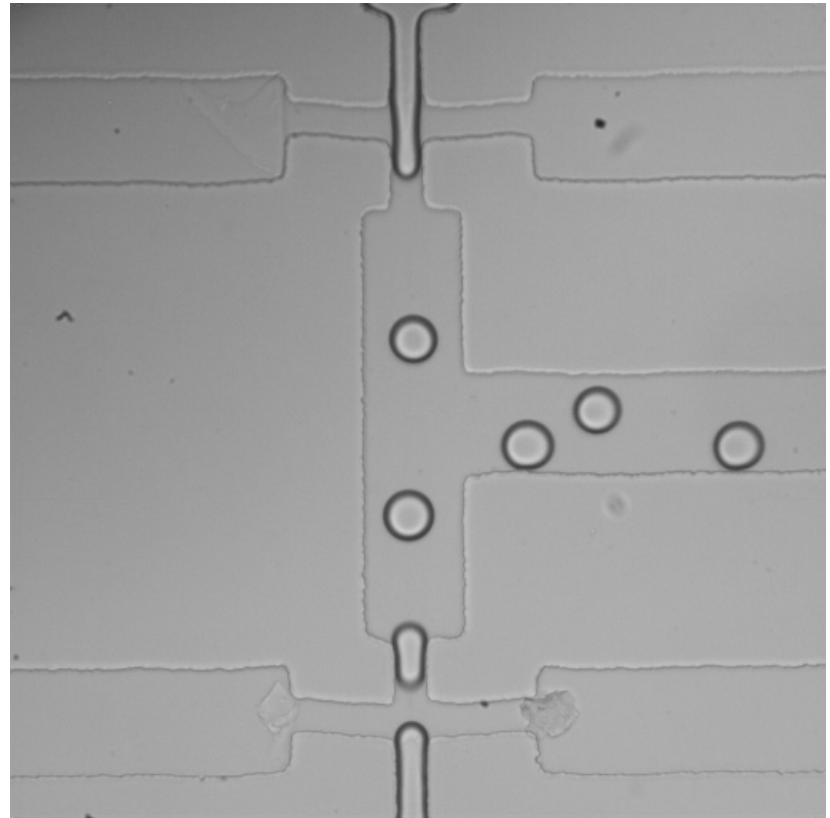
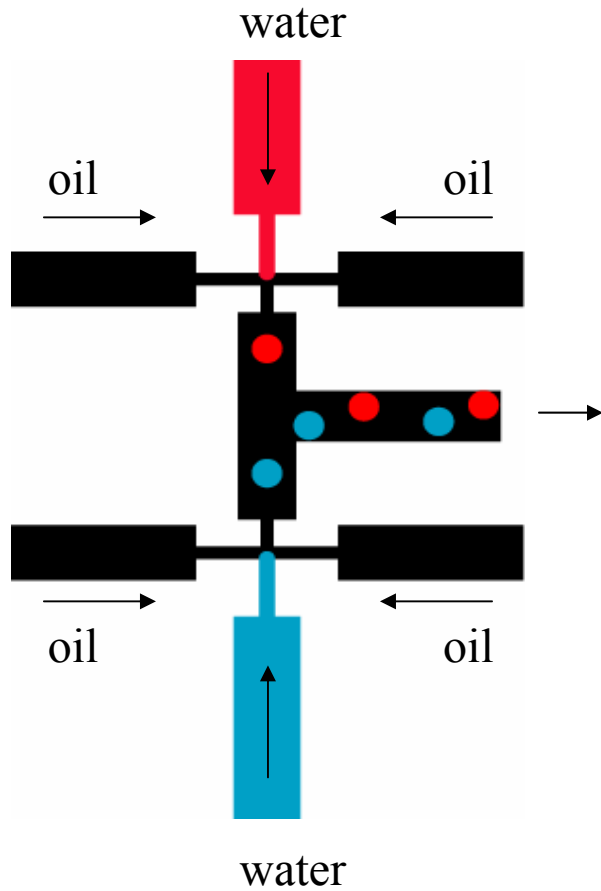


Controlled coalescence

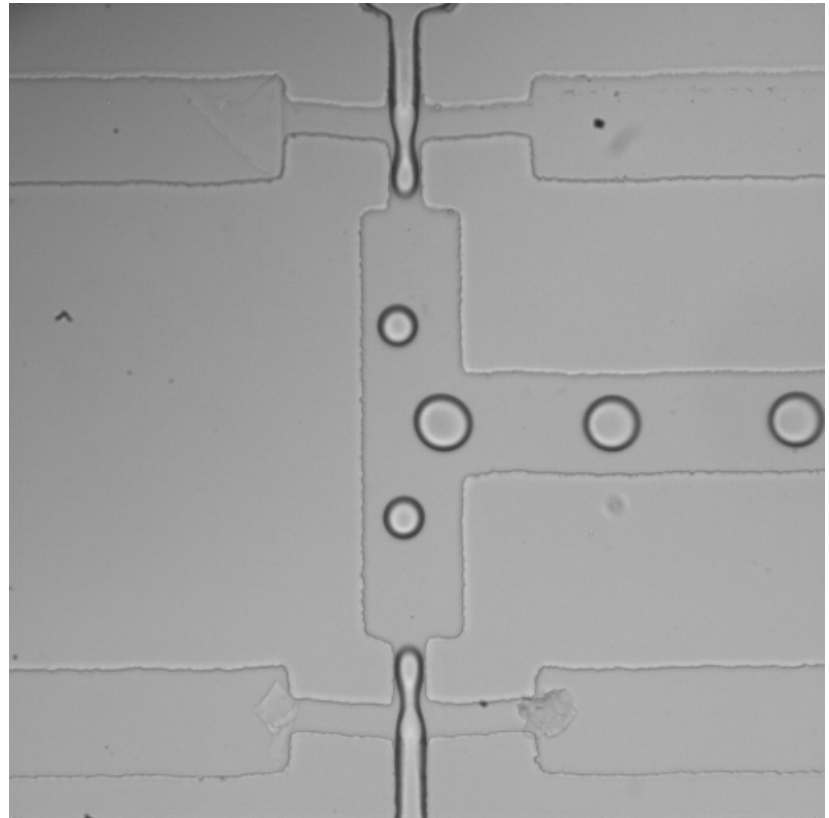
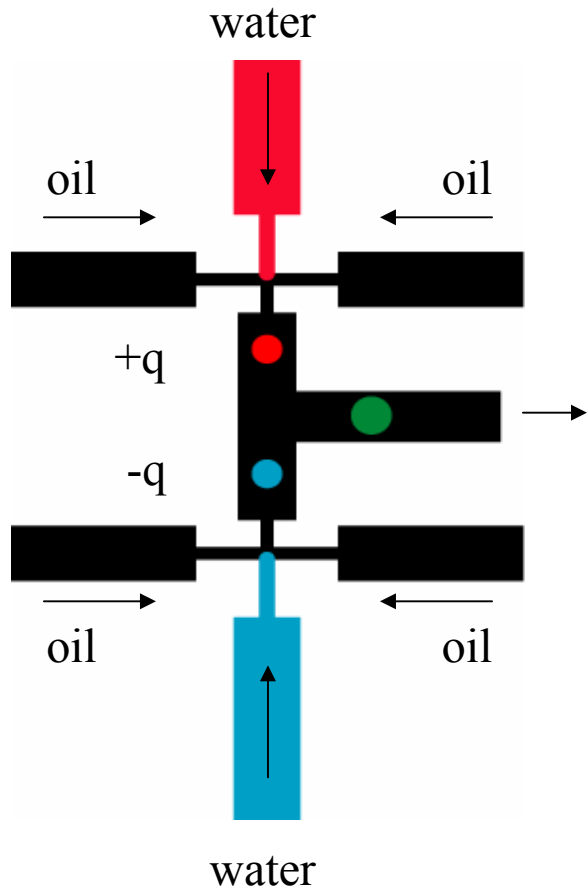
- Cross stream lines
- Overcome surface tension
- Time simultaneous arrival



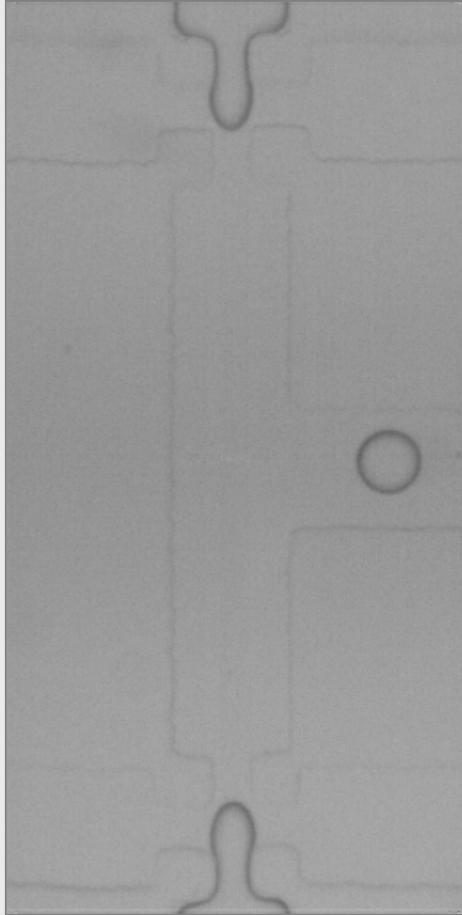
Uncharged droplets



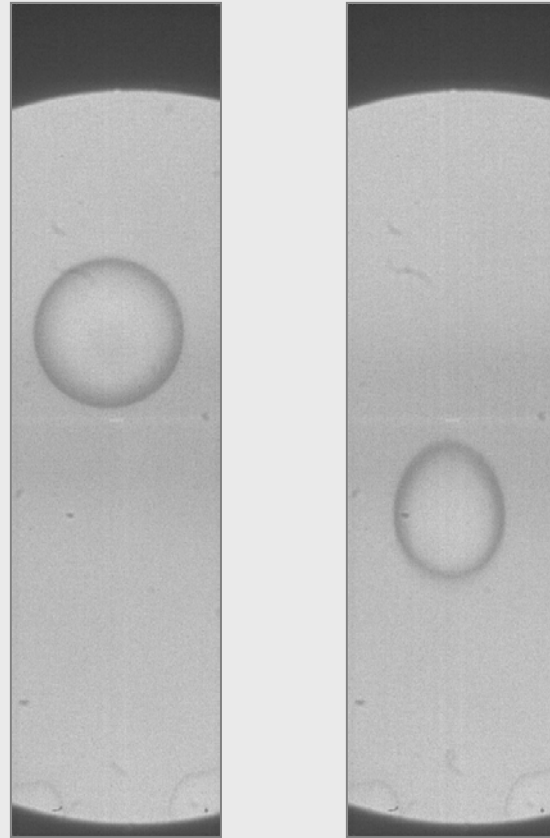
Charged droplets



Charged droplets under flow

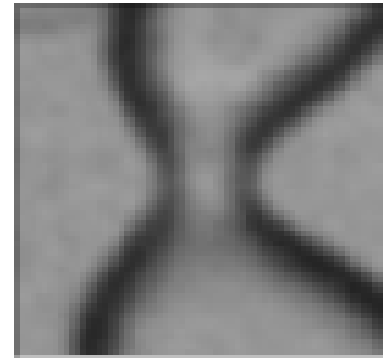
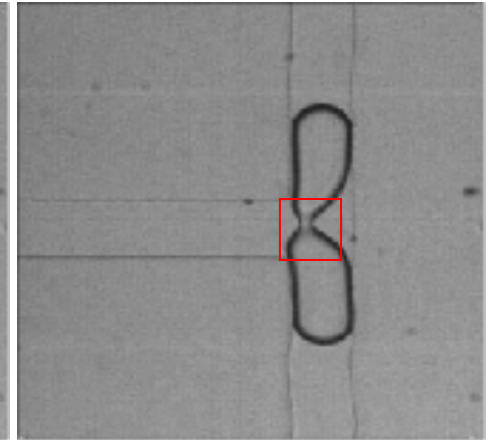
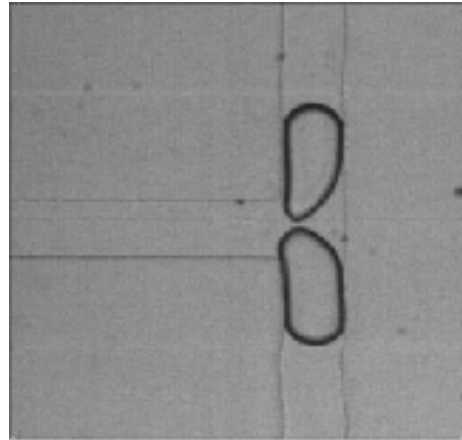
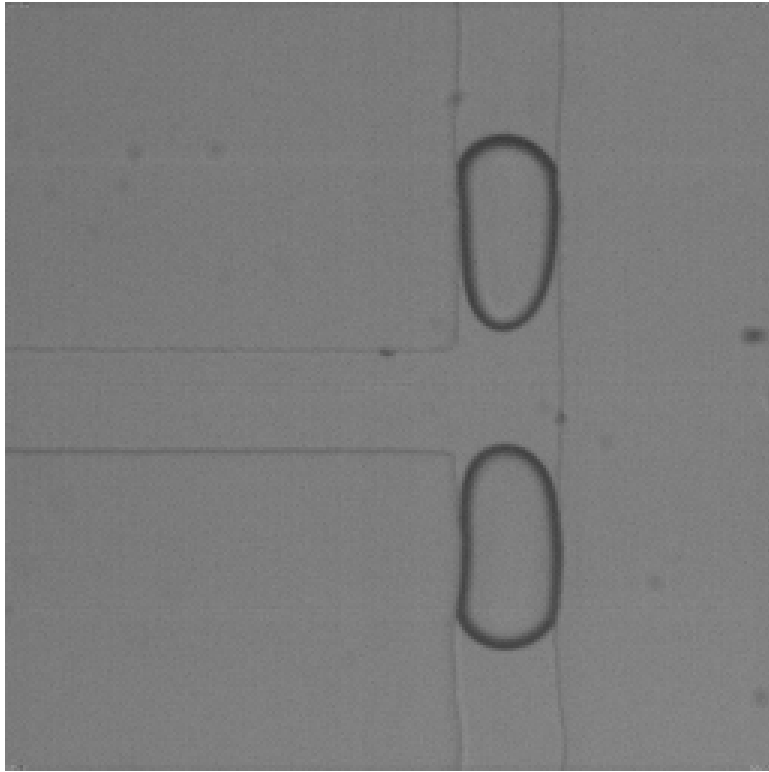


Oil flow rate: 100 $\mu\text{L/h}$
Water flow rate: 5 $\mu\text{L/h}$
Field: 1.6 $\text{V}/\mu\text{m}$



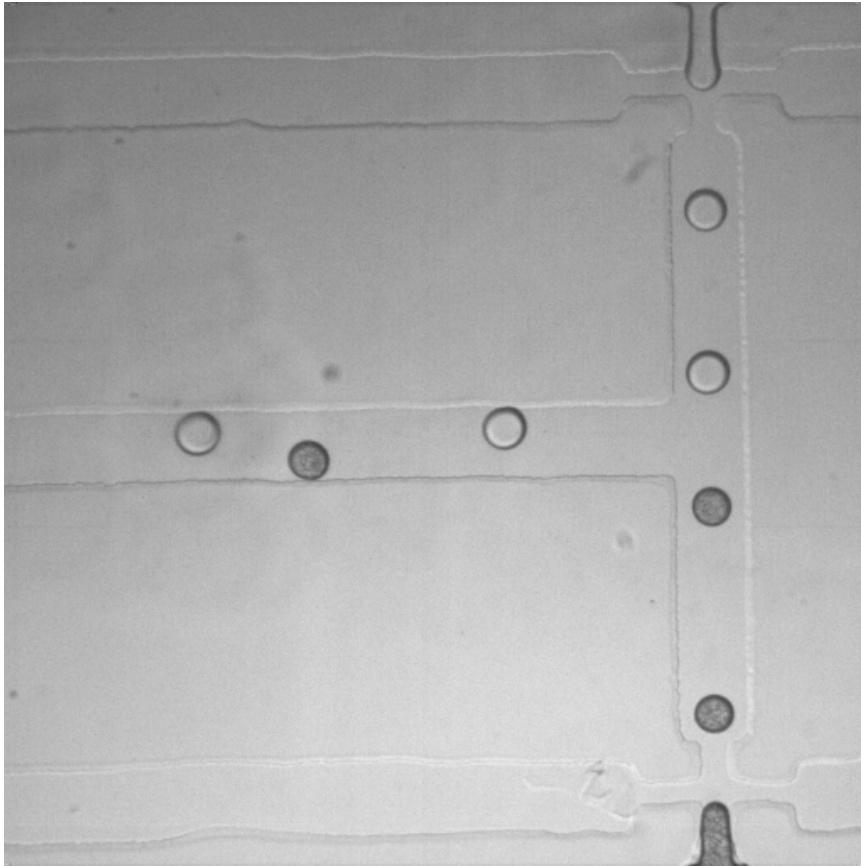
Oil flow rate: 100 $\mu\text{L/h}$
Water flow rate: 5 $\mu\text{L/h}$
Field: 0 – 1.8 $\text{V}/\mu\text{m}$

Fluid bridge formation

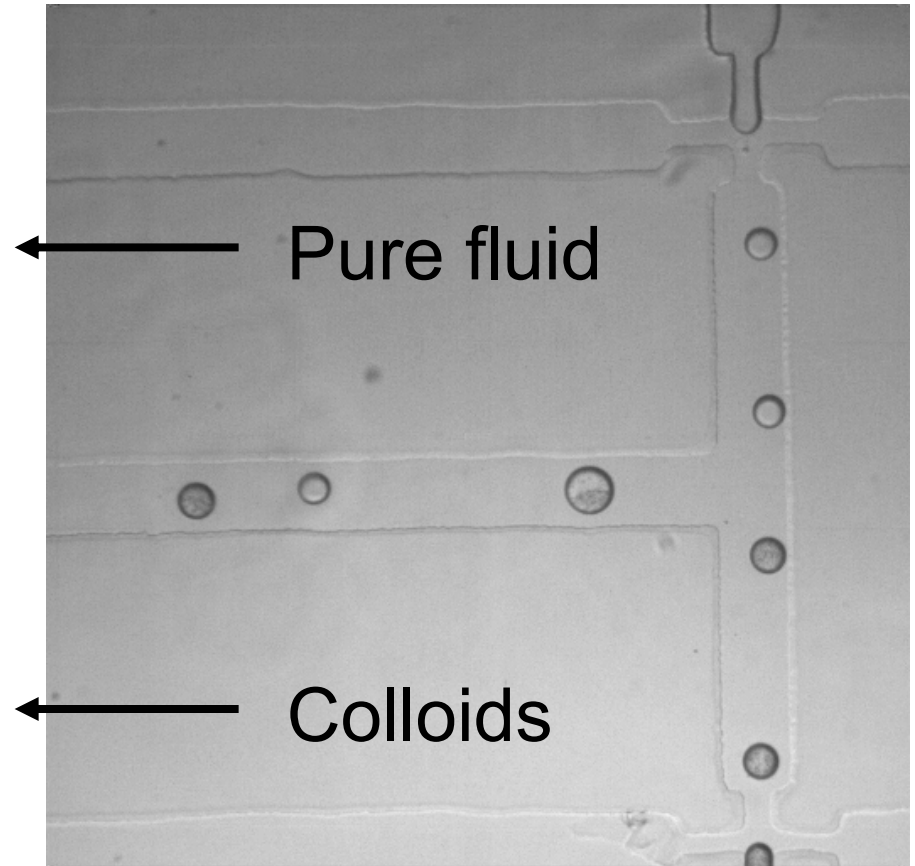


New materials: hemispheres

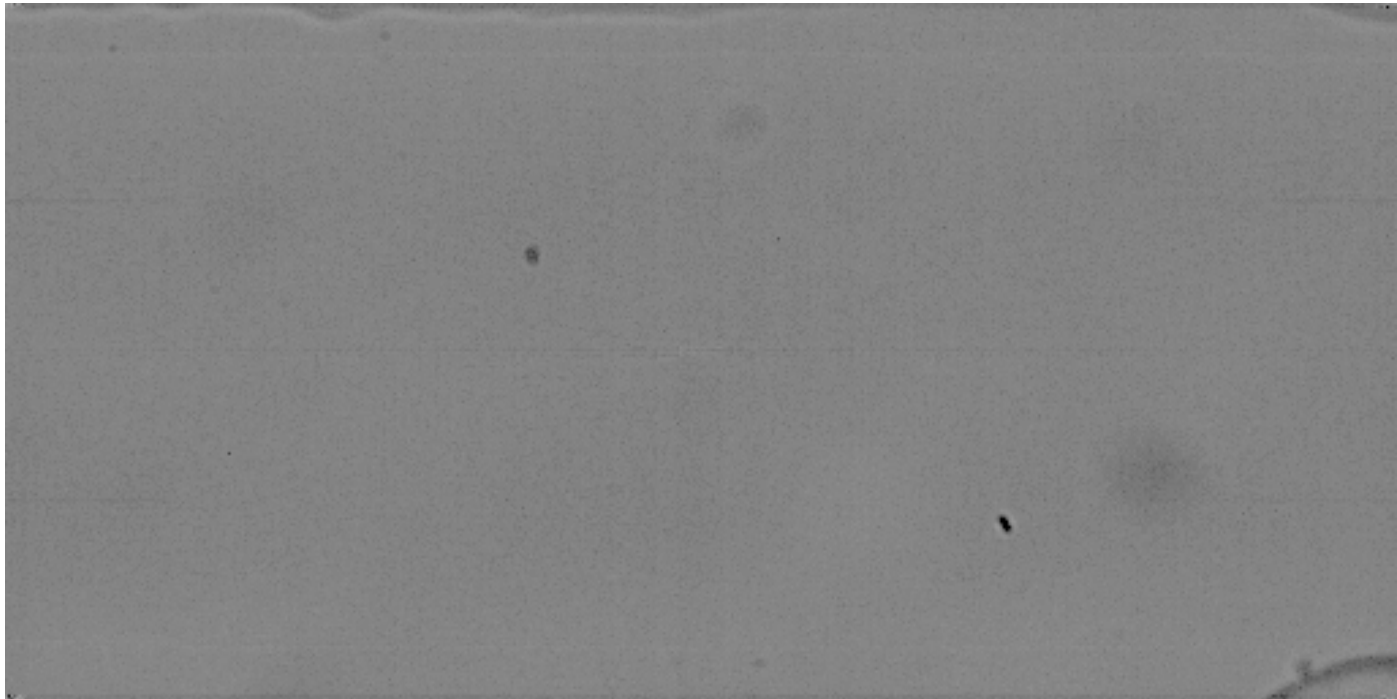
$E=0$



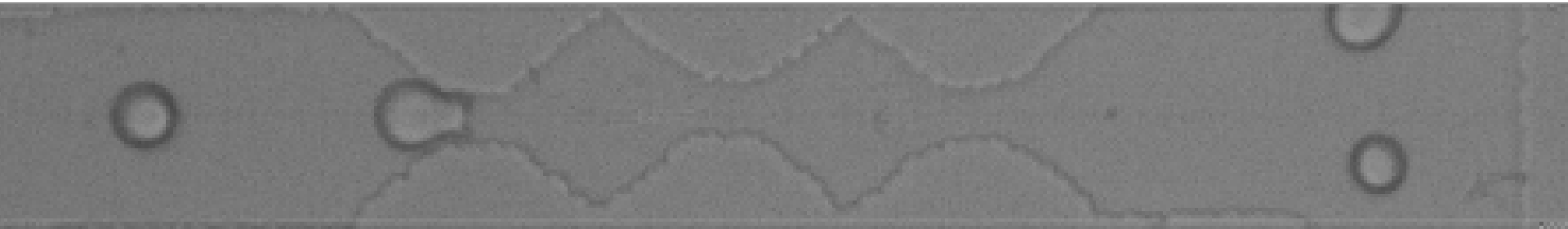
$E=1.2 \text{ V}/\mu\text{m}$



Separation of contents



Mixing scheme

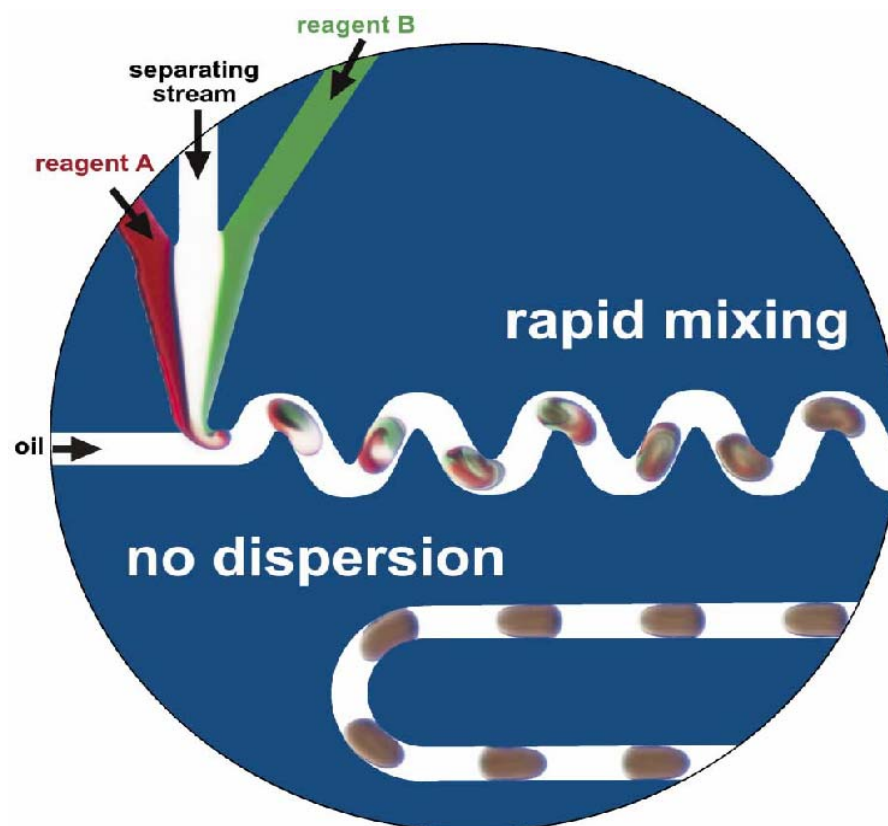


Studying Chemical Dynamics

Small volumes

- metering and transport of fluids

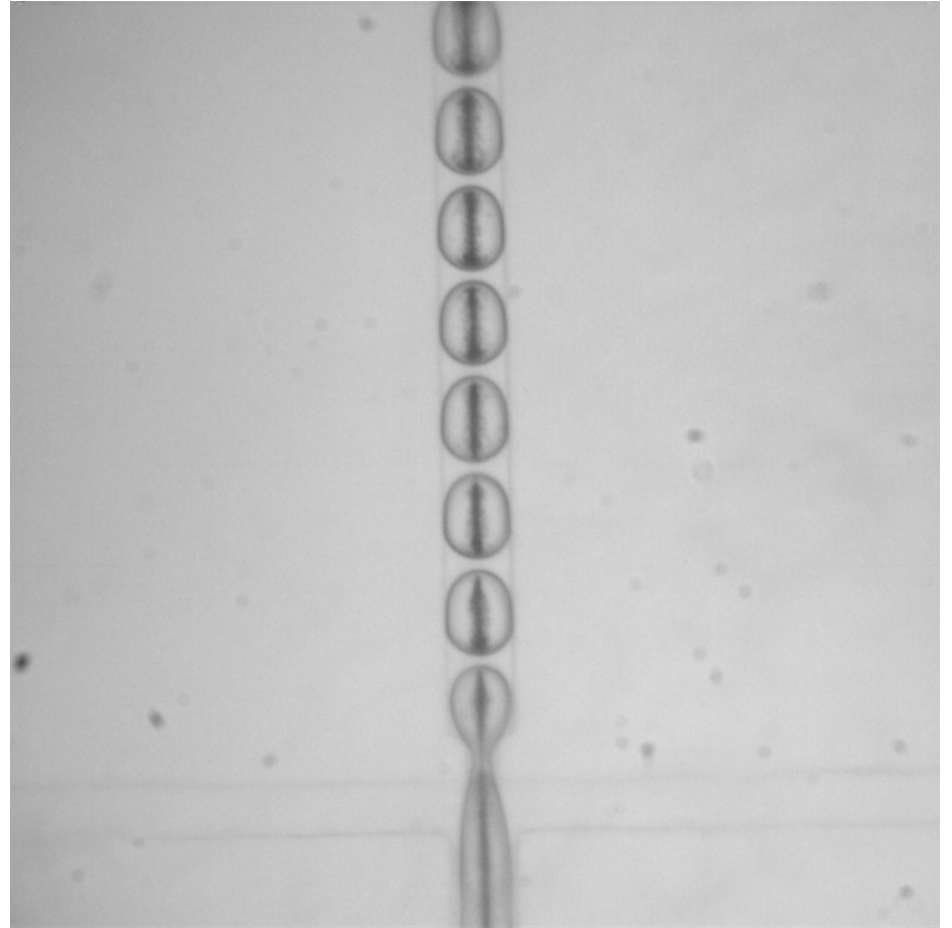
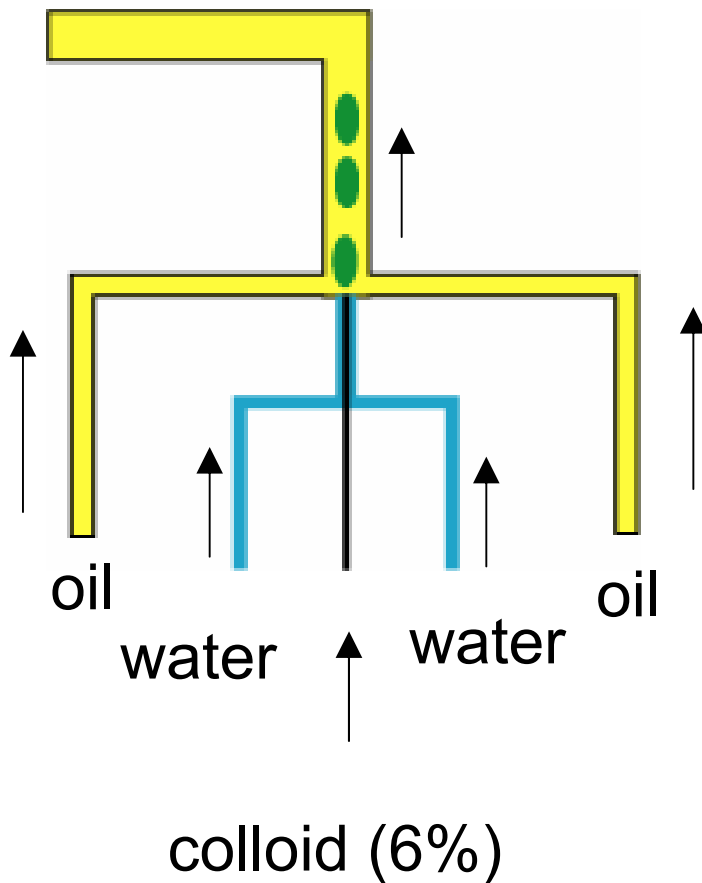
- reaction chambers



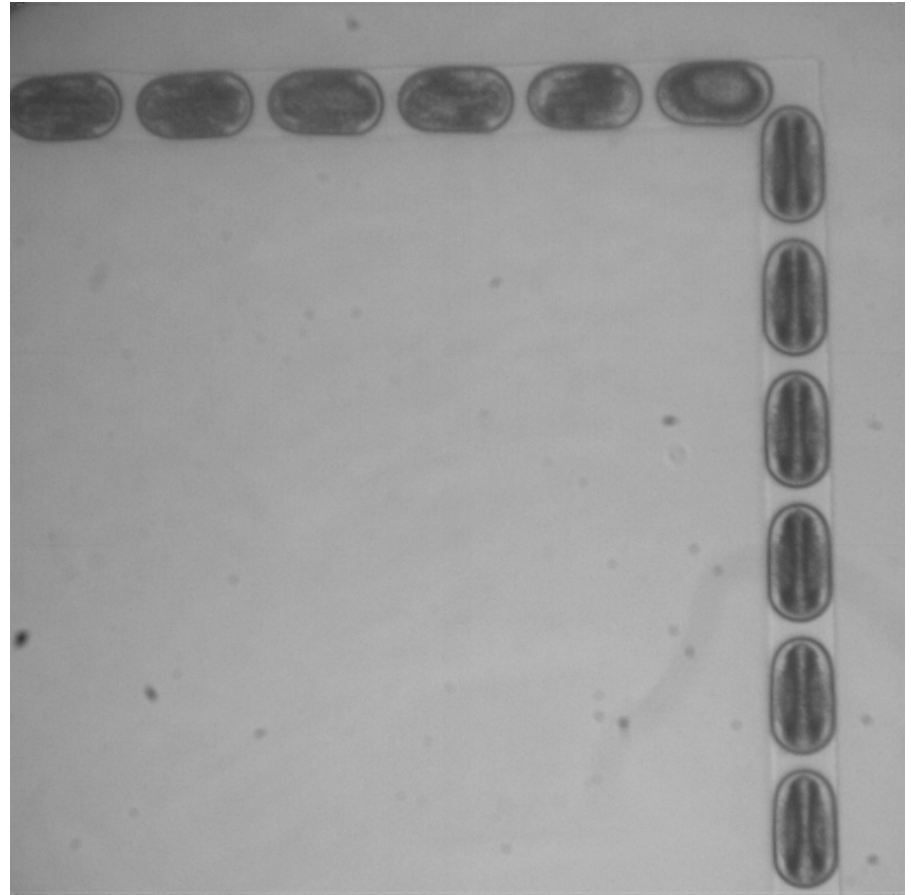
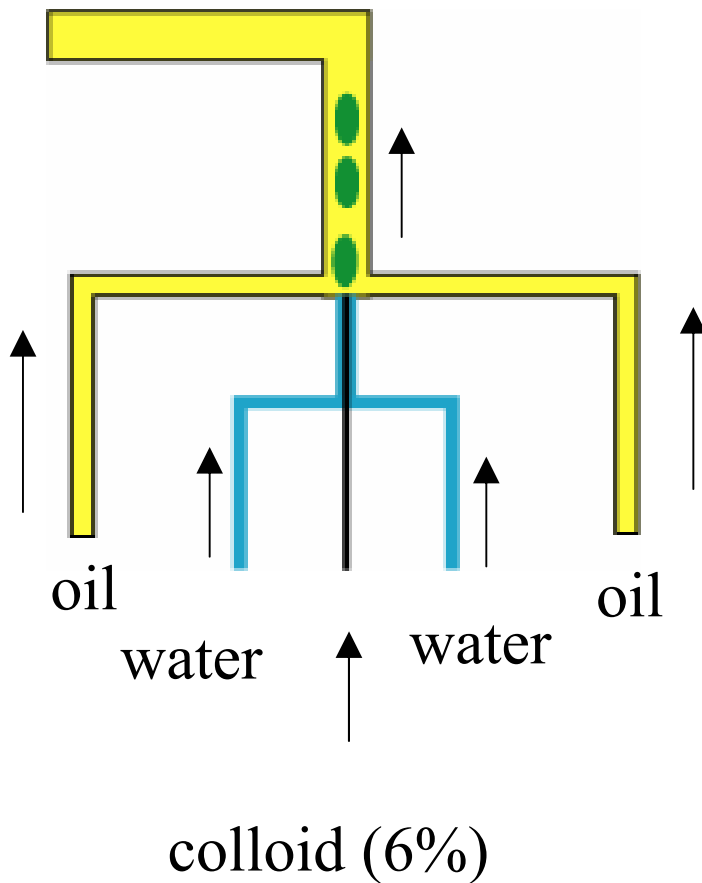
Distance = Time

H Song, JD Tice, and RF Ismagilov, *Angew. Chem. Int. Ed.* **42**, 768 (2003).

Emulsification with co-flow: micromixers and reactors

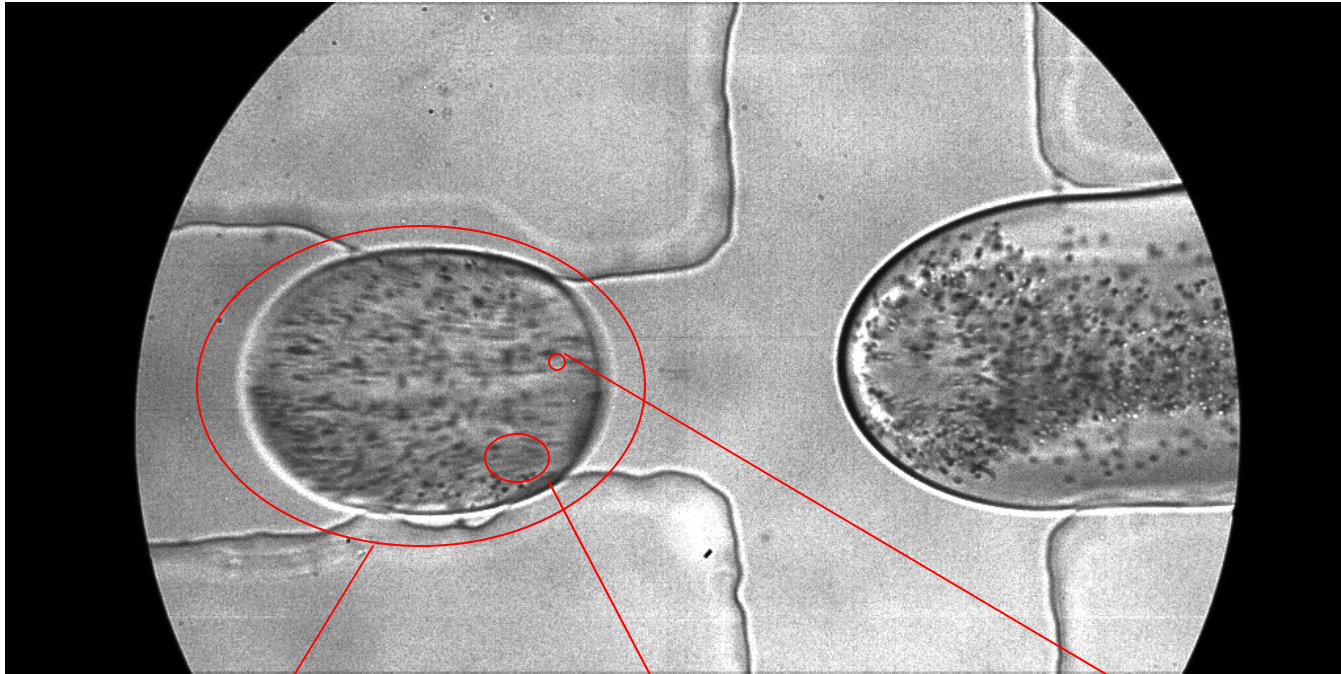


Emulsification with co-flow: micro-mixers and reactors



Drop formation

$$R_e = \frac{\text{momentum}}{\text{viscous force}} = \frac{\rho U a}{\eta}$$



Reynolds # drop in the channel

$a = 100 \mu\text{m}$

$\eta = 20 \text{ cp}$

$Re = 0.1$

Reynolds # volume element

$a = 100 \mu\text{m}$

$\eta = 1 \text{ cp}$

$Re = 2$

Reynolds # particle

$a = 1 \mu\text{m}$

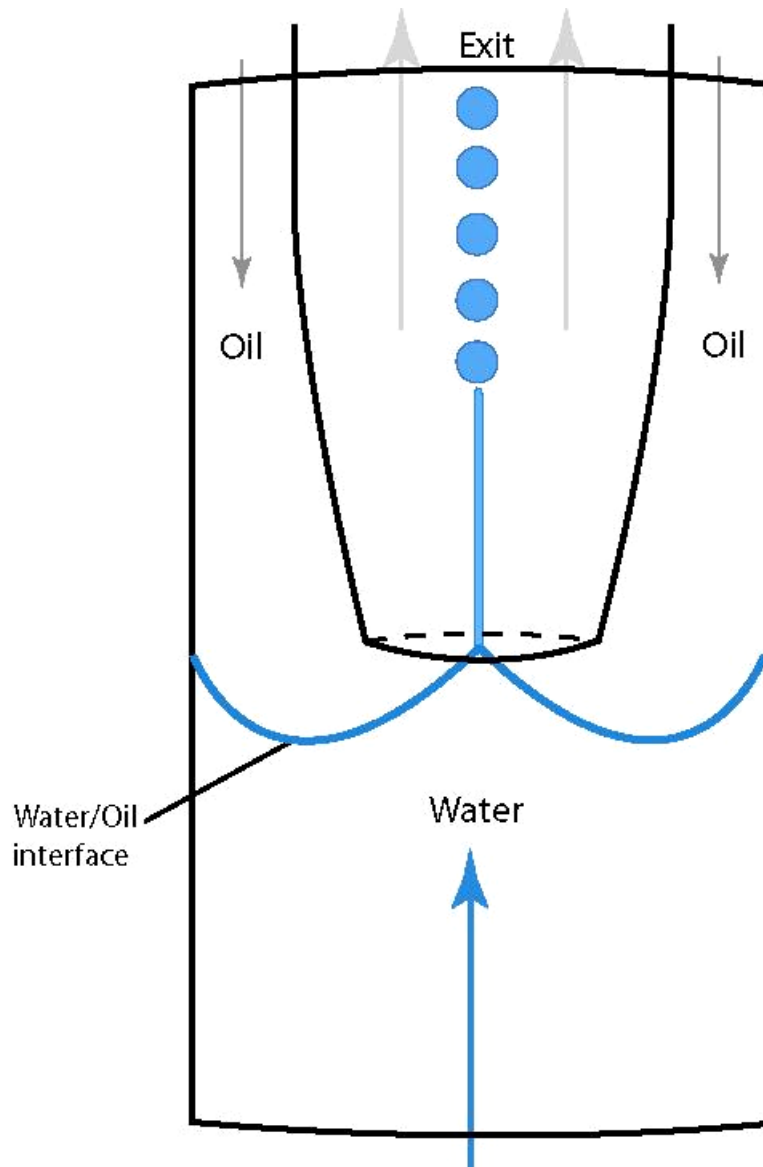
$\eta = 1 \text{ cp}$

$Re = 0.02$

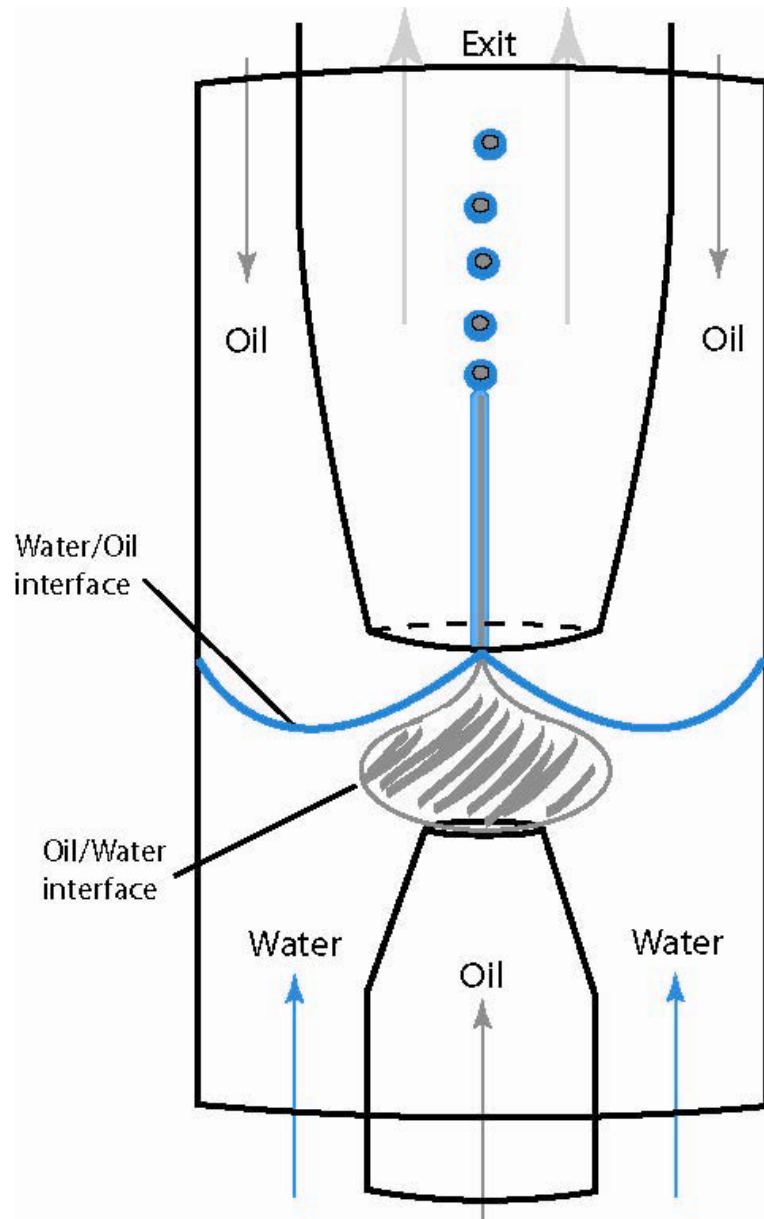
Microfluidics with Glass Tubes

- Fully flexible encapsulation demands 3D
- Wettability of PDMS is constraining
- Use glass tubes
- Three dimensional; water wet
- Maintain simplicity of soft lithography

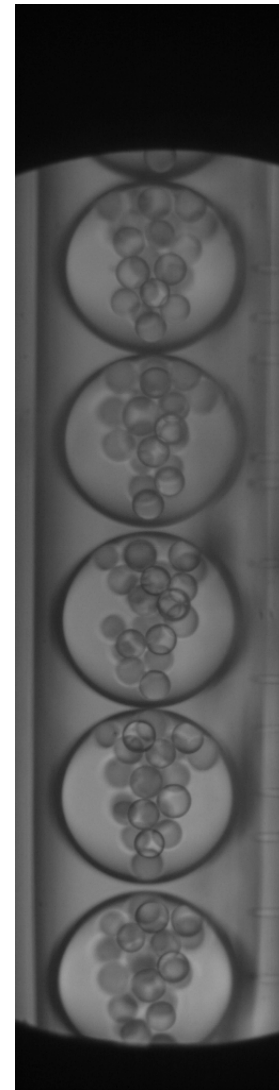
Opposing flow Emulsification



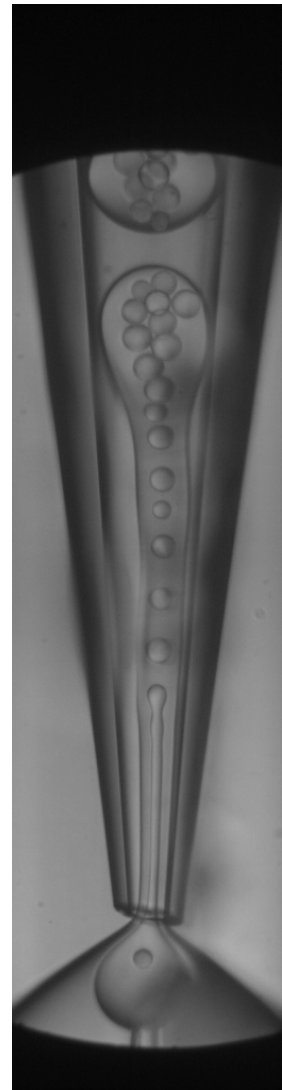
Controlled Multiple Emulsions



O/W/O

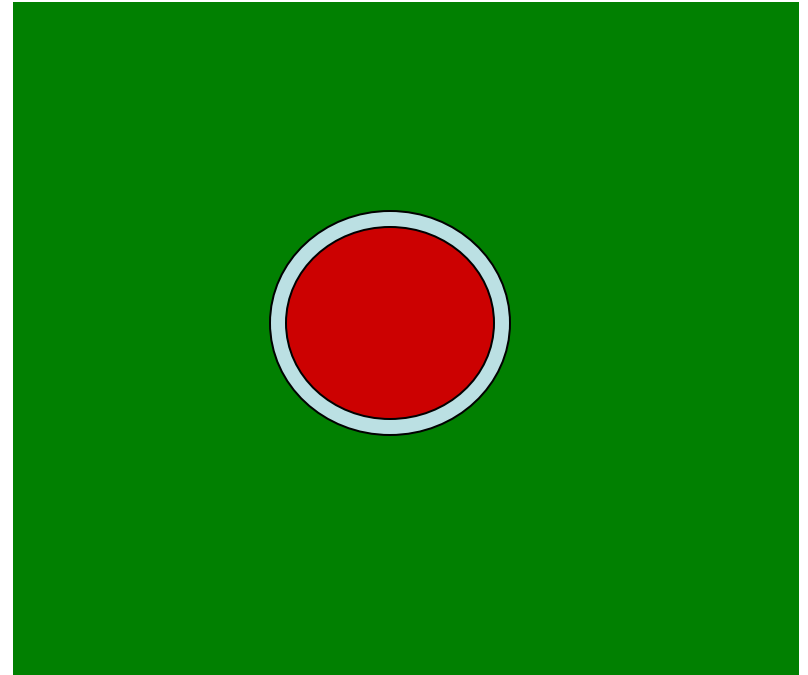
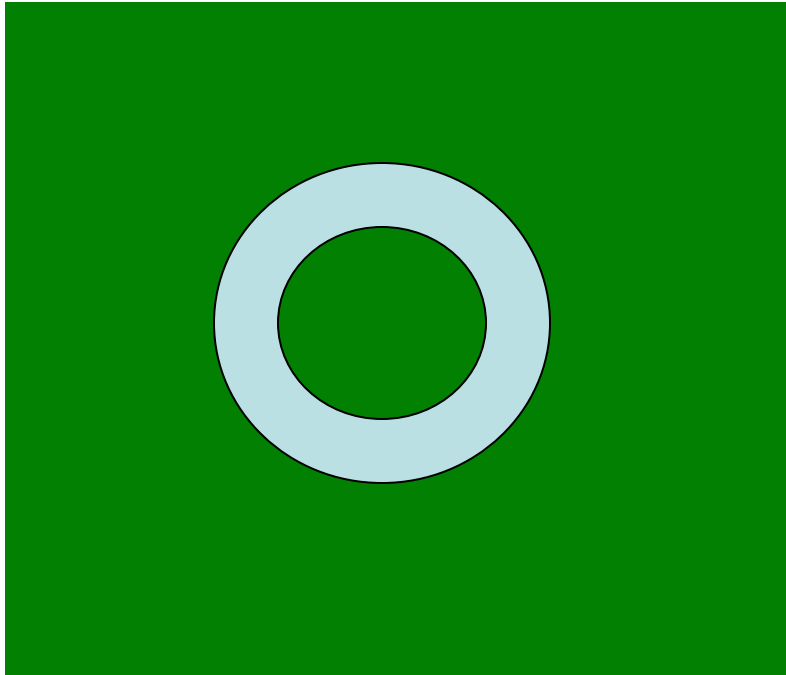


W/O/W



W/O/W

Controlled Encapsulants



Evaporate intermediate fluid
Vesicle for controlled encapsulation

Conclusions

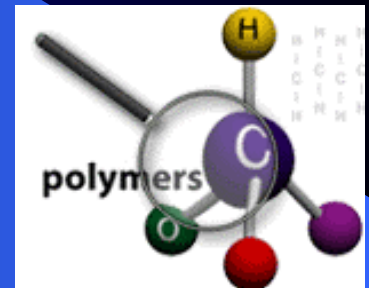
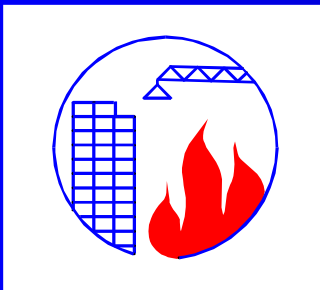
- Precision control of structured fluids
- Precision control of recombination
- Ideal for combinatorial techniques
- Control of structure
- Test concepts of structured fluid

Breakup of a Fluid Thread in a Confined Geometry

Jack F. Douglas, Polymers Division

Nicos S. Martys,
Materials and Construction Division

John G. Hagedorn, Mathematical and
Computational Sciences Division



Problem:

The breakup of fluid threads by capillary instability is ubiquitous in engineering, science and nature.

Ink-jet printing, coating optical fibers and wires with polymer films, late-stage liquid-liquid phase separation, ...

In many cases, thread breakup occurs under conditions of **geometrical confinement**.

Multiphase flows in synthetic and biological channels ranging in scale from oil pipelines to microfluidic devices-tertiary oil recovery, phase separation in films and porous media, stability of fibrous blend extrusion products, etc.

Study of thread breakup has a long history

First experimental reports

Savart (1833) , Magnus (1855)

Stability criterion / surface tension and shape

Plateau (1863)

First dynamical theory of breakup

Rayleigh (1879, 1892)

Viscosity mismatch of thread and surrounding fluid

Tomotika (1935)

**Full theory- viscosity mismatch, surface tension,
density and inertial effects**

Lee and Flumerfelt (1981)

Presence of surfactants and non-Newtonian fluids

Recent work by a variety of researchers

Observations of inhibited fluid thread breakup in confined geometries

D'Arcy Thompson, On Growth and Form (1917)

Emphasize effect on biological structures

Russel, Hodgson, Charles, Grover, *Canad. JChE* (1959)

Stable core annular oil-water flows / oil pipelines

Sung, Karim, Douglas and Han, *PRL* (1996)

Inhibition of capillary wave induced thread breakup in phase separating ultra-thin blend films

[Supression of capillary instability in $d = 2$ predicted by Miguel, Grant and Gunton, *PRA* (1985)]

Migler, *PRL* (2001); Hashimoto et al., *PRL* (1995)

String formation in blends under confinement and flow

Son, Martys, Hagedorn and Migler, *Macromol.* (2003)

Thread breakup under confinement between // plates

Influence of confinement on thread breakup-

Theoretical understanding

Geometrical confinement of an infinite Newtonian thread surrounded by another liquid in a coaxial pipe **does not provide stabilization against thread breakup under quiescent conditions.** Stabilization may occur **(Joseph et al.)** for a combination of confinement and flow conditions.

Lubrication theory calculations **(Hammond)** suggest a significant slowing down of the rate of thread breakup with confinement and numerical boundary integral calculations qualitatively support this prediction **(Newhouse and Pozrikidis).**

The present investigation focuses on the effect of confinement on the geometrical character and rate of the thread breakup instability using the Lattice Boltzmann model of multiphase fluid dynamics.

Advantages

Treat variable degree of fluid immiscibility (e.g. diffuse liquid-liquid interfaces) and polymer-surface interactions effects associated with compositional enrichment.

More easily treat singular dynamics of interfacial rupture and subsequent evolution of ruptured droplets.

Lattice-Boltzmann Model (Shan-Chen version)

Model is *coarse grained* description of liquid mixture

Considers evolution of *particle velocity distribution* $\mathbf{n}_a^i(\mathbf{x},t)$ of each component at each lattice position as a function of time, t . (D3Q19 model)

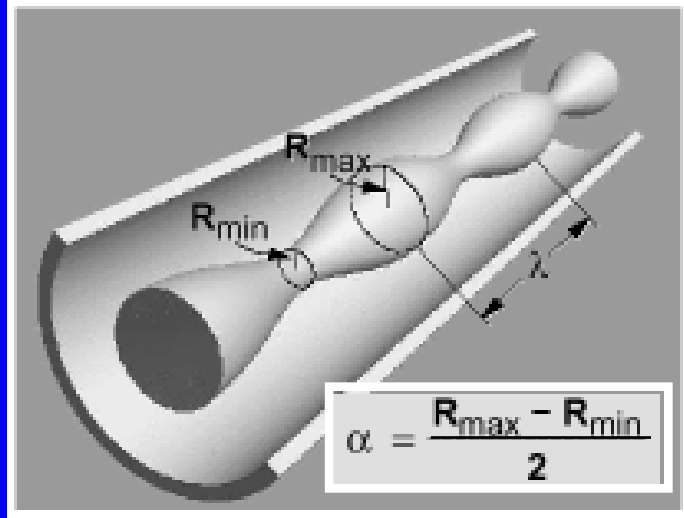
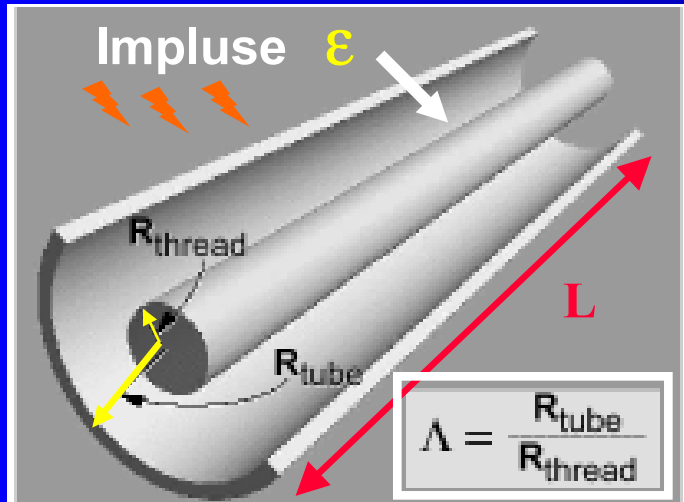
Collision operator $\Omega_a^i(\mathbf{x},t)$ describes the change of $\mathbf{n}_a^i(\mathbf{x},t)$ from its equilibrium value in the course of the fluid evolution.

Composition, velocities, temperature T and other properties are defined in terms of averages of $\mathbf{n}_a^i(\mathbf{x},t)$.

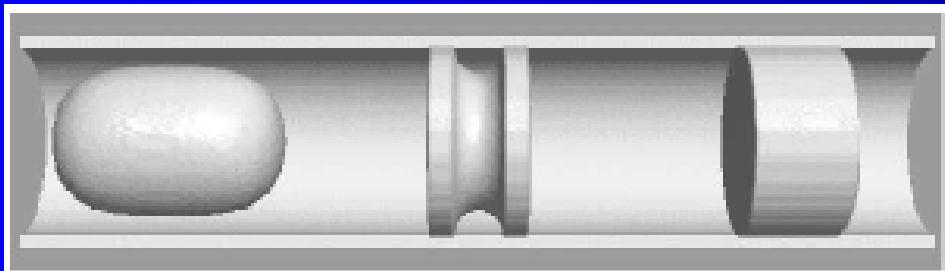
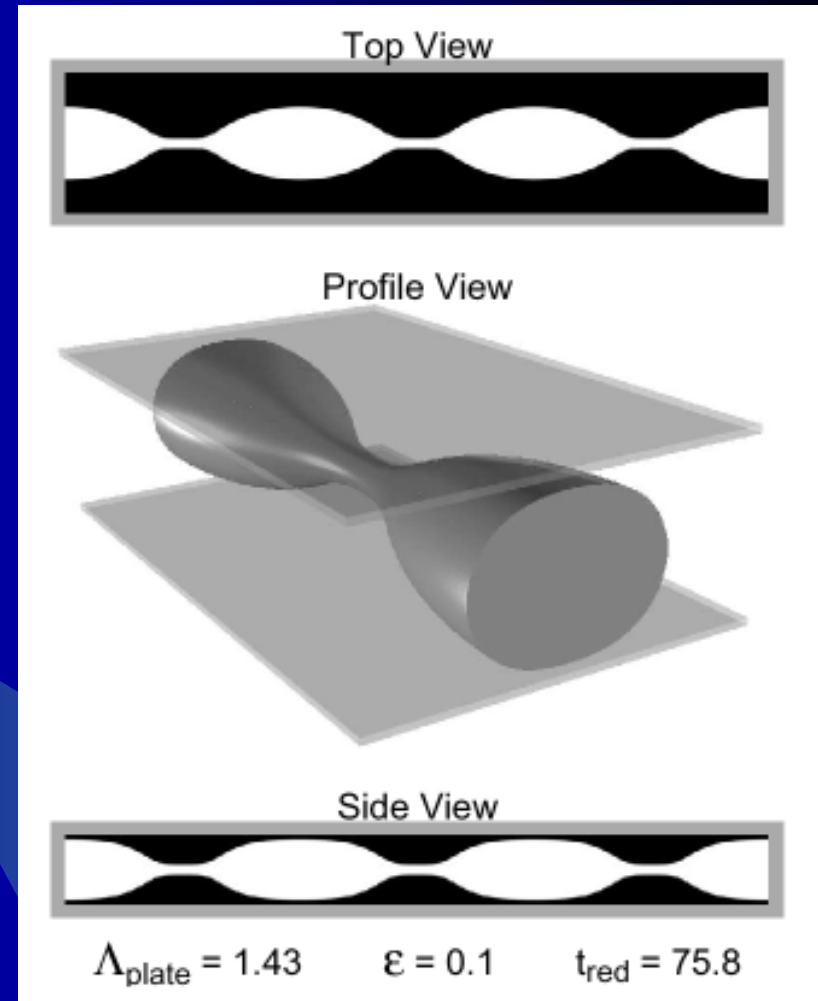
Interaction parameter G between components (Shan and Chen; 1992) added to cause phase separation upon cooling. Systematic study of the equilibrium fluid properties of this LB model (phase boundary, correlation length, surface tension) indicates *mean-field critical behavior*.

Martys and Douglas, *PRE* (1996)

Basic Geometrical Parameters



Long Threads
 $L \sim O(10 L_{\text{PR}})$

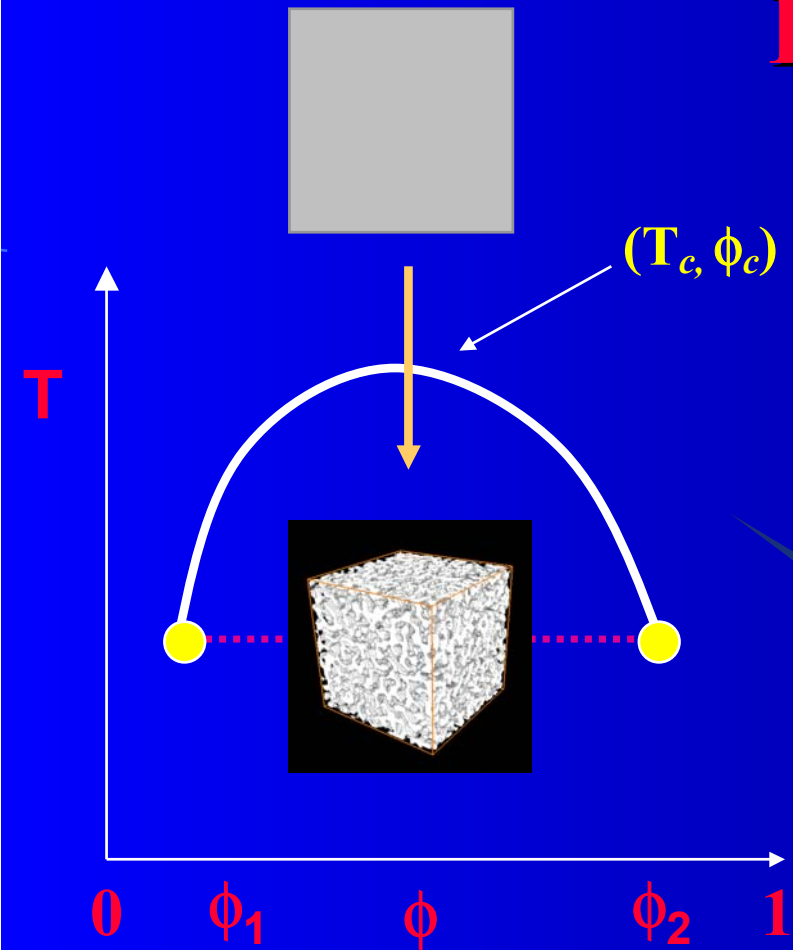


Newtonian fluids- confinement
 in tubes and between plates

Interactions

'Miscibility'

Phase separation occurs in the model upon cooling for a fixed value of G or for a critical value G_c at fixed T . Comparison to measurement is facilitated by expressing G and T in terms of a reduced variable τ_G that ranges between 0 and 1 in the two-phase region.



$$\tau_G \leftrightarrow |T - T_c| / T_c$$

$$\tau_G = 0.329, \phi_1 = 0.002, \phi_2 = 0.998$$

Martys and Douglas, *PRE* 63 031205 (2001)

Surface Interaction

contact angle

G_s



'stick' BC

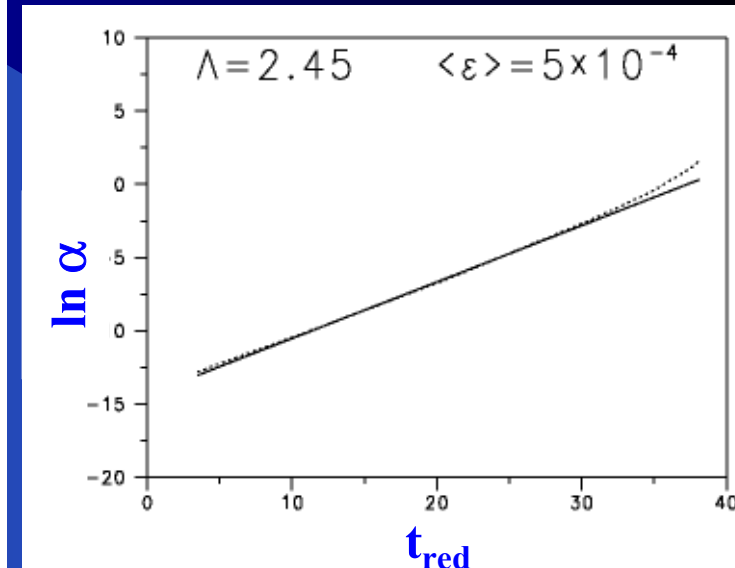
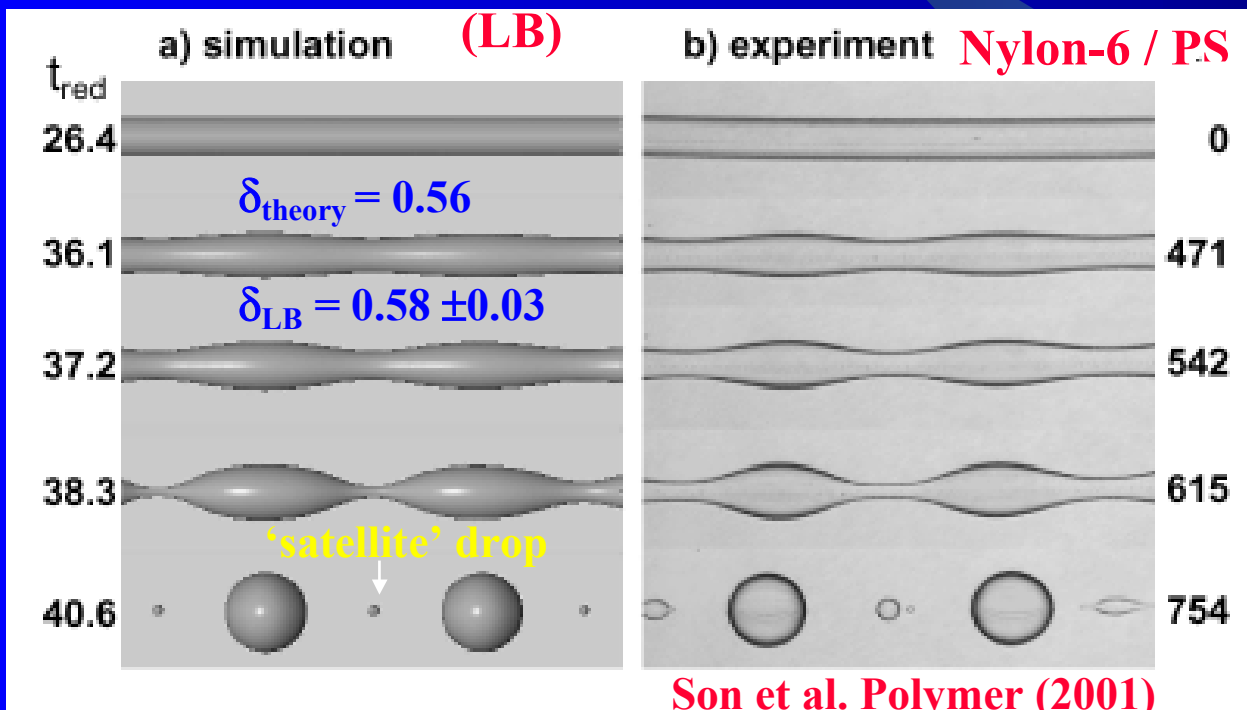
Thread Breakup in Bulk

Amplitude $\alpha(t)$ of a perturbation of the thread boundary

$$\alpha(t) = \alpha(0) \exp(q t), \quad t \rightarrow 0^+, \quad q_\infty = \sigma \Phi(\lambda_{\max}) / 2 \eta_m R_{\text{thread}}$$

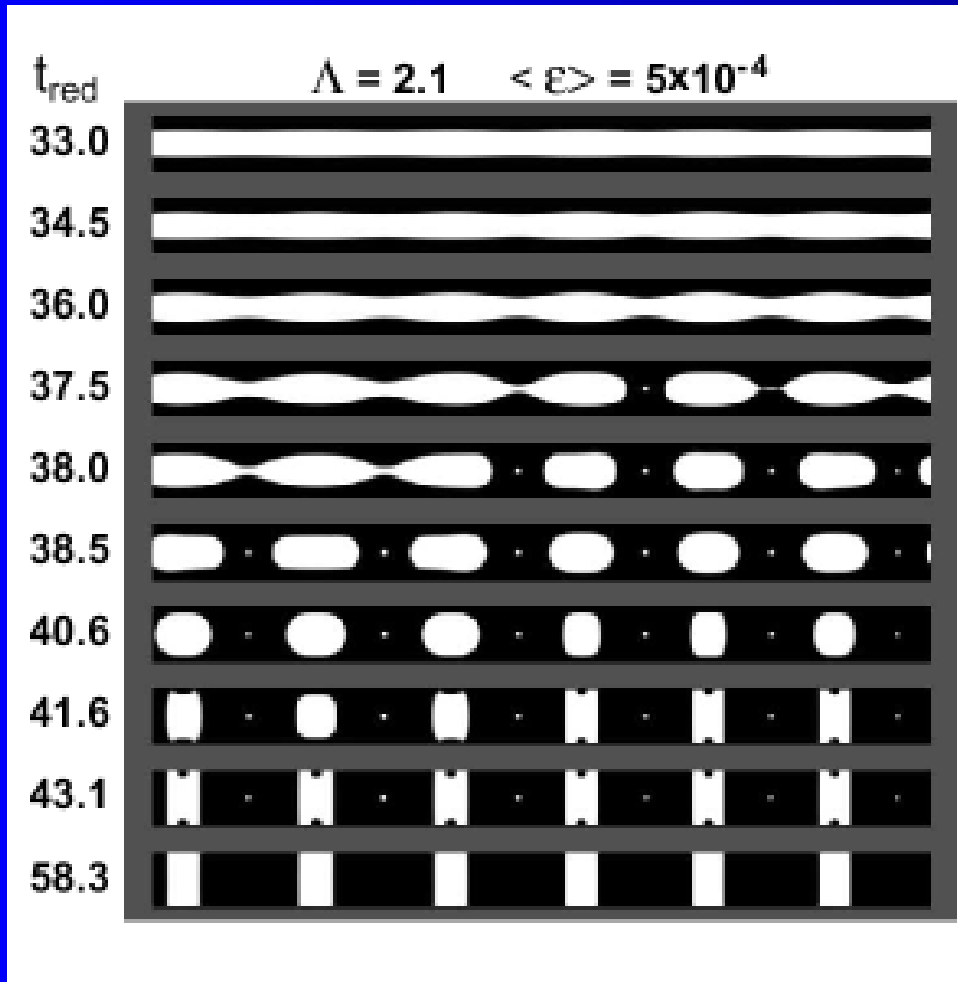
Growth rate q_∞ depends on the interfacial tension σ , shear viscosity η_m of the 'matrix' fluid, viscosity of the thread η_o .

$$\lambda_{\max} = 2 \pi R_{\text{thread}} / \delta, \quad \Phi(\lambda_{\max}, \eta_m / \eta_o = 1) = 0.0714, \quad t_{\text{red}} \equiv q_\infty t$$

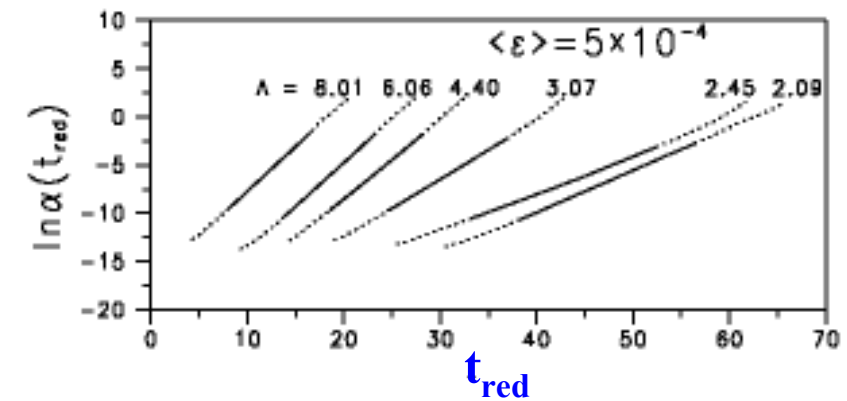


Confinement Effect on Thread Breakup

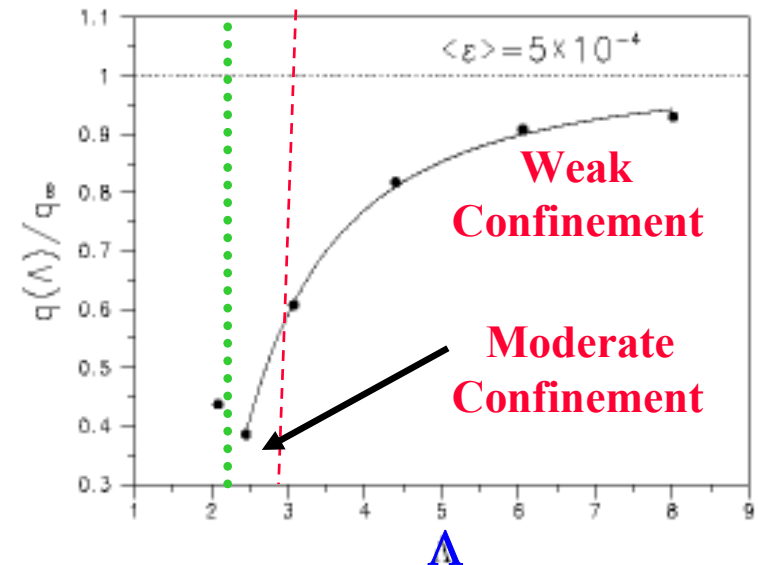
Weak and Moderate Confinement



Significant finite size effect!



$$q(\Lambda)/q_{\infty} \approx 1 - (3.680) \Lambda^{-2}$$

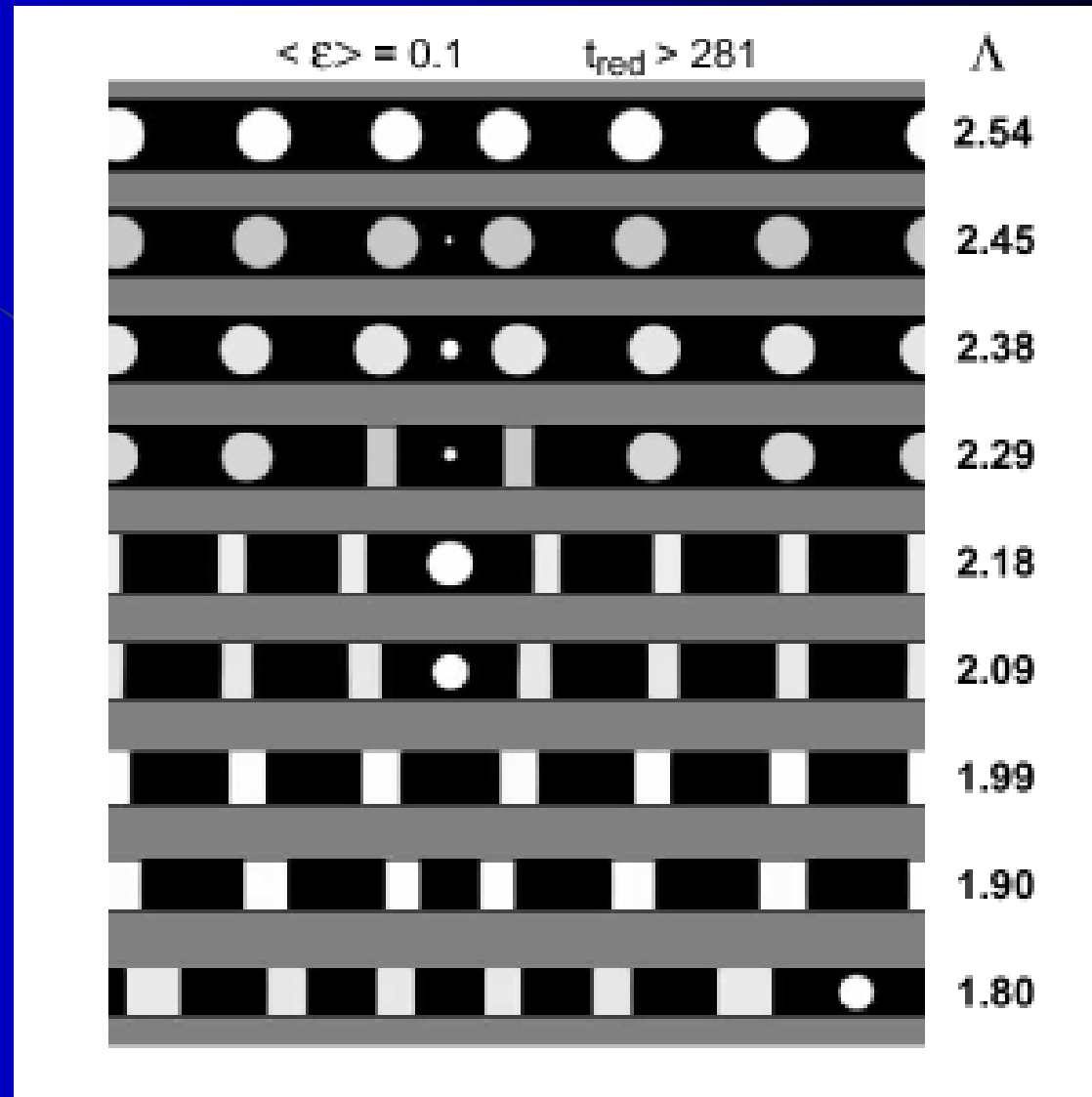


Confinement Effect on Thread Breakup

Weak Confinement- Droplet-Plug Transition

$$\Lambda_c \approx 2 + \varepsilon$$

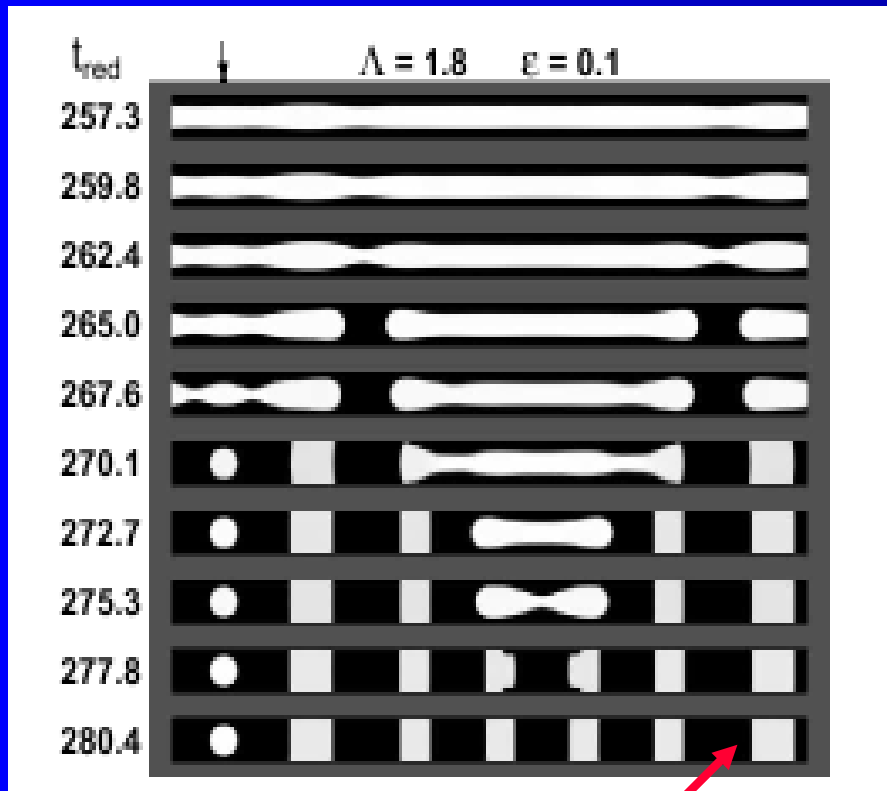
Volume Conservation



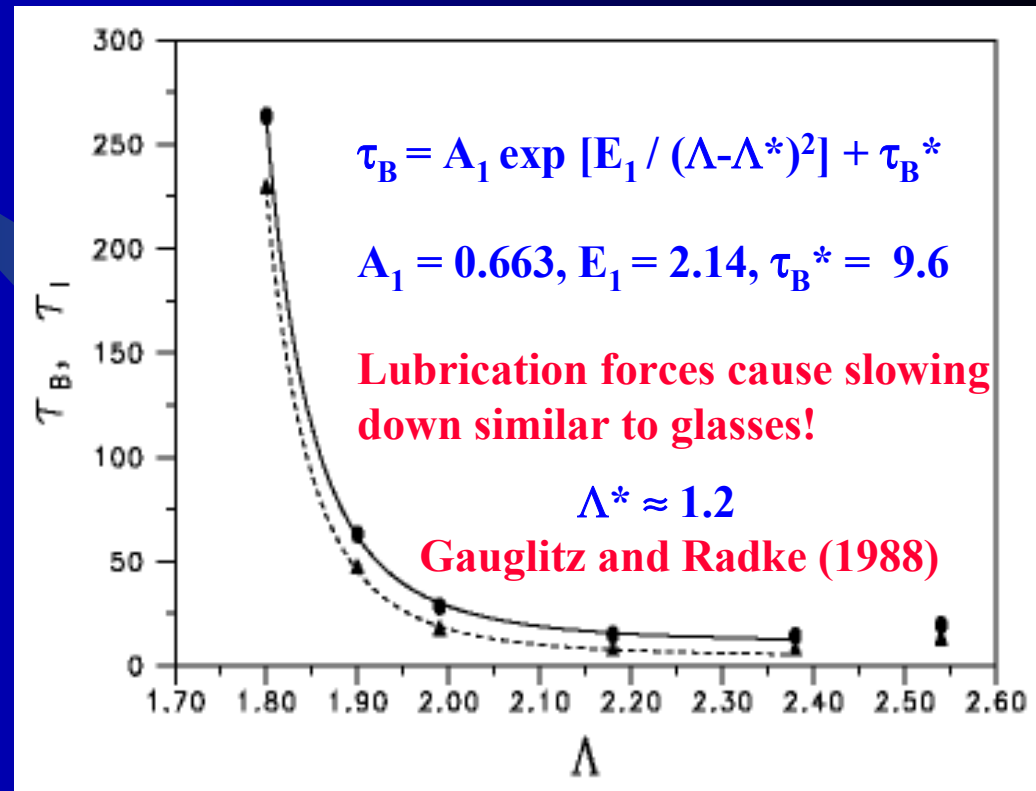
Confinement Effect on Thread Breakup

Strong Confinement

End-pinch Instability- 'kinetic stabilization'

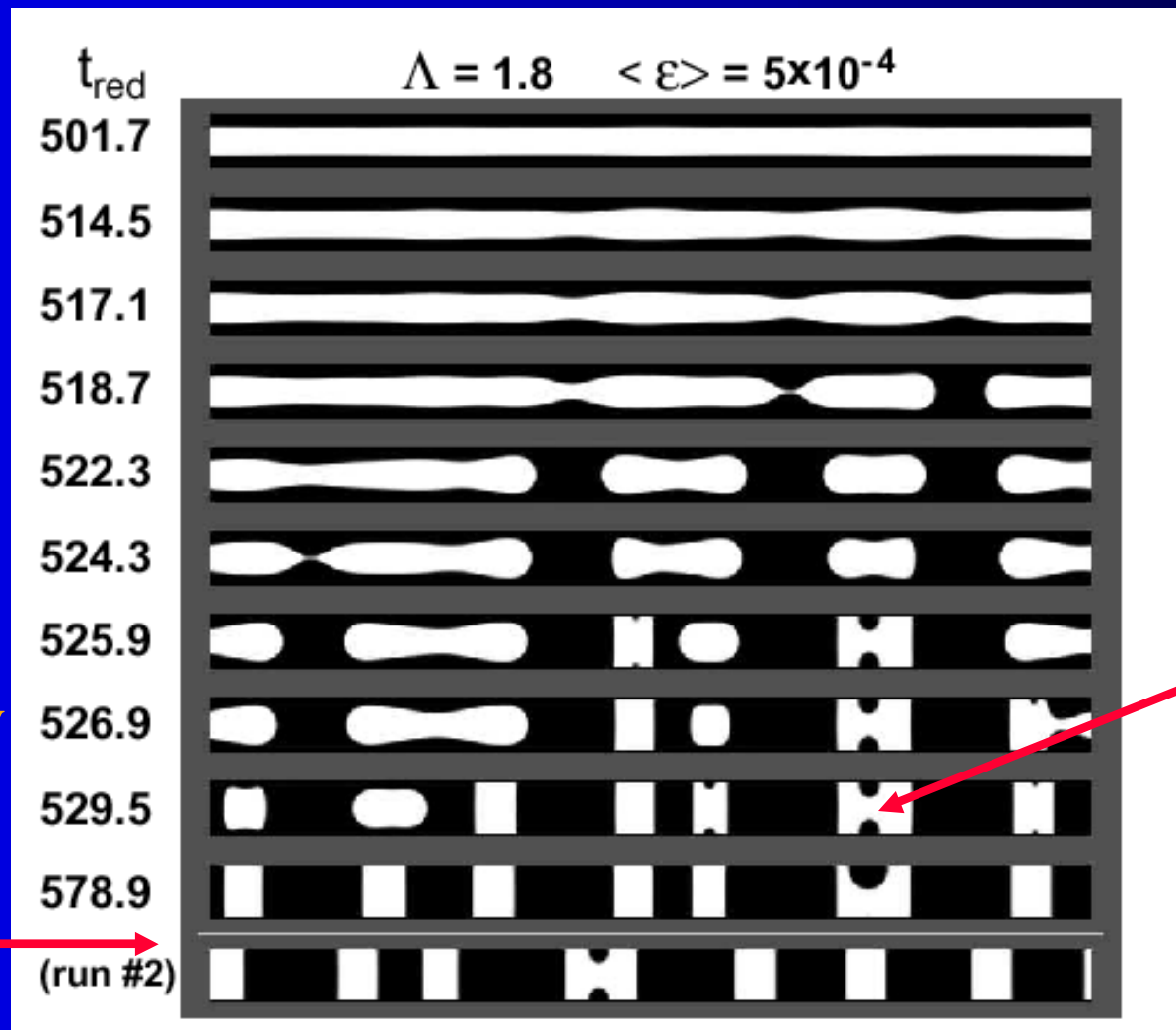


Jammin effect



Confinement Effect on Thread Breakup

Strong sensitivity to noise

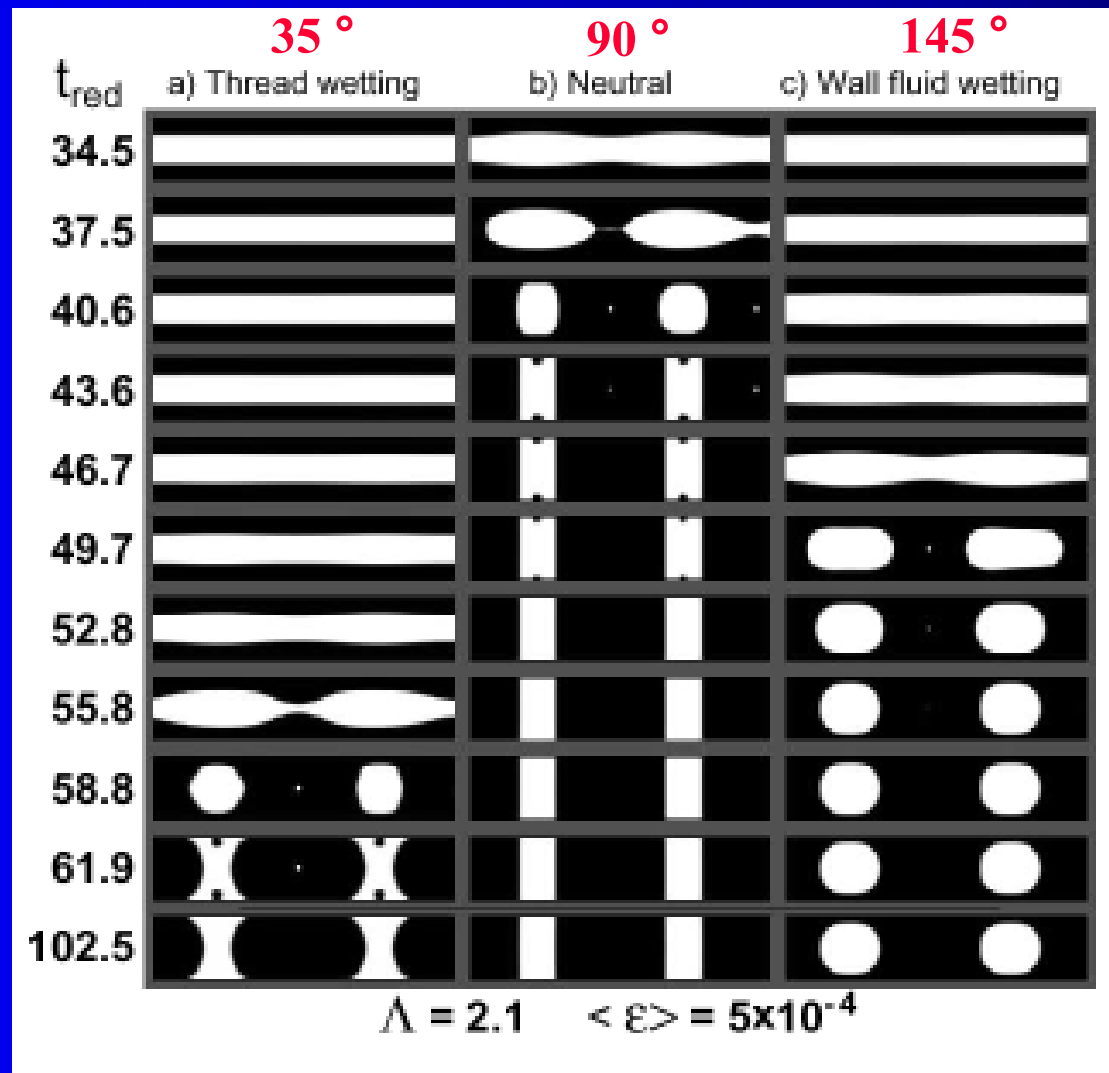


Final
Morphology
Dependent
On Run

Breakup of
plug collar

Confinement Effect on Thread Breakup

Effect of Surface Interaction- Strong Effect!

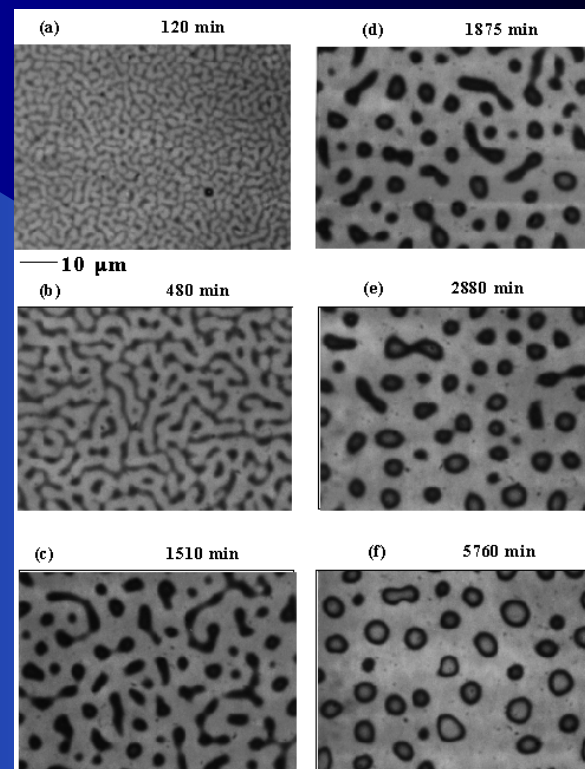
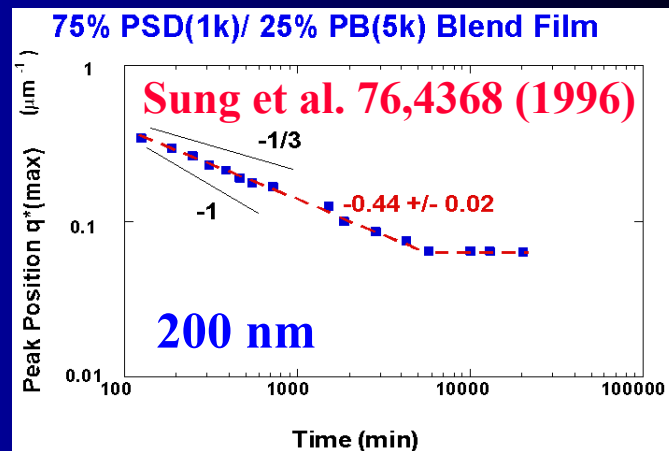
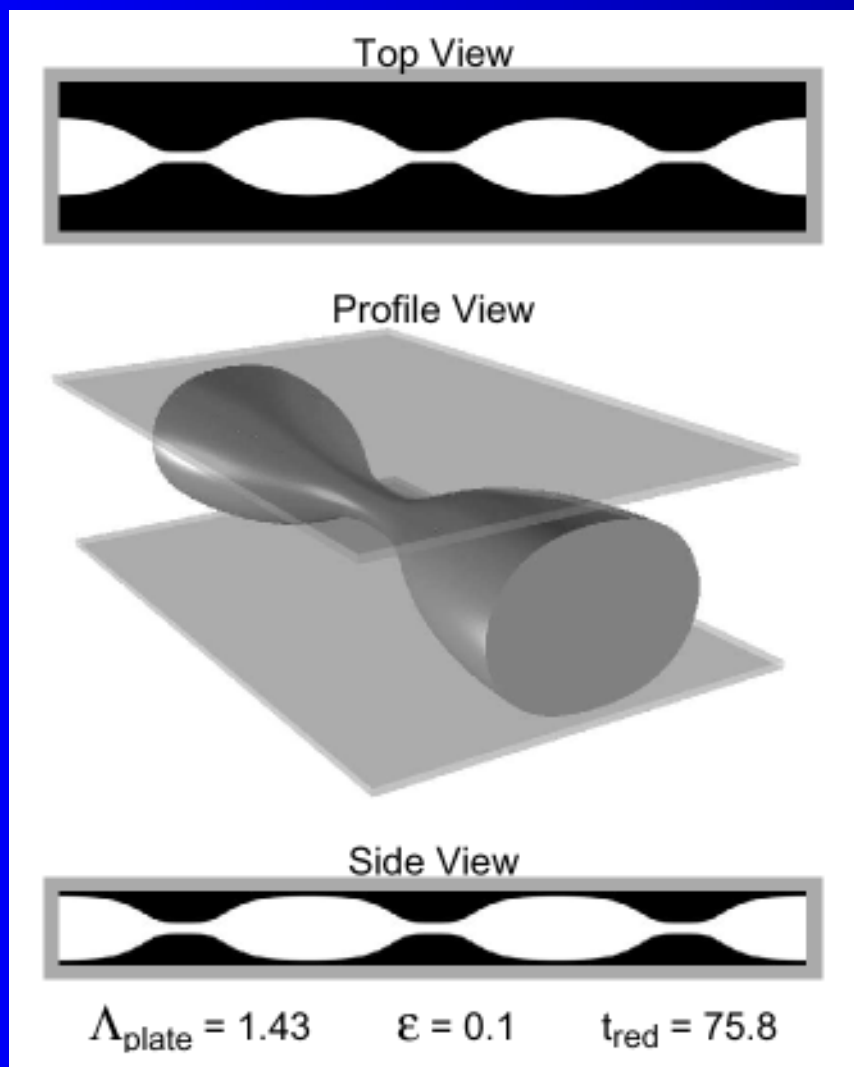


Dreyfus et al. *PRL*
144505 (2003)

Confinement Effect on Thread Breakup

Confinement between parallel plates

More confinement required to achieve a similar effect.

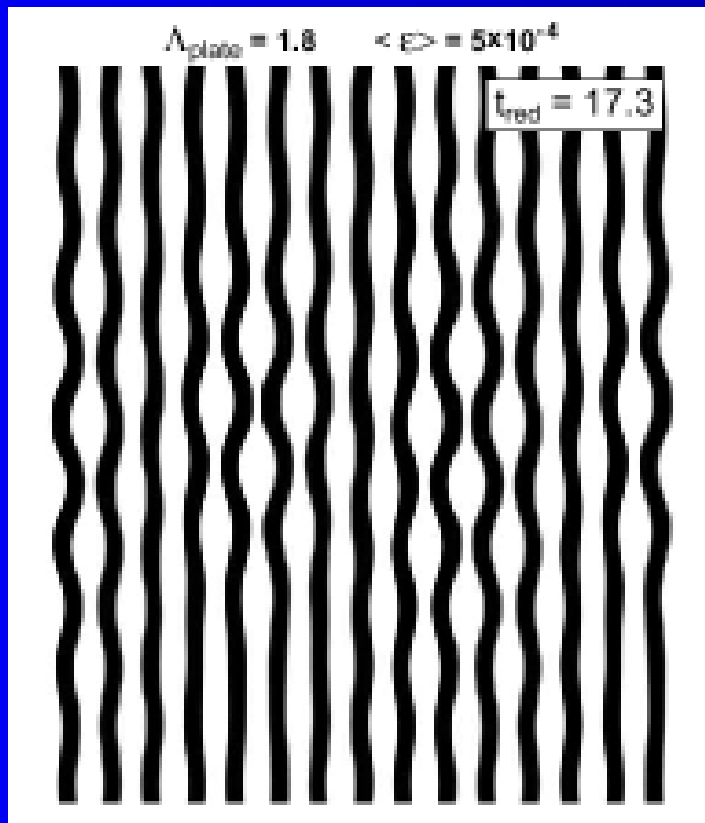


See Son et al. (*Macromolecules*, 2003)

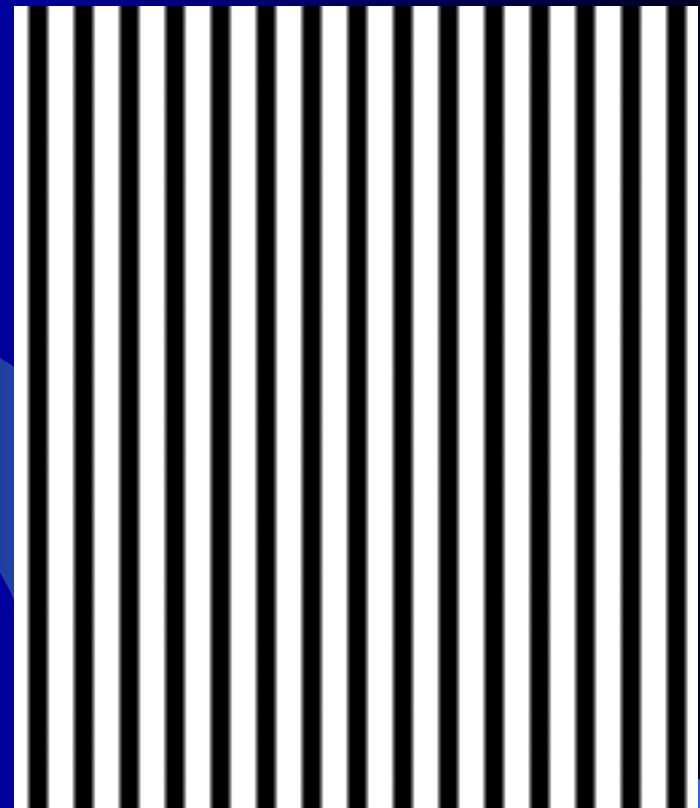
Confinement Effect on Thread Breakup

Multiple Confined Threads-Essential Aspects

Phase Locking Phase



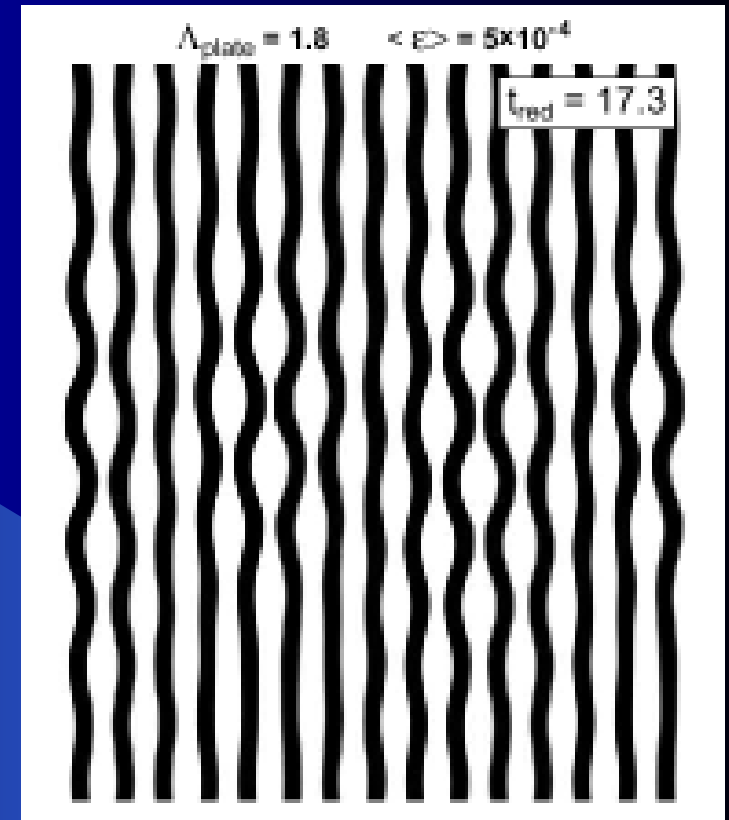
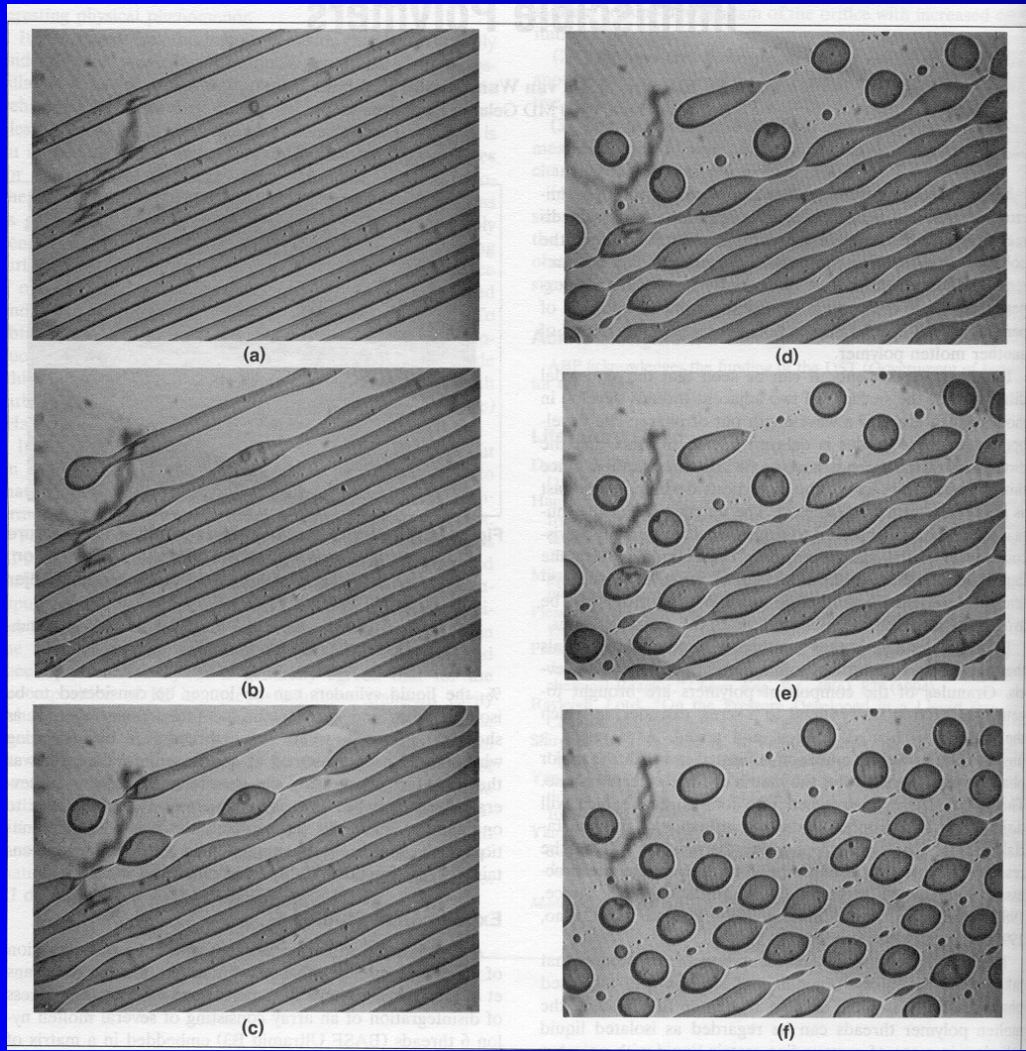
Collective Thread Breakup



Spacing = $1.7 R_{thread}$

Confinement Effect on Thread Breakup

Multiple Confined Threads- Expt vs. LB



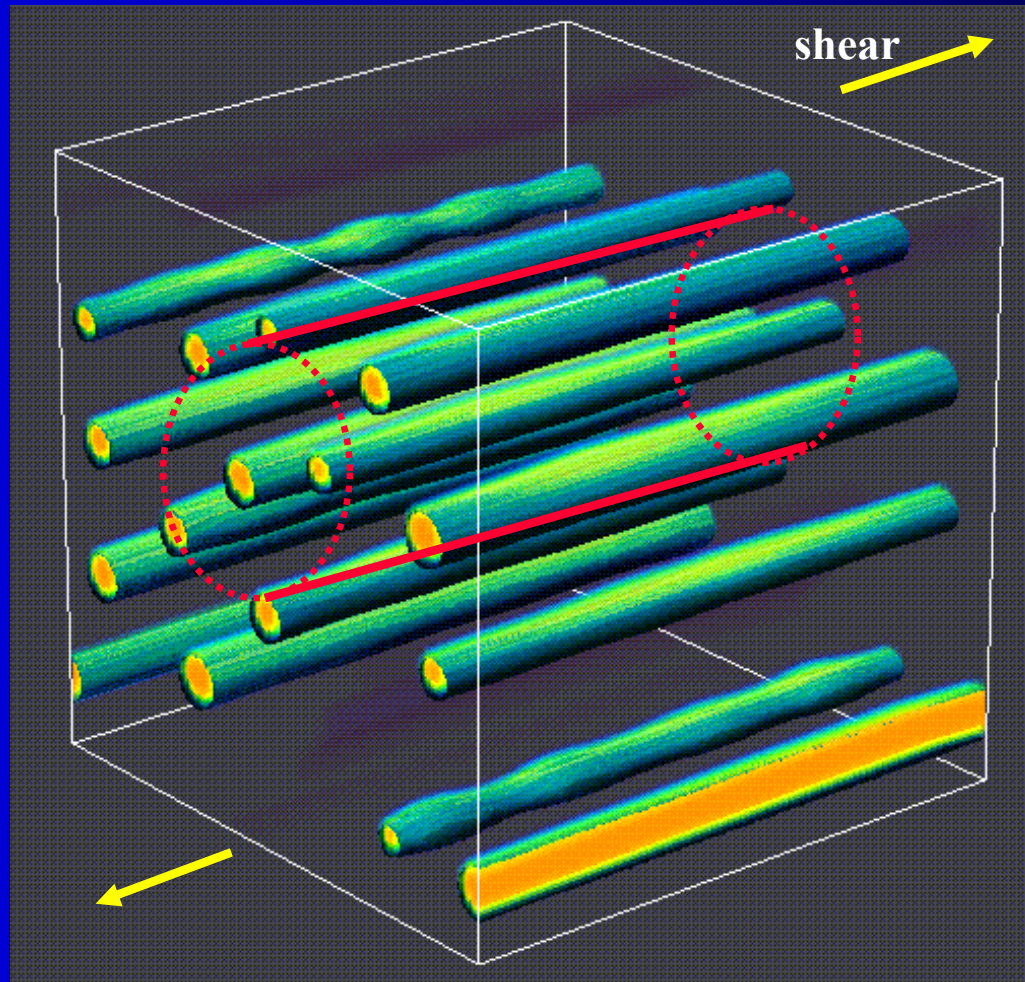
Nylon-6 / PS matrix

Elemans, Wunnik and van Dam, *AIChE J* 43 1649 (1997)

Confinement Effect on Thread Breakup

Multiple Interacting Threads- 'String Phase'

- Qualitative understanding into thread 'stability'



Flexible Boundaries

Martys and Douglas, *PRE* 63 031205 (2001)

Conclusions

- We observe a slowing down of the rate of thread breakup (**'kinetic stabilization'**) over a wide range of the confinement, $\Lambda = R_{\text{tube}} / R_{\text{thread}} \leq 10$ and find that the surface energies of the liquid components influence this effect. Tube and plate cases are basically similar.
- For moderate confinement, there is a **transition** in the late-stage morphology between 'capsules' (distorted droplets) and tube 'plugs'.
- Under strong confinement, thread breakup occurs through the propagation of a wave-like disturbance (**'end-pinch instability'**) initiating from the thread rupture point.
- Collective effects (**phase locking, out of phase undulations**) prevalent in multiple interacting thread breakup.

Ramifications for Microfluidics

- Rate of thread breakup and droplet retraction processes can be substantially influenced by finite size effects-

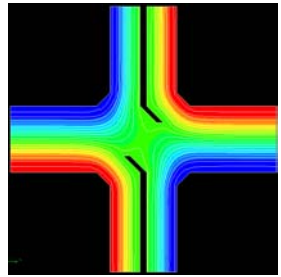
Limits scale of miniaturization

- Noise effects become more prevalent with confinement- Properties and breakup evolution become statistically defined
- Fluids tend to get 'stuck' through the formation of 'plugs' in tubes and 'ribbons' between plates

'Jammin Effect'

- Wall effects can have a large effect on the dynamics of thread breakup –

Influence of imperfect immiscibility



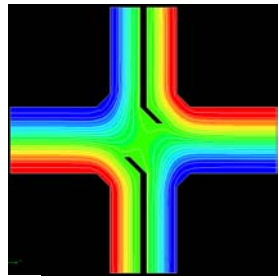
Pressure-driven 4-roll mill analog

A tool to measure interfacial properties

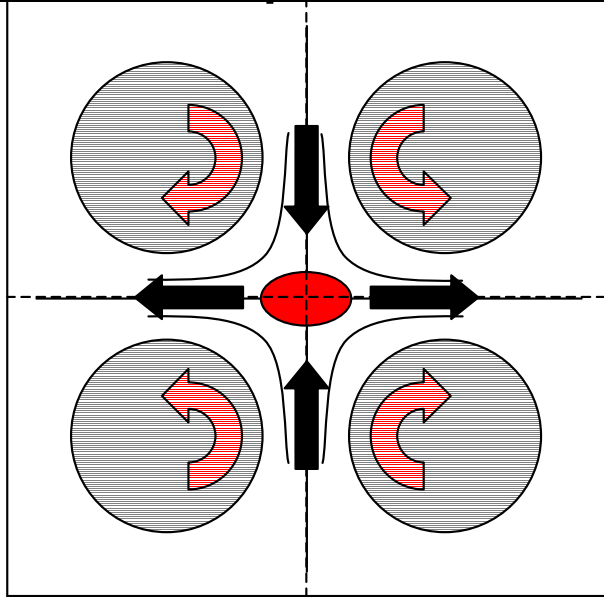
Steve Hudson, Fred Phelan, João Cabral
NIST, Polymers Division



Measure flow-induced properties



Macroscopic 4-roll mill



- Stagnation point.
- Adjustable flow type ξ : rotational, mixed and extensional flow. Pure shear is impossible.

Applications

Measure flow-induced ...

- molecular orientation
- particle dispersion and alignment nanotubes
- self-assembly and alignment
- drop deformation
- coalescence.

For example:

ξ affects the sharpness of the coil-stretch transition:

Babcock et al., Macromolecules (2003)

and earlier work by Leal et al.

$$\text{molecular extension} = f(\sqrt{\xi} Wi)$$

Flow type ξ and rate G :

$$\xi = \frac{|\lambda| - |W|}{|\lambda| + |W|} \quad G = |\lambda| + |W|$$

λ and W are the principal eigenvalues of the stretching and rotation tensors.

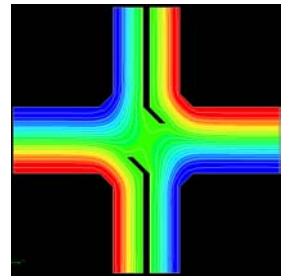
Extension: $\xi = 1$

Shear: $\xi = 0$

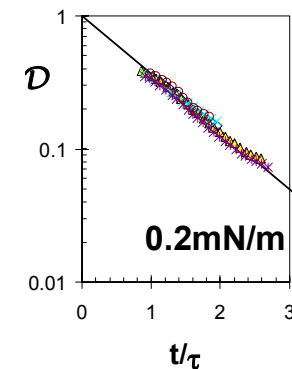
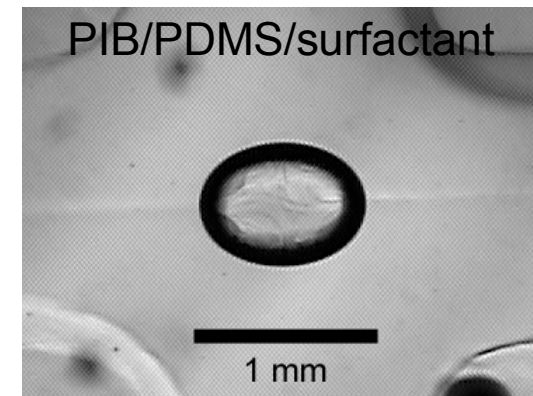
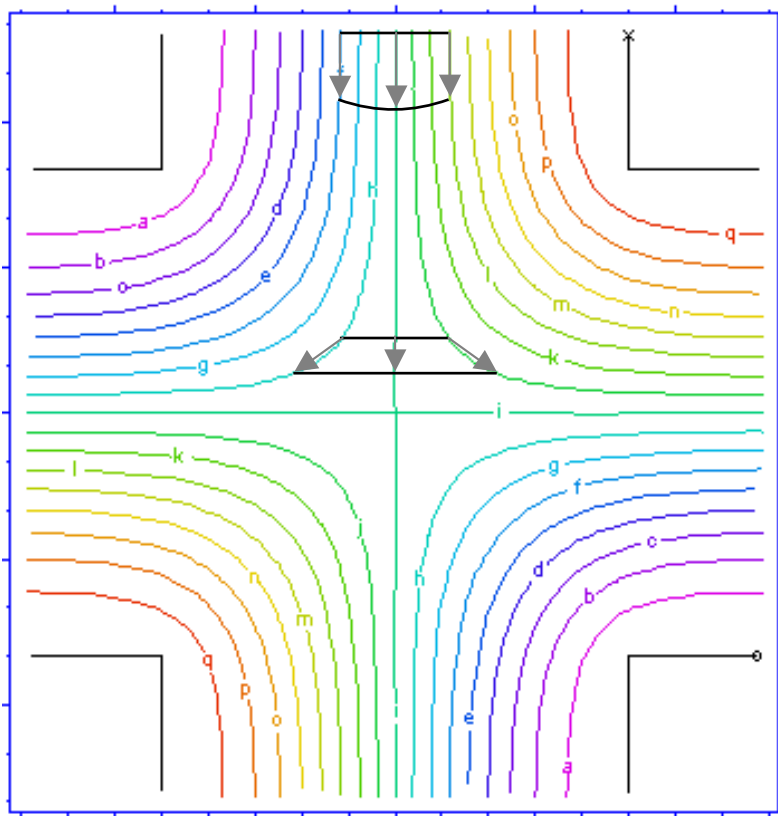
Rotation: $\xi = -1$



Using pressure-driven flow to stretch: Opposing jets

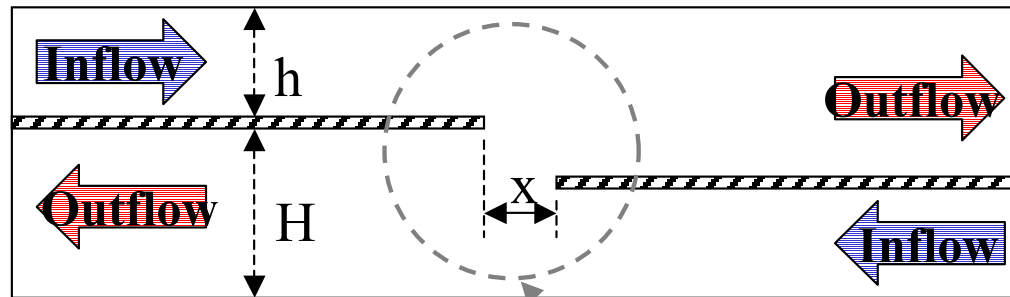
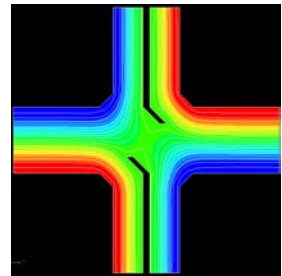


- Flow is “linear” near the stagnation point.
- Extensional flow stretches drops.

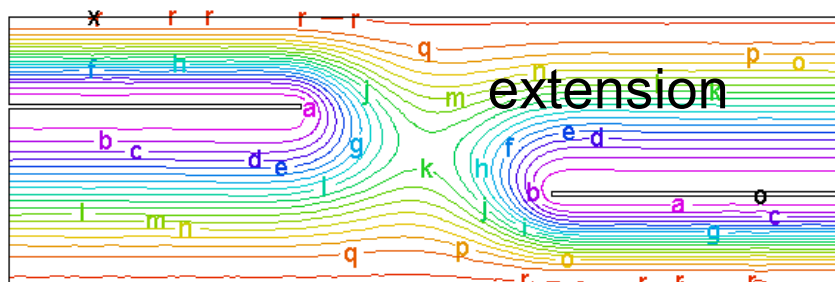




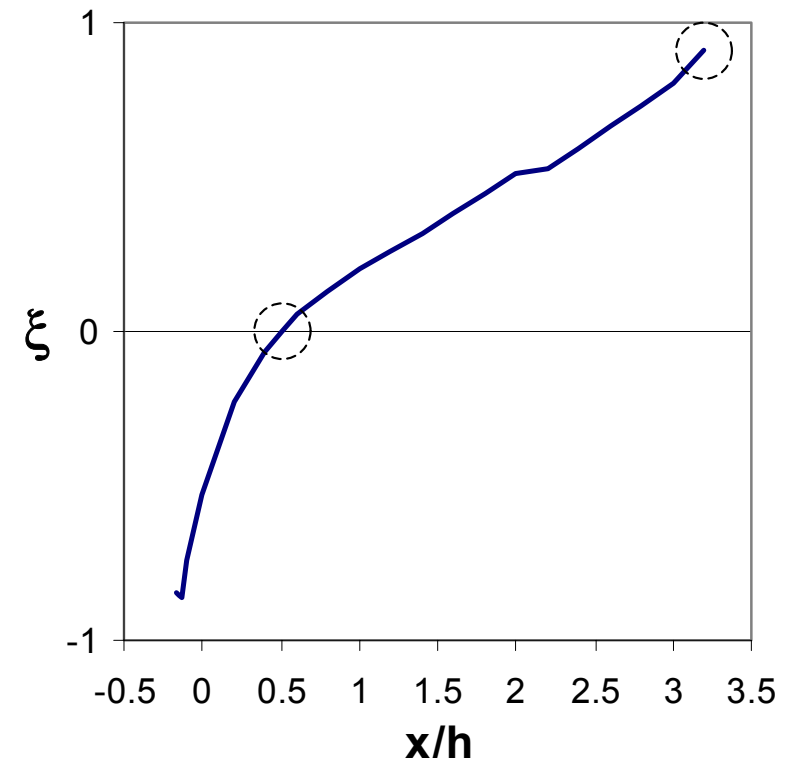
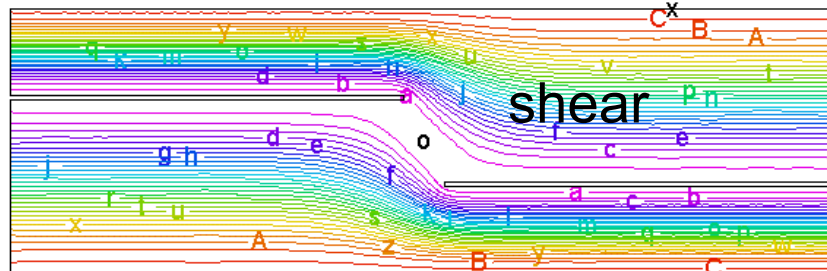
Using pressure-driven flow to rotate: Offset jets



Stagnation Region



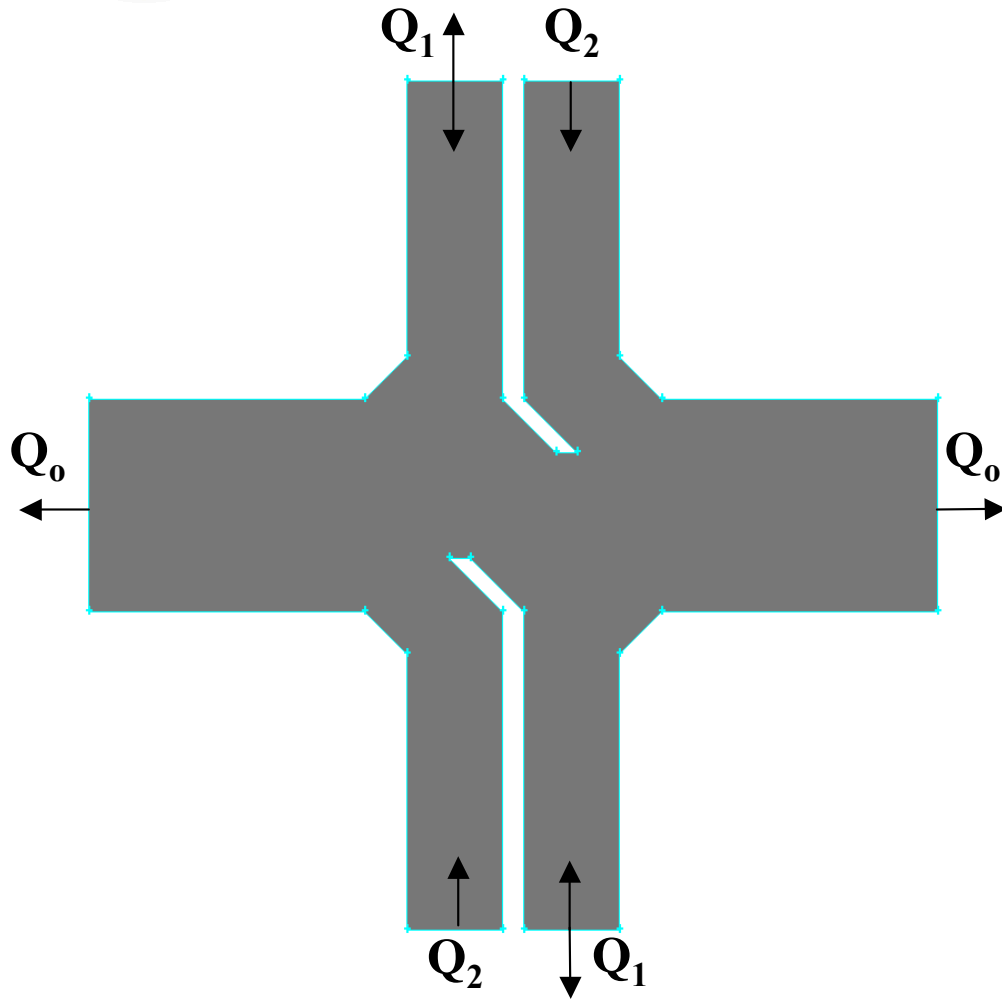
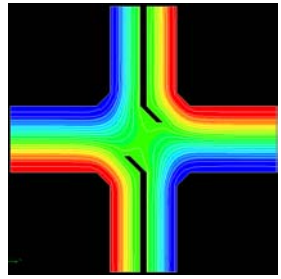
$H/h = 2$



- Flow type depends on fin placement.



Combined Geometry

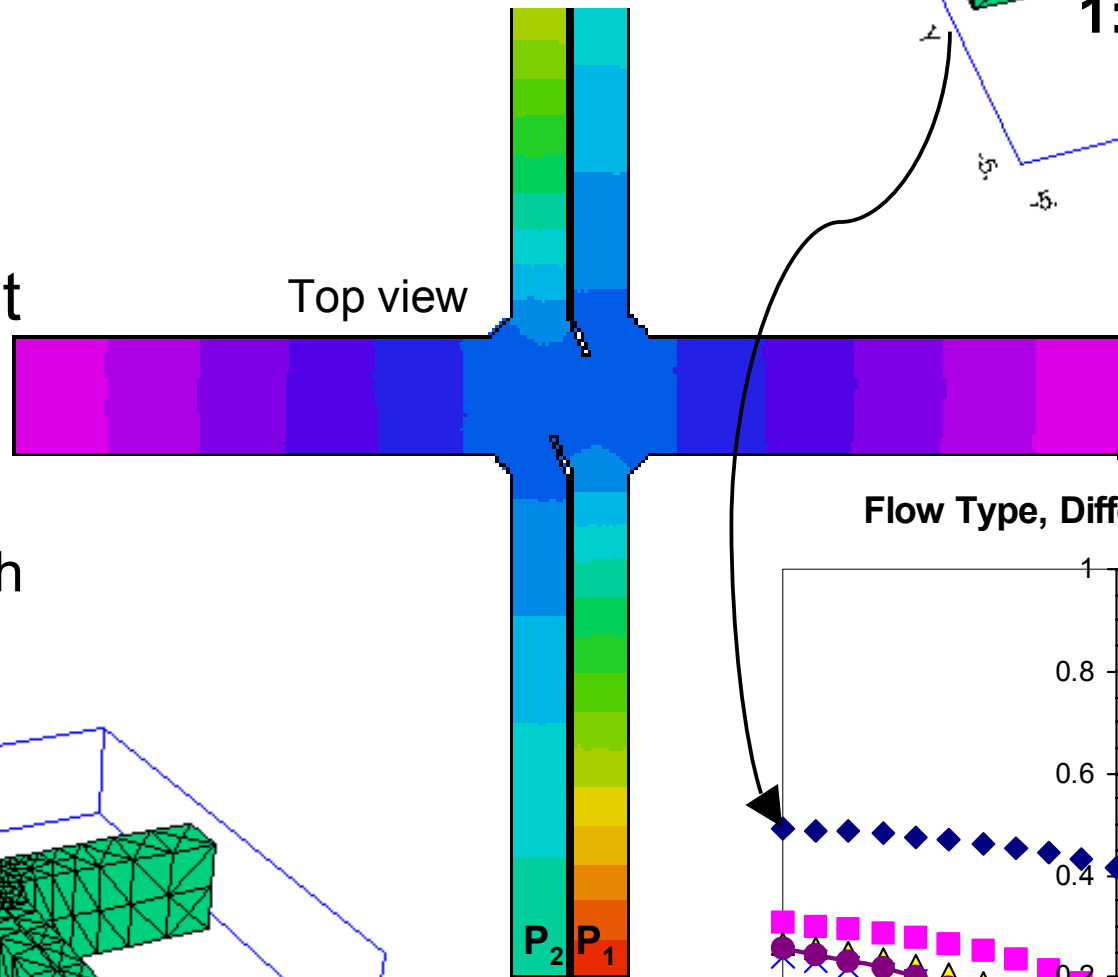


- Flow type controlled by Q_1/Q_2
- As before, the range of flow type accessible depends on placement of the flow divider fins.

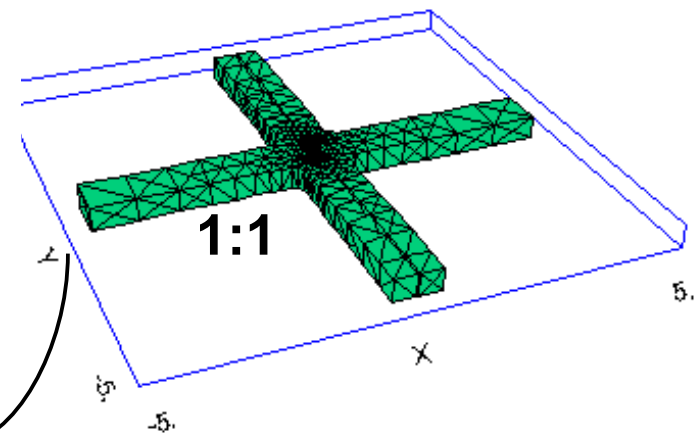
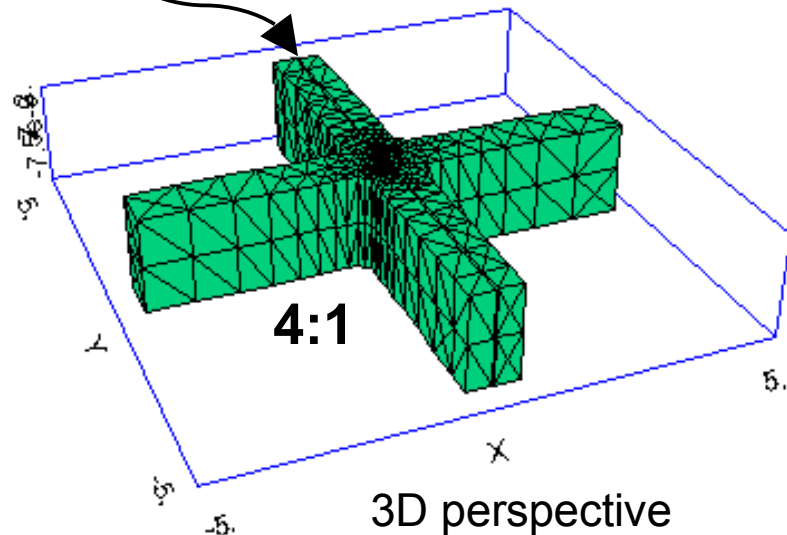


Fabrication challenge: High aspect ratio required

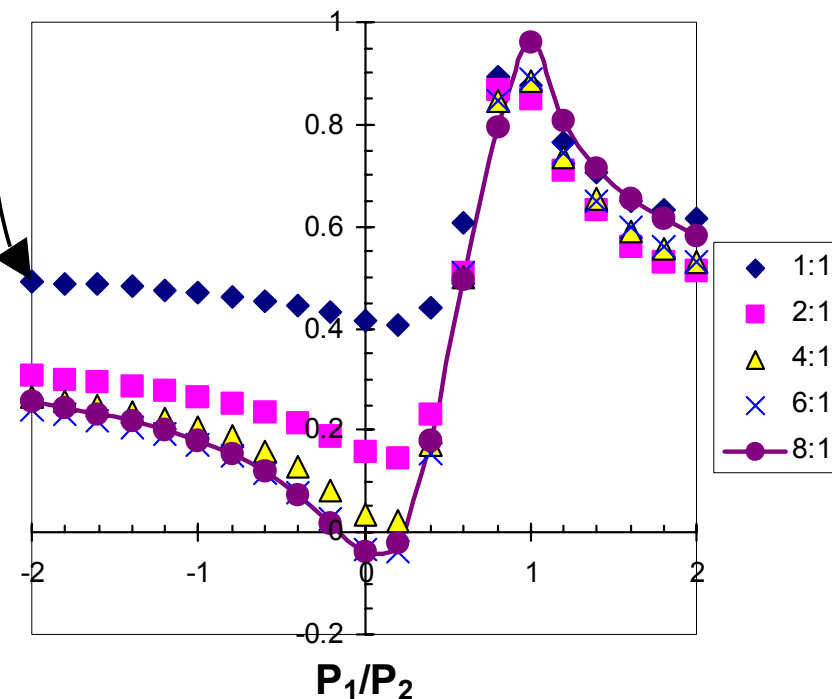
Finite element
calculations



Fin has very high
aspect ratio.



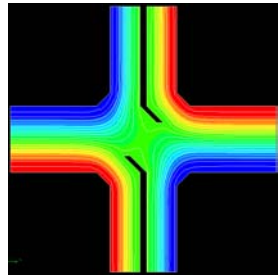
Flow Type, Different Height Channels



2D limit

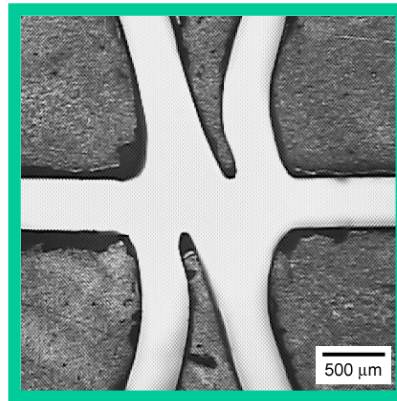
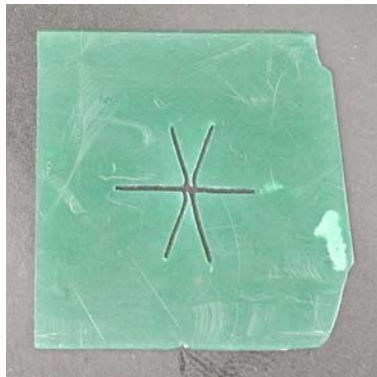


Device fabrication



Tall narrow fin: $\approx 10:1$ aspect ratio

- Engrave wax master.

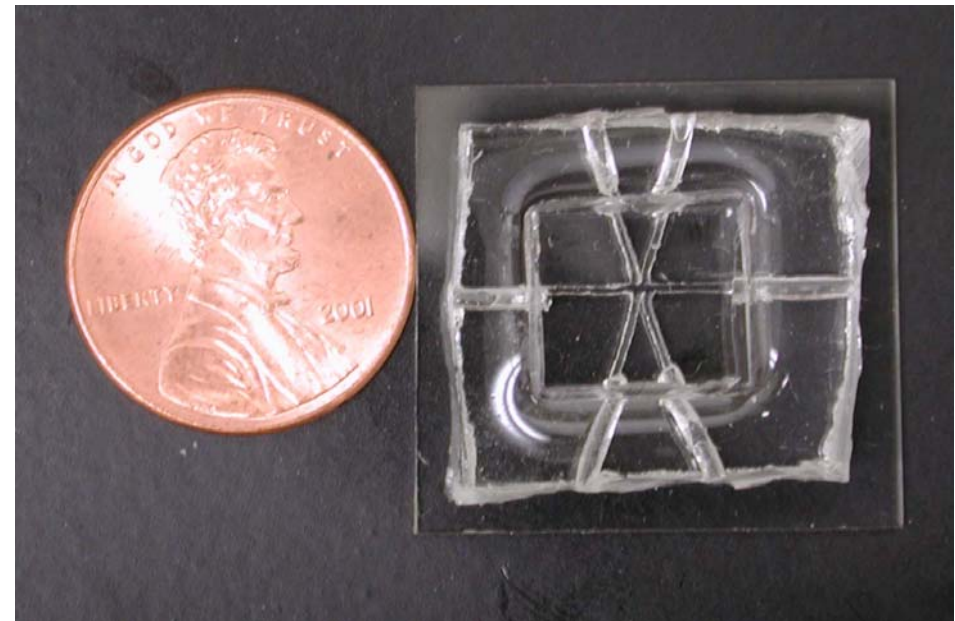


Channel dimensions:
 $400 \times 1100 \mu\text{m}$

Fin dimensions:
 $120 \times 1100 \mu\text{m}$

Masters were also made using a low-viscosity photo-activated optical adhesive, using a photolithographic process.

- Replicate twice with PDMS.

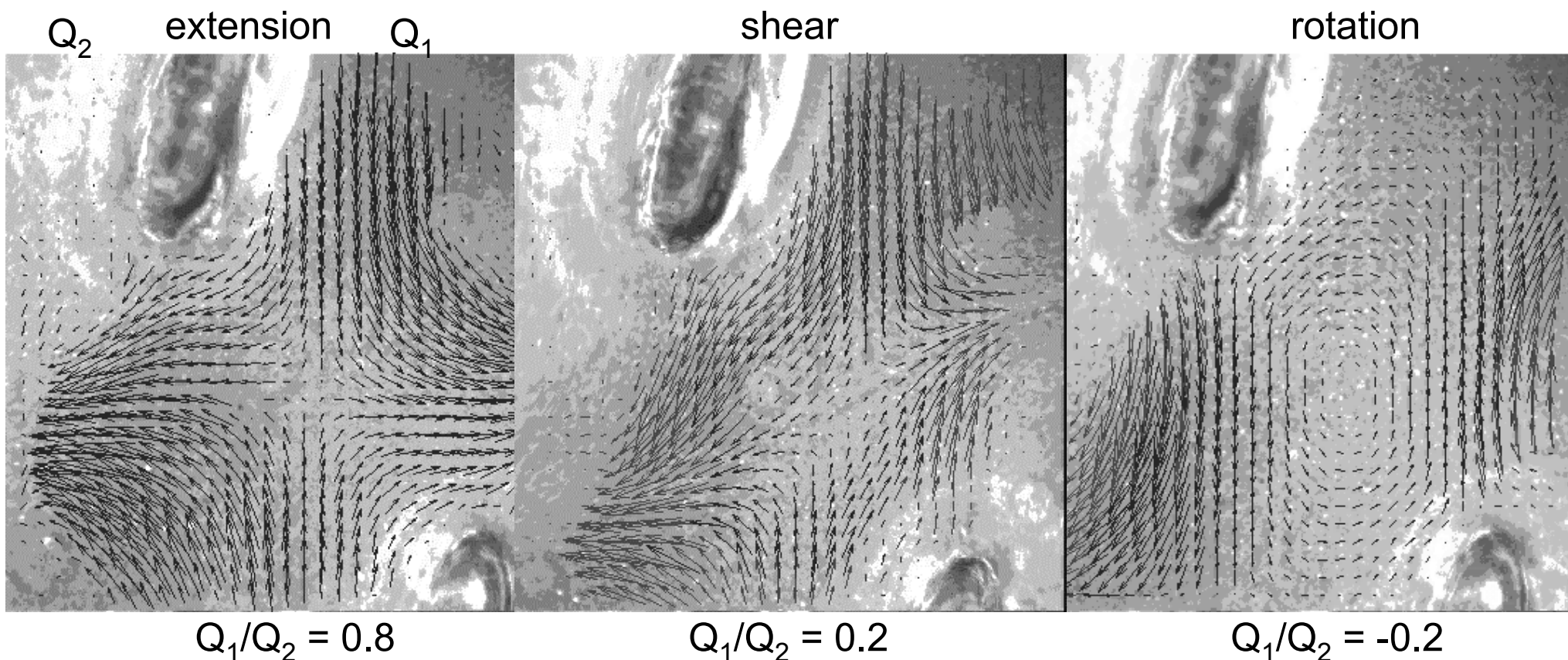
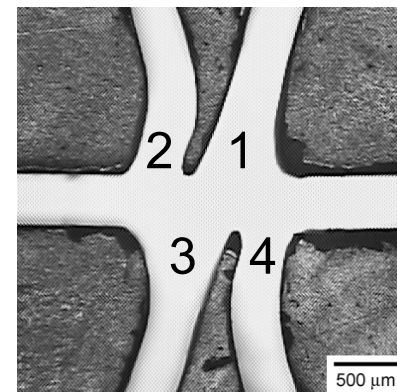


Adhesion of fin to glass substrate is robust to stresses above 10^4 Pa .



Device performance

- Particle image velocimetry to map flow field.
- A range of flow types is achieved.



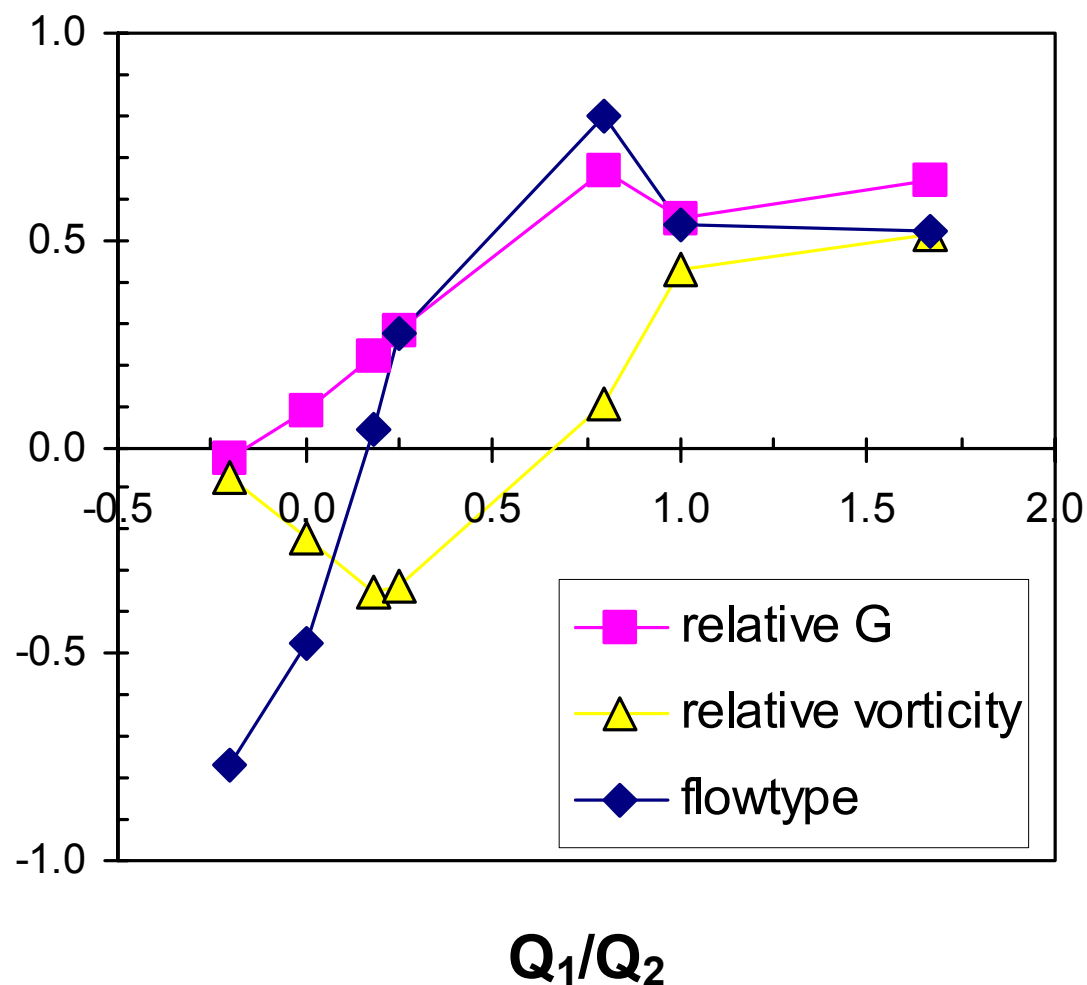
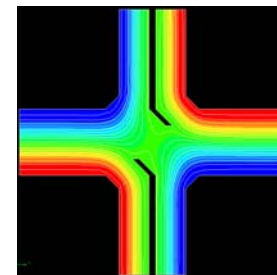
Fin: 120 x 1100 μm .
Channels: 400 x 1100 μm .

NCMC-4: Polymer Formulations Workshop
October 7, 2003

Emulsion: pdms-b-(peg-r-ppg) in ppg. 52 Pa s.
Phase-contrast imaging.
The flow rates, Q_i , were adjusted such that:
 $Q_1=Q_3$ and $Q_2=Q_4$.



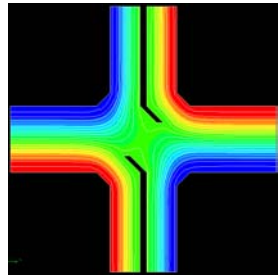
Device performance



- A wide range of flow type, including pure shear.
- Vorticity passes continuously through zero (i.e. pure extension). Clockwise and counter-clockwise rotation without reversing flow.



Device performance



- Device relaxation time

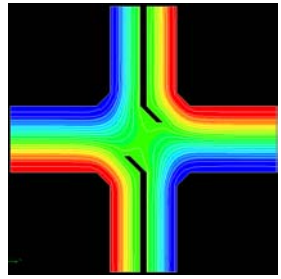
$$\tau_{device} = RC \quad R_{channel} \approx \eta \frac{12L}{wd^3}$$

- Control algorithms (for position and orientation)

$$G \leq 1 / \tau_{device}$$



Conclusions

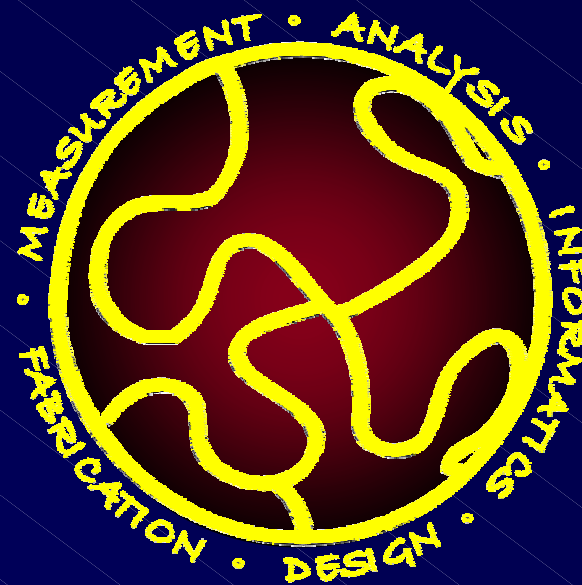


- Miniature analogue of the 4-roll mill has been developed.
- Pure shear flow is possible.
- Control algorithms can be implemented.

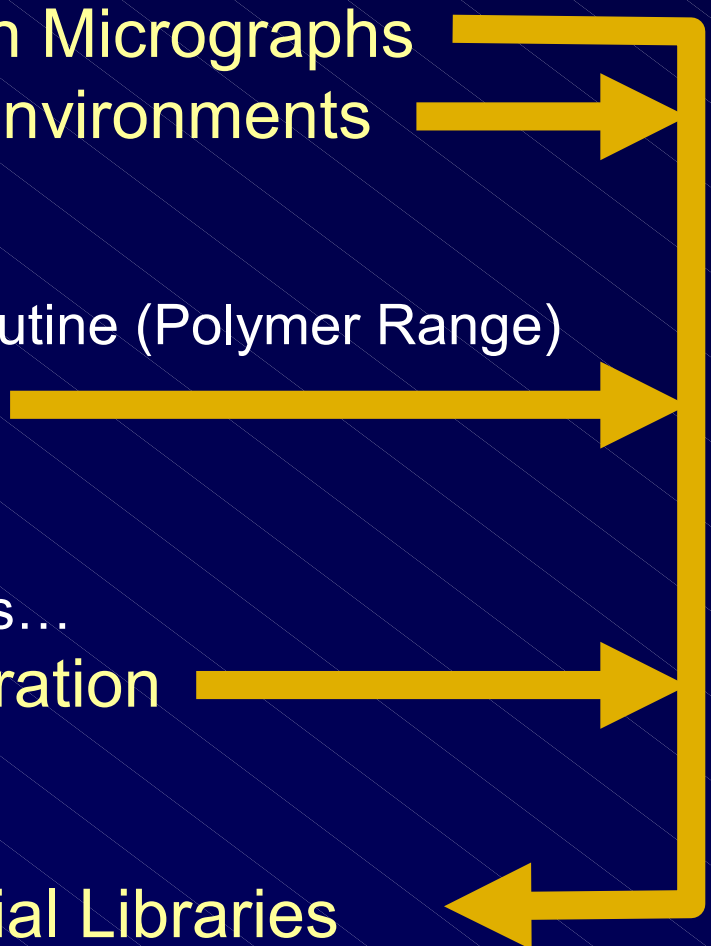
Scanning Probe Microscopy Research at the NIST Combinatorial Methods Center

Michael J. Fasolka
Mai Julthongpiput
Alamgir Karim, Eric J. Amis

*Gradient-based References and
Tools for Advanced SPM Measurements*



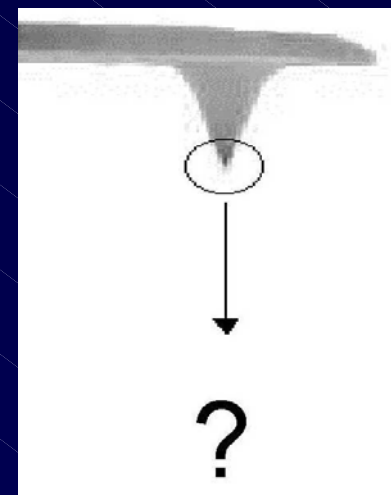
The Promise of Scanning Probe Microscopy (SPM):

- Routine Nanometer-scale Resolution Micrographs
 - Data Collection Under a Variety of Environments
 - In air (No HV required)
 - Under liquids - water and solvents
 - Higher Temperatures - Up to 250 C Routine (Polymer Range)
 - Topography + Sensitivity to Local:
 - Chemistry
 - Mechanical Properties / Adhesion
 - Magnetic and Optoelectronic Properties...
 - Automated or Semi-Automated Operation
 - Though not yet high-throughput...
 - Quantitative Analysis of Combinatorial Libraries
- 

Barriers to Quantitative SPM

What does SPM Micrograph Contrast Mean?

- **Probe (tip) Characterization**
 - Probe Shape / Size
 - Probe Quality (fabrication, modification)
 - Probe Contamination / Wear
- **Contrast Calibration**
 - Relationship to “traditional” measurement
 - Sensitivity / Resolution
 - Understanding of Tip/Surface Interactions, Artifacts
 - Instrument Parameters
- **Piezo/Lateral Length Calibration** ✓
 - NIST Calibrated AFM - T. Vorburger, MEL

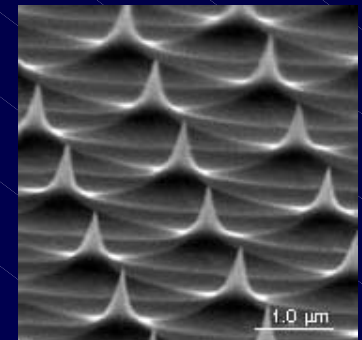


The Reference Specimen Paradigm

Highly designed substrates that aid in SPM measurements...

When scanned via SPM, a *reference specimen*...

- Characterizes the SPM probe and/or,
- Calibrates the Image Contrast



Well-designed Reference Specimens:

- Convenient / Easy to use
- Relate SPM data to other measurements
 - *E.g. NIST Traceable*
- *Ultimately, will reduce the cost of advanced SPM probes*

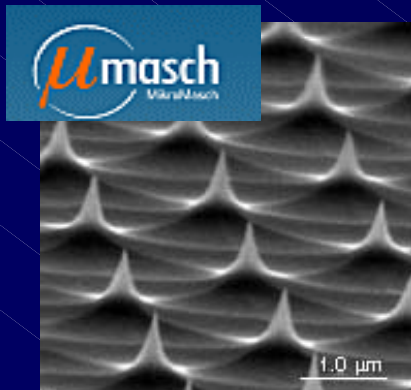
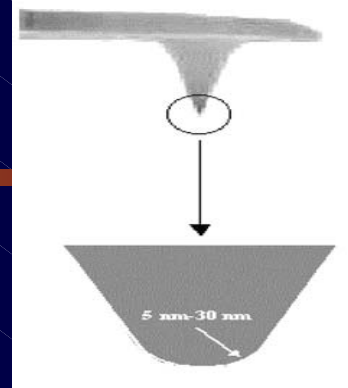


SEM of AFM Probe

The Reference Specimen Paradigm

Example: Quantification of AFM Topography

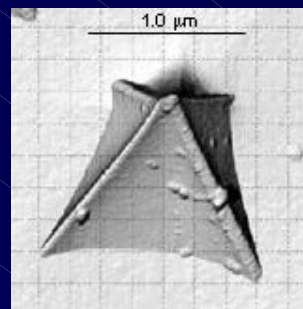
- Probe Characterization (tip shape, radius, quality)



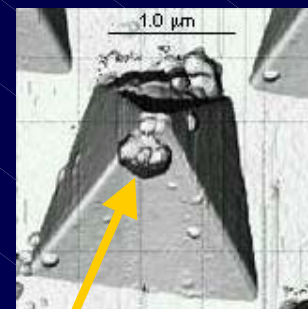
Ultrasharp reference specimen: Feature radius less than AFM tip radius



SPM of specimen yields...



3D image of tip shape



Shows tip wear, contamination

3D tip images can be used to “deconvolve” AFM micrographs to produce more accurate specimen topography data.

J.S. Villarrubia, NIST MEL

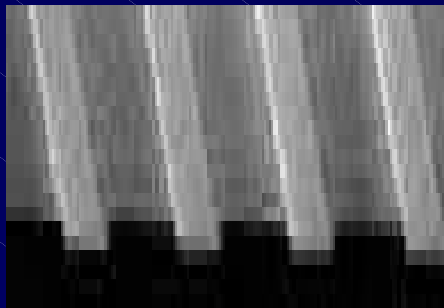
[J. Res. Natl. Inst. Stand. Technol. 102, 425 (1997)]

Includes code!

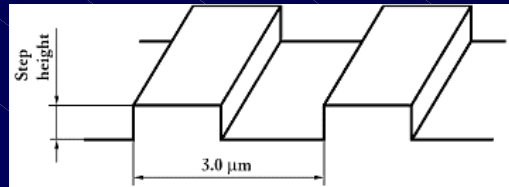
The Reference Specimen Paradigm

Example: Quantification of AFM Topography (cont.)

- Contrast Calibration (Height Data)



Step-height
reference
specimen



Step height is measured
by X-ray scattering,
ellipsometry...

- AFM image of reference specimen calibrates height data
- Reference specimen relates SPM data to other measurements
- Typically, several step heights are needed (*call for gradients...*)
- NIST research is central to SPM height calibration...

T.V. Vorburger et al NIST, MEL - Calibrated SPM/Step-Height Standards
R. Dixon, R. Koning, V. Tsai, J. Fu, and T. Vorburger, Dimensional metrology with
the NIST calibrated atomic force microscope, Proc. SPIE 3677, 20 (1999).

New NCMC Program: *Reference Specimens for Advanced SPM Techniques*

Outreach: Instrument Producers & Users

Hysitron: Nano-indentation Instruments

Digital Instruments/Veeco: SPM Instruments

New NCMC
Members!

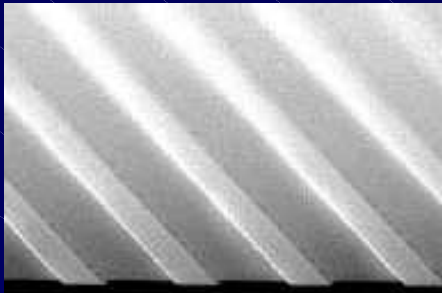
Research: Reference Specimen Design, Prototyping, Testing
For next generation SPM techniques that map...

- **Mechanical/Adhesion Properties**
 - Atomic Force Acoustic microscopy (AFAM), colloidal AFM, Phase
(*D. Hurley, P. McGuiggan, MSEL NIST*)
- **Chemistry/Surface Energy**
 - Chemical Force Microscopy (CFM)
(*T. Nguyen, X. Gu - BFRL; K. Briggman, J. Hwang - Physics, NIST*)
- **Electro-optical and Magnetic Properties...**

Reference Specimen Design/Prototyping

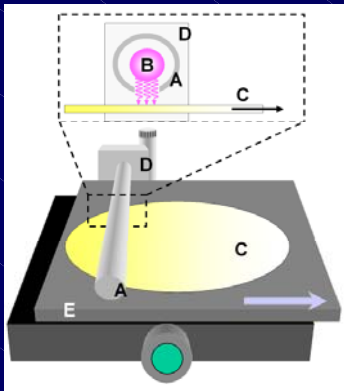
Duangrut “Mai” Julthongpiput

Bench top Micro/Nanopatterning



- Soft lithography (μcp)
- imprinting/embossing
- self-assembly

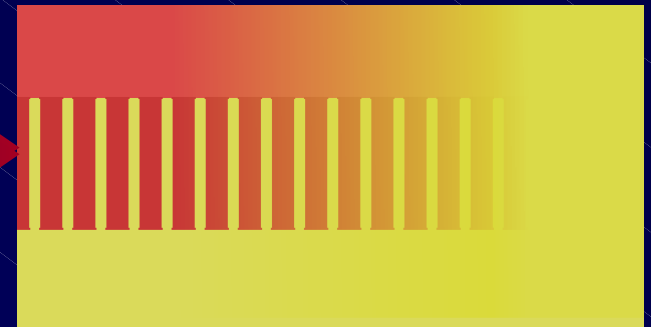
NCMC Gradient Toolbox



- ∇ surface energy
- ∇ composition
- ∇T processing
- ∇ crosslinking
- ∇ Thickness

Gradient Reference Specimens

*Many Conditions
Single Substrate*

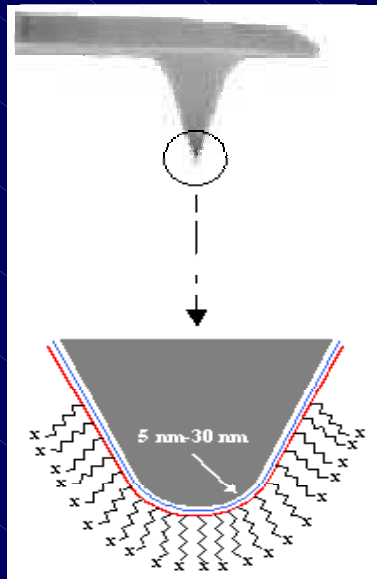


- Gradient Property Pattern
- “Internal Reference”
- Characterizes Probe
- Calibrates Contrast
- Technique Diagnosis

Chemical Force Microscopy (CFM)

C.D. Frisbie, L.F. Rozsnyai, A Noy, M.S. Wrighton, C.M. Lieber, 1994, *Science* 265:2071

A. Noy, D.V. Vezenov, and C.M. Lieber, *Annu. Rev. Mater. Sci.*, 1997, 27:381



AFM probe
modified with
SAM

Chemically Functionalized AFM probe with increased sensitivity to chemical differences:

- Tapping-Mode Phase imaging
- Friction Force Contact imaging

Barriers to a Better CFM:

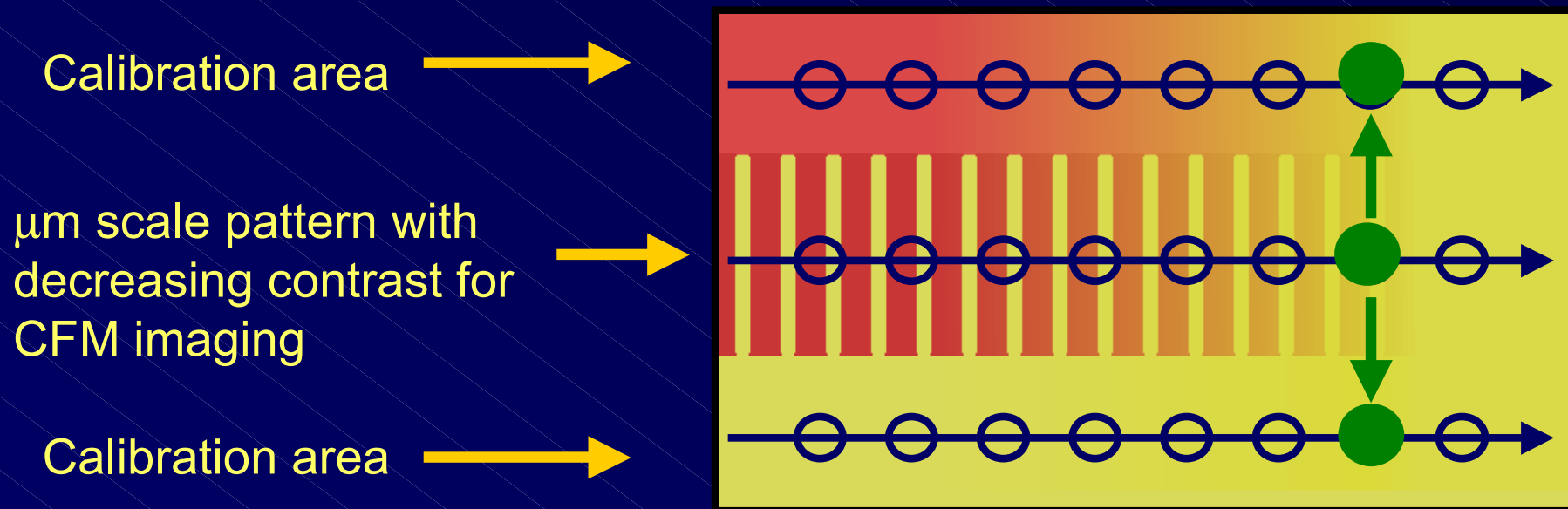
Moving CFM beyond the demonstration stage:

- Characterization of probe functionalization
Quality and Reliability of SAM
- Calibration of CFM Contrast
What does it mean?

Call for a reference specimen...

Gradient Reference Specimen for CFM

NIST ATP Program - with BFRL, Physics



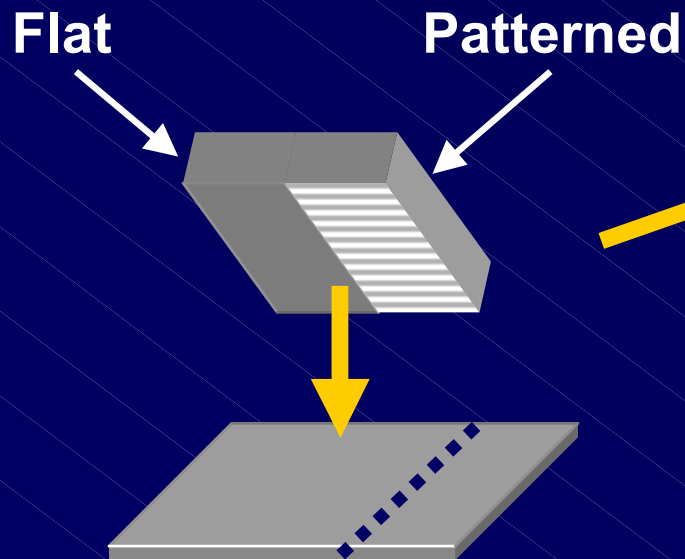
- Gradient of **Hydrophobic** and **Hydrophilic** domains
- Calibrates contrast w.r.t. traditional measurements.g. FTIR, contact angle
 - Illuminates **chemical sensitivity** (minimum contrast)
- Characterizes functionalized probe

Fabrication of CFM Reference Specimen

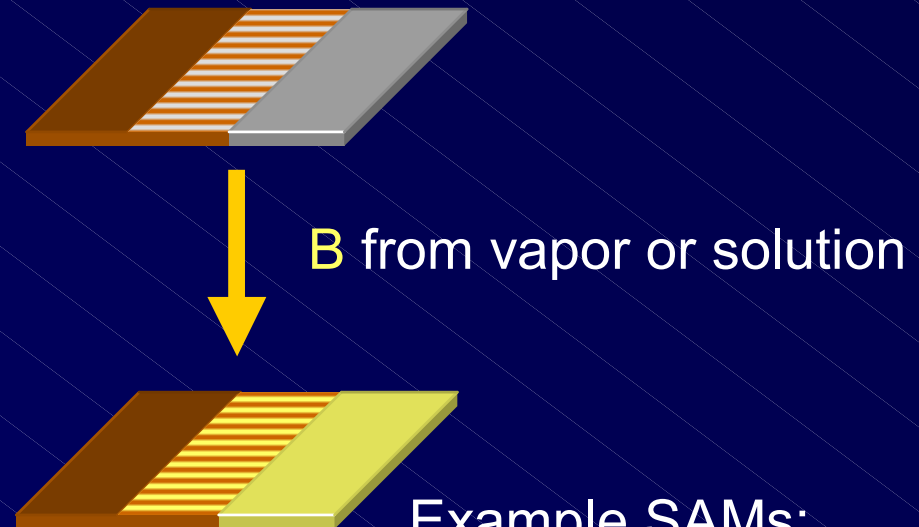
1. μ -contact print SAMs on substrate

Print with **SAM A**

Composite PDMS Stamp



Fill with **SAM B**



Example SAMs:

A: - $(\text{CH}_2)_{15}$ - CH_3

B: - $(\text{CH}_2)_{17}$ - COOH

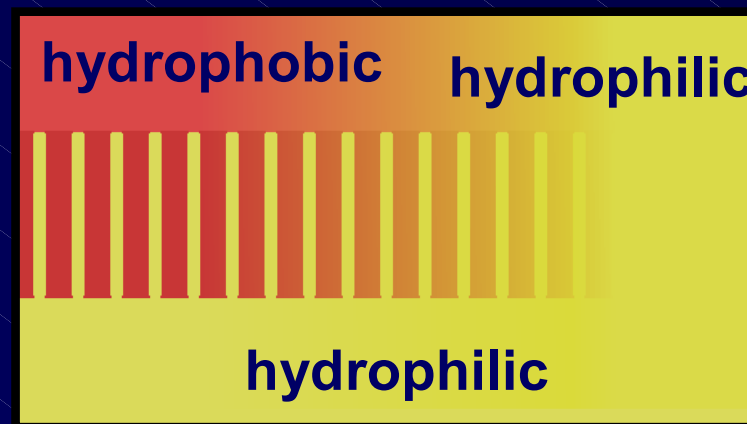
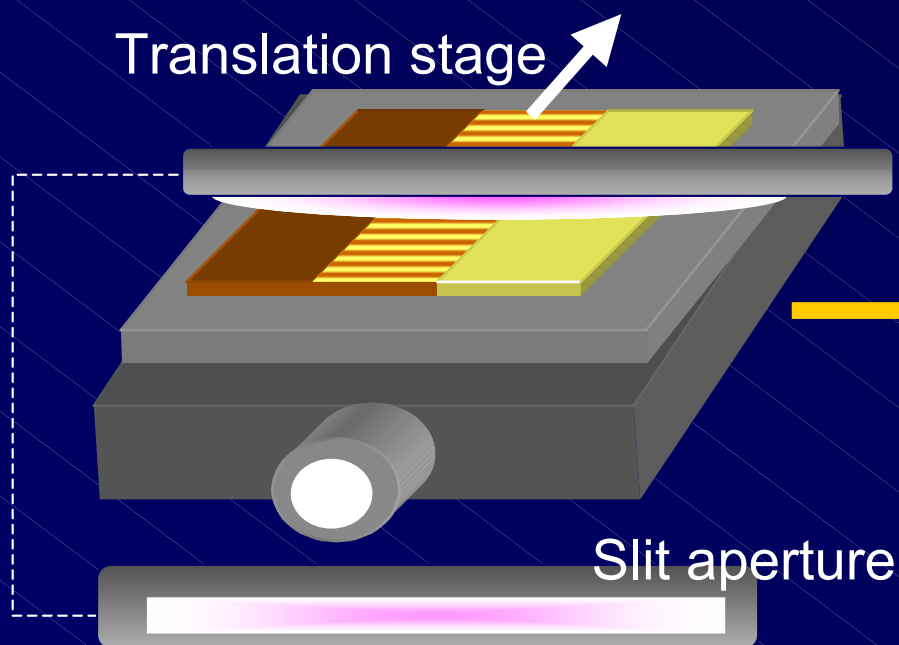
Fabrication of Reference Specimen

2. Application of UV-ozone exposure gradient

NCMC UVO Gradient Device

Exposure dependent SAM conversion

Translation stage

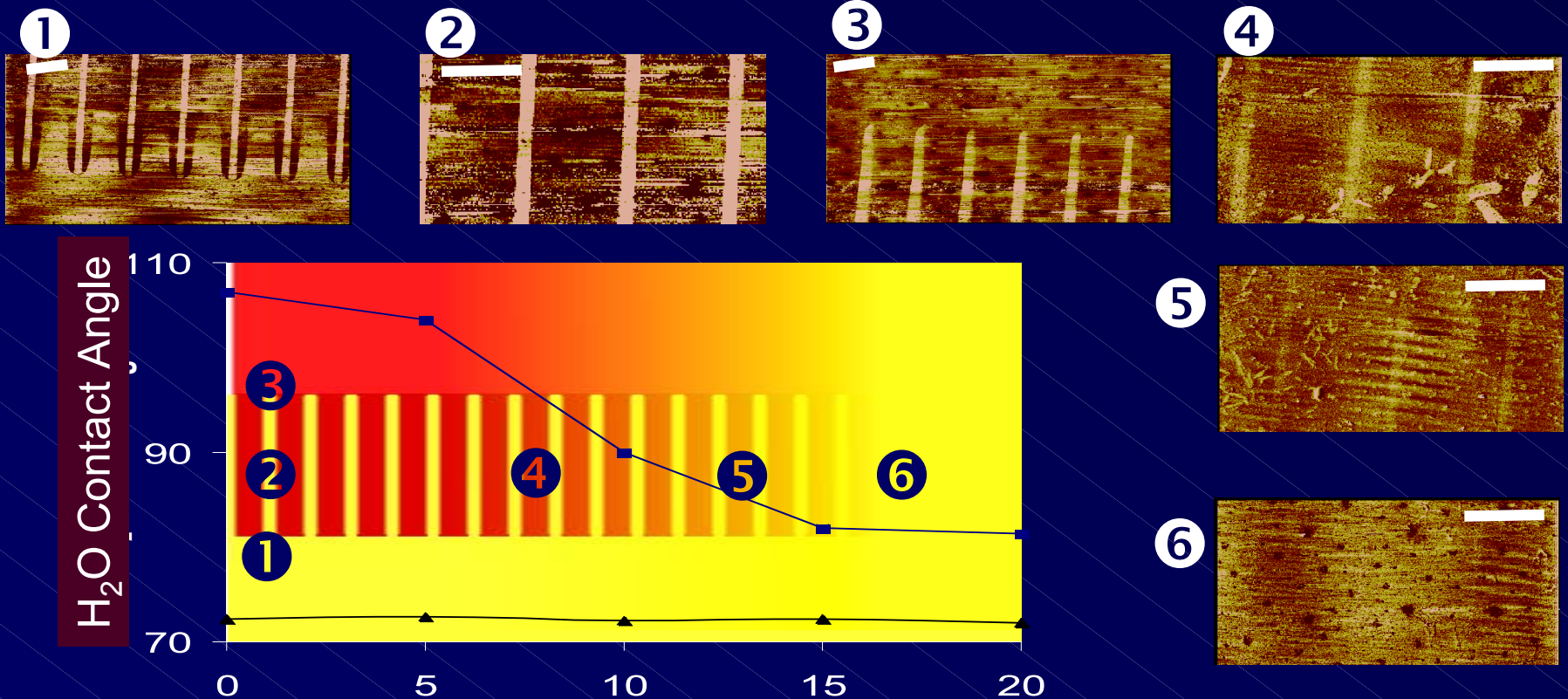


Complete Reference Specimen

- 192nm UV wand source
- O_3 and O generation

Gradient Reference Specimen Demonstration

Contact-Mode Friction AFM Images



Scale bars are 10mm
Images have equal z-scales

Print: $(\text{CH}_2)_{17}\text{-CH}_3$ SAM

Fill: $(\text{CH}_2)_{15}\text{-COOH}$ SAM

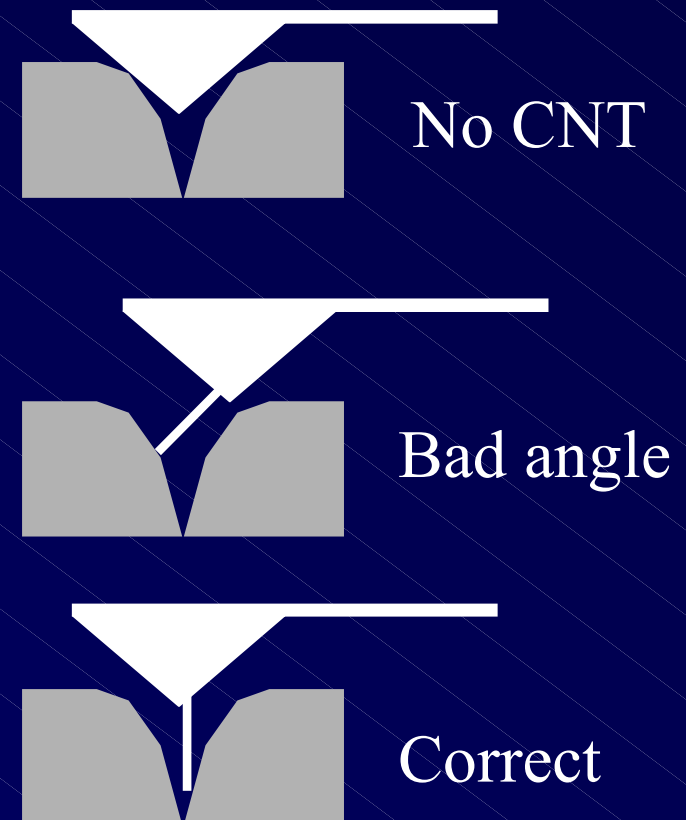
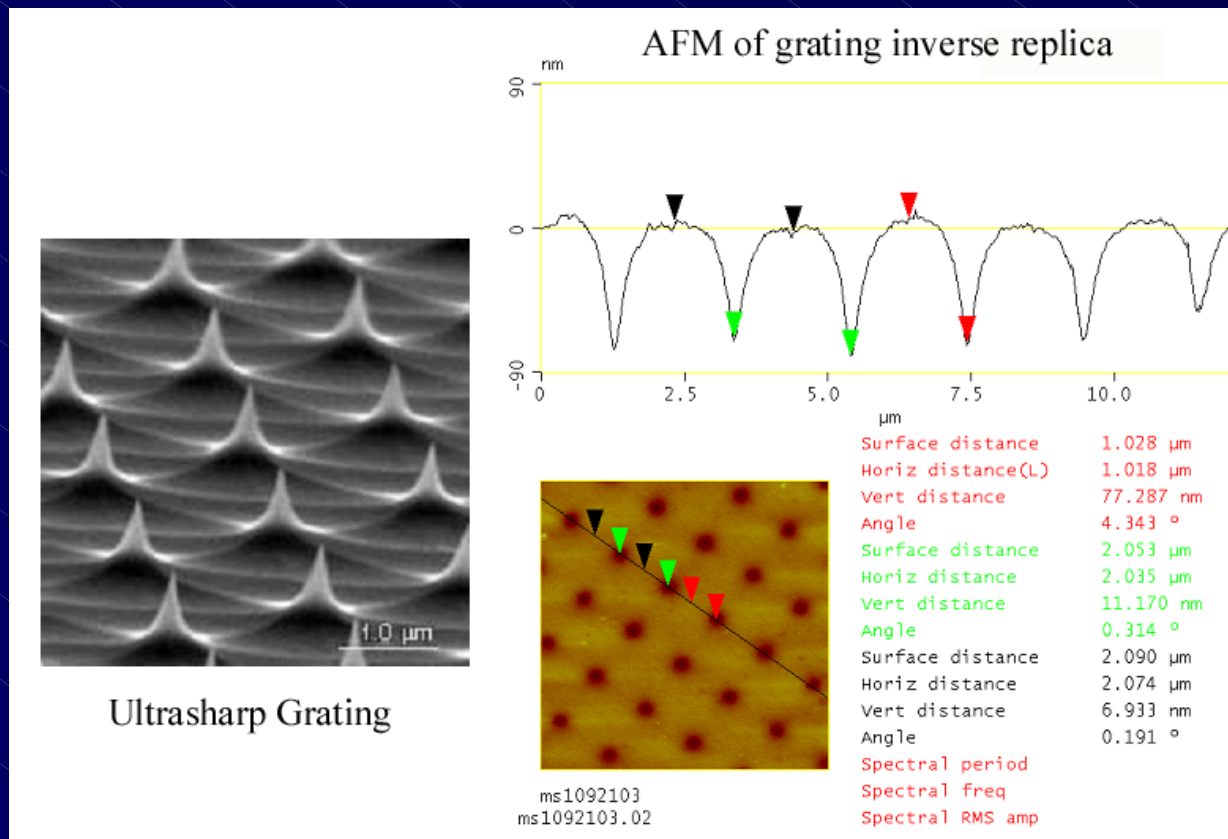
Linear UV Exposure Ramp: 0 - 60s



Reference Specimen for ultrasharp probes (e.g. CNT)

Probe Quality: Length and Angle of CNT on AFM tip

PDMS Casting of tip-reference substrate



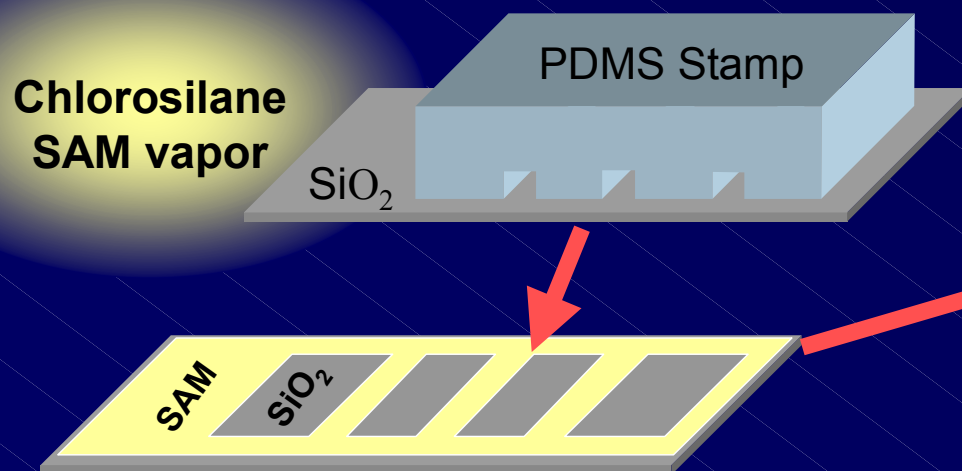
Current Direction: Making Specimens more Robust

Initial Prototypes: Thiol SAM Patterns on Gold **Easy but Fragile**

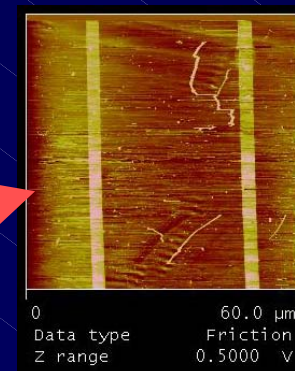
New Specimens: Chlorosilane Patterns on SiO_2 **Difficult but More Robust**

A new “ink-less” method for preparing SAM patterns on SiO_2 :

- Minimizes environment effects (less sensitive to H_2O)
- Better Reproducibility (No Inking of PDMS Stamp)
- Amenable to Multiple Specimen Processing
- Amenable to Gradient Processing



Vapor soft lithography!

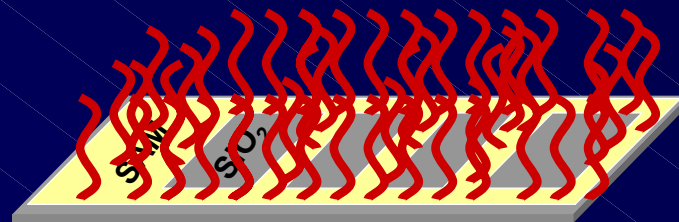
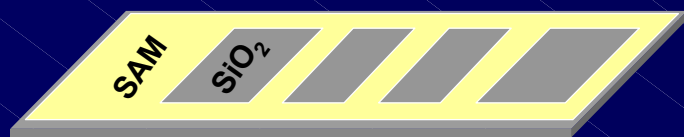


Friction AFM:
Fluorinated
chlorosilane SAM
pattern on SiO_2

The Future: Prospects and Portents

- A Suite of Reference Specimens for Advanced SPM
 - CFM - Chemical Imaging
 - AFAM/Colloidal AFM - Mechanical/Adhesion Imaging
 - Other Techniques - Optoelectronic, Magnetic...

Gradient SAMs → Platform for Gradient Graft Polymerization...
...surface complexity, versatility, robustness



- Gradient Surface Standards for a Wider Set of Technologies
 - Microfluidics - Mixing, Flow Control, Compatibility...
 - Adhesion – model surfaces
 - Bio-surfaces/Biomaterials

Useful for Many NCMC Projects

SPM Research at the NCMC

Collaborators:

NCMC / MSEL

Mai Julthongpiput (Polymers)

Patty McGuiggan (Polymers)

Donna Hurley and Paul Rice (Materials Reliability)

BFRL

Tinh Nguyen

Xiaohong Gu

Physics

Kimberly Briggman

Jeeseong Hwang

CFM Project

Funded by the
NIST ATP
Program

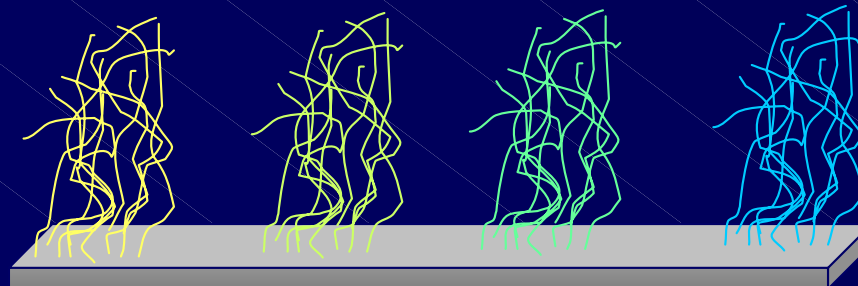
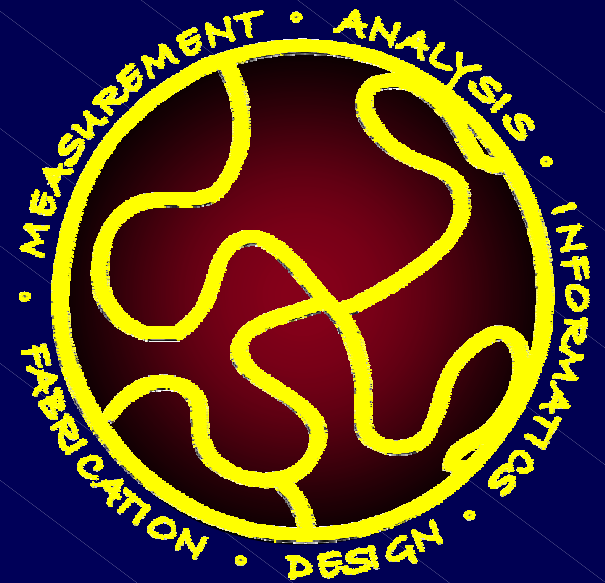
Discussion:
*Gradient Reference Surfaces
via Graft Polymerization*

Leaders/Moderators:

Kate Beers

Mike Fasolka

Eric Amis



Interaction of Complex Fluids with Surfaces

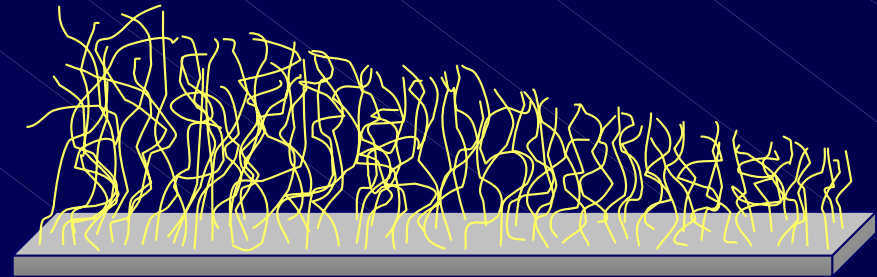
Calibrating interfaces with model substrates

Grafted Polymer

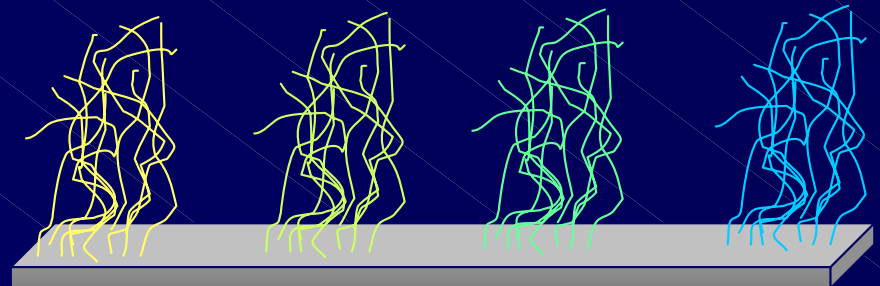
- More stable than SAMs
- Broader range of properties
 - Heterogeneity
 - Patterning
- Recently developed chemistry

Environments

- Fluidic channels
- Direct-write / Microelectronics
- Extruders
- Biosurfaces
- Inking/Printing



Tomlinson and Genzer, *Macromolecules*,
2003, 36, 3449.



Reference Surfaces: Parameters of Interest?

Fluid/Surface Interaction:

Compatibility
Adhesion
Selectivity

Test Fluid: Type? Components?

End Group:

Type?
Functionality?
Reactive?

Polymer Unit(s):

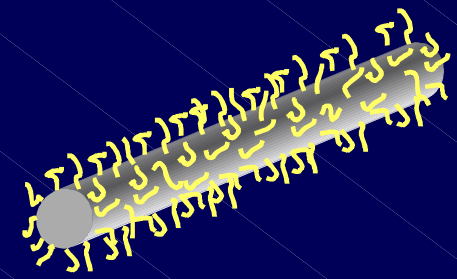
Polarity?
Functionality?
Charge?
Meso-Structure?
Crystalline...

Substrate

- Material? SiO_2 , Polymer...
- Geometry?
Planar
Fiber: textile, optical, hair...
Particle

Thickness

?

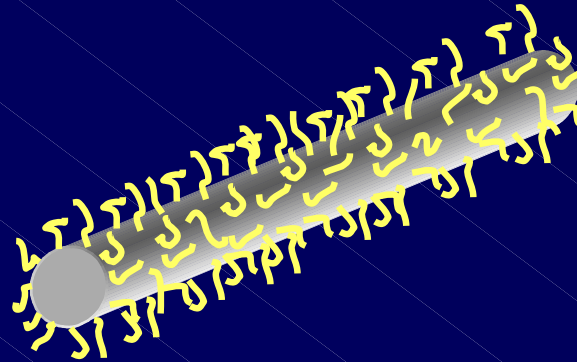


Modified Fiber Surfaces?

Polymer grafted fibers as model
interfaces

Environments

- Optical Fibers
- Hair
- Textiles



Recruitment focus this year: Instrument Producers

We are compiling a list of instrument producing companies that would be valuable additions to the NCMC.

Aims:

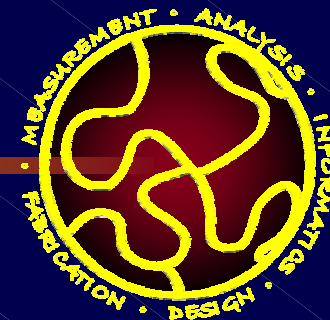
- Work together with these companies towards instrumentation that is better suited for Combi/High-Throughput Materials Research.
- A better foundation for Informatics Interchange Standards (CMRDS).

Submit suggestions to Mike Fasolka (mfasolka@nist.gov) ASAP. Add a contact if you have it...

Open Discussion Notes: Gradient Surfaces as Standards

- Physical-aging of organic based polymers is a big issue for some
- Properties of importance
 - Mechanical properties
 - Modulus
- Need to start with a primitive system, then work to more complicated
- Possible scenario: modulus change as a function of orientation (for a polymer in a given solvent)
- Question raised: What is the advantage of a gradient?
- What to study: All properties of interest and how they can be related
- Issue: Nano-porosity

Laboratory Tours:



We have arranged for 2 laboratory tours on Tuesday afternoon

High Throughput Flammability Testing and Gradient Extrusion Facilities

Rick Davis, Jeff Gilman - Building and Fire Research Lab

High Throughput Characterization of Metal Contacts to Wide-Band-Gap Semiconductors

Albert Davydov - Metallurgy Division, MSEL

Sign up for tours with Cher Davis by the end of today's meeting

- Tour groups will leave at 2pm and 3pm on Tuesday
- These are *in addition* to NCMC facilities Open House